

Solvated Electron

A symposium sponsored
by the Division of Physical
Chemistry at the 150th
Meeting of the American
Chemical Society, Atlantic
City, N. J., Sept. 15–16, 1965.

Edwin J. Hart, *Symposium Chairman*

ADVANCES IN CHEMISTRY SERIES

50

AMERICAN CHEMICAL SOCIETY

WASHINGTON, D. C. 1965

A. C. S. Editorial Library

Copyright © 1965

American Chemical Society

All Rights Reserved

Library of Congress Catalog Card 65-26801

PRINTED IN THE UNITED STATES OF AMERICA

**American Chemical Society
Library**

1155 16th St., N.W.

Washington, D.C. 20036

In Solvated Electron, Hart, E.
Advances in Chemistry; American Chemical Society, Washington, DC, 1965.

Advances in Chemistry Series

Robert F. Gould, *Editor*

Advisory Board

Fred Basolo

Raymond F. Boyer

Jack Halpern

George W. Irving

Amel R. Menotti

C. M. Sliepcevich

Leo H. Sommer

Fred R. Whaley

William A. Zisman

AMERICAN CHEMICAL SOCIETY PUBLICATIONS



FOREWORD

ADVANCES IN CHEMISTRY SERIES was founded in 1949 by the American Chemical Society as an outlet for symposia and collections of data in special areas of topical interest that could not be accommodated in the Society's journals. It provides a medium for symposia that would otherwise be fragmented, their papers distributed among several journals or not published at all. Papers are reviewed critically according to ACS editorial standards and receive the careful attention and processing characteristic of ACS publications.

P R E F A C E

The interaction of ionizing radiations with liquid water generates hydrated electrons (e_{aq}^-). Therefore, one may confidently say that about four billion years ago hydrated electrons first appeared on this planet. But so evanescent and elusive is this species that only in the present decade has it been identified positively. In contrast to this prodigious time lapse between formation and identification of hydrated electrons are the 43 years between the preparation of ammoniated electrons by Weyl in 1864 and their postulation by Kraus in 1907. Some 50 years later radiation chemists realized that the primary reducing species formed in irradiated water was the hydrated electron and not the hydrogen atom.

Current interest in the hydrated electron has sparked increased activity in the entire field of solvated electrons. If Conant and Hall had the hydrated electron at their disposal, they might have refrained from writing that "Much important chemistry has been obscured by our slavish devotion to water." Now, because of the interconversion of hydrogen atoms and hydrated electrons in alkaline solutions and because the hydrated electron is a primary product in many photochemical processes, intensified studies on aqueous systems at the experimental and theoretical levels may be predicted.

In the century since its discovery, much has been learned about the physical and chemical properties of the ammoniated electron and of solvated electrons in general. Although research on the structure of reaction products is well advanced, much of the work on chemical reactivity and kinetics is only qualitative in nature. Quite the opposite is true of research on the hydrated electron. Relatively little is known about the structure of products, but by utilizing the spectrum of the hydrated electron, the reaction rate constants of several hundred reactions are now known. This conference has been organized and arranged in order to combine the superior knowledge of the physical properties and chemical reactions of solvated electrons with the extensive research on chemical kinetics of the hydrated electron.

More and more it is becoming evident that the term "solvated electron" is but a mask for our ignorance of the actual structure of the species present in metal-solvent solutions. In their introductory paper entitled "Nature of Electronide and Spinide Solutions of Alkali Metals in Liquid Ammonia and Similar Solvents," Kraus and Evers propose a new nomenclature for identifying the species present. We are delighted that Professor Kraus, now in his 90th year, is able to give us the benefits of his experience and judgment in this area of research. Possibly only in

irradiated metal-free solutions, where the solvated electrons are free from attachment to positive ions, may the properties of these species be studied. At least, comparing the behavior of these solvated electrons with those of dilute metal solutions will improve our understanding of these more complex metal-ammonia systems.

The papers presented at the Solvated Electron Symposium at the 150th National Meeting of the American Chemical Society, September 1965, in Atlantic City, form the basis for this volume. In the first six papers, the present status of research on theory, structure, and reactions of solvated electrons, and of hydrated electrons are reported. The next eight papers, of a more detailed nature, deal with the electrical transport properties, conduction processes, volume expansion, spectroscopy, photochemistry, theory of electron transfer reactions, and structure of solvated electrons. The final seven papers deal principally with the hydrated electron. Properties discussed are its behavior in frozen aqueous solution, its optical generation, reaction with water, its behavior in the radiation "spur," its use in chemical analysis, and its reactions with substances of biological importance. Solvated electrons in general and hydrated electrons in particular are important, new, highly reactive ions. Because they are easily formed and can be studied by pulse radiolytic methods, significant contributions to our understanding of the mechanism of chemical reactions are expected in the present decade.

Argonne, Ill.
June 1965

EDWIN J. HART

Nature of Electronide and Spinide Solutions of Alkali Metals in Liquid Ammonia and Similar Solvents

CHARLES A. KRAUS and E. CHARLES EVERS

Laboratory for Research on the Structure of Matter, University of Pennsylvania, Philadelphia, Pa. 19104

The conductivity of salts in solvents of low dielectric constant, and of metals in liquid ammonia, exhibit minima which may be explained in terms of an equilibrium between ions and a coulombic compound of two ions, or "ion pairs." This equilibrium conforms to the law of mass action. At limiting conductance in solutions of sodium in liquid ammonia, part of the current is carried by metal ions, but seven-eighths is carried by electronides. Following the BLA model, it is assumed that when two ion pairs, consisting of a sodium ion and an electron, come together, the spins of the two electrons couple to form disodium spinide. Increase in conductivity past the minimum is assumed to be caused by dissociation of disodium spinide into sodium ions and spinions.

For this discussion, coulombic compounds between single electrons and metal ions shall be termed "electronides" and their negative ions "electronides"; similar compounds between metal ions and spin-coupled electrons shall be termed "spinides" and the negative ions "spinions."

Conductance and Structure

In the solid state a metallic element such as sodium consists of an ordered network of positively charged sodium ions and spin-coupled electrons which move freely through the field owing to the positive ions. In this state the conductance is high.

In the crystalline state sodium chloride consists of an ordered network of sodium and chloride ions. The ions in this network are almost completely fixed in position, and they have a very low conductance which, however, increases slightly with increased temperature. This conductance increase contrasts with the behavior of metallic sodium in which the conductance decreases with increasing temperature.

When sodium chloride is carried past its melting point, the molten compound becomes an excellent conductor, and conductance proceeds by an ionic process. As the current is passed between electrodes in the melt, reactions occur at the two electrodes, sodium metal being produced at the cathode and elemental chlorine at the anode.

By contrast, when current is passed through metallic sodium, whether solid or liquid, no electrochemical reactions occur. It is characteristic of metals that the current passes from one metal to another without any material effects.

Coulombic Interactions

When sodium chloride is dissolved in water at ordinary temperatures, it is practically completely dissociated into sodium and chloride ions which, under the action of an external field, move in opposite directions and independently of each other subject to coulombic interactions. If, however, sodium chloride is dissolved in a solvent of lower dielectric constant, and if the solution is sufficiently dilute, there is an equilibrium between ions and a coulombic compound of the two ions which are commonly termed "ion pairs." This equilibrium conforms to the law of mass action when the interaction of the ions with the surrounding ion atmosphere is taken into account. In solvents of very low dielectric constant, such as the hydrocarbons, sodium chloride is not soluble; however, many quaternary ammonium salts are quite soluble, and their conductance has been measured. Here at very low concentrations, there also is an equilibrium between ions and "ion pairs" which conforms to the law of mass action; but at higher concentration, in the neighborhood of $1 \times 10^{-4}N$, or below, a minimum occurs in the conductance. Thereafter, it may be shown that the conductance increases continuously up to the molten electrolyte, provided that a suitable electrolyte and solvent are employed which are miscible above the melting point of the electrolyte.

Sodium in Liquid Ammonia

Sodium is quite soluble in liquid ammonia, forming a saturated solution which contains 5.7 molecules of ammonia per atom of sodium. The density of the saturated solution is 0.578 g./cc. at $-33.8^{\circ}C.$; the specific conductance is 5047, and the atomic conductance is 0.800×10^4 . Considerable expansion occurs when a metal is dissolved in ammonia, and it may be pointed out that a saturated solution of lithium in ammonia is the lightest liquid known at room temperature, having a density of only 0.477 g./cc.

With decreasing concentration the atomic conductance of the sodium solution decreases to a minimum of 540 at 0.04*N*. Beyond the minimum, the conductance increases with increasing dilution and approaches a limiting value of 1022. It is obvious that between the minimum and infinite dilution, phenomena are occurring which are very similar to what one finds in all electrolyte solutions. In short, the conductance varies much like that of an ordinary electrolyte in liquid ammonia and similar solvents.

As stated above, the limiting conductance at infinite dilution has been determined to be 1022. The limiting conductance for the sodium ion is approximately 130. There can be no doubt therefore, that in a dilute solution of sodium or other alkali metal in liquid ammonia, part of the current is carried by metal ion. In the case of metallic sodium at the limiting conductance, one-eighth of the current is carried by the sodium ion; the other seven-eighths of the current is carried by the electrons. Thus, in a dilute solution, the conductance process is in part purely electrolytic.

Nature of the Current

Although seven-eighths of the current is carried by electrons, this process is not the same as that by which a current is carried in a metal. The low value of the conductance (about 900) of the electron in dilute solution shows clearly that in its motion, the electron interacts with solvent molecules in such a way as to reduce its mobility. The existence of such interaction between the electron and ammonia is confirmed by the magnetic resonance and optical properties of alkali metal solutions.

In one respect, the current passing through a solution of sodium in liquid ammonia is metallic in nature. The current passes from solution to metal and vice versa without any evidence of material effects at the electrodes. The process on electrolysis of a dilute sodium solution may be followed readily if the solutions used are sufficiently dilute so that the electrodes may be observed visually and the potential is sufficiently high to bring about concentration changes in a reasonable period of time.

On electrolyzing a solution of sodium in liquid ammonia in this way, the density of color owing to the presence of the metal increases at the cathode and, in time, the density of color in the anode compartment decreases. If the electrolysis is continued for a sufficiently long time, the metal is carried almost completely from anode compartment to the cathode compartment. In electrolyzing the solution the sodium ions are carried to the cathode where, when they reach the electrode, they permit spin-coupled electrons in the metal to come into the solution as single electrons.

BLA Model

As pointed out above, for a solution of say, sodium chloride in a solvent of lower dielectric constant than that of water, such as alcohol,

an equilibrium exists between ions and "ion pairs" which is formed as a result of coulombic interactions between the ions.

There is reason to believe that an equilibrium of this type exists between the sodium ions and the electron to form an "ion pair" as a result of coulombic interactions. If the conductance data for sodium are used to determine the equilibrium constant of sodium in liquid ammonia for computing the constant of the "ion pair" equilibrium, the experimental data do not conform to values required for such an equilibrium. This is because electrons in dilute solutions exhibit magnetic properties, from which we may conclude that, at very low concentrations, the electron has a spin of $1/2$ Bohr unit. It is, therefore, necessary to take into account the effect of the decreasing proportion of electrons that may be spin-coupled and interacting with the positive ions of the solvent. One of us (Evers) made the simplest possible assumption, following a model proposed by Becker, Lindquist, and Alder (BLA), namely that when two "ion pairs," consisting of a sodium ion and an electron, come together the spins of the two electrons couple to form disodium spinide, and that this coulombic compound is not dissociated into ions at low concentrations.

Calculations

Assuming that in equilibrium reactions the undissociated disodium spinide exists in equilibrium with the two sodium electronides which, in turn, are in equilibrium with the free ions, the dissociation constants and the limiting conductance Λ_0 of the metal in solution in liquid ammonia have been determined. For this purpose, the data employed were those which were originally obtained by one of us (Kraus) 50 years ago. The data in question were obtained in five independent series of measurements involving a total of 37 different observations which covered a range of concentration from $2.5 \times 10^{-5}N$ to near the minimum of approximately $0.04N$. The values obtained for the equilibria constants, ions to electronide, and electronide to spinide, and the limiting conductance value Λ_0 were, respectively, 7.23×10^{-3} , 27.0, 1022 based on the BLA model. On computing the conductance of these solutions of sodium in ammonia on the basis of the above constants, the calculated values differed from the observed values by a little less than 1% on the average. Considering the wide concentration range covered and their distributions, the data obtained certainly lend strong support to the underlying assumptions made in the calculations. Results obtained by Dye based on transport measurements and activity calculations, as well as resonance data, by Pitzer, Hutchison, Hughes, and others, also support this view.

Spinide Dissociation

At a concentration of approximately $0.04N$, solutions of sodium in liquid ammonia, like those of other alkali metals, pass through a minimum; thereafter the conductance increases very rapidly up to the saturated solution. This conductance increase beyond the minimum can

only be caused by the presence of a new "ionic" species whose mobility is not reduced by its interactions with the solvent molecules. The conductance increase probably is caused by the dissociation of the disodium spinide into sodium ions and spinions, and the latter ions do not interact appreciably with ammonia molecules at the minimum nor at concentrations beyond the minimum up to the saturated solution. Evidence exists that points toward the dissociation of the spinide and the formation of spinions moving freely through the solution much as they do in the metal. The amount of metal existing in the form of electronide in the neighborhood of the minimum cannot be very high since a very large amount is undoubtedly present as disodium spinide. The increased conductance can be caused only by the dissociation of the spinide.

To account for the dissociation of the spinide at higher concentration, we must consider the action of the ion field on the spinide. In electrolyte solutions where the minimum appears in solvents of low dielectric constant, the authors account for the increasing conductance of the electrolyte beyond the minimum by considering the action of the fields of individual ions on "ion pairs" which lie within the field. As Wien has shown, the dissociation of a partially dissociated electrolyte increases with the field if an external field is applied. Since the coulombic force acting between two ions is decreasing owing to the action of an ionic field, it may be dissociated into its components by the impact of a solvent molecule whose energy would not be high enough to bring about dissociation in the absence of a field. The authors have designated this action of the ionic fields on the dissociation of electrolytes as a micro Wien effect. It is obvious that, owing to the micro Wien effect, the dissociation of an electrolyte will increase very rapidly as ions are formed as a result of the ionic fields.

The role played by the micro Wien effect in dissociating the disodium spinide with increasing concentration beyond the conductance minimum is strongly indicated by the temperature coefficient of the conductance of solutions of sodium and potassium in liquid ammonia. Here we have data for the temperature coefficient of sodium and potassium from relatively dilute solutions up to saturation.

The fluidity of ammonia increases about 1.5% per degree, and in the dilute range the temperature coefficient of metal solutions is of this order of magnitude; but from a concentration of approximately 0.9*N* onward the temperature coefficient of sodium and potassium begins to increase, reaching a maximum of about 3.6% for sodium and 4.6% for potassium. The conductance increase owing to temperature increase can only be caused by an increased dissociation of sodium spinide. It follows that the conductance increase with increasing concentration of sodium solutions is to be expected and conforms with the assumptions of a micro Wien effect.

Conclusion

In this report we have emphasized the conductivity of these systems, only touching on other important physical properties. We have, how-

ever, attempted to introduce what we consider to be a logical method of naming certain species which have a high probability of existing in dilute solution; and we have proposed a mechanism to account for the minimum in the conductance curve, based on rather simplified concepts relating to the application of mass action theory.

RECEIVED May 13, 1965.

Theoretical Studies of Solvated Electrons

JOSHUA JORTNER* and STUART A. RICE

Institute for the Study of Metals and Department of Chemistry, University of Chicago, Chicago, Ill. 60637

Of the three models that have been proposed to explain the properties of excess electrons in liquid helium, two are considered in detail: (1) The electron is localized in a cavity in the liquid; (2) The electron is a quasi-free particle. The pseudopotential method is helpful in studying both of these models. The most useful treatment of electron binding in polar solvents is based on a model with the solution as a continuous dielectric medium in which the additional electron induces a polarization field. This model can be used for studies with the hydrated electron.

Theoretical and experimental studies of the bound and quasi-free states of excess electrons in liquids where no stable negative ions exist are of considerable interest in interpreting the electronic states of irregular systems. The following systems are relevant to the present discussion: (a) solutions of metals in ammonia, amines, and ethers (27); (b) the localized states of excess electrons in polar solvents, such as water and alcohols (15, 21, 29); (c) excess electrons in nonpolar solvents, such as He, Ar, etc (4, 30, 43); (d) metal-molten salt mixtures (17); (e) liquid metals (45). We shall limit our discussion to the study of metastable excess electron states in liquids corresponding to classes (b) and (c). However, some properties of systems containing a high density of excess electrons are of general interest and will also be included in this review.

We proceed by citing the following general questions:

1. What is the form of the general dispersion curve describing the momentum-energy relationship for a quasi-free electron in a liquid?

* Present address: Department of Chemistry, Tel Aviv University, Tel Aviv, Israel.

2. What are the conditions which lead to the localization of an excess electron in a liquid? The nature of the transition between localized and delocalized states—i.e., the dependence on the fluid density, temperature, and pressure—in a system where the interactions between excess electrons are negligible is of obvious interest.

3. What is the nature of the transition to the metallic state in a liquid containing a high density of excess electrons? When the concentration of excess electrons in a liquid is gradually increased, a transition from behavior characteristic of a localized state to that characteristic of a delocalized state is observed—e.g., in concentrated metal-ammonia solutions and in metal-molten salt mixtures.

4. What information about the dynamical and statistical geometry of the liquid state can be gained by studying the behavior of excess electrons in liquids?

It will be useful now to review some elementary facts regarding the structure of liquids at equilibrium. When a crystalline solid melts to form a liquid, the long range order of the crystal is destroyed. However, a residue of local order persists in the liquid state with a range of several molecular diameters. The local order characteristic of the liquid state is described in terms of a pair correlation function, $g_2(R)$, defined as the ratio of the average molecular density, $\rho(R)$, at a distance R from an arbitrary molecule to the mean bulk density, ρ , of the liquid

$$g_2(R) = \frac{\rho(R)}{\rho} \quad (1)$$

When $g_2(R)$ is unity everywhere, the fluid is completely disordered. Departures of $g_2(R)$ from unity measure the local order in the liquid. In general, $g_2(R)$ as a function of R consists of a series of rapidly damped maxima and minima. The positions of the maxima roughly correspond to the first several coordination shells, while the minima roughly correspond to the distances intermediate between the coordination shells. The area under a peak of $g_2(R)$ is related to the excess molecular density (relative to the bulk density) and is related to a rough coordination number. The radial distribution function specifies only the average local density, from which significant statistical fluctuations must occur owing to thermal motion. The thermal fluctuations are discernible in the broad diffuse peaks of $g_2(R)$ (compared to the precise order in the crystal) and in the rapid approach of $g_2(R)$ to unity as R increases beyond a few molecular diameters. A promising approach to the theory of liquids is through the direct evaluation of $g_2(R)$ without appealing to any special models. The molecular theory of liquids has recently been reviewed by Rice and Gray (40).

How is the molecular geometry of the liquid affected by the presence of an excess electron? Two extreme cases may be immediately distinguished: the free electron case and the localized electron case. The free electron may be adequately described by using a plane wave state. The physical significance of such a simple description is not trivial and will be clarified after the discussion of the pseudopotential theory. Here we

note that it is quite safe to assume that the liquid structure is not perturbed by a free electron. The electron can then be regarded as a quasi-free particle scattered from atoms in the liquid, with coherence between single scatterings from separate centers being accounted for in terms of the pair correlation function of the liquid. The structure factor for the scattering is thereby expressed in terms of the equilibrium radial distribution function.

In the case of a localized excess electron, the excess electron wave function tends toward zero for large distances from the center of localization and the liquid structure will be modified because of the following effects:

(a) Local conformational changes arising from short range electron-solvent repulsions can lead to cavity formation. This effect operates both in nonpolar liquids (e.g., liquid helium) and in polar liquids (e.g., ammonia).

(b) The long range polarization field induced by the excess electron may lead to marked structural changes in the fluid arising from electrostriction effects (operative in both polar and nonpolar liquids) and from the effects of rotational polarization (operative in a polar liquid such as water or ammonia).

The study of electron-solvent interactions in nonpolar monoatomic liquids (e.g., liquid rare gases) provides valuable information concerning the short range interactions between an excess electron and the solvent molecules. These studies provide an interesting model for electron localization arising from short range repulsions, as for liquid helium, and lead to a deeper understanding of the transition between the localized and delocalized states of an excess electron in simple fluids.

Bound and Free Excess Electron States in Liquid Rare Gases

Several experimental studies of the properties of excess electrons in simple monoatomic dense fluids have recently been completed. The most extensive data deal with liquid helium. However, some results for other liquid rare gases are also available. From these studies it is known that:

(a) The potential barrier of helium to electrons (42) is 1.3 ± 0.2 e.v. Under the experimental conditions employed the electrons move rapidly relative to the helium atoms so that the liquid does not rearrange in the process of electron injection.

(b) In the temperature range below the λ point of He the mobility, μ , is of the form $\mu \propto e^{\Delta/kT}$, where $\Delta/k = 8.1^\circ\text{K}$. The mobilities at low temperatures are high —e.g., at 0.4°K , $\mu = 10^4$ cm.²/volt sec. (31). This observation strongly implies that the dominant mechanism of dissipation involves interaction between electrons and rotons.

(c) Above the λ point of He(IV) and in He(III) above 1°K . the dissipative mechanism appears to be entirely different. The mobility of the electron is relatively low (of the order of 10^{-2} cm.²/volt sec.) and appears to depend on the density and the viscosity of the fluid (30).

(d) Ions create well defined quantized vortex rings in superfluid helium (38). The results of Rayfield and Reif are consistent with the hypothesis that both positive and negative ions in helium at 0.3°K. are accelerated by a field to a velocity where they can create a roton.

(e) Magnetic deflection experiments by Meyer (32) show that the effective mass of an electron in superfluid helium is large.

(f) In a recent study of the interaction of ions and quantized vortices in rotating He(II) Donnelly (9) showed that the experimental results can be interpreted adequately by assuming that the negative ion is characterized by a radius of 12 Å. and mass $m_i = 100 M$ in qualitative agreement with the localized model for the excess electron.

(g) Levine and Sanders (28) have demonstrated that as the density of He is increased in the gas phase at 4°K., a critical density is reached at which the mobility of the electron drops by a factor of 10^3 to 10^4 . These observations have been interpreted as indicating that the electron in He undergoes a transition from a delocalized state to a localized state as the He is compressed from gaseous densities to liquid densities.

(h) High electron mobilities have been observed recently by Schnyders, Rice, and Meyer (41) in liquid argon (400 cm.²/volt sec. at 80°K.) and in liquid krypton (500 cm.²/volt sec. at 120°K.). In liquid argon the mobility decreases with increasing temperature.

To date, three models have been proposed to explain the properties of excess electrons in liquid He:

(a) The electron is localized within a cluster of He atoms which, because of the effects of electrostriction, are at a higher density than the surrounding fluid (2). The size of the cluster is determined by assuming that the macroscopic equation of state may be extended to provide a valid density-pressure relationship (and hence phase equilibrium line) at the molecular level. Since it is unlikely that any complex of the form He_n^- is stable, this model will not be considered further.

(b) The electron is localized in a cavity in the liquid (11, 12, 24, 28, 36, 42). If the electron-atom repulsion is sufficiently strong, this state of local fluid dilation may lead to a stable state despite the large increase in the kinetic energy of the electron which accompanies the localization in the bubble.

(c) The electron is a quasi-free particle, basically in a plane wave state, and scattered by the atoms constituting the dense fluid (7, 8). When the electron-atom interaction is small, or is attractive because of a long range polarization interaction, this description will be accurate.

It is now known that the electron-He atom interaction energy is large and positive (20, 22). Experimental confirmation of this conclusion is provided by Sommers' experiment (42) which demonstrates that liquid helium (both above and below the lambda point) acts as an energy barrier of magnitude 1.3 e.v. for electrons. Because of the very large electron-helium atom interaction, the local structure of the liquid may be changed, and a substantially lower energy state is accessible to the electron if there can be created a cavity in the liquid sufficiently large to reduce the zero point energy of the localized electron without too much pressure-volume or surface tension work. This is the factor that leads to the failure of the

quasi-free electron model for an electron in liquid helium. The model in which the electron is localized in a bubble was first proposed by Ferrel, Feynman, and Kuper.

On the other hand, the interaction between an electron and an argon atom is strong and attractive, but of long range. Because of the sign and the range of the potential, no cavity formation is expected, and the quasi-free electron state should be energetically favored. Schnyders, Meyer, and Rice (41) have recently obtained preliminary data on the mobility of excess electrons in liquid argon. The magnitude of the mobility ($400 \text{ cm.}^2 \text{ v.}^{-1} \text{ sec.}^{-1}$ at $T = 90^\circ \text{K.}$) and its temperature dependence are consistent with the predictions of the free electron model.

Up to this point we have used rather crude terminology to describe the free electron state in simple liquids, and we are now faced with the following dilemma: is it possible to describe a free excess electron in a liquid in terms of a plane wave, neglecting the effect of the core electrons? Such a simple description is justified by the pseudopotential theory introduced by Phillips and Kleinman (37) and by Cohen and Heine (5).

The Pseudopotential

Electrons in a solid or a liquid may be separated into two groups: the core electrons which are the inner, tightly bound electrons with properties sometimes known by studying isolated atom or molecule, and the valence electrons which are the outer, relatively loosely bound electrons. The valence electrons are highly sensitive to the state of aggregation of the system. For our present discussion we might consider as valence electrons the outer 3s electron detached from a sodium atom in liquid ammonia, or the excess electron in a liquid rare gas.

The valence electron wave function ψ can be determined from the one-electron self-consistent field eigenvalue equation

$$(T + V)\psi = E\psi \quad (2)$$

where T is the kinetic energy operator, V the SCF potential energy, and E the valence electron energy. The valence electron energy must be determined in such a way that the Pauli exclusion principle is satisfied. This restriction is expressed mathematically in terms of the orthogonality relations between the core spin orbitals, X_c , and the valence electron eigenfunction—i.e.,

$$\langle \psi | X_c \rangle = 0 \quad (3)$$

for all X_c . Applying Equation 3 raises difficulties. It is most convenient to be able to ignore the oscillations introduced by the orthogonality condition (Equation 3) into the excess electron wave function within the core region, and use a smooth wave function; but we must still satisfy the restrictions imposed by the Pauli exclusion principle. This dilemma is resolved by introducing the pseudopotential. We introduce a pseudowave function, ϕ , for the valence electron, which is in one-to-one correspondence with the actual excess (or valence) electron wave func-

tion. The pseudowave function is not required to satisfy the orthogonality relation which implies that the valence electron must be excluded from the region of space occupied by the core electrons. The electron described by the pseudowave function ϕ is kept out of the core by adding a nonlocal repulsive potential, V_R , to the Hamiltonian, thereby defining the eigenvalue equation satisfied by ϕ to be

$$(T + V + V_R)\phi = E\phi \quad (4)$$

where the valence electron energy E is the same as in Equation 2. The potential $V + V_R$ defines the pseudopotential

$$V_{ps} = V + V_R \quad (5)$$

Cohen and Heine (5) have shown that there is no unique way to introduce ϕ and V_R by relaxing the orthogonality condition. They have taken advantage of this arbitrariness by requiring that V_R cancel the core contribution as much as possible. In particular, they have shown that the smoothest orbital (in the sense of having the lowest kinetic energy) is obtained from the following potential

$$V_R^{CH}\phi = -\sum_c X_c \langle X_c | V | \phi \rangle + \frac{\langle \phi | V + V_R | \phi \rangle}{\langle \phi | \phi \rangle} \sum_c \langle X_c | \phi \rangle X_c \quad (6)$$

The second term on the right hand side of Equation 6 is small and can be neglected. This form of the pseudopotential can be derived from the general expression obtained by Austin, Heine, and Sham (3):

$$V_R^{AHS}\phi = \sum_c X_c \langle X_c | F | \phi \rangle \quad (7)$$

where F is any arbitrary operator, by setting $F = -V$. We have thus managed to simplify the wave function by introducing the pseudopotential which depends on ϕ explicitly in two places: in the exchange potential and in V_R . The general expression for the pseudopotential for an excess electron state is conveniently displayed in the form:

$$V_{ps}\phi = (V_{coul} + V_{nuc} + V_{exc} + V_{pot})\phi - \sum_c \langle X_c | V_{coul} + V_{nuc} + V_{exc} + V_{pot} | \phi \rangle X_c \quad (8)$$

where V_{coul} , V_{nuc} and V_{exc} are the coulomb, nuclear, and exchange interaction potentials of the excess electron with the atomic or molecular core, and V_{pot} is the core polarization potential.

The pseudopotential method is extremely useful for studying both the free and localized states of excess electrons in liquids. In the case of the free electron states, a plane wave pseudowave function can be used. This formalism is also found to be extremely useful in studying localized electron states in simple liquids (—e.g., liquid helium). A direct solution to this problem in the SCF scheme is obviously impossible at present while the pseudopotential method makes the problem tractable.

The Free Electron Model

The assumption that an electron can be described as a quasi-free particle implies that the interaction between the electron and any atom in the liquid is weak. It is then necessary that the attractive potential of the nucleus experienced by the electron penetrating the atomic core and the long range core polarization potential will be balanced by the electron's increased kinetic energy in the nuclear region. This restriction implies that the pseudopotential of the atom should be small.

Pertinent information concerning the interaction of free electrons with rare gas atoms is obtained from low energy scattering data in the gas phase. Table I presents the scattering lengths, a , for the rare gas atoms, defined as

$$a = \lim_{k \rightarrow 0} \left(\frac{\tan \eta}{k} \right) \quad (9)$$

where k is the magnitude of the momentum vector and η the s wave ($l = 0$) phase shift (34, 44).

Table I. Scattering Lengths of Electrons by Rare Gas Atom

Atom	a^a a.u. <i>expt.</i>	a^b calculated
He	1.15 ± 0.05	1.19
Ne	0.2	...
Ar	-1.70	...
Kr	-3.7	...
Xe	-6.5	...

^a Experimental data from T. F. O'Malley (34).

^b Theoretical results for helium calculated using the pseudopotential method, Kestner *et al.* (23). For other calculations of the scattering length see R. W. LaBahan and J. Callaway, *Phys. Rev.* **135**, 1539 (1964).

It is apparent from these data that the relatively large and positive scattering length for the helium atom arises from orthogonality effects since the core polarization potential is small for He. For the cases of Ar, Kr, and Xe the scattering lengths are negative, so that the polarization potential overwhelms the short range repulsion effects. The scattering length for the neon atom is very small, indicating an almost complete cancellation between the positive contribution arising from orthogonality effects and the negative polarization potential.

From the gas phase scattering data we conclude that a plane wave state for the electron in liquid helium lies at positive energy relative to the vacuum level in agreement with Sommers' electron injection experiment. We proceed now to a semiquantitative treatment of free electron states in liquids characterized by a positive scattering length, which will be used to estimate the energy of interaction of a free electron with liquid helium (18).

The wave function of the electron is taken as

$$|k\rangle = \frac{1}{\sqrt{\Omega}} e^{ikz} \quad (10)$$

where r is the volume of the system. A first-order perturbation calculation can be used to obtain a rough estimate of the electron-liquid helium interaction. It is found that

$$E = \frac{\hbar^2 k^2}{2m} + \rho \langle k | V + V_R | k \rangle \quad (11)$$

where ρ is the number density of the fluid, and $V + V_R$ is the pseudopotential of a single atom. For $k = 0$ we get

$$E_0 = 4\pi\rho \int (V + V_R)r^2 dr \quad (12)$$

and E_0 is determined by the Fourier transform of the pseudopotential for $k = 0$. This transform is energy independent up to 0.5 e.v.

At low energies the pseudopotential is too large for the perturbation treatment to be applicable. We can then rewrite the Fourier transform of the pseudopotential in terms of the scattering length a , so that

$$\int (V + V_R)r^2 dr = \frac{\hbar^2 a}{2m} \quad (13)$$

leading to

$$E_0 = \frac{2\pi\hbar^2}{m} \rho a \quad (14)$$

This result properly accounts for single scattering effects. Equation 14 represents an optical approximation which underestimates the value of E_0 because the increase of the electronic kinetic energy associated with multiple scattering effects is not taken into account.

To obtain a rough estimate of the multiple scattering effects a model proposed by M. H. Cohen is useful (18). This model is based on the application of the Wigner-Seitz scheme to an electron in a helium crystal. Each helium atom is represented as a hard sphere characterized by a radius equal to the scattering length. The electron wave function will then be

$$\psi = \frac{\sin k(r - a)}{r} \quad (15)$$

The boundary conditions on ψ relate k with the equivalent sphere size, r_s ,

$$\tan k_0 (r_s - a) = k_0 r_s \quad (16)$$

while the lowest energy is given by

$$E_0 = \frac{\hbar^2 k_0^2}{2m} \quad (17)$$

Equation 16 can be readily solved for a hypothetical helium lattice with density equal to the liquid density. Table II summarizes the results of

the calculations for the free electron state in liquid helium. These results agree well with the experimental barrier energy for electron injection into the fluid.

Table II. Energy Calculations for Plane Wave Electrons in Helium

Density (a.u.) (liquid density) 4.2°K.	Energy (a.u.)			
	Born Approximation (1st Order Perturbation Theory)	Exact Single Scattering Result	Wigner-Seitz Model	Experiment (Sommer, 42)
0.2813×10^{-2}	0.0463	0.0221	0.0384	0.048 ± 0.008
0.2813×10^{-3}	0.00463	0.00221	0.00259	
0.1407×10^{-3}	0.00232	0.00111	0.00130	

Further information regarding the nature of the electron-helium interaction may be obtained from the mobility data. A mobility calculation based on single scattering is straightforward. A free electron has momentum $\hbar k$, where k is the electron wave vector. In the absence of concentration and temperature gradients the Boltzmann equation for an electron has a very simple form, providing certain conditions are satisfied. First, the energy surfaces in k space must be spherical. This is the case for a free electron, since the energy is given by $E_k = \hbar^2 k^2 / 2m^*$, where m^* is the effective mass of the electron. The second condition (which is also satisfied since the scattering potential is spherically symmetric) is that the scattering probability depend only on the angle between k and k' , where k is the electron wave vector before a collision with an atom and k' is the electron wave vector after the collision. Also note that $|k| = |k'| = k$ since the energy is conserved. The mobility is given from the Boltzmann equation as

$$\mu = \frac{4\pi e}{3} \left(\frac{\hbar}{m}\right)^2 \left(\frac{\beta\hbar}{2\pi m}\right)^{3/2} \int \exp\left(-\frac{\beta\hbar^2 k^2}{2m}\right) k^2 \tau(k) dk \quad (18)$$

where $\beta = 1/k_B T$, with k_B the Boltzmann constant, and T the absolute temperature. The relaxation time, $\tau(k)$, for the electron scattering is

$$\frac{1}{\tau(k)} = \int (1 - \cos\theta) Q(k, \theta) \sin\theta d\theta d\varphi \quad (19)$$

where $Q(k, \theta)$ is the differential transition probability that a particle with momentum $\hbar k$ is scattered through an angle θ into the volume element $\sin\theta d\theta d\varphi$,

$$Q(k, \theta) = \frac{2\pi}{\hbar} |\langle k' | \sum_i (V + V_R)_i | k \rangle|^2 N(E_k) \quad (20)$$

and the density of states—i.e., the total number of states available for the electron with energy between E_k and $E_k + dE_k$ is

$$N(E_k) = \frac{\Omega m k}{2\pi^2 \hbar^2} \quad (21)$$

The relaxation time can be separated into a form factor, $S(k)$, and an energy contribution, so that

$$\frac{1}{\tau(k)} = \frac{4Nm\hbar\Omega}{\hbar^3} \mu_k^2 S(k) \quad (22)$$

for very low energy electrons, and where

$$\mu_k = \Omega^{-1} \int e^{i\mathbf{k}\cdot\mathbf{r}} (V + V_R) d^3r \quad (23)$$

The form factor is defined in terms of the radial distribution function

$$S(k) = 1 + \frac{N}{\Omega} \int_0^\infty [g_2(R) - 1] \frac{\sin kr}{kr} 4\pi r^2 dr \quad (24)$$

To proceed, we need the value of $S(k)$ for very small k . Using the classical grand canonical ensemble (40) one can show that

$$S(k \rightarrow 0) = \frac{N\kappa_L}{\beta\Omega} \quad (25)$$

where κ_L is the isothermal compressibility of the liquid. No so-called quantum temperature is involved. This result is correct even in the limit of absolute zero.

The final result for the mobility (using the limit $u_k(k \rightarrow 0)$ and Equation 13 for the scattering length) is

$$\mu = \frac{e\beta^{3/2}}{12\sqrt{2} \pi^{5/2} m^{1/2} \kappa_L \rho^2 a^2} \quad (26)$$

At 4.2°K. we find $\mu = 36$ cm.²/volt sec. The experimental value is very different, being only 0.03 cm.²/volt sec. This discrepancy and its direction suggest that the electron is much more localized than a delocalized plane wave would allow. The analysis just described is applicable only when the electron atom pseudopotential is weak or attractive, and can therefore be used for studying low field mobility of excess electrons in liquid Ne, Ar, Kr, and Xe.

The Bubble Model for a Localized Electron in Liquid Helium

Simple cavity models have been used to study solvated electrons in liquid ammonia. In that case the dominant interactions arise from long range polarization effects, so that the energy of the localized state is not very sensitive to the fluid deformation in the vicinity of the localized charge. In the case of an excess electron in liquid helium, however, the electron-fluid interaction arises mainly from short range electron-atom interactions, and we shall show that the localized excess electron in a cavity in liquid helium lies lower in energy than the quasi-free electron.

We assume that the electron is in a localized state and can be described by a one-parameter smooth wave function of the form

$$\phi_{\zeta}(r) = \left(\frac{\zeta^3}{\pi}\right)^{1/2} e^{-\zeta|r-r_0|} \quad (27)$$

The wave function is referred to a coordinate system centered at r_0 , which is also taken to be the center of the cavity in the liquid. ζ is a variational parameter to be used in minimizing the energy.

The electronic energy of the system, for a constant fluid configuration, can now be displayed in the form

$$E_e(\zeta) = \frac{\hbar^2 \zeta^2}{2m} + \int v_{\zeta}(r) \rho(r) d^3r \quad (28)$$

where v_{ζ} is the diagonal matrix element of the pseudopotential (for the localized state),

$$v_{\zeta}(r) = \langle \phi_{\zeta} | V + V_R | \phi_{\zeta} \rangle \quad (29)$$

and $\rho(r)$ is the density of He atoms a distance r from the center of the cavity.

The total energy of the system of N He atoms and one electron, E_t , may be decomposed into the sum of the electronic energy, E_e , and the energy required for bubble formation, E_b .

$$E_t = E_e + E_b \quad (30)$$

The bubble energy is conveniently expressed as the sum of the pressure-volume work, ϵ_{PV} , the surface kinetic energy, ϵ_{SK} ; the surface potential energy, ϵ_{SP} , and the volume kinetic energy, ϵ_{VK} , arising from the removal of atoms from the cavity boundary to the bulk of the liquid.

Then

$$E_b = \epsilon_{PV} + \epsilon_{SK} + \epsilon_{SP} + \epsilon_{VK} \quad (31)$$

where the pressure-volume work is

$$\epsilon_{PV} = p \int \left(1 - \frac{\rho(r)}{\rho_0}\right) d^3r \quad (32)$$

and ρ_0 is the normal fluid density and p the pressure. The atom density function is taken to have the form

$$\begin{aligned} \rho(r) &= 0; \quad r < R_0 \\ \rho(r) &= \rho_0(1 - \{1 + \alpha(r - R_0)\}e^{-\alpha(r-R_0)}); \quad r > R_0 \end{aligned} \quad (33)$$

where R_0 is the cavity radius and α^{-1} the thickness of the boundary layer. The bubble size and shape and the excess electron charge distribution are now determined by the conditions that the total energy be stationary with respect to variation of the parameters ζ , α , and R_0 . Simple calculations have been performed on the basis of this model (18) assuming that $\epsilon_{VK} = 0$ and

$$\epsilon_{SK} + \epsilon_{SP} = 4\pi R_0^2 \gamma \quad (34)$$

where γ is the surface tension taken from the experimental data (6) or

Table III. Electronic Energies for a Localized State of an Electron in Liquid Helium (4.2°K., 1 atm)

R_0 a.u.	E_e (variation method) 10^{-2} a.u.	E_e (particle in box) 10^{-2} a.u.
0	5.40	
10	3.60	4.92
15	2.08	2.11
20	1.39	1.22
30	0.88	0.64
40	0.62	0.32
50	0.42	0.21

from the statistical model of Reiss *et al.* (39). However, it is not necessary to assume $\epsilon_{VK} = 0$. In a more elaborate theoretical analysis (16), a study of the structural changes in liquid helium in the vicinity of an excess electron was made using the formal similarity between the pair distribution function of an N boson system with the wave function, expressed as the product of pair wave functions, and the pair distribution function of a classical fluid. This analysis leads to an interfacial surface energy term which agrees well with the observed surface tension of liquid helium at 0° K. An important contribution to the bubble energy arises from the volume kinetic energy arising from the excess kinetic energy of the fluid atoms removed from the boundary layer. Table III summarizes the results of the theoretical treatment (18) of the ground state energy of a localized electron in liquid helium, and Table IV presents the comparison of the density dependence of the ground state energies of an excess electron in helium fluid. From these data we conclude that:

(a) The plane wave state is not the lowest energy state of an excess electron in liquid helium, and fluid deformation can lead to the formation of a stable localized state of the excess electron, where the excess electron wave function tends to zero at large distances from the trapping center. It becomes obvious now that the large repulsive pseudopotential and the small polarization potential of the helium atom lead to the strong short range repulsion which is responsible for electron localization in this system.

(b) It is instructive to compare the results of the present calculation of the electronic energy using the pseudopotential formalism with the simple model calculations based on the electron in a box model. For the case of a spherical box with infinite walls, $E_e = \pi^2/2R_0^2$ a.u. As is apparent from Table III, at the normal density of liquid He the results of our calculation are not appreciably different from those of the simple box model. However, at the lower fluid densities and for small R_0 , the box model is inadequate because it cannot account for the substantial charge leakage to the region outside the bubble.

(c) When the surface energy only is taken to account for the bubble energy, the calculated cavity radius is found to be 40 a.u. The increase of the kinetic energy of the fluid atoms removed from the bubble region is not taken into account in this simple model. This effect will increase the energy required for bubble formation, leading to the smaller value $R_0 = 24$ a.u. (16). This latter result is in good agreement with the results for the cross-section of electron quantized vortex interaction in superfluid He(II) (9).

(d) The mobility data for excess electrons in liquid helium above

the lambda point can be adequately described by classical hydrodynamics. The Stokes law mobility μ is

$$\mu = \frac{e}{6\pi R_0 \eta}$$

where η is the solvent viscosity. The calculated mobility for a negative ion in liquid helium at 4.2°K. and 1 atm. is $\mu = 0.024$ cm.²/volt sec., in excellent agreement with the experimental data (31).

(e) Finally, we must consider the transition from the quasi-free plane wave state to the localized state of an electron in helium. Sanders and Levine (28) have observed that as the density of He is increased in the gas phase at 4.2°K., a critical density is reached in the region $6 \times 10^{20} - 1.2 \times 10^{21}$ atoms/cc., at which the mobility of the electron drops three to four orders of magnitude to a value consistent with the mobility of an electron in the liquid. A theoretical study of the density dependence of the energies corresponding to the free and localized states of an electron in helium leads to a transition density of 1.0×10^{21} atoms/cc. at which the localized state becomes stabilized relative to the free state. This theoretical value agrees well with the experimental data. The result may be rationalized by noting that at relatively low densities the bubble is not the configuration of lowest energy because the volume work expended in creating a void is still large while the lowering of the localized state energy relative to the free plane wave state energy is small in view of the low density.

Table IV. The Density Dependence of the Well Depth for the Localized State of an Electron in Helium

ρ/ρ_0	$\Delta E \times 10^4$ a.u.	
	Isothermal 4.2°K.	Isobaric $p = 1$ atm.
0.050	2.0	..
0.071	8.0	5.7
0.083	12.4	9.9
0.100	18.4	15.0

$\Delta E = E_{FREE} - E_s$, where E_{FREE} is calculated from the variational method.
 ρ represents the fluid density, ρ_0 corresponds to the normal liquid helium density.
 ($\rho_0 = 1.92 \times 10^{22}$ atoms/cc.)

What predictions for new experiments are provided by the theoretical analysis presented herein? It would be extremely interesting to obtain direct spectroscopic evidence regarding the energy levels and charge distribution of the excess electron in liquid helium. Applying the pulse radiolysis technique, recently developed for studying bound electron states in polar solvents (—e.g., H₂O and aliphatic alcohols), should make the localized states of an excess electron amenable to spectroscopic study.

A rough estimate of the optical excitation energy can be obtained from the particle in a box model (18). The $1s \rightarrow 2p$ transition energy, $E_{1s \rightarrow 2p}$, is roughly given by

$$E_{1s \rightarrow 2p} = 1.046 E_c \approx 1.046 \pi^2/2R_0^2 \text{ a.u.}$$

For liquid helium at 4.2° K. and 1 atm. $E_{1s \rightarrow 2p} = 0.08$ e.v., so that the first optical transition is predicted to lie in the infrared region at about 1000 cm.⁻¹ The transition energy should be extremely sensitive to the

pressure in view of the pressure dependence of the cavity radius. Thus, at 4.2° K. and 100 atm $R_0 = 19$ a.u. and $E_{1s \rightarrow 2p} = 0.37$ e.v. (i.e., 3000 cm.⁻¹) while at $p = 5000$ atm. (which can be achieved at 40° K.) $R_0 = 9$ a.u. and $E_{1s \rightarrow 2p} = 1.9$ e.v. (—i.e., 15,000 cm.⁻¹). Another difficult but interesting experiment would be to study the electron paramagnetic resonance spectrum of the excess electron in liquid helium. The resonance line corresponding to the localized electron in He⁺ is expected to be extremely narrow but will be broadened in He³ by hyperfine interactions.

Localized Excess Electron States in Polar Solvents

The most useful phenomenological treatment of electron binding in polar solvents is based on a continuum model. The solution is approximated by a continuous dielectric medium, and the additional electron produces a polarization field. The charge distribution and energy levels of the electron depend on the interaction with this polarization field, which in turn depends on the charge density. It should be stressed that, in this treatment, the electron medium interaction energy arises from long range interactions and short range interactions are not included. Calculating the contribution of the self-consistent field potential (—i.e., the Hartree Fock pseudopotential) is quite straightforward, following the techniques described in this paper. However, calculating the polarization potential, which is considerably important for molecules such as H₂O or NH₃, is more complicated. Including polarization potential is crucial, as indicated by the scattering length of the isoelectronic (to NH₃) neon atom, where the repulsive contribution of the Hartree Fock pseudopotential is almost cancelled by the polarization potential.

We proceed now to outline a general treatment of the interaction of an excess electron with the polarization field of a polar liquid. The details of these calculations have been presented in a recent review from this laboratory (27).

Landau (26) proposed that an additive electron in a dielectric can be trapped by polarization of the dielectric medium induced by the electron itself. Applying the model to electrons in the conduction band of an ionic crystal is rather complicated since the translational symmetry of the solid must be considered and the interaction of the excess electron with the lattice vibrations must be treated properly (1, 13, 14).

It will be useful at this stage to consider some qualitative models which lead to an intuitive understanding of the problem. The properties of the electron are determined by the frequency of infrared oscillations, $\omega/2\pi$, of the medium. For low frequencies the excess electron velocity is much larger than the velocities of the ions, and the electron may be expected to follow adiabatically the fluctuations of the polarization field. Under these circumstances, the polarization field can be regarded as classical. At large distances the field produced by the electron is Coulombic, but owing to the finite spatial extension of the electron the potential is finite (not infinite) at small distances. If the electron is re-

garded as confined within a sphere of radius l , the potential energy is of the order of $-(e^2/l)(1/D_{op} - 1/D_s)$ while the kinetic energy is of the order of $\hbar^2/8ml^2$. A rough estimate for the self-energy of the electron in the lattice is then

$$\epsilon_1 \simeq \frac{\hbar^2}{8ml^2} - \frac{e^2}{l} \left(\frac{1}{D_{op}} - \frac{1}{D_s} \right) \quad (35)$$

The value of l which minimizes this energy is

$$l \sim \frac{\hbar^2}{8me^2} \left(\frac{1}{D_{op}} - \frac{1}{D_s} \right) \quad (36)$$

It should be noted that for ionic crystals $(1/D_{op} - 1/D_s) \sim 0.2$ to 0.4 ; hence, l may be smaller than the lattice parameter. The energy in this approximation is given by:

$$\epsilon_1 \sim - \frac{me^2}{8\pi^2\hbar^2} \left(\frac{1}{D_{op}} - \frac{1}{D_s} \right)^2 \quad (37)$$

The preceding (static) low frequency approximation is expected to break down when the frequency of the lattice vibrations is sufficiently large that the lattice can adjust to the motion of the electron. In this case the period of the lattice oscillations is less than the time taken by the electron to traverse the distance l . We now consider the dynamical problems arising when an electron with velocity v interacts with the vibrating lattice. The electron will exert a polarization field only at distances larger than v/ω . But the restriction of the electron in space requires that its de Broglie wavelength be of the order \hbar/mv . This distance must not exceed v/ω , so that $v \sim (\hbar\omega/m)^{1/2}$. If the kinetic energy of the electron is neglected (because of the relatively large spatial extension), the self-energy is represented by the potential energy owing to a charge distributed over a sphere of radius v/ω :

$$\epsilon_2 \simeq - \frac{e^2\omega}{v} \left(\frac{1}{D_{op}} - \frac{1}{D_s} \right) = -e^2 \left(\frac{m\omega}{2\pi\hbar} \right)^{1/2} \left(\frac{1}{D_{op}} - \frac{1}{D_s} \right) \quad (38)$$

It will be useful to express the self-energy of the polaron in the two models in units of a dimensionless coupling constant which is considerably important in polaron theory:

$$\alpha_P = e^2 \left(\frac{1}{D_{op}} - \frac{1}{D_s} \right) \left(\frac{m}{2\omega\hbar^3} \right)^{1/2} \quad (39)$$

The lower of the two solutions of Equations 37 and 38 is expected to be the better one. We thereby conclude that:

$$\epsilon_1 = -\alpha_P\hbar\omega; \quad \alpha_P < \frac{256}{25}$$

and

$$\epsilon_2 = -\frac{25}{256} \alpha_P^2\hbar\omega; \quad \alpha_P > \frac{256}{25} \quad (40)$$

For the case of typical ionic crystals $\alpha_P \approx 1-10$, and the weak coupling limit is applicable. The most important conclusion from this treatment is that the weak coupling limit leads to a perturbed Bloch type wave function characterized by equal probability for finding the electron at any point of the medium. Thus, in the case of the ionic crystals, the current description of the polaron is that of a mobile electron followed by lattice polarization.

In contrast, electron binding in polar solvents can be described as the extreme case in which a localized polaron exists since:

1) The binding energy of the excess electron is large (the heats of solution of an electron in water and in ammonia are of the order of 1.5 e.v.) so that the binding energy is much larger than the phonon energy of the medium.

2) Local changes caused by short range electron solvent repulsion (which may lead to cavity formation) and owing to the long range contribution of the rotational polarization of the dipolar medium lead to structural changes in the medium. The general description of the solvated electron in ammonia, involving an electron localized in a solvent cavity (of radius 3\AA .), is now well established (27). The factors governing the cavity size are better understood in view of the work on electron localization in liquid helium. Three notable differences should be pointed out:

a) The cavity size in the polar solvent should be much smaller than in liquid helium in view of the long range polarization effects.

b) The leakage of the excess electron charge density outside the cavity is much larger in liquid ammonia (about 30-40%) than in liquid helium. The electron helium pseudopotential is strongly repulsive (owing to a small polarization contribution) while core polarization effects are expected to be much more important in liquid ammonia or in water.

c) The contribution of the kinetic energy terms to the energy of cavity formation is unique in the case of liquid helium. In all other solvents the major contribution to the energy required for cavity formation is associated with the surface potential energy term, which can be associated roughly with the surface tension of the liquid.

It is interesting to consider the electron cavity size in other polar solvents relative to that in ammonia. For strongly hydrogen bonded solvents, such as water, the surface tension energy associated with cavity formation is larger than in liquid ammonia. It is thus reasonable to assume that the size of the electron cavity (if a cavity exists at all) will be substantially smaller in water than in liquid ammonia (19, 35).

Calculations based on the continuum dielectric model have been performed by the hydrated electron in the limit of zero cavity size (19). The general treatment is based on a variational calculation using hydrogenic type wave functions for the ground and the first excited states. This treatment is based on a Hartree Fock scheme, where the Coulomb and exchange interaction of the excess electron with the medium are replaced by the polarization energy of a continuous dielectric. The results obtained are summarized in Table V. The fair agreement obtained with

the experimental data indicates that the major contribution to electron binding in polar solvents arises from long range interactions.

Table V. Energy Levels of the Hydrated Electron

	<i>Theory</i> ^a	<i>Experiment</i>
Heat of solution	1.32 e.v.	1.6 e.v. ^b
First optical excitation energy	1.35 e.v.	1.7 e.v. ^c
Oscillator strength for optical transition	0.9	0.7 ^c

^a Calculated data from J. Jortner (19).

^b The experimental heat of solution was estimated from the measured rate constants of the reactions (29): $H_{30} + OH_{30}^- \rightleftharpoons H_{30}^+ + e_a$, and using the value of 260 kcal./mole for the heat of solution of the proton. For details of this calculation see J. H. Baxendale, *Radiation Res. Suppl.* **4**, 139(1964).

^c Spectroscopic data from 15, 21, and 29.

The Transition to the Metallic State

Solutions containing a high concentration of excess electrons display a transition to the metallic state. Thus, for sodium-ammonia solutions in the concentration region 1–6 *M* the specific conductance increases by about three orders of magnitude, and the temperature coefficient of the conductance is very small (27). Similar behavior is exhibited by other metal-ammonia solutions (but surprisingly, not by concentrated lithium-methylamine solutions!) (10) and by metal-molten salt solutions (17).

The metallic behavior of saturated metal-ammonia solutions can be rationalized using the simple assumptions:

(1) The conduction electrons of the metallic solution may be identified with the valence electrons of the alkali atoms.

(2) The conduction electrons move independently in the liquid. This latter assumption raises some difficulties, since the Coulomb interaction between the electrons is large. The difficulty is overcome by realizing that we need not consider the motions of electrons which are strongly correlated, but only the motions of Landau quasi particles (25), each electron being surrounded by a correlation hole. In more formal language, we may say that the quasi particles stand in one-to-one correspondence with the electrons and represent the elementary excitations of the Fermi liquid.

(3) The independent motions of the electrons can be described in the SCF scheme in terms of a one-electron hamiltonian.

(4) It is convenient to describe the conduction electrons with plane wave states, so that the potential for the one-electron problem is replaced by a proper pseudopotential.

(5) The conduction electrons are scattered by the alkali atoms, the coherence implicit in the radial distribution function. Unlike the case of the scattering of a single electron in a plane wave state by a liquid, discussed previously, in this case the structure factor $S(k)$ must be known up to the Fermi energy (which is 0.5 e.v. – 1 e.v. in saturated metal ammonia solutions).

The simple model described is successful in accounting for the properties of liquid metals (45) and has been applied with some success to the study of the conductivity of saturated metal-ammonia solutions (27).

The nature of the transition to the metallic state is not yet well understood, but it is useful at this stage to consider the arguments presented by Mott concerning this general problem (33). In a crystalline array of atoms, as the distance between the atoms is decreased a sharp transition to the metallic state is expected to occur. For a random array, the transition sharpness is lost because of the disordered atomic arrangement.

Mott describes the localized center in terms of an electron hole pair with a screened Coulombs potential

$$v_i(r) = -\frac{e}{Dr} \quad (41)$$

where D is the (high frequency) dielectric constant of the medium. When the system contains a considerable concentration of free carriers, N per unit volume, the Coulomb field will be replaced by a Debye-Hückel type potential arising from the Thomas Fermi screening by the free electron gas

$$v_d(r) = -\frac{e^2}{Dr} e^{-qr} \quad (42)$$

where the screening constant q is given by

$$q^2 = \frac{4me^2 N^{1/3}}{D\hbar^2} \quad (43)$$

The screened potential (Equation 42) does not lead necessarily to the formation of an electron-hole bound state. Indeed, the condition that electron-hole bound states will not form, is

$$q > me^2/D\hbar^2 \quad (44)$$

so that the critical concentration at which the transition to the metallic state will occur is approximately given by

$$N^{1/3} Da_H \gtrsim 0.25 \quad (45)$$

where $a_H = 0.528 \times 10^{-8}$ cm. is the Bohr radius. For saturated sodium-ammonia solutions, $N^{1/3} = 1.45 \times 10^7$ cm.⁻¹, then taking $D = 2$ we get $N^{1/3}Da_H = 0.15$. Since an exact theoretical estimate of the critical concentration is still impossible to obtain, this result seems to indicate that the concentration region in which a transition to the metallic state in metal-ammonia solutions occurs is not in disagreement with Mott's arguments.

It is, however, not clear at present whether such a model can be applied to metal solutions. It is worth mentioning again at this point that the specific conductivity of a saturated solution of lithium in methylamine (10) (concentration 5.5M) has been found to be 28 ohm⁻¹ cm.⁻¹, which is two orders of magnitude lower than that for a corresponding saturated metal-ammonia solution. This experimental result seems to indicate that the overlap between electron trapping centers may not be

the dominant factor in the transition to the metallic state for these systems.

Literature Cited

- (1) Allcock, G. R., *Advan. Phys.* **3**, 325 (1954).
- (2) Atkins, K. R., *Phys. Rev.* **116**, 1339 (1959).
- (3) Austin, B., Heine, V., Sham, L. J., *Phys. Rev.* **127**, 276 (1962).
- (4) Careri, G., Scaramuzi, F., Thompson, J. O., *Nuovo Cimento* **13**, 186 (1959).
- (5) Cohen, M. H., Heine, V., *Phys. Rev.* **122**, 1821 (1961).
- (6) Cook, G. A., "Argon, Helium, and the Rare Gases," Interscience, New York, 1962.
- (7) Davis, H. T., Rice, S. A., Meyer, L., *Phys. Rev. Letters* **9**, 81 (1962).
- (8) Davis, H. T., Rice, S. A., Meyer, L., *J. Chem. Phys.* **37**, 947 (1962); **37**, 2470 (1962).
- (9) Donnelly, R. J., *Phys. Rev. Letters* **14**, 39 (1965).
- (10) Evers, E. C., Young, A. E., Panson, A. J., *J. Am. Chem. Soc.* **79**, 5118 (1957).
- (11) Ferrel, R. A., *Phys. Rev.* **108**, 167 (1957).
- (12) Feynman, R. P., quoted in reference (24).
- (13) Frohlich, H., *Advan. Phys.* **3**, 325 (1954).
- (14) Frohlich, H., Pletzer, H., Zineau, S., *Phil. Mag.* **41**, 221 (1950).
- (15) Hart, E. J., Boag, J. W., *J. Am. Chem. Soc.* **84**, 4090 (1962).
- (16) Hiroike, K., Kestner, N. R., Rice, S. A., Jortner, J., Submitted to *J. Chem. Phys.*
- (17) Johnson, J. W., Bredig, M. A., *J. Phys. Chem.* **62**, 604 (1958).
- (18) Jortner, J., Kestner, N. R., Rice, S. A., Cohen, M. H., Submitted to *J. Chem. Phys.*
- (19) Jortner, J., *Radiation Res. Suppl.* **4**, 24 (1964).
- (20) Jortner, J., Kestner, N. R., Cohen, M. H., Rice, S. A., *The Electron Helium Atom Pseudopotential*, "New Developments in Quantum Chemistry," Istanbul Lectures, Academic Press, New York, 1965 (to be published).
- (21) Keens, L., *Nature*, **188**, 42 (1963).
- (22) Kestner, N. R., Jortner, J., Cohen, M. H., Rice, S. A., "Low Energy Elastic Scattering of Electrons and Positrons by Helium Atoms," *Phys. Rev.* (in press).
- (23) Kestner, N. R., Jortner, J., Rice, S. A., Cohen, M. H., *Phys. Rev.* (in press).
- (24) Kuper, C. G., *Phys. Rev.* **122**, 1007 (1961).
- (25) Landau, L., *Soviet Phys. JETP* **3**, 920 (1956); **5**, 101 (1957); **8**, 70 (1959).
- (26) Landau, L., *Physik Z. Sowjetunion* **3**, 664 (1933).
- (27) Lepoutre, G., Sienko, M. J., eds., "Metal-Ammonia Solutions," Benjamin Press, New York, 1964.
- (28) Levine, J., Sanders, T. M., *Phys. Rev. Letters* **8**, 159 (1962).
- (29) Matheson, M. S., Dorfman, L., "Progress in Chemical Kinetics," Vol. III (in press).
- (30) Meyer, L., Reif, F., *Phys. Rev.* **119**, 1164 (1960).
- (31) Meyer, L., Davis, H. T., Rice, S. A., Donnelly, R. J., *Phys. Rev.* **126**, 1927 (1962).
- (32) Meyer, L., Proceedings of the 9th Conference on Low Temperature Physics, Columbus, Ohio, 1964 (to be published).
- (33) Mott, N. F., *Phil. Mag.* **5**, 287 (1961).
- (34) O'Malley, T. F., *Phys. Rev.* **130**, 1020 (1963).
- (35) Onsager, L., *Radiation Res. Suppl.* **4**, 34 (1964).
- (36) Onsager, L., "New Developments in Quantum Chemistry," Istanbul Lectures, Academic Press, New York, 1965 (to be published).
- (37) Phillips, J. C., Kleinman, L., *Phys. Rev.* **116**, 287 (1959).
- (38) Rayfield, G. S., Reif, F., *Phys. Rev. Letters* **11**, 305 (1963).
- (39) Reiss, H., Frisch, H. L., Helfand, E., Lebowitz, J. L., *J. Chem. Phys.* **32**, 119 (1960).
- (40) Rice, S. A., Gray, P., "Statistical Mechanics of Simple Liquids," (in press).
- (41) Schnyders, H., Meyer, L., Rice, S. A. (to be published).
- (42) Sommer, W. T., *Phys. Rev. Letters* **12**, 271 (1964).
- (43) Williams, R. L., *Can. J. Phys.* **35**, 135 (1957).

(44) Wu, T., Ohmura, T., "Quantum Theory of Scattering," Prentice Hall, New York, 1962.

(45) Ziman, J. M., *Phil. Mag.* **6**, 1013 (1961).

RECEIVED May 17, 1965. Supported by the Directorate of Chemical Sciences of the Air Force Office of Scientific Research, The Petroleum Research Fund of the American Chemical Society, and the United States Public Health Service. This research has benefitted from using the facilities provided by ARPA for materials research at the University of Chicago.

The Structure and Kinetics of Metal-Ammonia Solutions

WILLIAM L. JOLLY

Department of Chemistry and Lawrence Radiation Laboratory, University of California, Berkeley, Calif.

Physical chemical studies of dilute alkali metal-ammonia solutions indicate the principal solution species as the ammoniated metal cation M^+ , the ammoniated electron e^- , the "monomer" M , the "dimer" M_2 and the "metal anion" M^- . Most data suggest that M , M_2 , and M^- are simple electrostatic assemblies of ammoniated cations and ammoniated electrons. The reaction, $e^- + NH_3 \rightarrow 1/2 H_2 + NH_2^-$ is reversible, and the directly measured equilibrium constant agrees fairly well with that estimated from other thermodynamic data. Kinetic data for the reaction of ethanol with sodium and for various metal-ammonia-alcohol reductions of aromatic compounds suggest that steady-state concentrations of ammonium ion are established. Ethanol-sodium reaction data allow estimation of an upper limit for the rate constant of $e^- + NH_4^+ \rightarrow 1/2 H_2 + NH_3$.

A wide variety of physical chemical techniques have been applied to the study of metal-ammonia solutions (23, 32). Some techniques have been useful as analytical methods for identifying dissolved species and studying equilibria involving these species. These techniques include, in the approximate order of decreasing usefulness, (a) conductivity measurements (concentration dependence and transference studies), (b) magnetic susceptibility measurements (both static and electron spin resonance (ESR)), (c) nuclear magnetic resonance (NMR) (Knight shifts), (d) vapor pressure measurements, and (e) optical spectroscopy. Another group of physical chemical techniques, including some already mentioned, have been useful for determining the structures of the dissolved species.

These include, again in the approximate order of decreasing usefulness, (a) optical spectroscopy, (b) density measurements, (c) NMR (Knight shifts), (d) conductivity measurements (mobilities and temperature coefficients), (e) ESR, and (f) thermochemistry. There is every reason to believe that in the future other techniques will be applied to these studies, and that a number of subtle features of the solutions will be uncovered.

Structure of Metal-Ammonia Solutions

First, let us consider the empirical formulas of the species which have been postulated to exist in alkali metal-ammonia solutions, and which have received the serious consideration of more than a few investigators. In this connection it is important to realize that identifying a species in terms of its empirical formula is not the same thing as determining its structure. In 1908 Kraus (30) proposed, on the basis of conductivity measurements and electrolytic experiments, that alkali metals exist in ammonia as monatomic species, M , in equilibrium with the corresponding cations, M^+ , and ammoniated electrons, e^- . In 1938 Huster (21) proposed, in order to account for the decrease in molar magnetic susceptibility with increasing concentration, that the cations and electrons are in equilibrium with the diamagnetic diatomic species M_2 . To explain similar magnetic data, Freed and Sugarman (14) and Ogg (33, 34) proposed the species e_2^{-2} (which generally has not been considered seriously since then), and Bingel (3) proposed the species M^- .

To account for both the conductivity data and the magnetic susceptibility data, Becker, Lindquist, and Alder (2) proposed that the following two equilibria be considered:



Arnold and Patterson (1) found that a better fit of the data could be obtained by considering three equilibria:



Let us consider the various structures which have been proposed for the species involved in the latter three equilibria. The only uncontroversial species is the metal cation, M^+ , which has always been assumed to be solvated by a shell of ammonia molecules with the negative ends of the ammonia dipoles (the nitrogen atoms) pointing toward the central cation.

The ammoniated electron, e^- , has been described by Ogg (35) and various other authors as an electron-in-a-cavity. In this model, the electron is stabilized in a large cavity by polarization and orientation of

the peripheral ammonia molecules. A "polaron" model due to Davydov (9) and Deigen (10), in which the electron is assumed to be stabilized by polarization of a continuous dielectric medium, is ruled out by density measurements which show that the electron occupies a very large volume.

The monomer species, M , has been described by Kraus (31) as an ion pair. Although he did not elaborate on its possible structure, one may assume that he pictured this species as two ammoniated ions held together by electrostatic forces. Douthit and Dye (12) pointed out that such a picture is consistent with the absorption spectra of sodium-ammonia solutions. Becker, Lindquist, and Alder (2) proposed an "expanded metal" model in which an electron was assumed to circulate in an expanded orbital on the protons of the coordinated ammonia molecules of an M^+ ion. The latter model is difficult to reconcile with optical, volumetric, and NMR data (16).

The dimer species, M_2 , was described by Huster (21) as a simple dissolved diatomic molecule. Such a species would be very unstable with respect to the ammoniated species, M^+ and e^- , and may be ruled out by thermochemical data. The "expanded metal dimer" model of Becker, Lindquist, and Alder, in which two ammoniated metal ions are held together by a pair of electrons in a molecular orbital located principally between the two ions, is just as difficult to reconcile with optical, volumetric, and NMR data as the expanded metal monomer. In order to account for the similar absorption spectra of e^- , M , M_2 (and any other species such as M^- or M_4 that might exist at moderate concentrations of metal), Gold, Jolly, and Pitzer (16) assumed that species such as M and M_2 consist of ionic aggregates in which the ammoniated electrons remain essentially unchanged from their state at infinite dilution.

Recently Golden, Guttman, and Tuttle (17) proposed that the M^- species is an ammoniated metal anion and that the M_2 species is an ion pair of this anion with the ammoniated metal cation. By using reasonable estimates of ionic ammoniation energies, it is possible to show that an ammoniated metal anion is thermodynamically plausible. However, the only experimental data which were used specifically to support the existence of this species were optical extinction coefficient data of Gold and Jolly (15). These data were obtained at 24,000 Å., which happens to be the longest wavelength investigated by Gold and Jolly because of limitations of the spectrophotometer and strong absorption by the solvent; hence the data may be spurious.

Blandamer *et al.* (4) have recently made a half-hearted effort to resurrect the e_2^{-2} species. They state that if a species such as M_2 or M^- contains two ammoniated electrons with sufficient overlap of the electronic wave functions to cause the species to exist in a singlet state, then only by a coincidence could the absorption spectrum be similar to that of the far-separated ammoniated electrons. They suggest that a comparable coincidence could just as well occur in the case of the e_2^{-2} species. Some clarification of the ionic aggregate model is therefore needed. It should be recognized that the optical absorption peak does shift slightly

with changing metal concentration, and that the energy difference between the singlet and triplet states of the electron pair is only required by the magnetic data to be greater than or of the order of magnitude of kT (0.5 kcal. or 170 cm.^{-1} at -33°C.). The equilibrium constants have been calculated generally assuming that M^- and M_2 are completely diamagnetic (corresponding to a singlet-triplet separation of at least several kT), but this is probably an unnecessary restriction. However, even if we assume that spin coupling in the ionic clusters causes the relative energies of the ground and excited states of the optical transition to change by three times kT , the calculated shift in absorption frequency is less than the 600 cm.^{-1} shift observed on going from very dilute solutions to 0.03 M (15). It should also be recognized that the magnetic coupling between the electrons may be enhanced by spin polarization of the intervening atoms, in much the same way that magnetic coupling occurs in antiferromagnetic compounds such as MnO and FeO (5).

Thermodynamic and Mechanistic Studies of Reactions

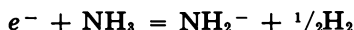
The reactivity of metal-ammonia solutions is a topic at least equal in importance to the structure of metal-ammonia solutions. The solutions have been used as reagents in an enormous number of syntheses, but very little quantitative systematization of the reactions has been achieved. However, in recent years significant progress has been made in the thermodynamics and kinetics of a few reactions of metal-ammonia solutions. These reactions are discussed in the remainder of this paper.

Thermodynamics. By correlating thermochemical and electrochemical data for liquid ammonia, it has been possible to estimate thermodynamic functions for a wide variety of ionic species in liquid ammonia at 25°C. (22, 24). The heats and free energies of formation and entropies (relative to H^+) for a few species are given in Table I. These values have been calculated from the data of references 6, 19, 20, and 24.

Table I. Thermodynamic Functions for Species in Liquid Ammonia at 25°C.

Species	ΔH°_f kcal./mole	ΔF°_f kcal./mole	S° cal./deg.-mole
H^+	0	0	0
NH_4^+	-16.1	-2.7	24.7
Na^+	-38.0	-43.6	15
K^+	-39.3	-47.0	25
NH_3	-16.1	-2.7	24.7
e^-	37.4	46	-13
NH_2^-	9.8	35.0	-15

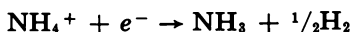
Using the data from Table I, an equilibrium constant of 10^6 is calculated for the reaction



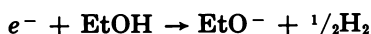
Thus, one predicts that a 1 M solution of potassium amide which is in equilibrium with 1 atm. of hydrogen will contain about $10^{-6} M$ ammoniated electron. By using ESR to determine the concentration of

ammoniated electrons, we have recently shown that this equilibrium can indeed be attained, and that the above equilibrium constant is correct within an order of magnitude (28).

Kinetics and Mechanisms. Ammonia ions react very rapidly with electrons in ammonia:



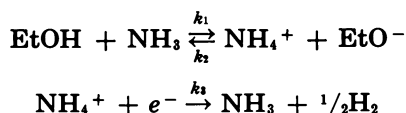
Although no one has succeeded in directly measuring the rate constant of this reaction, Kelly *et al.* (27) have reported some kinetic data which permit us to estimate an upper limit for the rate constant. These investigators followed the reaction of sodium with ethanol in liquid ammonia at -33.4°C . by measuring the evolved hydrogen as a function of time.



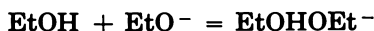
They noted that, during the first 25% of reaction, the reaction was first-order in alcohol and essentially zero-order in sodium. During the second 25% of reaction, the reaction did not appear to be of definite kinetic order, but during the last half of reaction, the reaction was much slower and was first-order in both alcohol and sodium, or second-order overall. These results at least qualitatively agree with the rate law

$$-\frac{d(\text{EtOH})}{dt} = \frac{k_1(\text{EtOH})(e^-)}{(k_2/k_3)(\text{EtO}^-) + (e^-)}$$

which corresponds to a mechanism involving a low steady-state concentration of ammonium ion:



In order to account quantitatively for the rate data over the entire extent of reaction, it is necessary to consider the fact that sodium ethoxide is only slightly soluble in ammonia, and that its solubility is markedly increased by the addition of ethanol. It happens that, in accounting for the kinetics, the following arbitrarily chosen equilibrium is satisfactory.



Probably other equilibria would serve just as well. Using an equilibrium constant of 10^3 for this reaction and a solubility product of 1.73×10^{-3} for sodium ethoxide, the constants $k_1 = 8 \times 10^{-3} \text{ sec.}^{-1}$ and $(k_2/k_3) = 6 \times 10^3$ were evaluated. The value for k_1 is fairly firm (and agrees with NMR data which indicate that the rate constant is less than 10 sec.^{-1}), but the value of (k_2/k_3) is dependent on an arbitrary choice, within limits, of the EtOHOEt^- equilibrium constant and the sodium ethoxide solubility product. In fact, the kinetic data are consistent with any value for

(k_2/k_3) greater than 10^3 . The experimental data of Kelly *et al.* are presented in Figure 1 as a plot of the fraction reaction *vs.* the logarithm of time. The curve through the experimental points corresponds to the rate constants and equilibrium constants given above. (A similar, less rigorous interpretation of the data has been published elsewhere (25).)

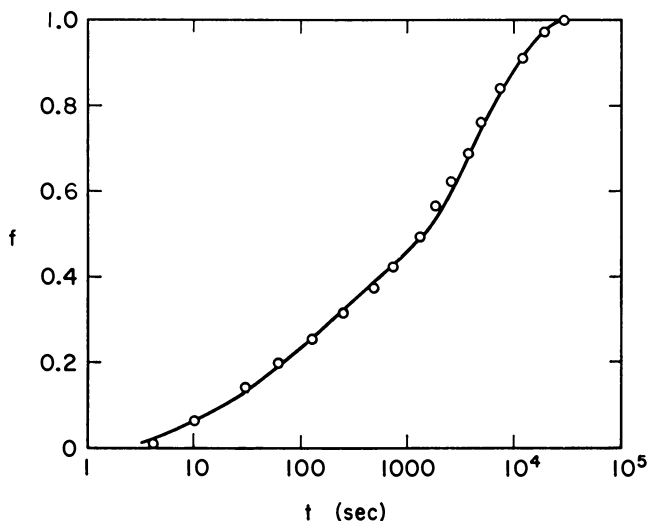
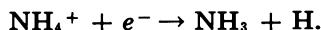


Figure 1. Fraction reaction *vs.* logarithm of time for the reaction of ethanol with sodium in liquid ammonia.

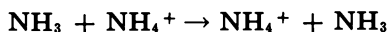
If the ionization constant for ethanol in liquid ammonia, k_1/k_2 , were known, it would be possible to calculate a value for k_3 , the $\text{NH}_4^+ + e^-$ rate constant. At present, the best we can do is estimate this ionization constant. Several types of evidence indicate that the pK values of normal acids are about eight units less in ammonia than in water. (For example, *p*-nitroacetanilide has a pK of 5.1 in ammonia (8) and a pK of about 13.2 in water.) Thus, since the aqueous pK of ethanol (7) is 17, we might estimate a pK of 9 for ethanol in liquid ammonia. However, the ethoxide ion is probably strongly hydrogen-bonded in aqueous solution and is probably abnormally stable in aqueous solution relative to ammonia solution. The analogous ion, hydroxide, is stabilized in water to such an extent that the pK value for water in ammonia (*ca.* 18) is greater than that in water (*ca.* 16) (22). The relative stabilization in water of the ethoxide ion is probably not as marked as that of the hydroxide ion; hence, we estimate a very approximate pK value of 13 for ethanol in liquid ammonia. (A pK value greater than 13 would correspond to the unlikely situation in which k_2 had a value greater than $10^{11} \text{ M}^{-1} \text{ sec}^{-1}$ —i.e., greater than that for a diffusion-controlled reaction.) This pK value, together with the data $k_1 = 8 \times 10^{-3}$ and $(k_2/k_3) > 10^3$, yields $k_3 < 10^8 \text{ M}^{-1} \text{ sec}^{-1}$. This result indicates that the $\text{NH}_4^+ + e^-$ reaction is not an ultra-fast, diffusion-controlled reaction like the $\text{H}_3\text{O}^+ +$

e^- reaction (18), and that the $\text{NH}_4^+ + e^-$ reaction has an appreciable activation energy. If we assume that the mechanism involves the formation of atomic hydrogen, then a lower limit for the activation energy should be obtained from the heat of the reaction



If we assume no solvation energy for atomic hydrogen in ammonia (and thus probably overestimate the heat) we calculate $\Delta H^\circ = 15$ kcal./mole for the latter reaction. It is hoped that the rate constant for the $\text{NH}_4^+ + e^-$ reaction soon will be evaluated by the same techniques of pulse radiolysis (18) or photolysis (36) which have been used to study the $\text{H}_3\text{O}^+ + e^-$ reaction.

Keenan *et al.* (26) carried out experiments designed to compare the rate of the $\text{NH}_4^+ + e^-$ reaction with that of the reaction:



They observed that, when a solution of lithium in tritiated ammonia was mixed with a solution of ammonium bromide in ordinary ammonia, the evolved hydrogen contained much less tritium than when a solution of lithium in ordinary ammonia was mixed with a solution of ammonium bromide in tritiated ammonia. These results were taken as evidence that the $\text{NH}_4^+ + e^-$ reaction is an order of magnitude faster than the $\text{NH}_4^+ + \text{NH}_3$ reaction. However when one considers that electrons in ammonia have an abnormally high mobility, and that they probably migrate without carrying ammonia molecules with them (11, 23), this interpretation seems doubtful. It is possible that the electrons diffused into the ammonium bromide solutions much more rapidly than the ammonium ions diffused into the lithium solutions, and that consequently the evolved hydrogen was always characteristic of the ammonium bromide solutions. Thus these experiments yield little information about the relative rates of the $\text{NH}_4^+ + e^-$ reaction and $\text{NH}_4^+ + \text{NH}_3$ reaction.

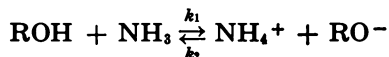
In view of the mechanism suggested above for the ethanol-sodium reaction, it seems likely that reduction of aromatic compounds by solutions of alcohols and alkali metals in liquid ammonia proceeds by a general mechanism involving a steady-state concentration of ammonium ion. Krapcho and Bothner-By (29) observed that the reduction of benzene and several substituted benzenes in lithium-alcohol-ammonia solutions,

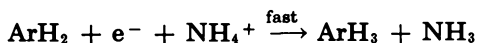
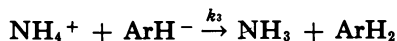
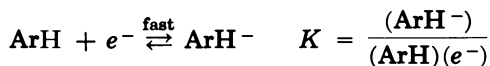


proceeds by the third-order rate law

$$-\frac{d(\text{ArH})}{dt} = k(\text{ArH})(\text{ROH})(e^-)$$

It can be shown that this rate law is consistent with the mechanism





By applying the steady-state approximation to the ammonium ion concentration, we calculate the rate law

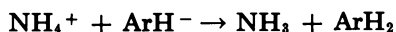
$$-\frac{d(\text{ArH})}{dt} = \frac{k_1 k_3 K (\text{ROH})(\text{ArH})(e^-)}{k_2 (\text{RO}^-) + k_3 K (\text{ArH})(e^-)}$$

which reduces to that found by Krapcho and Bothner-By when K is small and when the metal alkoxide is only slightly soluble. Their observation that the reduction rates with lithium, sodium, and potassium decrease in that order is predictable from the expected increase in solubility of the alkoxides in the same order. Eastham and Larkin (13) studied the reduction of the 1-naphthoxide ion with alcohol and potassium in ammonia. One would expect K to be relatively large for this substrate, and consequently one would predict that the rate law would reduce to

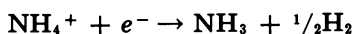
$$-\frac{d(\text{ArH})}{dt} = k_1 (\text{ROH})$$

In agreement with this rate law, Eastham and Larkin observed that addition of alkoxide had no effect on the reduction, but greatly retarded hydrogen evolution.

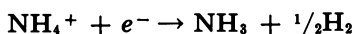
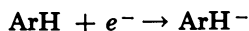
Many of these aromatic reductions proceed with almost quantitative yield, indicating that the reaction



proceeds much more rapidly than the reaction



However, when ammonium salts are added to solutions of aromatic compounds and alkali metals in ammonia, relatively poor yields of the reduced hydrocarbon are obtained. This result is probably because the rate constants of the reactions



are of comparable magnitude. When the ammonium ion concentration is low, hydrogen production does not compete seriously with the reduction. However, when the ammonium concentration is high, the hydrogen-producing reaction seriously competes with the rate of formation of ArH^- .

Literature Cited

- (1) Arnold, E., Patterson, A., Jr., *J. Chem. Phys.* **41**, 3089 (1964).
- (2) Becker, E., Lindquist, R. H., Alder, B. J., *J. Chem. Phys.* **25**, 971 (1956).
- (3) Bingel, W., *Ann. Physik* **12**, 57 (1953).
- (4) Blandamer, M. J., Catterall, R., Shields, L., Symons, M. C. R., *J. Chem. Soc.* **1964**, 4357.
- (5) Cotton, F. A., Wilkinson, G., "Advanced Inorganic Chemistry," pp. 593-4, Interscience, New York, 1962.
- (6) Coulter, L. V., Sinclair, J. R., Cole, A. G., Roper, G. C., *J. Am. Chem. Soc.* **81**, 2986 (1959).
- (7) Cram, D. J., *Chem. and Eng. News*, **93**, Aug. 19, p. 92 (1963).
- (8) Cuthrell, R. E., Fohn, E. C., Lagowski, J. J., "Abstracts of Papers," 145th Meeting, ACS, September 1963, p. 13N.
- (9) Davydov, A. S., *Zhur. Ekspit. i. Theoret. Fiz.* **18**, 913 (1948); Chem. Abstracts **45**, 10035ⁱ (1951).
- (10) Deigen, M. F., *Zhur. Ekspit. i. Teoret. Fiz.* **26**, 300 (1954).
- (11) Dewald, J. F., Lepoutre, G., *J. Am. Chem. Soc.* **78**, 2956 (1956).
- (12) Douthit, R. C., Dye, J. L., *J. Am. Chem. Soc.* **82**, 4472 (1960).
- (13) Eastham, J. F., Larkin, D. R., *J. Am. Chem. Soc.* **81**, 3652 (1959).
- (14) Freed, S., Sugarman, N., *J. Chem. Phys.* **11**, 354 (1943).
- (15) Gold, M. and Jolly, W. L., *Inorg. Chem.* **1**, 818 (1962).
- (16) Gold, M., Jolly, W. L., Pitzer, K. S., *J. Am. Chem. Soc.* **84**, 2264 (1962).
- (17) Golden, S., Guttman, C. Tuttle, T. R., Jr., *J. Am. Chem. Soc.* **87**, 135 (1965).
- (18) Gordon, S., Hart, E. J., Matheson, M. S., Rabani, J., Thomas, J. K., *J. Am. Chem. Soc.* **85**, 1375 (1963).
- (19) Gunn, S. R., Green, L. G., *J. Chem. Phys.* **36**, 368 (1962).
- (20) Gunn, S. R., Green, L. G., *J. Phys. Chem.* **64**, 1066 (1960).
- (21) Huster, E., *Ann. Physik* **33**, 477 (1938).
- (22) Jolly, W. L., *J. Phys. Chem.* **58**, 250 (1954).
- (23) Jolly, W. L., Chapter on "Metal-Ammonia Solutions" in Vol. 1 of *Progress in Inorganic Chemistry*, F. A. Cotton, ed., pp. 235-281, Interscience, New York, 1959.
- (24) Jolly, W. L., University of California Radiation Laboratory Report UCRL-2201, May, 1953; see also Latimer, W. M. and Jolly, W. L., *J. Am. Chem. Soc.* **75**, 4147 (1953).
- (25) Jolly, W. L., Hallada, C. J., Chapter on "Liquid Ammonia" in *Solvent Systems*, T. C. Waddington, ed., Academic, N. Y., 1965.
- (26) Keenan, C. W., Secor, H. V., Kelly, E. J., Eastham, J. F., *J. Am. Chem. Soc.* **82**, 1831 (1960).
- (27) Kelly, E. J., Secor, H. V., Keenan, C. W., Eastham, J. F., *J. Am. Chem. Soc.* **84**, 3611 (1962).
- (28) Kirschke, E. J., Jolly, W. L., *Science* **147**, 45 (1965).
- (29) Krapcho, A. P., Bothner-By, A. A., *J. Am. Chem. Soc.* **81**, 3658 (1959); *Ibid.*, **82**, 751 (1960).
- (30) Kraus, C. A., *J. Am. Chem. Soc.* **30**, 1323 (1908).
- (31) Kraus, C. A., *J. Chem. Education* **30**, 83 (1953).
- (32) Lepoutre, G., Sienko, M. J., "Metal-Ammonia Solutions; Physicochemical Properties," W. A. Benjamin, New York, 1964.
- (33) Ogg, R. A., *J. Am. Chem. Soc.* **68**, 155 (1946).
- (34) Ogg, R. A., *J. Chem. Phys.* **14**, 114, 295 (1946).
- (35) Ogg, R. A., *Phys. Rev.* **69**, 668 (1946).
- (36) Swenson, G. W., Zwicker, E. F., Grossweiner, L. I., *Science* **141**, 1042 (1963).

RECEIVED April 27, 1965. Performed under the auspices of the United States Atomic Energy Commission.

4

The Solvated Electron in Organic Liquids

LEON M. DORFMAN

Department of Chemistry, The Ohio State University, Columbus, Ohio

The optical absorption spectra of the solvated electron have now been reported for a number of organic liquids. The chemical reactivity in the aliphatic alcohols has been studied by the pulse radiolysis method. The absorption maxima for a series of five aliphatic alcohols are in the visible to near infra-red. These maxima show a red shift with decrease in the static dielectric constant. The solvated electron undergoes reactions of electron-ion combination, electron attachment, and dissociative electron attachment. Absolute rate constants have been determined for these reactions.

Solvation of the electron in a self-polarized liquid medium has only in recent years come to be recognized as a phenomenon of very general occurrence and importance. Although the solvated electron has been extensively investigated in alkali metal-ammonia solutions for over 50 years, direct observation of this species in a number of organic liquids is relatively new. The characteristic property of the solutions of alkali metals in ammonia, and in some amines, which makes these susceptible to study by conventional methods is, of course, the stability of the solvated electron. In most other liquids which have been investigated the solvated electron exhibits a very short natural lifetime and must be studied by fast reaction methods.

There are two parameters which appear to be of major importance in determining the occurrence and observability of electron solvation. The first is the polarizability of the liquid, as expressed by its dielectric behavior. On the basis of theory, which will be discussed later, a necessary condition for electron solvation appears to be that the static dielectric constant of the liquid be substantially greater than one. The second parameter, which seems at present to be unpredictable, is the natural lifetime of the solvated electron—i.e., its lifetime with respect to reaction with the solvent itself.

The solvated electron has been studied in a number of organic liquids, among which are the aliphatic alcohols (27, 28, 3, 26, 1, 17), some ethers (15, 5), and certain amines (9, 22, 2). Of these systems, it is only in the alcohols, to which this paper is principally but not exclusively directed, that both the chemical reactivity and the optical absorption spectrum of the solvated electron have been investigated in detail. The method used in these studies is that of pulse radiolysis (21, 11), developed some five years ago. The way was shown for such investigations of the solvated electron by the observation of the absorption spectrum of the hydrated electron (6, 18, 19) and by the subsequent kinetic studies (16, 12, 20) which are being discussed in other papers in this symposium.

Experimental

The pulse radiolysis method has been described in detail in some of the early papers (21, 11), in a brief review of the subject (13), and in a current comprehensive review (14). It is, in brief, a fast reaction method in which the external perturbation applied to the system is a microsecond pulse of electrons. The current is sufficiently high to produce an instantaneous concentration of transient species high enough to be observed by fast measurement of the optical absorption. Spectra may be recorded either photographically or spectrophotometrically. The kinetics are studied by fast spectrophotometry. Since a perturbing pulse as short as 0.4 μ sec. has been used, the time resolution has approached 10^{-7} sec. The flash photolysis method used in some of the other studies (17, 15) has been reviewed in detail (24).

Absorption Spectra in the Aliphatic Alcohols

The solvated electron in the aliphatic alcohols exhibits a broad optical absorption extending from the ultraviolet to the near infra-red with a maximum in the visible to the near infra-red. We have determined (26, 27, 28) the absorption spectrum in the series of five alcohols: methanol, ethanol, 1-propanol, 2-propanol, and ethylene glycol. In this series of similar liquids the static dielectric constant at 20° C. ranges from 38.7 for ethylene glycol to 19 for 2-propanol. The absorption spectra are shown in Figure 1. These spectra were obtained spectrophotometrically with individual points being determined from separate rate curves, although the spectra for ethanol (27, 28) and methanol (1) were first obtained spectrographically. At the short wavelength side, an appropriate correction was made for the alcohol radical (29).

The absorption maxima in Figure 1, which shows the decadic molar extinction coefficient plotted against wavelength, are at 5800, 6300, 7000, 7400, and 8200 Å. The determination of the maximum for methanol by Adams, *et al.* (1) is in close agreement with our value of 6300 Å.; that of Grossweiner, *et al.* (17) for ethanol by flash photolysis is in satisfactory agreement with our value of 7000 Å. It is immediately apparent that the maximum exhibits a red-shift with decrease in the static dielectric con-

stant. This is predicted by theory and provides an interesting correlation which will be discussed.

The half-width of all the absorption bands is approximately 1.5 e.v. When plotted on an energy scale the spectra are seen to be asymmetric on the high-energy side. If the asymmetric portion is deleted, the remaining symmetrically drawn peak has a half-width of about 1 e.v. for all five alcohols.

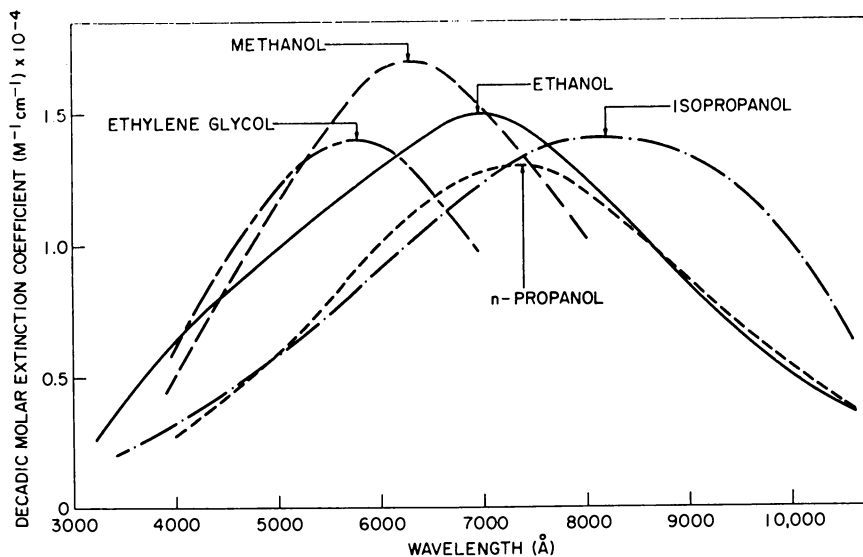


Figure 1. The absorption spectra of the solvated electron in the aliphatic alcohols at 23°C. The ordinate gives the decadic molar extinction coefficient. The wavelength is in angstrom units.

In addition to the absorption maximum, we have determined the molar extinction coefficient, the oscillator strength for the band, and the radiation chemical yield for the solvated electron in all five alcohols. These data are listed in Table I. The extinction coefficients at the maxima are similar for all five alcohols, and within experimental error of the value for the hydrated electron (19) which is 15,600 at 7200 Å, based (25) on $Ge_{\bar{a}q} = 2.6$. The oscillator strength ranges from 0.6 to 0.9. This high value strongly suggests that any further bands with appreciable oscillator strengths at energies in excess of 4 e.v., the short wavelength limit of our observations, are not likely to exist.

This observation is of interest with regard to the general question of whether there is any structure in the spectrum, and whether one may hope to resolve individual bands. Although the asymmetry of the spectrum hints at the possibility of an unresolved band or bands toward higher energy, it is evident from Figure 1 that no structure has been observed at room temperature with a wavelength resolution of 100–150 Å. There is thus no experimental evidence at present to support the possible existence

Table I. Optical Absorption Data and Radiation Chemical Yields for the Solvated Electron in the Aliphatic Alcohols at 23° C.

Compound	Absorption Maximum (A.)	ϵ_{10} at Maximum $M^{-1} cm.^{-1}$	Oscillator Strength	Radiation Yield (number/ 100 e.v.)
ethylene glycol	5800	14,000	0.7	1.2
methanol	6300	17,000	0.8	1.1
ethanol	7000	15,000	0.9	1.0
1-propanol	7400	13,000	0.6	1.0
2-propanol	8200	14,000	0.7	1.0

of a Rydberg series for this species, considered as a simple one-electron system (8) with a spherically symmetric ground state.

In view of the possibility that existing bands may simply be smeared out at room temperature by the thermal disorder in the liquid and the resulting fluctuations in the structure of the electron trap, Arai and Sauer (4) have determined the absorption spectrum of the solvated electron in ethanol at $-78^{\circ} C$. No structure was observed, so that evidence is lacking for a transition to a second level, $1s \rightarrow 3p$, even at the lower temperature. The absorption maximum was, however, found to be shifted from 7000 A. at $23^{\circ} C$. to 5800 A. at $-78^{\circ} C$. It is interesting to note that the half-width of the band remained the same, about 1.5 e.v., at the lower temperature.

Correlation With Theory

As has been pointed out, there is a red-shift in the absorption maximum with decrease in the static dielectric constant. That a correlation exists between the transition energy for the photoexcitation and the dielectric constant of the liquid may be seen in Figure 2. The shift in the maximum with temperature seems to be roughly in accord with this correlation as may be seen from the single point for ethanol at $-78^{\circ} C$. The straight line is drawn only to emphasize that a correlation exists and is not to be taken as an implication of a fundamental linear relationship.

To apply this series of observed transition energies as a test of a theory which was developed only as an approximation may be demanding a degree of sophistication of the theory which was not intended. However, this correlation, particularly with the expression derived by Davydov (8), is interesting.

The theory relates the energy states of the electron to the dielectric behavior of the continuous medium, assuming the electron to be bound in the potential field of the oriented dipoles. Davydov (8) has derived the expression:

$$\Delta E \text{ (e.v.)} = (0.071)(27.2)(1/D_{op} - 1/D_s)^2 [\mu/m] \quad (1)$$

where D_{op} and D_s are the optical and static dielectric constants respectively, and μ/m is the ratio of the effective mass of the electron in the liquid to its mass in the free state. μ/m is an unknown parameter. The correlation is shown in Table II, in which the calculated values are given

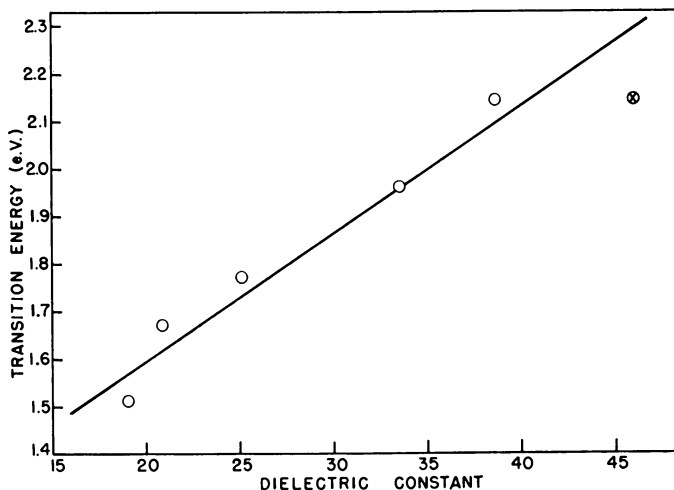


Figure 2. The optical transition energy (electron volts) for the solvated electron in the aliphatic alcohols as a function of the static dielectric constant of each liquid. \circ at 23°C ; \otimes at -78°C .

in terms of μ/m and as absolute values based on an arbitrary selection of $\mu/m = 3.6$ to fit the data for methanol. The trend from methanol through 2-propanol is in close agreement with experiment, but the value for ethylene glycol is not at all in accord with experiment. The agreement may be fortuitous since Equation 1 does not take into account any change in electronic polarization in the excited state.

Table II. Correlation of Optical Transition Energy of the Solvated Electron with Theory

Liquid	Transition energy ΔE (ev)	$D, 20^{\circ}\text{C}$.	Refractive index, n	ΔE calc. Equation 5	ΔE calc. Equation 5 $\mu/m = 3.6$
Ethylene Glycol	2.1 ₄	38.7	1.43	0.41(μ/m)	1.5
Methanol	1.9 ₆	33.6	1.33	0.54(μ/m)	2.0
Ethanol	1.7 ₇	25.1	1.36	0.48(μ/m)	1.7
1-Propanol	1.6 ₇	20.8	1.38	0.43(μ/m)	1.5
2-Propanol	1.5 ₁	19	1.38	0.43(μ/m)	1.5
Water	1.7 ₂	80	1.33	0.59(μ/m)	2.1
Ammonia	0.8 ₄	22	1.33	0.52(μ/m)	1.9 ^a

^a Agreement with experiment for liquid ammonia requires $\mu/m = 1.6$.

The data for water and ammonia, included for comparison are found not to be in accord with experiment. Agreement with experiment for liquid ammonia requires $\mu/m = 1.6$ in Equation 1.

Anbar and Hart (2) have demonstrated an interesting empirical correlation between the absorption maxima of the solvated electron in various solvents and those of the iodide ion in these same solvents. The halide ion spectra have also been discussed (23) in terms of a similar theory.

Chemical Reactivity in the Alcohols

The absolute rate constants were determined for a variety of reactions of the solvated electron in ethanol and methanol. Three categories of reaction were investigated: (a) ion-electron combination, (b) electron attachment, and (c) dissociative electron attachment. These bimolecular rate constants (3, 27, 28) are listed in Table III. The rate constants of four of these reactions have also been obtained for the hydrated electron in water. These are also listed in the table so that a comparison may be made for the four rate constants in the solvents ethanol, methanol, and water.

Table III. Absolute Rate Constants for Some Reactions of the Solvated Electron at 23° C.

<i>Reaction</i>	<i>Solvent</i>	<i>k</i> ($M^{-1} \text{ sec}^{-1} \times 10^{-10}$)
electron-ion combination		
$e_{\text{sol}}^- + \text{H}^+$	$\text{C}_2\text{H}_5\text{OH}$	2.0 ± 0.4
$e_{\text{sol}}^- + \text{H}^+$	CH_3OH	3.9 ± 0.9
electron attachment		
$e_{\text{sol}}^- + \text{O}_2$	$\text{C}_2\text{H}_5\text{OH}$	1.9 ± 0.3
$e_{\text{sol}}^- + \text{O}_2$	CH_3OH	1.9 ± 0.4
$e_{\text{sol}}^- + \text{diphenyl}$	$\text{C}_2\text{H}_5\text{OH}$	0.43 ± 0.07
$e_{\text{sol}}^- + \text{naphthalene}$	$\text{C}_2\text{H}_5\text{OH}$	0.54 ± 0.05
$e_{\text{sol}}^- + p\text{-terphenyl}$	$\text{C}_2\text{H}_5\text{OH}$	0.72 ± 0.06
$e_{\text{sol}}^- + \text{naphthacene}$	$\text{C}_2\text{H}_5\text{OH}$	1.02 ± 0.08
dissociative electron attachment		
$e_{\text{sol}}^- + \text{C}_6\text{H}_5\text{CH}_2\text{Cl}$	$\text{C}_2\text{H}_5\text{OH}$	0.51 ± 0.12
$e_{\text{sol}}^- + \text{C}_6\text{H}_5\text{CH}_2\text{Cl}$	CH_3OH	0.50 ± 0.12
$e_{\text{sol}}^- + (\text{C}_6\text{H}_5)_3\text{COH}$	$\text{C}_2\text{H}_5\text{OH}$	0.020 ± 0.004
reactions ^a of e_{aq}^-		
$e_{\text{aq}}^- + \text{H}^+$	H_2O	2.2 ± 0.2
$e_{\text{aq}}^- + \text{O}_2$	H_2O	2.0 ± 0.2
$e_{\text{aq}}^- + \text{naphthalene}$	H_2O	0.54 ± 0.15
$e_{\text{aq}}^- + \text{C}_6\text{H}_5\text{CH}_2\text{Cl}$	H_2O	0.55 ± 0.15

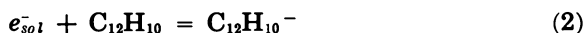
^a The literature sources of these rate constants are summarized in reference (14).

In the case of the reactions with the aromatic compounds, the nature of the reaction was established by observing the optical absorption spectrum of the transient product. Thus, in the reaction with diphenyl and *p*-terphenyl, the observation of the spectra of the mononegative ions (3) of these compounds establishes the occurrence of an attachment reaction. The rate constants for the reactions with diphenyl, naphthalene, *p*-terphenyl, and naphthacene increase in the order of increasing electron affinities of these compounds. In the case of the attachment reaction to oxygen, no attempt has been made to study the product ion in the alcohols. We have, however, obtained (7) the absorption spectrum of the O_2^- ion in aqueous solution.

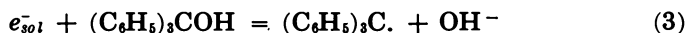
The occurrence of the dissociative electron attachment reactions was also established by direct observation of the transient product. Thus, the absorption spectra of the benzyl radical (21, 28) and the triphenyl methyl radical (28) were both observed. The other products formed in

these two elementary reactions are presumably the chloride ion and the hydroxyl ion, respectively.

Two of these reactions:



and

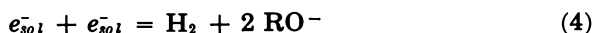


were used as the basis for determining the G value and the molar extinction coefficient of the solvated electron. In this determination (28, 26) the yield of the electron was related to the formation of the diphenylidene ion and the triphenyl methyl radical, based on the extinction coefficients of these species.

The reaction with hydrogen ion in a sense involves somewhat different species in the different solvents. Since the hydrogen ion is presumably solvated, it is in the form $CH_3OH_2^+$ in methanol and $C_2H_5OH_2^+$ in ethanol. It is interesting to note that, with one possible exception, the rate constants which have been determined in the three solvents, methanol, ethanol, and water, show no solvent effect. The reaction of the electron with hydrogen ion has a slightly higher rate constant in methanol. This is difficult to explain, and would appear not to be caused by the substantially lower viscosity of methanol since the other reactions in methanol exhibit no such difference.

Comparing the rate constants in the foregoing table with an approximate calculated value of the encounter rate is of interest. Taking the effective radius of the solvated electron as slightly less than 3 Å., and the diffusion coefficient in water as 10^{-4} cm.²/sec., it appears (14) that most of these rate constants are only very slightly lower than diffusion controlled. Only the reaction with triphenyl methanol is substantially slower than diffusion controlled.

The natural lifetime of the solvated electron in the alcohols has not yet been determined. The half-times have been reported (28) for the electron in irradiated methanol, ethanol, 1-propanol, and 2-propanol, without any additives, as ranging from 1.5 μ sec. to 5 μ sec. However, these values are likely to be very much lower than the true natural lifetimes since the observed rate curves included reaction with the counter ion, molecular products, and trace impurities which may be present. No evidence has been obtained for the reaction:



in the alcohols, which thus remains a subject for future investigation. The analogous reaction in water has been established by isotopic studies (12) as an elementary process.

The Solvated Electron in Other Organic Liquids

Since solutions of the alkali metals in various amines exhibit the formation of relatively stable absorbing species, there have been a number

of studies of the optical absorption spectra in these systems as well as of conductivity and ESR spectra. These are, of course, two-component systems, and the alkali metal, as a counter-ion, participates in the formation of optically absorbing species.

Dewald and Dye (9) have recently reported the absorption spectra over a broad range for the alkali metals in ethylenediamine. Their paper contains a useful summary of earlier work. Bands are observed at 6600 Å., 8500 to 8900 Å. and at 12,800 Å. The authors show that the bands at 6600 Å. and at 8500 to 8900 Å. involve the alkali metal. The suggestion is made that the band at 12,800 Å. is that of the solvated electron.

Ottolenghi *et al.* (22) have investigated both the optical spectra and the ESR spectra of the alkali metals in ethylamine. From the nature of the decay rates and the ESR spectra they conclude that the 6600 Å. band is to be assigned to the metal monomer and the 13,000 Å. band to the solvated electron.

In a pulse radiolysis study of ethylenediamine soon to be published, Anbar and Hart (2) find a conflicting result. These authors report a single broad absorption band with a maximum at 9200 Å. The absorption curve continues to fall off with increasing wavelength toward 11,500 Å., the sensitivity limit of their detector. In this system the counter-ion is the molecular ion of the solvent, and no alkali metal atom is present. The result raises a serious question about the assignment of the 13,000 Å. band to the solvated electron and calls for further study of these systems by the pulse radiolysis method.

Pulse radiolysis of dioxane (5) produces a broad, weak absorption in the visible which is suggested to be that of the solvated electron. No maximum was observed since this is at longer wavelengths than 8000 Å., the detection limit of the equipment used.

Eloranta and Linschitz (15) have investigated the flash photolysis of ether solutions of the alkali metals. The observed bands in tetrahydrofuran and dimethoxy ether are discussed in terms of the trapped electron pair species, e_2^- , which undergoes photodissociation:



Thus, in THF, the band at 9000 Å. is attributed to the trapped electron pair. The observations in water (12), relating to the electron-electron reaction, are of interest in this connection. Although our isotopic studies as well as the kinetics, support the occurrence of Reaction 4 in water, we may reach the following alternative conclusions regarding the species $(e_{aq}^-)_2$: (a) that if it is formed in water by Reaction 4, its lifetime is less than 0.2 $\mu\text{sec.}$, or (b) if this is not true, then the species does not absorb in the same region of the visible as does the hydrated electron.

It would appear at this stage that a good deal of useful information has yet to be obtained by the pulse radiolysis method concerning the absorption spectra of the solvated electron in various organic liquids. Such data would help to remove uncertainties regarding the assignment of bands and would serve as criteria for the validity of developing models.

It would seem from our correlations for the alcohols that the continuum model results in a valid expression for the energy states of the electron since the approximations arrived at by Platzman and Franck (23) and by Davydov (8) give the rough magnitude of the binding energy correctly, and the latter shows a trend with dielectric constant in accord with experiment. However, the theory is still in a rather primitive state, and other physical properties of the liquid, in addition to its dielectric behavior, may have to be taken into account.

Acknowledgment

I am indebted to my colleagues Drs. I. A. Taub, M. C. Sauer, Jr., and S. Arai, in cooperation with whom the foregoing work on the alcohols was carried out. It is a pleasure to acknowledge many stimulating discussions with Dr. R. L. Platzman, whose paper in 1953 was an important guidepost to radiation chemists on the road to the present developments.

Literature Cited

- (1) Adams, G. E., Baxendale, J. H., and Boag, J. W., *Proc. Roy. Soc. (London)*, **A277**, 549 (1964).
- (2) Anbar, M. and Hart, E. J., *J. Phys. Chem.* (in press).
- (3) Arai, S. and Dorfman, L. M., *J. Chem. Phys.* **41**, 2190 (1964).
- (4) Arai, S. and Sauer, M. C., Jr., (private communication).
- (5) Baxendale, J. H., Fielden, E. M. and Keene, J. P., *Science* (in press, 1965).
- (6) Boag, J. W. and Hart, E. J., *Nature* **197**, 45 (1963).
- (7) Czapski, G. and Dorfman, L. M., *J. Phys. Chem.* **68**, 1169 (1964).
- (8) Davydov, A. C., *Zh. Eksperim. i Teor. Fiz.* **18**, 913 (1948).
- (9) Dewald, R. R. and Dye, J. L., *J. Phys. Chem.* **68**, 121 (1964).
- (10) Dewald, R. R., Dye, J. L., Eigen, M. and de Maeyer, L., *J. Chem. Phys.* **39**, 2388 (1963).
- (11) Dorfman, L. M., Taub, I. A. and Bühler, R. E., *J. Chem. Phys.* **36**, 3051 (1962).
- (12) Dorfman, L. M. and Taub, I. A., *J. Am. Chem. Soc.* **85**, 2370 (1963).
- (13) Dorfman, L. M., *Science* **141**, No. 3580, 493 (1963).
- (14) Dorfman, L. M. and Matheson, M. S., *Progress in Reaction Kinetics*, Vol. 3, ed., G. Porter, Pergamon, London, 1965.
- (15) Eloranta, J. and Linschitz, H., *J. Chem. Phys.* **38**, 2214 (1963).
- (16) Gordon, S., Hart, E. J., Matheson, M., Rabani, J. and Thomas, J. K., *J. Am. Chem. Soc.* **85**, 1375 (1963).
- (17) Grossweiner, L. I., Zwicker, E. F. and Swenson, G. W., *Science* **141**, 1180 (1963).
- (18) Hart, E. J. and Boag, J. W., *J. Am. Chem. Soc.* **84**, 4090 (1962).
- (19) Keene, J. P., *Radiation Research* **22**, 1 (1964).
- (20) Keene, J. P., *Disc. Faraday Soc.* No. 36, 304 (1963).
- (21) Matheson, M. S. and Dorfman, L. M., *J. Chem. Phys.* **32**, 1870 (1960).
- (22) Ottolenghi, M., Bar-Eli, K., Linschitz, H. and Tuttle, T. R., Jr., *J. Chem. Phys.* **40**, 3729 (1964).
- (23) Platzman, R. L. and Franck, J., *Z. Physik* **138**, 411 (1954).
- (24) Porter, G., "Technique of Organic Chemistry," Vol. VIII, Part 2, p. 1055 Interscience, New York, 2nd ed., 1963.
- (25) Rabani, J., Mulac, W. A. and Matheson, M. S., *J. Phys. Chem.* **69**, 53 (1965).
- (26) Sauer, M. C., Jr., Arai, S. and Dorfman, L. M., *J. Chem. Phys.* **42**, 708 (1964).
- (27) Taub, I. A., Sauer, M. C., Jr., and Dorfman, L. M., *Disc. Faraday Soc.* No. **36**, 206 (1963).
- (28) Taub, I. A., Harter, D. A., Sauer, M. C., Jr., and Dorfman, L. M., *J. Chem. Phys.* **41**, 979 (1964).
- (29) Taub, I. A. and Dorfman, L. M., *J. Am. Chem. Soc.* **84**, 4053 (1962).

RECEIVED May 4, 1965.

The Hydrated Electron in Radiation Chemistry

MAX S. MATHESON

Chemistry Division, Argonne National Laboratory, Argonne, Ill.

The hydrated electron, e_{aq}^- is the major reducing species in water. A number of its properties are important either in understanding or measuring its kinetic behavior in radiolysis. Such properties are the molar extinction coefficient, the charge, the equilibrium constant for interconversion with H atoms, the hydration energy, the redox potential, the reaction radius, and the diffusion constant. Measured or estimated values for these quantities can be found in the literature. The rate constants for the reaction of e_{aq}^- with other products of water radiolysis are in many cases diffusion controlled. These rate constants for reactions between the transient species in aqueous radiolysis are essential for testing the "diffusion from spurs" model of aqueous radiation chemistry.

The faith of radiation chemists in the existence of the hydrated electron, e_{aq}^- , has varied through the years. In his book, published in 1947, Lea (27) proposed that electrons in irradiated water escaped the parent ion. Stein (40), in 1952, proposed that methylene blue in irradiated aqueous solutions might be reacting with e_{aq}^- , and Platzman (33), in 1953, reported his calculations on the mechanism of formation and some of the properties of the hydrated electron, including its blue color and the hydration energy of ~ 2 e.v. However, contrary to the situation in another discipline (32), in radiation chemistry "faith is" not "the evidence of things not seen," and these prophets were largely without honor in any country for several years. Finally, beginning with work by Hayon and Weiss (20), Baxendale and Hughes (3), and Barr and Allen (1) evidence rapidly accumulated (17, 30) supporting the existence of e_{aq}^- . The mounting tide of corroborating data culminated in (a) the demonstration that the major reducing species in irradiated neutral

water has unit negative charge (5, 7), and (b) the observation of the transient hydrated electron absorption spectrum in pulse radiolyzed aqueous solutions (4, 18, 24).

It now seems reasonably definite that an entity such as the hydrated electron exists. Further, the rate constants of reaction of e_{aq}^- with a large number of species have now been measured using the technique of pulse radiolysis. This paper describes some of the properties of e_{aq}^- and discusses the rate constants of reaction of e_{aq}^- with the other species produced in the pulse radiolysis of water. These rate constants are significant for any diffusion theory model of the radiolysis of water.

Properties of the Hydrated Electron

Absorption Spectrum of e_{aq}^- . The absorption spectrum of the hydrated electron is shown in Figure 1. The evidence that this spectrum is that of e_{aq}^- is at least four-fold. First, the spectrum is suppressed by known electron scavengers, such as H_3O^+ , O_2 , N_2O (4, 18). Second, it resembles in form the absorption bands of the solvated electron in liquid ammonia and methylamine (4, 18). Third, the rate constants calculated from the decay of this absorption in the presence of scavengers

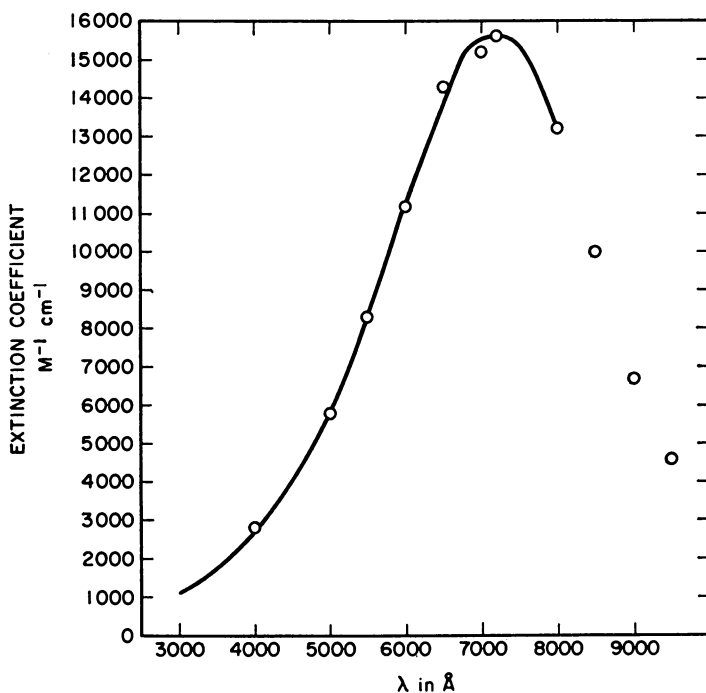
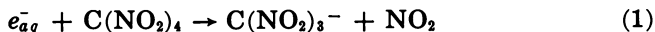


Figure 1. The absorption spectrum of the hydrated electron.

Data from Hart (17).

give rate constant ratios which agree with those obtained by competitive studies with these scavengers in steady radiolysis (15). Fourth, the absorbing species responsible for the absorption has unit negative charge (11, 15).

The molar extinction coefficient of e_{aq}^- at 5780 Å. has been measured (36) as $\epsilon_e^{5780} = 10,600 (\pm 10\%) M^{-1} \text{cm.}^{-1}$. This was done by using Reaction 1



and measuring the molar extinction coefficient of $\text{C}(\text{NO}_2)_3^-$ at 3660 Å. Then, with $\epsilon_{\text{NF}^-}^{3660}$ being known ($\text{NF}^- = \text{C}(\text{NO}_2)_3^-$), ϵ_e^{5780} was calculated from pulse radiolysis experiments using the initial absorption at 5780 Å., the final absorption at 3660 Å., with corrections for the small fraction of e_{aq}^- that reacted other than with $\text{C}(\text{NO}_2)_4$. $\text{C}(\text{NO}_2)_3^-$ does not absorb at 5780 Å. From ϵ_e^{5780} and the relative extinction coefficients (17, 24) as a function of wavelength ϵ_e^λ is determined at any wavelength. $\epsilon_e^{7200} (\text{max}) = 15,800 \pm 1600 M^{-1} \text{cm.}^{-1}$. From Figure 1, assuming $\epsilon_e^\lambda = 0$ at 1820 and 13,300 Å. the oscillator strength, f , was estimated to be 0.65, a value identical to that published for the solvated electron in ammonia (9).

Other Properties of e_{aq}^- . Table I lists various properties of the hydrated electron.

Table I. Properties of the Hydrated Electron

λ_{max}	7200 Å. (1.72 e.v.)
Molar extinction coefficient at 5780 Å.	10,600 ($\pm 10\%$) $M^{-1} \text{cm.}^{-1}$
at 7200 Å. (max)	15,800 $M^{-1} \text{cm.}^{-1}$
f = oscillator strength	0.65
Charge	-1
pK	9.7
Hydration energy (calc.)	≥ 1.72 e.v.
$E^0(e_{aq}^- + \text{H}_2\text{O}^+_{aq} \rightarrow \frac{1}{2} \text{H}_2 + \text{H}_2\text{O})$	≤ 2.67 volts
$\tau^{1/2}$ (pure water at pH 7.0)	
Limited mostly by $e_{aq}^- + \text{H}_2\text{O}^+_{aq}$	230 $\mu\text{sec.}$
Diffusion constant	$4.5 \times 10^{-5} (\pm 15\%) \text{ cm.}^2/\text{sec.}$
Mean radius of charged distribution (calc.)	2.5-3.0 Å.
$G_{e_{aq}^-}$ (in neutral water)	2.6 (reference 36)

The fact that the major reducing species in irradiated neutral water has unit negative charge (5, 7) has already been referred to. The evidence for this was obtained using the equation (5)

$$\log \frac{k}{k_0} = 1.02 Z_a Z_b \frac{\mu^{1/2}}{1 + \alpha \mu^{1/2}} \quad (2)$$

which is derived from the Debye-Hückel theory and the Brönsted model of ionic reactions. k is the rate constant for reaction between a and b with respective unit electronic charges Z_a and Z_b ; k_0 is the value of k at zero ionic strength; μ is the ionic strength, and α is a constant which depends upon the distance of closest approach of ions a and b.

In this earlier work under conditions of steady radiolysis the rate constants for reaction of e_{aq}^- with charged species were measured relative

to the rate constant for reaction of e_{aq}^- with an uncharged species as a function of ionic strength. More recently, this same equation has been applied using pulse radiolysis results in which the absolute rate constant for the reaction

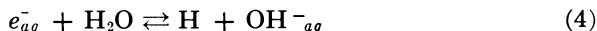


was measured over a range of ionic strengths (15). The radius of $\text{Fe}[\text{CN}]_6^{-3}$ was determined from mobility as 2.77 Å (14), and this was used as the radius of reaction for $\text{Fe}[\text{CN}]_6^{-3}$. Jortner (23) recently has used a dielectric continuum model and self-consistent field theory to estimate the electron-binding energy in water. He finds that the cavity that contains the electron in water is smaller than the cavity containing the electron in ammonia. Indeed, it is possible that there are no additional cavities needed in water to accommodate the electron. He calculated the mean radius for charge distribution in the ground state as 2.5–3.0 Å, and noted that this radius could be used for the reaction radius in the Debye equation for diffusion-controlled reactions of charged species. The encounter distance then for Reaction 3 will be about 6 Å, and for such an encounter distance α may be set equal to 2. Thus, in Figure 2 the log of k has been plotted against $\mu^{1/2}/(1 + 2\mu^{1/2})$.

In Equation 3, $\text{Fe}[\text{CN}]_6^{-3}$ has three negative charges. However, Dainton and Watt (6, 8) measured the rate constant for Reaction 3 relative to the rate constant for the reaction of e_{aq}^- with N_2O and plotted the logarithm of this ratio against $\mu^{1/2}/(1 + \mu^{1/2})$. They used a slope of +2, and they noted that in their solutions the $\text{Fe}[\text{CN}]_6^{-3}$ was largely combined in the form $\text{KFe}[\text{CN}]_6^{-2}$. Their work extended to much higher ionic strengths than the highest used to obtain the data in Figure 2.

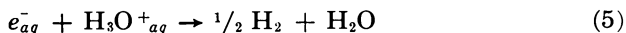
In reference (11) from the equilibrium constant of James and Monk (22), it was estimated that for points at $\mu^{1/2}/(1 + 2\mu^{1/2})$, less than 0.1 association of $\text{Fe}[\text{CN}]_6^{-3}$ was not important. In Figure 2 the experimental results are consistent with a slope of +3 at low ionic strength, with the slope falling off to a value of +2 in the region studied by Dainton and Watt (8). One can conclude from Figure 2 that the ionic strength effect is large and approximately that expected if the absorbing species has a charge of -1.

The pK for the hydrated electron is estimated from the individual rate constants in Reaction 4 as 9.7. However, even though



electrons can be converted to H atoms in pure neutral water, the reaction is sufficiently slow, that if any reactive electron scavenger is present in an irradiated aqueous solution, the electron will react with the scavenger before it is converted to an H atom.

The hydration energy of the electron and the redox potential of the reaction



are also included in Table I. These were calculated by Baxendale (2)

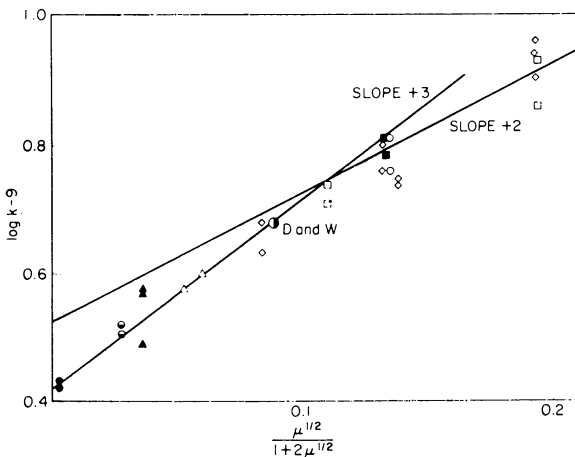
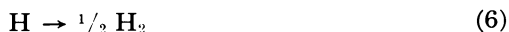


Figure 2. $\log k_3$ as a function of ionic strength, μ ; except where specified, 2.5×10^{-2} M CH_3OH was added to scavenge OH : ●, neutral, no other salt added to $\text{K}_3\text{Fe}(\text{CN})_6$; ○, pH 10.3; ▲, pH 10.47; △, neutral, $\text{K}_4\text{Fe}(\text{CN})_6$ added as salt and OH scavenger (No CH_3OH); ◇, pH 10.32 – 10.46, Na_2SO_4 ; ○ (with dot), value obtained from Dainton and Watt (8). □, pH 10.33, $\text{K}_4\text{Fe}(\text{CN})_6$; ■, pH 10.42, KClO_4 ; ○, pH 12.45. NaOH .

Reprinted with permission from Dorfman, L. M., and Matheson, M. S., Chapter on "Pulse Radiolysis" in *Progress in Reaction Kinetics*, Porter, G., ed., Pergamon Press, London 1965.

from the equilibrium constant for the equilibrium in Reaction 4. Using revised rate constants, particularly for the forward reaction (see Table II), E° for Reaction 5 is now 2.67 volts, whereas E° for H atoms is only 2.1 volts for Reaction 6 (2). The calculated hydration energy in Table I



is equal to the energy at the absorption maximum, 1.72 electron volts. The half-life of the hydrated electron in pure water is about 230 $\mu\text{sec.}$, with more than two-thirds of the electrons reacting in "pure" water by Reaction 5.

The diffusion constant, D_e , has only recently been measured. Schmidt and Buck (37) observed the formation and decay of the transient conductivity during and following the pulse irradiation of dilute aqueous barium hydroxide, pH 9.5. These workers fitted the curve of the transient conductivity, plotted as a function of time, by means of a computer. Necessary for this calculation were:

- (a) The G values for the molecular and radical products of water radiolysis.
- (b) The rate constants for reaction of these products among them-

selves which have been measured by various techniques, including that of pulse radiolysis with optical detection.

(c) The known mobilities of $\text{H}_3\text{O}^+_{\text{aq}}$ and OH^-_{aq} .

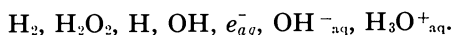
The equivalent ionic conductance of e^-_{aq} was determined as 170 (± 15) from which the mobility of e^-_{aq} , $\mu_e = 1.77 \times 10^{-3} \text{ cm}^2/\text{v}/\text{sec}$. (In this determination a given error in a G value or a rate constant introduces only a much smaller error into the equivalent ionic conductance of e^-_{aq} .) Since D_e and μ_e are related by the expression

$$D_e/\mu_e = kT/e \quad (7)$$

where k is the Boltzman constant, T is the temperature in $^\circ\text{K}$., and e is the electronic charge, the diffusion constant $D_e = 4.5 \times 10^{-5}$ ($\pm 15\%$) cm^2/sec . This value is about half the value previously supposed (11, 39).

Rate Constants of the Hydrated Electron

About 10^{-8} sec. after the deposition of energy in water by a fast moving electron, the products of radiolysis are believed to be



Rapid reactions occur between many of these species and the rate constants for such reactions are summarized in Table II. The rate constants for Reactions 8 thru 15, plus 19 and 21, were determined by the technique of pulse radiolysis. In fact, the hydrated electron Reactions 10 thru 13, plus Reactions 15 and 21, were determined in one system (31). In this system, high concentrations of H_2 (100 atm.) converted OH to H and high concentrations of OH^-_{aq} eliminated $\text{H}_3\text{O}^+_{\text{aq}}$. In addition, at high pH, Reaction 15 converted H to e^-_{aq} . Thus, by using pHs 13.3 and 10.5 and employing H_2 pressures of 100 and 0 atm., it was possible to emphasize Reactions 10, 11, 12, and 13 in turn so that the rate constant of each could be measured by computer fitting of absorption decay curves, using known G values for the above products and rate constants already known or else determined in this system. The rate constant for Reaction 15 was measured at pH 11.6 and 100 atm. H_2 by finding a pulse intensity at which the formation by Reaction 15 initially equalled the decay by other reactions, the reaction rates for decay being calculated from the measured rate constants, the known G values for the products of radiolysis, and the initial optical density owing to e^-_{aq} . Similarly, for Reaction 21, a pulse intensity was found at pH 13.3 and 1 atm. H_2 for which the initial rate of decay of absorption was zero, the rate-controlling step for the formation of e^-_{aq} in the sequence 21 and 15 being 21.

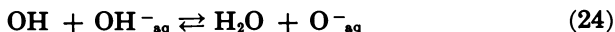
The rate constants for 8 and 9 were determined by pulse radiolysis by adding known amounts of excess acid or H_2O_2 and measuring the pseudo-first order decay of hydrated electron absorption (15, 25). The rate constant for recombination of OH radicals (Reactions 19) was deter-

Table II. Rate Constants in Pulse Radiolyzed Water^a

Reaction	Equation	Rate Constant $M^{-1} \text{ sec.}^{-1}$	pH	Reference ^b
$e_{aq}^- + H_2O^+_{aq} \rightarrow H + H_2O$	(8)	$(2.07 \pm 0.08) \times 10^{10}$	2.1–4.3	(25)
$e_{aq}^- + H_2O_2 \xrightarrow{H_2O} OH + OH^-_{aq}$	(9)	$(1.23 \pm 0.14) \times 10^{10}$	7	(15)
$e_{aq}^- + e_{aq}^- \xrightarrow{H_2} 2OH^-_{aq}$	(10)	$(0.9 \pm 0.15) \times 10^{10}$ $(1.1 \pm 0.15) \times 10^{10}$	10.9 13.3	(16) (31)
$e_{aq}^- + H \xrightarrow{H_2O} H_2 + OH^-_{aq}$	(11)	$(2.5 \pm 0.6) \times 10^{10}$	10.5	(31)
$e_{aq}^- + OH \xrightarrow{H_2O} OH^-_{aq}$	(12)	$(3.0 \pm 0.7) \times 10^{10}$	10.5	(31)
$e_{aq}^- + O^-_{aq} \xrightarrow{H_2O} 2OH^-_{aq}$	(13)	$(2.2 \pm 0.6) \times 10^{10}$	13	(31)
$e_{aq}^- + H_2O \rightarrow H + OH^-_{aq}$	(14)	(16 ± 1)	8.4	(19)
$H + OH^-_{aq} \rightarrow e_{aq}^- + H_2O$	(15)	$(1.8 \pm 0.6) \times 10^7$	11.6	(31)
$H + H \rightarrow H_2$	(16)	2×10^{10}	2.1	(41)
$H + OH \rightarrow H_2O$	(17)	$(0.7-3.2) \times 10^{10}$	3	(42)
$H + H_2O_2 \rightarrow OH + H_2O$	(18)	$(9.0 \pm 1) \times 10^7$	2.1	(41)
$OH + OH \rightarrow H_2O_2$	(19)	$(1.26 \pm 0.16) \times 10^{10}$	7	(34, 35)
$OH + H_2 \rightarrow H + H_2O$	(20)	4.5×10^7	7	(38)
$O^-_{aq} + H_2 \rightarrow H + OH^-_{aq}$	(21)	$(8 \pm 4) \times 10^7$	13.3	(31)
$OH + H_2O_2 \rightarrow H_2O + HO_2$	(22)	4.5×10^7	7	(38)
$H_2O^+_{aq} + OH^-_{aq} \rightarrow 2H_2O$	(23)	1.43×10^{11}	7	(12, 13)

^a 20°–25°C.^b For other references for these rate constants see Dorfman and Matheson (11).

mined in a pulse radiolytic competition of $OH + OH$ with $OH +$ ferrocyanide (34, 35), the rate constant for $OH +$ ferrocyanide being known and again fitting the optical density vs. time curve with a computer. The pK of OH was also determined as 11.9 ± 0.2 in this latter system, where the pK is the pH at which $[OH] = [O^-_{aq}]$ in the equilibrium



For the other reactions in Table II, the rate constants were measured by other techniques as described in the references cited.

Discussion of Hydrated Electron Rate Constants

Comparison with Diffusion Controlled Encounter Rates. The rates for many of the e_{aq}^- reactions in Table II are very fast, exceeding $10^{10} M^{-1} \text{ sec.}^{-1}$, and therefore, may be limited by the rates of diffusion-controlled encounters. The equation from which the diffusion-limited rate constants may be calculated for ionic species is due to Debye (10)

$$k_{eX} = \frac{4\pi r_{eX} D_{eX} N}{1000} \left\{ \frac{Z_e Z_X e^2}{r_{eX} E k T} / \left(\exp \left[\frac{Z_e Z_X e^2}{r_{eX} E k T} \right] - 1 \right) \right\} \quad (25)$$

The term on the right, outside the braces, is the diffusion-limited rate for encounters of uncharged species e and X whose total diffusion constant is D_{eX} and whose encounter radius is r_{eX} . N is Avogadro's number

and k_{ex} will be in units of $M^{-1} \text{sec}^{-1}$. The term in braces is the Debye correction on the diffusion-limited encounter rate if e and X have charges $Z_e e$ and $Z_X e$ respectively, the force between them is coulombic, and E is the effective dielectric constant of the solution. k is the Boltzmann constant, T is the absolute temperature, and e is the charge on the electron.

In Table III, the diffusion limited rate of encounter has been calculated for four e_{aq}^- reactions and the results compared with experimental values. As might be expected, the measured D_e gives better agreement than had been obtained by similar comparisons before (11, 39). In particular, the rate constant for reaction of e_{aq}^- with the uncharged species O_2 calculated from $4\pi r_{eO_2} D_{eO_2} N/1000$ is in good agreement with the experimental value. The reaction radii or diffusion constants for H and OH in water are not known exactly, but the values listed for their experimental rate constants and the results calculated for O_2 suggest that a similar agreement between k (observed) and k (calculated) would result if these quantities were known. For $e_{aq}^- + e_{aq}^-$ and $e_{aq}^- + H_3O^+_{aq}$, the observed reactions are one-half and one-fifth as fast as the calculated diffusion limited rates of encounter. First, it must be admitted that we do not know precisely what to use for the reaction radii of either e_{aq}^- or $H_3O^+_{aq}$. In addition, at the short distances involved at the moment of reaction, the effective dielectric constant E is probably not 80, the static dielectric constant of water, which has been used in Equation 25. Only for the reaction $e_{aq}^- + H_3O^+_{aq}$ has an activation energy been measured. E_{act} for this reaction is 3.2 kcal./mole (43), and is in fact very close to the $E_{act} = 3.5$ kcal./mole estimated for Reaction 23 from the data in (13), $H_3O^+_{aq}$ is the most rapidly diffusing species in both of these reactions. These values are of the order of magnitude expected for a diffusion-controlled reaction and, therefore, the activation energy does not in itself explain why the experimental rate is less than the calculated diffusion-controlled rate for Reaction 8. It might be expected that there would be an entropy change also, owing to the reorganization in the hydration spheres of the two reactants in Reaction 8.

Table III. Comparison of Diffusion Controlled and Experimental Rate Constants

Reaction	r_x^a	D_x^b	k^c	
			calc.	obs.
$e_{aq}^- + O_2$	1.6 ^d	2.4 ^e	2.31	2.0 ^g
$e_{aq}^- + e_{aq}^-$	2.7	4.7	0.94	0.45
$e_{aq}^- + H_3O^+_{aq}$	2.5 ^d	9.3 ^f	10.3	2.1
$e_{aq}^- + Cu^{++}$	0.7 ^d	0.7 ^d	5.4	3.3 ^h

^a In units 10^{-8} cm.

^b In units 10^{-5} cm.²/sec.

^c In units $10^{10} M^{-1} \text{sec}^{-1}$ For $e_{aq}^- + e_{aq}^-$ $k =$ number of successfully reacting collisions and is k_{10} not $2k_{10}$.

^d See Table VII reference (11).

^e Data from Himmelblau (21).

^f Data from Schwarz (39).

^g Data from Gordon *et al.* (15) and Keene (25).

^h Data from Gordon *et al.* (16).

Significance of Rate Constants for the Diffusion Theory of Water Radiolysis. Magee (28) and Hart (17) are among those who

have described the sequence of events in which a fast electron deposits energy in water. These descriptions lead to the concept of localized energy deposition in small volumes, with the resulting formation of $\text{H}_3\text{O}^{+\text{aq}}$, OH, and e_{aq}^- in spurs of about 10–20 Å radius. These species diffuse and at the same time may encounter each other in the spur and react before diffusing into the bulk of the solution. The spurs, of course, vary in size and in number of species per spur. Nevertheless, using an average number of radicals per spur and an average spur radius, one can, by using the diffusion model (26), calculate G values which agree reasonably with experiment for all the species on the right in the process



This process is supposed to summarize the situation existing at the end of the sequence of events in which energy was deposited locally. The $\text{H}_3\text{O}^{+\text{aq}}$, OH, and e_{aq}^- present at the time the secondary electrons become hydrated ($\sim 10^{-11}$ sec. after energy deposition) diffuse and react with each other, until finally the products indicated on the right appear in the bulk of the solution (about 10^{-8} sec. after energy deposition). Since the first attempts to explain the formation of molecular and radical products in water by the diffusion model, our knowledge of aqueous radiation chemistry has been considerably increased. Many of the parameters in the diffusion equation were originally unknown, but now all of the rate constants are known and a beginning has been made in determining precise values of the diffusion constants. It may be possible that, when the radius of the spur remains as the only unknown parameter which enters into the diffusion equation, one will be able to calculate not only the radius of the spur, but also determine whether or not there are different radii of distribution for e_{aq}^- and for OH and $\text{H}_3\text{O}^{+\text{aq}}$. That is to say, conceivably, one will be able to distinguish between the theory of Platzman (33), in which the electrons are thermalized and hydrated at some distance from the parent-ion, and the theory of Magee (29), in which the thermalized electron is recaptured by the parent-ion to form an excited molecule, perhaps H_3O , which then thermally dissociates to give a hydrated electron near the positive ion.

Literature Cited

- (1) Barr, N. F., Allen, A. O., *J. Phys. Chem.* **63**, 928 (1959).
- (2) Baxendale, J. H., *Rad. Res. Suppl.* **4**, 139 (1964).
- (3) Baxendale, J. H., Hughes, G., *Z. Phys. Chem. (Frankfurt)* **14**, 306 (1958).
- (4) Boag, J. W., Hart, E. J., *Nature* **197**, 45 (1963).
- (5) Czapski, G., Schwarz, H. A., *J. Phys. Chem.* **66**, 471 (1962).
- (6) Dainton, F. S., *J. Leeds Univ. Union Chem. Soc.* **5**, 3 (1963).
- (7) Dainton, F. S., Collinson, E., Smith, D. R., Tazuké, S., *Proc. Chem. Soc.* **1962**, 140.
- (8) Dainton, F. S., Watt, W. S., *Proc. Roy. Soc.* **275A**, 447 (1963).
- (9) Das, T. P., *Advances in Chemical Physics*, Vol. 4, p. 303, Interscience, New York, 1962.
- (10) Debye, P., *Trans. Electrochem. Soc.* **82**, 265 (1942).
- (11) Dorfman, L. M., Matheson, M. S., Chapter on "Pulse Radiolysis" in *Progress in Reaction Kinetics*, Porter, G., ed., Pergamon, London, 1965.
- (12) Eigen, M., DeMaeyer, L., *Z. Elektrochem.* **59**, 986 (1955).

- (13) Ertl, G., Gerischer, H., *Z. Elektrochem.* **66**, 560 (1962).
- (14) Gibby, C. W., Monk, C. B., *Trans. Faraday Soc.* **48**, 632 (1952).
- (15) Gordon, S., Hart, E. J., Matheson, M. S., Rabani, J., Thomas, J. K., *J. Amer. Chem. Soc.* **85**, 1375 (1963).
- (16) Gordon, S., Hart, E. J., Matheson, M. S., Rabani, J., Thomas, J. K., *Discuss. Faraday Soc.* **36**, 193 (1963).
- (17) Hart, E. J., *Ann. Rev. of Nucl. Science* **15**, (1965).
- (18) Hart, E. J., Boag, J. W., *J. Am. Chem. Soc.* **84**, 4090 (1962).
- (19) Hart, E. J., Gordon, S., Fielden, E. M. (unpublished).
- (20) Hayon, E., Weiss, J., *Proc. 2nd Int'l. Conf. Peaceful Uses Atomic Energy, Geneva* **29**, 80 (1958).
- (21) Himmelblau, D. M., *Chem. Rev.* **64**, 527 (1964).
- (22) James, J. C., Monk, C. B., *Trans. Faraday Soc.* **46**, 1041 (1950).
- (23) Jortner, J., *Rad. Res. Suppl.* **4**, 24 (1964).
- (24) Keene, J. P., *Nature* **197**, 47 (1963).
- (25) Keene, J. P., *Rad. Res.* **22**, 1 (1964).
- (26) Kuppermann, A., *Actions Chimiques et Biologiques des Radiations, V^e Série*, Haissinsky, M., ed., Academic, New York, 1961. (In this reference the diffusion model is discussed at length.)
- (27) Lea, D. E., *Actions of Radiation on Living Cells*, The MacMillan Co., New York, p. 47 (1947).
- (28) Magee, J. L., *Ann. Rev. Phys. Chem.* **12**, 389 (1961).
- (29) Magee, J. L., *Rad. Res. Suppl.* **4**, 20 (1964).
- (30) Matheson, M. S., *Ann. Rev. Phys. Chem.* **13**, 77 (1962).
- (31) Matheson, M. S. and Rabani, J., *J. Phys. Chem.* **69**, 1324 (1965).
- (32) Paul, St., *Epistle to the Hebrews*, Chapter 11, Verse 1.
- (33) Platzman, R. L., *Physical and Chemical Aspects of Basic Mechanisms in Radiobiology* Publ. No. 305, 34 (U. S. Nat'l. Research Council, 1953).
- (34) Rabani, J., Matheson, M. S., *J. Am. Chem. Soc.* **86**, 3175 (1964).
- (35) Rabani, J., Matheson, M. S., *J. Chem. Phys.* (to be submitted).
- (36) Rabani, J., Mulac, W. A., Matheson, M. S., *J. Phys. Chem.* **69**, 53 (1965).
- (37) Schmidt, K. H., Buck, W. L., unpublished results.
- (38) Schwarz, H. A., *J. Phys. Chem.*, **66**, 255 (1962).
- (39) Schwarz, H. A., *Rad. Res. Suppl.* **4**, 89 (1964).
- (40) Stein, G., *Discussions Faraday Soc.* **12**, 227 (1952).
- (41) Sweet, J. P., Thomas, J. K., *J. Phys. Chem.* **68**, 1363 (1964).
- (42) Thomas, J. K., *Trans. Faraday Soc.* **61**, 702 (1965).
- (43) Thomas, J. K., Gordon, S., Hart, E. J., *J. Phys. Chem.* **68**, 1524 (1964).

RECEIVED May 3, 1965. Based on work performed under the auspices of the United States Atomic Energy Commission.

Reactions of the Hydrated Electron

MICHAEL ANBAR

The Weizmann Institute of Science, Rehovoth, and the Soreq Nuclear Research Center, Yavneh, Israel

Many reactants, both organic and inorganic, react with e_{aq}^- at specific rates higher than that of $e_{aq}^- + H_2O$ but slower than diffusion-controlled rates. For these, correlations have been found between the reactivity toward e_{aq}^- and the availability of a vacant orbital on the reactant. The first product of the reaction with e_{aq}^- , which contains an additional electron, may be of limited stability, but it is always formed as an intermediate. It was suggested that the electron transfer from e_{aq}^- to any reactant is an extremely fast process which is never rate determining. Consequently, those reactions which are not diffusion controlled involve pre-equilibria with reactants which have an electron configuration that allows the incorporation of an additional electron.

The development of chemistry in the 20th century has been dominated and motivated by the electronic theory of the chemical bond and the role of electrons in chemical reactivity. The electronic structure of the chemical bond could be deduced by more or less direct methods, such as electronic excitation spectra, dipole moments, or paramagnetism; but there was no direct indication for the transfer of electrons in chemical reactions. Using isotopic techniques it has been possible to demonstrate bond cleavage and atom transfer reactions, but it is impossible to label an electron and trace its transfer from one molecule to another. It was not until the discovery of the radiolytically produced solvated electron that electron transfer processes could be examined directly and unambiguously.

By studying the reactions of solvated electrons, which are by definition electron transfer processes, it has become possible to analyze basic postulates in modern chemistry. These include the contribution of molecular properties to electron transfer reactions, such as intramolecular electron distribution, electron affinity, and redox potentials. Since electron transfer reactions are, by definition, the most elementary reduction processes, studying these reactions tests the validity of theories of redox processes. The investigations have resulted in a gratifying agreement with the predictions of the prevailing theories. The sensational finding from studies of solvated electron reactivity is just the nonsensational fact that the unit negative charge, bound to its medium only by its energy of solvation, behaves as expected for an electron, thus confirming our basic views on molecular structure and chemical reactivity.

An additional product of these studies was the characterization of many reduced species which have never before been produced or investigated. It may be concluded that the discovery of the solvated electron with its characteristic spectrum of absorption is one of the great achievements in chemistry of the last few decades—not only because it demonstrated the existence of a most elementary chemical species, but also because it firmly establishes the role of electron transfer in chemical reactivity.

The following review will summarize and systematize the available knowledge on the chemical reactivity of solvated electrons and the products of their reactions. Since most of the work was carried out with solvated electrons in aqueous solutions, we shall confine ourselves mainly to hydrated electrons. We do not intend to discuss the interaction of solvated electrons with their solvents since this will be covered in other chapters.

Hydrated Electrons and their Kinetic Behavior

The Formation of Solvated Electrons and the Methodology of Investigating their Kinetics. Solvated electrons have been produced in polar, nonreactive solvents like water, ammonia, alcohols, and aliphatic amines by various processes:

(1) They may be formed by the solvation of radiolytically generated secondary electrons after these undergo thermalization (106, 123). This has been demonstrated in water (66, 83, 84) in alcohols (117) and in ethylenediamine (12). The presence of long-lived trapped electrons has been demonstrated in radiolyzed alkaline ice (71, 86), and their behavior was found to be analogous to e_{aq}^- .

(2) Hydrated electrons were suggested as being formed photochemically from species which possess an absorption band corresponding to charge transfer to the solvent (80). This has been confirmed by demonstrating that the spectrum of hydrated electrons formed on photolysis of an extensive series of anions is similar to that of e_{aq}^- produced by radiolysis (61, 94). The photolysis of halide ions in ethanol gave analogous results, yielding solvated electrons with an absorption spectrum similar to that obtained by radiolysis (62).

(3) Solvated electrons in ammonia are formed in equilibrium with metal ions dissolved in this medium (76). Analogous behavior was reported for ethylenediamine (42). On mixing ethylenediamine solutions of alkali metals with water, hydrated electrons were claimed to be formed as transients (43).

(4) Hydrated electrons are also formed as a product of the interaction of hydroxide ions with hydrogen atoms. This reaction was first established kinetically (4, 6, 81, 82, 99) and then corroborated spectrophotometrically using flash radiolysis (95, 96). It should be noted that the rate of the $\text{H} + \text{OH}^- \rightarrow e_{aq}^-$ reaction is only $1.8 \times 10^7 \text{ M}^{-1} \text{ sec}^{-1}$ (96); thus, this step may become rate determining in many reactions with reactive substrates.

The participation of hydrated electrons as transients in certain electrode processes as well as in the reaction of alkali metals with water remains an open question and requires further investigation.

The kinetic behavior of solvated electrons has been followed directly using flash radiolysis (44, 45, 58) or flash photolysis technique (62, 94, 107). The former method is more universally applicable owing to the high absorption coefficient of e_{solv}^- in a spectral region where most reactants contribute little to the overall optical density. Stopped-flow spectrophotometry has also been applied in the specific case of the $e_{aq}^- + \text{H}_2\text{O}$ reaction (43), but it is not applicable to reactions where the e_{solv}^- half-life is below 0.1 msec.

In all the direct kinetic measurements e_{solv}^- is generated in minute concentrations of 10^{-8} – 10^{-6} M , while the other reactants are present in excess, so that a pseudo first-order disappearance of e_{solv}^- is followed. The disappearance of e_{aq}^- by the reactions $e_{aq}^- + e_{aq}^-$ or $e_{aq}^- + \text{radicals}$ follows second-order kinetics.

Before direct kinetic techniques were adapted to studying the reactions of e_{aq}^- , the only experimental approach was competition kinetics, based on determining the yield of products. The major drawback of these methods is the presumption that the products analyzed have been formed in the primary step of the reaction. In many cases however, the final product analyzed is formed in a secondary or tertiary step, and the effect of additives on its yield does not necessarily reflect their interference with the primary step. Taking even rather recent results obtained by this method, significant discrepancies may be encountered between rate data derived from competition kinetics and those obtained by direct measurement (4, 105, 111).

In many cases excellent agreement has been found between relative rates derived from competition kinetics and from direct measurement—e.g., for the ratio $k(e_{aq}^- + \text{NO}_2^-)/k(e_{aq}^- + \text{acetone})$ (112). If, on the other hand, large discrepancies are observed for relative reaction rates, this would imply that secondary reactions contribute to the formation of the products. Competition kinetics may therefore find their justification in the study of the chemical behavior of secondary products. For $e_{solv}^- + \text{X}$ reactions, this means studying the chemical behavior of X^- . In any case it should be remembered that competition kinetics require

several cross-checks with competitors of different chemical characteristics before it is established that the given yield originates from a primary reaction only.

The Chemical Reactivity of e_{aq}^- . The chemical behavior of solvated electrons should be different from that of "free" thermalized electrons in the same medium. Secondary electrons produced under radiolytic conditions will thermalize within 10^{-13} sec., whereas they will not undergo solvation before 10^{-11} sec. (106). Thus, any reaction with electrons of half-life shorter than 10^{-11} sec. will take place with nonsolvated electrons (75). Such a fast reaction will obviously not be affected by the ultimate solvation of the products, since the latter process will be slower than the interaction of the reactant with the thermalized electron. This situation may result in a higher activation energy for these processes compared with a reaction with a solvated electron. No definite experimental evidence has been produced to date for reactions of thermalized nonsolvated electrons, although systems have been investigated under conditions where electrons may be eliminated before solvation (15).

Once the electron becomes hydrated, its charge is spread out over a number of water molecules (106, 123, 124, 85) with a hydration energy of approximately 40 kcal./mole (26). It takes the hydrated negative charge about 3.10^{-9} sec. to attain equilibrium with its ionic environment; consequently, any reaction that proceeds faster than this will involve a hydrated electron without its normal gegen-ion sphere. This has been experimentally demonstrated both for radiolytically and for photolytically produced electrons (36, 38). Since photolytically produced hydrated electrons were shown to have a normal ionic environment, it must be concluded that the "cages" suggested for these species (80) are an expression of the nonhomogeneous distribution of the $I_2^- + e_{aq}^-$ pairs in the photolyzed solution rather than cages in the classical sense (101).

After 3.10^{-9} sec. the hydrated electron attains its final configuration in solution, with an outer sphere of positive ions which affects its reactivity according to the classical Brønsted-Bjerum theory of ionic reactions. This has been demonstrated both in competition studies (34, 37) and by following the effect of ionic strength on the rate of the $e_{aq}^- + Fe(CN)_6^{-3}$ reaction (59). Very high concentrations of electrolytes invariably were found to diminish the reaction rates of e_{aq}^- with charged and noncharged reactants (12). If the shifts in the absorption spectrum of e_{aq}^- in these media are considered as indicating an increase in the energy of hydration, the decrease in the reactivity of e_{aq}^- is not surprising. The stabilization of e_{aq}^- in concentrated solutions may be considered analogous to the behavior of trapped electrons in ice (85, 86). Alternatively, the rate decrease may be caused by the fact that the required rearrangement of solvent molecules around the activated complex is partially inhibited in concentrated solutions of electrolytes (47). It is interesting to note at this point that the reaction rates of e_{solv} in alcohols with different substrates are identical, within the experimental error, with those measured for e_{aq}^- (9, 117). The energy of solvation of the electron is also comparable in both media.

Diffusion-Controlled Reactions. The specific rates of many of the reactions of e_{aq}^- exceed $10^9 M^{-1} \text{sec.}^{-1}$, and it has been shown that many of these rates are diffusion controlled (92, 113). The parameters used in these calculations, which were carried out according to Debye's theory (41), were a diffusion coefficient of 10^{-4}sec.^{-1} (78, 113) and an effective radius of 2.5–3.0 Å. (77). The energies of activation observed in e_{aq}^- reactions are also of the order encountered in diffusion-controlled processes (121). A very recent experimental determination of the diffusion coefficient of e_{aq}^- by electrical conductivity yielded the value $4.7 \pm 0.7 \times 10^{-5} \text{cm.}^2 \text{sec.}^{-1}$ (65). This new value would imply a larger effective cross-section for e_{aq}^- and would increase the number of diffusion-controlled reactions. A quantitative examination of the rate data for diffusion-controlled processes (47) compared with that of e_{aq}^- reactions reveals however that most of the latter reactions with specific rates of $< 10^{10} M^{-1} \text{sec.}^{-1}$ are not diffusion controlled.

Taking the experimental value for the $e_{aq}^- + e_{aq}^-$ reaction in dilute solution as $4.5 \times 10^9 M^{-1} \text{sec.}^{-1}$ (58, 96) and assuming that this reaction is diffusion controlled with a diffusion coefficient $D = 5 \times 10^{-5} \text{cm.}^2 \text{sec.}^{-1}$ (a value which has been used in the following calculations unless otherwise indicated), one arrives at a distance of closest approach (r) of about 3 Å., which is the value obtained by theoretical calculations (77). The rate of $e_{aq}^- + \text{I}_2$ is $5.2 \times 10^{10} M^{-1} \text{sec.}^{-1}$ (122), and yields a value for r of about 9 Å. Another example of a diffusion-controlled reaction with a neutral molecule is the reaction of e_{aq}^- with tetranitromethane, which proceeds at a rate of $4.6 \pm 0.5 \times 10^{10} M^{-1} \text{sec.}^{-1}$ (109). A series of neutral reactants which react with e_{aq}^- with a specific rate of about $3 \times 10^{10} M^{-1} \text{sec.}^{-1}$ includes H atoms (58), OH radicals (58, 96), NO (58), CS_2 (68), CCl_4 (68), and CHCl_3 (68), all of which might be expected to react with e_{aq}^- on encounter. Taking $r = 5$ Å., which is a reasonable value for these reactants, and a diffusion coefficient for these reagents of $3 \times 10^{-5} \text{cm.}^2 \text{sec.}^{-1}$ one finds that these reactions are diffusion controlled. The $e_{aq}^- + \text{O}_2$ reaction may also be expected to be diffusion controlled. However, in view of the fact that NO, which has similar dimensions, reacts with a significantly higher specific rate, it may be suggested that the $e_{aq}^- + \text{O}_2$ reaction has some geometrical restrictions and is not purely diffusion controlled. Taking, on the other hand, $e_{aq}^- + \text{H}_2\text{O}_2$, which react with a specific rate $1.23 \pm 0.14 \times 10^{10} M^{-1} \text{sec.}^{-1}$ (59), one finds $r = 2.5$ Å., which implies (47) that this reaction is not diffusion controlled. This applies to any neutral molecule reacting with e_{aq}^- at a specific rate lower than $2 \times 10^{10} M^{-1} \text{sec.}^{-1}$.

Turning now to monovalent cations, for a cation of low mobility, $2 \times 10^{-5} \text{cm.}^2 \text{sec.}^{-1}$, and an effective radius of 5 Å. (116) so that, $r = 8$ Å., a diffusion-controlled reaction with e_{aq}^- , assuming $D = 5 \times 10^{-5} \text{cm.}^2 \text{sec.}^{-1}$ would proceed at a specific rate of $7 \times 10^{10} M^{-1} \text{sec.}^{-1}$. Several monovalent complex cations were found to react at about this rate (11, 115), and their reactions may be considered as examples of diffusion-controlled processes. A complete overlap of e_{aq}^- and the reactant ($r = 0$) and taking $D = 5 \times 10^{-5} \text{cm.}^2 \text{sec.}^{-1}$ would result in $k = 3 \times 10^{10} M^{-1}$

sec.⁻¹ Thus, any lower rates for monovalent cations cannot be considered as diffusion limited. The value reported for methylene blue (28) namely, $3.4 \times 10^{11} M^{-1} \text{sec.}^{-1}$, seems to be out of line with all other information available, and it would require a diffusion coefficient of $3.10^{-4} \text{cm.}^2 \text{sec.}^{-1}$ for e_{aq}^- .

The most interesting case in the group of monovalent cations is the reaction $H^+ + e_{aq}^-$ which can be shown is definitely not diffusion controlled. The effective radius of $H_3O_4^+$ is 4 A. (47), thus giving r a value of > 6 A., and taking into consideration the high diffusion coefficient for H^+ in water and $D = 5 \times 10^{-5} \text{cm.}^2 \text{sec.}^{-1}$, a limiting value of $1.1 \times 10^{11} M^{-1} \text{sec.}^{-1}$ is obtained, compared with the experimental value of $2.3 \times 10^{10} M^{-1} \text{sec.}^{-1}$ (122). It should also be noted that a similar value, $2.0 \pm 0.4 \times 10^{10} M^{-1} \text{sec.}^{-1}$, is obtained in ethanol (117) for $e_{solv}^- + H^+$ despite the large difference in dielectric constants.

The diffusion-controlled upper limits for divalent and trivalent cations having an effective radius of 4 A., ($r = 7$ A.) is 7.2×10^{10} and $1.0 \times 10^{11} M^{-1} \text{sec.}^{-1}$, respectively. Only a few of the divalent and trivalent cations examined approach these values. In order to assume that the highest of the measured values are diffusion controlled—e.g. $Co(NH_3)_6^{+3}$ ($k = 9 \times 10^{10} M^{-1} \text{sec.}^{-1}$) (11) and Cd^{+2} ($k = 5 \times 10^{10} M^{-1} \text{sec.}^{-1}$) (11), one has to assign to e_{aq}^- a diffusion coefficient of $5 \times 10^{-5} \text{cm.}^2 \text{sec.}^{-1}$

A small monovalent anion with an effective radius of 2.5 A. like NO_3^- would yield a diffusion-controlled limit of $1.1 \times 10^{10} M^{-1} \text{sec.}^{-1}$, which is in excellent agreement with the experimental value for this ion (122). From the measured data one may conclude that the rate of $O^- + e_{aq}^-$ ($k = 2.2 \pm 0.6 \times 10^{10}$) (96) is diffusion controlled and that O^- is perhaps hydrated. Other examples of diffusion-controlled reactions are $e_{aq}^- + MnO_4^-$, ($k = 2.2 \times 10^{10} M^{-1} \text{sec.}^{-1}$) (122), $e_{aq}^- + C(NO_2)_3^-$, ($k = 3.0 \pm 0.5 \times 10^{10} M^{-1} \text{sec.}^{-1}$) (109), and most probably $e_{aq}^- + Cr(C_2O_4)_2(H_2O)_2^-$, ($k = 2 \times 10^{10} M^{-1} \text{sec.}^{-1}$) (115).

A divalent anion with an effective radius of 7 A., would be expected to react with a diffusion-controlled rate of $2 \times 10^{10} M^{-1} \text{sec.}^{-1}$. A slightly higher value has been observed (122) for $Cr_2O_7^{-2}$ and it implies a certain hydration sphere around the oxyanion (116). A smaller anion with an effective radius of 5 A. will have a diffusion-controlled rate of $1 \times 10^{10} M^{-1} \text{sec.}^{-1}$. This actually has been observed for $S_2O_8^{-2}$ ($k = 1.1 \times 10^{10} M^{-1} \text{sec.}^{-1}$) (122).

For a trivalent anion with an effective radius of 9 A. the diffusion-limited rate is $1.5 \times 10^{10} M^{-1} \text{sec.}^{-1}$. This value, within experimental error, has been observed for $Cr(C_2O_4)_3^{-3}$ (115). $Cr(CN)_6^{-3}$ reacts with a comparable rate ($k = 1.5 \pm 0.2 \times 10^{10} M^{-1} \text{sec.}^{-1}$) (11) although it has evidently a smaller radius.

Assuming the possibility of overlap in the reactions of e_{aq}^- with anions ($r \rightarrow 0$), much lower values of diffusion-controlled rates can be derived. This approach is, however, untenable in view of the cases of agreement with reasonable values of r cited above. It may be concluded therefore that the twenty reactions quoted, namely, $e_{aq}^- + e_{aq}^-$, I_2 , $C(NO_2)_4$, H , OH , CS_2 , $CHCl_3$, CCl_4 , NO , O_2 , $Cr(en)_2Cl_2^+$, $Co(en)_2Cl_2^+$,

Ti^+ , NO_3^- , O^- , MnO_4^- , $\text{C}(\text{NO}_2)_3^-$, $\text{S}_2\text{O}_8^{2-}$, $\text{Cr}_2\text{O}_7^{2-}$, $\text{Cr}(\text{CN})_6^{3-}$ and $\text{Cr}(\text{C}_2\text{O}_4)_3^{3-}$ are exceptionally fast reactions which approach the diffusion-controlled limit, while the great majority of rate data reported on e_{aq}^- reactions refer to reactions which are not diffusion controlled.

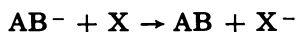
The Reactivity of Different Chemical Species toward Hydrated Electrons and the Products of these Reactions

Introduction. Over 300 different chemical compounds have been investigated up to now for their reactivity with e_{aq}^- (21, 45). Since e_{aq}^- is the most elementary chemical species it was worthwhile examining its reactivity toward different chemical species. The rates of interaction of the reactants investigated with e_{aq}^- range from $16 M^{-1} \text{sec}^{-1}$ to diffusion-controlled processes. Although many of the compounds examined show very high reactivities toward e_{aq}^- , only a few actually reach the diffusion-controlled limit, as pointed out previously. Comparing specific rates yields invaluable information on the chemical reactivity of different compounds in electron transfer processes as long as the reactions are not diffusion controlled. There is no reactant other than e_{aq}^- which could be investigated for its reactivity toward such a large variety of species following one and the same basic process. It is not surprising therefore, that, since the development of kinetic methods for investigating reactions with hydrated electrons in 1962, so many compounds have been examined for their reactivity.

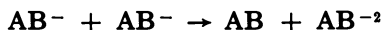
The reaction of e_{aq}^- with any neutral chemical species may be expressed by the following general formulation



The primary product AB^- may be stable and show up as the final product, or it may be unstable and dissociate to give stable negative ion B^- and a radical A , or a stable molecule A and a radical ion B^- . AB^- may react with water to give $\text{ABH} + \text{OH}^-$, and ABH may or may not undergo further chemical changes. When another reagent is present, AB^- may eventually transfer an electron to it.

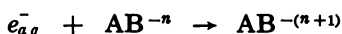
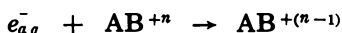


In some cases another AB^- will take the place of X , which means a disproportionation of AB^- .



AB^{2-} may be stable or it may dissociate to give two stable species $\text{A} + \text{B}^{2-}$ or $\text{A}^- + \text{B}^-$.

The reaction of e_{aq}^- with a charged ion will follow an analogous course



$AB^{+(n-1)}$ and $AB^{-(n+1)}$ may be stable species or may subsequently undergo chemical changes analogous to those cited above for AB^- .

It has been suggested that certain species formed on association with e_{aq}^- have no chemical stability at all and may be considered merely as transition states, as in the dissociative electron capture reactions observed in the gas phase (49, 51, 72, 90). It should be noted that there is an intrinsic difference between the capture of an electron in the gas phase and an interaction with e_{aq}^- in aqueous solutions. In the gas phase one also obtains in the first stage $e^- + AB \rightarrow AB^-$. If the bond energy $A-B^-$ is smaller than the electron affinity of the molecule, the energy gained in the electron capture may be dissipated either by radiative processes or by dissociation (110). The cross-section for capturing a thermalized electron in the gas phase is very small, even for molecules of the high electron affinity (48, 51, 72). In solution, AB^- is stabilized by solvation, and it may dissipate any excess energy by collisions with its close neighbors in its hydration shell. These two factors increase the probability of interaction with "thermal" electrons from negligible values to collision frequencies. Taking, for example, the $e^- + I_2$ reaction in the gas phase (51), the cross-section for thermal electrons is very small, and furthermore no I_2^- is formed since even a slight excess energy induces its dissociation in the gas phase. The $e^- + I_2 \rightarrow I + I^-$ as well as the $e^- + RCl \rightarrow R + Cl^-$ reactions apparently require an electron with a minimum kinetic energy for completely dissociating the activated complex (48, 110). In aqueous solutions, on the other hand, the $e_{aq}^- + I_2$ reaction is diffusion controlled, and I_2^- is produced quantitatively (122). Br_2^- and Cl_2^- were also shown to be relatively stable species in solvated form (24, 94), whereas their existence in the gas phase could not be demonstrated. As we shall see later in discussing the experimental data, evidence is accumulating that an AB^- intermediate is formed in practically all e_{aq}^- reactions, and no dissociative electron capture takes place in aqueous solutions. If this intermediate undergoes monomolecular dissociation in less than 10^{-8} sec. (which still leaves 10^6 vibrations of the bond before rupture plus ample time for solvation) it will escape all presently available detection techniques based on physical properties, and its scavenging by the most reactive additives requires rather high concentrations ($>0.1 M$). Such additives are likely to react also with e_{aq}^- or with other primary species and interpreting the results obtained by competition kinetics may become extremely difficult. Intermediates which persist for 10^{-6} sec. or longer are easily detected by competition kinetics, and many of those which persist longer than 10^{-5} sec. can be detected directly and characterized by physical methods.

In the following sections we shall systematize and try to interpret the information available on the reactivity of different chemical species toward e_{aq}^- and the products of these reactions. Since specific rate constants of e_{aq}^- reactions have been previously tabulated (21, 45) we do not intend to cite them here.

Free Radicals and Other Paramagnetic Reagents. The first group of reactants to be considered will be atoms and molecules which

contain an unpaired electron. These include the primary and secondary products of radiolysis: e_{aq}^- , H, OH, HO₂, O⁻, and O₂⁻, organic free radicals such as CH₂OH or (CH₃)₂COH, stable chemical species like NO or NO₂, and biradicals like O₂.

The $e_{aq}^- + e_{aq}^-$ reaction proceeds at a diffusion-controlled rate (96). As theoretically predicted (e_{aq}^-)₂ is utterly unstable (77, 123), and it might convert into two H atoms, a H⁻ ion, or an H₂ molecule. It has been demonstrated unambiguously that the $e_{aq}^- + e_{aq}^-$ reaction produces hydrogen, and the hydrogen produced does not originate from the recombination of two H atoms or from $e^- + H$ in a cage (46, 96). Since it is hard to believe that an H₂ molecule is formed in a single step, it may be suggested that H⁻ is formed as an intermediate. It may be speculated that a second electron interacting with the region of negative charge, which constitutes e_{aq}^- , results in detaching an OH⁻ ion, leaving a hydride ion to interact with water and give H₂. The formation of H⁻ from $e_{aq}^- + e_{aq}^- + H_2O \rightarrow H^- + OH^-$ is thermodynamically feasible, taking ΔF of e_{aq}^- as 57.5 kcal./mole (64) and ΔF of H⁻, H₂O, and OH⁻ as 51.9, -56.7 and -37.6 kcal./mole, respectively (88). Therefore, this would be a plausible mechanism for the formation of H₂. However it would be hard to prove the presence of H⁻ as an intermediate since it reacts with water at a diffusion-controlled rate. This can be deduced from the H/D isotope effects involved in the reaction of LiH with H₂O in tetrahydrofuran (23).

The $e_{aq}^- + H$ reaction, which also proceeds at a diffusion-controlled rate (58), most probably produces H⁻ as a primary product. The reaction $e_{aq}^- + H \rightarrow H^-$ has a negative ΔF of 54 kcal./mole (neglecting the energy of hydration of H which is small) (26) and the final product will be H₂. As already pointed out, it is hard to prove the existence of hydride ions as intermediates in aqueous solutions. It should be noted here that although the reactions $e_{aq}^- + e_{aq}^-$ and $e_{aq}^- + H$ were shown to produce H₂, these reactions probably are not the source for the formation of the "molecular" hydrogen in the radiolysis of water (16, 114).

The $e_{aq}^- + OH$ and $e_{aq}^- + O^-$ reactions are also diffusion controlled (96), and the product is obviously OH⁻. No information is available on the reaction rate of HO₂ and O₂⁻ with e_{aq}^- because it is difficult to maintain electrons in the presence of the oxygen or H₂O₂ necessary for producing O₂⁻.

Free radicals produced from alcohols by hydrogen abstraction—e.g., CH₂OH and CH₃CHOH, show a low reactivity toward e_{aq}^- (47, 58). This property may be correlated with the fact that CH₂OH tends to act as an electron donor toward alkyl bromides, inducing their debromination (22); in other words, CH₂OH tends to convert to a carbonium rather than to a carbanion. Furthermore, CH₂OH radicals tend to dimerize rather than to disproportionate (50), which again reflects their reluctance to act as electron acceptors. This inertness of CH₂OH as an electron acceptor makes methanol an ideal additive for scavenging OH and H radicals, producing a free radical which does not interact with e_{aq}^- .

Two other paramagnetic reactants which react with e_{aq}^- at close to diffusion-controlled rates are NO and O₂. It has been already pointed out that whereas NO reacts with a diffusion-controlled specific rate of $3.14 \pm 0.2 \times 10^{10} M^{-1} \text{sec.}^{-1}$ (58), O₂ reacts with a rate of $1.88 \pm 0.2 \times 10^{10} M^{-1} \text{sec.}^{-1}$ (92) and may therefore have some geometrical restrictions. The product of $e_{aq}^- + \text{NO}$ is most probably NO⁻ which on reaction with NO may yield N₂O. This requires experimental verification. The formation of O₂⁻ from $e_{aq}^- + \text{O}_2$ has been demonstrated unambiguously by the fact that the rate of appearance of O₂⁻ is identical with the rate of disappearance of e_{aq}^- in its reaction with O₂ (60). O₂⁻ disappears by disproportionation to O₂ + H₂O₂. O₂⁻ was shown to accept an electron from H₂O₂, following the reactions $\text{O}_2^- + \text{H}_2\text{O}_2 \rightarrow \text{O}_2^{-2} + \text{H}_2\text{O}_2^+ \rightarrow \text{HO}_2^- + \text{HO}_2 \rightarrow \text{H}_2\text{O}_2 + \text{O}_2^-$, thus inducing isotopic exchange of oxygen without "scrambling" (8).

In conclusion, it may be stated that all the paramagnetic reactants examined, with the exception of alkyl radicals, accommodate the electron from e_{aq}^- in their orbitals at a diffusion-controlled rate.

Water, H₂O⁺ and Brönsted Acids. The most important reagent in the chemistry of e_{aq}^- is obviously the solvent, water. Were it not for the relatively low reactivity of e_{aq}^- with H₂O most of our information on hydrated electrons would be merely hypothetical. Fortunately the rate of the $e_{aq}^- + \text{H}_2\text{O} \rightarrow \text{H} + \text{OH}^-$ reaction is slow enough to enable one to examine the kinetic behavior of any solute reacting with e_{aq}^- at a rate over $10^5 M^{-1} \text{sec.}^{-1}$

The rate of the $e_{aq}^- + \text{H}_2\text{O}$ reaction has been determined by many investigations. Since this reaction follows first-order kinetics, any impurity present will add to its apparent rate. With increasing care in purifying the solvent, the upper limit of the specific rate of the $e_{aq}^- + \text{H}_2\text{O}$ reaction has been reduced to $16 \pm 1 M^{-1} \text{sec.}^{-1}$ (67), which is in excellent agreement with the value obtained by stopped-flow kinetics when a metal solution in ethylenediamine was mixed with H₂O (43). These observations suggest that the apparent isotope effect reported in D₂O (33), was probably caused by a difference in the purity of the solvents used. The new value for $k_{e_{aq}^- + \text{H}_2\text{O}}$ decreases the calculated redox potential of e_{aq}^- from 2.7 (26) to 2.5 volts (64). If one assumes that e_{aq}^- reacts with Mg⁺², although extremely slowly ($k < 10^5 M^{-1} \text{sec.}^{-1}$) (12), just as it reacts with Mg⁺² in ice (98), one may conclude that $E^\circ_{e_{aq}^-} > 2.4$ volts, which implies $k_{e_{aq}^- + \text{H}_2\text{O}} \geq 2 \times 10^{-2} M^{-1} \text{sec.}^{-1}$. In order to test this experimentally, reactive trace impurities in water must be $< 10^{-10} M$.

The mechanism of the $e_{aq}^- + \text{H}_2\text{O}$ reaction is not clear. It is evident that the reaction may take place only with solvated electrons, and it requires the solvation of the hydroxide ions to make it thermodynamically feasible (66). As will be seen later the reaction cannot be regarded as a proton transfer by a weak Brönsted acid to e_{aq}^- . Adhering to the formal scheme $e_{aq}^- + \text{AB} \rightarrow \text{AB}^- \rightarrow \text{A} + \text{B}^-$ one would expect an electron to be absorbed in one of the higher unoccupied orbitals of H₂O. A dissociative state of H₂O⁻ exists at about 4 e.v. (87) which yields $\text{H} + \text{OH}^-$; however,

in view of the relatively low activation energy of the $e_{aq}^- + \text{H}_2\text{O}$ reaction (122) there is little probability that this state is involved in the mechanism. It should be noted that the activation energy of 4.6 kcal./mole was derived using the decay rate of e_{aq}^- as $2.3 \times 10^4 \text{ sec.}^{-1}$, compared with the recently observed value of $8.8 \times 10^2 \text{ sec.}^{-1}$. If the measured rate includes a reaction with a trace impurity which accounts for 96% of the e_{aq}^- decay and which has a much lower activation energy, then the actual ΔE of the $e_{aq}^- + \text{H}_2\text{O}$ reaction becomes much higher. This point awaits experimental verification. In any case the activation energy involved in the $e_{aq}^- + \text{H}_2\text{O}$ reaction is not the ΔE of diffusion, as the two reactants are continuously in intimate contact. This means that a certain amount of energy has to be put into the negatively charged region in water in order to localize an electron on an OH, which undergoes hydration to give OH_a^- , leaving a free hydrogen atom.

The reaction of e_{aq}^- with H_3O^+ is not a diffusion-controlled process, despite its high rate ($k = 2.3 \times 10^{10} \text{ M}^{-1} \text{ sec.}^{-1}$) (47, 59). The final product of this reaction is a hydrogen atom. The reaction is not a proton transfer from H_3O_4^+ to e_{aq}^- , but includes the formation of a long-lived intermediate, H_3O . In other words, the mechanism involves accommodating an electron on H_3O_4^+ . Since the vacancy in electron density in H_3O_4^+ is spread out over many atoms and since the negative charge of the hydrated electron is also spread out, it is not surprising that e_{aq}^- is not absorbed by H_3O_4^+ on each encounter. Since the reaction has the same activation energy as diffusion-controlled processes (122), about 20% of the encounters of e_{aq}^- with H_3O_4^+ result in its absorption to form H_3O .

Evidence for the formation of H_3O_{aq} as intermediate may be derived from competition kinetics. When the scavenging reactivity of H_3O^+ toward e_{aq}^- was compared with acetone by competition (79), it was found half as effective as expected from the specific rate constants obtained directly. This may suggest the reaction $\text{H}_3\text{O} + (\text{CH}_3)_2\text{CO} \rightarrow \text{H}_3\text{O}^+ + (\text{CH}_3)_2\text{CO}^-$. In another study, the competition for e_{aq}^- between H_3O^+ and N_2O showed the latter to be more effective as expected from the known rate data (4, 111), suggesting again $\text{H}_3\text{O} + \text{N}_2\text{O} \rightarrow \text{H}_3\text{O}^+ + \text{N}_2\text{O}^-$.

An H/D isotope effect in forming H atoms from $e_{aq}^- + \text{H}_3\text{O}^+$ has been observed. After correction for the "residual hydrogen," the value is 3.8, in excellent agreement with the value of 3.77 obtained for photolytically produced e_{aq}^- (16). If hydrogen in the $\text{H}_3\text{O}^+ + e_{aq}^-$ reaction is produced by proton transfer, the expected isotope effect would not exceed that in the $\text{H}_3\text{O}^+ + \text{OH}^-$ reaction, namely 1.5 (53, 54, 103). On the other hand, if the H_3O is formed from H_3O_4^+ with an isotope effect of 1.4 (54), after which it decomposes in a slow step, the isotope effect on the hydrogen atoms may be of the magnitude measured. It has also been suggested that H_3O is formed in spur reactions as a precursor of H_2 and H atoms (91, 114, 120).

It has been proposed (79) that e_{aq}^- reacts with Brönsted acids following the Brönsted general acid catalysis law. The work was based on the competition of four acids with acetone and with I^- for e_{aq}^- . The acids

were H_3O^+ , HF, H_2PO_4^- and NH_4^+ , the effective rates of which were in the ratio $1:5 \times 10^{-3}$; 10^{-3} and 1.5×10^{-4} . Using the recent value for the $e_{aq}^- + \text{H}_3\text{O}^+$ reaction rate one obtains 10^8 , 2×10^7 and $3 \times 10^6 M^{-1} \text{sec.}^{-1}$ for HF, H_2PO_4^- and NH_4^+ , respectively (the pK's of which are 3.45, 7.21, and 9.25, respectively). It has since been found, however, that other Brönsted acids within the given range of pK's do not react with e_{aq}^- at all—e.g., citric acid (122) (pK = 3.08, 4.74, 5.40), lactic acid (69) (pK = 3.08), oxalic acid (5, 69) (pK = 1.23, 4.19), and carbonic acid (122, 111) (pK = 10.25). Furthermore it was shown by pulse radiolysis that H_2PO_4^- reacts with e_{aq}^- at a rate of $1.5 \times 10^9 M^{-1} \text{sec.}^{-1}$, (122)—i.e., 200 times faster than calculated from competition kinetics. It may be concluded that the hypothesis of a general acid catalysis contradicts the experimental evidence and must therefore be rejected.

Hydrated electrons react with many Brönsted acids. This reaction is not a proton transfer process but an incorporation of the electron into the acid to form an AH^- ion radical, which may subsequently undergo decomposition. This decomposition may occasionally yield a hydrogen atom, but in many cases other pathways of dissociation have been observed.

Starting with acetic acid, it has been shown that only part of the acid, which reacts with e_{aq}^- at a moderate rate of $1.76 \pm 0.3 \times 10^8 M^{-1} \text{sec.}^{-1}$ (122) produces hydrogen (119), the other mode of decomposition being $\text{CH}_3\text{COOH}^- \rightarrow \text{CH}_3\text{CO} + \text{OH}^-$ (27). This observation has been confirmed, and a $G(\text{H}) = 1.1 \pm 0.1$ originating from AcOH has been determined (19). Formic acid behaves in an analogous manner, interacting with e_{aq}^- at a rather high rate, $1.43 \pm 0.1 \times 10^8 M^{-1} \text{sec.}^{-1}$ (122) to yield primarily $\text{HCO} + \text{OH}^-$, indicating the formation of HCOOH^- as intermediate (63).

Ammonium ions produce hydrogen atoms on interaction with e_{aq}^- but the H/D isotope effect involved in producing these H atoms (H/D = 4.36 after correction for the "residual H," H/D = 4.33 for photolytically produced e_{aq}^- (16)) indicates the formation of NH_4 as intermediate which then dissociates to $\text{NH}_3 + \text{H}$. These assumptions are in accord with the observed behavior of alkyl ammonium ions which, on interaction with e_{aq}^- produce alkyl radicals rather than H atoms (52): $\text{RNH}_3^+ + e_{aq}^- \rightarrow \text{RNH}_3 \cdot \rightarrow \text{NH}_3 + \text{R}$. Hydroxyl ammonium ions behave similarly yielding NH_2 radicals rather than H atoms (52, 89): $\text{NH}_2\text{OH}^+ + e_{aq}^- \rightarrow \text{NH}_2\text{OH} \cdot \rightarrow \text{NH}_2 + \text{H}_2\text{O}$.

The discrepancy in the rate data for H_2PO_4^- (79, 122) may be explained by the possible reactions $\text{H}_2\text{PO}_4^{-2} + (\text{CH}_3)_2\text{CO} \rightarrow \text{H}_2\text{PO}_4^- + (\text{CH}_3)_2\text{CO}^-$ and $\text{H}_2\text{PO}_4^{-2} + \text{NO}_2^- \rightarrow \text{H}_2\text{PO}_4^- + \text{NO}_2^{-2}$ which proceed with comparable efficiency (it is interesting to note that the e_{aq}^- rate constants for acetone and NO_2^- are also comparable) (21). On the other hand, it seems that $k_{(\text{H}_2\text{PO}_4^{-2} + \text{Fe}(\text{CN})_6^{-1})} / k_{(\text{H}_2\text{PO}_4^{-2} + \text{acetone})} > k_{(e_{aq}^- + \text{Fe}(\text{CN})_6^{-1})} / k_{(e_{aq}^- + \text{acetone})}$, probably because of the significant difference in salt effect on the reactions of monovalent and divalent anions.

The formation of AH^- and its decomposition without producing H atoms may take place even with a strong acid like HSO_4^- (pK = 1.92)

which was shown (in ice) to form HSO_4^- , which decomposes to $\text{SO}_3^- + \text{OH}^-$ rather than to $\text{H} + \text{SO}_4^{2-}$.

It may be concluded that as a rule an electron is accommodated on the acid molecule which subsequently dissociates, in the absence of other reagents, to give the most stable fragments. In the case of oxygen-containing acids, the hydration energy of OH^- is generally greater than that of the anion of the given acid and the free energy of formation of the corresponding free radical is lower than that of a hydrogen atom. It is not surprising, therefore, that AOH^- dissociates to $\text{A} + \text{OH}^-$ rather than to $\text{AO}^- + \text{H}$. An exception to this behavior is $\text{H}_2\text{PO}_4^{2-}$ which ultimately dissociates quantitatively to give $\text{HPO}_4^{2-} + \text{H}$. This is to be expected since the energy of dissociation of a P—O bond in phosphate is significantly higher than that of an OH bond (35). Oxygen free acids like ammonium or alkylammonium ions also dissociate to give those fragments whose formation requires the least energy and which are best stabilized by solvation.

Bi- and Triatomic Molecules. The most abundant triatomic molecule, H_2O , and the biatomic paramagnetic O_2 and NO have been discussed previously. Here we shall examine a number of other simple reactants.

Hydrogen shows no reactivity toward e_{aq}^- (96) which is not surprising since $e_{aq}^- + \text{H}_2 \rightarrow \text{H}_2^- \rightarrow \text{H} + \text{H}^-$ is thermodynamically unfeasible. The reactivity of nitrogen toward e_{aq}^- has not been examined but such a reaction seems rather unlikely in view of the inertness of the nitrogen molecule as an electron acceptor. CO which is isoelectronic with N_2 has a longer bond length (116), a finite dipole moment, with the oxygen positively polarized (104), and a much higher electron affinity (110). This results in a much higher reactivity toward e_{aq}^- , with $k = 1.10^9 M^{-1} \text{sec}^{-1}$ (69). The product of the $e_{aq}^- + \text{CO}$ reaction is probably CO^- which reacts with water to give HCO . The latter species is capable of abstracting an OH from H_2O_2 yielding formic acid; alternatively, it dimerizes to glyoxal (69). The chain reaction of CO in alkaline solution to yield formate ions (125) suggests that CO^- is capable of abstracting an OH radical from H_2O . CO^- was not detected in the gas phase by electron impact (49), although it must be formed as an intermediate.

N_2O reacts with e_{aq}^- at a high rate ($k = 8.7 \pm 0.6 \times 10^9 M^{-1} \text{sec}^{-1}$) (58, 84), yielding nitrogen and OH radicals as the final products (40). N_2O^- , which is formed as an intermediate, has been shown to have a lifetime long enough to participate in various chemical reactions. N_2O^- or N_2OH show a strong oxidative reactivity in many reactions. This behavior gave the impression that OH radicals are produced instantaneously as a product of a dissociative electron capture by N_2O (38). It was shown however that the OH-like behavior of N_2O^- or N_2OH does not hold quantitatively; thus $k_{(\text{OH} + \text{iPrOH})} / k_{(\text{OH} + \text{en})} > k_{(\text{N}_2\text{O}^- + \text{iPrOH})} / k_{(\text{N}_2\text{O}^- + \text{en})}$ (20), (en = ethylenediamine) $k_{(\text{OH} + \text{Tl}^+)} / k_{(\text{OH} + \text{iPrOH})} \gg k_{(\text{N}_2\text{O}^- + \text{Tl}^+)} / k_{(\text{N}_2\text{O}^- + \text{iPrOH})}$ (20), and that $k_{(\text{OH} + \text{Br}^-)} / k_{(\text{OH} + \text{R})} > k_{(\text{N}_2\text{O}^- + \text{Br}^-)} / k_{(\text{N}_2\text{O}^- + \text{R})}$ (22), where the product R is the same in both reactions. It was further found that N_2O^- reduces I_2 and Br_2 and that $k_{(\text{N}_2\text{O}^- + \text{Br}_2)} > k_{(\text{N}_2\text{O}^- + \text{I}_2)}$ (22),

whereas $k_{(e_{aq}^- + Br_2)} < k_{(e_{aq}^- + I_2)}$ (7). The increase in $G(I_2)$ under N_2O when the I^- concentration is increased from 10^{-4} to 10^{-3} (18) may be attributed to the competition between $N_2O^- + I^- \rightarrow I + N_2 + H_2O$ and $N_2O^- + I_2 \rightarrow N_2O + I_2^-$. Under the experimental conditions, where the concentration of I_2 did not exceed $10^{-5} M$, the I_2 could not possibly compete with N_2O ($1.6 \times 10^{-2} M$) for e_{aq}^- . N_2O^- is a rather mild reducing agent, reducing I_2 and Br_2 but not RBr (22). N_2O^- was also shown to reduce Cu^{+2} (39). It thus appears that N_2O^- or N_2OH may persist at least 10^{-7} sec. and may act both as an oxidizing and as a reducing agent. As an oxidizing agent, N_2O^- tends toward hydrogen abstraction rather than to electron transfer. This is apparent from all cases where competition kinetics were studied. Regarding the case of *iPrOH vs. ethylenediamine* (19) it was shown that *iPrOH* reacts with OH radicals by electron transfer, whereas the oxidation of ethylenediamine proceeds by hydrogen abstraction. The reaction of N_2O^- with Tl^+ and Br^- vs. RH corroborate the same conclusion.

CO_2 , which is isoelectronic with N_2O and has a similar linear configuration (116), reacts with e_{aq}^- at a surprisingly similar rate $k = 7.7 \pm 1.1 \times 10^9 M^{-1} sec^{-1}$ (58). The presence of the product, CO_2^- , has been demonstrated in a number of studies. CO_2^- was shown to add to organic radicals to form carboxylates (111, 112, 125, 126). It has been pointed out that the $CO_2^- + CH_2OH$ reaction must proceed extremely fast ($> 10^9 M^{-1} sec^{-1}$) to compete with the recombination reactions $2 CO_2^- \rightarrow (CO_2)_2^{-2}$ and $2 CH_2OH \rightarrow (CH_2OH)_2$ (121). In studying the competition between CO_2 and N_2O for e_{aq}^- it was shown that N_2O is three times more efficient as a scavenger of e_{aq}^- (111). This is not in accord with the direct rate measurements for the $e_{aq}^- + CO_2$ and $e_{aq}^- + N_2O$ reactions, and may be explained by an efficient electron transfer from CO_2^- to N_2O that is, $CO_2^- + N_2O \rightarrow CO_2 + N_2O^-$. The efficiency of CO_2^- as a reducing agent has been demonstrated in many reactions; CO_2^- was found to reduce H_2O_2 (3, 74), I_2 and Br_2 , as well as RBr , NO_3^- , and Cu^{+2} (22). It was shown that $k_{(CO_2^- + I_2)}/k_{(CO_2^- + H_2O_2)} < k_{(e_{aq}^- + I)}/k_{(e_{aq}^- + H_2O_2)}$, $k_{(CO_2^- + Cu^{+2})}/k_{(CO_2^- + RBr)} > k_{(e_{aq}^- + Cu^{+2})}/k_{(e_{aq}^- + RBr)}$ and $k_{(CO_2^- + NO_3^-)}/k_{(CO_2^- + RBr)} < k_{(e_{aq}^- + NO_3^-)}/k_{(e_{aq}^- + RBr)}$ (22).

The conjugate acid of CO_2^- , namely $COOH$ generally acts as an oxidizing agent. It oxidizes H_2O_2 (74), I^- , but not Br^- (22); thus, its oxidation potential may be estimated. No oxidizing properties of CO_2^- could be detected (22), and from the fact that it dimerizes to oxalate ions rather than disproportionates, it may be concluded that this species is inefficient as an electron acceptor.

CS_2 , the analogue of CO_2 , reacts with e_{aq}^- at a faster rate ($k = 3.1 \pm 0.3 \times 10^{10} M^{-1} sec^{-1}$) (68) which is diffusion controlled. It is not surprising that the $C=S$ bond is more reactive toward e_{aq}^- than the carbonyl bond, since the lower electronegativity of the sulfur atom makes its additional orbitals more liable to accommodate an additional electron. It is very likely that a long lived CS_2^- is produced, which eventually is reduced to carbon monosulfide; however this requires verification. It

would also be worthwhile to look for CS_2^- spectrophotometrically using pulse radiolytic techniques.

We shall conclude the discussion in this section with the reaction $e_{aq}^- + I_2 \rightarrow I_2^-$ which proceeds at a diffusion-controlled rate (122). In this reaction, I_2^- was shown to be formed at a rate equal to the rate of disappearance of e_{aq}^- . I_2^- may act as an iodine atom carrier on interaction with organic radicals (22) and will be reduced easily by e_{aq}^- or H atoms. Ultimately, it disproportionates to give $I_3^- + I^-$.

Nonmetallic Inorganic Anions. Many nonmetallic anions are nonreactive toward e_{aq}^- . These include F^- , Cl^- , Br^- , I^- , CN^- , CNS^- , CNO^- , N_3^- , and OH^- (21) which have no electron vacancy, and moreover, exhibit a charge transfer to the solvent. Obviously the formation of an X^{-2} from these ions is not feasible. Another group of inert anions includes oxyanions of nonmetals in their highest state of oxidation for example SO_4^{-2} , ClO_4^- , HPO_4^{-2} , PO_4^{-3} , CO_3^{-2} (21). It has been reported that HCO_3^- reacts with e_{aq}^- (108); however, the results can easily be explained by the amount of CO_2 present in equilibrium under the given conditions. All these ions except ClO_4^- have rather low oxidation potentials (88) and are thus very reluctant to accept an additional electron. It is hard however to explain the difference between ClO_4^- and NO_3^- , the latter reacting with e_{aq}^- at a diffusion-controlled rate. The difference in the kinetic behavior of ClO_4^- and NO_3^- may stem from the fact that the chlorine atom in ClO_4^- is formally negatively charged (104), whereas the nitrogen in NO_3^- is positively charged. Furthermore, the planar structure of NO_3^- with partial π bonding, facilitates the interaction between e_{aq}^- and the central atom, which is sterically hindered in the tetrahedral ClO_4^- .

The product of the $e_{aq}^- + NO_3^-$ reaction is hydrated NO_2 which has been detected spectrophotometrically (28) and whose presence could also be inferred from the behavior of the $I^- - I_2 - NO_3^-$ system (22, 100).

NO_2^- reacts with e_{aq}^- at a rate which is slower than that of NO_3^- (122), which is still unexpectedly high in view of the $NO_2^- - NO$ redox potential (+ 0.46 volts) (88). This high rate may be explained by the exposure of the positively charged nitrogen in the angular structure of the nitrite ion and by the stability of the NO_2^{-2} ion which has been produced from $e_{aq}^- + NO_2^-$ in liquid ammonia (127). This is another example of the fact that the reactivity of a compound toward e_{aq}^- is not a linear function of its redox potential.

Another series of anions which react with e_{aq}^- at fast, though not diffusion-controlled rates, are ClO_3^- , BrO_3^- and IO_3^- ; the specific rates are 0.023 (7, 28, 122), 2.1, and $7.7 \times 10^9 M^{-1} sec.^{-1}$ respectively (11). A large increase in reactivity is observed on passing from ClO_3^- to BrO_3^- , in spite of the rather small difference in redox potential (88). Again this may be caused by the partial negative charge on the Cl atom (104). The Br—O bond length in BrO_3^- , 1.78 Å. (116), is very near to the normal single bond length 1.80 Å. (104), implying a partial positive charge on the bromine, which is thus more liable to accommodate an additional negative charge.

The interaction of e_{aq}^- with ClO_3^- produces ClO_3^{-2} or ClO_2 , the appearance of which has been observed by pulse radiolysis (28). Analogously, BrO_3^{-2} or BrO_2 is produced from BrO_3^- . This transient has been observed by pulse radiolysis (7), and its chemical properties were examined in the I^- - I_2 system (22). It was found that BrO_3^{-2} oxidizes five equivalents of I^- in neutral solution; on the other hand, it reduces I_2 to I_2^- .

The transients of I(IV) and I(VI) formed by the reaction of e_{aq}^- with IO_3^- and IO_4^- , respectively, still await investigation.

Sulfite ions were found to have a low reactivity toward e_{aq}^- with $k < 10^7 M^{-1} \text{sec.}^{-1}$ (7). Tellurite ions are more reactive with $k = 6 \times 10^8 M^{-1} \text{sec.}^{-1}$ (33) in line with the behavior of group VII. The high reactivity of persulfate ions (122), which react at a diffusion-controlled rate is not surprising. A transient, presumably SO_4^- formed from $\text{S}_2\text{O}_8^{-3} \rightarrow \text{SO}_4^{-2} + \text{SO}_4^-$ has been observed by pulse radiolysis (28).

To sum up, oxyanions are liable to accommodate an additional electron on interaction with e_{aq}^- , if the central atom has an available orbital. This parameter, not the redox potential, determines the reactivity toward e_{aq}^- . In all cases investigated AO^{-n} yielded $\text{AO}^{-(n+1)}$ which occasionally may lose H_2O to give $\text{AO}^{-(n-1)}$.

Metal Ions and Metal Ion Complexes. Alkali metal and alkaline earth ions (with the possible exception of Mg^{+2}) do not react with e_{aq}^- . This is expected in view of the redox potential of the hydrated electron, $E^\circ = +2.5$ volts (64). It is expected however that e_{aq}^- will react with Mg^{+2} at a slow rate ($k < 10^5 M^{-1} \text{sec.}^{-1}$ has been observed (12)). The formation of Mg^+ in irradiated ice (98) suggests that a similar reaction may also take place in aqueous solution. All other metal ions are liable to be reduced by e_{aq}^- . The specific rates of $e_{aq}^- + \text{M}_n^{+n}$ range from $7 \times 10^{10} M^{-1} \text{sec.}^{-1}$ for Tl^+ down to $7.7 \times 10^7 M^{-1} \text{sec.}^{-1}$ for Mn_n^{+2} (11, 28). It has been suggested that the reactivity of metal ions is linearly correlated with their M^{+2} - M^+ redox potentials (45, 122). This assumption was primarily based on the behavior of the rare earth series where such a correlation was found to hold for Sm^{+3} , Yb^{+3} , and Eu^{+3} . However, this linear free energy correlation does not hold even for the aquo complexes of a limited series of divalent ions (45). Furthermore, comparing amino complexes with aquo complexes of the same central atom it is found that the two types of complexes react at comparable rates (11), whereas the redox potentials of the amino complexes as a rule, have lower values owing to the stabilization of the higher states of oxidation by the amino ligands. A related parameter suggested was the electron affinity which, in the case of divalent ions, is equal to the second ionization potential (45). This relation is also open to serious criticism. Whereas qualitatively the order of reactivity is $\text{Mn}^{+2} < \text{Fe}^{+2} < \text{Zn}^{+2} < \text{Co}^{+2} < \text{Ni}^{+2} < \text{Cu}^{+2} < \text{Cr}^{+2}$ (21), the order of electron affinity of these equivalent ions is $\text{Mn}^{+2} < \text{Fe}^{+2} < \text{Cr}^{+2} < \text{Co}^{+2} < \text{Zn}^{+2} < \text{Ni}^{+2} < \text{Cu}^{+2}$. Plotting $k_{(e_{aq}^- + M^{+2})}$ vs. electron affinity one can easily see that the best-fitting curve would require Cu^{+2} to react at collision frequency (about an

order of magnitude faster than observed), whereas Cr^{+2} would be expected to react two orders of magnitude slower than observed.

In view of the large difference in the reactivity of Cr^{+2} and Mn^{+2} aquo complexes it seems that the reactivity of the metal complex toward e_{aq}^- is not related to the energy required to remove a second $4s$ electron. The similar reactivity of aquo and amino complexes makes the correlation between reactivity and redox potentials rather unlikely. As an alternative mechanism, we suggest that the availability of a vacant d orbital on the central atom and the energy gain on adding an electron are the major factors which determine the reactivity of transition metal ions.

Taking the same series Cr^{+2} , Mn^{+2} , Fe^{+2} , Co^{+2} , Ni^{+2} , Cu^{+2} , Zn^{+2} one sees that adding an electron to the $3d^4 \text{Cr}^{+2}$ results in a maximum gain in exchange energy since the electron spin is parallel to the four spins on the metal (102). This could explain the high reactivity of Cr^{+2} toward e_{aq}^- ($k = 4.2 \times 10^{10} M^{-1} \text{sec.}^{-1}$) (11). The next metal in this series is $3d^5 \text{Mn}^{+2}$. A sixth electron added must have its spin antiparallel to all the electrons already present, and so it is not stabilized at all (102), resulting in a very low reactivity toward e_{aq}^- ($k = 7.7 \times 10^7 M^{-1} \text{sec.}^{-1}$) (28). Adding an electron to $3d^6 \text{Fe}^{+2}$ results in some gain in exchange energy, which increases for $3d^7 \text{Co}^{+2}$ and $3d^8 \text{Ni}^{+2}$. In the case of $3d^9 \text{Cu}^{+2}$ the gain in exchange energy is maximal, as in Cr^{+2} , and indeed Cu^{+2} approaches Cr^{+2} in its specific rate: 3.3×10^{10} as compared with $4.2 \times 10^{10} M^{-1} \text{sec.}^{-1}$ respectively (21). $3d^{10} \text{Zn}^{+2}$ is obviously expected to have a low reactivity since all the $3d$ orbitals are filled and the extra electron is placed in the N shell.

Comparing the reactivity of two metal ions of the same group in the periodic table invariably shows that the member of the higher series is more reactive. This is true for Cd^{+2} compared with Zn^{+2} ; Pd^{+2} compared with Ni^{+2} ; Pb^{+2} compared with Sn^{+2} ; as well as for Sb^{+5} compared with As^V (11). This effect is most probably caused by the higher availability of vacant electron orbitals, as well as by an increased polarizability of the molecule into which the hydrated electron is to be incorporated on encounter.

The presence of ligands may affect the reactivity of the central atom in two ways: first, by changing the ligand field as well as the electron density of the d electrons through σ and π bonding, and second, by acting as a bridge for electron transfer to the central atom. Ligands of high nephelauxic power (102) like CN^- will exert their action by the first mechanism. By covalent interaction with the d orbitals they will partially inhibit the addition of an extra electron to the central atom. This may explain the general tendency of cyano complexes to be less reactive compared to halo complexes (11). Since cyanide ions induce a strong ligand field, they will also change the spin distribution in the d orbitals. It is expected therefore, that ferrocyanide ions should be quite unreactive toward e_{aq}^- ($k < 10^7$), owing to the fact that the additional electron has to enter a vacant e_g orbital with a high Δ . On the other hand $\text{Mn}(\text{CN})_6^{-4}$ is expected to be more reactive than Mn_q^{+2} , owing to the spin coupling

which makes the accommodation of an additional electron rather favorable.

Ligands which do not strongly interact with the d orbitals, like fluoride, chloride, or iodide ions, may affect the reactivity of a complex toward e_{aq}^- by channeling the electron from the solvent to the central atom. Different ligands examined showed the following efficiency of acting as bridges for electron transfer: $I > Cl > F > H_2O > NH_3 \sim RNH_2 > CN^- > OH^-$ (11). This sequence is different from that observed for the reactivity of H atoms toward the same compounds and it was concluded that H atoms react with transition metal complexes by atom rather than by electron transfer (17).

The effect of OH^- and O^{-2} on the reactivity of complexes deserves special mention. It was found that some hydroxy complexes—e.g., $Al(OH)_4^-$ and $Zn(OH)_4^{-2}$, are extremely inert to attack by e_{aq}^- (11). Since no orbitals are involved in these cases, it must be concluded that OH^- is an extremely poor bridge for electrons. Hydroxy complexes which still contain water in their inner sphere, like cuprate (II), chromate (III), or plumbate(II) do not differ as much from their corresponding aquo complexes. The inhibitory effect of O^{-2} on the reactivity of the central atom is not sufficient to suppress the reactivity of the metal ions in their higher states of oxidation. Thus we find that MnO_4^- or $Cr_2O_7^{-2}$ react at diffusion-controlled rates (122).

We can conclude the discussion on the reactions of metal ions and their complexes with e_{aq}^- by noting that these reactions are, in fact, electron transfer processes and provide us with an ideal tool to examine the theories on electron transfer to inorganic species. It is gratifying to see that the behavior of the different metals and ligands as reflected in the e_{aq}^- reactions is in good agreement with the prevailing theories on electron transfer to transition metal complexes (11).

The primary product of the reaction of M_{aa}^{+2} with e_{aq}^- is obviously $M^{+(n-1)}$. In the case of $Co(III)$, $Cr(III)$, $Eu(III)$, $Fe(III)$, or $Cu(II)$ the product of lower valency is relatively stable and can be isolated. This has actually been carried out for $Eu^{+3} + e_{aq}^-$, where Eu^{+2} was identified as the primary product by pulse radiolysis (56). In the case of Zn^{+2} , Cd^{+2} , Mn^{+2} , Co^{+2} , and Ni^{+2} the corresponding M^+ ions have limited stability and can be detected only as transients. The spectra of Zn^+ , Mn^+ , Cd^+ , Co^+ , and Ni^+ were determined by pulse radiolysis (1, 30). A transient was also observed in the $PtCl_4^{-2} + e_{aq}^-$ reaction (28). These transients were found to decay by second-order kinetics, suggesting a disproportionation reaction $M^+ + M^+ \rightarrow M^{+2} + M^0$. The existence of Zn^+ and Cd^+ was confirmed by electron spin resonance in irradiated ice (98). These transient ions live long enough to react with additives, which permit their chemical behavior to be examined. Zn^+ , Cd^+ , and Tl^0 were found to induce debromination of RBr (22), most probably by an electron transfer $Zn^+ + RBr \rightarrow R + Br^- + Zn^{+2}$ or alternatively by an atom transfer $Zn^+ + RBr \rightarrow RBrZn^+ \rightarrow R + ZnBr^+$. Interestingly enough, Cu^+ formed from $Cu^{+2} + e_{aq}^-$ was found to reduce organic radicals, probably by electron transfer (13), as well as to de-

halogenate very reactive alkyl halides (22). Since reagent Cu^+ does not participate in such reactions at the given rates, it must be concluded that Cu^+ formed in neutral solution at very low concentrations is in a reactive chemical form with a higher reduction potential than reagent Cu^+ .

Some of the transient metal ions may react with water to give hydrogen. The reaction of Mn^+ with water produces H_2 and not hydrogen atoms, implying a hydride transfer mechanism: $\text{Mn}(\text{H}_2\text{O})_n^+ + \text{H}_2\text{O} \rightarrow \text{Mn}(\text{OH})(\text{H}_2\text{O})_{n-1}^{+2} + \text{H}_2 + \text{OH}^-$ (14).

Aliphatic Compounds. Saturated hydrocarbons as well as alcohols, amines and ethers are unreactive toward e_{aq}^- , as are also their fluoro derivatives (43, 69, 10). This is not surprising since the elements of the first series when bound by σ bonds have no vacant orbital to accommodate an additional electron. Hydrocarbons cannot solvate electrons because of their low polarity, but alcohols and amines can be used in pure form as solvating media for electrons (12, 43, 45). If our hypothesis on the role of solvation of OH^- in the $e_{aq}^- + \text{H}_2\text{O}$ reaction is correct, it is expected that, if alcohols are purified to eliminate the last traces of electron scavengers, e_{sol}^- will survive in them much longer than in water, owing to the lower stability of alkoxy ions in alcohols. The same should be true of alkyl amines and diamines.

Olefins show some reactivity toward e_{aq}^- (for $e_{aq}^- + \text{CH}_2:\text{CH}_2$ $k = 7.6 \times 10^6 \text{ M}^{-1} \text{ sec.}^{-1}$) (28). Conjugated olefins are more reactive—e.g., $k_{e_{aq}^-} + \text{butadiene} = 2.4 \times 10^8 \text{ M}^{-1} \text{ sec.}^{-1}$ (68, 69). The accommodation of an electron on an olefin molecule may be looked on as analogous to the addition of a nucleophilic reagent (73). In the latter case, it has been shown that if the carbon is activated by electron withdrawing groups it can be directly attacked by nucleophiles. e_{aq}^- is probably the most efficient nucleophile, thus it may interact with a carbon atom adjacent to any double bond, provided this is not specially deactivated. Conjugation will obviously increase the chances of having the carbon positively polarized; thus, it will increase its reactivity toward e_{aq}^- . The same reasoning may be extended to the reactivity of e_{aq}^- with carbonyl carrying compounds. These were found to be fairly reactive, and the same reactivity was observed for aldehydes and ketones (after correction for the nonreactive hydrates) (68, 69). The carbon on a carbonyl is positively polarized and may be attacked by a powerful nucleophile like e_{aq}^- . If this carbon is deactivated by an electron donating group like an hydroxy, alkoxy, or amino group, its reactivity toward e_{aq}^- will be inhibited. The lower reactivity of acetic acid as compared with that of acetone ($k = 0.18 \times 10^9$ and $5.6 \times 10^9 \text{ M}^{-1} \text{ sec.}^{-1}$ respectively) (116, 11) is probably owing to the electron donating power of the hydroxy group. Acyl amides are also expected to exhibit a low reactivity as can be deduced from the relatively low reactivity of thiourea ($k = 2.9 \times 10^9 \text{ M}^{-1} \text{ sec.}^{-1}$) (69) as compared with that of acetone. The high reactivity of acrylamide (69) is due to conjugation. The effect of an alkoxy group on the electrophilic reactivity of the carbon of a carbonyl group can be demonstrated by the low reactivity of esters compared with aldehydes and ketones (69). The decrease in the positive character of the carbonyl carbon

owing to adjacent electronegative groups may account for the even lower reactivity of lactic (69), citric (122), and oxalic (69) acids as compared with acetic acid (121). Carboxylate ions are still less reactive toward e_{aq}^- (69). This is in accord with the fact that the carbon atom of the carboxylate is completely deactivated toward nucleophiles. When the carbonyl bond has added a water molecule, obviously there is no room for any further nucleophilic attack on the carbon. This explains the extremely low reactivity of formaldehyde toward e_{aq}^- (58).

The products of reaction of e_{aq}^- with olefins are carbanions which react with the solvent within less than 10^{-11} sec. (47) to give the corresponding hydrogen adducts $>C=C< + e_{aq}^- \rightarrow (>C=C<)^- + H^+ \rightarrow >C-CH<$. In the case of acetone, the adduct $(CH_3)_2CHO$ was observed spectrophotometrically by pulse radiolysis and was found to be identical to the radical obtained from isopropyl alcohol by hydrogen abstraction (60). $(CH_3)_2CO^-$ was also detected by electron spin resonance in ice (86). Kinetic analysis has shown that $(CH_3)_2CHO$ acts as an electron donor which induces the debromination of RBr (22). The products of the reactions of carboxylic acids and e_{aq}^- have been discussed previously.

Another group of aliphatic compounds which has been thoroughly investigated for their reactivity toward e_{aq}^- are the haloaliphatic compounds (10, 115). It has been found that the reactivity of these compounds increases in the order $Cl < Br < I$ (10). This indicates that e_{aq}^- interacts with the halogen atoms and not with the adjacent carbon, as the inductive effect on the carbon follows the opposite sequence. It was further shown that neighboring groups which increase the positive polarization of the halogen increase its reactivity toward e_{aq}^- (10). In other words, it may be assumed that e_{aq}^- is accommodated on the halogen forming RX^- , and that this process is favored by additional orbitals on the halogen and by the withdrawal of electrons through the inductive effect of neighboring groups. It was suggested that the effect of near-by groups is caused by their weakening of the $C-X$ bond which undergoes cleavage in the rate-determining step: $RX + e_{aq}^- \rightarrow R + X^-$ (93), RX^- being only an activated complex and not an intermediate. In deciding between the two theories, the reactivity of CF_3Cl was investigated. The $C-Cl$ bond in this compound is of comparable strength to that in CH_3Cl (35). On the other hand, the Cl atom is extremely positively polarized. It was found that CF_3Cl undergoes dechlorination by e_{aq}^- . From the effect of pH on the extent of dechlorination $k_{(e_{aq}^- + CF_3Cl)}$ was determined and found to be $1.5 \pm 0.5 \times 10^{10} M^{-1} sec^{-1}$ (21). Taking into consideration the short $C-F$ bond (1.3A) (116), this reaction may be considered to be diffusion controlled, like $e_{aq}^- + CCl_4$ or $CHCl_3$ (10). It proceeds, therefore, more than two orders of magnitude faster than the reaction with RCH_2Cl . This supports the mechanics of accommodating an electron on the halogen, forming RX^- as intermediate. This mechanism finds further support in the existence of CCl_4^- in the gas phase (110). RX^- undergoes very fast dissociation to $R + X^-$, which is facilitated by the hydration of the halide ion. It was shown

that e_{aq}^- quantitatively dehalogenates monochloroacetate (70) as well as α -bromopropionate (22), and it seems reasonable to assume that halide ions and R radicals are the only products of $e_{aq}^- + RX$ reactions.

Various other aliphatic compounds carrying different functional groups have been examined (21), but no systematic study was carried out to justify the discussion of the reaction mechanism.

Aromatic Compounds. The reactivity of aromatic compounds toward hydrated electrons has been extensively investigated (9, 68, 69, 115), and this group of organic compounds is the largest one for which a unified theory of reactivity could be developed. It has been shown that the reactivity of these compounds toward e_{aq}^- is a function of the electron density in the π orbitals of the aromatic rings, as expressed by Hammett's σ -function. This correlation was found to hold over four orders of magnitude of specific rates, from phenol which reacts at $4 \times 10^6 M^{-1} \text{ sec.}^{-1}$ up to nitrobenzene, with a rate constant of $3 \times 10^{10} M^{-1} \text{ sec.}^{-1}$, which is practically diffusion controlled (9). It is suggested that e_{aq}^- reacts with aromatic compounds as a most reactive nucleophile which attacks a positive center on the ring. The probability of formation of such a center is inversely proportional to the density of the π electrons, just as the probability of an electrophilic attack is directly proportional to it. A detailed discussion of these findings is found in (9). Iodine and bromine atoms were found to facilitate the absorption of the electron to a greater extent than warranted by their contribution to the π electron density in the ring. It is suggested that they act here as bridges for an electron transfer to the ring, just as they do in their role of ligands to a transition metal (11).

The primary product of the $e_{aq}^- + \text{aryl H}$ reaction is an aryl H^- ion. The fate of this ion is determined by the substituents. In the case of aryl iodides a quantitative deiodination has been observed: $\text{PhI} + e_{aq}^- \rightarrow \text{PhI}^- \rightarrow \text{Ph} + \text{I}^-$ (7). This pattern is likely to be true also of bromo and chloro derivatives, all of which are expected to decompose at a rate $>10^9 \text{ sec.}^{-1}$. It is also possible that these carbanions react with water to give cyclohexadienyl radicals which undergo subsequent elimination of HCl. The carbanions of nitro derivatives are stabilized by resonance and they may eventually dissociate to give a nitrite ion and a phenyl radical, or disproportionate to yield nitroso benzene. A long-lived transient product from trinitrophenol has been observed by pulse radiolysis (55). The carbanions of aromatic carboxylic acids are also stabilized by resonance and transients have been observed for benzoic (7), trimesic (55), and the phthalic acids (60). The fate of these transients is unknown, but no decarboxylation takes place as a result of the e_{aq}^- reaction (97). It is most likely that they react with water to give a cyclohexadienyl radical and a hydroxyl ion. These radicals may then undergo recombination or disproportionation. Polycyclic structures also stabilize the aromatic carbanions. Diphenylide, anthracenide and terphenylide ions were observed by pulse radiolysis (25, 118). These ions react with alcohols to give a hydrogen adduct and an alcoholate ion (25). Alpha and beta naphthols also produce a transient which can be detected by pulse radioly-

sis (7, 55). Another transient observed by pulse radiolysis is the benzophenone negative ion Ph_2CO^- (2).

To conclude this section we note that whereas a fair amount of information is available, on the reactivity of aromatic compounds toward e_{aq}^- , little is known about the products of these reactions.

Heterocyclic Compounds. A rather large number of heterocyclic compounds has been investigated for their reactivity toward e_{aq}^- (21, 68, 115). There is less basic information available on heterocyclic compounds as compared with the aromatic systems, thus it is much more difficult to derive correlations between the reactivity toward e_{aq}^- and certain other properties of these compounds.

It is evident that cyclization of a conjugated system by a hetero atom reduces its reactivity. Going from butadiene ($k = 8 \times 10^9 M^{-1} \text{sec.}^{-1}$) (68, 69) to furan ($k = 3.10^6 M^{-1} \text{sec.}^{-1}$) (115) there is a decrease of three orders of magnitude in reactivity. This may be caused by the reluctance of the oxygen to become positively polarized, which disturbs the conjugation (104), as well as to the inductive effect of the etheric oxygen which diminishes the positive character of the terminal carbon. The sulfur analog of furan, thiophene, shows a higher reactivity as expected ($k = 6.5 \times 10^7 M^{-1} \text{sec.}^{-1}$) (115). On the other hand, pyrrole, which is expected to show an intermediate reactivity between that of furan and thiophene, as far as its effect on conjugation is concerned, exhibits a significantly lower reactivity ($k = 6.0 \times 10^5 M^{-1} \text{sec.}^{-1}$) (115). This suggests that the inductive effect of the lone pair on the nitrogen is more pronounced than the inductive effect of the etheric oxygen.

The replacement of a carbon atom by a tertiary nitrogen, when going from pyrrole to imidazole, increases the reactivity by two orders of magnitude ($k = 3.7 \times 10^7 M^{-1} \text{sec.}^{-1}$) (115). The same effect of tertiary nitrogen is observed when comparing pyridine with benzene ($k = 1 \times 10^9$ and $1 \times 10^7 M^{-1} \text{sec.}^{-1}$, respectively) (68) and thiazole with thiophene ($k = 4.5 \times 10^9$ and $6.5 \times 10^7 M^{-1} \text{sec.}^{-1}$ respectively) (115). It may be suggested that the $>\text{C}=\text{N}-$ bond is polarized in a way similar to that of the carbonyl bond, and the carbon is therefore a far better electrophilic center than in a $>\text{C}=\text{C}<$ bond. In other words, whereas a heteroatom adjacent to a $\text{C}=\text{C}$ double bond tends to deactivate the carbon as electrophile, the presence of a heteroatom as part of a double bond accentuates the positive character of the carbon. The deactivating action of an $>\text{NH}$ group when in a heterocyclic structure can be demonstrated again when comparing the reactivities of styrene and indole (1.1×10^{10} and $7 \times 10^8 M^{-1} \text{sec.}^{-1}$ respectively) (69). The electron donating power of the $>\text{NH}$ group in indole is large enough to deactivate two $\text{C}=\text{C}$ systems; thus indole has the same reactivity as expected for *o*-amino benzoic acid (9).

When going to more complex heterocyclic compounds—e.g., purines and pyrimidines, one sees that the effect of the $-\text{N}=\text{C}<$ system is most pronounced and that all these compounds are highly reactive toward e_{aq}^- ($k > 10^{10} M^{-1} \text{sec.}^{-1}$) (68). Like in the case of the carbonyl group the $\text{C}=\text{N}-$ group is deactivated by electron donating groups bound to

the carbon. The deactivating action of OH groups adjacent to the C=N bond is demonstrated in the case of uric acid when compared with purine (69).

The products incorporating an electron into heterocyclic systems have not been investigated. Transients have been observed by pulse radiolysis in the cases of adenine, purine, and cytosine (55).

Concluding Remarks

One may look upon the research into e_{aq}^- reactions from two standpoints. One is the standpoint of the radiation chemist or radiation biochemist who is interested in the radiolytic damage caused by e_{aq}^- as compared with other radiolytic species. The other is the approach of the chemist who may use the reactivity of e_{aq}^- to investigate the electronic structure of chemical species and test the theories on the role of electron transfer in chemical reactions. The species e_{aq}^- is important to the chemist from still another angle: being the purest and simplest reducing agent it may be used to produce reduced chemical species, some of them only as short-lived transients, which have never before been synthesized.

As far as the radiation chemist is concerned there is today more quantitative information available on the reactivity of different substrates with e_{aq}^- than there is on any other radiation-induced process. With this information in hand one can predict the radiolytic behavior of a large variety of solute systems in aqueous solution. Since one of the major objectives of radiation chemistry is to provide clues for the understanding of radio-biological processes, this goal is achieved by the quantitative study of the reaction of the primary products of radiolysis with different substrates. This information may allow us to predict the behavior of more complicated biochemical systems. It has been shown, for instance, that the reactivity of certain components in biochemical systems—e.g., purines and pyrimidines is orders of magnitude higher than that of other components in the system. Thus, these compounds are liable to undergo much more extensive radiolytic damage. The reactivity of transition metals in complexed form also has interesting radiobiological implications, as these may sensitize or deactivate various biochemical systems to radiolytic damage. Even the reactivities of simple compounds like O_2 and CO_2 have important radiobiological implications.

In comparison with the abundant information on the reactivity of different compounds toward e_{aq}^- , there is a lack of information on the products of these reactions. It has been shown throughout this review that some of these products are extremely reactive oxidizing or reducing agents. The formation of such products may occasionally reverse the radiolytic damage or sometimes enhance it. The characterization of the reactive intermediates formed from solutes is the major task of radiation chemistry of aqueous solutions in the coming decade. Pulse radiolysis is the most appropriate tool for this type of investigation.

As far as general chemistry is concerned, it has been shown that the reactivity of different chemical species toward e_{aq}^- is a function of the

availability of a vacant orbital on the substrates as well as of the gain in free energy on incorporation of an additional electron. A more quantitative approach might confirm the following reasoning. The reactions of e_{aq}^- with organic and inorganic reactants may be considered as a limiting case of nucleophilic substitution $A + BC \rightarrow ABC^\ddagger \rightarrow AB + C$; $e_{aq}^- + BC \rightarrow BC^-$. BC^- is formed here as an intermediate rather than a transition state, owing to the ease of incorporation of an electron into any vacant orbital of BC , compared with the formation of a definite chemical bond with an atom A . At first sight it would appear that the rate-determining step here involves the electronic rearrangements in BC which allow the incorporation of an electron into its orbital. However, since both processes, the internal electronic rearrangements in BC and the incorporation of the electron into it, should take place within $<10^{-14}$ sec., like any allowed electronic transition, one has to explain the measured rates of the e_{aq}^- reactions in terms of pre-equilibria. In other words, it is assumed that BC is in dynamic equilibrium with BC' and BC' always reacts with e_{aq}^- at a diffusion-controlled rate. Consequently, the rate of e_{aq}^- reactions is a measure of the equilibrium constant $K = BC'/BC$ which obviously depends on the distribution of electrons within the molecule, including all resonating electronic configurations. (Following this argument one has to drop the idea of polarization of the substrate molecule by e_{aq}^- (10), as the e_{aq}^- - BC interaction is not rate determining.) In other words, the reactivity of a compound toward e_{aq}^- is a quantitative measure of the molecular electronic arrangements in the molecule which allow the addition of an external electron into a vacant orbital.

If the rate of e_{aq}^- reactions, which are not diffusion controlled, is determined by a pre-equilibrium, the temperature dependence of these reactions should involve the ΔE of the latter. As this equilibrium involves primarily electronic rearrangements, it is expected to have a rather small temperature coefficient. Moreover, it is likely that an increase in temperature will decrease the probability of localization of a vacant orbital. These assumptions have been corroborated by showing that the activation energy of the $e_{aq}^- +$ phenylacetate ($k = 1.4 \times 10^7 M^{-1} \text{sec.}^{-1}$ at 25°C.) is less than 2.5 kcal./mole (22)—i.e., less than that of a diffusion-controlled reaction (122).

The studies of e_{aq}^- reactivity have shown results consistent with the accepted theories on atomic and molecular structure and on chemical reactivity. In the years to come, it is hoped that confidence in the e_{aq}^- reaction as a diagnostic tool in the methodology of chemistry will grow and e_{aq}^- will become a common reagent in the laboratories of both the inorganic and the organic chemists.

Literature Cited

- (1) Adams, G. E., Baxendale, J. H., Boag, J. W., *Proc. Chem. Soc.* **1963**, 241.
- (2) Adams, G. E., Baxendale, J. H., Boag, J. W., *Proc. Roy. Soc. A* **277**, 549 (1964).
- (3) Adams, G. E., Hart, E. J., *J. Am. Chem. Soc.* **84**, 3994 (1962).
- (4) Allan, J. T., Beck, C. M., *J. Am. Chem. Soc.* **86**, 1483 (1964).

- (5) Allan, J. T., Getoff, N., Lehmann, P., Nixon, K., Scholes, G., Simic, M., *J. Inorg. Nucl. Chem.* **19**, 204 (1961).
- (6) Allan, J. T., Robinson, M. G., Scholes, G., *Proc. Chem. Soc.* **1962**, 381.
- (7) Anbar, M., unpublished result.
- (8) Anbar, M., Guttman, S., Stein, G., *J. Chem. Phys.* **34**, 703 (1961).
- (9) Anbar, M., Hart, E. J., *J. Am. Chem. Soc.* **86**, 5633 (1964).
- (10) Anbar, M., Hart, E. J., *J. Phys. Chem.* **69**, 271 (1965).
- (11) Anbar, M., Hart, E. J., *J. Phys. Chem.* **69**, 973 (1965).
- (12) Anbar, M., Hart, E. J., *J. Phys. Chem.* **69**, 1244 (1965).
- (13) Anbar, M., Levitzki, A., *Radiation Res.*, in press.
- (14) Anbar, M., Meyerstein, D., *Proc. Chem. Soc.*, **1963**, 23.
- (15) Anbar, M., Meyerstein, D., *J. Phys. Chem.* **68**, 1713 (1964).
- (16) Anbar, M., Meyerstein, D., *J. Phys. Chem.* **69**, 698 (1965).
- (17) Anbar, M., Meyerstein, D., *Nature* **206**, 825 (1965).
- (18) Anbar, M., Meyerstein, D., Neta, P., *J. Phys. Chem.* **68**, 2967 (1964).
- (19) Anbar, M., Meyerstein, D., Neta, P., to be published.
- (20) Anbar, M., Munoz, R. A., Rona, P., *J. Phys. Chem.* **67**, 2708 (1963).
- (21) Anbar, M., Neta, P., *Int. J. Appl. Rad. and Isotopes* **16**, 227 (1965).
- (22) Anbar, M., Neta, P., to be published.
- (23) Anbar, M., Taube, H., to be published.
- (24) Anbar, M., Thomas, J. K., *J. Phys. Chem.* **68**, 3829 (1964).
- (25) Arai, S., Dorfman, L. M., *J. Chem. Phys.* **41**, 2190 (1964).
- (26) Baxendale, J. H., *Radiation Res. Suppl.* **4**, 139 (1964).
- (27) Baxendale, J. H., *Radiation Res. Suppl.* **4**, 114 (1964).
- (28) Baxendale, J. H., *et al.*, *Nature* **401**, 468 (1964).
- (29) Baxendale, J. H., Dixon, R. S., *Proc. Chem. Soc.* **1963**, 148.
- (30) Baxendale, J. H., Fielden, E. M., Keene, J. P., *Proc. Chem. Soc.* **1963**, 242.
- (31) Bell, R. P., "The Proton in Chemistry," Chapter 6, Cornell University Press, Ithaca, 1959.
- (32) Benson, S. W., "The Foundations of Chemical Kinetics," McGraw-Hill, New York, 1960.
- (33) Brown, D. M., Dainton, F. S., Keene, J. P., Walker, D. C., *Proc. Chem. Soc.* **1964**, 266.
- (34) Collinson, E., Dainton, F. S., Smith, D. R., Tazuke, S., *Proc. Chem. Soc.* **1962**, 140.
- (35) Cottrell, T. L., "The Strengths of Chemical Bonds," Butterworths, London 1958.
- (36) Coyle, J. P., Dainton, F. S., Logan, S. R., *Proc. Chem. Soc.* **1964**, 219.
- (37) Czapski, G., Schwarz, H. A., *J. Phys. Chem.* **66**, 471 (1962).
- (38) Dainton, F. S., *Discuss. Faraday Soc.* **36**, 300 (1963).
- (39) Dainton, F. S., *Radiation Res. Suppl.* **4**, 71 (1964).
- (40) Dainton, F. S., Peterson, D. B., *Proc. Roy. Soc. A* **267**, 443 (1962).
- (41) Debye, P., *Trans. Electrochem. Soc.* **82**, 265 (1942).
- (42) Dewald, R. R., Dye, J. L., *J. Phys. Chem.* **68**, 121 (1964).
- (43) Dewald, R. R., Dye, J. L., Eigen, M., de Maeyer, L., *J. Chem. Phys.* **39**, 2388 (1963).
- (44) Dorfman, L. M., *Science*, **141**, 493 (1963).
- (45) Dorfman, L. M., Matheson, M. S., in "Progress in Chem. Kinetics," G. Porter, ed., Vol. III, Pergamon Press, London 1965.
- (46) Dorfman, L. M., Taub, I. A., *J. Am. Chem. Soc.* **85**, 2370 (1963).
- (47) Eigen, M., Kruse, W., Maass, G., de Maeyer, L., "Progress in Reaction Kinetics," G. Porter, ed., Vol. II, Pergamon Press, London, 1964.
- (48) von Engel, E., "Ionized Gases," Chapter 6, Oxford University Press, 1955.
- (49) Field, F. H., Franklin, J. L., "Electron Impact Phenomena," Chapter 4, Academic Press, New York, 1957.
- (50) Fricke, H., Hart, E. J., Smith, H. P., *J. Chem. Phys.* **6**, 229 (1938).
- (51) Frost, D. C., McDowell, C. A., "Adv. in Mass Spectrometry," J. D. Waldron, ed., Vol. I, Pergamon Press, 1959.
- (52) Garrison, W. M., *Radiation Res. Suppl.* **4**, 158 (1964).
- (53) Gold, V., *Trans. Faraday Soc.* **56**, 255 (1960).
- (54) Gold, V., *Proc. Chem. Soc.* **1963**, 141.
- (55) Gordon, S., *Radiation Res. Suppl.* **4**, 21 (1964).
- (56) Gordon, S., private communication.
- (57) Gordon, S., Hart, E. J., (to be published) as reported by M. S. Matheson and J. Rabani (96).

- (58) Gordon, S., Hart, E. J., Matheson, M. S., Rabani, J., Thomas, J. K., *Disc. Faraday Soc.* **36**, 193 (1963).
- (59) Gordon, S., Hart, E. J., Matheson, M. S., Rabani, J., Thomas, J. K., *J. Am. Chem. Soc.* **85**, 1375 (1963).
- (60) Gordon, S., Hart, E. J., Thomas, J. K., *J. Phys. Chem.* **68**, 1262 (1964).
- (61) Grossweiner, L. I., Swenson, G. W., Zwicker, E. F., *Science* **141**, 1042 (1963).
- (62) Grossweiner, L. I., Zwicker, E. F., Swenson, G. W., *Science* **141**, 1180 (1963).
- (63) Hart, E. J., *Radiation Res. Suppl.* **4**, 87 (1964).
- (64) Hart, E. J., *Science* **146**, 19 (1964).
- (65) Hart, E. J., private communication.
- (66) Hart, E. J., Boag, J. W., *J. Am. Chem. Soc.* **84**, 4090 (1962).
- (67) Hart, E. J., Gordon, S., Fielden, E. M., to be published.
- (68) Hart, E. J., Gordon, S., Thomas, J. K., *J. Phys. Chem.* **68**, 1271 (1964).
- (69) Hart, E. J., Thomas, J. K., Gordon, S., *Radiation Res. Suppl.* **4**, 79 (1964).
- (70) Hayon, E., Allen, A. O., *J. Phys. Chem.* **65**, 2181 (1961).
- (71) Hendriksen, T., *Radiation Res.* **23**, 63 (1964).
- (72) Hickam, W. M., Berg, D., "Adv. in Mass Spectrometry," Vol. I, Pergamon Press, 1959.
- (73) Hine, J., "Physical Organic Chemistry," 2nd ed., McGraw-Hill, New York, 1962.
- (74) Husain, A., Hart, E. J., *J. Am. Chem. Soc.* **87**, 1180 (1965).
- (75) Hutchinson, F., *Radiation Res. Suppl.* **4**, 137 (1964).
- (76) Jolly, W. L., *Progress in Inorg. Chemistry* **1**, 235 (1959).
- (77) Jortner, J., *Radiation Res. Suppl.* **4**, 24 (1964).
- (78) Jortner, J., *Radiation Res. Suppl.* **4**, 110 (1964).
- (79) Jortner, J., Ottolenghi, M., Rabani, J., Stein, G., *J. Chem. Phys.* **37**, 2488 (1962).
- (80) Jortner, J., Ottolenghi, M., Stein, G., *J. Phys. Chem.* **66**, 2029 (1962).
- (81) Jortner, J., Rabani, J., *J. Am. Chem. Soc.* **83**, 4368 (1961).
- (82) Jortner, J., Rabani, J., *J. Phys. Chem.* **66**, 2081 (1962).
- (83) Keene, J. P., *Nature* **197**, 47 (1963).
- (84) Keene, J. P., *Radiation Res.* **22**, 1 (1964).
- (85) Kevan, L., *J. Am. Chem. Soc.* **87**, 1481 (1965).
- (86) Kevan, L., Moorthy, P. N., Weiss, J. J., *J. Am. Chem. Soc.* **86**, 771 (1964).
- (87) Laidler, K. J., "The Chemical Kinetics of Excited States," Chapter 4, Oxford University Press, 1955.
- (88) Latimer, W. M., "Oxidation Potentials," 2nd ed., Prentice Hall, New York, 1952.
- (89) Lefort, M., Tarrago, X., *J. Inorg. Nucl. Chem.* **16**, 169 (1961).
- (90) Lind, S. C., "Radiation Chemistry of Gases," Reinhold, New York, 1961.
- (91) Magee, J. L., *Radiation Res. Suppl.* **4**, 20 (1964).
- (92) Matheson, M. S., *Radiation Res. Suppl.* **4**, 1 (1964).
- (93) Matheson, M. S., private communication.
- (94) Matheson, M. S., Mulac, W. A., Rabani, J., *J. Phys. Chem.* **67**, 2613 (1963).
- (95) Matheson, M. S., Rabani, J., *Radiation Res.* **19**, 180 (1963).
- (96) Matheson, M. S., Rabani, J., *J. Phys. Chem.* **69**, 1324 (1965).
- (97) Matthew, R. W., Sangster, D. F., to be published.
- (98) Moorthy, P. N., Weiss, J. J., *Nature* **201**, 1317 (1964).
- (99) Nehari, S., Rabani, J., *J. Phys. Chem.* **67**, 1609 (1963).
- (100) Neta, P., Thesis, Rehovoth, 1965.
- (101) Noyes, R. M., *J. Am. Chem. Soc.* **79**, 551 (1957).
- (102) Orgel, L. E., "An Introduction to Transition Metal Chemistry," Chapter 3, Methuen, London, 1960.
- (103) Parlee, E. L., *J. Am. Chem. Soc.* **81**, 263 (1959).
- (104) Pauling, L., "The Nature of the Chemical Bond," 3rd ed., Cornell Univ. Press, Ithaca, 1960.
- (105) Pikaev, A. K., Glazunov, P. Ya., Spitsyn, V. I., *Doklady Akad. Nauk USSR* **151**, 1387 (1963).
- (106) Platzman, R. L., *Basic Mechanisms in Radiobiology*, Natl. Res. Council Publ. **305**, 34 (1953).
- (107) Porter, G., in "Investigation of rates and mechanisms of reactions," S. L. Friess, E. S. Lewis and A. Weissberger, eds., 2nd ed., p. 1055, Interscience, New York, 1963.

- (108) Rabani, J., *J. Am. Chem. Soc.* **84**, 868 (1962).
(109) Rabani, J., Mulac, W. A., Matheson, M. S., *J. Phys. Chem.* **69**, 53 (1965).
(110) Reed, R. I., "Ion Production by Electron Impact," Academic Press, New York, 1962.
(111) Scholes, G., Simic, M., *J. Phys. Chem.* **68**, 1731 (1964).
(112) Scholes, G., Simic, M., Weiss, J. J., *Disc. Faraday Soc.* **36**, 214 (1963).
(113) Schwarz, H. A., *Radiation Res. Suppl.* **4**, 89 (1964).
(114) Sworski, T. J., *J. Am. Chem. Soc.* **86**, 5034 (1964).
(115) Szutka, A., Thomas, J. K., Gordon, S., Hart, E. J., *J. Phys. Chem.* **69**, 289 (1965).
(116) "Tables of Intramolecular Distances," L. E. Sutton, ed., Spec. Publ. **11**, The Chemical Society, London, 1958.
(117) Taub, I. A., Harter, D. A., Sauer, M. C., Dorfman, L. M., *J. Chem. Phys.* **41**, 979 (1964).
(118) Taub, I. A., Sauer, M. C., Dorfman, L. M., *Disc. Faraday Soc.* **36**, 206 (1963).
(119) Thomas, J. K., *Radiation Res. Suppl.* **4**, 87 (1964).
(120) Thomas, J. K., *Radiation Res. Suppl.* **4**, 113 (1964).
(121) Thomas, J. K., *Radiation Res. Suppl.* **4**, 151 (1964).
(122) Thomas, J. K., Gordon, S., Hart, E. J., *J. Phys. Chem.* **68**, 1524 (1964).
(123) Weiss, J., *Nature* **186**, 751 (1960).
(124) Weiss, J. J., *Nature* **199**, 589 (1963).
(125) Weiss, J. J., *Radiation Res. Suppl.* **4**, 141 (1964).
(126) Weiss, J. J., *Radiation Res. Suppl.* **4**, 150 (1964).
(127) Wells, A. F. "Structural Inorganic Chemistry," 3rd ed., p. 624, Oxford Univ. Press, 1962.

RECEIVED May 5, 1965.

Electrical Transport Properties of Metal-Ammonia and Metal-Amine Solutions

DONALD S. BERNIS

Division of Laboratories and Research, New York State Department of Health and Department of Biochemistry, Albany Medical College, Albany, N. Y.

The electrical transport properties of alkali metals dissolved in ammonia and primary amines in many ways resemble the properties of simple electrolytes except that the anionic species is apparently the solvated electron. The electrical conductance, the transference number, the temperature coefficient of conductance, and the thermoelectric effect all reflect the presence of the solvated electron species. Whenever possible the detailed nature of the interactions of the solvated electrons with solvent and solute species is interpreted by mass action expressions.

The properties of electrolyte solutions have presented an intriguing problem ever since they were first explored by Faraday over a century ago. Electrolytes are distinguished from molecular compounds in solution by the fact that the compounds dissociate into atoms or groups of atoms bearing electrical charges, termed ions. These ions possess properties that permit us, by means of an external field, literally to reach into the solution and move them about, and in that way learn something about their interactions. In part, the origins of physical chemistry rest with the early investigation of the conductance of electrolyte solutions. Similarly, the origins of the studies of solvated electrons or metals in amine solvents lie in the precise electrical transport experiments begun over 50 years ago by Kraus (24). Kraus' early experiments and subsequent interpretation made it quite clear that, in solutions of alkali and alkaline earth metals in ammonia and the amines, one ionic species, the cation, is a metal ion, and the anionic species is some form of solvated electron. More sophisticated experimental techniques have greatly added to our knowledge of solvated electron properties; however, it is

still worthwhile to glean information from low field conductivity, transference number, and Wien effect experiments. From these experiments one may learn something about the interactions of the electron with the solvent and the rest of the solute species.

In attempting to clarify most of the electrical transport experiments, a dilemma arises that may be considered inherent in the properties of these solutions. Metal-ammonia and metal-amine solutions in the dilute concentration region exhibit quasi-electrolyte behavior. This is advantageous in applying much of current electrolyte theory to explain the behavior of these systems and, therefore, we apply the current mechanisms of electrolyte solutions to our treatment of metal-ammonia solutions. The ideal behavior of dilute electrolyte solutions, namely the interaction of the ionic species, is generally explained by using the Debye-Hückle theory. The deviation from ideal behavior by the properties of a dilute electrolyte solution is generally attributed to the association of ions into pairs or larger clusters. The definition of an ion pair or higher cluster, or for that matter the tacit assumption that these species exist, can tend to restrict the interpretation of the transport properties of the solutions. In our discussion we shall knowingly step into this trap at some times because we believe that the proposed complex is realistic and at other times because the author's ideas on this subject are not sufficiently sophisticated to propose a convincing alternative. The question should be kept in mind, however, whether ion pairs and other association complexes exist or whether the observed results can be explained on the basis of interactions without using complexes. Both methods should be considered (17).

Conductance

The equivalent conductance *vs.* concentration curve in the dilute region for salts (binary electrolytes) is quite similar to that for the alkali metals in ammonia and amine solvents in the dilute region. For example, if we examine the data below 10^{-2} *N* for solution of sodium in NH_3 , potassium in ethylenediamine, lithium in methylamine, and at the same time solutions of KNO_3 in NH_3 and KNO_3 in H_2O , we may begin to understand the similar behavior of solutions of the salts and metals. A plot of Λ/Λ_0 is particularly revealing for making this comparison (Figure 1). The behavior of all of these solutions is somewhat analogous. Certainly the equivalent conductance of each is significantly different (Table I) owing to the differences in anionic transport species and in viscosity of the solvents as a result of temperature and type. The Λ/Λ_0 behavior for salts and metals in the several solvents is, however, quite similar. A more accurate comparison of limiting conductance may be made by using the Walden product $\lambda_0^{+\eta}$ for the cationic species involved. This is not a straightforward calculation and requires some gross assumptions. At present we can only compare $\Lambda_0\eta_0$ for metallic species from solvent to solvent. Even the reported conductance studies of Cafasso and Sundheim (5) for potassium in 1,2-dimethoxyethane are apparently comparable

to the lithium in the CH_3NH_2 system. However, the work is on saturated solutions, and the system is reported to be diamagnetic, arousing interesting speculation concerning the conduction process. Further investigation of this type of system is necessary.

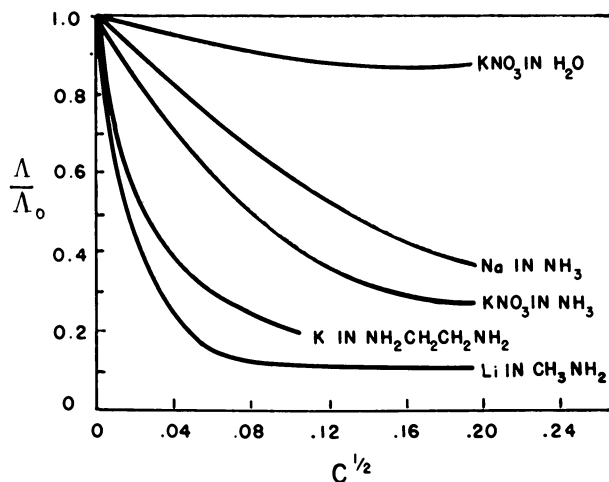


Figure 1. Δ/Δ_0 as a function of $C^{1/2}$. A comparison of the behavior of alkali metals in amine solvents with the behavior of salts in aqueous and nonaqueous systems. KNO_3 in H_2O and in NH_3 (48); sodium in NH_3 (15); potassium in $\text{NH}_2\text{CH}_2\text{CH}_2\text{NH}_2$ (11); lithium in CH_3NH_2 (3).

Table I. Mass Action Constants and Conductivity Data

Metal or Salt	Solvent	Λ_0	K_1	K_2	Λ_{070}	References
Na	NH_3 (-33°)	1022	7.23×10^{-3}	27.0	2.61	(15)
	NH_3 (-37°) ^a		9.2×10^{-3}	18.5		
	NH_3 (-37°) ^b		9.6×10^{-3}	23.0		
Li	CH_3NH_2 (-78°)	228	5.5×10^{-5}	5.42	2.07	(3)
Li	NH_3 (-72°)	555	1.28×10^{-3}	4.33	2.8	(34)
K	$\text{NH}_2\text{CH}_2\text{CH}_2\text{NH}_2$	139 ^c	1.54×10^{-4}		2.14	(11)
Rb	$\text{NH}_2\text{CH}_2\text{CH}_2\text{NH}_2$	117 ^c	1.69×10^{-4}		1.80	(11)
Cs	$\text{NH}_2\text{CH}_2\text{CH}_2\text{NH}_2$	204 ^c	1.44×10^{-4}		3.14	(11)
KNO_3	NH_3 (-40°)	331				(48)
KCl	NH_3 (-33°)	348	8.7×10^{-4}			(19)
NaBr	NH_3 (-33°)	314	2.9×10^{-3}			(19)
KNO_3	H_2O (25°)	145				(48)

^a Transference data

^b Activity data

^c Room temperature

The general shape of the equivalent conductance *vs.* concentration plot for metal-ammonia solutions is shown by the behavior of sodium in NH_3 at -33°C . in Figure 2. The conductance behavior of metal-ammonia solutions is quite analogous to the behavior of electrolytes in solvents of low dielectric constant. The dilute region equivalent conductance decreases with increasing concentration, eventually goes

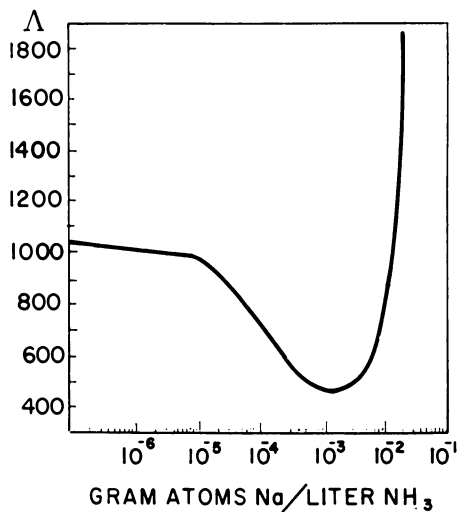


Figure 2. Equivalent conductance as a function of concentration for sodium in NH_3 at -34° from the data of Kraus (26, 30).

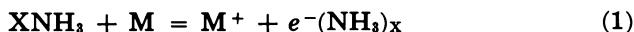
through a minimum, and begins to increase (22, 29). The large, almost exponential increase in conductivity observed in the concentrated metal-ammonia solutions is peculiar to these solutions and is caused by the appearance of essentially metallic conduction properties. Both metal-ammonia and amine solutions and simple electrolyte solution conductance properties in the dilute region can be analyzed by comparing the experimental slope to that predicted from the Onsager-Debye-Hückle equation. All the experimental curves for those metal-ammonia and metal-amine systems investigated lie between the slopes predicted for 1-1 and 1-2 electrolytes. Such behavior is generally interpreted in terms of electrostatic interactions leading to the formation of uncharged, nonconducting species—ion pairs. The appearance of the conductance minimum in simple electrolyte systems has been explained by Kraus and Fuoss (29) in terms of charged ion triplets. The competition for removal of charged species by ion pair formation and the appearance of other charged species from ion triplet formation are used to explain the appearance of the conductance minimum. In metal-ammonia solutions the appearance of the conductance minimum has been explained in terms of competition between the metal ion-electron interaction which removes conducting species and the onset of metallic type behavior. The formation of higher aggregates that conduct can also be invoked. Sukhotin (50) and Kenausis, Evers, and Kraus (22) have each contributed information for electrolyte solutions that seriously questions the ion triplet interpretation of Kraus and Fuoss (29). Evers and co-workers suggest that under normal circumstances in the dilute concentration region the energy of the Coulombic interaction of anion and cation in forming an ion pair is sufficiently

greater than the energy supplied by solvent collisions with the ion pair; hence, the relative stability of the ion pair. If an ion pair happens to lie in the field of an ion, it may be dissociated by the thermal impact of a molecule whose energy is less than that required in the absence of a field. Both ions of the pair are acted upon by a force of the same order of magnitude but of opposite direction, and the Coulombic force holding them together is reduced. This effect may be viewed in somewhat the same way as the Wien effect (52) when an external field is applied to an electrolyte system. Wien has shown that when an external field is applied to a solution of a partially associated electrolyte, the degree of association decreases with an increasing field. The dissociation of ion pairs in the field of ions has been aptly termed the "microscopic Wien effect of the ion fields." The frequency of this effect necessarily increases with, and is roughly proportional to, the concentration of ion pairs and free ions, and thus would be properly considered in the concentration region of the observed conductance minimum in electrolyte systems. The suggestion of a "microscopic Wien effect" in explaining the conductance minimum in metal-ammonia solutions is a very inviting speculation. The effect could indeed be more pronounced in these systems. Further investigation along this line is certainly worth pursuing since it is an appealing physical explanation which may be useful in explaining other phenomena in the concentration region where it is applicable (14).

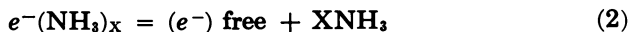
The deviations of experimental slopes for dilute solutions of metal-ammonia and metal-amine conductance plots from the limiting Onsager slope can be used conveniently to calculate association constants for the postulated, nonconducting species responsible for the deviations. Precise association constants of sufficient magnitude may be taken somewhat as confirming the probable existence of the postulated complexes.

Heavy reliance on precise association constants calculated from this type of interpretation can be dangerous as indicated by the recent work of Kay and Dye (21) in simpler systems. Indeed, interactions not accounted for in the conventional Debye-Hückle sense are indicated; however, chemical complexes are not to be taken as a unique interpretation.

Analyzing the conductance data for sodium in NH_3 solutions led to the original mass action equilibria postulate of Kraus (27). It was originally proposed that metal in NH_3 solutions behave as weak electrolytes or ionogens, producing metal ions and solvated electrons in accord with the equation

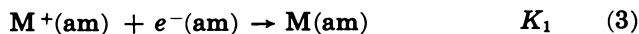


To explain the properties of more concentrated solutions it was suggested that solvated electrons were released to form electrons essentially free in the metallic sense.



More sophisticated extensions of the original Kraus theory are numerous and are dealt with in other chapters. Another equilibrium is necessary to

explain the magnetic properties that in more concentrated solutions indicate the presence of diamagnetic species. One can represent the two necessary equations agreed upon by most theories as



with no further comment as to the fine structure of the species. We are concerned merely with the evidence from electrical transport experiments that such postulated equilibria are indeed feasible.

Assuming that electrolyte theory is applicable to metal solutions permits the calculation of the equilibrium constants K_1 and K_2 from the conductance data. It is also instructive to evaluate the mass action constants K_1 , for salts in NH_3 and in amines for purposes of comparison (Table I). For NaCl (28) in NH_3 , $K_1 = 1.45 \times 10^{-3}$ as compared to 7.23×10^{-3} for sodium in NH_3 (15). For tetra-*n*-butylammonium picrate in methylamine (16) at -78°C ., $K_1 \sim 8 \times 10^{-5}$ compared to $K_1 = 5.8 \times 10^{-5}$ for lithium in CH_3NH_2 at -78°C . (3). Note that in both cases the constants for salts and metals are of the same order of magnitude. This is apparent support for applying the same mechanism in both systems, namely, ion association. The applicability of electrolyte theory to metal solutions should be considered in light of the evidence that electron conduction in these solutions probably does not proceed by what may be called classical ion transport. We may refer to the solvated electron as possessing an excess mobility over that of ordinary ion transport. Many mechanisms have been invoked with a tunneling mechanism most favored. For our purposes (to be compatible with electrolyte theory) we may hope that, in the concentration region under consideration, the conduction mechanism remains essentially unchanged with changing concentration; consequently, a mobility decrease with increasing concentration will be experienced by the electron largely owing to the interaction with metal ions in accord with the Onsager equation. One can gather support for this proposal from the fact that Onsager's equation may be used in connection with aqueous solutions of acids, where the protons probably migrate by a "Grotthus" mechanism. Further support is found in the fact that the Walden product $\Lambda_0\eta_0$ for sodium in NH_3 solution at -34°C ., 2.6 is very close to that obtained with solutions of lithium in methylamine at -78°C . (3). Longo (34) and Evers indicate for the lithium in NH_3 system, at -71°C ., $\Lambda_0\eta_0 = 2.8$. Recent work of Dye and Dewald (11) on metals in ethylenediamine reports the apparent $\Lambda_0\eta_0$ values for these systems are in the region of 1.80 - 3.0; Dye and Dewald believe (11) the amine systems differ significantly in the prevalence of stable species from the NH_3 solutions. It is thus interesting that the $\Lambda_0\eta_0$ values agree with those from NH_3 solutions. The close correlation of Walden products in all of the systems (Table I) does seem to support the suggestion that the conductance depends on viscosity. This would indeed permit interpretation on a classical electrolyte basis.

The two mass action equilibria previously indicated have been used in conjunction with a modified form of the Shedlovsky conductance function to analyze the data in each of the cases listed in Table I. Where the data were precise enough, both K_2 and K_1 were calculated. As mentioned previously, the K_1 's so evaluated are practically the same as those obtained for ion pairing in solutions of electrolytes in ammonia and amines. This is encouraging since it implies a fairly normal behavior (in the electrolyte sense) for dilute solutions of metals. Further support of the proposed mass action equilibria can be found in the conductance measurements of sodium in NH_3 solutions with added salt. Berns, Lepoutre, Bockelman, and Patterson (4) assumed an additional equilibrium between sodium and chloride ions, associated to form NaCl , to compute the concentration of ionic species, monomers, and dimers when the common ion electrolyte is added. Calculated concentrations of conducting species are employed in the Onsager-Kim extension of the conductance theory for low-field conductance of a mixture of ions. Values of $[\text{Na}]_{\text{total}}$ ranging from 5×10^{-4} to 6×10^{-2} and of the ratio of NaCl to $[\text{Na}]_{\text{total}}$ ranging from zero to 28.5 are included in the calculations.

Panson and Evers (37) have reported measurements of the effect of temperature on the conductance of lithium in methylamine, and Naiditch (36) has recently reported similar measurements for sodium in NH_3 solutions at elevated temperatures. Phenomenologically, these results are quite similar to those observed for solutions of normal electrolytes. Maxima are observed in conductance-temperature curves for the more dilute solutions. In the case of conventional electrolytes, maxima such as these may be interpreted as being caused by enhanced ion interaction induced by a lowering of the dielectric constant. With completely dissociated electrolytes the conductance change parallels the change in fluidity of the solvent medium, conductance increasing with increasing temperature. In the higher concentration regions with salts such as aqueous KCl , the temperature coefficient of conductance is high but decreases with increasing temperature. In principle at least, in all solvents, regardless of dielectric constant, if the temperature is raised sufficiently high, the conductance reaches a maximum value, then decreases. This decrease in conductance with increasing temperature is generally taken as direct evidence that the conducting species is removed through ion association as a result of a decrease in dielectric constant of the solvent medium. For example, with aqueous KCl at concentrations between $0.1N$ and $3.0N$ the maximum appears around 300°C . At $0.002N$ there is no maximum up to 306°C . The lower the concentration, the higher is the temperature of the maximum. This is to be expected since ion interaction becomes less significant at lower concentrations and disappears at infinite dilution. In nonaqueous media of intermediate dielectric constant the maxima become more accessible at lower temperatures and lower concentrations. For example, a $0.03N$ KI solution in NH_3 exhibits a maximum at 10°C .; in methylamine this is found at -45°C . The effect does become more complex with solvents like methylamine. For the lithium in methylamine the maximum occurs at -20°C . at $0.005N$;

at 0.02*N* the maximum has moved to -5°C . The trend apparently continues. One postulates that conducting species are being removed through mass action effects as the temperature is being raised.

Changes in properties of the solvated electron in the metal-ammonia and metal-amine systems are indicated by changes in the temperature coefficient of resistance of these solutions when examined as a function of concentration. Kraus and Lucasse (31, 32) and others have reported for sodium in NH_3 solution that a maximum in the temperature coefficient of resistance occurs in the region of $C = 0.9$ in the temperature interval from -32.5°C . to 40°C . Solutions of potassium in NH_3 behave similarly. The appearance of a maximum in the temperature coefficient-concentration curves seems to be related to the appearance of metallic-like properties. For sodium in NH_3 solutions at -34°C . at a concentration of approximately 0.6*N* the conductance-concentration curve begins to increase exponentially with increasing concentration. At the same time, the temperature coefficient has gone through a maximum and begins to decrease rapidly reaching small values toward saturation; in fact, it would appear that the coefficient might even become negative, which is characteristic of the metallic state, if the concentration could be increased slightly above the saturation value. The appearance of a minimum in the Δ - C curve and maximum in the resistivity concentration curve evidently results from two competing processes. At low metal concentrations electrostatic interactions and/or association effectively remove conducting species, leading to a decrease in conductance with an increase in concentration. At higher concentration the "micro Wien" effect releases solvated electrons from the ion pairs. These effects are finally overcome at still higher concentration by electrons free to move in the metallic sense.

Arnold and Patterson (1, 2) explain the conductance in the intermediate concentration region, including the conductance minimum, by using a tunneling mechanism in terms of the interaction of F , F' , and F_2 centers, electrons, and metal ions. Introducing the F' center may be considered comparable to using an M^- or ion triplet. This species apparently becomes important in the conductance minimum region and is of increasing interest in attempts to demonstrate complete compatibility of conductance and magnetic studies. The necessity of proposing an M^- species may be thought of in terms of the dilemma that Sukhotin (50, 51) presents in conventional 1-1 electrolyte solutions. Sukhotin demonstrated that in nonaqueous electrolyte solutions the appearance of the observed conductance minima can be explained without postulating the presence of ion triplets. An increase in the apparent dielectric constant of the electrolyte solutions, with increasing concentration of electrolyte, is observed in the region of the conductance minimum. This is reflected in a decrease of the ionic activity coefficient with increasing concentration and, therefore, an increase in the concentration of conducting species. This coincides with the appearance of the conductance minimum. The use of the dielectric constant-activity coefficient effect or the "micro Wien" effect could possibly explain the observed conductance minimum

for sodium in NH_3 and other metal-amine solutions without postulating an M^- species. However, the magnetic data would seem to be more easily interpreted with the M^- species.

Recent field dependent experiments for the sodium in NH_3 system by Schettler and Patterson (46) show an unexpectedly large and complex field influence on the conductance of dilute solutions of sodium in liquid ammonia at -33°C . Two distinctive effects are noted. One occurs at very low fields, 2.5 v./cm., and results in an increase, within one microsecond, of the conductance by 2–3% over the observed value on a commercial bridge at 0.2 v./cm. and 1,592 c.p.s.

The second effect results when the field increases by factors of ten from the 2.5 v./cm. value. The conductance, measured at a given time following the pulse application, increases abruptly and reaches a near limiting value. The effect is many times larger than that observed in any previous electrolytic measurements and cannot be explained on the basis of any currently accepted theory for the influence of high fields. This, when understood, may give added insight into the solvated electron interactions.

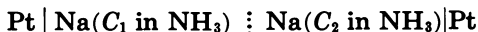
EMF and Transference Numbers

Studies by Pleskov and Monoszon (38–44) established much of what we know about standard potentials in liquid NH_3 . The type of cell used in these studies may be represented by



From the known potential of the lead-lead nitrate electrode, the standard potentials of the cations could be calculated if several assumptions are made (10). The results give reliable values for the free energies of formation for most of the alkali ions. Determining the value of E° for an inert metal in contact with the solvated electron requires a somewhat sophisticated experimental apparatus. The obvious use of the free metals as an electrode is impossible because of their high solubility, and the problems involved in using amalgam electrodes have apparently never been resolved. Inert metals, such as platinum and tungsten, are suitable since they are reversible to the solvated electron, and polarization effects at all investigated concentrations of metal-ammonia solutions are absent.

The first estimate of the transference number of the electron was contributed by C. A. Kraus in 1914 (25). Using the concentration cell,



he measured the e.m.f. as a function of concentration. The data were used to estimate the transference number of the negative species (the electron) which demonstrates that this species carried most of the current, about seven-eighths. Evers and Klein (23) have come to similar conclusions for solutions of lithium in methylamine. Unfortunately, these "transference numbers" are based on the assumption that the activity coefficient is independent of concentration. This was acknowledged at

the time as necessary approximation. Direct transference measurements have been made by the moving boundary technique by Dye and his co-workers (12). These have been combined with e.m.f. measurements to compute the activity coefficients. The transference number as a function of concentration for sodium in NH_3 solutions has been calculated from both the e.m.f. data of Kraus (25) and Dye *et al.* (12) (see Figure 3). The transference numbers determined from the e.m.f. method are higher than those determined with the moving boundary technique. This difference in transference number can be accounted for by activity coefficient behavior not taken into account by the e.m.f. method (13, 49). The concentration variation of transference numbers of potassium and sodium in NH_3 solutions is surprisingly similar, although the intercepts as determined from data for salts are significantly different (45).

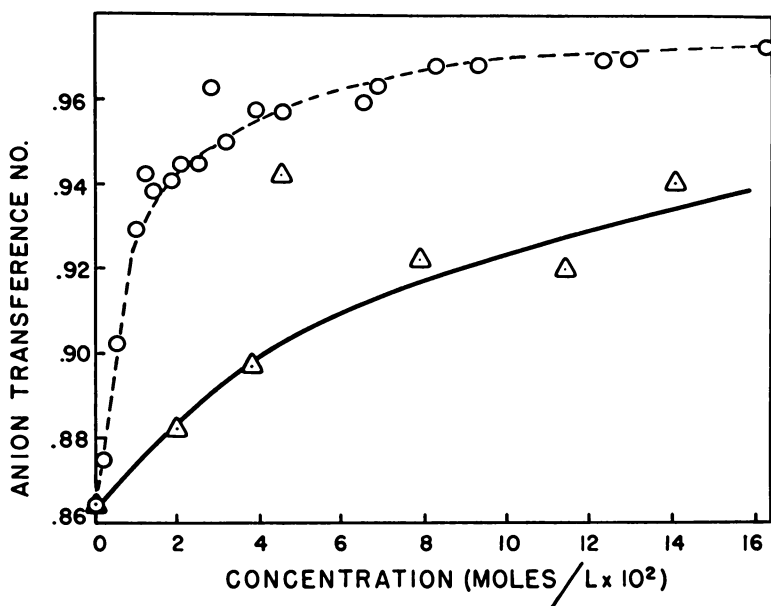


Figure 3. Anion transference number as a function of concentration for sodium in NH_3 ; O calculated from the e.m.f. data of Kraus assuming activity coefficients of unity; Δ from moving boundary experiments of Dye *et al.* (12).

When the transference numbers are combined with equivalent conductances, the results are as expected (Figure 4). The cationic conductance decreases monotonically with increasing concentration while the anionic conductance goes through a minimum. Applying the mass action equilibria to these data is as successful as it was with the conductance data. Conductance, transport, and activity data give good fits using reasonably constant and consistent values of K_1 and K_2 . The activity coefficients obtained from these data for K correlate quite well with the dilute solution points of Marshall (35) obtained from vapor pressure measurements.

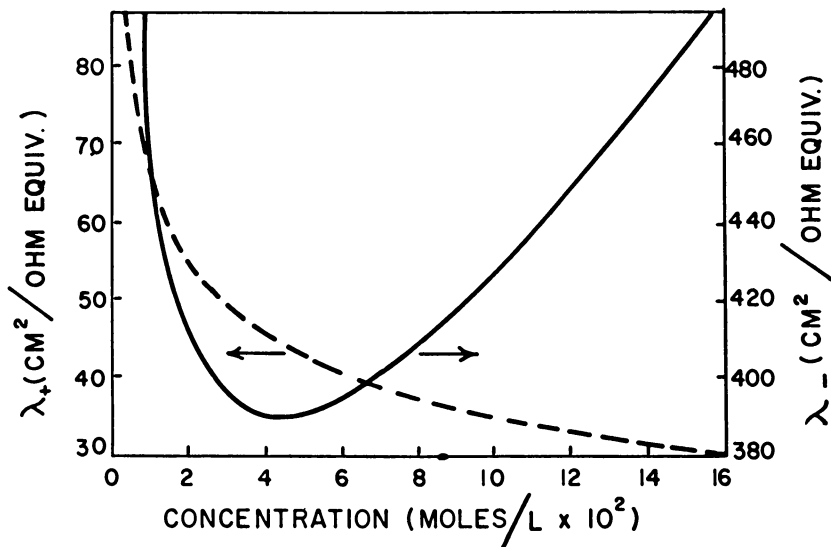
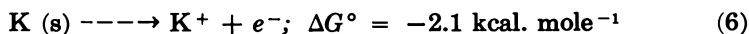
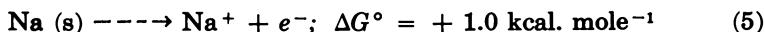
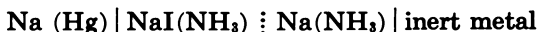


Figure 4. Anionic and cationic conductances as a function of concentration for sodium in NH_3 solutions as calculated using transport data (12).

Dye has also used the sodium and potassium data to calculate ΔG° values:



These values refer to the hypothetical one molal standard state for the ions. The difference between these values, $3.1 \text{ kcal. mole}^{-1}$, should represent the difference in free energy of formation of Na^+ and K^+ . The value given by Jolly (20) and Coulter (6, 7) for this difference is $+ 3.4 \text{ kcal. mole}^{-1}$ in good agreement as is the value of $\Delta G^\circ = - 3.14$ very accurately determined by Schug and Friedman (47) for the reverse reaction. Russell and Sienko (45) used the cells



to estimate the standard potential and ΔG° for the Na process. Drastic assumptions were necessary to complete the calculation; however, their value, $\Delta G^\circ = 2.4 \text{ kcal. mole}^{-1}$, agrees well with the other quoted values.

A chronopotentiometric method has been used by Gordon and Sundheim (18) to measure the anionic diffusion for the potassium in NH_3 solution in the presence and absence of salt. The limiting value of diffusion coefficient for the electron is in the region of $14.5 \times 10^{-5} \text{ cm.}^2/\text{sec}$. This agrees with values derived from Dye (12). The anionic diffusion coefficient is several times larger than that for the neutral metal species. Gordon and Sundheim, however, do not believe that there is necessarily

any indication of a different diffusion mechanism for anion and neutral species. Similarly the activation energies for diffusion are not greatly different for the electron and neutral combination. The activation energies are not consistent with the proposal of a conduction band in dilute solutions, and interpretation in terms of tunneling is not necessary. A unique diffusion process is not involved.

Thermoelectric Effect

Dewald and Lepoutre (8, 9, 33) have investigated the thermoelectric power of metal-ammonia solutions in great detail. Concentrated solutions exhibit thermoelectric properties in very good accord with predictions based on a degenerate electron gas model. The thermoelectric power of these solutions is of the order of magnitude characteristic of typical metals (1–10 μ volts/degree). It was also noted that the thermoelectric power increases monotonically as the concentration decreases, indicating that conduction in these solutions is by means of electrons ("N" type conduction). In dilute solutions, the thermoelectric power for both potassium and sodium at -33°C . also indicates a monotonic increase with decreasing metal concentration. Furthermore, below 0.1M the data for potassium and sodium are indistinguishable within experimental error. The behavior is analogous to measurement results on silicon and germanium as well as dilute aqueous work. The variation of thermoelectric power with concentration in the dilute region is almost logarithmic. The slope is about twice what would be predicted from the Nernst equation. Dewald and Lepoutre claim that deviations in the aqueous work and the metal-ammonia work are not entirely accountable in terms of activity and association effects. Thermoelectric effect experiments of Lepoutre and Dewald with mixed salt-metal-ammonia solution do, however, indicate a pronounced ion-electron interaction. At -78°C . the same positive temperature dependence and fairly large logarithmic dependence on metal concentration are present. A significant difference between the potassium and sodium curves over the entire concentration region is noted. This suggests that the specific nature of the positive ion has an important bearing on the electronic properties of the dilute solutions. One would expect increased ion-electron interactions at lower temperatures owing to less thermal energy; however, a higher dielectric constant at lower temperatures would tend to decrease the interaction. The effect of salt added to sodium in NH_3 solutions at -33°C . is noteworthy. There is a very large increase in thermoelectric power, which is the direction expected if the salt were decreasing the concentration of electrons by a common ion effect. The observed change is about ten times that predicted simply by such a mechanism. It is concluded that the very large salt effect may be found in changes in heats of transport of the charged species. The suggestion is made that the apparent anomaly of large dilution effects and large salt effects can be explained by assuming that the transport heat of the electrons is negative; that is, when the electrons move through a solution, heat is transported

in the opposite direction. This could arise if the primary mode of electron transport were by a tunneling or jump mechanism; in making transitions from one polarization center to another, an electron would then leave the dipole polarization energy of the center behind and, with the electron gone, this energy would eventually be transformed into heat. In its "new" environment the electron would polarize the solvent at the expense of thermal energy of the surroundings. Polarization energy would thus flow in a direction opposite to electron flow. It should be noted that this postulate leads to S° for the electron in ammonia in strong disagreement with estimate by other methods (33).

The common facts that obviously permeate all aspects of the transport properties of metal-ammonia and metal-amine systems are:

(1) Phenomenologically, in dilute solutions the metal-ammonia and metal-amine solutions have transport properties quite similar to electrolytes in similar solvents, and consequently the types of interactions involved are probably similar.

(2) The anionic species is responsible for the anomalously large conductance and thermoelectric effects, and is definitely some form of solvated electron.

(3) The further anomaly in all measurements is that the electron appears to have an "extra mobility" over that normally associated with anionic or cationic species. This behavior resembles that associated with the "solvated proton" in aqueous solutions.

Acknowledgment

We wish to thank Dr. E. C. Evers and Dr. H. Friedman for reading the manuscript and making valuable suggestions.

Literature Cited

- (1) Arnold, E., Patterson, A. J., "Calculation of Conductivity in Sodium-Liquid Ammonia Solutions" in "Metal-Ammonia Solutions, Physicochemical Properties," Colloque Weyl, G. Lepoutre, M. J. Sienko, eds., p. 160, Benjamin Press, New York, 1964.
- (2) *Ibid.*, p. 285.
- (3) Berns, D. S., Evers, E. C., Frank, P. W., Jr., *J. Am. Chem. Soc.* **82**, 310 (1960).
- (4) Berns, D. S., Lepoutre, G., Bockelman, E. A., Patterson, A. J., *J. Chem. Phys.* **35**, 1820 (1961).
- (5) Cafasso, F. A., Sundheim, B. R., *J. Chem. Phys.* **31**, 809 (1959).
- (6) Coulter, L. V., *J. Phys. Chem.* **57**, 553 (1953).
- (7) Coulter, L. V., Maybury, R. H., *J. Am. Chem. Soc.* **71**, 3394 (1949).
- (8) Dewald, J. F., Lepoutre, G., *J. Am. Chem. Soc.* **76**, 3369 (1954).
- (9) *Ibid.*, **78**, 2956 (1956).
- (10) Dye, J. L., "Electrochemical Properties of Metal-Ammonia Solutions: E.M.F. and Transference Numbers" in "Metal-Ammonia Solutions, Physicochemical Properties," Colloque Weyl, G. Lepoutre, M. J. Sienko, eds., p. 137, Benjamin Press, New York, 1964.
- (11) Dye, J. L., Dewald, R. R., *J. Phys. Chem.* **68**, 135 (1964).
- (12) Dye, J. L., Sankuer, R. F., Smith, G. E., *J. Am. Chem. Soc.* **82**, 4797 (1960).
- (13) Dye, J. L., Smith, G. E., Sankuer, R. F., *J. Am. Chem. Soc.* **82**, 4803 (1960).
- (14) Evers, E. C., University of Pennsylvania, Philadelphia, private communication.
- (15) Evers, E. C., Frank, P. W., Jr., *J. Chem. Phys.* **30**, 61 (1959).
- (16) Filbert, G., unpublished observations, University of Pennsylvania.

- (17) Friedman, H. L., *Ann. Rev. Phys. Chem.* **12**, 171 (1961).
- (18) Gordon, R. P., Sundheim, B. R., *J. Phys. Chem.* **68**, 3347 (1964).
- (19) Hnizda, V. F., Kraus, C. A., *J. Am. Chem. Soc.* **71**, 1565 (1949).
- (20) Jolly, W. L., *Chem. Rev.* **50**, 351 (1952).
- (21) Kay, R. L., Dye, J. L., *Proc. Natl. Acad. Sci.* **49**, 5 (1963).
- (22) Kenausis, L. C., Evers, E. C., and Kraus, C. A., *Proc. Natl. Acad. Sci.* **48**, 121 (1962).
- (23) Klein, H. M., Ph.D. dissertation, University of Pennsylvania (1957).
- (24) Kraus, C. A., *J. Am. Chem. Soc.* **30**, 1323 (1908).
- (25) Kraus, C. A., *J. Am. Chem. Soc.* **36**, 864 (1914).
- (26) Kraus, C. A., *J. Am. Chem. Soc.* **43**, 749 (1921).
- (27) Kraus, C. A., *J. Franklin Inst.* **212**, 537 (1931).
- (28) Kraus, C. A., Bray, W. C., *J. Am. Chem. Soc.* **35**, 1315 (1913).
- (29) Kraus, C. A., Fuoss, R. M., *J. Am. Chem. Soc.* **55**, 21 (1933).
- (30) Kraus, C. A., Lucasse, W. W., *J. Am. Chem. Soc.* **43**, 2529 (1921).
- (31) Kraus, C. A., Lucasse, W. W., *J. Am. Chem. Soc.* **44**, 1941 (1922).
- (32) Kraus, C. A., Lucasse, W. W., *J. Am. Chem. Soc.* **44**, 1949 (1922).
- (33) Lepoutre, G., Dewald, J. F., *J. Am. Chem. Soc.* **78**, 2953 (1956).
- (34) Longo, F., Ph.D. Thesis, University of Pennsylvania, 1963.
- (35) Marshall, P. R., *J. Chem. Eng. Data* **7**, 399 (1962).
- (36) Naiditch, S., "Electrical Conductivities of Sodium-Ammonia Solutions," in "Metal-Ammonia Solutions. Physicochemical Properties," Colloque Weyl, G. Lepoutre, M. J. Sienko, eds., p. 113, Benjamin Press, New York, 1964.
- (37) Panson, A. J., Evers, E. C., *J. Am. Chem. Soc.* **82**, 4468 (1960).
- (38) Pleskov, V. A., *Acta Physicochim.*, URSS **6**, 1 (1937).
- (39) Pleskov, V. A., *Acta Physicochim.*, URSS **21**, 235 (1946).
- (40) Pleskov, V. A., *J. Phys. Chem. (USSR)* **9**, 12 (1937).
- (41) Pleskov, V. A., *J. Phys. Chem. (USSR)* **20**, 163 (1946).
- (42) Pleskov, V. A., Monoszon, A. M., *Acta Physicochim. (USSR)* **2**, 615 (1935).
- (43) Pleskov, V. A., Monoszon, A. M., *J. Phys. Chem. (USSR)* **6**, 1290 (1935).
- (44) Pleskov, V. A., Monoszon, A. M., *J. Phys. Chem. (USSR)* **6**, 1286 (1935).
- (45) Russell, J. B., Sienko, M. J., *J. Am. Chem. Soc.* **79**, 4051 (1957).
- (46) Schettler, P., Patterson, A. J., *J. Am. Chem. Soc.* **87**, 392 (1965).
- (47) Schug, K., Friedman, H., *J. Am. Chem. Soc.* **80**, 45 (1958).
- (48) Shedlovsky, T., *J. Am. Chem. Soc.* **54**, 1411 (1932).
- (49) Smith, G. E., Ph.D. Dissertation, Michigan State University, 1963.
- (50) Sukhotin, A. M., *Zhur. Fiz. Khim.* **33**, 72 (1959).
- (51) Sukhotin, A. M., *Zhur. Fiz. Khim.* **34**, 63 (1960).
- (52) Wien, M., Schiele, *J. Physik. Z.* **32**, 545 (1931).

RECEIVED April 27, 1965.

Conduction Processes in Concentrated Metal-Ammonia Solutions

J. C. THOMPSON

Department of Physics, University of Texas, Austin, Tex. 78712

The metallic nature of concentrated metal-ammonia solutions is usually called "well known." However, few detailed studies of this system have been aimed at correlating the properties of the solution with theories of the liquid metallic state. The role of the solvated electron in the metallic conduction processes is not yet established. Recent measurements of optical reflectivity and Hall coefficient provide direct determinations of electron density and mobility. Electronic properties of the solution, including electrical and thermal conductivities, Hall effect, thermoelectric power, and magnetic susceptibility, can be compared with recent models of the metallic state.

The concentrated ($>0.4M$) metal-ammonia solutions were first called "metallic" by Kraus in 1921 (7). On several recent occasions the term "semiconductor" has implicitly been substituted for "metal" in interpreting various data (1, 2). Since Kyser and Thompson (8) have established the truly metallic nature of the solutions by measuring the free carrier concentration, it is worthwhile to re-examine the relative data and interpret it in terms of liquid metal theory.

The first conclusion is that solvated electrons no longer exist in appreciable quantities. The most direct determination has been by Beckman and Pitzer (2) who do not find the famous 1.5μ peak at concentrations above $1M$. Indeed, it would be difficult to understand how the solvation layer might be maintained around electrons with the high thermal velocities characteristic of a degenerate electron gas. One may also note that at the concentrations in question the mole ratio r_1 (= moles solvent/mole solute) is rapidly approaching unity, so that fewer solvent molecules are available for the solvation process. At the onset of the

metallic state r_1 is still ~ 50 . The solvated electron disappears, not by a gradual erosion of solvating layers, but in a rapid reaction which may be represented by:



where n is the number of solvating ammonia molecules. The process is not that simple, however; at concentrations below the metallic range there is evidence for at least two classes of bound electrons. The spectral evidence of Beckman and Pitzer implies the usual electron-in-a-cavity to be present; at least the 1.5μ absorption is still present. At the same time the conductance data imply that electrons exist, bound by only 0.2 e.v. (1). The latter class, of course, is responsible for the conductivity since thermal energies are inadequate to release electrons from the relatively immobile solvated state.

The analysis to be presented is based on the results of Kyser and Thompson (8), which are summarized briefly, then discussed in turn with the other properties of the solutions.

Kyser and Thompson, using the Hall effect, measured the free electron concentration directly. They find, at concentrations above 4 mole % in sodium or lithium solutions, that all metal valence electrons are free. Furthermore, the numbers of free electrons do not vary with temperature, though there is a slight temperature variation of number density (number of electrons/cc.) owing to the thermal expansion of the liquid as a whole. Hence, we must use the metal concentration and the electron concentration as identical, within the precision of their experiment. The precision puts a limit of one in 100 electrons per metal atom in any bound state—e.g., monomer, dimer, or other cluster. The bound electrons, if any, are bound by energies so great that a 30 degree temperature rise does not free a measurable number. A saturated solution is in this sense no different from any other solution in the concentration range above the metallic transition. The final model is just that proposed by K. S. Pitzer in 1958 (12). We must consider a form of "liquid sodium," or other metal, as simple as the pure metal, but with a widely varying ionic and electronic density, and imbedded in a dielectric medium.

Electronic Properties

The electrical conductivities of several alkali metals dissolved in liquid ammonia are shown in Figure 1 (7, 11, 15). The strong variation of the conductivity, σ , with concentration has been most difficult to explain. This difficulty can be assessed by referring to a simple model of conductance, the Thomas-Fermi model of a screened Coulomb potential (19). This model has been used in describing semiconductors as well as in theories of metal-ammonia solutions (1).

The scattering center is the metal ion, the Coulomb potential of which is screened in the manner of the Debye-Hückel theory of weak electrolytes. The screened potential has the form

$$\psi = \frac{-e}{4\pi\epsilon r} e^{-\lambda r} \quad (2)$$

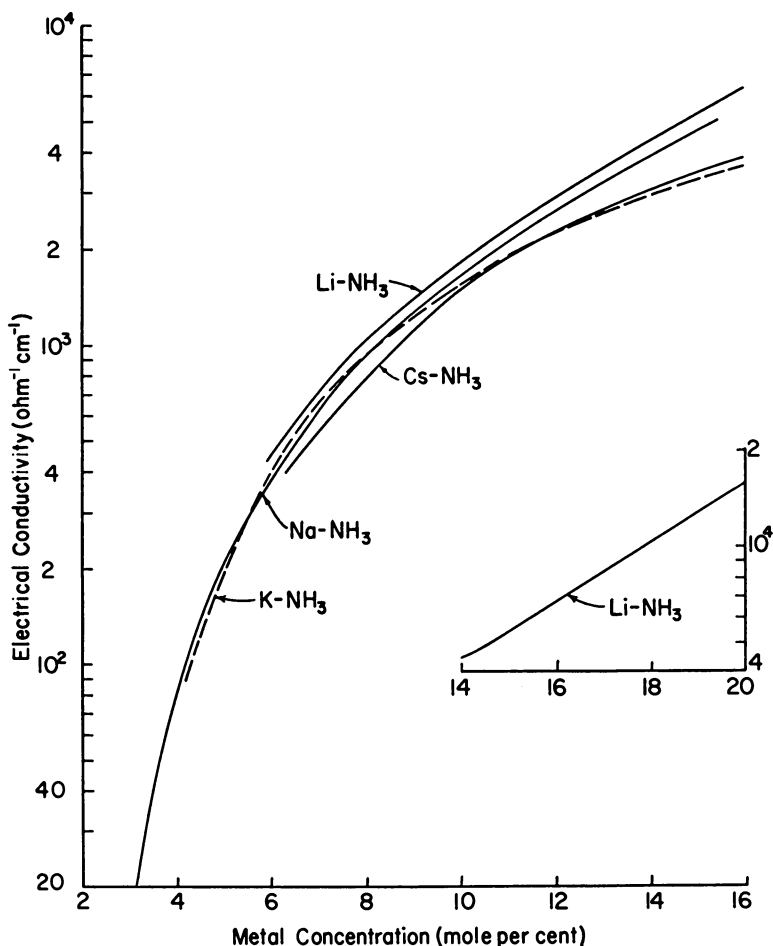


Figure 1. *Electrical conductivity vs. concentration for several alkali metals dissolved in liquid ammonia at 33°C.*

Data points have been omitted for clarity. The inset shows data for concentrated lithium-ammonia solutions.

where λ is the screening constant, the reciprocal of the screening length, and ϵ is the permittivity. For such a potential the scattering cross-section is easily calculated to be (15)

$$f(\theta) = \left| \frac{2me^2}{4\pi\epsilon\hbar^2(k^2 + \lambda^2)} \right|^2 \quad (3)$$

for an electron wave with wave number k . The mean free path, Λ , is then (18)

$$\frac{1}{\Lambda} = 2\pi n_s \int_0^\pi (1 - \cos \theta) f(\theta) \sin \theta d\theta \quad (4)$$

where n_s is the number density of scatterers. The factor $(1 - \cos \theta)$ enters because small-angle scattering does not remove momentum from the stream of particles. It is customary to assume elastic scattering so that

$$\left(\frac{k}{k_0}\right)^2 = 2(1 - \cos \theta) \quad (5)$$

where k_0 is the Fermi wave number

$$k_0 \equiv (3\pi^2 n_0)^{1/3} \quad (6)$$

Now, the mean free path is found to be

$$\frac{1}{\Lambda} = \frac{n_s m^2 e^4}{8\pi \epsilon^2 \hbar^4 k_0^4} \left[\ln\left(\frac{4k_0^2}{\lambda^2} + 1\right) - \frac{4k_0^2/\lambda^2}{1 + 4k_0^2/\lambda^2} \right] \quad (7)$$

As in standard kinetic theory the conductivity, σ , is

$$\begin{aligned} \sigma^{-1} &= \frac{\hbar k_{02}}{n_0 e^2} \frac{1}{\Lambda} \\ &= \frac{m^2 e^2 n_s}{24\pi^3 \epsilon^2 \hbar^3 n_0^2} \left[\ln\left(\frac{4k_0}{\lambda^2} + 1\right) - \frac{4k_0^2/\lambda^2}{1 + 4k_0^2/\lambda^2} \right] \end{aligned} \quad (8)$$

for degenerate statistics. This very fine result is meaningless until we know λ .

The primary particle involved in the screening process is the mobile electron. One has then the problem of a self-consistent calculation of the charge distribution in the neighborhood of a test charge. The Thomas-Fermi approach to this problem is the analog of the Debye-Hückel calculation wherein allowance has been made for the Pauli exclusion principle. From any standard text one can obtain the Poisson equation (19)

$$\begin{aligned} \nabla^2 \psi &= -\rho/\epsilon = \frac{e}{\epsilon} (n - n_0) \\ &= \frac{en_0}{\epsilon} \left[\left(1 + \frac{e\psi}{\zeta_0}\right)^{3/2} - 1 \right] \end{aligned} \quad (9)$$

where $\rho = e(n - n_0)$ is the charge density; n_0 is the uniform charge density in the absence of the test charge; $n = n(r)$ is the nonuniform charge density produced by the test charge; K_ϵ is the dielectric constant ($\epsilon = K_\epsilon \epsilon_0$); and ζ_0 is the Fermi energy (or electrochemical potential) of the degenerate electron gas and is given by

$$n_0 = \frac{8\pi}{3h^3} (2m\zeta_0)^{3/2}. \quad (10)$$

The symbols \hbar , e , m have their usual meaning. One now linearizes the equation for ψ by assuming:

$$\left(\frac{e\psi}{\zeta_0}\right)^2 \ll 1 \quad (11)$$

gives:

$$\nabla^2 \psi = \frac{en_0}{\epsilon} \left(\frac{3e\psi}{2\zeta_0} \right) \quad (12)$$

which if $\psi = \psi(r)$ only, takes the form:

$$\frac{d^2\psi}{dr^2} + \frac{2}{r} \frac{d\psi}{dr} = \frac{3e^2 n_0}{2\epsilon\zeta_0} \psi \quad (13)$$

and is easily solved to yield:

$$\psi = -\frac{e}{4\pi\epsilon r} e^{-\lambda r} \quad (14)$$

where, using (10),

$$\lambda^2 = \frac{\epsilon\hbar^3}{4\pi e^2 (2m)^{3/2} \zeta_0^{1/2}} \quad (15)$$

We define the Fermi wave number, k_0 by

$$\hbar k_0 = (2m\zeta_0)^{1/2}, \quad (16)$$

and obtain, finally,

$$\lambda^2 = \frac{\pi^2 \epsilon \hbar^2}{e^2 m k_0} \quad (16a)$$

All of this is based on the linearization procedure in Equation 11. If one examines this condition, the restriction turns out to be quite tight. We may approximate ψ by $e/4\pi\epsilon r_0$, where r_0 is the ionic spacing (19). Then Equation 11 takes the form:

$$(e^2/4\pi\epsilon r_0 \zeta_0)^2 \ll 1 \quad (11a)$$

but $r_0 = (n_0)^{-1/3}$ and on substituting from Equation 10 we find, ignoring the overall square,

$$\frac{me^2}{2 \cdot 3^{2/3} \cdot \pi^{7/3} \hbar^2 \epsilon} \frac{1}{n_0^{1/3}} \ll 1 \quad (11b)$$

We may now put in such constants as are available and find

$$r_0 \ll 2.53 \cdot 10^{-8} \frac{K_e}{m^*/m} \text{ cm.} \quad (11c)$$

where m^*/m is the ratio of effective electron mass to free electron mass. In the simplest case, $K_e = m^*/m = 1$; hence $r_0 \ll 2.5$ A. In Figure 2 are plotted several simple parameters of an electron gas, including r_0 . One sees at once that Equation 11c is not satisfied unless $K_e/(m^*/m) \gtrsim 10$, and the situation worsens as the electron concentration decreases. One may parenthetically note that in the very dilute ($10^{-4}M$) electron gas, the Thomas-Fermi result goes over into the Debye-Hückel formula

which is then justified on the basis that the thermal energy, kT , is to exceed $e^2/4\pi\epsilon r_0$, which condition obtains at high dilutions.

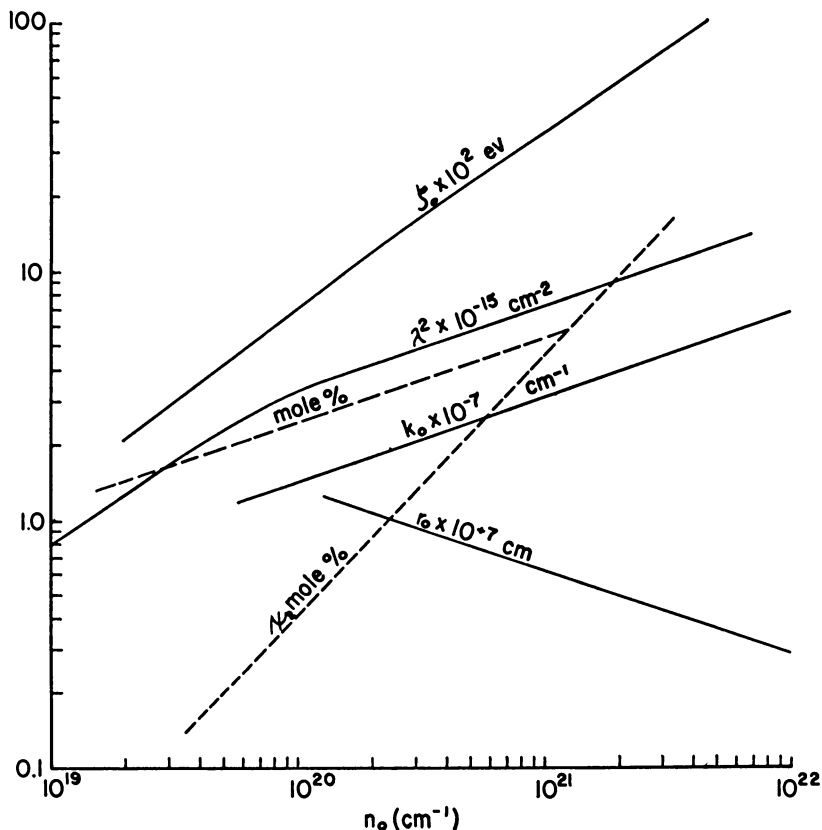


Figure 2. Several parameters of an electron gas as a function of the density of electrons.

ζ_0 is the Fermi energy; r_0 is the interparticle spacing; k_0 is the Fermi wave number; and λ is the Thomas-Fermi screening length. The dashed line shows the sodium concentration which yields n_0 free electrons (as determined from the Hall coefficient); the dotted line is the metal concentration.

In applying these ideas to metal solutions in ammonia, the restrictions on the Thomas-Fermi screening approach have generally been ignored. At metallic concentrations the concentration of free ammonia molecules is low, and the dielectric constant is near unity; the pure ammonia value of K_e is only applicable when solvent molecules are not polarized by the ions. If we choose m^*/m less than unity, then fitting the theory to experimental data on conductivity becomes impossible. For the calculated conductivity to agree with the measured conductivity, we require

$$\frac{K_e}{m^*/m} \cong 10$$

at saturation and much less than 10 below saturation. This requirement contravenes the condition for a linear version of the Poisson equation.

The failure is not limited to metal-ammonia solutions nor to the linear Thomas-Fermi theory (19). The metals physicist has known for 30 years that the theory of electron interactions is unsatisfactory. E. Wigner showed in 1934 that a dilute electron gas (in the presence of a uniform positive charge density) would condense into an "electron crystal" wherein the electrons occupy the fixed positions of a lattice. Weaker correlations doubtless exist in the present case and have not been properly treated as yet. Studies on metal-ammonia solutions may help resolve this problem. But one or another form of this problem—the inadequate understanding of electron correlations—precludes any conclusive theoretical treatment of the conductivity in terms of, say, effective mass at present. The effective mass may be introduced to account for errors in the density of states—not in the electron correlations.

Pohler and Thompson (13) have treated the ionic potential by an OPW formalism. In that calculation, screening was computed with a Hartree-Fock formalism. The electron correlations are still not included properly. Further criticism may be aimed at their calculation. They took the wave functions of the core electrons and renormalized them so that they were spread over the greater volume available to the ion in solution. There is no guarantee that the procedure used properly allowed for the increased orbital angular momentum produced by the spreading process. This effect should be less on the, intrinsically larger, cesium ion than on the lighter alkali metals. Thus, no meaningful conclusions can be drawn from their computation, either as to magnitude or trend.

An omission has been made in deriving Equation 4. The relative positions of the scattering centers are important and may be included by multiplying $f(\theta)$ by $a(\theta)$ [= $a(k)$] where $a(\theta)$ is the Fourier transform of the radial distribution function of the solution (20). This quantity is usually determined from x-ray diffraction data. All of the temperature dependence of σ depends upon $a(k)$. We cannot explain the temperature variation of σ by density changes or by an alternation in the scattering process. Only through changes in the relative positions of the scattering centers does the temperature influence the conduction process. Thus, the fact that conductivity increases with temperature in the range below 0° C., need not force us to assume a semiconductor-like description of the solution. Even pure zinc shows such behavior just above its melting point (3). These conclusions are independent of the details of the scattering process—i.e., of $f(\theta)$, and are not altered by the failure of the theory of the screening.

Let us turn now to the other conclusions which can be based on free electron theory. The Hall effect measurements of Kyser and Thompson permitted the computation of the free electron concentration. The Hall effect is produced by a balance between the magnetic force (Lorentz force) on a current carrier and the electric force produced by a displaced charge density within a conductor. For a charge, q , moving

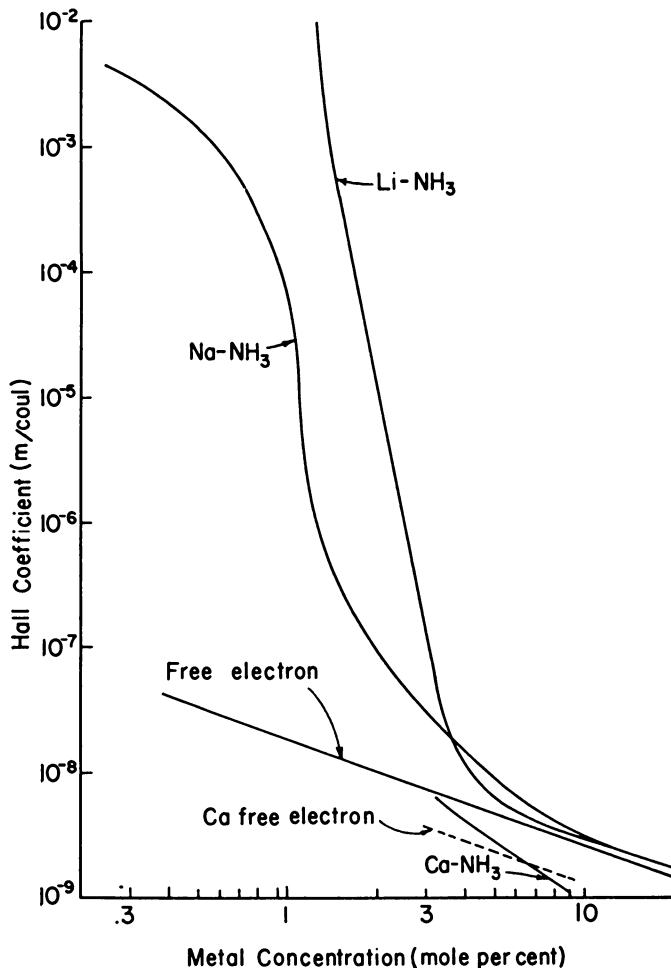


Figure 3. The Hall coefficient of lithium, sodium, and calcium solutions in ammonia.

with drift velocity, v_d , in a current element the force due to a magnetic field, \underline{B} , is

$$\underline{F} = qv_d \times \underline{B} \quad (17)$$

This is balanced by the Hall electric field, E_H , so that

$$qE_H = qv_d \times \underline{B} \quad (18)$$

If the conductor (assumed rectangular) has a cross section $A = t \cdot w$, where t is the thickness and w is the width, then the current is

$$\underline{I} = qv_d An \quad (19)$$

where n is the carrier concentration and the Hall voltage is $V_H = E_H w$.

Substitution yields

$$\begin{aligned} \frac{V_H}{w} &= \frac{IB}{qnA} \\ &= \frac{IB}{qnwt} \end{aligned} \quad (20)$$

when $B \perp I$. One obtains finally

$$\begin{aligned} V_H &= \frac{1}{qn} \frac{IB}{t} \\ &= R_H \frac{IB}{t} \end{aligned} \quad (21)$$

If I , B , t , and $|q|$ are known, then n and the sign of q are determined from V_H and R_H is called the Hall coefficient. The results of Kyser and Thompson are shown in Figure 3. At metal concentrations above five mole % all valence electrons in Li, Na, or Ca solutions are found to be free. It is furthermore found, as noted earlier, that R_H is temperature independent. Figure 4 shows the small variation observed and the change expected when the known density variation with temperature is

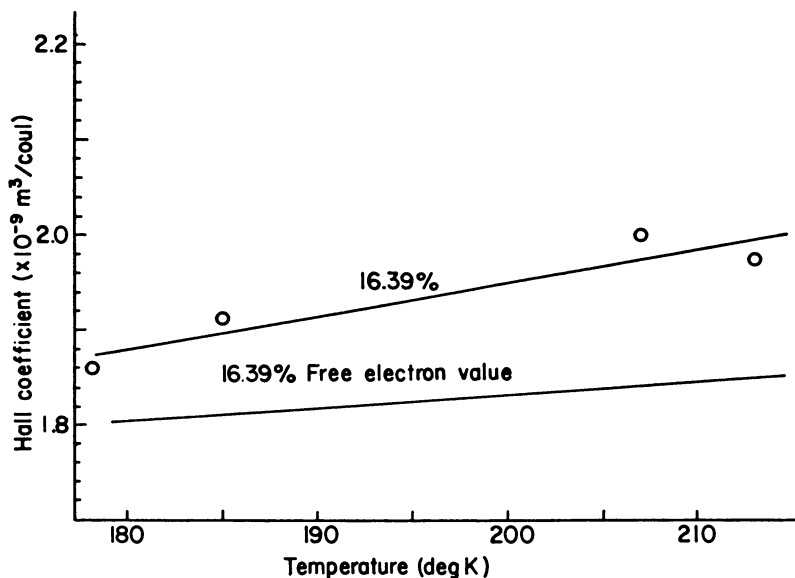


Figure 4. The temperature dependence of the Hall coefficient of concentrated lithium-ammonia solutions.

included. The small discrepancy is assigned to a small error in determining t . These results indicate that the bronze solutions are metallic in every sense of the word. Previous efforts to make the Thomas-

Fermi calculations agree with experiment by postulating a temperature variation to n are shown to be wrong.

Kyser and Thompson (9) have also searched for an effect of B upon σ : magnetoresistance. None was found within the precision of measurement and over the metallic concentration range. This provides further evidence for the metallic nature of the solutions since no magnetoresistance is to be expected for a simple metal with a spherical Fermi surface. That is, if the electron energy has the same dependence upon wave number regardless of propagation direction, there should be no magnetoresistance. Such isotropy is, of course, expected in a liquid. However, if tunneling or hopping were the charge transfer process instead of free electron drift, a magnetoresistance might occur.

Let us look now to the thermoelectric power. For a simple metal with a spherical Fermi surface the thermopower depends only on the electron concentration (18). The relationship is:

$$\epsilon = \frac{\pi^2 k^2 T}{3 e \xi_0} = -2.45 \times 10^{-2} \frac{T}{\xi_0} \mu V/\text{deg.} \quad (22)$$

where ξ_0 is the Fermi level (in e.v.), as given by Equation 10. We may calculate ϵ using the electron concentration shown in Figure 3. The results of this calculation are compared with the measurements of Dewald and Lepoutre (4) in Figure 5. The discrepancy appearing there is of the same order as that found in pure, solid sodium. One of two modes of analysis is customarily used when dealing with the thermopower of metal (10). If a small impurity is present, and if this impurity contributes a second scattering mechanism for the electrons, then one may apply Matthiessen's rule: $\rho = \rho_1 + \rho_2$. The net resistivity is ρ ; the contributions from the host and impurity are ρ_1 and ρ_2 . One then finds the thermopower, ϵ , to be

$$\epsilon = \epsilon_2 + (\epsilon_1 + \epsilon_2) \frac{\rho_1}{\rho} \quad (23)$$

Equation 23 goes by the name, Gorter-Nordheim rule; it indicates that a plot of ϵ vs. $\sigma (=1/\rho)$ will be linear. On the other hand, if one has a single scattering mechanism and two groups of carriers (two bands), then the conductivities rather than resistivities are added: $\sigma = \sigma_1 + \sigma_2$. In the two-band model the thermopower is:

$$\epsilon = \epsilon_2 + (\epsilon_1 - \epsilon_2) \frac{\sigma_1}{\sigma} \quad (24)$$

and one expects ϵ vs. $\rho (=1/\sigma)$ to be linear. Neither of the two approaches is successful when attempted on the metallic sodium-ammonia solutions. That is, the linear relation is not found in either case. This does not rule out the presence of a single carrier and a single scattering center. Rather the absence of multiple carriers or scatters is indicated. This observation supports the contention that the material is basically a simple metal.

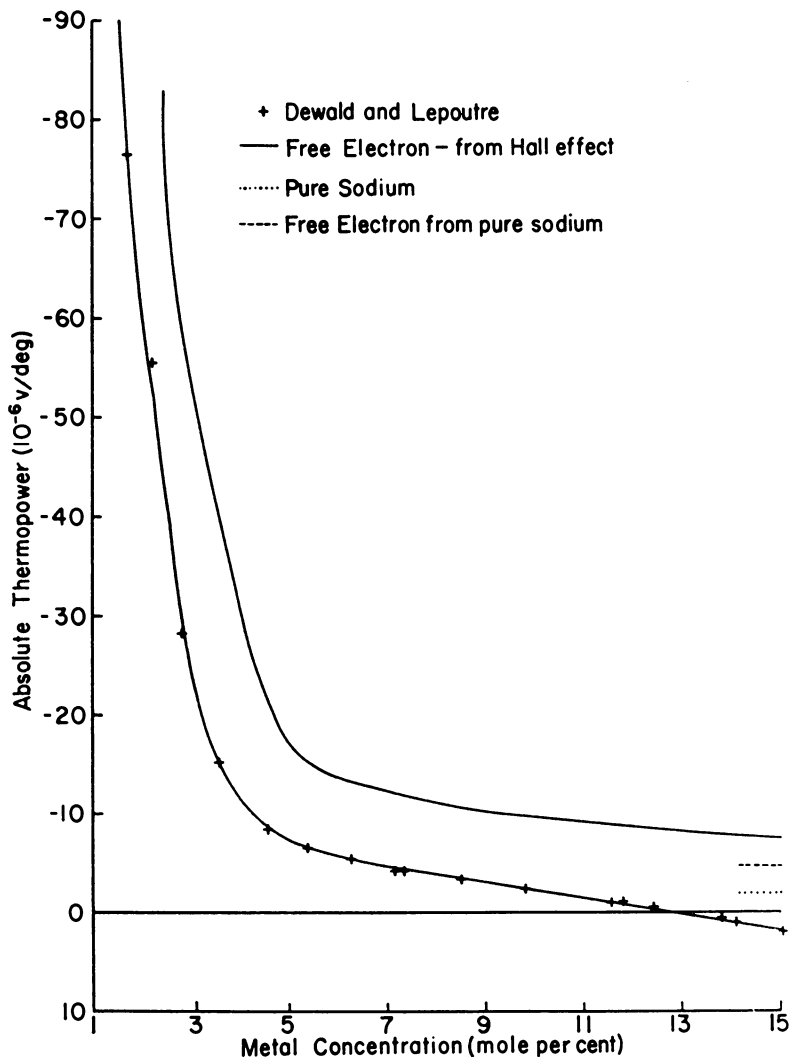


Figure 5. The thermoelectric power of concentrated sodium-ammonia solutions from experiment and as calculated for a free electron gas.

The dotted lines to the right of the saturation line refer to pure solid sodium.

The magnetic susceptibility is also derived from the electron density. There are two contributions (19): the Pauli paramagnetism and the Landau diamagnetism. The former is given by

$$\chi_p = \frac{3}{2} \frac{n_0 \mu_B^2}{\xi_0} \quad (25)$$

and the latter by

$$\chi_d = - \frac{n_0 \mu_B^2}{2\xi_0} \quad (26)$$

where μ_B is the Bohr magneton. In the free electron gas one has $\chi_d = -1/3\chi_p$; the total susceptibility is:

$$\chi = \chi_p + \chi_d = \frac{n_0 \mu_B}{\xi_0} \quad (27)$$

However the electron effective mass enters the two terms in different ways. The spin magnetic moment is fixed; hence m^*/m enters χ_p only through the Fermi energy. The diamagnetism is the result of the force exerted on the electron by an applied field; the angular velocity change derived from this force depends on m^*/m . Combining these results gives:

$$\chi^* = \frac{n_0 \mu_B^2}{2\xi_0} \left[3 \frac{m^*}{m} - \frac{m}{m^*} \right] \quad (28)$$

Combining Equations 27 and 28 one finds

$$\frac{\chi^*}{\chi} = \frac{1}{2} [3m^*/m - m/m^*] \quad (29)$$

A change of sign is possible for small m^*/m . In particular, if the electrons are bound, the Landau turn is dropped. If we turn now to the value of χ_p

$$\chi = 1.47 \times 10^{-14} n_0^{1/3} \quad (30)$$

in cgs. units. Converting to mass units:

$$\chi = \frac{1.47 \times 10^{-14}}{\rho} \quad (30a)$$

where ρ is the density. Finally, for the susceptibility per gram atom metal one multiplies by the molecular weight. In a sodium solution the equivalent molecular weight is

$$S = x_1 17.03 + x_2 23$$

and to obtain the sodium fraction, divide by x_2 :

$$\chi = \frac{1.47 \times 10^{-14} S}{\rho x_2} (n_0)^{1/3} \quad (30b)$$

Equation 30b duplicates Yost and Russell (17), though we shall not apply it to such a wide concentration range. One may now construct χ as a function of x_2 . The graph of this function is shown in Figure 6 along with the meagre data. The rapid rise of χ below 1.3% does not match the rapid drop found from Equation 30b. Caution is necessary in applying Equation 30b since the assembly is no longer degenerate, the

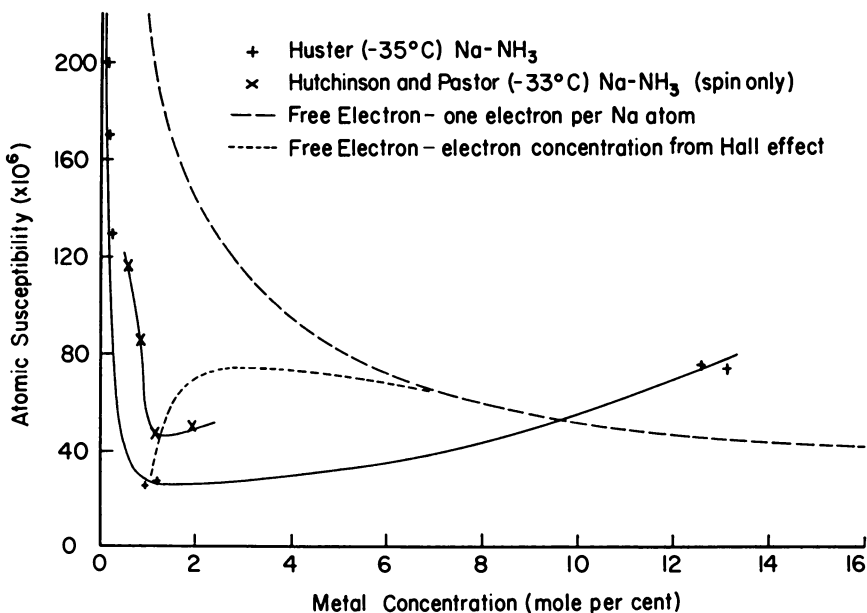


Figure 6. The atomic susceptibilities of sodium in ammonia.

The dotted line shows the free electron theory. Note the absence of data between two and 12 mole %.

Landau derivation of the diamagnetism no longer applies, and contributions from the orbital motion of the electrons may be expected. Here, as before, the free electron model only reproduces the broad trends of the data. Both model and the sparse data are essentially flat at concentrations above two mole %; the free electron model should not be used at lower concentrations. The magnitudes agree as well as for the pure solid metal.

Since the thermal conductivity is limited by the same scattering mechanism as the electrical conductivity we are also unable to make any calculation. Nevertheless, if a mean free path exists, then the Wiedemann-Franz law (19) must hold:

$$\frac{\kappa}{\sigma T} = L_0 \quad (31)$$

where κ is the thermal conductivity and $L_0 = 2.45 \times 10^{-8} \frac{\text{watt-ohm}}{\text{deg.}^2}$

is the Lorenz number. Even in pure metals, deviations from L_0 occur though the value of $\kappa/\sigma T$ is usually close to L_0 . Figure 7 shows $\kappa/\sigma T$ as a function of concentration for lithium-ammonia solutions (14, 16). The measured values all are low though there is an upward trend with increasing concentration. Error bars appropriate to the thermal conductivity used in the calculation would be about $\pm 0.2 \times 10^{-8} \text{ watt } \Omega/\text{deg.}^2$ in width.

In pure metals the deviation from L_0 is usually interpreted as evidence for inelastic scattering processes contributing to the resistivity. In the absence of any valid calculation of the conductivity such a conclusion is hard to justify in the present case.

The optical data will not be discussed here. Beckman and Pitzer analyzed their reflectance data in terms of thermally activated electrons; the Hall effect data are inconsistent with this interpretation. An effective mass could be introduced to bring their data into concert with the Drude (free electron) model, but would add little to our understanding.

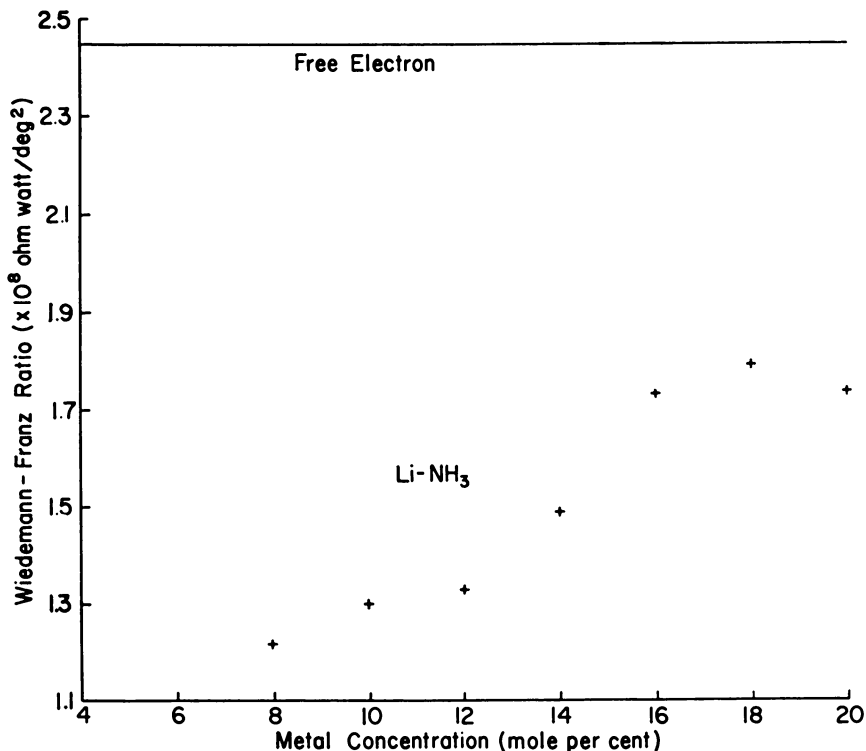


Figure 7. The Wiedemann-Franz ratio for solutions of lithium in ammonia at -33°C . The Lorenz number is 2.45×10^{-8} watt Ω/deg^2 .

The futility of an effective mass analysis, alluded to above, may be demonstrated by referring to the thermopower and susceptibility. Each of these quantities may be used to determine an effective mass if calculation and measurement are reconciled by varying m^*/m . One finds that χ requires $m^*/m > 1$, while ϵ requires $m^*/m < 1$. A more sophisticated approach is doubtless needed.

Conclusions

Simple models of electron behavior fail to describe quantitatively metal-ammonia solutions. Though the solutions show qualitatively the

properties predicted by a free electron model and a simple scattering law, no single parameter has been found to bring quantitative agreement. The obvious, single, parameter—effective mass—shows opposite trends when adjusted in a search for agreement.

Any prospective quantitative theory of the metallic state must include a proper treatment of the two (at least) types of bound electron levels present in the nonmetallic state. In addition, a proper theory of electron transport must be developed for situations wherein electron-electron interactions are important.

Acknowledgment

The author gratefully acknowledges the valuable conversations with many of his colleagues, including J. D. Gavenda, L. M. Falicov, D. S. Kyser, W. E. Millett, and C. M. Thompson.

Literature Cited

- (1) Arnold, E., Patterson, A., *J. Chem. Phys.* **41**, 3089, 3098 (1964).
- (2) Beckman, T. A., Pitzer, K. S., *J. Phys. Chem.* **65**, 1527 (1961).
- (3) Cusack, N. E., *Rept. Prog. Phys.* **26**, 361 (1963).
- (4) Dewald, J. F., Lepoutre, G., *J. Am. Chem. Soc.* **76**, 3369 (1954).
- (5) Huster, E., *Ann. Physik* **33**, 477 (1938).
- (6) Hutchinson, C. A., Pastor, R. C., *J. Chem. Phys.* **21**, 1959 (1953).
- (7) Kraus, C. A., *J. Am. Chem. Soc.* **43**, 754 (1921); **43**, 2533 (1921).
- (8) Kyser, D. S., Thompson, J. C., *J. Am. Chem. Soc.* **86**, 4509 (1964).
- (9) Kyser, D. S., Thompson, J. C., *J. Chem. Phys.* **41**, 1162 (1964).
- (10) MacDonald, D. K. C., "Thermoelectricity," p. 103, Wiley and Sons, New York, 1962.
- (11) Morgan, J. A., private communication.
- (12) Pitzer, K. S., *J. Am. Chem. Soc.* **80**, 5046 (1958).
- (13) Pohler, R. F., Thompson, J. C., *J. Chem. Phys.* **40**, 1449 (1964).
- (14) Schroeder, R. L., private communication.
- (15) Schiff, L. I. "Quantum Mechanics," First ed., p. 168, McGraw-Hill, New York, 1949.
- (16) Varlashkin, P. G., Thompson, J. C., *J. Chem. Phys.* **38**, 1974 (1963).
- (17) Yost, D. M., Russell, H., "Systematic Inorganic Chemistry," p. 142, Prentice Hall, Englewood, 1946.
- (18) Ziman, J. M., "Electrons and Phonons," Clarendon Press, Cambridge, 1960.
- (19) Ziman, J. M., "Principles of the Theory of Solids," Cambridge University Press, Cambridge, 1964.
- (20) Ziman, J. M., *Phil. Mag.* **6**, 1013 (1961).

RECEIVED May 3, 1965. Supported by the Office of Naval Research and the R. A. Welch Foundation.

The Volume Expansion of Alkali Metals in Liquid Ammonia

WILLIAM H. BRENDLEY, JR. and E. CHARLES EVERS

*Laboratory for Research on the Structure of Matter,
University of Pennsylvania, Philadelphia, Pa. 19104*

The volume expansions of alkali metals in liquid ammonia are discussed in the light of the current available data. Special emphasis is made of the anomalous volume minimum found with sodium-ammonia and potassium-ammonia solutions. Recent studies of potassium in ammonia at -34° C. were found to exhibit a large minimum in the volume expansion, ΔV , vs. concentration curve. The results of these findings were compared with the previous results of potassium in ammonia at -45° C. The volume minimum was found to be temperature dependent in that the depth of the minimum increased and shifted to higher concentrations with increasing temperature. No temperature effect was observed on either side of the minimum. These findings are discussed in light of the Arnold and Patterson and Symons models for metal-ammonia solutions.

Solutions of alkali metals in liquid ammonia at all concentrations, with the exception of cesium, are less dense than either of the constituents. This behavior for metal ammonia solutions is unique in that the expansion in volume is much larger than that shown on forming solutions of normal electrolytes or non-electrolytes.

In very dilute metal solutions where dissociation is considered complete, the alkali metal ion is considered to be a normal solvated ion, as in electrolytic solutions, and it is generally conceded that the large volume change is to be ascribed chiefly to the solvated electron. As the concentration is increased it is quite obvious from conductance and magnetic data that metal ions interact with electrons to form some sort of an ion pair and also that electrons couple to form spin-paired species. The manner in which these species form is not entirely clear, nor is their

structure, but there is still an expansion in volume which exceeds the volume of solvent plus metal. The effect also persists at high metal concentrations where the solutions exhibit unquestionably metallic properties. However, the volume expansion is not uniform on going from extremely dilute solutions to saturation. In the case of sodium and potassium solutions, a pronounced minimum is found in the region of concentration where the conductance passes through a minimum, and a maximum is observed in the volume change at high metal concentration.

A large volume expansion for solutions of sodium in ammonia was first reported by Kraus and Lucasse (17). Since this initial report, many investigations have been made of the volume expansion for a number of alkali metal-ammonia solutions. The techniques employed in these investigations have varied from density measurements for concentrated solutions using the Westphal Balance or Pycnometer to dilatometric studies for dilute solutions, which measure the volume expansion directly.

The volume expansion per gram atom of metal, ΔV , as used in this report, will be defined as:

$$\Delta V = \frac{V_{\text{soln.}} - [V_{\text{NH}_3} + V_{\text{metal}}]}{\text{gram-atom metal}}$$

where V_{NH_3} is the volume of the liquid ammonia in the solution at the temperature studied, V_{metal} is the volume of the metal, and $V_{\text{soln.}}$ is the volume of the solution. One might also express the data in terms of the apparent molar volume of metal. In this case the volume change would be computed as the volume of solution, $V_{\text{soln.}}$, minus the volume of ammonia, V_{NH_3} , per gram atom of metal. While either method may be used, we feel the former is more appropriate since we do not know the partial molar volumes of the constituents. Owing to the metastability of the metal-ammonia solutions, meticulous and detailed experimental procedures are discussed in great detail in the doctoral dissertation of Brendley (3) and in the book, "Metal-Ammonia Solutions" (7).

A brief summary of the data from various sources will be presented below and some of these data will be discussed in more detail in a following section.

Lithium

Lithium, the smallest atom in Group I of the periodic table, exhibits the largest volume expansion of the alkali metals in liquid ammonia. Johnson, Meyer, and Martens (14) studied the density of lithium solutions at -33.2°C . They reported a maximum in the volume expansion *vs.* concentration curve at 1.262*N*. The ΔV value at the maximum is 46.59 cc./gram-atom. Gunn and Green (10) have reported volume changes for lithium in ammonia at 0°C . The volume change results of Gunn at 0°C . are much lower than the volume change data of Johnson at -33°C . The results of these investigations are plotted in Figure 1. It should be noted that a line has been drawn through the points obtained

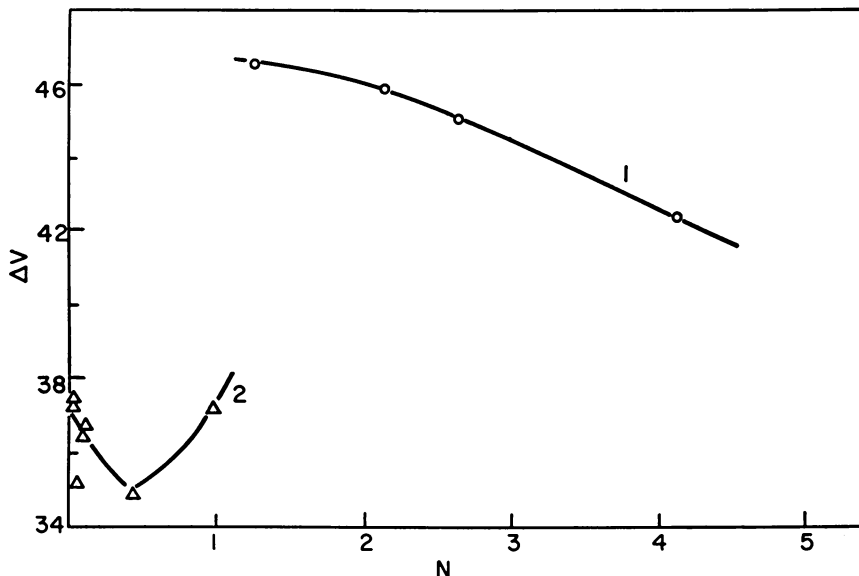


Figure 1. A comparison of the temperature effect on the volume change for lithium in liquid ammonia as a function of concentration

Curve 1—○—Johnson, Meyer, Martens at -33.2°C ., curve 2—△—Gunn and Green at 0°C .

dilatometrically by Gunn and Green. It would seem that a shallow minimum in the curve occurs at $0.408N$.

Sodium

Sodium has been the subject of extensive volume change investigations. Figure 2 presents the volume change *vs.* concentration curve for many of these studies. Kraus' results (18) (curve 6) shows the volume expansion passes through a maximum at approximately $2.9N$ at -33°C . The ΔV value at the maximum is 44.98 cc./gram-atom. This value is near the same concentration as the high ΔV value reported by Huster (12) (curve 4) from rather scanty data. Curve 7 and curve 3 are plots of the data reported by Kikuti (16) at -30°C . and 0°C ., respectively. Curve 5 is a plot of the data of Johnson and Meyer (15) at -33°C .; curve 2 is that of Gunn and Green (10) at 0°C . Kikuti's data (curve 3), obtained at higher concentrations, has been extended by a dotted line to meet Gunn's results at lower concentrations. This extrapolation seems to indicate a weak minimum in the curve at 0°C . which covers a fairly wide concentration range.

Curve 1 is a plot of data from the investigation of Filbert (8) at -45°C . Filbert's results show a pronounced minimum in the volume expansion *vs.* concentration curve at $0.04N$. The ΔV value at the minimum is 30 cc./gram-atom as compared with the limiting value of approximately 42 cc./gram-atom at infinite dilution.

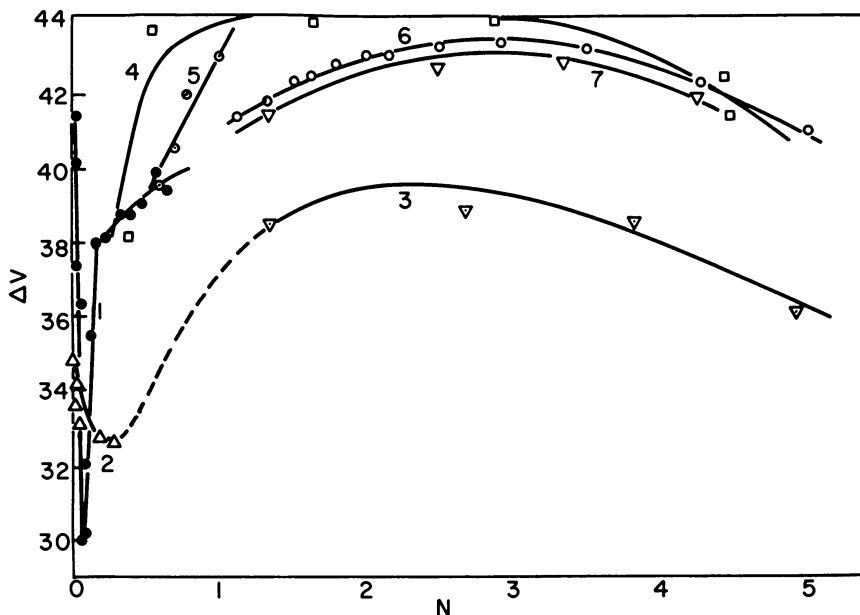


Figure 2. A comparison of the effect of temperature on the volume change for sodium in liquid ammonia as a function of the concentration

- | | |
|--|---|
| ● Filbert at -45°C .—curve 1 | □ Huster at -33°C .—curve 4 |
| ○ Kraus at -33°C .—curve 6 | △ Gunn and Green at 0°C .—curve 2 |
| ○ Johnson and Meyer at -33°C .—curve 5 | ▽ Kikuti at -30°C .—curve 7 |
| | ▽ Kikuti at 0°C .—curve 3 |

Figure 3 is the volume change *vs.* concentration curve for sodium in ammonia in the dilute and transition concentration region. This figure includes the data of Filbert and Orgell (21) (open circles) which confirms the minimum. The data of Filbert and of Gunn and Green at -45°C . are presented in Figure 4.

Potassium

Potassium in liquid ammonia exhibits a maximum in the volume expansion *vs.* concentration curve at 3.16N. The ΔV value at the maximum is 29.62 cc./gram-atom. Figure 5 shows some of the investigations for the potassium-ammonia system. Curve 4 is the data of Johnson and Meyer at -33.8°C . Curve 1 is the data of Orgell (21) at -45°C . Curves 2 and 3 are the investigations of Hutchison and O'Reilly (13) at -33° and 0°C ., respectively. The results of Hutchison and O'Reilly at the two temperatures again indicate that the volume expansion at the higher temperature is below that of the volume change at the lower temperature. Figure 6 is the volume change *vs.* concentration data on an expanded scale for the dilute and transition concentration range. Curve 4 is the data of Hutchison and O'Reilly (13) for potassium in ND₃ at 0°C . Comparing curve 3 with curve 4 shows that the expansion is

greater in ND_3 . The one point, Δ , in Figures 5 and 6 is the determination of Gunn at 0°C . Figure 7 is the data of Orgell (21) at -45°C . showing the existence of a sharp, narrow minimum for potassium in ammonia. More recently, Brendley and Evers (3) have studied the volume expansion of potassium-ammonia solutions at -34°C . using a dilatometric technique. The results of this investigation are shown in Figure 8. A broad, deep minimum in the volume change *vs.* concentration curve occurs at approximately $0.02N$. The ΔV value at the minimum is approximately 4.0 cc./gram-atom , and the limiting value of ΔV at infinite dilution extrapolates to approximately $26.0\text{ cc./gram-atom}$. Figure 9 is a graph giving a plot of the volume change as a function of the logarithm of the concentration for potassium in ammonia at -34°C . The circles are the dilute and transition concentration region studies of Brendley (3); the triangles are the data of Hutchison and O'Reilly (13), and the squares are data for the more concentrated region studied by Johnson and Meyer (15). Figure 10 compares the effect of temperature on the expansions. The squares represent Orgell's data for potassium-ammonia solutions at -45°C ., and the circles represent the data of Brendley for potassium-ammonia solutions at -34°C . The following conclusions are evident:

(a) The volume minimum is temperature dependent. It appears to shift to higher concentrations with an increase in temperature. The

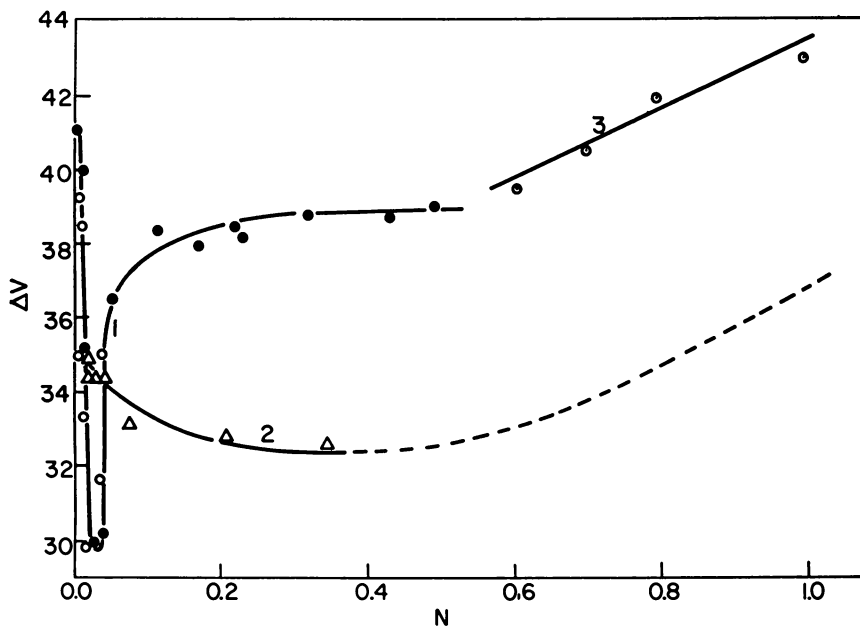


Figure 3. Dilute region, Na in NH_3

● Filbert at -45°C .
○ Orgell at -45°C .

○ Johnson & Meyer at -33°C .
△ Gunn & Green at 0°C .

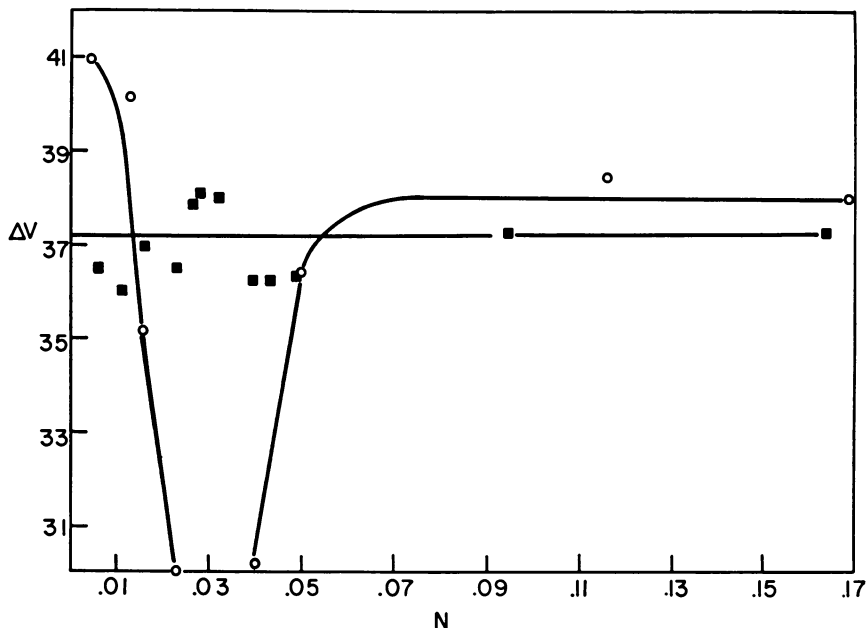


Figure 4. The volume change of sodium in liquid ammonia at -45°C . as a function of the concentration

○ Data of Filbert; ■ Data of Gunn and Green

minimum at -45°C . occurs at $0.01N$, and the minimum at -34°C . occurs at $0.02N$.

(b) The width and depth of the minimum are also affected by temperature. The width of the minimum at -45°C . is very narrow compared to the width of the minimum at -34°C . The depth of the minimum changes from approximately $12.0\text{ cc./gram-atom}$ at -45°C . to approximately 4.0 cc./gram-atom at -34°C . for the potassium-ammonia system. This is a remarkable three-fold increase in the depth of the minimum with only an 11 degree increase in temperature.

(c) Changing the temperature had very little effect on the volume change on either side of the minimum. In both experiments the extrapolated value of ΔV is $26.0\text{ cc./gram-atom}$ at infinite dilution. At concentrations above the minimum the two curves seem to superpose, that is to say, the effect of temperature appears to be rather small in this region.

Cesium

The only investigation of the volume behavior of cesium in ammonia solutions was the density study of Hodgins (11) at -50°C . His results are shown in Figure 11. The expansion at high concentrations is the lowest observed of all the alkali metals. The cesium-ammonia solutions show a continuous decrease of ΔV with concentration from a value of 16 cc./gram-atom at $4.32N$ to approximately 3 cc./gram-atom at $1.23N$.

No maximum is found up to the highest concentration measured. This is roughly what one would expect if the maximum appears at higher concentrations with increasing atomic number.

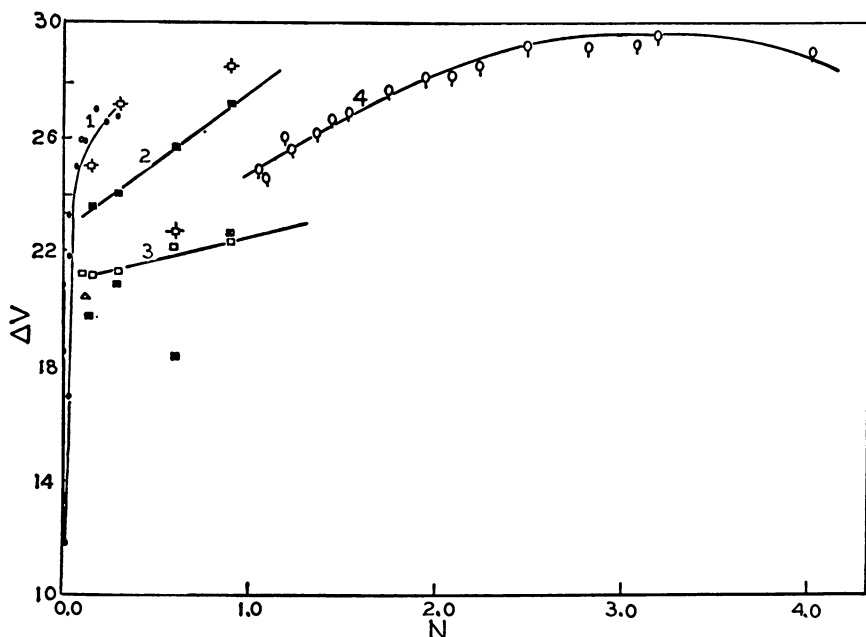


Figure 5. A comparison of the temperature effect of potassium in liquid ammonia

Curve 1—○—Orgell at -45°C .

Curve 2—■—Hutchison and O'Reilly at 33°C .

Curve 3—□—Hutchison & O'Reilly at 0°C .

Curve 4—○—Johnson & Meyer at -33.8°C .

□—Hutchison & O'Reilly, ND_3 at 0°C .

⊠ Hutchison & O'Reilly at 20°C .

△ Gunn & Green at 0°C .

Discussion

A fairly comprehensive review of the information on the volume expansion exhibited by metal solutions may be found in the paper of R. Catterall (4). Our purpose here is to emphasize our most recent work on these solutions, namely, to discuss the expansion studies of potassium in liquid ammonia at -34°C . and to compare these results with the earlier investigations obtained at -45°C .

It is observed from Figure 12 that at infinite dilution the apparent molar volume of all alkali metals in ammonia approach roughly the same value. This suggests complete dissociation of metal into metal ions and solvated electrons as has been demonstrated by conductivity and other measurements. As we continue to increase the concentration from infinite dilution, a rather peculiar phenomenon has been shown to occur

with sodium and potassium solutions. In a narrow concentration region the volume expansion decreases rapidly, passes through a minimum, and increases again. This minimum was totally unexpected and does not agree with the present data from optical measurements (9). Three independent investigations have found a volume minimum for sodium and potassium at different temperatures. No model proposed to date can adequately explain this phenomenon.

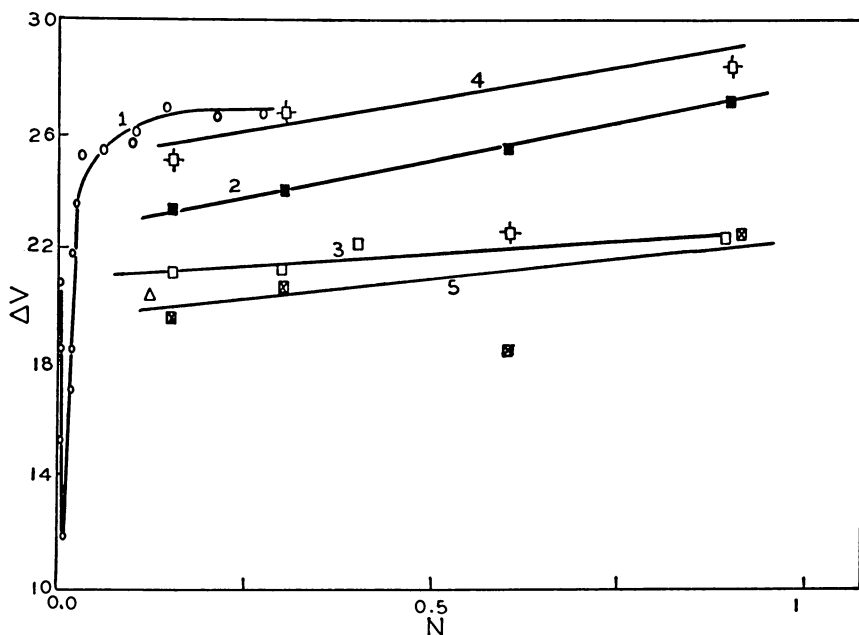


Figure 6. Comparison of volume change for potassium in liquid ammonia (dilute & transition concentration region)

Curve 1—○—Orgell at 45°C.

Curve 2—■—Hutchison & O'Reilly at -33.2°C.

Curve 3—□—Hutchison & Reilly at 0°C.

Curve 4—◻—Hutchison & O'Reilly in ND_3 at 0°C.

Curve 5—◻—Hutchison & O'Reilly at 20°C.

△ Gunn & Green at 0°C.

Let us again review the previous findings for the volume expansion of sodium and potassium in liquid ammonia. Filbert (8) reported a volume minimum for sodium in ammonia at -45°C . at approximately $0.03N$. Orgell (21) confirmed the existence of this minimum for sodium in ammonia at -45°C . and extended his study to potassium in ammonia at the same temperature. Potassium-ammonia solutions were found to exhibit a minimum at $0.01N$ which was quite sharp and not nearly as broad as the minimum for sodium at -45°C . More recently, Brendley has investigated the volume expansion of potassium in ammonia at -34°C . Once again a pronounced minimum was found. The potassium data at -45°C . and -34°C . showed differences in the position and

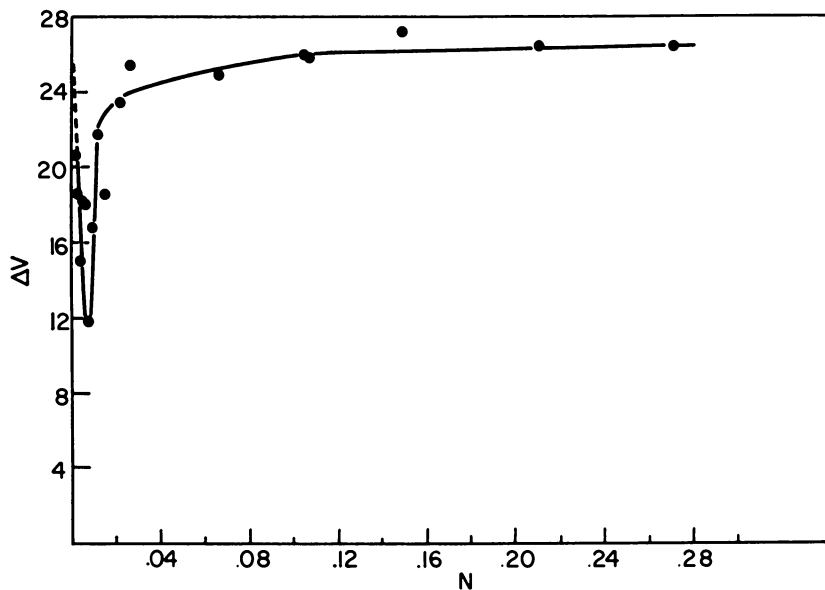


Figure 7. Volume expansion of potassium in liquid ammonia at -45°C . (data of Orgell)

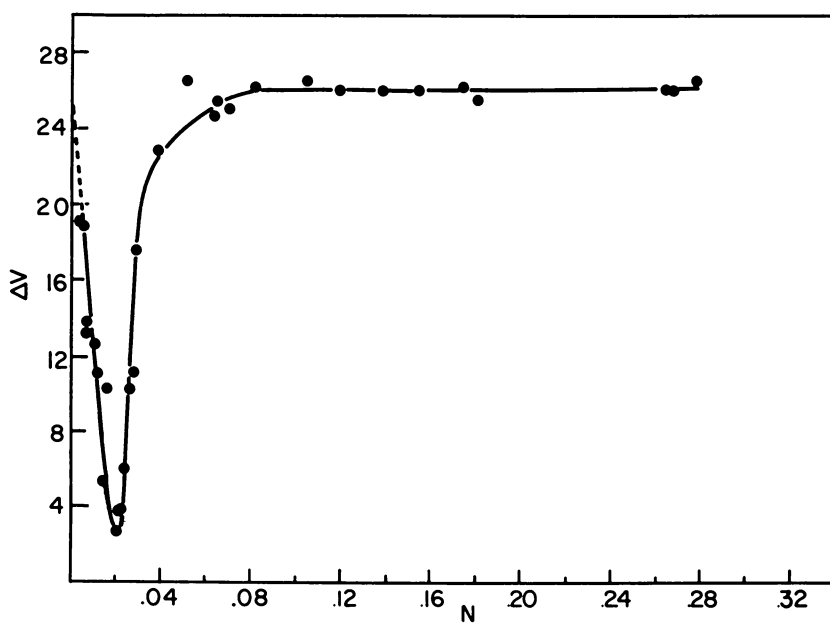


Figure 8. The volume expansion of potassium in liquid ammonia at -34°C . (data of Brendley)

depth of the volume minimum, but the values of the volume expansion on either side of the minimum were nearly the same as shown in Figure 10. Increasing the temperature from -45°C . to -34°C . caused the minimum to shift to higher concentrations, going from $0.01N$ to $0.02N$. The increase in temperature also caused a three-fold increase in the depth of the minimum. Orgell reported a minimum ΔV value of approximately 12 cc./gram-atom at -45°C ., while Brendley found a minimum ΔV of approximately 4 cc./gram-atom at -34°C . The depth of the minimum may also be defined in terms of the deviation from the almost constant value on either side of the minimum. This gives a deviation of 14 cc./gram-atom at -45°C . and 22 cc./gram-atom at -34°C . for a ratio of 1.5.

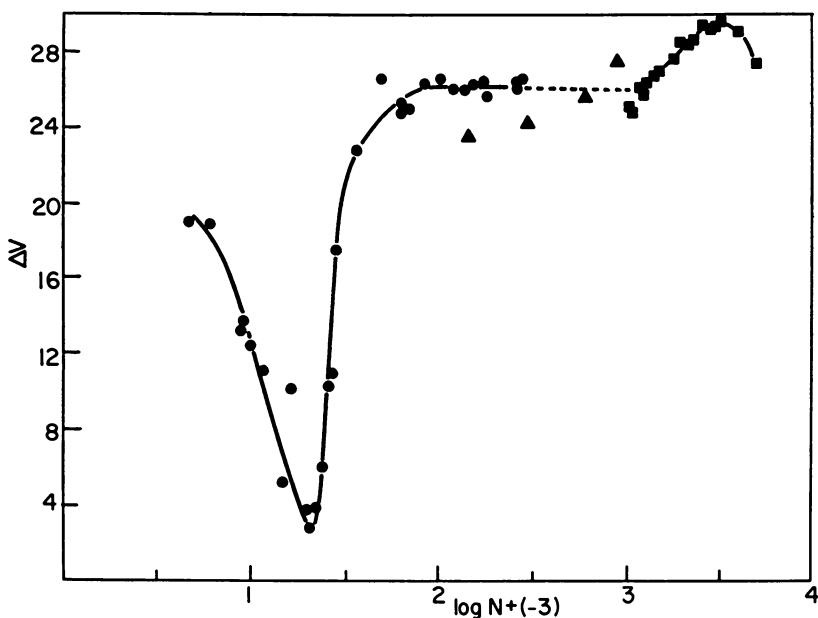


Figure 9. A comparison of the volume expansion of potassium in liquid ammonia as a function of the logarithm of the concentration

●—Brendley at -34°C .

▲—Hutchison & O'Reilly at -33.2°C .

■—Johnson & Meyer at -33.8°C .

Whatever causes the minimum, it is the electron which is intimately involved—that is, the volume increase depends primarily on the electron. This electron can be the “solvated electron” in its dissociated state or the electron bound in some type of association.

While the conductivity decrease may be explained adequately by the Becker, Lindquist, and Alder model (2), and while the magnetic features may be explained adequately by the cavity model proposed by Ogg (19), neither model will serve to explain all the properties of these solutions.

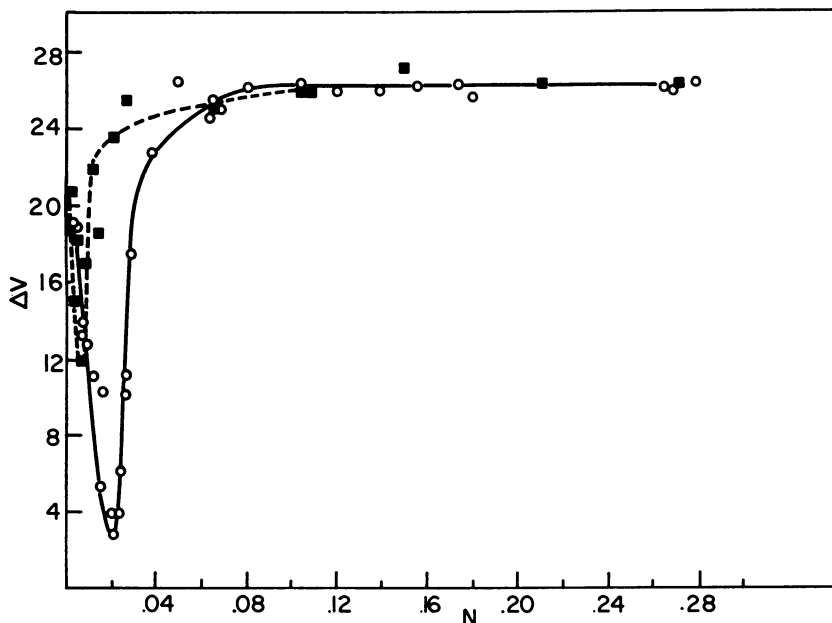
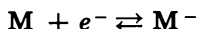


Figure 10. A comparison of the temperature effect on the volume change of potassium in liquid ammonia

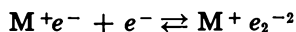
■—Orgell at -45°C ., ○—Brendley at -34°C .

Recently Arnold and Patterson (1) and Symons (22) have introduced new species for their metal-ammonia models. The Arnold and Patterson model employs an equilibrium between a monomer and an electron.

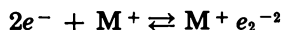


This is a monomer unit associated in some manner with an electron giving a diamagnetic species. The Arnold and Patterson model, obtained from theoretical considerations, helps to reconcile the magnetic and conductance data of metal-ammonia solutions.

Symons and Catterall have proposed a confined model for metal



or



solutions based on their recently performed optical and electron resonance studies.

Either the equilibria of Arnold and Patterson or Symons and Catterall could explain the large decrease in the volume occupied by electrons, because the electron center would now contract. The confined species of Symons and Catterall occurs in a narrow, critical concentration region and is found to shift to higher concentrations with increasing temperature. It is interesting to note that recently O'Reilly (20) has found that the

Knight shifts for the metal nucleus in metal-ammonia solutions are not interpretable in terms of the two equilibria of the Becker, Lindquist, and Alder Model, but can be accommodated by an equilibrium of the type:



where M^- is either the species of Symons' confined model or that proposed by Arnold and Patterson. It seems inconceivable to neglect the existence of this species in light of the recent evidence supporting it.

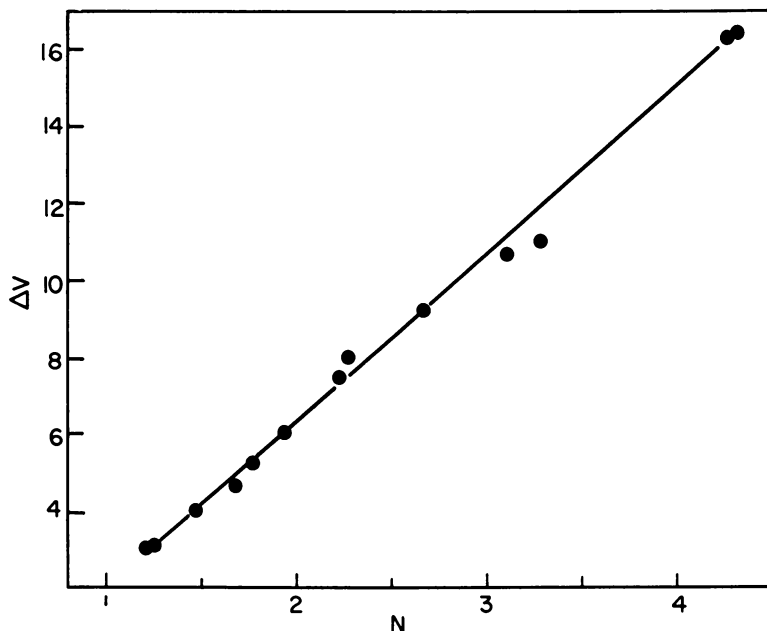


Figure 11. The volume change of cesium in liquid ammonia at -50°C . (data of Hodgins)

Another interesting observation is the change in the depth of the volume minimum with an increase in temperature as found with potassium solutions. It might be expected that ion-clustering would be favored over some type of e_2 centers at higher temperatures and hence, a shallower minimum. However, Catterall and Symons (5) have found that the electron-iodide interaction is stronger at higher temperatures than at lower ones. This would imply a higher concentration of e_2 centers relative to spin-paired separate electrons in a quadrupolar state and hence, a deeper depth in the minimum at higher temperature.

Intuitively, one may feel that the electron becomes associated with the metal cation as the concentration is increased, and further increase in concentration may cause the formation of e_2 centers. O'Reilly (20) has recently found that rubidium and cesium solutions are markedly less spin-paired than lithium, sodium, or potassium. This may suggest that

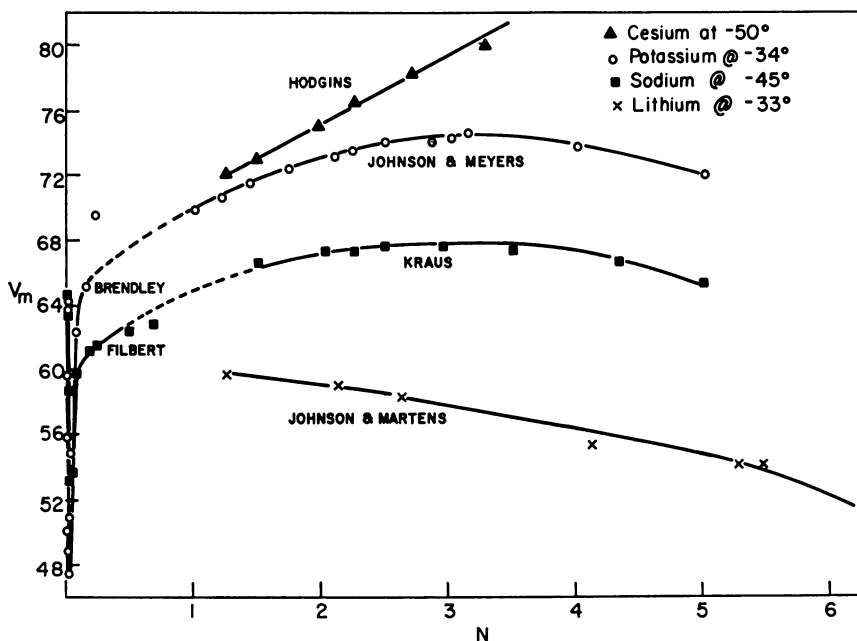


Figure 12. The apparent molar volumes of alkali metals in liquid ammonia

Table I. Volume Minima of Alkali Metals in Ammonia

Metal	Temperature	V_{\min} Conc.	Investigator
Na	-45°	0.03N	Filbert
K	-45°	0.01N	Orgell
K	-34°	0.02N	Brendley
K	0°	0.06N	Theoretical*
K	25°	0.14N	Calculations of Catterall

* Reference (6)

Table II. Comparative Data for the Alkali Metals in Liquid Ammonia

Metal	Conc. at Saturation	ΔV at Saturation	Conc. at Maximum	ΔV Maximum	ΔV Minimum	ΔV Infinite Dilution
Lithium ^a	7.58	34.18	1.26	46.59	35 ^b	46
Sodium ^a	5.01	41.97	2.96	44.98	30	42 ^c
Potassium ^a	5.09	27.28	3.16	29.62	12, ^c 4 ^d	26 ^{a,d}
Cesium ^e	—	—	4.32*	16.40*	—	—

^a at -33° C.

^b at 0° C.

^c at 45° C.

^d at -34° C.

^e at -50° C.

* Maximum value reported

a minimum in the volume change *vs.* concentration curve would occur at higher concentrations.

Table I is a composite of the actual observed volume minima for alkali metals in ammonia and the theoretical calculations made for the temperatures, 0° C. and 25° C.

Table II is a summary of some of the comparative data for alkali metal-ammonia solutions.

We have attempted to review briefly the volume expansion work and to introduce our most recent experimental findings. Needless to say we have not arrived at a theoretical model to explain the anomalous volume expansion behavior. It has been our objective to stimulate and whet the experimental and theoretical appetites of others to pursue a logical deduction and interpretation of these findings.

Literature Cited

- (1) Arnold, E., Patterson, A. J., *J. Chem. Phys.* **41**, 3089 (1964).
- (2) Becker, E., Lindquist, R. H., Alder, B. J., *J. Chem. Phys.* **25**, 971 (1956).
- (3) Brendley, W. H., Doctoral Dissertation, Univ. of Penna., 1965.
- (4) Catterall, R., "Metal-Ammonia Solutions," p. 41-48, Benjamin Press, New York, 1964.
- (5) Catterall, R., Symons, M. C. R., *J. Chem. Soc.* **1964**, 4342.
- (6) Catterall, R. to Brendley, W., Private Communication (1964).
- (7) Evers, E. C., Orgell, C. W., Filbert, A. M., "Metal-Ammonia Solutions," p. 65-75, Benjamin Press, New York, 1964.
- (8) Filbert, A. M., Doctoral Dissertation, Univ. of Penna., 1962.
- (9) Gold, M., Jolly, W. L., Pitzer, K. S., *J. Am. Chem. Soc.* **84**, 2264 (1962).
- (10) Gunn, S. R., Green, L. G., "Apparent Molar Volume of Salts and Metals in Liquid Ammonia at 0° C.," UCRL-6432 (1961).
- (11) Hodgins, J. W., *Can. J. Res.* **27B**, 869 (1949).
- (12) Huster, E., *Ann. d. Physik* **33**, 477 (1938).
- (13) Hutchison, C. A., O'Reilly, D. E., *J. Chem. Phys.* **34**, 163 (1961).
- (14) Johnson, W. C., Meyer, A. W., Martens, R. D., *J. Am. Chem. Soc.* **72**, 1842 (1950).
- (15) Johnson, W. C., Meyer, A. W., *J. Am. Chem. Soc.* **54**, 3621 (1932).
- (16) Kikuti, S., *J. Soc. Chem. Ind. (Japan)*, **42**, suppl. binding, 15 (1939).
- (17) Kraus, C. A., Lucasse, W. W., *J. Am. Chem. Soc.* **43**, 2538 (1921).
- (18) Kraus, C. A., Carney, G. S., Johnson, W. C., *J. Am. Chem. Soc.* **49**, 2206 (1927).
- (19) Ogg, R. A., *Phys. Rev.* **69**, 668 (1946).
- (20) O'Reilly, D. to Catterall, R., Private Communication (1964).
- (21) Orgell, C. W., Doctoral Dissertation, Univ. of Penna., 1962.
- (22) Symons, M. C. R., Blandamer, M. J., Catterall, R., Shields, L., *J. Chem. Soc.* **1964**, 4357.

RECEIVED May 13, 1965. Supported in part by the National Science Foundation and in part by the Laboratory for Research on the Structure of Matter, University of Pennsylvania.

Spectroscopy of Dilute Metal-Deuteroammonia Solutions

D. F. BUROW and J. J. LAGOWSKI

Department of Chemistry, The University of Texas, Austin, Tex.

The spectra of dilute solutions of lithium, sodium, potassium, calcium, and barium in liquid deutero-ammonia indicate that the absorbing species is the same in each case. The dependence of the shape, intensity, and energy of the absorption band on temperature was investigated for sodium-ND₃ solutions. The data are discussed in terms of the electron-in-a-cavity model. No spectral evidence was found for the presence of new species in ND₃ solutions containing mixtures of sodium and sodium iodide.

The properties of solutions of the active metals in liquid ammonia depend strikingly upon concentration. The more concentrated systems have a bronze color and have been described as pseudo-metals; on the other hand, the more dilute solutions have a very intense blue color. There seems to be little doubt that the properties of the more dilute solutions arise, not from the dissolved metal species, but from some ill-defined species which is best described (18) as a "solvated electron." Numerous investigators have attempted to describe the properties of these dilute solutions on the basis of models of the solvated electron which fall into two general categories: the cavity model (15, 21) and the expanded metal model (1). Spectroscopic methods appear to offer a relatively unambiguous means of studying these solutions since many substances (—e.g., metallic electrode surfaces) appear to catalyze the decomposition of metal-ammonia solutions into the corresponding amide. The intense blue color associated with the dilute solutions immediately suggests that they absorb radiation in the red or infrared region of the spectrum. Jolly and his co-workers (9, 10) and Douthit and Dye (6), who have made quantitative measurements on dilute solutions in this spectral region, report that solutions in the concentration range 10^{-1} to $10^{-3}M$ possess an intense ($\epsilon \sim 4 \times 10^4$) broad absorption band with a maximum near 15,000 Å. A shift in the band maximum to higher energy

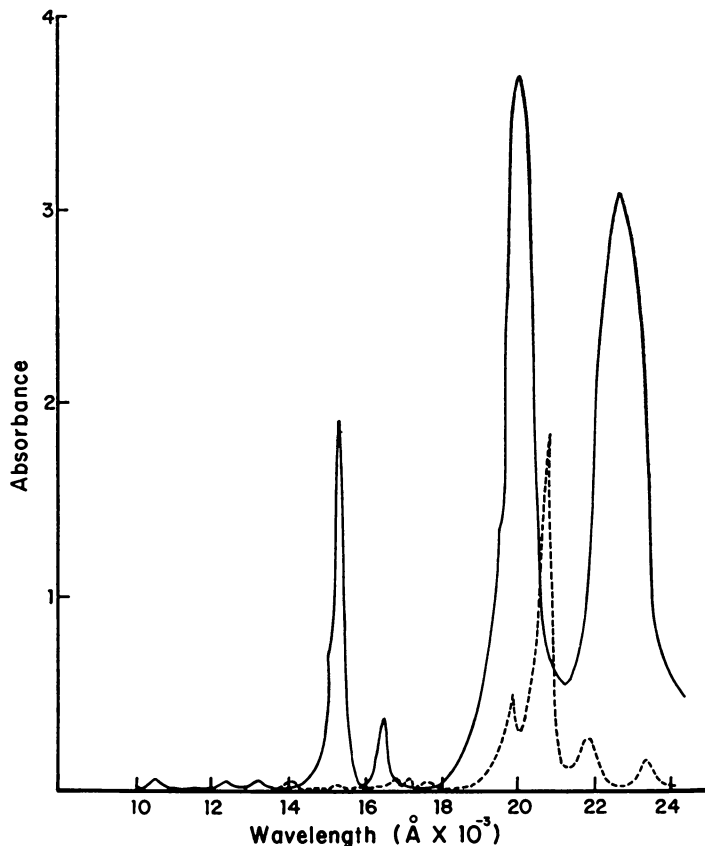


Figure 1. The spectra of liquid NH_3 (—) and liquid ND_3 (---) determined with a one mm. path length cell at -70°C .

has been reported (9, 22) for sodium-ammonia solutions in the presence of sodium iodide. However, the existence of a second band centered at about 12,500/cm. (8000 Å.) for sodium-ammonia solutions containing sodium iodide, and attributed to the formation of a metal ion-iodide ion-paired species which contains the solvated electron (3, 22), has not been substantiated (6, 9, 10).

The primary goal of this investigation was the spectrophotometric characterization of the "solvated electron" in very dilute ND_3 solutions. Since the occurrence of equilibria between the solvated electron and various other species might accentuate ambiguities in interpreting measurement results on more concentrated solutions, absorption data have been obtained on solutions that are an order of magnitude less concentrated than those previously reported (6, 9, 10). An absorption cell with a path length of approximately 1 mm. is the most convenient to use with metal solutions in the concentration range 10^{-4} to $10^{-6}M$.

Unfortunately, liquid ammonia possesses a very intense absorption band at 15,320 Å. ($2\nu_1$ and/or $2\nu_3$) so that this region is inaccessible for quantitative measurements even with a 1 mm. cell. If ND_3 is used as the solvent instead of NH_3 , no intense overtone or combination bands of the solvent occur in the spectral region of interest (Figure 1). The spectra of dilute solutions of lithium, sodium, potassium, calcium, and barium in liquid ND_3 , and the perturbations arising from concentration changes, temperature changes, and the presence of "inert" salts have been investigated.

Experimental

Spectra were determined with a Cary Model 14 recording spectrophotometer using a specially constructed vacuum-jacketed, strip-silvered, dewar system incorporating a 1.07 mm. path length optical cell with silica windows (Figure 2). Neutral density screens designed for use with the Cary Model 14 were calibrated and used in the reference beam of the spectrophotometer for solutions with an absorbance greater than 2. The exterior silica windows were attached to the ground glass flanges of the dewar with picein sealing compound, and the lower portion of the dewar system was embedded with polyurethane foam in an aluminum box designed to fit snugly in the sample compartment of the spectrometer. After evacuating the dewar jacket with an oil diffusion pump overnight, the vessel could be used for several weeks without condensation forming on the outer windows. The temperature of solutions in the cell was monitored with a tissue implantation thermistor (Yellow Springs Instruments) calibrated against the vapor pressure of pure ammonia.

Small samples of metal and salts were introduced into the cell with the aid of a winch mechanism (Figure 3a), care being taken to keep the nylon line from prolonged immersion in the solutions. Large samples of salt were introduced into the cell using the apparatus shown in Figure 3b. Either the winch or the salt delivery system was attached to the optical dewar at point "A" of Figure 2 and could be taken into a helium-filled dry box fitted with a vacuum entry port. The atmosphere in this box was equilibrated with a liquid sodium-potassium alloy and was periodically circulated through an activated charcoal trap immersed in liquid nitrogen. (All the alkali and alkaline earth metals except rubidium have been handled in this dry box with little or no observable reaction on freshly cut surfaces.) Samples were weighed in the dry box with a Cahn Electrobalance, Model M-10.

Deuteroammonia was prepared by the reaction of D_2O with Mg_3N_2 . The latter compound was prepared by passing dry prepurified nitrogen over reagent grade magnesium heated to 1100°C . in a vacuum-tight steel pipe. The powdered Mg_3N_2 was placed in a clean dry lecture bottle and heated *in vacuo* at 400°C . to decompose any $\text{Mg}(\text{OH})_2$ formed during the preparation of the nitride. The cylinder was then filled with helium cooled to -196°C . and a deficiency of D_2O (deuterium content, 99.5%) was introduced with a syringe. After several days at 25°C . the reaction was complete, and the ND_3 was transferred to a storage cylinder. Analysis of the ND_3 by infrared and NMR spectroscopy and by mass spectrometry indicated that less than 2% hydrogen was present.

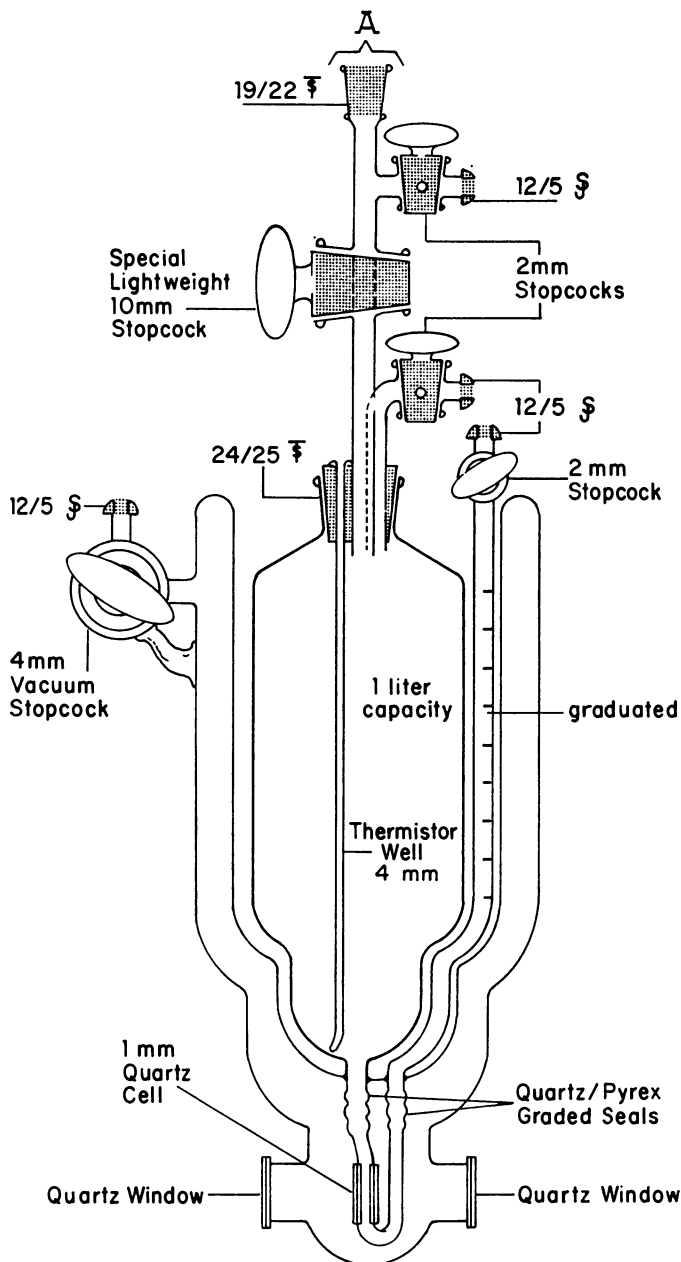


Figure 2. Spectrophotometric Dewar system.

The ammonia was commercial refrigeration grade which was distilled into and stored in small stainless steel cylinders containing sodium metal, from which it was distilled as necessary. The ammonia used in

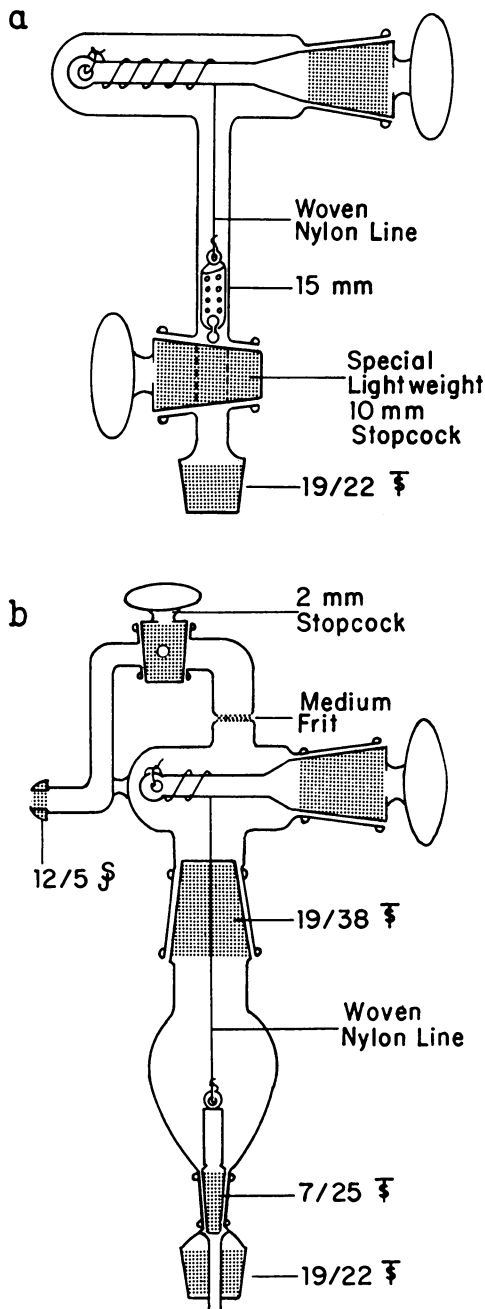


Figure 3. (a) Winch mechanism. (b) Salt delivery assembly.

these experiments was redistilled from sodium in the vacuum system immediately prior to use.

Sodium and potassium were distilled into ampoules and stored in the dry box. Lithium and the alkaline earth metals were the best grade available commercially and were used without further purification. Reagent grade sodium iodide was dried at 300°C. *in vacuo*, recrystallized from anhydrous liquid ammonia, and heated to 200°C. *in vacuo* prior to use. The recrystallization procedure eliminated the rapid fading of dilute sodium-ammonia solutions containing sodium iodide which had been dried in the conventional manner.

A special cleaning procedure was developed which virtually eliminated the characteristic decomposition of dilute metal-ammonia solutions. The optical cell was evacuated with a diffusion pump for several hours, about 50 ml. of anhydrous ammonia condensed onto the walls of the apparatus, and this wash ammonia was forced into a waste flask containing sodium and cooled with dry-ice. The optical cell was rinsed a total of four times. Approximately 500 ml. of anhydrous ammonia was condensed into the cell, about 5 mg. of potassium was introduced into the cell with the winch assembly (Figure 3a), and the solution was allowed to remain in the cell for at least 48 hours. The metal-ammonia solution was then forced from the cell into the waste flask; the cell was rinsed four times with anhydrous ammonia and evacuated before introducing ND₃.

Discussion

The unique properties of dilute metal-ammonia solutions depend not upon the nature of the metal species, but upon the solvated electron common to all these solutions. Thus, the electron-in-a-cavity model (17, 19, 21) seems best suited to describe the species present in these solutions since the model is independent of the type of cation present. Jortner and his associates (15, 16) have extended this model by assuming that the cavity arises from polarization of the medium by the electron. The energy levels of the bound electrons are obtained by using a potential function containing the static and optical dielectric constants of the bulk medium as parameters. Using one-parameter hydrogen-like wave functions for the first two bound states of the electron, the total energy of the *i*th state is expressed as

$$E_i = W_i + S_i'$$

where W_i is the energy of level *i* and S_i' is the energy contribution of the electronic polarization. The absorption band in the near infrared region for metal-ammonia solutions is attributed to a transition between the ground state and the first excited state. Values chosen for the cavity radius close to those deduced from molar volume measurements give the energy of the absorption band, the temperature variation of λ_{\max} , and the heat of solvation of the electron with reasonable accuracy.

Since it appears that the dielectric constant of the medium plays an important role in the existing models for metal-ammonia solutions, and experimental data are not available for the static (D_s) or optical di-

electric constants (D_{op}) of ND_3 , it was necessary either to measure or estimate values for these parameters. The value of D_{op} for H_2O is 1.779 at 20°C . and that for D_2O is 1.764 at 20°C . (13). Hence, the assumption that D_{op} for NH_3 is equal to D_{op} for ND_3 should not introduce a large error into any calculations for the ND_3 system. The static dielectric constant of liquid ND_3 as a function of temperature was measured using the heterodyne beat method (4) at 500 kilocycles; the values obtained are given in Table I. Temperature control was accomplished by using standard slush baths, and the temperature of the system was obtained from the vapor pressure of ND_3 .

It was essential that the apparatus be cleaned by the procedure described in the experimental section before quantitative optical measurements could be made on the metal-ammonia solutions. Significant decomposition arises from reaction of the metal solution with water adsorbed on the surface of the glass (23); a similar phenomenon was observed for solutions of strongly basic species in liquid ammonia (5). The rinsing and aging procedure apparently replaces adsorbed water and/or hydroxyl species on the surface of the glass with ammonia. Removing the rinse-ammonia from the cell by distillation rather than as liquid was a noticeably less effective procedure. Since the surface of the cell became contaminated quickly on exposure to the atmosphere with species that react with the metal solutions, it would appear that removing water molecules by displacement with less polar ammonia molecules proceeds more slowly than the reverse process. After a cell had been cleaned by this procedure, the decomposition rate of a $10^{-6}M$ metal- ND_3 solution was reduced to such a level that no detectable decomposition occurred within 20 hours. Since the aging solutions ($10^{-3}M$ metal in NH_3) retained their deep blue color over a period of 48 hours, this clearly indicates that the NH_3 solutions possess a similar stability.

Table I. Dielectric Constants of Liquid NH_3 and ND_3

$T, ^\circ\text{C}$.	Static dielectric constant	
	NH_3^a	ND_3
-74 ± 1	...	26.0 ± 0.2
-72 ± 1	25.5 ± 0.2	...
-63 ± 1	24.5 ± 0.2	25.0 ± 0.2
-50 ± 1	23.3 ± 0.2	23.8 ± 0.2
-45 ± 1	22.7 ± 0.2	23.1 ± 0.2
-37 ± 1	21.8 ± 0.2	22.1 ± 0.2

^a The following static dielectric constants have been reported for NH_3 : 25 at -77.7°C . (11), 23.8 at -50°C . (8), 22.5 at -40°C . (8), 22.4 at -33.4°C . (11), and 22 at -33°C . (13).

Ordinarily, high temperature and ultraviolet radiation seem to promote the decomposition of metal-ammonia solutions. However there is evidence that these factors merely accelerate decomposition which was initially begun by catalytic amounts of contaminants on the walls of the containers. A silica tube was rinsed with liquid ammonia, the rinse-ammonia removed by evaporation, and the tube evacuated; a concentrated blue metal-ammonia solution ($\sim 1M$) was prepared in the tube,

and the tube sealed. After four weeks irradiation under intense ultra-violet light at 35° C. the solution faded; in similar tubes which had not been rinsed with ammonia the solutions faded within a few days. It appears that metal-ammonia solutions are more stable than previously reported.

The spectra of solutions of lithium, sodium, potassium, calcium, and barium in liquid ND₃ (Figure 4) in the concentration range 5 – 50 × 10⁻⁶M are identical within experimental error, indicating that the absorbing species is the same in each case. The only absorption band present occurs at 13,800 Å. (7246/cm.) at -70° C. for the concentration range investigated (Figure 4). As with NH₃ solutions, the bands for ND₃ solutions are symmetrical when absorbance is plotted against wave

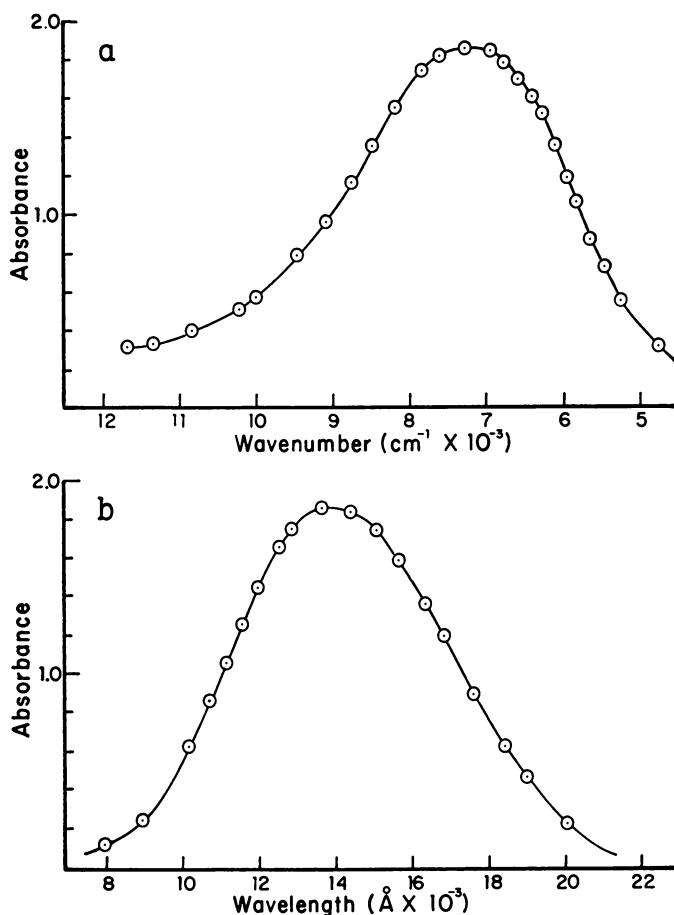


Figure 4. A typical spectrum of a metal-ND₃ solution at -70°C. (3.52×10^{-4} M sodium): (a) absorbance vs. wave number ($\nu_{\max} = 7245/\text{cm.}$); (b) absorbance vs. wavelength ($\lambda_{\max} = 13,800 \text{ \AA.}$).

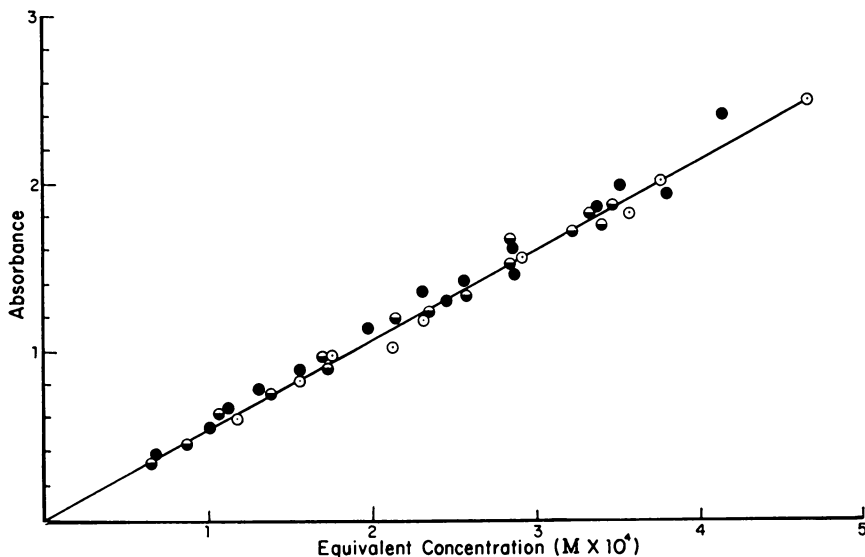


Figure 5. Absorbance vs. concentration for metal-ND₃ solutions at 13,800 Å. at -70°C.: ● lithium; ◐ sodium; ○ barium.

number. The wavelength of the absorbance maximum is independent of concentration within the given range at a given temperature. Douthit and Dye (6) and Jolly *et al.* (14) report that for more concentrated metal-ammonia solutions the maximum absorbance varies with concentration [7100/cm. (14,085 Å.) for 10⁻³M solutions to 6500/cm. (15,380 Å.) for 10⁻¹M solutions] at -65° C. Preliminary measurements made in this laboratory indicate that the absorbance maximum for metal-ammonia solutions of ca. 10⁻⁴M is between 14,000 Å. (7143/cm.) and 14,500 Å. (6896/cm.). Unfortunately these measurements on NH₃ solutions are ambiguous because solvent bands are present. In any event, the absorbance maximum observed for the ND₃ solutions occurs at higher energy than that observed in NH₃ solutions. Preliminary calculations using Jortner's model, appear to indicate that the difference in the energy of transition between NH₃ and ND₃ solutions may be accounted for solely by the difference in the dielectric constants of the two solvents.

The absorbance at the band maximum for solutions of lithium, sodium, and barium in ND₃ is a linear function of the concentration, and extrapolation of the linear function to zero concentration predicts zero absorbance (Figure 5 and Table II). The molar extinction coefficients as calculated by the least squares method for solutions of lithium, sodium, and barium in ND₃ at -70° C. are given in Table II. If it is assumed that barium loses two electrons upon solvation, the molar extinction coefficients of lithium, sodium, and barium solutions are the same to within the estimated error of measurement (4%). The residual absorbance, as calculated from the least squares analysis, in each case is

zero within experimental error. These observations suggest that the species giving rise to the absorption band is not significantly involved in equilibrium processes at these concentrations.

Table II. Molar Extinction Coefficients^a at -70°C . for ND_3 Solutions of Lithium, Sodium, and Barium

	<i>Li</i>	<i>Na</i>	<i>Ba</i> ^b
$\epsilon_{\text{max}}(13,800 \text{ \AA.})$	4.84×10^4	4.99×10^4	5.00×10^4
Absorbance at zero concentration ^c	0.040	0.001	-0.050

^a Calculated by the method of least squares.

^b Assumes barium loses two electrons.

^c Calculated from the least square intercept.

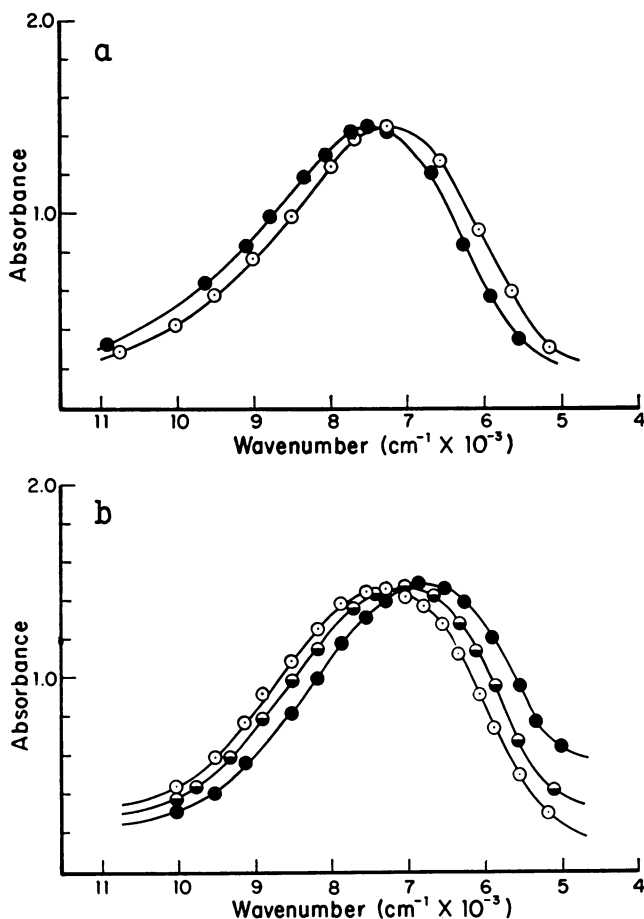


Figure 6. (a) Salt effect on the spectrum of a $2.83 \times 10^{-4} \text{ M}$ solution of sodium in ND_3 at -70°C . (b) Temperature effect on the spectrum of a $2.83 \times 10^{-4} \text{ M}$ solution of sodium in ND_3 at ○ -69°C .; ● -52.5°C .; ● -30.5°C .

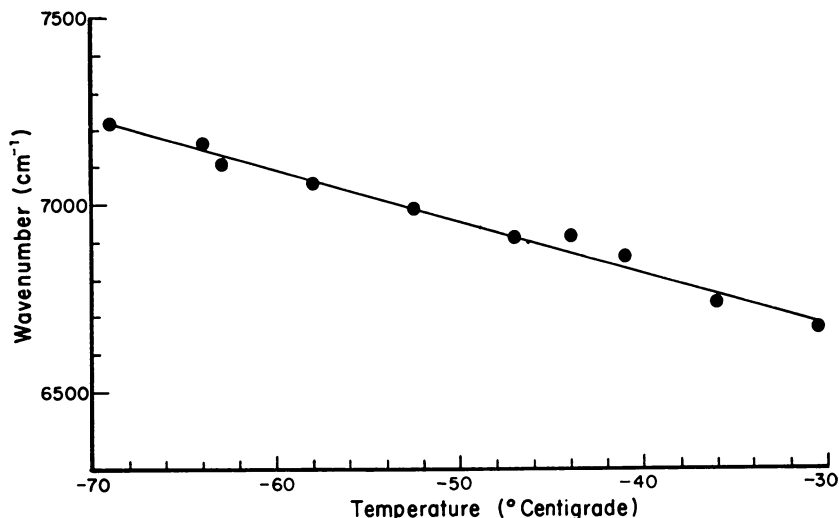


Figure 7. The temperature dependence of λ_{\max} of a $2.83 \times 10^{-4} M$ solution of sodium in ND_3 .

The molar extinction coefficient in ND_3 is about 10% larger than that previously reported for NH_3 solutions (9, 10). Perhaps the density of the solutions could account for the discrepancy since the densities of NH_3 and ND_3 at $-33.7^\circ C.$ are 0.68 and 0.80 g./cc., respectively (12). Since the solutions under consideration are very dilute, their densities are approximately that of the solvent itself. However, the molar volume of the solvent is a more significant parameter since the solvation of the electron would be expected to be the same in each solvent. The molar volume of NH_3 ($-33.7^\circ C.$) is 24.3 cc./mole and that of ND_3 ($-33.7^\circ C.$) is 25.0 cc./mole (12). These quantities differ by only 3% and are in the wrong direction to account for the observed difference in intensity. It is possible that the transition responsible for the absorption is less forbidden in liquid ND_3 than in liquid NH_3 , but the most likely explanation is that some decomposition to amide had already occurred when the measurements in NH_3 were made.

The dependence of the shape, intensity, and energy of the absorption band on temperature was investigated using a $2.83 \times 10^{-4} M$ solution of sodium in liquid ND_3 . The spectrum of this solution at several temperatures is shown in Figure 6b. A plot of the energy of the absorption maximum vs. temperature is shown in Figure 7, and a least squares treatment of these data indicates that the temperature dependence of the band maximum is $-14.3/cm./deg.$ Values of $-9.7/cm./deg.$ for sodium (6), $-9.1/cm./deg.$ for potassium (2), and $-12.7/cm./deg.$ for the alkali metal solutions (9) in liquid ammonia have been reported. No detectable decomposition of the solution occurred during the four hours required to take the measurements between -69° and $-31^\circ C.$ The intensity of the band, as measured by both the absorbance (1.48 ± 0.04)

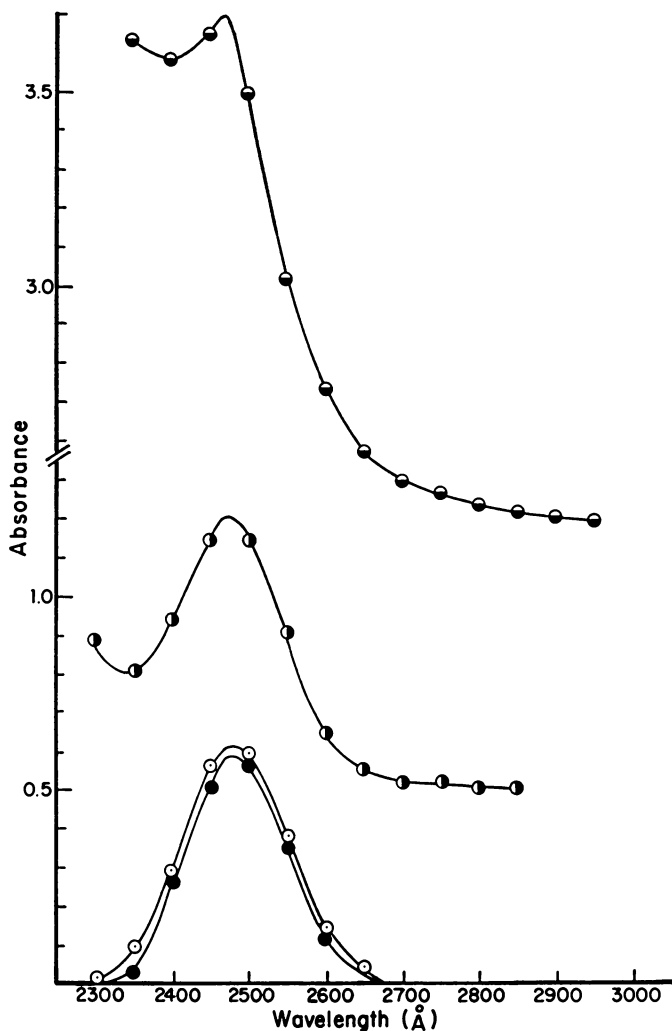


Figure 8. Charge-transfer-to-solvent spectrum of iodide ion in liquid NH_3 : \circ $6 \times 10^{-4} M \text{ NaI}$; \bullet $6 \times 10^{-4} M \text{ NaI}$ and $1.3 \times 10^{-3} M$ sodium; \circ $6 \times 10^{-4} M \text{ NaI}$ and $1.2 \times 10^{-2} M$ sodium; \bullet $6 \times 10^{-4} M \text{ NaI}$ and $9 \times 10^{-2} M$ sodium.

at the maximum and the oscillator strength at each measured temperature, remained constant. The oscillator strength at all temperatures measured was calculated to be $7.7 \pm 0.3 \times 10^{-2}$ using the expression given by Dunn (7). This behavior seems unusual since it might be expected that the change in density of the solvent brought about by a change in temperature would affect the absorbance. Increased molecular vibration at the higher temperatures might be expected to cause band broadening, but the constant oscillator strength suggests that this

is not the case. Preliminary calculations using the cavity model indicate that the change in $\bar{\nu}_{\max}$ with temperature cannot be attributed wholly to the change in the dielectric constant of the medium.

It is generally agreed that the presence of excess "inert" salt in a metal-ammonia solution shifts the center of the absorbance band to higher energy. This phenomenon is also observed in sodium-ND₃ solutions (Figure 6a). Symons (3, 22) observed a shoulder on the high energy side of the absorbance band in sodium-ammonia solutions which contained a large excess of sodium iodide. However, this shoulder was not observed in the spectra of solutions of sodium in ND₃ ($1 - 50 \times 10^{-5}M$) which contained 0.6 - 1.2M sodium iodide. Symons attributes this shoulder to the absorption of a sodium ion-iodide ion-paired species which contains an extra electron, and the formation of such a species might be expected to affect the charge-transfer-to-solvent (CTS) band of the iodide ion in liquid ammonia (20). The CTS transition of the iodide ion in liquid ammonia occurs at approximately 2475 Å. at -70° C. The CTS spectrum of a $6 \times 10^{-4}M$ solution of sodium iodide in liquid ammonia was unchanged as the concentration of sodium metal was varied from 1.3 - $900 \times 10^{-3}M$, except that the background absorbance owing to the presence of sodium increased (Figure 8). We were unable to find spectral evidence for the formation of any new species in liquid ammonia solutions containing mixtures of sodium and sodium iodide in the concentration range indicated.

Literature Cited

- (1) Becker, E., Lindquist, R. H., Alder, B. J., *J. Chem. Phys.* **25**, 961 (1956).
- (2) Blades, H., Hodgins, J. W., *Can. J. Chem.* **83**, 411 (1955).
- (3) Caterall, R., Symons, M. C. R., *J. Chem. Soc.* **1964**, 4343.
- (4) Chien, Jen-Yuan, *J. Chem. Ed.* **24**, 494 (1947).
- (5) Cuthrell, R. E., Ph.D. Dissertation, The University of Texas, 1964.
- (6) Douthit, R. C., Dye, J. L., *J. Am. Chem. Soc.* **82**, 4472 (1960).
- (7) Dunn, T. M., "Modern Coordination Chemistry," J. Lewis and R. G. Wilkins, eds., p. 276, Interscience, New York, 1960.
- (8) Fish, K., Miller, R. C., Smyth, C. P., *J. Chem. Phys.* **29**, 745 (1958).
- (9) Gold, M., Jolly, W. L., *Inorg. Chem.* **1**, 818 (1962).
- (10) Hallada, C. J., Jolly, W. L., *Inorg. Chem.* **2**, 1076 (1963).
- (11) "Handbook of Chemistry and Physics," 41st ed., Chemical Rubber Publishing Co., Cleveland, Ohio, 1959.
- (12) Hutchison, C. A., Jr., O'Reilly, D., *J. Chem. Phys.* **34**, 163 (1961).
- (13) Jolly, W. L., *Chem. Rev.* **50**, 35 (1952).
- (14) Jolly, W. L., Hallada, C. J., Gold, M., "Metal Ammonia Solutions," G. LePoutre and M. J. Sienko, eds., p. 174, Benjamin, New York, 1964.
- (15) Jortner, J., *J. Chem. Phys.* **30**, 839 (1959).
- (16) Jortner, J., Rice, S. A., Wilson, E. G., "Metal Ammonia Solutions," G. LePoutre and M. J. Sienko, eds., p. 222, Benjamin, New York, 1964.
- (17) Kaplan, J., Kittel, C., *J. Chem. Phys.* **21**, 1429 (1953).
- (18) Kraus, C. A., *J. Franklin Inst.* **212**, 537 (1931).
- (19) Lipscomb, W. N., *J. Chem. Phys.* **21**, 52 (1953).
- (20) Nelson, J. T., Cuthrell, R. E., Lagowski, J. J., unpublished results.
- (21) Ogg, R. A., *J. Am. Chem. Soc.* **68**, 155 (1946); *J. Chem. Phys.* **14**, 144 (1946); *Ibid.*, **14**, 295 (1946).
- (22) Symons, M. C. R., *Quart. Rev.* (London) **13**, 99 (1959).
- (23) Warshawsky, I., *J. Inorg. Nuclear Chem.* **25**, 601 (1963).

RECEIVED April 30, 1964. This study was sponsored by the National Science Foundation.

Theoretical Study of Electron Transfer Reactions of Solvated Electrons

R. A. MARCUS

Noyes Chemical Laboratory, University of Illinois, Urbana, Ill. 61803

The assumptions, equations and several applications of a recently formulated theory of electron transfer reactions of solvated electrons are outlined. The relationship of the reorganization terms to those of ordinary electron exchange and electrochemical reactions is described, together with the role played by an effective standard free energy of reaction. Applications include prediction of conditions under which chemiluminescence might be found and description of conditions under which reactions might not be diffusion-controlled.

For purposes of this monograph we summarize the concepts and principal assumptions of an electron transfer theory (5), together with the additional ones used to formulate a treatment of electron transfer reactions of solvated electrons (8). The final equations and several applications are also described, but the detailed mathematical derivation is given elsewhere (8).

Electron Transfer Mechanism

The theory stems from the writer's work on simple electron transfer reactions of conventional reactants (5). A simple electron transfer reaction is defined as one in which no bonds are broken or formed during the redox step; such a reaction might be preceded or followed by bond-breaking or bond-forming steps in a several-step reaction mechanism. Other chemical reactions involve rupture or formation of one or several chemical bonds, and only a few coordinates suffice to establish their essential features. In simple electron transfers in solution, on the other hand, numerous coordinates play a role. One cannot then use the usual two-coordinate potential energy contour diagram (4) to visualize the

course of the reaction, but must resort to some other pictorial method such as the use of profiles of a potential energy surface.

In the postulated mechanism of simple electron transfer reactions, a weak coupling of the "redox orbitals" of the two reactants is assumed (5), and fluctuations of translational, rotational, and vibrational coordinates leading from those characterizing stable configurations of reactants to those describing stable configurations of products is described in terms of potential energy surfaces. A surface for the reactants, plotted *vs.* the many relevant coordinates of the system, intersects one for the products, and a profile of these surfaces is given in Figure 1. The intersection is split in the usual quantum mechanical manner by a coupling of the redox orbitals (5).

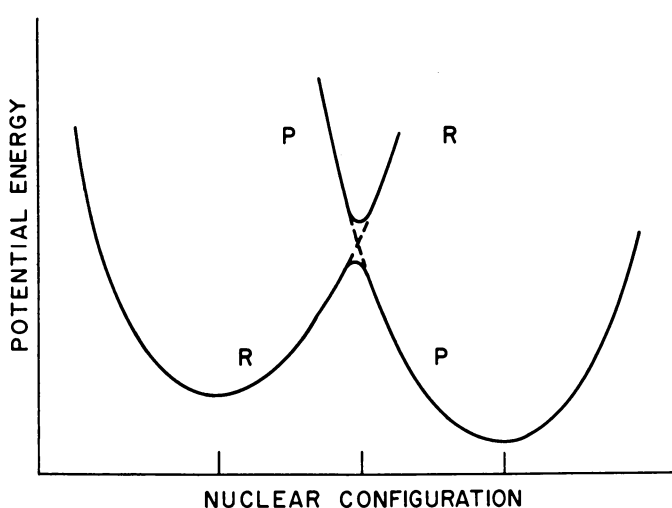


Figure 1. Profile of potential energy surface of reactants (R) and that of products (P) plotted vs. configuration of all the atoms in the system. The dotted lines refer to a system having zero electronic interaction of the reacting species. Each adiabatic surface is indicated by a solid line.

Accordingly, reaction can occur if the system reaches the intersection region during a fluctuation, and if the electronic coupling is large enough to cause the system to remain on the lowest surface during the crossing of the intersection. The configurations occurring at the intersection constitute the "activated complex" for the reaction. They define a hypersurface in this many-dimensional configuration space. The theoretical problem of calculating the reaction rate is largely that of calculating the chance of crossing this hypersurface in unit time. The coordinates undergoing some or appreciable change during the simple electron transfer include the separation distance of the reactants, bond distances in a reactant (those in an inner coordination shell for example), and orientations of solvent molecules. All of these coordinates contribute to

the "reaction coordinate" leading from reactants through activated complex to products.

Special Features for Solvated Electron Reactions

In addition to the above features which electron transfer reactions of solvated electrons and ordinary electron transfers have in common, those of the solvated electron possess several novel aspects:

(1) The electronic wave function of a solvated electron, spread over several solvent molecules, should be very sensitive to orientation fluctuations of these molecules, unlike that of an ordinary reactant.

(2) The solvated electron "disappears" into the other reactant so that there is a change in number of reacting particles.

(3) Unlike many of the conventional electron transfers, many reactions of the solvated electron are diffusion controlled.

Because of (1) the mean kinetic energy of the solvated electron changes appreciably during the orientation fluctuations required for the system to reach the intersection hypersurface. Such changes are included in Figure 1, which represents a plot of the total electronic energy of the system as a function of the atomic coordinates.

Item (2) contributes to the calculated free energy of formation of the product from a system coming from the intersection.

Because of (3), the observed rate constant k_{obs} is given by

$$\frac{1}{k_{\text{obs}}} = \frac{1}{k_{\text{diff}}} + \frac{1}{k_{\text{act}}} \quad (1)$$

where k_{diff} and k_{act} are diffusion-controlled and activation-controlled rate constants. According as $k_{\text{diff}} \gg k_{\text{act}}$ or $k_{\text{act}} \gg k_{\text{diff}}$, k_{obs} equals k_{act} or k_{diff} , respectively (7).

Assumptions

The mathematical derivation of the theoretical expression for k_{act} for solvated electron transfers has been given elsewhere (8). The following assumptions were the principal ones made, of which (a) to (c) are standard in activated complex theory:

(a) The adiabatic (Born-Oppenheimer) approximation is used to treat the electronic-nuclear motion. (In the vicinity of the intersection hypersurface, nonadiabatic effects arise only if the splitting is very small. The factor κ in Equation 2 is then less than unity and is calculated by various nonadiabatic methods. Normally, the reaction is assumed to be adiabatic ($\kappa \sim 1$.)

(b) Classical equilibrium statistical mechanics is used to calculate the probability of reaching the intersection hypersurface. Any vibrational quantum effects which occur are treated approximately in the usual way for activated complex theory.

(c) The rate is given by the number of "first passages" of a system across the intersection surface per unit time.

(d) Highly specific interactions of the two reactants (—e.g., steric effects) are assumed to contribute primarily to the work w required to bring the reactants together.

(e) The solvent polarization (outside any inner coordination shell) caused by the two reactants is treated by dielectric continuum theory. (Statistical mechanics was used for conventional electron transfers and can be used to replace the continuum theory when this refinement becomes appropriate.)

(f) In the hydrogen-bonded solvents of present interest the electron is assumed to be in a cavity-free medium. Arguments were given to suggest that when a solvent cavity for the electron occurs it will primarily affect the numerical value of λ_e^∞ in Equation 3 rather than the functional form of those final equations (8).

In addition, two approximations were introduced (5) which simplified the equations considerably. They are easily avoided as described later. The equations then become more complex.

(g) The vibrations of the second reactant are treated as harmonic oscillators.

(h) A symmetrized vibrational potential energy function is used for reactants and products. The minor error introduced thereby has been estimated elsewhere (5).

A solvated electron in a polar solvent has a high classical frequency of motion in its "orbit." Accordingly, the rotating or librating solvent molecules of the system see it primarily as some diffuse charge distribution. The molecules orient themselves toward this diffuse charge in a way consistent with their thermal motion and with their bonding to other molecules. The valence and inner electrons of these molecules are polarized by the instantaneous field of the solvated electron when they are some distance from the electron. If they are too close to it they cannot follow the motion of the instantaneous field, as uncertainty principle arguments show (8). A quantum mechanical continuum estimate of the radius of this dynamical sphere of exclusion of electron polarization and of the contribution to the interaction energy was made (8). When the radius is small relative to the circumference of the "orbit" of the electron the radius does not influence the numerical value of λ_e^∞ in Equation 3. More refined models for the solvated electron would also recognize any vibronic effects, since the estimated frequency of electronic motion (8) is not far from that of polar OH vibrations of the medium.

Calculation of k_{act}

The rate constant k_{act} is given by Equation 2, on the basis of assumptions (a) to (c) and the introduction of certain comparatively minor approximations (5, A). (In the present paper a reference labelled by a letter refers to a comment in the Appendix.)

$$k_{act} = Z\kappa\rho e^{-\Delta F^*/kT} \quad (2)$$

where ΔF^* is the free energy of formation from reactants of a system centered on the intersection hypersurface and Z is a collision frequency

between uncharged species. (Z is about 10^{11} liters/mole/sec. The charge effects on collision frequency are included in ΔF^* .) ΔF^* is computed for the most probable separation distance contributing to reaction. ρ is a ratio of certain root mean square displacements and is taken to be about unity (5, A).

Statistical mechanics was used to calculate the probability of occurrence of the necessary fluctuations in vibrational coordinates. Continuum theory was used to calculate the free energy of formation of any nonequilibrium state of polarization of the medium in the presence of the electron, and quantum mechanics to calculate changes in the kinetic energy and solvation free energy of the electron owing to changes in solvent polarization (8). In this way the free energy was calculated for a system having the electronic charge distribution of the reactant and having Boltzmann-type polarization and vibrational distribution functions. Similarly, for the same distribution of coordinates the free energy was calculated for a system having the electronic configuration of the product. However, as Figure 1 illustrates, these two free energies are equal when each system is constrained to be centered on the intersection hypersurface: the potential energy, averaged over the given distribution, is the same, because of the intersection, and the entropy of a system is determined only by the configurational distribution and so must also be the same for two systems having the same such distribution. The kinetic energy of any nucleus is also the same in the two systems.

Minimization of the free energy of this arbitrary state of a system containing the reactants, subject to the condition of equality of the two free energies, yields an expression for the free energy of the reactants in this centered distribution and, thereby, for ΔF^* . The functional form of the equation for ΔF^* is given by Equation 3, and that for ΔF^{*p} , the free energy of formation of the centered distribution from the product, is given by Equation 4 (8).

$$\Delta F^* = w + m^2 \left[\left(1 - \frac{m^2}{2} \right) \lambda_e^\infty + \lambda_2^\infty + \Delta \lambda_R \right] \quad (3)$$

$$\Delta F^{*p} = (m + 1)^2 [(1 - m^2) \lambda_e^\infty + \lambda_2^\infty + \Delta \lambda_R], \quad (4)$$

where w is the work required to bring the reactants together to a mean separation distance R in the activated complex. (Both coulombic and noncoulombic terms can contribute to w .) λ_e^∞ is an "intrinsic reorganization factor," which can be expressed in terms of the properties of the solvated electron (8). λ_2^∞ is an "intrinsic reorganization factor" of the second reactant and depends only on the properties of that reactant, such as differences in equilibrium bond lengths and orientation polarization in the oxidized and reduced forms (8). The ∞ superscript indicates that the quantities are evaluated for reactants far apart, and $\Delta \lambda_R$ is the change in the sum of intrinsic reorganization factors from $(\lambda_e^\infty + \lambda_2^\infty)$ to $(\lambda_e^R + \lambda_2^R)$. In terms of continuum theory $\Delta \lambda_R$ for the one-electron transfer equals $-e^2(D_{op}^{-1} - D_s^{-1})/R$, where D_{op} and D_s denote the optical

and static dielectric constants, respectively, and where e is the electronic charge (8). The quantity m is the solution of

$$\Delta F^* - \Delta F^{*p} = \Delta F^{\circ'}_{\text{int}} - w. \quad (5)$$

In this last equation $\Delta F^{\circ'}_{\text{int}}$ is the "standard" free energy of reaction $\Delta F^{\circ'}$ in the prevailing medium, corrected for the translational free energy loss when the "oriented center," in which the electron formerly resided, disappears during the formation of product from the centered distribution on the hypersurface. This corrected $\Delta F^{\circ'}$ constitutes the "driving force" for reaction at the mean separation distance R :

$$\Delta F^{\circ'}_{\text{int}} = \Delta F^{\circ'} - \Delta F^{\circ}_{\text{trans}} \quad (6a)$$

$$= \Delta F^{\circ'} - RT \ln [(2\pi m_p kT)^{3/2} 1000 / h^3 N_a] \quad (6b)$$

for a standard state of $1M$, where m_p is the effective mass for translation of the solvated electron (the "polaron") and N_a is Avagadro's number. The value of $\Delta F^{\circ}_{\text{trans}}$ is 5.3 kcal./mole if m_p is $3/N_a$ grams/molecule (B).

The functional form of Equations 3 and 4 differs somewhat from that found earlier (5) for conventional electron transfers, the difference arising from the sensitivity of the wave function to changes in solvent polarization. Equations 3 and 4 simplify on close examination: These reactions are extremely rapid because the solvated electron is a very strong reducing agent, so that $\Delta F^{\circ'}$ is very negative. In this case, ΔF^* is very small and, therefore, m^2 is seen from Equation 3 to be small. In fact, for the usual reactions of the solvated electron *a posteriori* numerical calculations from the observed rates show that $m^2 \ll 1$, and so m^2 can be neglected in the coefficients of λ_e° in Equations 3 and 4.

The equations then become

$$\Delta F^* = w + m^2 \lambda \quad (7)$$

$$m = -\frac{1}{2} \left(1 + \frac{\Delta F^{\circ'}_{\text{int}} - w}{\lambda} \right) \quad (8)$$

where

$$\lambda = \lambda_e^R + \lambda_2^R \quad (9)$$

These equation are now similar to those derived earlier for conventional electron transfer reactions (5).

The value for λ_2^R is the same as that for this same reactant in an ordinary homogeneous or electrochemical electron transfer occurring at the same R and can be estimated from them, as described later (6). $\Delta F^{\circ'}_{\text{int}}$ is known for many reactions of the solvated electron, and w can be estimated approximately. Accordingly, a theoretical value of ΔF^* can be calculated from Equation 7 once λ_e^R is known. Either λ_e^R can be calculated from other sources (it depends on the model of the solvated electron) or a value can be used which best fits data on k_{act} for several reactions, or both. In making such calculations it should be noted that ΔF^* is not highly accurately given by Equation 7, because of the various

approximations. It is more realistic to compare theoretical and experimental values for ΔF^* , therefore, rather than those for k_{act} .

The work term w makes a relatively minor contribution to ΔF^* . In numerical calculations it is usually assumed to be electrostatic in origin and to be given roughly by the shielded coulombic formula, $w^r = (e_1 e_2 / DR) \exp(-\kappa R)$, where e_1 and e_2 are the charges of the reactants, D is the dielectric constant and κ the Debye kappa. (In very dilute solutions $\exp(-\kappa R) \cong 1$.)

Dependence of k_{act} on $\Delta F^{o'}$. Possible Chemiluminescence.

To explore the behavior of ΔF^* with $\Delta F^{o'}$ it is convenient to rewrite Equations 7 and 8 as

$$\Delta F^* = w + \frac{\lambda}{4} \left[1 + \frac{\Delta F^{o'}_{int} - w}{\lambda} \right]^2 \quad (10)$$

The value of $\Delta F^* - w$ is seen to decrease at first as $\Delta F^{o'}$ becomes increasingly negative, to pass through a minimum at $(\Delta F^{o'}_{int} - w) = -\lambda$, and then to increase as $\Delta F^{o'}$ becomes still more negative. The physical origin of the behavior is seen from Figure 1: As $\Delta F^{o'}$ is made more negative the product surface in Figure 1 is lowered relative to the R surface, and ΔF^* becomes smaller at first, because the intersection occurs at lower energies on the R surface. This effect of $\Delta F^{o'}$ on ΔF^* is the normal one, and the configurations at the intersection are seen to be a compromise between the stable ones of the initial state and the stable ones of the final state. When $\Delta F^{o'}$ becomes still more negative, the intersection is seen to occur to the left of the minima of the R and P surfaces in Figure 1, at higher and higher parts of the initial R surface as $\Delta F^{o'}$ becomes increasingly negative. The configurations at the intersection are no longer compromise ones. This latter $\Delta F^{o'}$ region might be called the abnormal $\Delta F^{o'}$ region.

When $\Delta F^{o'}$ is sufficiently negative ΔF^* becomes large, and either the reaction with the solvated electron should become very slow or a reaction should occur by other paths, two of which are the following:

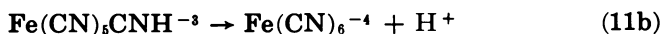
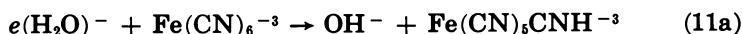
(a) Formation of electronically-excited states and possible chemiluminescence (8):

Although the intersection of the R surface with the surface for the electronic ground state of the product occurs at high $\Delta F^{o'}$'s when $\Delta F^{o'}/\lambda$ becomes very negative (slightly more negative than -1), the calculations given below indicate that an intersection with a surface in which the product is excited may then occur at low $\Delta F^{o'}$; chemiluminescence may therefore result:

For formation of the excited state of the product ΔF^* is again given by Equation 10, with λ_2^R and $\Delta F^{o'}_{int}$ now referring to formation of this excited state. For example, in a reaction for which $\Delta F^{o'}_{int}$ is as negative as -4 e.v., and in which the fluorescence occurs at say 6000 Å. (2 e.v.), the $\Delta F^{o'}_{int}$ for formation of the excited state is then only -2 e.v. or even less. If $\lambda/4$ for both reactions is about 0.4 e.v. and if, for present pur-

poses we neglect w , then ΔF^* for a reaction leading to the ground and excited state of the product is 0.9 e.v. and 0.025 e.v., respectively. In the first case the reaction is much too slow for measurement in these systems and in the second case it would occur with ease, the barrier ΔF^* being about 0.6 kcal./mole.

(b) Atom transfer reaction: In principle, it is possible that an atom transfer reaction such as Equation 11 can occur when the second reactant is an atom transfer acceptor or is otherwise reactive to the atom. To be sure, there is no evidence as yet for such reactions of the solvated electron. By suitable choice of reactant they could be avoided.



Estimating $\Delta F^{\circ'}_{\text{int}}$ and λ

From measured forward and reverse rate constants of the reaction of a solvated electron with water Baxendale (1) estimated the standard potential for the solvated electron. Use of a more recent rate constant (3) and correction (8) for a certain omitted entropy change yields a value, $E^{\circ'}_e = +2.7$ volts, for the standard oxidation potential of the solvated electron. To calculate $\Delta F^{\circ'}_{\text{int}}$ for a reaction from a difference of the standard oxidation potentials of the two reactants, $E^{\circ'}_e - E^{\circ'}_2$, the $\Delta F^{\circ'}$ must be corrected for the $\Delta F^{\circ}_{\text{trans}}$ of about 5 kcal./mole. This correction can be made (8) by taking the effective $E^{\circ'}_e$, $E^{\circ'}_{\text{eff}}$, for a solvated electron to be 2.9 volts.

$$\Delta F^{\circ'}_{\text{int}} = -eF(E^{\circ'}_{\text{eff}} - E^{\circ'}_2) \quad (12)$$

In homogeneous electron exchange reactions between two species differing only in their valence states, ΔF^* is given by Equation 10 with λ equal to $2\lambda_2^R$ and $(\Delta F^{\circ'}_{\text{int}} - w)$ replaced by $\Delta F^{\circ'} - w^r + w^p$ (5). (w^r and w^p denote the work required to bring the reactants together to the mean separation distance R , and the products to this R , respectively.) $\Delta F^{\circ'}$ is zero for a simple electron exchange reaction and w^r equals w^p for it, since the products are chemically indistinguishable from the reactants.

$$\Delta F^*_{\text{ex}} = w^r + \frac{\lambda_2^R}{2} \quad (13)$$

The separation distance R should affect primarily the orientation polarization contribution to λ rather than the vibrational contribution from the inner coordination shell (5). If R is about the same for this reaction as it is for reaction with the solvated electron then λ_2^R is the same. The difference in λ_2^R would probably be relatively minor in any case for typical R 's.

Since ΔF^*_{ex} equals $-RT \ln(k_{\text{ex}}/10^{11} M^{-1} \text{sec.}^{-1})$, λ_2^R can be estimated from the electron exchange rate constant k_{ex} when correction of ΔF^*_{ex} is made for w^r or when w^r is small enough to be neglected. Values of ΔF^*_{ex} have also been obtained indirectly from measurements of rate

constants of other redox reactions involving the species, particularly in (2), where tests of this evaluation are described.

In electrochemical electron transfer reactions, the value of the rate constant k_{ei} at zero activation overpotential yields a value of ΔF^*_{ei} . The latter equals $-RT \ln(k_{ei}/10^4 \text{ cm. sec.}^{-1})$, and the theoretical expression for ΔF^*_{ei} is (5)

$$\Delta F^*_{ei} = \frac{w^r + w^p}{2} + \frac{\lambda_2^R}{4} \quad (14)$$

Correction of this ΔF^*_{ei} for the work terms then yields a value of λ_2^R . The consistency of Equations 13 and 14 has received some experimental support (9), though further work is desirable. Examples of some approximate values of λ_2^R computed in these ways are (C): $\text{Co}(\text{NH}_3)_6^{+2,3}$ (~ 60 kcal./mole), $\text{Fe}(\text{phen})_3^{+2,3}$ (~ 15 kcal./mole), $\text{Eu}^{+2,3}$ (~ 40 kcal./mole).

The value of λ_e^R for the solvated electron has been estimated in several ways (8, 10). By assuming that diffusion of the solvated electron in water occurs as a site-to-site electron transfer and using an expression for ΔF^* for a unimolecular electron transfer reaction (5); Sutin estimated (10) a lower bound of 5 kcal./mole for λ_e^R from the known diffusion constant. The writer has estimated (8) a value of roughly 15 kcal./mole to fit the rate constant for reaction of the solvated electron with Sm^{+3} , assuming that λ_2^R was about the same as that for another rare earth, Eu^{+3} . An estimate of λ_e^R can also be made from spectral and solvation data, but depends on the detailed model used for the solvated electron (8) and neglects the "electron affinity" of the first excited state of the solvated electron. (This electron affinity describes local interactions; these are not covered by simple polaron theory.) The latter estimated value of λ_e^R is rough but is consistent with the value just cited and with a value estimated *a priori* (8). At the same time this second estimate from the data yields a rough and perhaps not reliable value of the "electron affinity" of the ground state of the solvated electron (8).

From Equation 10 an estimate can be made of an error in calculated ΔF^* owing to an error in λ . If the errors are denoted by δ 's we have

$$\delta \Delta F^* = - \left(1 + \frac{\Delta F^{\circ'}_{\text{int}} - w}{\lambda} \right) \frac{\Delta F^{\circ'}_{\text{int}}}{2\lambda} \delta \lambda \quad (15)$$

For example, an error of 5 kcal./mole in λ introduces an error of 0.6 kcal./mole in ΔF^* , when $\Delta F^{\circ'}_{\text{int}}/\lambda \cong -0.6$. Similarly the error in ΔF^* owing to an error in $\Delta F^{\circ'}_{\text{int}}$ is

$$\delta \Delta F^* = \left(1 + \frac{\Delta F^{\circ'}_{\text{int}} - w}{\lambda} \right) \frac{\delta \Delta F^{\circ'}_{\text{int}}}{2} \quad (16)$$

An error of 2 kcal./mole in $\Delta F^{\circ'}_{\text{int}}$ introduces an error of 0.9 kcal./mole in ΔF^* when $\Delta F^{\circ'}_{\text{int}}/\lambda \cong -0.6$. However, one sees from Equations 15 and 16 that the sensitivity of ΔF^* to a change in λ or $\Delta F^{\circ'}_{\text{int}}$ depends on the value of $\Delta F^{\circ'}_{\text{int}}/\lambda$. We have selected a typical value.

Further Applications

The prediction (8) of possible chemiluminescence at suitable $\Delta F^{\circ'}_{\text{int}}/\lambda$'s has already been discussed. Applications of the equations have also been made to calculations of rate constants for reactions of solvated electrons, using λ_2^R 's estimated as above (8, 10). If, when $\Delta F^{\circ'}_{\text{int}}$ is very negative, the calculated rates are too low, the explanation may lie in the formation of excited states or, in some cases, in atom transfers. A search for the predicted chemiluminescence is under way (11). It would be favored by a reaction for which λ_2^R is small enough that $\Delta F^{\circ'}_{\text{int}}/\lambda$ is quite negative for formation of the ground state of the product. Interestingly enough, it is possible to vary ΔF° systematically without varying λ , simply by varying a substituent in a large organic ligand (2). Thus, a control of the relative values of ΔF° 's for reactions leading to ground and excited states becomes possible and so, thereby, does the yield of any chemiluminescence.

To investigate reactions of solvated electrons in the borderline region of diffusion and activation control there are two regions of $E^{\circ'}$ for the second reactant which are of interest, for typical λ 's. Estimated from Equation 10, neglecting w , these are: $E^{\circ'}_2 > ca. 1.5$ to 2 volts (8) and $E^{\circ'}_2 < ca. -0.5$ to -1.0 volts for a typical λ of about 55 kcal./mole. The former region, particularly, would be expected to yield the most reliable empirical values of λ_e^R , since they involve compromise configurations in the activated complex, just as k_{ex} and k_{ei} do. The resulting λ_e^R 's may be compared with those obtained from the second $E^{\circ'}_2$ region. In cases which involve appreciable changes in bond lengths of a reactant, it may be necessary to replace the harmonic oscillator approximation (g) by use of anharmonic potential energy functions. (Approximation (h) is automatically replaced at the same time.) For this purpose one may replace Equation 10 by an equation derived earlier for ordinary electron transfer reactions (6) as the derivation of Equation 10 from Equation 3 and as the similarity of Equation 10 to the equation for conventional electron transfers both indicate.

Appendix

(A) In activated complex theory the rate constant can be expressed in terms of the free energy F^\ddagger of a system hypothetically constrained to exist on a certain hypersurface, the "activated complex," cf. Marcus, R. A., *J. Chem. Phys.* **41**, 2624 (1964). F^\ddagger can be expressed in terms of the free energy F^* of a system centered on that hypersurface (5). The difference between F^\ddagger and F^* contributes a factor to ρ . A second factor in ρ arises from the fluctuations in the separation distance of the reactants in the activated complex (5).

(B) Theoretical values of m_p and λ_e^∞ would depend on the model of a solvated electron. The value of m_p used in the text is at best rough (8), but $\Delta F^{\circ}_{\text{trans}}$ is relatively insensitive to it in the region of interest.

American Chemical Society
Library

1155 16th St., N.W.

In Solvated Electron; Hart, E.
Washington, D.C. 20036

A theoretical value of $\Delta F^{\circ'}$ would also depend on the model, but fortunately its experimental value is known instead.

(C) Values of λ_2^R for $\text{Co}(\text{NH}_3)_6^{+2, +3}$ and for $\text{Eu}^{+2, +3}$ were estimated from k_{ei} in (9), neglecting w because of the high salt concentrations. The value of $\text{Fe}(\text{phen})_3^{+2, +3}$ was estimated from the value assigned to k_{ex} in (2), neglecting w . Only a lower limit for k_{ex} , quoted in (2), is known. A possible noncoulombic source of w for certain $\text{Fe}(\text{phen})_3^{+3}$ reactions is noted in (2) and (9) and, if correct, may apply to reaction between $e(\text{aq})$ and $\text{Fe}(\text{phen})_3^{+3}$. Data on other k_{ex} 's and k_{ei} 's are given in (2) and (9) and in various other articles.

Literature Cited

- (1) Baxendale, J. H., *Radiation Res. Suppl.* **4**, 139 (1964).
- (2) Campion, R. J., Purdie, N., Sutin, N., *Inorg. Chem.* **3**, 1091 (1964).
- (3) Dorfman, L. M., Matheson, *Progr. Reaction Kinetics* **3** (in press).
- (4) e.g. Glasstone, S., Laidler, K. J., Eyring, H., "The Theory of Rate Processes," p. 96, McGraw-Hill, New York, 1941.
- (5) Marcus, R. A., *Ann. Rev. Phys. Chem.* **15**, 155 (1964); *J. Chem. Phys.* **43**, (1965).
- (6) Marcus, R. A., *Discuss. Faraday Soc.* **29**, 21 (1960). (The term involving $(\Delta e)^2(D_{op}^{-1} - D_{op}^{-1})/2a_1$ there is to be replaced by λ_{∞} and the Δq_i 's now refer only to the second reactant.)
- (7) Marcus, R. A., *Discuss. Faraday Soc.* **29**, 129 (1960).
- (8) Marcus, R. A., *J. Chem. Phys.* **43**, (1965).
- (9) Marcus, R. A., *J. Phys. Chem.* **67**, 853, 2889 (1963).
- (10) Sutin, N., in "Symposium on Exchange Reactions," International Atomic Energy Agency, Brookhaven, June 1965.
- (11) Sutin, N., Schwarz, H. A., private communication.

RECEIVED May 3, 1965. Supported by a grant from the National Science Foundation.

The Photochemistry of Metal Solutions, III: Formation of Metal Solutions from Alkali Amides, in Ethylamine and Ammonia

MICHAEL OTTOLENGHI and HENRY LINSCHITZ

Department of Chemistry, Brandeis University, Waltham, Mass.

Ultraviolet (UV) irradiation of decomposed alkali metal solutions in ethylamine or ammonia regenerates the original species. The reaction has been studied using both steady and flash excitation. In ammonia the reaction is ascribed to electron transfer from excited amide ion to solvent, followed by competitive combination between electron and amine radical, or two amine radicals. In ethylamine, it seems that an electron is transferred from amide to cation within an excited ion pair. Flashing bleached ammonia solutions with light near $500\text{ m}\mu$ produces a new short-lived transient, absorbing at $510\text{ m}\mu$. Photoregeneration of bleached ethylamine solutions is accompanied by irreversible formation of a band of $265\text{ m}\mu$. Extinction coefficients are given for the amides and for the metal monomer and dimer species in ethylamine.

The formation of solvated or hydrated electrons by photoionization of various negative ions, in suitable organic solvents or in water, has been observed by several workers using either rigid solvent or flash technique (8, 11, 15, 20, 22). In developing a general understanding of electron behavior in liquids, one must ultimately obtain data, either by photoionization or by radiolysis (9, 16, 26), over the widest possible range of solvent media. Photoionization studies on simple ions in liquid ammonia or amines are of special interest, particularly in obtaining comparisons with the results in water (15, 16, 22), and in connection with the closely related problem of the structure of metal solutions. Such studies on amides are described in this paper.

We have recently reported a new photochemical reaction, in which faded alkali metal solutions in ethylamine are regenerated by UV ir-

radiation (23). Flash-photolysis experiments on such solutions in ethylamine and ammonia were also described. We present now a more complete account of this work, including measurements of the extinction coefficients of potassium amide and of monomer and dimer species in alkali metal solutions.

Experimental

Preparation of Samples. Metal solutions were prepared on the vacuum line as in our previous work (24), in thoroughly flamed-out pyrex ampoule assemblies, equipped as needed with various side arms and tubes for bulb-to-bulb distillation of metal, for absorption and flash-photolysis cells, for catalytic decomposition of solution, and for final freezing out of solutions before analysis. Preparations were sealed off under "stick" vacuum. Ethylamine and ammonia were Matheson products and were degassed and dried over lithium before distilling through glass wool plugs into the working ampoule. The concentrations of ethylamine solutions were readily controlled by varying the contact time between solvent and metal mirror. Preparing very dilute metal-ammonia solutions is more difficult, owing to the rapid dissolution of metal. Accordingly, such solutions were prepared by distilling small amounts of metal onto a glass bead containing an iron core and transferring this bead magnetically into the ammonia bulb (28). Potassium-ammonia solutions were bleached by standing overnight at -78°C . over electrolytically blackened platinum foil in a side bulb separated from the rest of the assembly by a sintered disc. Ethylamine solutions were decomposed in less than an hour over blackened platinum at room temperature, or simply by standing for several hours.

Photochemical Technique. Flash-photolysis apparatus and procedures have been described previously (24). For work in liquid ammonia, the photolysis cell was first cooled in the flash Dewar and cold solution, then poured in from the storage bulb. No difficulty was experienced in the transfer through the short length of connecting tubing, and frosting of the cell windows was thus avoided. The spectral region of exciting light was controlled either by dyed cellophane filters (Rosco Labs, N. Y.) wrapped around the Dewar, or by interposing four 2 in. \times 2 in. Corning filters between the four flash lamps (21, 24) and the photolysis cell assembly. These filters were supported in a square frame, mounted symmetrically around the central focus of the four-leaved elliptical reflector (21). Steady irradiations were carried out in pyrex cells, about 10 cm. from a Hanovia type HS 150-watt mercury arc.

Analysis of Solutions. (a) AMIDES—The amide concentration in decomposed metal-ethylamine solutions was determined by titration, using bromcresol green-methyl orange indicator (2). The solution, in a side arm of the ampoule, was cooled in dry ice-acetone, the side arm cut off and immediately connected to the vacuum line via a short length of rubber tubing, and the solvent distilled into another calibrated tube. The amount of solvent was determined either by volume or by weighing the tube while cold. A known amount of degassed water was then distilled onto the amide residue and aliquots removed for titration with 500N HCl, either directly or after gently boiling for five minutes in a small Erlenmeyer. Blanks gave negligible corrections. Boiling reduced

the titer of the aliquots by half ($\pm 2\%$), corresponding to the expected amount of free ammonia or amine produced on amide hydrolysis. Samples which were immediately acidified and then back-titrated with sodium hydroxide gave results agreeing with the direct titrations.

(b) **FREE METAL**—Ethylamine solutions were analyzed for alkali metal by measuring hydrogen gas evolution upon adding water or standing over platinum catalyst at room temperature. After decomposition, samples were degassed by thoroughly agitating, freezing, and opening the sample to the McCleod gauge. Four or five such cycles were generally required to remove the hydrogen completely.

Results

Ethylamine Solutions. (a) **PHOTOREGENERATION OF BLEACHED SOLUTIONS**—The absorption spectra of alkali metals in ethylamine have been discussed in previous publications (24, 25). Briefly, three characteristic bands are found, absorbing at about 650 (V), 850 (R) and 1300 (IR) $m\mu$, and attributed respectively to metal monomers, dimers, and solvated electrons. In potassium solutions, the equilibria favor the V-band, while in rubidium the R-band is most prominent, except at extreme dilutions.

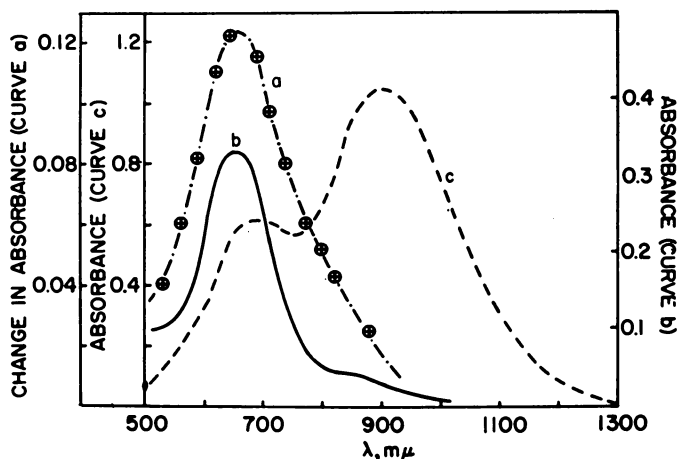


Figure 1. Spectra of decomposed K- and Rb-ethylamine solutions after irradiation.

- Absorbance change on flashing bleached K-ethylamine solution 5 msec. after flash; 11°C .
- Bleached K-ethylamine solution, after 5-min. irradiation with Hanovia HS arc; 1 cm. pyrex cell; -78°C .
- Bleached Rb-ethylamine solution, after 7-min. irradiation with Hanovia arc; room temperature.

Irradiation of decomposed metal solutions in borosilicate or quartz, using the medium pressure arc, develops a deep blue color with approximately the same stability as a solution obtained directly by metal-solvent contact. (In recycled solutions, in which fading is catalyzed by accumulated decomposition products, room temperature half-lives may be as short

as 10–15 minutes.) Typical spectra of irradiated solutions are shown in Figure 1, which includes also results obtained by flash illumination. In the case of potassium, the absorption consists mainly of the 650 $m\mu$ V-band, while in rubidium the 850 $m\mu$ R-band predominates, with V also present. Both spectra in this region are completely analogous to those of the original undecomposed solution. Moreover, the same constant absorbance ratio, $D^{2}_{600\ m\mu}/D_{1000\ m\mu}$, establishing a monomer-dimer equilibrium (25), is found in the photochemically colored solutions as in the original systems (Figure 2). Finally, the ESR absorption of a

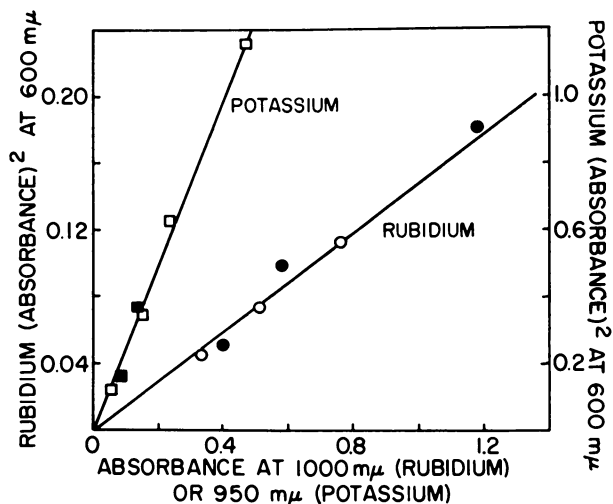


Figure 2. Ratio ($D^{2}_{600\ m\mu}/D_{1000\ m\mu}$) in K- and Rb-ethylamine solutions; room temperature.

- Rb original solution, colored by contact with metal, and allowed to fade.
- K, as above.
- Rb bleached solution, UV irradiated and allowed to fade.
- K, as above.

bleached and irradiated potassium-ethylamine solution is identical to that of an undecomposed solution of the same optical absorbance (Figure 3). The spectrum consists of four equidistant lines with a hyperfine splitting of 9.5 gauss, typical of the monomeric (V-band) species (4). We thus conclude that UV irradiation of bleached alkali metal solutions in ethylamine regenerates the same components which are present in the original system before decomposition.

(b) FLASH EXCITATION OF BLEACHED METAL-ETHYLAMINE SOLUTIONS—Flash experiments were performed to search for possible intermediates in the photoregeneration reaction. The situation is complicated by the fact that both the V and R bands themselves undergo reversible photobleaching (24). Thus, flash excitation of the V-band results in immediate formation of the IR-band and growing-in of the R-band, which then decays back to the original equilibrium amount of V. In K-ethyl-

amide solutions, the first flash regenerates sufficient 650 m μ absorption so that subsequent flashes show the full pattern of the reversible photobleaching reaction, superimposed on further photoregeneration. Care was therefore taken to ensure that metal decomposition was complete in preparing



Figure 3. ESR signal following UV irradiation of bleached K-ethylamine solution; Strand Labs Model 601 X-band spectrometer, 3200 gauss; room temperature.

amide test solutions and that no trace of V-band contamination was present before excitation. Despite such precaution, a marked growing-in of the 650 m μ absorption is still observed even on the first flash. This process is accurately first-order, and in a typical potassium-ethylamide solution, at 11° C. the rate constant for V-band appearance is 1.85×10^4 sec.⁻¹ A transient absorption at 850 m μ is also seen, whose decay closely matches the V-band appearance. (In the example cited, $k_{850 \text{ m}\mu} = 1.90 \times 10^4$ sec.⁻¹) These rate constants are similar to those measured for the R \rightarrow V conversion in our previous work on reversible photobleaching of metal solutions (24). The observed growing-in at 650 m μ in flashed amide solutions may therefore be caused not by a true V precursor, but simply by a secondary reversible photobleaching of the V-band by the same flash which forms the band in the primary regeneration reaction. In agreement with this, extrapolating the kinetic plots for 650 m μ appearance back to zero time after the flash shows an initial jump in absorbance, and the ratio $(\Delta D_{\text{initial}}/\Delta D_{\text{final}})_{650 \text{ m}\mu}$ increases toward unity as the flash intensity is decreased (Table I). It is also found that the ratio of absorbance change at 850 m μ to that part of the 650 m μ absorbance which grows in $(\Delta D_{\text{final}} - \Delta D_{\text{initial}})_{650 \text{ m}\mu}$ is closely similar to the corresponding ratio obtained in reversible V-band flash-photolysis (24).

We therefore conclude that no directly formed precursor of the V-band is seen in our experiments, and the photoregeneration reaction must occur in times shorter than the flash duration (3 μ sec).

(c) SPECTRA AND EXTINCTION COEFFICIENTS OF AMIDE AND METAL SOLUTIONS—The spectrum of decomposed potassium solutions in ethylamine consists of two partially overlapping bands with maxima at 320 and 265 m μ , respectively, at room temperature (Figure 4). The relative intensity of the bands, prior to any photoregeneration, varies from sample to sample, but no clear correlation could be made between this intensity ratio and such variables as concentration or mode of decomposition of the metal solution. The 265 m μ band is practically temperature inde-

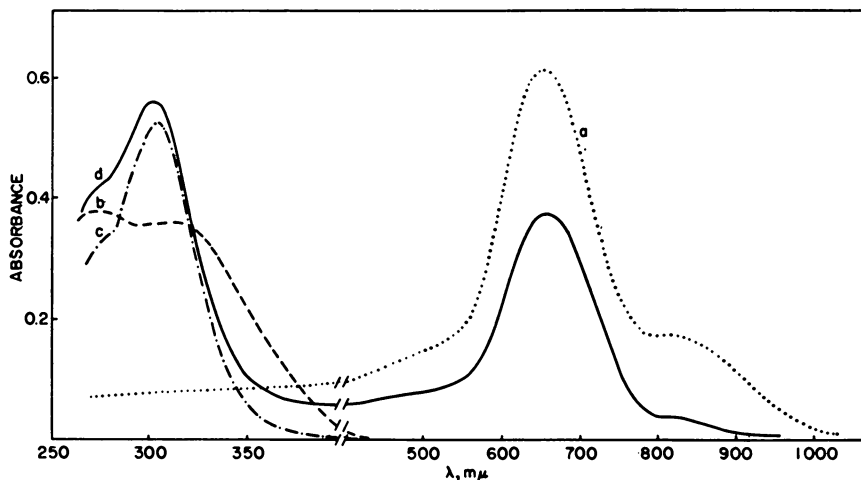


Figure 4. Effects of temperature and UV irradiation on decomposed K-ethylamine solutions; 1 cm. pyrex cell.

- a) Original solution, prior to bleaching; -78°C .
- b) Decomposition products after several bleaching-regeneration cycles; room temperature.
- c) Above, at -78°C .
- d) After 20-min. irradiation with Hanovia arc; -78°C .

pendent, while the $320\text{ m}\mu$ band shifts strongly toward the blue ($d\nu/dT = -15\text{ cm.}^{-1}\text{ deg.}^{-1}$) and sharpens markedly as the temperature is lowered (Figure 4, b and c). At -78°C ., the peak moves to $305\text{ m}\mu$. On the basis of the similarity in both location and temperature dependence of the $320\text{ m}\mu$ band in ethylamine and the amide band in liquid ammonia (see below), we attribute the $320\text{ m}\mu$ absorption to potassium ethylamide. Titration of samples showing relatively little $265\text{ m}\mu$ absorption gives $\epsilon = (2.7 \pm 0.4) \times 10^3$ for the molar decadic extinction coefficient of potassium ethylamide at $320\text{ m}\mu$, at room temperature, and $\epsilon = (3.7 \pm 0.7) \times 10^3$ at $305\text{ m}\mu$ and -78°C .

These results combined with the photochemical transformations (formation of V-band from amide and conversion of R to V in reversible bleaching) permit evaluation of the extinction coefficients of the metal monomer (V) and dimer (R) in ethylamine. The photoregeneration of a decomposed potassium ethylamide solution at -78°C . is shown in Figure 4. Curve-a is the spectrum of the original metal solution, curve-c, after decomposition, and curve-d, following irradiation. The change at $305\text{ m}\mu$ in the photoregeneration reaction is assumed to be the sum of the decrease in amide absorption and increase in the overlapping high-energy tail of the V-band (24), any changes owing to the $265\text{ m}\mu$ species being neglected. The increase owing to the V-band is obtained from the measured absorbance rise at $650\text{ m}\mu$ (Figure 4, d) and the ratio $D_{650}/D_{305} = 7.0 \pm 0.3$ for the V-band at -78°C . determined from Figure 4, a. For example, from observed absorbance increases of 0.38 at $650\text{ m}\mu$ and

Table I. Effect of Flash Intensity on Development of 650 m μ Band.
K-EtNH in Ethylamine, Conc. = $1.3 \times 10^{-3}M$; Temp. = 11° C.

Flash Energy, Joules	ΔD_{650}^a (initial)	ΔD_{650} (final)	$\frac{\Delta D_i}{\Delta D_f}$
150	0.054	0.364	0.15
100	0.030	0.132	0.23
50	0.008	0.021	0.38
20	0.004	0.007	0.6

^a By extrapolation of growing-in kinetics to $t = 0$.

0.030 at 305 m μ , we obtain $\Delta D_{\text{amide}} = -0.023$ for the corrected bleaching of the amide. (A corrected increase of the same magnitude (~ 0.02) is observed at 305 m μ when a V-band ($D = 0.44$) is allowed to bleach.) Taking $-\Delta C_{\text{amide}} = \Delta C_{\text{monomer}}$, we estimate the value $\epsilon = (6 \pm 2) \times 10^4$ for the molar decadic extinction coefficient of the V-band at 650 m μ and -78°C . The rather large uncertainty arises from the smallness of the absorbance change at 305 m μ compared with that at 650 m μ . In these photoregeneration experiments the extent of conversion reaches a steady state ($\Delta_{650}^{\text{max}} \approx 0.4$ for the situation in Figure 4) owing to thermal back reaction to the amide and inner filtering by the accumulated V-band, so that the precision of this method for determining $\epsilon_{\text{monomer}}$ is further limited.

As a check on these relationships and assumptions, the extinction coefficient of the potassium monomer was obtained by directly analyzing potassium-ethylamine solutions (showing low 265 m μ absorption) by determining hydrogen evolution following addition of water. This gave $\epsilon = (4.9 \pm 0.7) \times 10^4$ at 650 m μ and -78°C ., which is quite close to the photoregeneration value and somewhat more reliable.

Reversible bleaching experiments, in which the R-band decays to form the V-band, give a ratio of $\Delta D_{850}/\Delta D_{650} = 0.92$ at -78°C . Assuming that this is a dimer \rightarrow monomer conversion, we thus obtain $\epsilon_{\text{R-band}} = (4.9 \times 10^4) (2) (0.92) = (9.0 \pm 2) \times 10^4$, for the molar extinction coefficient of the dimer at its absorption peak, at -78°C . Table II summarizes these values and corresponding extinction coefficients in ammonia.

Table II. Summary of Molar Decadic Extinction Coefficients

Species	Solvent	λ (m μ)	Temp. °C.	$\epsilon \times 10^{-3}$	Method
K-EtNH	Ethylamine	305	-75°	3.7 ± 0.7	titration
		320	room	2.7 ± 0.4	titration
V (monomer)	Ethylamine	650	-75°	60 ± 20	photochem.
			-78°	49 ± 7	H ₂ evol.
R (dimer)	Ethylamine	850	-78°	90 ± 20	photochem.
		K-NH ₂	Ammonia	335	-48°

(d) DEVELOPMENT OF THE 265 m μ BAND—The intensity of the 265 m μ band increases as the solution undergoes repeated cycles of photoregeneration and thermal decomposition. If irradiation is conducted at room temperature, the rate of the thermal back reaction is sufficiently fast so that free metal does not accumulate. Thus, steady irradiation at room

temperature is the equivalent of repeated regeneration-bleaching cycles at lower temperature. Figure 5 shows the results of such irradiation. In passing from the initial (curve-a) to the final spectrum (curve-c), the amount of 265 m μ absorption is roughly trebled, while the amide (appearing merely as a shoulder on curve-c) remains about constant. Since the total metal ion concentration is not changed in the process, we conclude that the 265 m μ absorption cannot be a metal-containing compound.

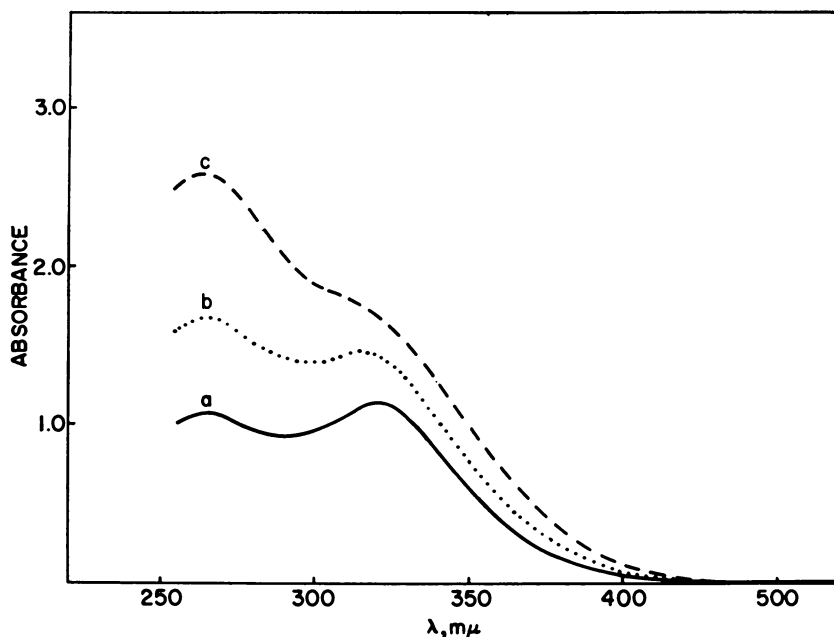


Figure 5. Formation of 265 m μ band on room temperature irradiation of bleached K-EtNH₂.

- a) Bleached solution, before irradiation.
- b) After 8-min. irradiation with Hanovia arc.
- c) After 30-min. irradiation with Hanovia arc.

Liquid-Ammonia Solutions—Spectrum and Photolysis of Potassium Amide. Figure 6 shows the spectrum of a bleached solution of potassium in ammonia, at -48°C . Only a single peak due to the amide is seen at 335 m μ before the ammonia cutoff. The molar decadic extinction coefficient, as determined by titration, is $\epsilon = (1.0 \pm 0.2) \times 10^4$ at -48°C . and 335 m μ . (A careful Beer's Law check on the 335 m μ band has not yet been made.) The temperature coefficient of the peak is $-20 \text{ cm.}^{-1} \text{ deg.}^{-1}$ (3), which is close to the value given above for the long-wave band in decomposed ethylamine solution.

Flash-photolysis of potassium amide solutions gives different photochemical patterns, depending on the excitation wavelength. Flash excitation through Corning #9863 filters (passing 240–400 m μ and far red

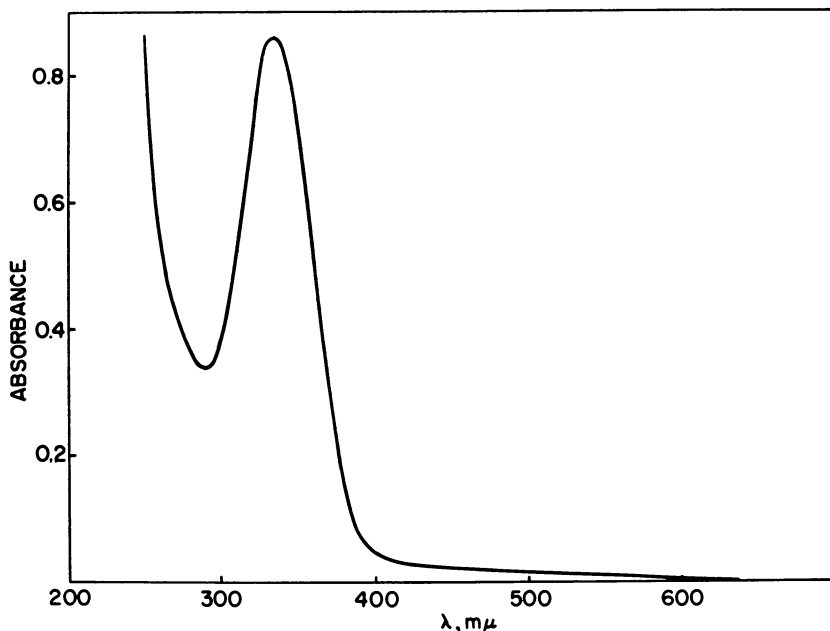


Figure 6. Absorption spectrum of potassium amide in liquid ammonia (decomposed $K-NH_3$ solution); $-48^\circ C$.

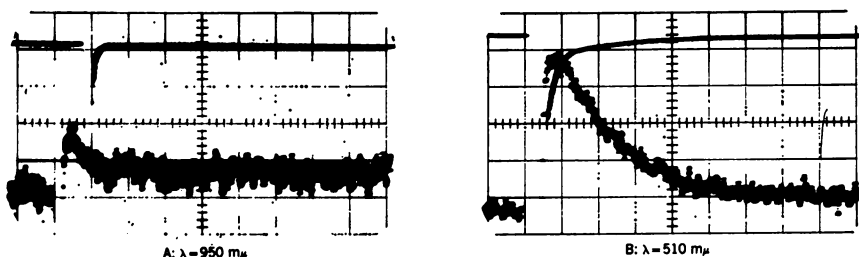


Figure 7. Flash transients in potassium amide-ammonia solutions; original amide absorbance, $D_{335} = 0.78$; sweep = $50 \mu sec./cm.$; V_0 = deflection before flash; upper sweep, blank; lower sweep, measuring light on; both sweeps at indicated gain; temperature $-65^\circ C$.

Experiment	λ ($m\mu$)	V_0 (volts)	Gain, V/cm.
a	950	4.0	0.50
b	510	12.0	0.10

beyond $680 m\mu$) results in absorbance changes illustrated in the oscillograms of Figure 7a. The flash transient disappears in two stages, an initial fast decay, with half-life around $40 \mu sec.$, and a residual very slow decay (longer than one minute). In fresh, dilute samples, where the blue color is still somewhat unstable, the "long-lived" transient disappears much more quickly. The kinetics of the two decays are difficult to

establish owing to the short lifetime (of the fast component) and the high noise-level in the far red where the absorbance changes are largest.

The spectra of the fast- and slow-decaying transients appear to be the same, as shown in Figure 8 (solid curves). The range of our measurements was limited to wavelengths below 1000 $m\mu$. Within this range, the spectra of both short- and long-lived flash transients closely match the high energy absorption tail of sodium or potassium metal solutions in liquid ammonia at the same temperature (10). Thus, as in the ethylamine case, it is possible to regenerate the original blue solution by UV illumination of the metal amide. However, despite the demonstration of long-lived far red absorption in flash-regenerated ammonia solutions, we have not been able to obtain metal absorption measurable in a Cary model 14 spectrophotometer, even after prolonged illumination.

Flash experiments using unfiltered excitation give results entirely similar to those described for UV excitation alone, except that an additional transient band, peaking at 510 $m\mu$, is superimposed on the far red absorption (Figures 7, b and 8, dotted curve). At 510 $m\mu$, our photometer permits good kinetic analysis even of very small absorbance changes (Figures 7 and 8), and it is found that the decay of the transient is strictly first-order, with $k = 1.2 \times 10^4 \text{ sec}^{-1}$ at -65°C . Flash excitation through 96% silica filters having the same UV cutoff as the 9863 glass, reproduces the results with unfiltered light. The additional 510 $m\mu$ band must therefore be caused by light of longer wavelength than 400 $m\mu$, rather than to high energy excitation shorter than 240 $m\mu$. Borosilicate filters (cutoff at 300 $m\mu$) leave the 510 $m\mu$ transient unchanged, but reduce both long- and short-lived far red intermediates by the same factor of 70%. A yellow filter, transmitting above 490 $m\mu$, entirely eliminates the far red transients, but still leaves 60% of the 510 $m\mu$ band, and with a filter cutoff at 550 $m\mu$, only 10% of the 510 $m\mu$ transient remains. Thus, the far red transient is formed by excitation on the high energy side of the amide band, while the 510 $m\mu$ intermediate results from excitation in the long low-energy tail seen in Figure 6. Whether this absorption is some other decomposition product is not yet clear. The possibility that the 510 $m\mu$ band results from excitation of the far red product is eliminated by the filter experiments, and also by the appearance of this band on flashing solutions that had been very carefully decomposed by long standing over catalyst. There is some indication that the yield of the 510 $m\mu$ transient relative to the far red band increases with increasing amide concentration.

Discussion

A complete interpretation of these experimental results must account for differences in the photoregeneration reaction in ethylamine compared with ammonia. These include the different spectra of the flash transients and their relation to the stable metal species, the appearance of two decay stages of the flash intermediate in ammonia instead of one very slow decay in ethylamine, the irreversible appearance

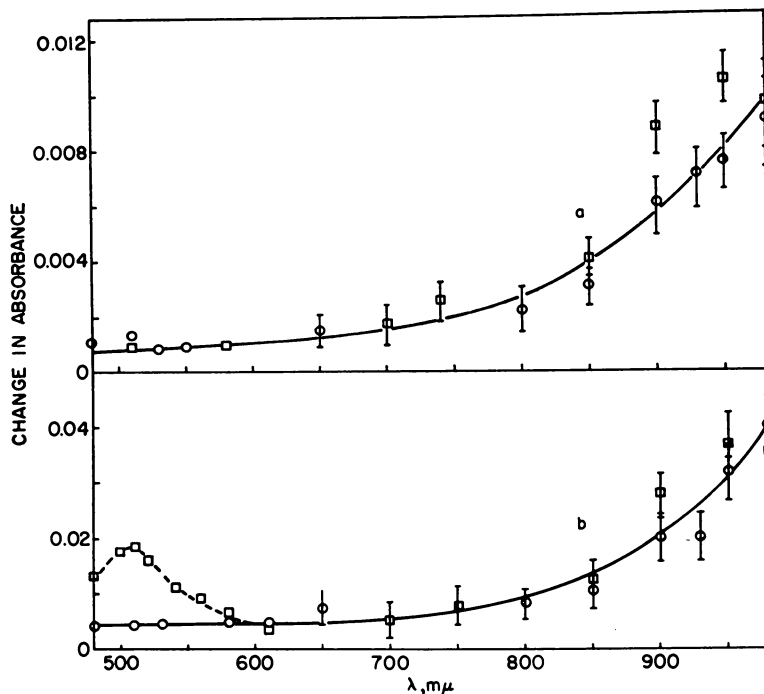


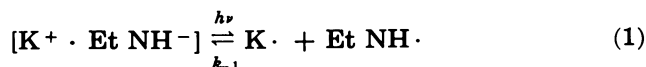
Fig. 8. Spectra of flash intermediates in potassium amide-liquid ammonia; $D_{385\text{ m}\mu} = 0.78$; -65°C .

Upper curve (a)—Residual absorption, measured 400 μsec after flash—
 ○—Excited through 9863 filter.
 □—No filter.

Lower curve (b)—Total initial absorption, measured 20 μsec . after flash—
 ○—Excited through 9863 filter.
 □—No filter.

of the 265 $\text{m}\mu$ band in irradiated ethylamine solutions, and the overall fact that photoregeneration effects in ammonia are much smaller and of shorter duration than in ethylamine.

There can be little question that excitation of metal amide is the initial step in both solvent systems. However, it is not clear at the outset whether ion pairs or free ions are involved. No direct measurements of the dissociation constant of potassium ethylamide in ethylamine are available. In ammonia, the value $K = 7.3 \times 10^{-5} M$ has been obtained (17) from conductivity data at -33.5°C . The temperature coefficient of K appears to be small (18), and this value will be assumed also at -78°C . In ethylamine, the dissociation constant must be considerably smaller than this, and in the concentration range of our experiments in ethylamine (0.5 to $1.5 \times 10^{-3} M$) most of the salt will be present as ion pairs. We therefore write for the ethylamine reaction:



and



This ascribes the photoregeneration reaction to an electron transfer from amide to potassium ion occurring in the excited state of the ion pair. Such a picture is consistent with the immediate appearance ($\tau < 10^{-8}$ sec.) of the 650 m μ cation-centered monomer band, on flashing potassium ethylamide in ethylamine. The monomer is stabilized by the irreversible removal of EtNH \cdot radicals in the reaction forming the 265 m μ band.

The presence of this band in the original (unilluminated) bleached solution may perhaps be understood as a consequence of the thermal decomposition reaction sequence:

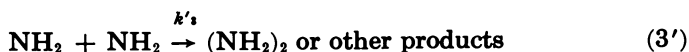


In this case, the ethylamine radical is formed by hydrogen abstraction from the solvent, instead of dissociation of the excited (charge-transfer) state of the amide ion pair.

The compound responsible for the 265 m μ absorption has not yet been identified. The obvious assignment to *sym*-diethylhydrazine is contradicted by the absorption spectrum of an authentic sample of the hydrazine (supplied by Merck, Sharp and Dohme, Montreal), which shows no sign of a peak at 265 m μ . Instead, the spectrum in ethylamine solvent has a broad maximum at 358 m μ and rises steeply near the solvent cutoff at 250 m μ . We assume, therefore, that in Reaction 2, the ethylamine radical is scavenged by the solvent, to yield other ultimately stable products. In liquid ammonia, hydrogen and amide appear to be the only decomposition products, implying that the process $\text{H} + \text{NH}_3 \rightarrow \text{H}_2 + \text{NH}_2$ does not occur. The relative inefficiency of this process compared to H atom recombination in liquid ammonia is also indicated by radiation chemical studies (6).

In our liquid ammonia experiments the amide concentration ($1.5 - 8 \times 10^{-5} M$) is in a range in which appreciable ionic dissociation occurs. Negative ions in aqueous solution are well known to yield solvated electrons upon excitation in their charge-transfer bands (7, 15, 19, 22), and one may expect the same process to operate also for NH_2^- in ammonia. The large blue shift of the amide peak with decreasing temperature (3) supports the view that the absorption is a charge-transfer band (27). We therefore write for potassium amide in liquid ammonia (e signifies the solvated electron):





Reaction 1' represents formation of the initial far red transient, Reaction 2' the initial fast decay stage and 3' accounts for the residual far red absorption as those electrons which escape recombination with amine radicals.

Figure 8 shows that the residual solvated electron concentration at the end of the fast decay process is about 30% of the initial yield. On the time scale of our flash observations, cage and geminate recombination effects play no role, and the measured ratio of long- to short-lived product thus is fixed by the ratio of k_2' to k_3' . Without solving the above kinetic scheme in detail, it is evident that k_2' and k_3' are of the same order of magnitude. This result is in general agreement with previous measurements on the rate of electron capture in solution (11).

The solvated electrons in the flash transient may be present either as free or paired ions. The extent of pairing may be estimated in a given experiment from the extinction coefficient of the solvated electron (taken to be 1.0×10^4 at $980 \text{ m}\mu$) (10), from the potassium amide dissociation constant and from the ion pair dissociation constant for the process $[\text{M}^+ e^-] \rightarrow \text{M}^+ + e^-$. Taking this to be about $3 \times 10^{-3} M$ (1, 12, 14), we find for a typical flashed solution in which $\Delta D_{980} \approx 0.02$ and $D_{335} = 0.9$, that the ratio (unpaired/paired) solvated electrons is about 30. This result is difficult to confirm, at least by spectroscopic methods, owing to the obedience to Beer's Law in the pairing region (13).

There remains the question of the $510 \text{ m}\mu$ transient. We have seen that the photoregeneration reaction produces the thermodynamically stable species appropriate to each solvent, the cation-centered monomer ($650 \text{ m}\mu$ band) in potassium-ethylamine and the far red solvated electron in potassium-ammonia. The as yet unidentified cation-centered monomer in ammonia (5) should have a high-energy absorption and short lifetime, and it is tempting to ascribe the $510 \text{ m}\mu$ intermediate to this species. Following its presumed formation by charge-transfer within an ion pair (long-wave tail of the amide absorption band?), this species might be expected to decay to the stable solvated electron. However, repeated and careful search gave no evidence for a growing-in of the far red transient in flash regenerated potassium amide solutions. It is clear that further spectroscopic and photochemical studies are needed over a wider concentration range.

Acknowledgment

We wish to thank Dr. K. Bar-Eli and Prof. T. R. Tuttle for their assistance at various stages of this research.

Literature Cited

- (1) Arnold, E., Patterson, A., *J. Chem. Phys.* **41**, 3089 (1964).
- (2) Bar-Eli, K., personal communication.
- (3) Bar-Eli, K., Ph.D. Thesis, Rehovoth, Israel (1962).
- (4) Bar-Eli, K., Tuttle, T. R., *J. Chem. Phys.* **40**, 2508 (1964).
- (5) Becker, E., Lindquist, R. H., Alder, B. J., *J. Chem. Phys.* **25**, 971 (1956).
- (6) Cleaver, D., Collinson, E., Dainton, F. S., *Trans. Faraday Soc.* **56**, 1640 (1960).
- (7) Dobson, G., Grossweiner, L. I., *Radiation Research* **23**, 290 (1964).
- (8) Dobson, G., Grossweiner, L. I., *Trans. Faraday Soc.* **61**, 708 (1965).
- (9) Dorfman, L. M., *Science* **141**, 493 (1963).
- (10) Douthit, R. C., Dye, J. L., *J. Am. Chem. Soc.* **82**, 4472 (1960).
- (11) Eloranta, J., Linschitz, H., *J. Chem. Phys.* **38**, 2214 (1963).
- (12) Evers, E. C., Frank, P. W., *J. Chem. Phys.* **30**, 61 (1959).
- (13) Gold, M., Jolly, W. L., Pitzer, K. W., *J. Am. Chem. Soc.* **84**, 2264 (1962).
- (14) Golden, S., Guttman, C., Tuttle, T. R., *J. Am. Chem. Soc.* **87**, 135 (1965).
- (15) Grossweiner, L. I., Swenson, G. W., Zwicker, E. F., *Science* **141**, 805, 1180 (1963).
- (16) Hart, E. J., Boag, J. W., *J. Am. Chem. Soc.* **84**, 4090 (1962).
- (17) Hawes, W. H., *J. Am. Chem. Soc.* **55**, 4422 (1933).
- (18) Higginson, W. C. E., Wooding, N. S., *J. Chem. Soc.* **1952**, 766.
- (19) Jortner, J., Ottolenghi, M., Stein, G., *J. Phys. Chem.* **68**, 274 (1964).
- (20) Linschitz, H., Berry, M., Schweitzer, D., *J. Am. Chem. Soc.* **76**, 5833 (1954).
- (21) Linschitz, H., Sarkanen, K., *J. Am. Chem. Soc.* **80**, 4826 (1958).
- (22) Matheson, M., Mulac, W. A., Rabani, J., *J. Phys. Chem.* **67**, 2613 (1963).
- (23) Ottolenghi, M., Bar-Eli, K., Linschitz, H., *J. Am. Chem. Soc.* **87**, 1809 (1965).
- (24) Ottolenghi, M., Bar-Eli, K., Linschitz, H., *J. Chem. Phys.* (in press).
- (25) Ottolenghi, M., Bar-Eli, K., Linschitz, H., Tuttle, T. R., *J. Chem. Phys.* **40**, 3729 (1964).
- (26) Ronayne, M. R., Guarino, J. P., Hamill, W. H., *J. Am. Chem. Soc.* **84**, 4230 (1962).
- (27) Stein, G., Treinin, A., *Trans. Faraday Soc.* **55**, 1091 (1959).
- (28) Warshawsky, I., "Metal Ammonia Solutions," ed. Lepoutre and Sienko, p. 167, W. A. Benjamin, New York, 1964.

RECEIVED May 14, 1965. Supported by a grant from the U. S. Atomic Energy Commission to Brandeis University (No. AT-30-1-2003).

Kinetics of Electron-Attachment Reactions in Ethylenediamine

LARRY H. FELDMAN, ROBERT R. DEWALD¹ and JAMES L. DYE

Department of Chemistry, Michigan State University, East Lansing, Mich.

Rate studies of the reaction between cesium and water in ethylenediamine, using the stopped-flow technique, have been extended to all alkali metals. The earlier rate constant ($k \approx 20 M^{-1} \text{ sec.}^{-1}$) and, in some cases, a slower second-order process ($k \approx 7 M^{-1} \text{ sec.}^{-1}$) have been observed. This is consistent with optical absorption data and agrees with recent results obtained in aqueous pulsed-radiolysis systems. Preliminary studies of the reaction rate of the solvated electron in ethylenediamine with other electron acceptors have been made. The rate constant for the reaction with ethylenediammonium ions is about $10^5 M^{-1} \text{ sec.}^{-1}$. Reactions with methanol and with ethanol show rates similar to those with water. In addition, however, the presence of a strongly absorbing intermediate is indicated, which warrants more detailed examination.

The discovery by radiation chemists of solvated electrons in a variety of solvents (5, 16, 20, 22, 23) has renewed interest in stable solutions of solvated electrons produced by dissolving active metals in ammonia, amines, ethers, etc. The use of pulsed radiolysis has permitted workers to study the kinetics of fast reactions of solvated electrons with rate constants up to the diffusion-controlled limit (21). The study of slow reactions frequently is made difficult because the necessarily low concentrations of electrons magnify the problems caused by impurities, while higher concentrations frequently introduce complicating second-order processes (9). The upper time limit in such studies is set by the reaction with the solvent itself.

¹Present Address: Tufts University, Medford, Mass.

Before any measurements had been made of the properties of hydrated electrons, a program of study was begun at the Max Planck Institut für physikalische Chemie in Göttingen, Germany, suggested by M. Eigen, involving reactions of stable solvated electrons with water in amine solvents (6). Only a few homogeneous rate studies had previously been made using metal-ammonia solutions (12). It appeared that these sources of relatively stable solvated electrons could prove very useful in studying reactions by the stopped-flow technique with second-order rate constants from 10^{-2} to $10^6 M^{-1} \text{sec.}^{-1}$

To avoid the problems associated with working at high pressures or low temperatures, amine solutions which are stable at room temperatures under low pressure were investigated. Ethylenediamine was selected as a promising solvent for these studies. Because it was well known (2, 13) that alkali metals have more complex spectra in amine solutions than in ammonia, it was first necessary to study extensively the nature of these solutions (7, 8). Such studies are still being pursued in several laboratories (19), and there is by no means universal agreement on the species present in solution.

Since we follow changes in absorption spectra during reaction, it would be most desirable to know the nature of the species responsible for the various absorption peaks. Three types of absorption maxima are encountered in most amine solvents in contrast to the single absorption maximum in metal-ammonia solutions. An absorption maximum at $650 - 700 m\mu$ is found for lithium, sodium, potassium, and sometimes rubidium. The position and shape of this maximum depend upon the solvent, but seem to be independent of the metal used. The source of this absorption is a subject of considerable speculation, but it has been variously associated with an M_2^+ species (11) or with a "monomer" (19) consisting of an electron trapped in the field of a solvated metal ion. An intermediate absorption, at 840 to $1030 m\mu$ (strongly dependent upon metal) is commonly found in solutions of potassium, rubidium, and cesium. It has been suggested that this absorption is caused by dissolved molecules of the alkali metals, similar to those found in the gas phase (11). The third, and broadest absorption maximum occurs at $1300-1500 m\mu$ and the shape and position appear to be independent of metal. Conductance and spectral data, as well as solubilities (7, 8) strongly indicate that the species responsible for this absorption are "ammonia-like," and may reasonably be called "solvated electrons." Except at the lowest concentrations, these solvated electrons interact with each other and with the cation to form loose aggregates (15). The aggregates would be expected to have different conductance and magnetic properties, but nearly the same spectral properties as the dissociated solvated electron.

Recently, Anbar and Hart have studied the properties of an electron pulse-generated species in ethylenediamine (1). They observe only one band with a maximum at $920 m\mu$ and a $2\mu\text{sec.}$ half-life and attribute this to the solvated electron. This does not agree with the previous assignment based on spectra and conductivity (7, 8). Because the spectra

depend upon the nature of the cation and there is the possibility of metal carry-over during distillation of the solvent, this system should be studied further (perhaps by adding other alkali metal salts) before any definite assignment can be made. In addition, optical spectra of stable, very dilute metal solutions in ethylenediamine should be obtained.

With spectral properties as complex as these, one can anticipate at the outset that kinetic studies will yield complex results. This prediction is in fact borne out. The gross features permit easy evaluation of, for example, the reaction rate of "solvated electrons" with water; but working out the kinetics in detail is quite another matter. This paper reports our experiments and results to date using these methods.

Experimental

The reactive nature of these solutions, coupled with their inherent instability owing to reaction with the solvent itself, forces workers in this field to take extreme pains in purifying the materials and cleaning the apparatus. In our laboratory we have found what we believe to be an effective cleaning procedure for glassware (7). First, the items are rinsed briefly with a hydrofluoric acid detergent cleaning solution (5% hydrofluoric acid, 33% concentrated reagent grade nitric acid, 2% acid soluble detergent, and 60% distilled water), then ten times or more with distilled water. Next, they are filled with fresh aqua regia and heated to boiling, followed by ten more rinses with distilled water, then by several rinses and/or soakings in double-distilled conductance water. After each use and a preliminary cleaning, they are heated in an annealing oven at 550° C. before being cleaned as described above.

High vacuum techniques are used wherever possible with well trapped mercury vapor diffusion pumps giving pressures between 10^{-5} and 10^{-6} torr. Dow Corning high vacuum silicone grease is used on all stopcocks which come in contact with liquid; Apiezon N grease is used elsewhere. Apiezon T grease is used on movable tapers and ball joints, and Apiezon W wax is used on all fixed joints. Ethylenediamine (Matheson, Coleman, and Bell 98–100%) was purified in either of two ways. The first method (7) involves distillation at atmospheric pressure in a nitrogen stream, followed by reaction with alkali metals and repeated vacuum distillations. In the second method (for which we are indebted to Prof. Paul Sears of the University of Kentucky), ethylenediamine was purified in a large separatory funnel by slowly freezing it and then melting and discarding the core. The process was repeated at least four times and resulted in a pure product without the difficulties involved in distillation. Following freeze-purification, the ethylenediamine was put over lithium and sodium, vacuum distilled onto a potassium mirror, and then distilled into a flask equipped with a sidearm for liquid withdrawal.

The alkali metals were obtained from the following sources: sodium—J. T. Baker; potassium—Mallinckrodt; rubidium—Fairmount Chemical Co.; cesium—a gift from the Dow Chemical Co.; and lithium—Lithium Corp. of America. The lithium was washed with dry benzene and cut in a dry box when necessary. The other metals were cleaned, cut, and then degassed and distilled under high vacuum. Repeated vacuum distillations were used to obtain small metal samples in

sealed ampoules which were then used to make up metal solutions. Water solutions in ethylenediamine were made from freshly distilled conductance water which was degassed by repeated freezing and pumping and vacuum distilled. Next it was either vacuum distilled directly into a solution make-up flask or was used to prepare fragile glass ampoules which could be used to make up water solutions of lower concentration. Absolute methanol was distilled from a magnesium-magnesium sulfate mixture and then degassed and vacuum distilled. Spectral grade absolute ethanol was distilled from sodium metal, then degassed and vacuum distilled. A solution of ethylenediammonium chloride was prepared by introducing a known amount of Matheson hydrogen chloride gas into a solution make-up flask. An ammonium bromide solution was made using the reagent grade salt. A cesium hydroxide solution was prepared using a cesium mirror onto which water, treated as above, was distilled. (The concentration of cesium hydroxide is uncertain because a small amount of a liquid-phase separated when added to ethylenediamine.)

Nitrogen (Matheson, pre-purified) was used as a covering gas for all liquids. It was further purified by passing it over copper turnings in a tube furnace, an Ascarite column, a dry ice trap, and finally through a silica gel column at liquid nitrogen temperature in which some condensation occurred. This nitrogen was then stored in two-liter bulbs on the vacuum line.

The stopped-flow method of Chance (3), as modified by Gibson (14), has been used considerably since its inception (4). It is particularly useful for studying reactions with half-times from 2 msec. up to 100 sec. and requires relatively small amounts of reagents. Precision is good, and the method requires only a rapid measurement of concentration changes.

In our studies, the intense absorption of the metal-amine solutions in the near infrared provides an excellent property to monitor. A stopped-flow system, similar to that which has since been described by Dulz and Sutin (10), was constructed. (The pushing is done manually; a Bausch and Lomb grating monochromator and an RCA7102 or 6199 photomultiplier tube are used, depending upon spectral region.) A four jet Plexiglas mixing chamber, which has four inlet holes of 0.5 mm. bore each arranged almost tangentially about a 1.0 mm. central hole, was used. This cell is capable of a mixing efficiency of better than 98% in 2 msec., as measured by an acid-base reaction. The mixing cell was mounted vertically to eliminate bubbles. It was gradually attacked by the solutions and had to be changed every few runs. The entire system including the syringes, could be evacuated to about 10^{-4} torr. The system was thermostated at $25.0^\circ \pm 0.2^\circ$ C. Up to five reactant solutions could be delivered to the syringe, and dilutions could be made in a buret. Metal solutions were prepared immediately prior to a run, and only one concentration of metal solution was used in each run. When flow was stopped, a micro-switch triggered the time base of a Tetrionix Model 564 Storage Oscilloscope. The vertical deflection on the scope, produced by the output of the photomultiplier at a given fixed wavelength, was proportional to the light intensity over at least two decades. The trace was then photographed using a Polaroid camera with Type 146L transparency film. These transparencies were enlarged and traced on graph paper. Absorbance and log absorbance as functions of time were calculated using a Control Data 3600 computer.

Results

The reactions of all the alkali metals with water, of cesium and rubidium with methanol, of cesium with ethanol, and of cesium with HCl and with NH_4Br have been examined. Figure 1 shows a typical oscilloscope trace, and Figure 2 shows a plot of log absorbance vs. time for this trace. The reaction is pseudo-first-order in metal (since solute concentration is ten or more times greater than metal concentration), and the overall rate constants and their order in solute are obtained by varying solute concentration.

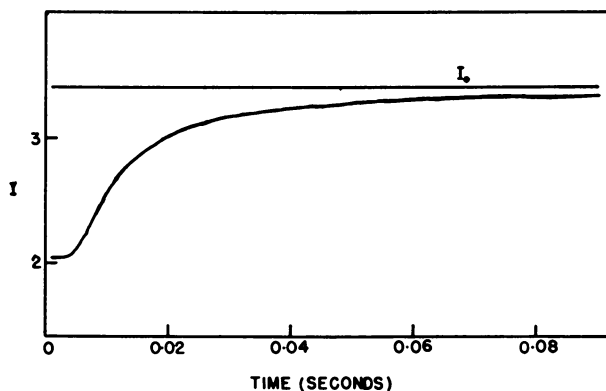


Figure 1. Enlargement of a typical oscilloscope trace; reaction of cesium with water in ethylenediamine.

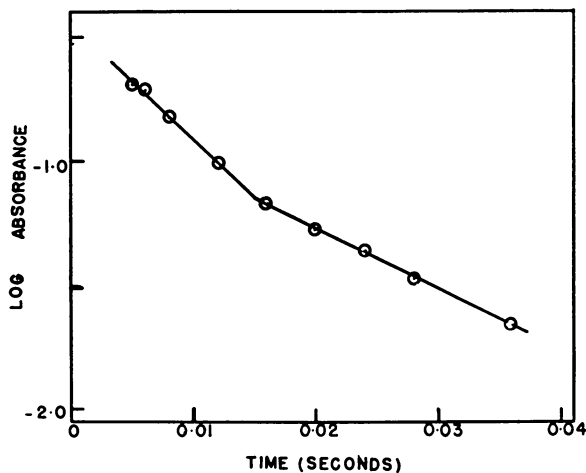


Figure 2. Log Absorbance vs. time for a typical cesium and water trace showing two rates.

Water. The reaction of cesium with water in ethylenediamine was carried out over a wide range of water concentrations using several dif-

ferent metal concentrations, and the results are given in Table I. Limits of error given in this paper are average deviations from the mean. The major absorbance change occurred with a second-order rate constant of $20.2 \pm 4.8 M^{-1} \text{ sec.}^{-1}$. In most cases, analysis of the complete trace showed that a slower competitive reaction also was present with a rate constant of $6.9 \pm 2.2 M^{-1} \text{ sec.}^{-1}$. In two runs with low water concentrations a small initial absorbance change occurred with a faster rate constant, varying from 38 to $200 M^{-1} \text{ sec.}^{-1}$. Preliminary studies of one run each were made using rubidium and potassium solutions with results paralleling those of cesium.

Table I. Cesium-Water Rate Constants

Water Conc. (M)	Run	Cesium Conc. (M)	k ($M^{-1} \text{ sec.}^{-1}$)
0.0230	1.1	$4.1 \times 10^{-4*}$	$17.2 \pm 1.4^{**}$
			...
0.0244	0.1	$\approx 2.5 \times 10^{-4}\dagger$	$26.0 \pm 1.1^{**}$
			...
0.0244	0.3	$2.9 \times 10^{-4*}$...
			8.36 ± 1.8
0.341	0.1	$\approx 2.5 \times 10^{-4}\dagger$	$20.3\dagger\dagger$
			6.05 ± 0.41
0.341	0.3	$2.9 \times 10^{-4*}$	$21.2\dagger\dagger$
			5.00 ± 0.90
0.670	1.1	$4.1 \times 10^{-4*}$	14.5 ± 4.3
			4.47 ± 1.5
5.60	1.1	$4.1 \times 10^{-4*}$	27.1 ± 1.5
			7.58 ± 3.1
6.11	0.3	$2.9 \times 10^{-4*}$	22.4 ± 2.8
			5.63 ± 0.43
$\approx 4(\text{CsOH present})$	0.3	$2.9 \times 10^{-4*}$	≈ 18.8
			$\approx 11.5\dagger\dagger$

*—by analysis †—from absorbance ††—one trace.
**—fast rate constant also observed.

The results obtained with sodium and water differ somewhat from those described above. Three runs were made, and except for three traces of the last run only a single rate was observed. Figure 3 shows a plot of $\log \kappa$ (where κ is the pseudo-first-order rate constant) vs. \log [water concentration]. The order in water found from this plot is 1.6 compared to a value of 1.1 for the slowest rate of cesium with water also shown in Figure 3.

Lithium is the most difficult of the alkali metals with which to obtain stable solutions since it cannot be distilled in glass. Three runs were carried out with lithium and water, but the results are inconclusive. In the first run, lithium prepared by evaporating a lithium-ammonia solution was used, and in the other runs the lithium was cut in a dry box and introduced into the ethylenediamine just prior to the run by means of a break-seal sidearm. The first two runs appeared to yield three rate constants, with values around 100, 20, and $7 M^{-1} \text{ sec.}^{-1}$, respectively and involved both infrared and visible absorptions. In the third run, a very dilute solution showing no infrared absorbance was used and resulted in a single rate constant of about $30 M^{-1} \text{ sec.}^{-1}$, obtained by following the decay of the 660 $m\mu$ absorbance.

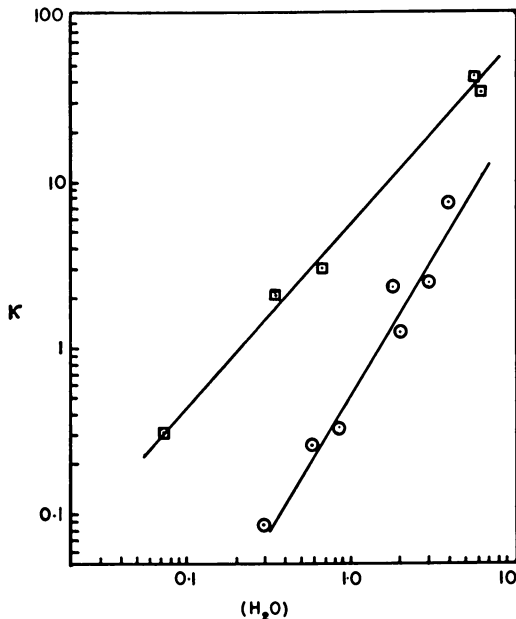


Figure 3. Comparison of $\log \kappa$ vs. $\log [H_2O]$ for sodium and cesium: ○, sodium and water; □, slowest rate of cesium and water.

Methanol. Rubidium reacted with one methanol concentration, and two runs were made with cesium using several concentrations of methanol. While reaction times were comparable to those observed in the water reactions, several marked differences were apparent. In some cases two rates were observed, but the constants were not reproducible. More striking was the fact that the shapes of the traces themselves differed from picture to picture, and with dilute solutions seemed to indicate that an absorbing intermediate was formed. For these reasons we do not report any rate constants at this time.

Ethanol. Two runs with cesium and ethanol were carried out. Once again the overall reaction times were comparable with those using water. Traces giving two rate constants of 17.0 ± 3.8 and $5.4 M^{-1} \text{ sec.}^{-1}$ were observed in some cases. The lower rate constant was obtained from a $\log \kappa$ vs. $\log [EtOH]$ plot which had a slope of unity. Several traces exhibited nonreproducibility similar to that observed with methanol.

Hydrogen ions. Hydrogen chloride and cesium reacted in ethylenediamine, and several traces were obtained. A rate constant of $1.7 \pm 0.2 \times 10^5 M^{-1} \text{ sec.}^{-1}$ was observed.

Ammonium ions. Ammonium bromide reacted with cesium, but the reaction was too rapid to be studied in our system, even at an ammonium concentration of $10^{-4} M$. This indicates that the bimolecular rate constant is greater than $10^6 M^{-1} \text{ sec.}^{-1}$

Discussion

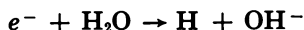
Earlier work (6) using this method yielded a second-order rate constant of $24.7 \pm 1.5 M^{-1} \text{ sec.}^{-1}$ for the reaction of dilute solutions of cesium with water in ethylenediamine. On the basis of optical absorption spectra (7) and other evidence (8, 11), it was assumed that this reaction was that of the solvated electron as well as loosely bound electrostatic aggregates of electrons and cations with water. This permitted correlation with the results of aqueous radiation chemistry.

Absorbance studies show considerable overlap of the different spectral bands in metal-ethylenediamine solutions. It appears likely that the simultaneous first-order processes in reducing water and other solutes result from different reaction rates of the various species. With this assumption, and using Beer's Law for the individual species, one obtains

$$k_a^{\text{true}} = k_a^{\text{app}} + \frac{B_0}{A_0} (k_a^{\text{app}} - k_b)$$

where k_a^{app} is the observed higher rate constant, k_b is the lower rate constant, A_0 and B_0 are the initial absorbances of species *A* and *B*, respectively, and k_a^{true} is the corrected value of k_a .

Previous studies show that at least three different absorbing species are needed to describe the metal-ethylenediamine systems. It is also likely that the primary step in the reaction with water,



is followed by rapid abstraction of an alpha-hydrogen atom from ethylenediamine, resulting in a free radical which can react further, either with another radical or with the reducing species. Because of these complexities it is hazardous to assign the several rate processes to particular species at this time. At least for the reaction of cesium solutions with water, the second-order rate constant of about $20 M^{-1} \text{ sec.}^{-1}$ seems to be compatible with the previous assignment to the solvated electron (and loose aggregates). If this is the case, the slower reaction ($k \simeq 7 M^{-1} \text{ sec.}^{-1}$) might be assigned to the reaction of the dimer, Cs_2 .

The rapid decrease in absorbance observed at the beginning of some traces ($k = 40$ to $200 M^{-1} \text{ sec.}^{-1}$) might be caused by reaction with impurities. This would require occasional impurity concentrations in excess of 10^{-4} molar, however. Further study is necessary to determine the origin of this process. Blank determinations of the rate of absorbance change upon mixing with the pure solvent indicate that autodecomposition is much slower than the rate of reaction with the lowest water concentration used.

All reactions were found to be first-order in the absorbance, and all reactions except that of sodium solutions with water seem to be first-order in water. In considering the apparent 3/2 order in water for the latter, it must be recalled that sodium solutions show only a single absorption band with a maximum at $660 \text{ m}\mu$. The nature of this reaction is

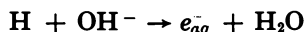
not known, and indeed the nature of the major species in solutions of sodium in ethylenediamine is not understood at present.

Although the detailed nature of the reactions with methanol and ethanol remains unknown, it is clear from these studies that the reaction rate of solvated electrons with these alcohols is not very different from that with water. Pulse radiolysis studies (24) show minimum half-times of 1.5 and 3 μ sec. for the disappearance of the electron peak in the pure alcohols; but this does not represent reaction of the electron with the alcohol since no attempt was made to remove the counter ion or other radiolysis products.

A very fast second-order disappearance of hydrated electrons with the production of molecular hydrogen has been observed in water using pulse radiolysis (9). In our system this reaction would be expected to cause large deviations from first-order behavior at high water concentrations. The absence of such deviation shows that this reaction depends strongly upon the solvent structure and not merely upon the concentration of water molecules.

While the reaction of the solvated electron with hydrogen ions is near the diffusion-controlled limit in aqueous and alcoholic systems (24), the reaction with hydrogen chloride in our system, which presumably gives ethylenediammonium ions, is much slower with $k = 1.7 \times 10^6 M^{-1} \text{ sec.}^{-1}$. Interestingly, the reaction with ammonium ions is at least an order of magnitude faster than this, indicating that appreciable proton transfer from ammonium ion to ethylenediamine does not occur.

Although the work of Jortner and Rabani (17) and of Matheson and Rabani (18) would indicate the reaction



to be relatively fast, we found that adding OH^- had no apparent effect on the rate of reduction of water. This probably means that hydrogen atoms are short lived in ethylenediamine and react rapidly with the solvent to produce molecular hydrogen. The production of one-half mole of H_2 for each mole of metal reacted would indicate that the radicals resulting from hydrogen abstraction react further with electrons or other reducing species.

In order to study absorbance change as a function of wavelength, we are currently modifying the flow apparatus to include a Perkin-Elmer Model 108 Rapid-Scan Monochromator. This will allow us to study absorbance as a function of both wavelength and time and should help in the assigning of decay rates of the various bands. It should also allow us to detect absorbing intermediates with lifetimes of a few milliseconds or longer.

It is clear that the study of solvated electron reaction rates, using metal-amine solutions as the source of electrons, is currently in the early stages of development, and the conclusions drawn must be very limited in scope. If the species present in metal solutions in ethylenediamine and other amines can be firmly identified, the techniques described in this paper should prove useful for studying reactions of solvated electrons with

second-order rate constants as large as $10^6 M^{-1} \text{sec.}^{-1}$. This should serve to complement studies of radiation-produced electrons which can conveniently cover the range from about 10^6 to $10^{11} M^{-1} \text{sec.}^{-1}$.

Acknowledgments

This research was supported by the U. S. Atomic Energy Commission (Contract AT-(11-1) - 958). The authors would like to thank Messrs. Seer and Eklund of the Michigan State University Glass Shop for their cooperation. We also acknowledge the assistance of Messrs. Hansen and Wreede during the course of this investigation.

Literature Cited

- (1) Anbar, M., Hart, E. J., *J. Phys. Chem.* **69**, 1244 (1965).
- (2) Blades, H., Hodgins, J. W., *Can. J. Chem.* **33**, 411 (1955).
- (3) Chance, B., *J. Franklin Inst.* **229**, 455, 613, 737 (1940).
- (4) Chance B., *et al.*, eds., "Rapid Mixing and Sampling Techniques in Biochemistry," Academic Press, New York, 1964.
- (5) Czapski, G., Schwarz, H. A., *J. Phys. Chem.* **66**, 471 (1962).
- (6) Dewald, R. R., Dye, J. L., Eigen, M., deMaeyer, L., *J. Chem. Phys.* **39**, 2388 (1963).
- (7) Dewald, R. R., Dye, J. L., *J. Phys. Chem.* **68**, 121 (1964).
- (8) Dewald, R. R., Dye, J. L., *J. Phys. Chem.* **68**, 128 (1964).
- (9) Dorfman, L. M., Taub, I. A., *J. Am. Chem. Soc.* **85**, 2370 (1963).
- (10) Dulz, G., Sutin, N., *Inorg. Chem.* **2**, 917 (1963).
- (11) Dye, J. L., Dewald, R. R., *J. Phys. Chem.* **68**, 135 (1964).
- (12) Eastham, J. F., Larkin, D. R., *J. Am. Chem. Soc.* **81**, 3652 (1959).
- (13) Eding, H. J., Ph.D. Dissertation, Stanford University, 1952.
- (14) Gibson, Q., *J. Physiol.* **117**, 49P (1952).
- (15) Gold, M., Jolly, W. L., Pitzer, K. S., *J. Am. Chem. Soc.* **84**, 2264 (1962).
- (16) Hart, E. J., Boag, J. W., *J. Am. Chem. Soc.* **84**, 4090 (1962).
- (17) Jortner, J., Rabani, J., *J. Phys. Chem.* **66**, 2081 (1962).
- (18) Matheson, M. S., Rabani, J., *J. Phys. Chem.* **69**, 1324 (1965).
- (19) Ottolenghi, M., Bar-Eli, K., Linschitz, H., Tuttle, Jr., T. R., *J. Chem. Phys.* **40**, 3729 (1964).
- (20) Sauer, Jr., M. C., Arai, S., Dorfman, L. M., *J. Chem. Phys.* **42**, 708 (1965).
- (21) Spinks, J. W. T., Woods, R. J., "An Introduction to Radiation Chemistry," Chapter 8, Wiley, New York, 1964.
- (22) Taub, I. A., Dorfman, L. M., *J. Am. Chem. Soc.* **84**, 4053 (1962).
- (23) Taub, I. A., Sauer, Jr., M. C., Dorfman, L. M., *Disc. Faraday Soc.* **1963**, 206.
- (24) Taub, I. A., Harter, D. A., Sauer, Jr., M. C., Dorfman, L. M., *J. Chem. Phys.* **41**, 979 (1964).

RECEIVED May 6, 1965.

Solvent Dimer Model for Solvated Electrons

LIONEL RAFF and HERBERT A. POHL*

Department of Chemistry, Oklahoma State University, Stillwater, Okla.

A dimer model consisting of two solvent molecules with an attached electron is presented as a representation of the solvated electron system. Simple molecular orbital theory, using scaled H_2^+ wave functions, is employed to evaluate the geometries, binding energies, and electronic transition energies for several series of homologous compounds. The results predict a general decrease of optical transition energies and binding energies with dipole moment of the solvent. The calculated transition energies when compared with existing experimental data give the trend expected from chemical experience, but tend generally to overestimate the magnitudes.

The experimental study of the physical and chemical properties of the ionic species known as the solvated electron goes back many years (3, 5, 8, 9, 10). It includes the interesting aspects of solutions of alkali metals in liquid ammonia and amines (5) and of irradiated water (8). Considerable experimental data is available, but the nature of the binding of the electron in the solvents is still controversial. The most widely discussed model is one suggested by Landau (18) and by Ogg (21) in which the electron is pictured as being in a cavity bound by the polarization of the dielectric medium. Ogg computed the cavity radius and binding energy using a simplified model of an electron in a "spherical" box. This calculation was much refined by Lipscomb (19) to include electrostriction, electronic polarization, and surface energy. Kaplan and Kittel (17) proposed that binding of the electron took place in a cavity orbital associated with many (ca.50) protons of the NH_3 solvent molecules. Jortner (12, 13, 14, 15) proposed a model for very dilute solutions of the solvated electron, e_{solv} , in which the electron is removed from the metal

* Department of Physics

cation and trapped in a cavity by polarization of the medium. This concept of "an electron trapped by digging its own hole" is that introduced by Landau (4) in which the medium is regarded as a continuous dielectric.

A totally different view was proposed by Becker, Lindquist, and Alder (2) who considered the electron to be trapped at a solvated cation site in which the solvated metal cation has its valence electron localized on the protons of the ammonia molecules of the innermost solvation layer. This species, with its valence electron in a sort of enlarged Rydberg orbital, may then dissociate or undergo dimerization.

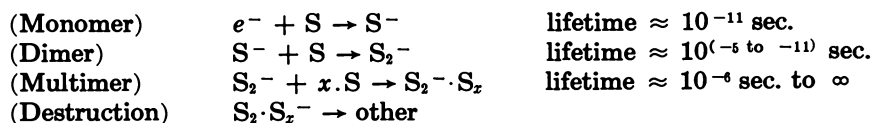
We wish here to inquire if a molecular view of the basic e_{min}^- species might be taken. We shall postulate, as in the cavity model, that the solvated electron is removed from the metal cation, but we shall assume instead a molecular model—one in which several solvent molecules are bound, forming the basic unit.

The Model

We have in mind the following model: the energetic electron as first produced—e.g., on irradiating a solvent—is preliminarily trapped or localized in the neighborhood of the positive regions of the dipoles of the polar solvent with the emission of energy by photons, etc., characteristic of the trap depth. Massey (20) notes that electron attachment for H_2O begins at an electron beam energy of 0.1 e.v. and continues to increase in cross-section with increasing beam energy up to 2.0 e.v. The existence of the H_2O^- ion is thus implied. Following this quasi-localization of the electron, rapid reorientation of a local solvent molecule occurs to form a deeper trap. These deeper traps can be viewed as analogs of the hydrogen molecule ion (dimeric traps). From dielectric relaxation measurements (4), it is known that the relaxation times of solvent dipoles (such as H_2O) is of the order 10^{-9} to 10^{-10} sec., so that it seems likely that the conversion of monomeric traps to the dimeric type takes place on such a time scale.

Further clustering of the solvent molecules near the deeper trap then occurs almost simultaneously causing a modest further increase of the trap depth.

The scheme may be written as:



where S represents a solvent molecule and x is a small integer.

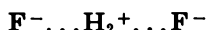
The longer term properties of the solvated electron depend essentially, in this view, on the character of the dimer and multimer. For simplicity in calculating the transition energy between the ground and first excited state we shall examine the dimer states alone, although the spectroscopic properties of the solvated dimer can be expected to be some-

what modified from this by the accumulation of other solvent molecules owing to ion-dipole and ion-induced dipole forces.

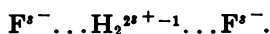
Specifically, for the calculation we choose a dimer model consisting of opposed molecular dipoles bound by a delocalized electronic charge, having a center of gravity lying between the positive ends of the original molecular dipoles. For example, the simplest case, $(\text{HF})_2^-$, could be written diagrammatically as:



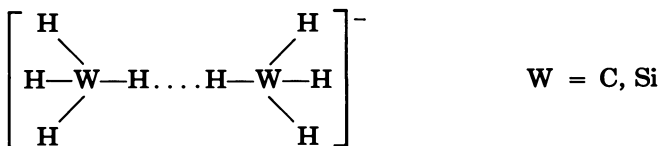
This proposed structure can be alternately viewable as resembling that of a perturbed H_2^+ ion—e.g.,



or one with a scaled nuclear charge,



Analogous structures are proposed for other members of the homologous series of the solvated electron family:



Calculation

A full quantum mechanical calculation of the simplest dimer ion is a formidable task (—e.g., $[\text{F}-\text{H} \dots \text{H}-\text{F}]^-$ with 21 electrons). We are forced to examine the matter using various approximations. Using a molecular orbital approach we can view the problem as one of five electrons associated with the several atomic cores. For $[\text{F}-\text{H} \dots \text{H}-\text{F}]^-$, the simplest MO could be built from 2 p_z orbitals on F and 1s orbitals on H, as in Table I. By symmetry, the orbital coefficients for the two F atomic orbitals will be identical in magnitude as will those of the two H atomic orbitals. The orbital coefficients, c_{ij} , can thus be chosen to be positive definite if the sign convention in Table I is used. The MO's should be

chosen orthogonal to each other and to all other MO's of the molecule ion.

Table I. LCAO MO Scheme for $[\text{F}-\text{H} \dots \text{H}-\text{F}]^-$

MO Wave Function	Energy Level	No. of Nodes	No. of Elec- trons	Sym- metry	Orbital Coefficient for AO's			
					F (1)	H (2)	H (3)	F (4)
ψ_1	1	0	2	<i>g</i>	$+C_{11}$	$+C_{12}$	$+C_{12}$	$+C_{11}$
ψ_2	2	1	2	<i>u</i>	$+C_{21}$	$+C_{22}$	$-C_{22}$	$-C_{21}$
ψ_3	3	2	1	<i>g</i>	$+C_{31}$	$-C_{32}$	$-C_{32}$	$+C_{31}$
ψ_4	4	3	(1*)	<i>u</i>	$+C_{41}$	$-C_{42}$	$+C_{42}$	$-C_{41}$

In a first-order approximation one may view the problem in a one-electron approximation, fixing attention on the fifth electron, that in the lowest "upper" molecular orbital, ψ_3 ; and then argue that on physical grounds one expects $C_{31}^2 < C_{32}^2$ —i.e., this electron orbital will have the electron charge distribution gathered more strongly on the electropositive hydrogen rather than on the electronegative fluorine cores. As a crude approximation we can set $0 \leq C_{31}^2 \ll C_{32}^2$ so that the problem then further reduces to that of a perturbed H_2^+ ion (Orthogonality of the MO's is then lost in this very rough approximation).

The effective charge, Z_{eff} , at the screened protons can be estimated as

$$Z_{\text{eff}} = (\mu_{\text{bond}}/d_{\text{bond}}) \cdot |e|$$

where

μ_{bond} = dipole moment of the H—X, H—Y, or H—Z bond

d_{bond} = bond length

$|e|$ = electronic charge, 4.80×10^{-10} e.s.u.

An excellent summary of the arguments for and against using dipole moments to estimate the effective charge in sigma-bonded systems is give by Del Re (6).

The Hamiltonian chosen is that for an electron in an LCAO-MO of two scaled hydrogenic functions seeing a potential at the four nuclei of $\text{F}-\text{H} \dots \text{H}-\text{F}$ of Z_{F1} , Z_{H2} , Z_{H3} , Z_{F4} , respectively. Preliminary calculation for $Z_{\text{F1}} = Z_{\text{F2}} = -1$, $Z_{\text{H2}} = Z_{\text{H3}} = +1$ showed the effect on the transition energy, ΔE , to be affected in a minor way (25%) by including Z_{F} terms; hence, these were dropped. The calculation then reduced to that for an electron seeing a potential at two shielded positive nuclei. The ground state energy, E_s , for an electron in the field of two positive charges, Z_{H2} and Z_{H3} using the LCAO-MO approximation can be shown to be

$$E_s = -\frac{Z^2}{2} + \frac{Z^2}{1 + \Delta} \left\{ \frac{1}{ZR} [Z(1 + \Delta) - 1] - (1 + ZR)e^{-\Delta R} + (1 + 1/ZR)e^{-2\Delta R} \right\} \quad (1)$$

It has a minimum (in a.u.) at $\partial E_s/\partial R = 0$. (a.u. = atomic units)

This requires

$$\frac{\partial E_s}{\partial R} = 0 = (1 + \Delta) \left\{ \frac{1}{R^2} \left[\frac{1}{Z} - (1 + \Delta) \right] + Z^2 R e^{-sR} - e^{-2sR} [2Z + Z/R + 1/ZR^2] \right\} + \Delta^1 \left\{ \frac{1}{ZR} + e^{-sR}(1 + ZR) - e^{-2sR}(1 + 1/ZR) \right\} \quad (2)$$

$$\text{where} \quad \Delta = e^{-sR} [1 + ZR + Z^2 R^2/3] \quad (3)$$

$$\text{and} \quad \Delta^1 = -e^{-sR} Z^2 R (1 + Z)/3.0 \quad (4)$$

This can be solved numerically for $R = R_e$ at given Z . Using R_e , one evaluates E_s and $\Delta E = E_A - E_s$, the transition energy, where

$$\Delta E = \frac{2Z^2}{1 + \Delta^2} \{ e^{-sR_e} (1 + ZR_e) + \Delta [-1/ZR_e + e^{-2sR_e} (1 + 1/ZR_e)] \} \quad (5)$$

The calculated values for the proton-proton separation, R_e , the binding energy, E_s , and the optical transition energy, ΔE , are given in Table I.

Table II. Rough Estimates for the Characteristics of the Various Dimer Species of the Solvated Electron

Mole- cule	Bond Length of H-X, A. (ref. 22)	Bond Moment, debyes (ref. 23)	Effective Charge, Z_{eff}	Proton-Proton Separation, R_e , a.u., calc.	E_s , e.v., calc.	ΔE , e.v., calc.	ΔE , e.v., obsd.
H_2^+			1	2.14 (2.00 obsd., ref. (11))	-15.53	9.66	11.83 (ref. 1)
HF	0.92	1.94	0.440	2.78	-4.58	3.69	
HCl	1.27	1.08	0.177	4.32	-0.95	0.86	
HBr	1.42	0.78	0.115	5.47	-0.43	0.41	
HI	1.61	0.38	0.049	8.97	-0.09	0.09	
H_2O	0.96	1.51	0.330	3.16	-2.84	2.39	1.19 (ref. 7)
H_2S	1.34	0.68	0.106	5.73	-0.37	0.35	
H_2N	1.014	1.27	0.260	3.55	-1.89	1.63	0.85 (ref. 16)
H_3P	1.42	0.36	0.053	8.56	-0.10	0.10	

Discussion

We have suggested that the solvated electron species can be assumed to be basically a skeleton of two opposed solvent dipoles bound by a localized electron and solvated by further solvent molecules. Using a very rough quantum mechanical treatment, in which the extra electron is treated as localized as in a scaled hydrogen molecule ion orbital perturbed by the remainders of the solvent dipole, and with the scaling chosen essentially proportional to the dipole moment of the solvent molecule, we find the binding energies and transition energies of the solvated electron to be qualitatively reasonable in magnitude. Moreover, the trend in the calculated properties in all cases examined is found

to vary among the several homologous series (—e.g., HX, H₂Y, H₃Z) in a manner in accord with that predicted by chemical experience. In addition, the crude model used in a calculation which contains no empirical parameter yields values for the optical transition energies, ΔE , in reasonable agreement with experiment (see Table II, values for H₂O and H₃N). From a theoretical point of view this indicates that the various approximations involved in the model have a similar effect within the series. From the fact that the calculated transition energies are predicted to within 90% or better without the arbitrariness of adjustable parameters in the model it may be concluded that the approximations are compatible and well suited to describe the solvated electron systems.

Further, the results can suggest to the experimentalist the optical region for absorption by still other possible species of the solvated electron.

Calculations using an improved basis set for the MO's and alternate Hamiltonians for the paired dipole skeleton of the solvated electron are in progress and will be reported at a later date.

Acknowledgment

The authors express their thanks to Professors Kimio Ohno, and Frank E. Harris, and to Dr. Hans Looyenga and Fil. lic. Karl Berggren for many fruitful discussions. One of us (H.A.P.) would like to thank Professor Per O. Löwdin for his encouraging interest and for the opportunity of working in the stimulating atmosphere of the Uppsala University Quantum Chemistry Group in Sweden.

Literature Cited

- (1) Bates, D. B., Ledsham, K., Stewart, A. L., *Phil. Trans. Roy. Soc. London* **246**, 215 (1953).
- (2) Becker, Lindquist, and Alder, *J. Chem. Phys.* **25**, 971 (1956).
- (3) Boag, J. W., Hart, E. J., *Nature* **197**, 45 (1963).
- (4) Bottcher, C. J. F., "Theory of Electric Polarization," p. 234, Elsevier Press, 1952.
- (5) Das, T. P., *Adv. Chem. Phys.* **4**, 303 (1962) (review).
- (6) Del Re, G., *J. Chem. Soc.* **1958**, 4031.
- (7) Grossweiner, L. I., Swenson, G. W., Zwicker, E. F., *Science* **141**, 805, 1042 (1963).
- (8) Hart, E. J., *Science* **146**, 19 (1964).
- (9) Hart, E. J., Boag, J. W., *J. Am. Chem. Soc.* **84**, 4090 (1962).
- (10) Hart, E. J., Platzman, R. L., "Mechanisms in Radiobiology," Errara and Forsberg, eds., Academic Press, New York, 1961.
- (11) Hylleraas, E. A., *Z. Physik* **71**, 739 (1931).
- (12) Jortner, J., *J. Chem. Phys.* **30**, 839 (1959).
- (13) Jortner, J., *Ibid.* **37**, 2506 (1962).
- (14) Jortner, J., Ottolenghi, M., Stein, G., *J. Phys. Chem.* **66**, 2029, 2037 (1962).
- (15) Jortner, J., *Mol. Phys.* **5**, 257 (1962).
- (16) Jortner, J., *Rad. Res. Suppl.* **4**, 24 (1964).
- (17) Kaplan, J., Kittel, C., *J. Chem. Phys.* **21**, 1429 (1953).
- (18) Landau, L., *Physik Z. Sowjetunion* **3**, 664 (1933).
- (19) Lipscomb, W. N., *J. Chem. Phys.* **21**, 52 (1953).
- (20) Massey, H. S. W., "Negative Ions," p. 76, Cambridge University Press, 1950.

- (21) Ogg, R., *Phys. Rev.* **69**, 669 (1946).
- (22) Pauling, L., "The Nature of the Chemical Bond," p. 226, 3rd ed., Cornell University Press, Ithaca, 1960.
- (23) Smyth, C. P., "Dielectric Behavior and Structure," p. 244, McGraw-Hill, New York, 1955.

RECEIVED May 3, 1965. Supported in part by the Oklahoma State Research Foundation.

Formation and Reactions of Electrons and Holes in γ -Irradiated Ice and Frozen Aqueous Solutions

P. N. MOORTHY* and J. J. WEISS

Laboratory of Radiation Chemistry, School of Chemistry, The University, Newcastle upon Tyne, 1, England

Paramagnetic species formed by reactions of the radiation-produced transient species in ice and frozen aqueous systems have been studied by ESR technique. The radiation-produced electrons have been found to react e.g. with acidic solutes to form H-atoms and with group II(b) metal ions to give the corresponding univalent radical ions, while the holes can react with anions such as SO_4^{-2} and H_2PO_4^- giving the radical ions SO_4^- and HPO_4^- . Evidence that the electron and hole are coupled to each other, and may in fact exist in irradiated pure ice primarily in an (exciton-like) bound state has been discussed. The present work provides evidence for the reactions of the radiation-produced positive holes apart from the reactions of the electrons.

The study of the radiolysis of ice and frozen aqueous solutions is not only of intrinsic interest but may also serve to elucidate the views put forward to explain the radiation-induced chemical changes in water and aqueous solutions. From the latter studies (see e.g. Matheson (43) for a recent review) there is now good evidence for the primary chemical species H, OH, $(\text{H}_2\text{O})^-$ (or e_{aq}^-), H_3O^+ , H_2 , and H_2O_2 , of which the hydrogen atoms, the hydroxyl radicals, and the electrons (designated variously as negative polarons or hydrated electrons) are only of transitory existence. One possible way of studying transient species would be to produce them in a rigid ice matrix at low temperatures and use physical methods such as light absorption and electron spin resonance (ESR) to identify them.

* Permanent address: Chemistry Division, Atomic Energy Establishment Trombay, Bombay, India.

The first report of an ESR signal in γ -irradiated ice by Smaller and Matheson (65) demonstrated the feasibility of this method for studying ice radiolysis. Subsequently, Livingston, Zeldes, and Taylor (40) found a doublet ESR spectrum with a splitting of ~ 506 Gauss in γ -irradiated perchloric, sulfuric, and phosphoric acids at 77° K. In H_2SO_4 , diluted with D_2O , the doublet was replaced by a triplet, thus indicating the species responsible for these spectra to contain one interacting proton (or deuteron). The g -factor for the resonance was found to be close to the free electron value, while the hyperfine energy separations differed from the value for the free hydrogen atom (or deuterium) by less than 1%. These observations strongly suggested that this paramagnetic species was the free hydrogen atom. In γ -irradiated pure ice at 77° K., Livingston, Zeldes, and Taylor (41) were unable to detect this doublet; instead, another ill-resolved doublet, split by about 40 Gauss was observed, and this showed anisotropy in the single crystal. This was tentatively attributed to the OH radicals. Ghormley and Stewart (18) observed an ultraviolet absorption spectrum with maximum at 280 μ in γ -irradiated ice and attributed this to the OH radicals. Irradiation and ESR examination of ice at 4° K. (52, 62) revealed the presence of both doublets. On heating to 77° K., the H-atom doublet was found to decay irreversibly, while the intensity of the 40 Gauss doublet was reduced only slightly. Irreversible decay of the latter doublet occurred only on heating to $\sim 110^\circ$ K. (61). Although there is no direct proof that the 40 Gauss doublet is the OH radical, Siegel *et al.* (61) have put forward a number of arguments to support this. From a single crystal study McMillan, Matheson, and Smaller (44) have evaluated the hyperfine and g -tensors for this spectrum. Determination of the yields (G -values) of the H-atoms in the irradiated acids and of the H-atoms and OH radicals in ice have also been made. Livingston and Weinberger (42) found $G(\text{H}) = 1.33$ in glassy 0.129 mole fraction sulfuric acid. In ice irradiated at 4° K., Siegel *et al.* obtained $G(\text{H}) \approx G(\text{OH}) \approx 0.8\text{--}0.9$, while at 77° K., $G(\text{H}) = 0$ and $G(\text{OH}) \approx 0.6$ (61, 62). A recent redetermination (45) of the absolute yields employing DPPH as the reference standard gave results in good agreement with the data of Livingston and Weinberger (42), while the values reported by Siegel *et al.* (61, 62) were found to be too high by a factor of about two.

However, the mechanism of the radiation-induced formation and stabilization of hydrogen atoms in the acidic systems at 77° K. and the fate of the charged intermediate species still remained unsettled. A number of investigations have been carried out in recent years, notably by Schulte-Frohlinde and Eiben (57, 58), Ershov *et al.* (16), and Weiss and co-workers (32, 33, 46, 47, 48, 49, 50). The former two groups have been mainly concerned with the problem of stabilizing the electrons in alkali hydroxide glasses, whereas Weiss *et al.* have investigated frozen aqueous solutions of a number of compounds of widely different chemical nature, including the alkali hydroxides. The physical nature of the charged species in irradiated ice, and their chemical reactions in frozen aqueous solutions form the subject matter of the present article.

**Reactions of the Electrons: Radiation-Induced
Hydrogen Atom Formation in Frozen Aqueous Solutions**

In order to elucidate the mechanism of formation and stabilization of hydrogen atoms in γ -irradiated ice matrices at 77° K., Kevan, Moorthy, and Weiss (32) carried out detailed investigations on frozen solutions of different types of compounds such as the acids and acidic, neutral, and basic salts. In all cases, solutions covering a range of concentrations (from $\sim 0.01M$ up to the highest attainable) were studied, and ESR spectra were recorded over a range of ~ 300 Gauss on either side of the field corresponding to free electron resonance. Some representative spectra are given in Figure 1. In the case of pure ice itself, the ESR signal is an

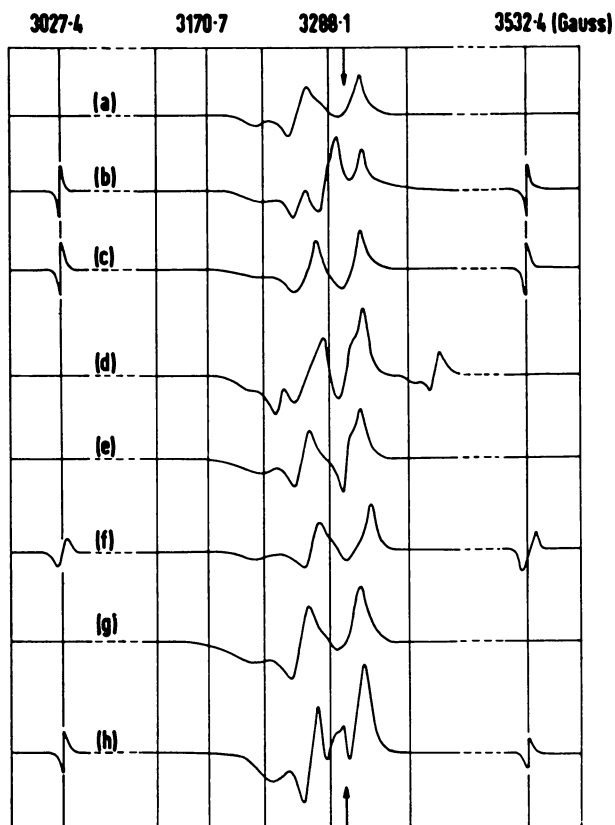


Figure 1. ESR spectra of γ -irradiated frozen aqueous systems at 77°K.; (a) H_2O ; (b) $0.5M H_2SO_4$; (c) $0.5M H_3PO_4$; (d) $0.1M HNO_3$; (e) $0.1M HCO_2H$; (f) $1M Na_2SO_4$; (g) $1M NaCl$; (h) $0.5M Na_2CO_3$.

ill-resolved doublet with a separation of about 40 Gauss, attributed to the OH radical (61), but as the solute concentration increases, superimposed resonances appear. Nevertheless, the low field line of the OH doublet

(at ~ 3264 Gauss) is relatively unperturbed and therefore easily recognizable in all cases except with H_3PO_4 , NaH_2PO_4 , and Na_2HPO_4 in which case the new resonance itself is a doublet with about the same splitting and g factor as the OH radical doublet. With the exception of HNO_3 , HCO_2H , $\text{CH}_3\text{CO}_2\text{H}$, NaNO_3 , and NaCl a second 1:1 doublet with a splitting of about 506 Gauss is also recognizable. In the corresponding heavy water solutions this doublet was replaced by a 1:1:1 triplet with a splitting of ~ 76 Gauss, thus indicating hyperfine interaction of the unpaired electron in the radical with one proton ($I = 1/2$) or deuteron ($I = 1$). The hyperfine energy separations and g -factors evaluated from the appropriate Breit-Rabi equation (13) were found to be close to the free H (or D) atom hyperfine energy separations (51), and free electron g factor respectively. It is to be inferred, therefore, that the 506 Gauss doublet in the aqueous systems and the 76 Gauss triplet in the deuterio aqueous systems are caused by the radiation-produced hydrogen or deuterium atoms.

The presence of OH or OD radicals in these systems is not surprising since they are present in irradiated pure ice itself at this temperature. Other resonances close to the free spin field position differ from one solute to another, and are discussed in the next section. A more significant observation is the presence of H atoms in a number of widely different systems and yet their absence in pure ice itself.

Origin of H Atoms. A comparison of the H atom yields in the pure solute and the frozen aqueous solution indicated that the hydrogen atoms are not formed as a result of the direct action of radiation on the solute itself. In fact, it has been found by Livingston and Weinberger (42) that at high acid concentrations the H atom yields actually decrease, whereas on the basis of a direct effect an increase would be expected. Livingston and Weinberger (42) suggested that the acids may act in some way as physical traps, immobilizing the H atoms primarily formed according to:



The findings of Siegel *et al.* (62) that the 500 Gauss doublet characteristic of the H atoms is found in pure ice irradiated and examined at 4°K . but disappears on warming would, at first sight, support this explanation. The "trap theory" would also explain the concentration dependence of the H atom yields in the different acids; thus with increasing acid concentration, the trap concentration would also increase proportionately, and hence, also the hydrogen atom yield. At high acid concentrations, however, the decrease in the relative proportion of water could lead to a lower rate of hydrogen atom formation according to Equation 1, and hence the H atom yield could decrease although the trap concentration is still increasing. As a result of these two opposing effects the yield could pass through a maximum at some intermediate acid concentration as observed experimentally.

In order to test the validity of the trap theory Kevan, Moorthy, and Weiss (32) compared the H atom yields in a number of different systems.

The results are given in Table I. Although the absolute G values may be subject to systematic errors of up to $\pm 50\%$, the relative values in the different systems are significant to $\pm 10\%$ except in those cases where the yields are less than 0.05 where the limits of error may be $\pm 20\%$. Nevertheless, these results show that the "trapping ability" of the solutes, if such is the case, is vastly different for the different compounds, being, in fact, absent in the case of chloride, nitrate, nitric, formic, and acetic acids. However, these differences in the "trapping abilities" of different solutes are not explicable on the basis of the trap theory.

Table I. Hydrogen Atom Yields in Different γ -Irradiated Aqueous Solutions at 77° K.

<i>Solute (1M)</i>	<i>H atom yield G (atoms/100 e.v.)</i>
Nil	0
HClO ₄	2.07
H ₂ SO ₄	0.43
H ₃ PO ₄	0.25
HNO ₃	0
HCl	0.03
HCO ₂ H	0
CH ₃ CO ₂ H	0
NaHSO ₄	0.14
NaH ₂ PO ₄	0.27
KH ₂ PO ₄	0.27
NH ₄ H ₂ PO ₄	0.25
NaClO ₄	0.02
Na ₂ SO ₄	0.04
NaNO ₃	0
NaCl	0
Na ₂ HPO ₄	0.07
Na ₃ PO ₄	0.03
NaHCO ₃	0.01
Na ₂ CO ₃	0.006

To explain Livingston and Weinberger's observation of the variation of the H atom yields (and of the hydrogen gas yields after thawing) with acid concentration, Sharpaty (63) suggested that the H atoms originating from ice radiolysis according to Equation 1 are not found in pure ice at 77° K. because of rapid recombination according to:



at temperatures above $\sim 20^\circ$ K. When the anions ClO₄⁻, SO₄⁻² and PO₄⁻³ are present, these were supposed to capture the OH radicals, thus suppressing the recombination reaction. The inadequacy of this theory is, however, revealed when the H atom yields in the different solutions are compared (Table I). Up to $\sim 3M$ solute concentration, the yields vary linearly, as shown for a few representative cases in Figure 2. From the results given in Table I, it is seen that, for the same anion, the H atom yields are much higher with the acid as a solute than with the corresponding salt. The fact that acids like H₂SO₄ and H₃PO₄ are incompletely dissociated and consequently at 1M the anion concentration in the acid is less than in the corresponding salt, does not invalidate the above

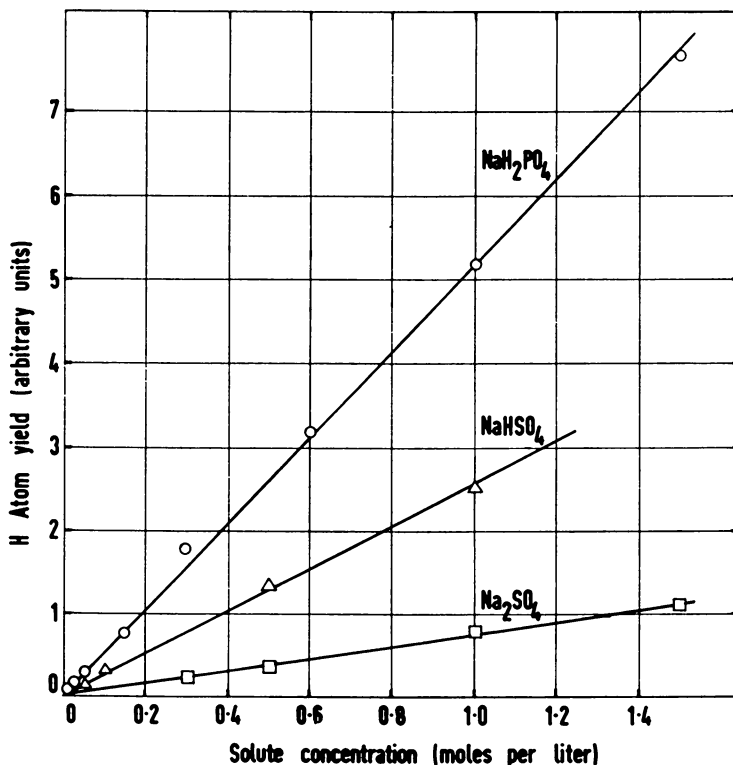


Figure 2. Dependence of H atom yields on solute concentration in γ -irradiated frozen aqueous solutions at 77°K.

argument, since the linear variation of the yield with solute concentration (Figure 2) suggests that at a salt concentration corresponding to the anion concentration in 1M acid, the yield would be still less than for 1M salt. Moreover, from experiments performed at 4° K., Siegel *et al.* (62) have found the yields of H and OH radicals to be $G \approx 0.4$ whereas in the acids the H atom yields increase to a maximum value as high as $G \approx 2$.

Recognizing the importance of the electron in the radiation chemical reactions in aqueous solutions led Weiss (70) to propose a new explanation for the presence of H atoms in the acidic ices at 77° K. In the case of aqueous solutions at room temperature it had been shown (4), that under acidic conditions the electrons are converted to H atoms according to:



The symbol $(\text{H}_2\text{O})_n^-$ or more simply $(\text{H}_2\text{O})^-$ is used to denote that the electron in water does not exist as a water anion H_2O^- but is delocalized over a number of water molecules (71). Weiss extended this idea to the case of ice and frozen aqueous solutions and suggested that the H atoms observed in the irradiated acids arise as a result of

Reaction 3 occurring in ice, when an acid is present. It is to be inferred that the H atoms formed according to Reaction 1 and observed in ice at 4° K. with a yield of $G(\text{H}) \approx 0.4$ contribute little, if any, to the H atom yields in the acids at 77° K. With certain modifications to be discussed below, the concept of the radiation-produced electron as one of the reactive intermediates in the radiolysis of frozen aqueous solutions explains many experimental results.

As the results summarized in Table I indicate, hydrogen atoms are also observed in solutions of the neutral salts such as NaClO_4 , Na_2SO_4 , and of the basic salts Na_2HPO_4 , NaHCO_3 , Na_3PO_4 , and Na_2CO_3 where Reaction 3 evidently cannot occur. Moreover, although 1M solutions of HClO_4 , H_2SO_4 , H_3PO_4 , and HCl contain a sufficiently high hydrogen ion concentration to convert all the electrons into H atoms, the H atom yields in these systems show marked differences. Also the above theory does not satisfactorily explain the effect of HNO_3 and H_2O_2 on the H atom yields as observed by Livingston and Weinberger (42). Although it would appear that these solutes can act as electron scavengers, comparing the rate constants for the reaction of the electron with H^+ and other scavengers such as NO_3^- and H_2O_2 (6, 9, 21, 22, 66, 67, 68) shows that low concentrations of NO_3^- and H_2O_2 cannot compete with H^+ for the electrons. Although the absolute values of the rate constants for the reactions of the electron may be different in the solid and liquid phases, it is reasonable to assume that they would follow the same trend. The relative rate constants evaluated in the case of a few scavengers and compared with the liquid phase results justify this assumption. The alternative possibility that the H atoms first formed according to Reaction 3 react with these scavengers can be ruled out on the basis of the low reactivities of H atoms with these solutes even in fluid solutions at room temperature (21, 22).

Mechanisms of H Atom Formation and Stabilization. Detailed investigations of the effect of a number of electron scavengers on the H atom yields in the different systems were carried out by Kevan, Moorthy, and Weiss (33) in order to find if more than one mechanism is responsible for H atom formation and stabilization in these systems. These results are summarized in Table II. It will be seen that the H atom yields are affected by the scavengers only in certain solutions, but not in others. The scavengers chosen are such as to be much more reactive towards the electron (rate constants of the order of 10^9 – $10^{10} M^{-1} \text{sec.}^{-1}$) than towards H atoms (10^6 – $10^8 M^{-1} \text{sec.}^{-1}$). It therefore appears that there are at least two mechanisms operating to form and stabilize H atoms in these systems. Further, as a general rule, H atoms appear to be formed by reaction of the electron only in the case of mononegative inorganic oxyanions. However, no hydrogen atom signals were found in the case of NO_3^- or NO_2^- as solutes, and also with the simple inorganic ions such as Cl^- and the organic anions such as HCO_2^- .

To explain these observations Kevan, Moorthy, and Weiss (33) proposed that in the case of the anions HSO_4^- , H_2PO_4^- , HCO_3^- , and the corresponding acids as well as with HClO_4 , the hydrogen atoms are formed not only by Reaction 3, but also by reaction of the electron with the

Table II. Effect of Different Electron Scavengers on H Atom Yields in γ -Irradiated Frozen Aqueous Solutions at 77° K.

Solute Acceptor	H_2SO_4 or $NaHSO_4$		H_3PO_4 or NaH_2PO_4		$NaHCO_3$	$NaClO_4$	Na_2SO_4	NaH_2PO_4 or Na_3PO_4		Na_2CO_3
	$HClO_4$	$NaHSO_4$	NaH_2PO_4	Na_3PO_4						
$NaNO_3$	+	+	+	+	+	-	-	-	-	
$NaNO_2$	dec	dec	+	+	+	-	-	-	-	
$Cr_2O_7^{-2}$ or CrO_4^{-2}	+	+	+	+	+	-	-	-	-	
$FeSO_4$...	+	ppt	ppt	+	-	ppt	ppt	ppt	
$CuSO_4$	+	+	ppt	ppt	+	-	ppt	ppt	ppt	
$ClCH_2CO_2H$...	+	+	...	+	-	
CH_3COCH_3	+	+	+	+	+	-	-	-	-	

+ : H atom yields are decreased markedly even by small concentrations ($\sim 0.01M$) of the acceptor solute.

- : H atom yields are not affected even by a high concentration ($\sim 1M$) of the acceptor solute.

dec: Decomposition occurs on mixing the solutions.

ppt: Precipitation occurs on mixing the solutions.

...: No data.

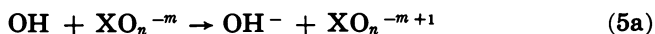
anions (HX^-) and with the undissociated acid molecules H_2X according to:



Consideration of the H atom yields at 1M $HClO_4$, H_2SO_4 , H_3PO_4 , HCl , HSO_4^- , and $H_2PO_4^-$ (Table I) would however indicate that Reaction 3 is rather insignificant as compared to reactions 4(a) and (b). As $HClO_4$, H_2SO_4 , and HCl are "strong" acids, the H atom yields in 1M solutions of these acids should have been nearly equal if H atoms were to be formed by Reaction 3, whereas, in fact, the observed yields are considerably different for these acids. Also, the H atom yield in the weaker acid H_3PO_4 , is higher than in HCl . These differences can be explained on the basis of Reaction 4. The H—O bond in the oxyacids is more polar than the H—Cl bond, so that an electron transfer reaction would occur more readily with the oxyacids than with HCl , thus accounting for the higher H atom yield in the former. Among the oxyacids themselves the polarity of the H—O bond would decrease in the order $HClO_4 > H_2SO_4 > H_3PO_4$, which is also the order of decreasing H atom yields. The effect of electron scavengers on the H atom yields can be considered as a competition between Reaction 4 and the reaction of the electrons with the scavenging solute. The $H_2PO_4^-$ ion (and presumably also HSO_4^- , HCO_3^- , and the undissociated acid molecules) is about two orders of magnitude less reactive than solutes such as NO_2^- , NO_3^- , CH_3COCH_3 , CrO_4^{-2} so that even at concentrations of $\sim 0.01M$ the latter solutes are able to compete for the electrons with the acids and acidic solutes present at $\sim 1M$ concentration.

In the case of Na_2SO_4 , Na_2HPO_4 , Na_3PO_4 , and Na_2CO_3 as the solutes, Kevan, Moorthy, and Weiss (33) suggested that the H atoms formed by Reaction 1 in the hydration shell of the anion are protected from the recombination reaction as a result of the possibility of the reaction of the OH radicals with the respective anions. A reaction in the hydration shell is proposed because this process does not appear to occur in the bulk of

the solution at 77° K. Thus, the OH radical yield at 77° K. is unaffected by the presence of these solutes, and this is as expected, since the OH radicals are not mobile at this temperature. Nevertheless, such a reaction may occur in the hydration shell because of the proximity of the OH radical to the anion. On the basis of this mechanism it can also be seen why the H atom yield ($\sim 0.02-0.04$) in the case of SO_4^{-2} , PO_4^{-2} , CO_3^{-2} , and HPO_4^{-2} as solutes is much smaller than the atomic hydrogen yield in pure ice at 4° K. (~ 0.4): in the latter case the H, OH radical pairs formed according to Equation 1 throughout the bulk contribute to the hydrogen atom yield, whereas in these solutions at 77° K. only the relatively few water molecules in the hydration shells of the anions are effective, the hydrogen atoms produced in the bulk disappearing by recombination (Equation 2). Although this may not seem quite conclusive, some experimental evidence to support the reaction of OH radicals (in the hydration shell) with the anions is suggested from the ESR spectra of these solutions obtained upon irradiation at 77° K. (Figure 3), which reveal the presence of additional resonances. If these new signals are assigned to the reaction product of the anion with the OH radical, it must be further concluded that these reaction products are not necessarily the radical ions formed according to: (XO_n^{-m} acid anion).



Thus, in the case of SO_4^{-2} , the additional resonance either at 77° K. or the one left after warming to $\sim 110^\circ$ K. (when the OH radical signal disappears) is not the same as the one more conclusively attributed to the SO_4^- radical ion. On the other hand, in the case of HPO_4^{-2} , the signal closely resembles the one attributed to the HPO_4^- radical ion. It is possible that, in the case of SO_4^{-2} , the reaction is a simple addition through hydrogen bonding:



However, from pulse radiolysis studies of aqueous solutions definite evidence for processes such as 5 has been obtained recently (2), and the rate constant for the reaction with CO_3^{-2} has been shown to be $2 \times 10^8 \text{ M}^{-1} \text{ sec}^{-1}$. Thus, Reaction 5 or 5a can be justifiably assumed to occur between the anions SO_4^{-2} , HPO_4^{-2} , PO_4^{-3} , and CO_3^{-2} and the OH radicals formed according to Equation 1 in the hydration shell of these ions.

The behavior of perchlorate would at first appear to be anomalous. Thus although in this case, H-atoms are expected to be formed and stabilized in the same way as in SO_4^{-2} , HPO_4^{-2} , PO_4^{-3} , and CO_3^{-2} , yet it is found (Table II) that the H atom yield is decreased in the presence of electron scavengers. To explain this behavior Kevan, Moorthy, and Weiss, (32) suggested that here the H atoms must be formed in the hydration shell of the anion by reaction of the electron with H^+ , the concentration of which in the hydration shell could possibly be higher than in the bulk. An alternative mechanism has been recently proposed by Kevan (31), according to whom the electron reacts with the anion to give an

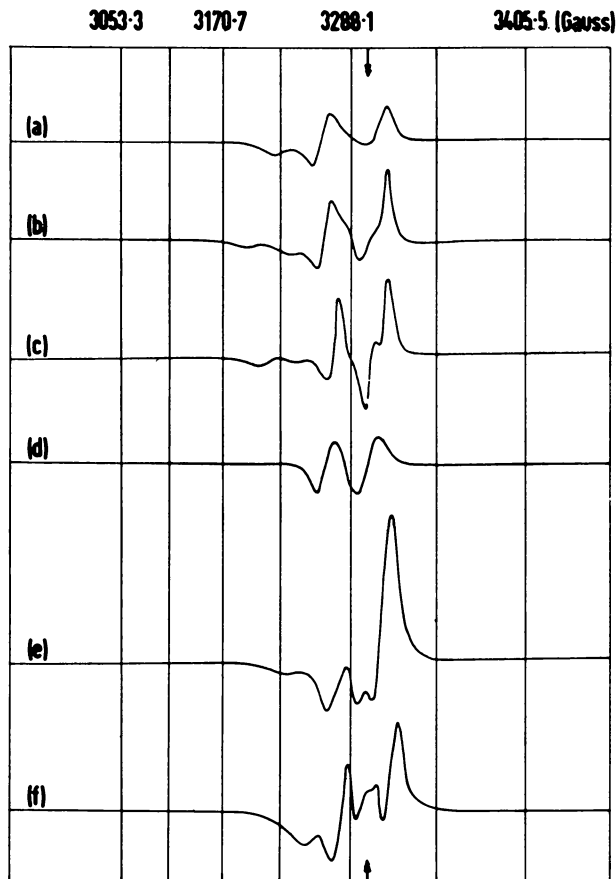
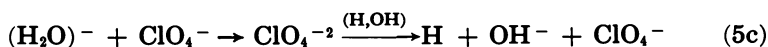


Figure 3. ESR spectra of γ -irradiated frozen aqueous systems at 77°K.; (a) H_2O ; (b) 2M Na_2SO_4 ; (c) 2M Na_2SO_4 after annealing; (d) 2M Na_2HPO_4 ; (e) 2M Na_3PO_4 ; (f) 0.5M Na_2CO_3 .

intermediate dinegative ion followed by an electron transfer from the latter to the OH radical of an H, OH pair formed in the hydration shell:



As a result, an equivalent number of H atoms are protected from the recombination Reaction 2. There is however no direct experimental evidence to support either of these mechanisms. Also, results of scavenging experiments do not reveal whether part of the H atoms in the case of HSO_4^- , $H_2PO_4^-$, HCO_3^- originate from either of the above mechanisms, since H atoms formed according to Reactions 4 and 5c are indistinguishable from the point of view of electron scavenging. A mechanism represented by Equation 5c would also lead to the conclusion that ClO_4^- has electron scavenging properties, although to a very small degree. In

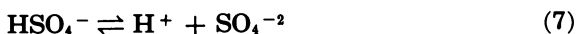
the case of SO_4^{-2} , HPO_4^{-2} , PO_4^{-3} , and CO_3^{-2} as solutes, the absence of any detectable decrease in the H atom yields in the presence of electron scavengers indicates that H atoms are formed almost entirely according to Equations 5a or 5b. This would mean that the di- and trinegative oxyanions exhibit little, if any, electron scavenging properties. A similar conclusion is also arrived at if one considers the variation of H atom yields with acid concentration reported by Livingston and Weinberger (42). Their results in the region of high acid concentration (e.g., at 0.25 mole fraction) indicate that, although in the case of HClO_4 the H atom yield has dropped by nearly an order of magnitude from its maximum value at ~ 0.12 mole fraction, the decrease is much less with H_2SO_4 and almost nonexistent in the case of H_3PO_4 . This inability of the di- and trinegative oxyanions to function as electron acceptors has been attributed (31, 33) to the relatively greater Coulombic repulsion experienced by the electron as it approaches the polynegative ions. This must not, however, be taken as the sole criterion for assessing an ion for its ability as an electron acceptor. Thus it is found that $\text{Cr}_2\text{O}_7^{-2}$ or CrO_4^{-2} are good electron scavengers, comparable with NO_3^- , NO_2^- , and acetone (Table III). A process similar to the one represented by Reaction 5c also cannot occur in the case of the halide ions which, because of their inert gas like electron configuration have little electron affinity, and this may account for the absence of H atoms in the case of the halides (Table I). Organic anions such as HCO_2^- react only slowly with the electron even in aqueous solutions. Further, in the case of these organic ions, even if H atoms were to be formed in their hydration shell by any of the mechanisms represented by Equations 5a to 5c they would be lost by the dehydrogenation reaction:



Liquid phase results (22) also indicate that the corresponding organic acids are very reactive towards the electron, the H atom however not being one of the reaction products.

Hitherto, H atom formation and stabilization has been postulated to occur through Reaction 5a or 5b only in the case of the di- and trinegative oxyanions SO_4^{-2} , HPO_4^{-2} , PO_4^{-3} , and CO_3^{-2} , but not in the case of HSO_4^- , H_2PO_4^- , HCO_3^- , and ClO_4^- . This is justified by the experimental results on the effect of electron scavengers on the H atom yields in the different systems. Thus it was found that with H_2PO_4^- , HCO_3^- and ClO_4^- as solutes, sufficiently high ($\sim 0.1M$) concentrations of electron scavengers such as NO_3^- reduced the H atom yield to below the detection limit of $G(\text{H}) \approx 10^{-4}$. In the case of HSO_4^- as solute, however, there was a residual yield of H atoms ($G \approx 0.02$) even at scavenger concentrations as high as $1.0M$ NO_3^- . Moreover, it was found that this residual H atom signal exhibited microwave power saturation characteristics identical with those from the Na_2SO_4 system, but different from the behavior exhibited by the H atom signals in the NaHSO_4 system in the absence of any scavenger. This conclusively establishes that the residual H atom yield in the case of the NaHSO_4 systems, is

caused by the H atoms stabilized according to Equation 5a or 5b in the hydration shell of the SO_4^{-2} ions present in the system as a result of the dissociation equilibrium:



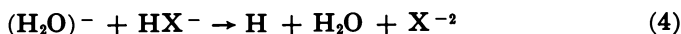
Since nearly 50% of the solute exists as SO_4^{-2} , the observed residual yield in 1M NaHSO_4 (—i.e., in presence of high scavenger concentration) is in agreement with $G(\text{H}) \approx 0.04$ in 1M Na_2SO_4 itself. With H_2PO_4^- or HCO_3^- as solutes the absence of a residual nonscavengeable H atom yield can be attributed to the much smaller dissociation of these anions and the low H atom yields attainable in the HPO_4^{-2} and CO_3^{-2} systems. The ions HSO_4^- , H_2PO_4^- , HCO_3^- , and ClO_4^- themselves appear to be incapable of stabilizing H atoms by the process represented by Equation 5a or 5b. This has been attributed (31) to the fact that Reaction 5a is favored only in the case of the di- and trinegative oxyanions because of the resulting Coulombic repulsion, which is not operative in the case of a mononegative anion in such a reaction. This would also explain why H atoms are not stabilized by such a mechanism in the case of alkali halides as solutes.

From the preceding discussion it may be inferred that in frozen aqueous solutions there are basically two different mechanisms by which H atoms can be formed: (1) by reaction of the electron with acid anions according to Equation 4, and (2) by direct "radiolysis" of water molecules according to Equation 1. Earlier investigations of aqueous solutions at room temperature have also lead to the same conclusion (70). Although there are no experimental data from either the room temperature studies or from those on the frozen solutions, as to the actual nature of the second process, it is believed (70) that it is the dissociation of excited water molecules formed in the tracks of the fast electrons.

Nature of the Mobile Species. In considering the effect of scavengers on the H atom yields it has been assumed that the mobile species reacting with the acceptor molecules are the electrons and not the H atoms as suggested previously (42). This assumption is justified on the grounds that the substances which inhibit H atom formation are specific electron scavengers, such as CH_3COCH_3 , $\text{ClCH}_2\text{CO}_2\text{H}$ and Fe^{+2} , the reactivity of which towards H atoms is very low even in aqueous solutions at room temperature, and therefore should be almost negligible in the frozen matrix. In contrast, these scavengers have a very high reactivity towards the electrons, thus supporting the view that the latter are the reactive species involved. Moreover it is found experimentally that the H atom yields fit a linear plot over a wide range of solute concentration. Although H atoms formed in the bulk according to Equation 1 and diffusing to a "trap" associated with the anion, could lead to the observed linear dependence such a scheme can be ruled out since the maximum H atom yield observed in the acids at 77° K., ($G(\text{H})_{\text{max}} \approx 2$ in HClO_4) is about an order of magnitude higher than the H atom yield in pure ice at 4° K. attributable to the process represented by Equation 1. Moreover, such a view would be inconsistent with the observed dif-

ferences in the effect of electron scavengers in the case of HSO_4^- , H_2PO_4^- , HCO_3^- , and ClO_4^- on the one hand, and SO_4^{2-} , HPO_4^{2-} , CO_3^{2-} , and PO_4^{3-} on the other. It is therefore concluded that the reactive species involved in these reactions are the electrons. More direct evidence to support this is provided by identifying the additional paramagnetic species formed in the presence of certain electron scavengers which can be attributed to the reaction products of the electron with these scavengers. Thus, in presence of the group II(b) metal ions, Mg^{+2} , Zn^{+2} , Cd^{+2} , and Hg^{+2} , an ESR spectrum is found which is unambiguously attributable to the corresponding monovalent ions formed as a result of the reaction of the electrons with the divalent cations while, in presence of $\text{Cr}_2\text{O}_7^{2-}$, a spectrum owing to a pentavalent chromium species is found. Similarly, in the case of acetone as scavenger, the acetone negative ion has been identified (33).

Rate Constants. The effect of electron scavengers on the H atom yields can be considered as a competition between Reactions 4 and 8: (S, electron scavenger).



Making the usual assumption of a stationary state for the concentration of the transient species one obtains:

$$\frac{d[(\text{H}_2\text{O})^-]}{dt} = EI - k_r[(\text{H}_2\text{O})^-] - k_4[(\text{H}_2\text{O})^-][\text{HX}^-] - k_8[(\text{H}_2\text{O})^-][\text{S}] = 0 \quad (9)$$

E , the efficiency of electron formation by the action of radiation, is the number of electrons formed per 100 e.v. of energy absorbed, and I is the dose rate in units of 100 e.v. 1^{-1} sec.^{-1} ; $k_r [(\text{H}_2\text{O})^-]$ is a term to account for the disappearance of the electrons in the absence of any scavengers; the nature of this process is not relevant to the present discussion and will be considered later. The H atom yield is then given by:

$$G(\text{H}) = \frac{1}{I} \frac{d[\text{H}]}{dt} = k_4 \frac{[(\text{H}_2\text{O})^-][\text{HX}^-]}{I} = \frac{Ek_4[\text{HX}^-]}{k_r + k_4[\text{HX}^-] + k_8[\text{S}]} \quad (10)$$

In the absence of the electron acceptor, this becomes:

$$G(\text{H})_0 = \frac{Ek_4[\text{HX}^-]}{k_r + k_4[\text{HX}^-]} \quad (11)$$

Comparing the last two equations shows that, for any given concentration of HX^- , the H atom yield will be progressively reduced with increasing concentration of the scavenger in agreement with experiment. From the last two equations it can also be deduced that

$$\frac{G(\text{H})_0 - G(\text{H})}{G(\text{H})} = \frac{k_8[\text{S}]}{k_r + k_4[\text{HX}^-]} \quad (12)$$

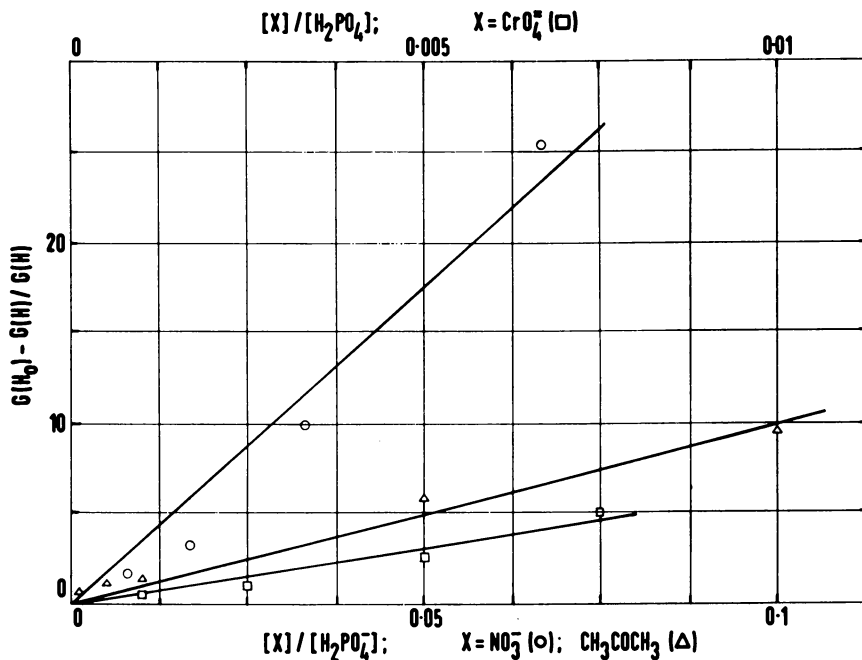


Figure 4. Comparison of the relative reaction rates of the electron with different acceptors in γ -irradiated frozen aqueous solutions at 77°K.

Table III. Comparison of the Relative Rates of Reactions of the Electron with Different Scavengers in Liquid and Frozen Aqueous Systems

Scavenger S	Aq. soln. (20° C.) ^a	Frozen aq. soln. (-196° C.)
CrO ₄ ⁻²		610
NO ₃ ⁻	1300	350
NO ₂ ⁻	770	185
CH ₃ COCH ₃	570	100

^a From reference (27).

Under conditions such that $k_4[\text{HX}^-] \gg k_r$, this can be approximated as:

$$\frac{G(\text{H}_0) - G(\text{H})}{G(\text{H})} \simeq \frac{k_8[\text{S}]}{k_4[\text{HX}^-]} \quad (12a)$$

so that it is possible to evaluate the rate constant ratio (k_8/k_4) for a given scavenger from a plot of $G(\text{H})_0 - G(\text{H})/G(\text{H})$ vs. $[\text{S}]/[\text{HX}^-]$. A few such plots are shown in Figure 4 which show that the experimental results follow the behavior predicted by Equation 12 reasonably well. For a given hydrogen atom-producing solute, and for different scavengers the rate constant ratios (k_8/k_4) should give a measure of the relative efficiencies of these acceptors. The rate constant ratios for a number of scavengers in the frozen aqueous NaH_2PO_4 solutions as evaluated from the plots in Figure 4 are given in Table III and are compared with the

data for aqueous solutions at room temperature. From these results it is apparent that the relative efficiencies of the different scavengers follow the same trend in both phases.

Variation of H Atom Yields with Solute Concentration. Equation 11 also predicts that at low concentrations of HX^- such that $k_r \gg k_4 [\text{HX}^-]$, the H atom yield should vary linearly with the solute concentration. This is in agreement with the experimental results plotted in Figure 2 in the case of NaHSO_4 and NaH_2PO_4 ; other solutes such as HClO_4 , H_2SO_4 , and H_3PO_4 exhibit a similar behavior. Although one would expect that at high solute concentrations (such that $k_r \ll k_4 [\text{HX}^-]$) the H atom yield should approach a limiting value, solubility limitations do not permit experimental verification. In the case of the acids, Livingston and Weinberger's data (42) suggest that, even if one were able to investigate the high concentration region, other factors would introduce complications. Thus, the progressive decrease in the mole fraction of water in the system with increasing solute concentration and the possibility that the anions of these acids may function as electron scavengers to a varying degree can lead to a decrease in the H atom yields in the region of acid concentrations where they should have attained a limiting value. As a result, the yield *vs.* acid concentration plots show a maximum at some intermediate concentration which is different for the different acids. From the maximum $G(\text{H})$ which is found to be highest in the case of HClO_4 (42) a lower limit to the value of E can be given as ~ 2 electrons per 100 e.v.

With Na_2SO_4 , Na_2HPO_4 , Na_3PO_4 , and Na_2CO_3 as solutes where the mechanism of hydrogen atom formation and stabilization is different, the observed linear dependence of the H atom yields of the solute concentration is as expected on the basis of the proposed mechanism. Thus, since the probability of forming an H,OH radical pair in the hydration shell of the anion (—e.g., by dissociation of an excited water molecule) would be proportional to the anion concentration, and since the stabilization of the H atom is postulated as the result of the reaction of the OH radical with the anion in whose hydration shell it is formed, it follows that the yield should be proportional to the solute concentration.

Phase Effects. In the range of solute concentrations employed by Kevan, Moorthy, and Weiss (32) only opaque polycrystalline specimens were obtained on rapidly freezing the aqueous solutions. This method is believed to result in a homogeneous distribution of the solute within the specimens. Both Livingston and Weinberger (42) and Henriksen (23) have investigated the phase effects on the H atom yields in γ -irradiated acids. In regions of acid concentration where one can obtain either glassy or polycrystalline specimens, depending on the technique employed, they find that the H atom yields in the crystalline phase are considerably lower than in the glassy phase. From the method of preparation described by these authors, which in the case of crystalline specimens was to cool the solution very slowly or to induce crystallization by seeding, it appears that in such systems a considerable fraction of the solute could have crystallized as a separate phase, thus leading to a rather low acid con-

centration in the remaining "solution phase," a factor which could account for the low yields in the crystalline system. However, one cannot rule out the alternate possibility that in the glassy phase the electrons are more mobile than in the crystalline systems. This would be equivalent to saying that for the glassy phase k_4 is higher than for the crystalline phase, so that for a given acid concentration $G(H)$ would be higher in the glassy phase.

Dose Saturation. Livingston and Weinberger (42) as well as Kevan, Moorthy, and Weiss (33) found that on prolonged irradiation the hydrogen atom concentration in the acids and acid salt solutions attain a limiting value proportional to the solute concentration. A few typical plots are given in Figure 5. In order to explain this behavior, Kevan, Moorthy, and Weiss suggested that the following reaction occurred in competition with Reaction 4:



Equation 9 then takes the form:

$$\frac{d[(\text{H}_2\text{O})^-]}{dt} = EI - k_r[(\text{H}_2\text{O})^-] - k_4[(\text{H}_2\text{O})^-][\text{HX}^-] - k_{13}[(\text{H}_2\text{O})^-][\text{H}] = 0 \quad (9a)$$

from which one obtains:

$$[(\text{H}_2\text{O})^-] = \frac{EI}{k_r + k_4[\text{HX}^-] + k_{13}[\text{H}]} \quad (14)$$

Under conditions such that $k_r \gg k_4[\text{HX}^-]$, it would follow that $k_r \gg k_{13}[\text{H}]$, since $[\text{HX}^-] \gg [\text{H}]$. Equation 14 can then be approximated as

$$[(\text{H}_2\text{O})^-] \approx \frac{EI}{k_r} \quad (14a)$$

The rate of formation of H atoms is given by

$$\frac{d[\text{H}]}{dt} = k_4[(\text{H}_2\text{O})^-][\text{HX}^-] - k_{13}[(\text{H}_2\text{O})^-][\text{H}] \quad (15)$$

which on integration becomes

$$[\text{H}]_t = \frac{k_4}{k_{13}} [\text{HX}^-] \left[1 - \exp \left\{ - \frac{EI k_{13} t}{k_r} \right\} \right] \quad (16)$$

From the last equation it is seen that as the total dose (*I.t.*) tends to become large such that $\frac{EI k_{13}}{k_r} t \gg 1$, the H atom concentration tends to a limiting value of $[\text{H}]_t = \frac{k_4}{k_{13}} [\text{HX}^-]$, which is in agreement with the plots shown in Figure 5.

Moorthy and Weiss (49) have also studied photochemical charge transfer reactions in frozen aqueous solutions. With I^- and Fe^{+2} as the

ultraviolet absorbing solutes they found that the excited ion formed on light absorption can transfer an electron to a nearby acceptor molecule. When the acids HClO_4 , H_2SO_4 , H_3PO_4 , and HCl are used as electron acceptors, one of the products of the electron transfer reaction is the hydrogen atom. From a study of the hydrogen atom quantum yields, it has been concluded that the efficiencies of these acids are the same as in the case of γ -radiolysis—i.e., in the order of $\text{HClO}_4 > \text{H}_2\text{SO}_4 > \text{H}_3\text{PO}_4 > \text{HCl}$.

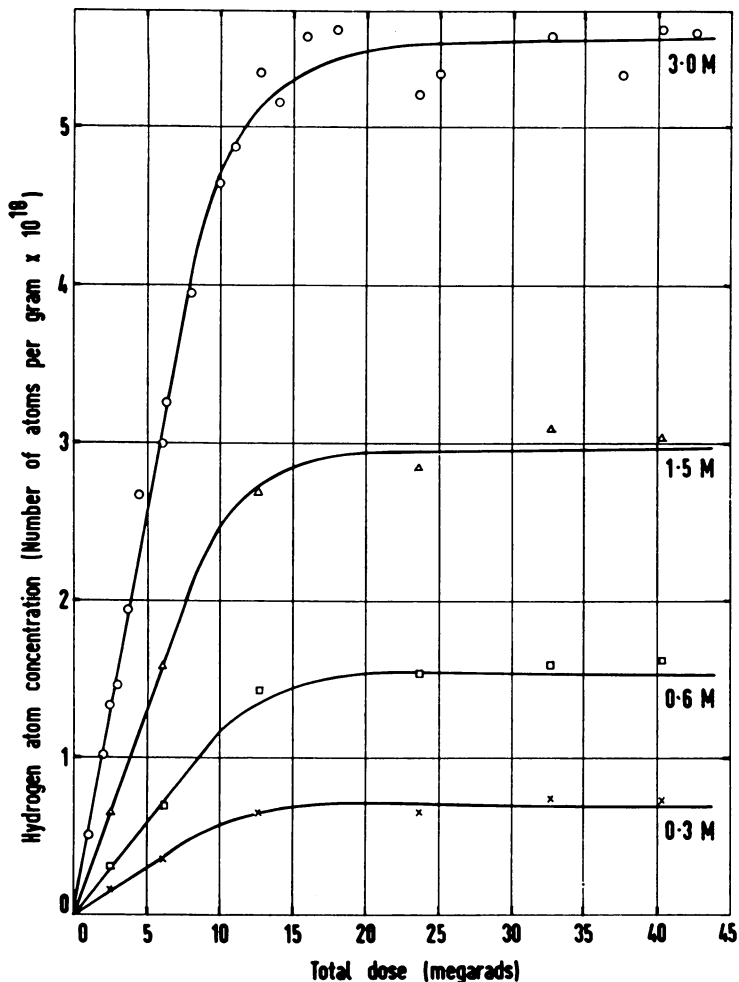
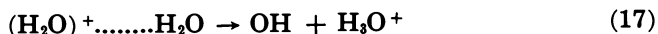


Figure 5. Dose saturation plots for H atoms in γ -irradiated frozen aqueous NaH_2PO_4 solutions at 77°K .

Reaction of the Positive Holes Formed in the Radiolysis and Photolysis of Frozen Aqueous Solutions at 77°K .

The postulation of the reactions of the electrons with certain solutes as discussed above naturally raises the question regarding the fate of the

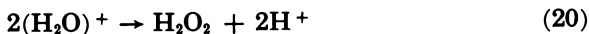
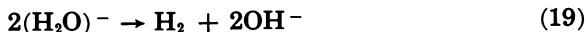
simultaneously formed counterparts—the holes (positive polarons). In the case of liquid water, it is generally supposed that these are much shorter lived than the electrons and are converted into OH radicals by reaction with the neighboring hydrogen-bonded water molecules (24).



Consequently, their reactions with the solutes might not be observable. In support of this view are quoted (24) the high rate constant for the corresponding ion-molecule reaction in the gas phase and the similarity of the ratios of rate constants for reactions of radiolytically and photochemically produced "OH radicals" with H_2 and H_2O_2 , and the absence of salt effects on the competition reactions of Br^- and $\text{C}_2\text{H}_5\text{OH}$ for the "OH radicals" produced in water radiolysis. Weiss (70) has suggested that in a polar medium like water, the positive hole may not be quite as unstable because of the possibility of delocalization of the positive charge in the medium in the manner of what can be called a "positive polaron." The experimentally observed orientation effects in the radiation-induced hydroxylation reactions of cholesterol and related compounds and of monosubstituted benzene derivatives have been quoted to support this view (72). For pure water it was suggested (72) that in the absence of any scavenger, most of the primarily formed positive and negative polarons will recombine according to the reaction:



and that species of the same sign can also interact to some extent giving rise to the molecular products according to:



Positive "Holes" in Ice. In the radiolysis of ice and frozen aqueous solutions, we note that the OH radical yield in pure ice even at 4°K . is only $G \approx 0.4$ whereas the yield of the electrons, as deduced from the H atom studies at 77°K ., is at least as high as $G \approx 2$. If, as is sometimes believed in the case of the liquid phase, the holes are all converted to OH radicals according to Reaction 17 within a very short time after their formation, then one might have found a value of at least $G \approx 2$ for the OH radical yield in pure ice at 4°K . This divergence between the OH yields suggests that in the solid phase at 4° – 77°K ., either Reaction 17 does not occur, or the electron and the hole recombine in the absence of scavengers. It is also found (45) that the OH radical yield is unaffected by the presence of a variety of powerful electron acceptors, from which it follows that the positive holes escaping the recombination reaction do not form OH radicals. As will be discussed in this and subsequent sections, there is good evidence that in the solid phase at 77°K . the positive hole is sufficiently stable to be able to enter into chemical reactions. In fact, the reactions of the electrons and holes seem to be interdependent; this aspect will be discussed later. In the following, the usual solid state

terminology "hole" will be employed to denote a mobile radiation produced positive charge in ice, while Weiss' notation, $(\text{H}_2\text{O})^+$, (abbreviation for $(\text{H}_2\text{O})_n^+$) will be retained to suggest the nature of the matrix as well as to emphasize that the charge is not localized on a single water molecule.

The only previous conjecture regarding the possible existence of the hole in irradiated ice is that of McMillan *et al.* (44) who suggested that the broad resonance on the low-field side of the OH radical doublet spectrum (—e.g., Figure 1(a)) could be caused by this species. Although the observed g -factors: $g_{\parallel} = 2.00$ and $g_{\perp} = 2.04$ (44) would agree with this suggestion in the sense that the corresponding g -factor shifts from the free electron value are as expected for an electron deficient center, it has been found (45) that the intensity of this broad resonance remained unaffected in the presence of various solutes of widely different chemical nature, which included efficient hole acceptors such as the Fe^{+2} ion. Further, assignment of this resonance to the holes naturally raises the question regarding a signal which could be assigned to the electrons. It cannot be argued that the latter are all converted rapidly into H atoms since the H atom yield observed in pure ice at 4° K. is considerably lower than the yield of the electrons as deduced from the H atom yields in the acids at 77° K. It is therefore concluded that this broad resonance is not caused by the radiation-produced holes in ice, and that ESR signals in pure ice owing to electrons and holes as such have not been observed.

Solutes capable of reacting with the electrons and holes can compete with the recombination Reaction 18 to varying degrees depending on their reactivities. Furthermore, when the electron reacts with a solute—e.g., an acid or an acid salt, an equivalent number of holes should escape this recombination process. If these are not converted to OH radicals, they must be either present as such or should react with the solute itself to give some more or less characteristic paramagnetic species. As mentioned above, new ESR signals in addition to those of H atom and OH radical are in fact found in these systems.

Formation of SO_4^- Radical Ion. In the case of H_2SO_4 or NaHSO_4 as solute, a typical ESR spectrum obtained on γ -irradiation at 77° K. is shown in Figure 6a. (In this and subsequent figures the H atom doublet, even when present, is not shown. Wherever necessary, relevant comments are made in the text.) The concentration chosen is such that the new signal at 32881 Gauss does not obscure the low field line of the OH doublet at 3264.6 Gauss. On annealing at $\sim 110^\circ$ K., the OH radical doublet disappears, as in pure ice (61) leaving behind the signal at 3288.1 Gauss (Figure 6c). Comparing this resonance in the H_2O and D_2O matrices (Figure 7) shows that the shapes in the two cases are essentially the same, except that in the D_2O matrix the individual "kinks" are better resolved. This is as expected on the basis of line broadening owing to magnetic dipolar interactions of the unpaired electron with the surrounding nuclei—protons or deuterons in the present case. There is no sign of any nuclear hyperfine structure arising from interaction with the proton or the deuteron. The overall shape can be considered as arising from randomly oriented radicals with an anisotropic g -tensor

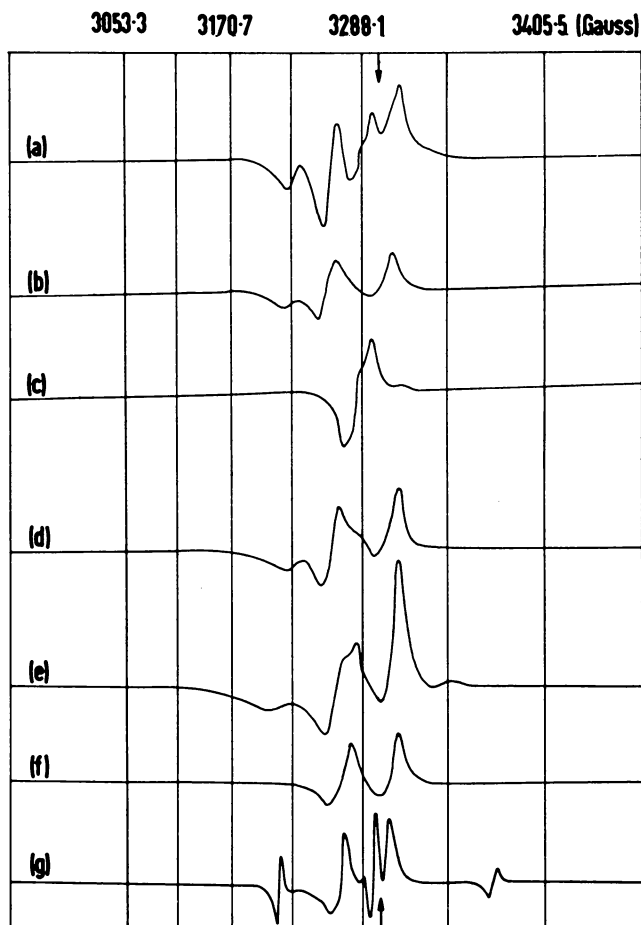


Figure 6. ESR spectra of γ -irradiated frozen aqueous systems at 77°K.: (a) 0.5M NaHSO₄; (b) H₂O; (c) 0.5M NaHSO₄ after annealing; (d) 0.5M NaHSO₄, 0.01M FeSO₄; (e) 2M HClO₄; (f) 1M NaH₂PO₄; (g) 1M NaH₂PO₄ in D₂O.

(35), and the principal g -factors computed on the basis of this interpretation are listed in Figure 7. Since the g -factors are larger than the free electron value, it can be concluded that the spectrum is caused by an electron deficient center. This, together with the absence of proton (or deuteron) hyperfine structure, suggests that either this species is the radiation produced hole itself, in which case the absence of nuclear hyperfine structure could be attributed to a delocalization of the positive charge, or the species is the SO₄⁻ radical ion formed by reaction of the hole with the solute anion according to:



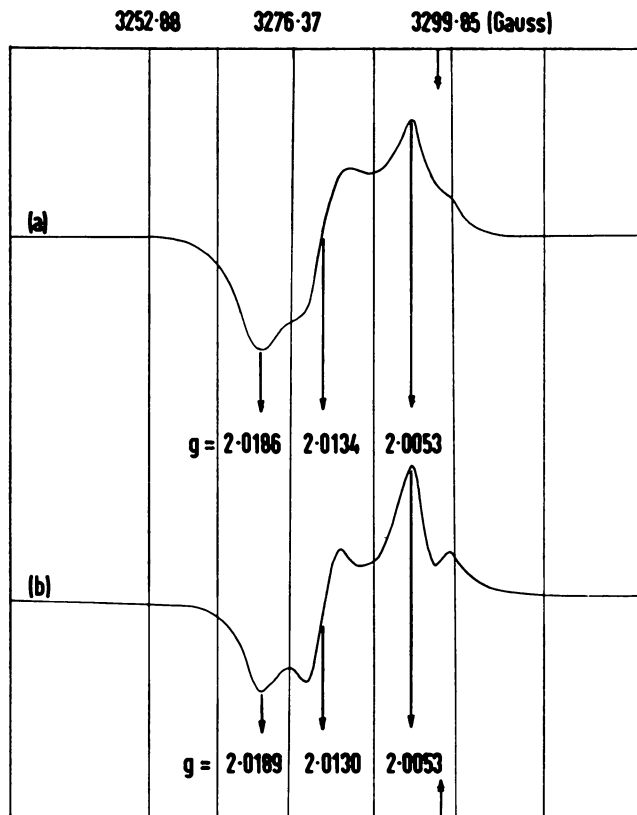


Figure 7. The SO_4^- radical ion ESR spectrum in H_2O and D_2O matrices at 77°K .: (a) 1M NaHSO_4 in H_2O after annealing; (b) 1M NaHSO_4 in D_2O after annealing.

In support of these conclusions it was found that the line at 3288.1 Gauss is absent in NaHSO_4 or H_2SO_4 systems containing a small concentration ($\sim 0.01\text{M}$) of Fe^{+2} (as sulfate) as the hole scavenger (Figure 6d). On annealing the NaHSO_4 or H_2SO_4 specimens (free of Fe^{+2}) it is found that the disappearance of the H and OH doublets is accompanied by an increase in the intensity of the signal at 3288.1 Gauss. As the H atoms and OH radicals could dehydrogenate the HSO_4^- ion to form SO_4^- during the annealing process it may be supposed that the radiation-induced species is also SO_4^- formed according to Reaction 21. Further evidence suggesting that the resonance is not caused by the hole as such is obtained when the spectrum of Figure 6a is compared with those obtained in the case of H_3PO_4 (or NaH_2PO_4) and HClO_4 as solutes (Figures 6e and f). It is found that the line at 3288.1 Gauss found in the case of H_2SO_4 (or NaHSO_4) is not a common feature of these spectra.

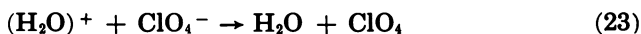
Formation of HPO_4^- Radical Ion. With H_3PO_4 (or NaH_2PO_4) as the solute the spectrum is a doublet with a splitting of about 35 Gauss

superimposed on the OH radical doublet (Figure 6f). Because of the closeness of the hyperfine splittings and the g -factors of the two doublets, they appear as one doublet in the spectrum of Figure 6f, although it is seen to be clearly different from the spectrum of pure ice itself (Figure 6b). The conclusion that the new signal is also a doublet is based on the following observations: on annealing at $\sim 110^\circ$ K. (at which the OH radicals decay) the shape of the spectrum remains essentially unchanged. This means that either the OH radicals do not decay in this system at $\sim 110^\circ$ K., or that the doublet which is superimposed on the OH doublet is much more intense than the latter. The first possibility can be ruled out since the OH radicals have been found to decay irreversibly on annealing at $\sim 110^\circ$ K. in a wide variety of systems such as the dilute H_2SO_4 (or NaHSO_4) system mentioned above. In the case of the H_2SO_4 and NaOH systems to be discussed later, no OH radicals are found in the glassy specimens (obtained above 5M concentration), whereas the doublet under consideration is found even in glassy H_3PO_4 specimens and has the same shape as in the crystalline specimens obtained at lower solute concentrations. The 35 Gauss doublet, with the same shape, is also found in the case of NaH_2PO_4 or D_3PO_4 in the D_2O matrix along with the D atom and OD radical triplets (Figure 6g), and remains unchanged on annealing till the D and OD signals disappear. This last observation, viz., that a doublet and not a triplet is obtained on deuterium substitution, shows that the hyperfine structure is not caused by interaction with the proton (or the deuteron) but by the other nucleus of spin $1/2$ in the system. This hyperfine interaction with the P^{31} nucleus in the solute also indicates that the observed spectrum is not caused by the radiation-produced hole itself. Again, a reaction similar to the one proposed above is indicated:



The observed doublet spectrum is therefore assigned to the radical ion HPO_4^- . In support of this conclusion may be mentioned the observation of a 30 Gauss doublet found in irradiated NaH_2PO_4 and KH_2PO_4 crystals (25) and attributed to the same radical ion.

Formation of ClO_4 Radical. In the case of HClO_4 as a solute the observed spectrum is rather complex (Figure 8f) and less informative. As will be shown later, the two outer lines together with two more lines actually obscured by the rest of the spectrum in the middle can be considered to constitute a quartet expected for the radical ClO_4 formed according to:



A quartet is expected for this radical from hyperfine interaction with Cl^{35} and Cl^{37} nuclei, both of which have a spin of $3/2$, and nearly equal magnetic moments.

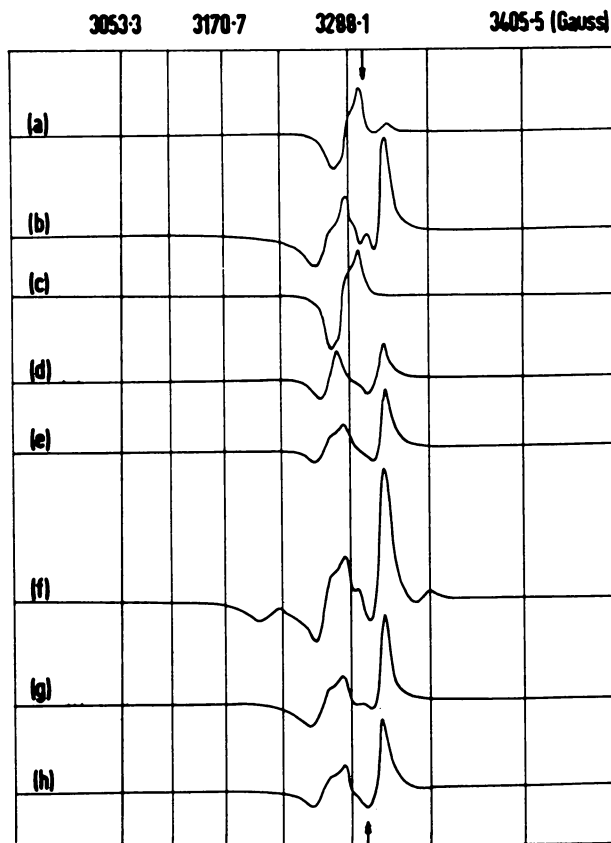


Figure 8. ESR spectra of γ -irradiated frozen aqueous systems at 77°K.: (a) 5M H_2SO_4 ; (b) 5M H_2SO_4 after photobleaching; (c) 5M H_2SO_4 after photobleaching and annealing; (d) 5M H_3PO_4 ; (e) 5M H_3PO_4 after photobleaching; (f) 5M $HClO_4$; (g) 5M $HClO_4$ after photobleaching; (h) 0.5M $Ce(ClO_4)_4$ in 5M $HClO_4$, 2537 Å. UV irradiated.

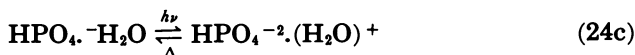
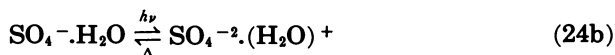
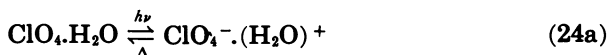
Absorption Spectra. The specimens of H_2SO_4 (or $NaHSO_4$) and H_3PO_4 (or NaH_2PO_4) in ice matrices take on characteristic colors on irradiation, the former turning yellow and the latter pink. From spectrophotometric measurements performed on glassy specimens these colors have been found to correspond to broad absorption maxima centered around 445 and 525 $m\mu$, respectively. The observed "blue shift" in the absorption maximum on going from H_3PO_4 to H_2SO_4 would suggest that in the case of $HClO_4$, where no visible coloration occurs, the absorption lies in the ultraviolet region. Bleaching experiments described below indicate that this absorption has a long tail in the visible region.

Reversible Photochemical Bleaching in Acid Glasses. Photo-bleaching and thermal annealing experiments on initially γ -irradiated (at 77° K.) glassy specimens of oxyacids have led to some interesting observations (48). With glassy specimens of H_2SO_4 as noted before, the OH radical doublet is not found, the spectrum (Figure 8a) consisting essentially of the SO_4^- line at 3288.1 Gauss. There is a much weaker line at 3317.5 Gauss, and this actually forms part of a more complex pattern partly obscured by the more intense SO_4^- line. That this weak line and the associated complex pattern do not form part of the SO_4^- line could be demonstrated both by the bleaching and the annealing experiments. In the former, it was found that only the SO_4^- line and the $445\text{ m}\mu$ absorption band disappear, while the line at 3317.5 Gauss increases in intensity and the full spectrum to which this line belongs appears, without interference from the SO_4^- line (Figure 8b). On subsequent annealing, the pattern shown in Figure 8b including the line at 3317.5 Gauss disappears, while the $445\text{ m}\mu$ absorption band and the SO_4^- line at 3288.1 Gauss are restored (Figure 8c); the resulting spectrum is similar to the initial one (Figure 8a) except that the weak line at 3317.5 Gauss has now disappeared. Annealing performed before bleaching also results in the same spectrum as given in Figure 8c. The two processes of alternate annealing and bleaching can be carried out repeatedly with little loss in the intensity of the spectra at each stage. The above results also show that the $445\text{ m}\mu$ absorption band is to be attributed to the SO_4^- radical ion.

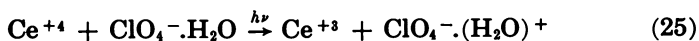
γ -Irradiated glassy H_3PO_4 systems exhibit a similar behavior; the HPO_4^- ESR doublet (Figure 8d) and the $525\text{ m}\mu$ absorption band disappear on photobleaching, and the spectrum shown in Figure 8e results; on annealing, the original doublet and the absorption band reappear, although in this case the efficiency of the thermal restoration process is less than in the case of H_2SO_4 . In both cases, however, complete restoration of the spectra characteristic of the SO_4^- and HPO_4^- radicals occurs even at 77° K., although at a much slower rate. Finally, in the case of HClO_4 , exposure to visible light causes the outer two lines in the complex spectrum of Figure 8f to disappear, leaving behind the pattern shown in Figure 8g. However, in this case, heat treatment either before or after bleaching leads to irreversible changes.

The "Trapped" Hole. Comparing Figures 8b, e, and g reveals that the ESR spectra obtained after bleaching are very similar in all the three cases. An identical spectrum is also obtained on ultraviolet irradiation (at $\lambda = 2537\text{ \AA}$.) of frozen aqueous systems of $\text{Ce}(\text{ClO}_4)_4$ in HClO_4 (Figure 8h). Such a close similarity suggests the species responsible for the spectra to be very similar. Moreover, the complete reversibility (at least in the case of H_2SO_4 and H_3PO_4) of the bleaching and thermal restoration processes, together with the earlier conclusion that the species ClO_4^- , SO_4^- , and HPO_4^- are formed by reaction of the radiation-produced hole with the respective anions according to Equations 21–23 suggests that the processes occurring during bleaching and thermal treatment are

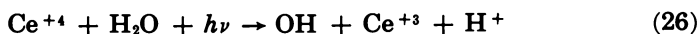
simple charge transfer reactions involving the positive hole. Such reactions can be formally represented by Equations 24.



where the symbols on the right imply a hole trapped in the hydration shell of the respective oxyanion. Such an interpretation is also supported by the result of the photolysis experiment mentioned above in the case of ceric perchlorate where the photochemical reaction:



can be expected to occur. In fact, in aqueous solutions at room temperature the photochemical liberation of oxygen from ceric solutions has been explained by Weiss and Porret (69) on the basis of the primary process:



The analogy between Reactions 25 and 26 is apparent when one notes that in aqueous solutions $(\text{H}_2\text{O})^+$ can be converted to OH radicals by proton transfer from a water molecule (Equation 17).

The characteristic shape of the ESR spectrum of the trapped hole in the different systems is not caused by nuclear hyperfine interaction since $\text{Cl}^{35,37}$ ($I = 3/2$), S^{32} ($I = 0$) and P^{31} ($I = 1/2$) have different nuclear spins, yet the spectra are almost identical in all the three cases (Figure 8). Also, photobleached specimens of H_3PO_4 in H_2O and D_3PO_4 in D_2O exhibit identical ESR spectra, and hence there is no hyperfine interaction with the H or D nuclei. The shapes can be attributed to randomly oriented species with g -factor anisotropy.

In order to elucidate the role of the anions in stabilizing the trapped holes, Moorthy and Weiss (50), in their studies on the photolysis of $\text{Ce}(\text{ClO}_4)_4$ in HClO_4 , followed the quantum yield of the trapped holes as a function of HClO_4 and ClO_4^- concentration. From the results of these experiments given in Table IV, it is apparent that in the perchlorate system the traps for the holes are associated with the ClO_4^- ion. For analogy, one may infer that in the H_2SO_4 and H_3PO_4 systems the traps must be similarly associated with the HSO_4^- (or SO_4^{-2}) and H_2PO_4^- (or HPO_4^{-2} or PO_4^{-3}) ions. From this, some conjecture regarding the nature of the trapped hole in these systems may be made. The isoelectronic ions ClO_4^- , SO_4^{-2} , and PO_4^{-3} have for their central atoms the configuration:

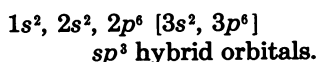


Table IV. Variation of the Relative Quantum Yield of the Trapped Holes with the Concentration of HClO_4 and ClO_4^- in Ultraviolet Irradiated Ce^{+4} (0.02M, as the perchlorate) in HClO_4

Concentrations (molarity)		Relative quantum yield (arbitrary units)
HClO_4	NaClO_4	
1.0	0.0	17.8
1.0	0.8	25.4
1.8	0.0	20.0
1.0	1.9	66.5
2.9	0.0	23.8
1.0	3.8	56.0
4.8	0.0	24.6
^a 9.5	0.0	63.0

^a Glassy specimen, all others polycrystalline.

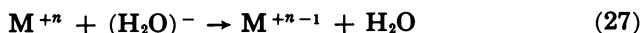
When the radiation-produced hole abstracts an electron from one of the sp^3 hybrid orbitals, the resulting radicals ClO_4 , SO_4^- , and HPO_4^- have an unpaired electron in this orbital, which because of its partial s character can experience hyperfine interaction with the central nucleus, if this has a nonzero spin as in the case of ClO_4 and HPO_4^- . For the latter, a doublet spectrum is observed as expected ($I = 1/2$ for P^{31}). In the case of ClO_4 the two outer lines in the complex pattern of Figure 8f which disappear on optical bleaching can be the outer pair of lines of the expected quartet ($I = 3/2$ for Cl^{35} and Cl^{37}) the central two lines being obscured by the more intense spectrum of the trapped hole. If an electron is transferred from the hydration shell to the half-filled sp^3 hybrid orbital of the radicals ClO_4 , SO_4^- , and HPO_4^- , (—e.g., when they absorb a light quantum according to the scheme represented by Equation 24), the resulting species can be considered to be a hole trapped in an expanded $3d$ orbital of the central atom of the respective ions, delocalized over the water molecules in the hydration shell. In such a species, hyperfine interaction with the central nucleus is not expected.

From the results discussed above it is to be inferred that in the frozen aqueous solutions there is good evidence for the radiation-produced positive species reacting to form free radicals identifiable by ESR. Photobleaching of the radicals so produced as well as ultraviolet photolysis of the Ce^{+4} ion lead to the formation of what must be considered to be a trapped hole.

Radiation-Induced Reduction of Metal Ions in Frozen Aqueous Solutions

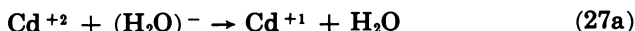
The radicals ClO_4 , SO_4^- , and HPO_4^- described in the previous section represent a few examples of the formation of normally unstable oxidation states of the nonmetallic elements $\text{Cl} (+8)$, $\text{S} (+7)$ and $\text{P} (+6)$ from the corresponding stable, lower oxidation states. In a rigid matrix such as ice, particularly at low temperatures (—e.g., 77°K .) these reactive species, once formed, may not be able to take part in chemical reactions. Nevertheless, as seen in the previous section, charge transfer reactions such as those between the solute ions and the primarily formed charged intermediates of ice radiolysis may occur relatively rapidly even under these

conditions. At sufficiently high temperatures when molecular motions set in—i.e., near the phase transition point of ice ($\sim 193^\circ \text{K.}$) the reactive species formed in these processes are found to decay irreversibly, presumably by chemical reaction with the surrounding molecules. The present section will describe a few more examples of the formation of such species in which, however, the lower, normally unstable oxidation states result from a capture of the radiation produced electron by a metal ion as represented by the general equation:



The normally stable oxidation states of the Group II(b) elements in the periodic table is the +2 state, although in the case of the heaviest member Hg, the +1 state is also stable in a few compounds, where the ion exists in a dimeric form Hg_2^{+2} . The possible role of the +1 states of Cd, Zn, and Mg as reactive intermediates of transitory existence have often been postulated (14). More definite evidence of the formation of the +1 states of Cd and Zn, but not of Mg, was obtained by Adams, Baxendale and Boag (1) by the pulse radiolysis technique.

Cd^{+1} Radical Ions. From the results given in Table IV it is found that the presence of Cd^{+2} in H_2SO_4 or $NaHSO_4$ solutions markedly depressed the H atom yield obtainable on γ -irradiation at 77°K. , a behavior analogous to that of the other electron scavengers. It is thus apparent that the reaction



can compete with the H atom-producing Reaction 4.

Table V. Effect of Cd^{+2} on the H atom Yield in γ -Irradiated 0.5M H_2SO_4 at 77°K.

Cd^{+2} (moles/liter)	$G(H)$ in 0.5M H_2SO_4
0	0.14
0.00075	0.07
0.0025	0.04
0.005	0.03
0.025	0.01 ^a

^a Residual yield (See p. 190-191).

Further, examination of the ESR spectrum of these systems in the region corresponding to free electron resonance revealed the presence of a new signal (in addition to the OH radical doublet and the SO_4^- line at 3288.1 Gauss) which could be attributed to the Cd^{+1} ion. The ESR spectrum of γ -irradiated 0.1M $CdSO_4$ has the same features (Figure 9a). Here the 500 Gauss split broad lines constituting the H atom doublet are not shown. As explained above in the case of SO_4^{-2} as solute, these H atoms are formed in a process which does not involve the electron and therefore are unaffected by the presence of Cd^{+2} . Comparing this spectrum with that of the OH radical spectrum in pure ice (Figure 6b) clearly reveals the presence of the low-field line of the OH radical doublet at 3264.6 Gauss. Superimposed on the high-field line at ~ 3311.6 Gauss is the intense signal attributable to the Cd^{+1} ion. In comparison with the spectrum ob-

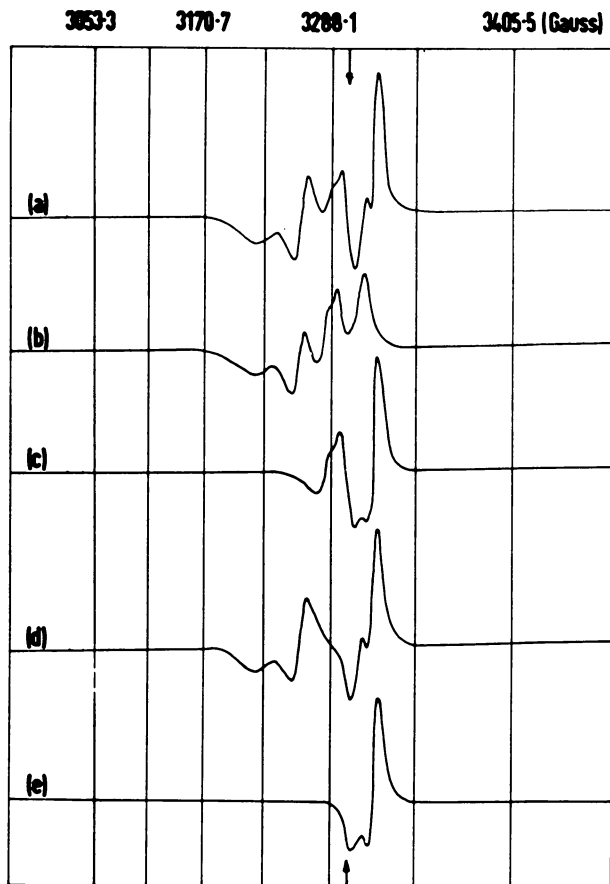
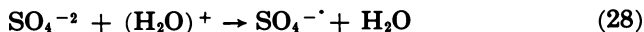


Figure 9. ESR spectra of γ -irradiated frozen aqueous systems at 77°K .: (a) 0.2M CdSO_4 ; (b) 0.5M NaHSO_4 ; (c) 0.2M CdSO_4 after annealing; (d) 0.2M CdSO_4 , 0.02M FeSO_4 ; (e) 0.2M CdSO_4 , 0.02M FeSO_4 after annealing.

tained in the case of 0.5M NaHSO_4 (Figure 9b) the presence of the SO_4^- line at 3288.1 Gauss with its characteristic shape is evident; the formation of the SO_4^- radical ion in the present system must evidently be attributed to the reaction of a radiation-produced hole according to:



On annealing at $\sim 110^\circ\text{K}$., only the OH radical doublet decays leaving behind the SO_4^- and Cd^{+1} lines at 3288.1 and 3311.6 Gauss, respectively (Figure 9c). As in the case of NaHSO_4 , when $\sim 0.02\text{M FeSO}_4$ is also present in 0.2M CdSO_4 , the SO_4^- line is not found (Figure 9d and e), which confirms the occurrence of Reaction 28 in the present case. In the $0.2\text{M CdSO}_4 + 0.02\text{M FeSO}_4$ system, the spectrum remaining on anneal-

ing until the OH radicals decay is that owing to the Cd^{+1} species (Figure 9e). The shape of this spectrum corresponds to that of a species with g -factor anisotropy randomly oriented in the matrix (35) and the principal g -factors computed on the basis of Kneubühls' analysis were found to be $g_1 = g_2 = 1.9880$, $g_3 = 1.9989$ so that $g_{av} = 1.9916$. This indicates that the species responsible for the spectrum is an electron excess center in support of the mechanism proposed for its formation (Equation 27a).

Reaction 27 is similar to the H atom forming Reaction 4 in the case of the acids and acid anions discussed previously. An expression similar to Equation 11 would result for the yields of the M^{+1} ions formed in Reaction 27. At low concentration of the solute the primary recombination of the electrons and holes is predominant compared to their reactions with the solute ions and the yield of the monpositive ions is given by:

$$G(M^{+1}) \approx E k_{27}[M^{+2}] \quad (29)$$

where k_{27} is the rate constant of Reaction 27, and E is the efficiency for the formation of electrons and holes by the primary action of the radiation. From Equation 29 it follows that at low solute concentrations the yield of M^{+1} ions should vary linearly with the concentration; the experimental data have been found to fit a linear plot.

Mg^{+1} and Zn^{+1} Radical Ions. With ZnSO_4 and MgSO_4 as solutes essentially similar spectra as in the case of CdSO_4 were obtained although the SO_4^- line and the signals attributable to the Zn^{+1} and Mg^{+1} ions were found to be of much weaker intensity. As the rate constants at room temperature reveal (9), Zn^{+2} reacts with electrons almost an order of magnitude slower than Cd^{+2} , and the reactivity of Mg^{+2} may be expected to be even less. From Equation 29 it is seen that at a given solute concentration the yield of the $+1$ ions is proportional to the rate constant of the corresponding divalent ion with the electron. This would explain the relatively lower intensity of the spectra of Zn^{+1} and Mg^{+1} as compared with Cd^{+1} . A lower yield of the M^{+1} ions also means that the yield of the SO_4^- ions will be correspondingly lower, since only the holes escaping the primary recombination reaction with the electrons can react to form this radical ion.

Hg^{+1} Radical Ion. Frozen aqueous solutions of mercurous salts (such as the nitrate) do not exhibit an ESR signal as the ion is present in a dimeric form. However, radiation-induced reduction of the $+2$ state in the ice matrix should lead to a different situation. Here the $+1$ ions, once formed, cannot dimerize; under this condition the Hg^{+1} ion should exhibit an ESR spectrum like the other members of the group. This was, in fact, found to be the case, as is evident from Figure 10a which is the ESR spectrum of an acidic ($1M \text{H}_2\text{SO}_4$) solution of $0.1M \text{HgSO}_4$ after γ -irradiation at 77°K . The spectrum consists of a signal attributable to the Hg^{+1} ion in addition to the resonances from the radicals OH and SO_4^- . Similarly on annealing, only the SO_4^- and Hg^{+1} signals are left behind (Figure 10e) while in the presence of $\sim 0.01M \text{FeSO}_4$, only the former is found to have disappeared (Figures 10d and e).

Pentavalent Chromium. The radiation-induced formation of unstable lower oxidation states is not limited to the cations. As an example of the anions, CrO_4^{-2} or $\text{Cr}_2\text{O}_7^{-2}$ have been investigated. In acid media, the presence of dichromate markedly decreases the H atom yields, while in alkali hydroxide solutions an absorption band ($\lambda_{\text{max}} = 585 \text{ m}\mu$) and a characteristic ESR signal both attributable to the trapped

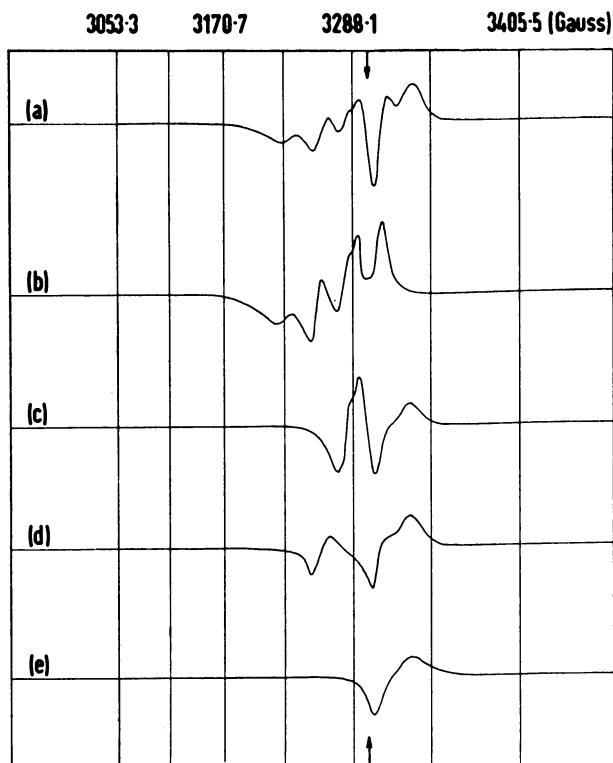


Figure 10. ESR spectra of γ -irradiated frozen aqueous systems at 77°K .: (a) $\sim 0.1\text{M HgSO}_4$; (b) 0.5M NaHSO_4 ; (c) $\sim 0.1\text{M HgSO}_4$ after annealing; (d) $\sim 0.1\text{M HgSO}_4$, 0.01M FeSO_4 ; (e) $\sim 0.1\text{M HgSO}_4$, 0.01M FeSO_4 after annealing.

electron are decreased in intensity (Table VI) in the presence of chromate ions. Comparing the resulting ESR spectra with those obtained in the absence of the electron scavenger reveals the presence of a characteristic ESR signal on the low g -factor side of the free electron position (Figure 11) which can therefore be attributed to a $\text{Cr}(+5)$ species formed according to Equation 27. The line shapes and the principal g -factors (Table VII) of the $\text{Cr}(+5)$ species in the different matrices are close to the values reported for this species formed by chemical reduction (37).

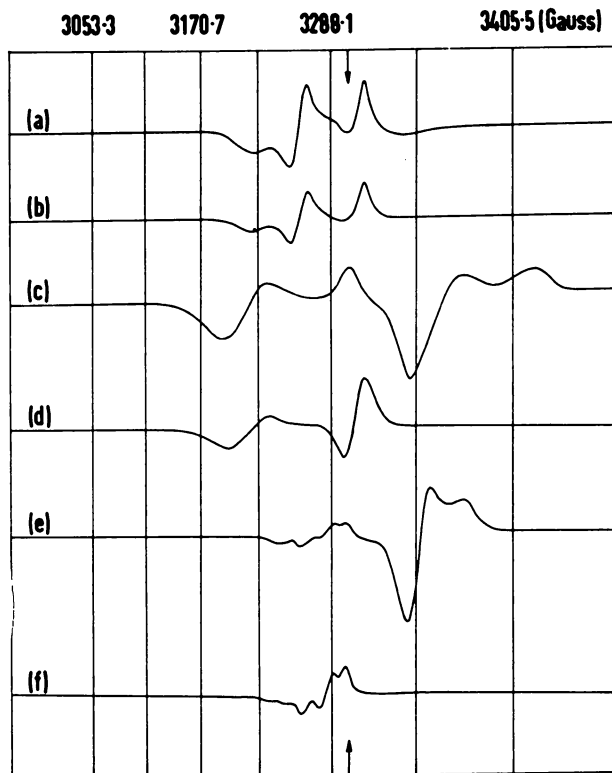


Figure 11. ESR spectra of γ -irradiated frozen aqueous systems at 77°K.: (a) 0.2M CrO_4^{-2} ; (b) H_2O ; (c) 0.1M CrO_4^{-2} , 2M NaOH after annealing; (d) 2M NaOH after annealing; (e) 0.1M CrO_4^{-2} , 2M HClO_4 after annealing; (f) 2M HClO_4 after annealing.

Table VI. Effect of Chromate on the Yields in Acidic and Alkaline-Systems at 77° K.

System	CrO_4^{-2} concentration (moles liter ⁻¹)	G-value (of H atoms or trapped electrons)
1M HClO_4	0	2.07
1M HClO_4	0.1	0.41
1M NaHSO_4	0	0.14
1M NaHSO_4	0.1	0.02 ^a
1M NaH_2PO_4	0	0.27
1M NaH_2PO_4	0.1	0
2M NaOH	0	0.34
2M NaOH	0.2	0

^a Residual yield.

Reactions of Electrons and Holes in Frozen Aqueous Solutions of Alkali Hydroxides

There have been several attempts to identify the radiation-produced electrons in ice, whose role in water radiolysis has been well established by

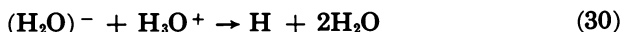
Table VII. Principal *g*-Factors for the Cr(V) Species in Different Matrices at 77° K.

<i>Matrix</i>	<i>g</i> -factors	
	<i>g</i>	<i>g</i> _⊥
2 <i>M</i> HClO ₄	1.9755	1.9547
1 <i>M</i> NaHSO ₄	1.9755	1.9575
1 <i>M</i> NaH ₂ PO ₄	1.9864	1.9222
2 <i>M</i> NaOH	1.9758	1.9332
^a CH ₃ CO ₂ H	1.959	1.970
^a CF ₃ CO ₂ H	1.961	1.977
^a (CO ₂ H) ₂ /CH ₃ CO ₂ H	1.962	1.978

^a Data taken from (37).

conventional chemical methods. Although the formation and reactions of the electrons in water have now been more directly established by the pulse radiolysis technique (20, 30), there is also considerable interest in identifying them by ESR mainly because this can provide an unambiguous and independent proof of their formation and structure in irradiated ice. The experimental difficulties associated with the application of this technique to water have not yet been fully overcome, and therefore most of the work has been carried out in ice. The ESR examination of γ -irradiated pure ice however, showed only the OH radicals at 77° K. (61) and H atoms and OH radicals at 4° K. (62) but no signals attributable to the electrons. This would indicate either that the electrons are not formed in irradiated ice, or that if present, unfavourable relaxation mechanisms obscure their ESR signals, or that the electrons disappear very rapidly as a result of subsequent reactions. However, from the results discussed above it is evident that there can be little doubt as to the formation of electrons in irradiated ice and frozen aqueous solutions. Existing experimental data at different temperatures (61) and over a wide range of microwave power (45) as well as the effect of deuterium substitution (62) shows the second of the above alternatives to be rather unlikely.

One is therefore led to believe that chemical reactions occurring during the irradiation are the main cause of the absence of ESR signals of the electrons in irradiated ice. Such reactions can be basically of three types: (1) between the electron and other radiation produced species, (2) between the electrons and trace impurities, (3) some form of "self destruction" of the electrons. Until recently the widely held belief was that traces of O₂ and CO₂ present even in pure water normally used for radiation chemical work act as efficient electron scavengers. This was logical since the high reactivity of these molecules towards electrons (20) has been established. Since ice specimens prepared from triple distilled water degassed under high vacuum by the freeze-pump-thaw technique showed exactly the same ESR spectrum as those prepared from water not subjected to this treatment, at least the presence of traces of oxygen can be ruled out; the same could be shown for CO₂. In the "self-destruction" hypothesis it was argued (16, 57, 58, 59) that the electrons might be converted to H atoms by the reaction:



In either case, it was thought that increasing the pH should suppress such a process, and the electrons were therefore expected to be stabilized in alkaline systems. It will be shown later that this is basically an incorrect explanation but, nevertheless, an ESR signal and optical absorption at $\sim 585 \text{ m}\mu$ both tentatively attributed to "stabilized free electrons" were first reported by Schulte-Frohlinde and Eiben (57) in γ -irradiated frozen alkali hydroxide solutions. Since then there have been a number of investigations of these systems in different laboratories from different viewpoints. Thus, for example, Blandamer *et al.* (12) have attempted to explain the absorption spectra of γ -irradiated alkali hydroxide glasses at 77° K . by the so-called "confined model." On the other hand, in the present work the aim has been primarily to elucidate the mechanism of the radiolysis of frozen aqueous solutions along the lines developed in the previous sections. From the results discussed above it is apparent that in the case of frozen aqueous solutions both the electrons and holes, formed as a result of the primary action of radiation on ice, play a significant role. It will also be apparent that the absence of ESR signals attributable to the electrons and holes in γ -irradiated pure ice should be attributed to a rapid recombination of these species in the absence of suitable solutes acting as scavengers.

The Spectra. The ESR spectrum of $3M$ NaOH after γ -irradiation at 77° K . is shown in Figure 12a. Similar spectra are also obtained in the case of LiOH and KOH as solutes. The spectra obtained at all solute concentrations up to $\sim 5M$ are qualitatively similar; however, at concentrations below $\sim 0.5M$ the distinguishing features are much less apparent because of the relatively low intensities of the signals. Comparing the spectrum of γ -irradiated alkaline ice with that of pure ice (Figure 12b) reveals the presence of two new signals in the former, one at ~ 3300 Gauss (designated as line A) and the other at ~ 3208 Gauss (designated as line B) in addition to the OH-radical doublet. On annealing at $\sim 110^\circ \text{ K}$. till the OH radical signals decay completely, the spectrum shown in Figure 12c, (scanned at 77° K .) consisting only of the two new lines mentioned above, is obtained. The annealing process also leads to a considerable enhancement in the intensity of line B, whereas the other line is almost unaffected. In contrast, solutions of alkali hydroxide of concentration $>5M$ always give glassy transparent specimens on rapid cooling in liquid nitrogen, and these specimens on γ -irradiation at 77° K . give a spectrum consisting only of the two new lines mentioned above, the OH radical doublet being absent. On annealing, these glassy specimens at $\sim 110^\circ \text{ K}$. (for a period comparable to the time required for the decay of the OH radicals in the case of the crystalline specimens) no change in the intensities of either of these two lines was found.

All specimens, whether glassy or not, take on a blue color on γ -irradiation, and from experiments performed on glassy specimens this color has been found to correspond to a broad absorption maximum centered around $585 \text{ m}\mu$ (28, 57, 58, 59). Similar results are also obtained with the alkali hydroxides in D_2O ; here the line at ~ 3300 Gauss (—i.e., line A) is considerably narrower than the corresponding line in the H_2O matrix,

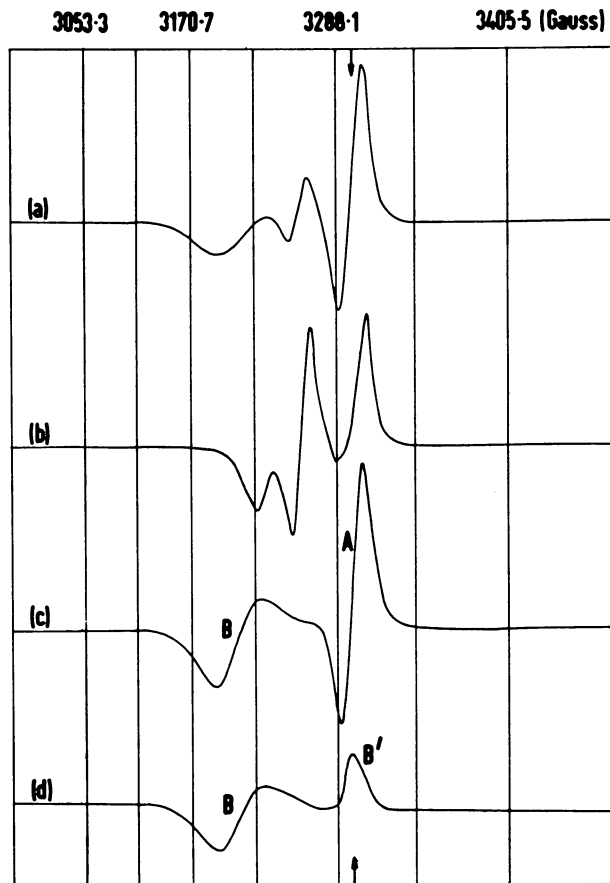


Figure 12. ESR spectra of γ -irradiated frozen aqueous systems at 77°K .: (a) 3M NaOH; (b) H_2O ; (c) 3M NaOH after annealing; (d) 3M NaOH after annealing and photobleaching.

Table VIII. Line Widths and g -Factors for the Trapped Electrons and O^- Radical Ions^a in γ -Irradiated Alkali Hydroxide Solutions at 77°K .

System	Trapped electrons			O^- radical ions		
	g -factor ^b	g -shift $-\Delta g$ $\times 10^3$	Line width ^c ($\pm 1.0\text{ G}$)	g -factor	g -shift $+\Delta g$ $\times 10^3$	Line width ^c ($\pm 2.0\text{ G}$)
LiOH- H_2O	2.0010	1.3	17.6	2.0578	55.5	51.0
NaOH- H_2O	2.0006	1.7	15.9	2.0597	57.4	50.5
KOH- H_2O	2.0003	2.0	14.7	2.0615	59.2	49.5
LiOH- D_2O	2.0005	1.8	5.3	2.0577	55.4	45.0
NaOH- D_2O	2.0003	2.0	6.3	2.0593	57.0	42.7
KOH- D_2O	1.9999	2.4	5.5	2.0605	58.3	41.8

^a As will be evident from the discussion to follow, line A is attributable to trapped electrons and the spectrum comprising lines B and B' to the O^- radical ions.

^b Relative error ± 0.0001 , absolute error ± 0.0003 .

^c Full width at half maximum.

Relative error ± 0.0003 , absolute error ± 0.0006 . The g -factor given here corresponds to the center of line B.

whereas the breadth of line B is only slightly decreased. That these lines are due to two different species is shown by the results of the following experiments. On exposure of the irradiated specimens to visible light the 585 μ absorption band and line A both disappear while the other line is almost unaffected. The former observation also indicates that line A and the blue color are to be attributed to the same species. The microwave power saturation characteristics of the two lines are markedly different: over the microwave power region 1 μ W–5 mW, line B does not show any power saturation at all, while the other line exhibits this behavior at power levels 50 μ W (Figure 13). Experiments on the effect of different electron scavengers to be described below also lead to the same conclusion since only one of the lines is found to be decreased in intensity. From Figure 12d it is also seen that an asymmetric “kink” persists near 3300 Gauss even after bleaching till the blue color disappeared completely. The shape of the last spectrum corresponds to that of randomly oriented species with g-factor anisotropy. The “kink” near 3300 Gauss is designated here as line B'. It will be shown later that this entire spectrum BB' belongs to one species.

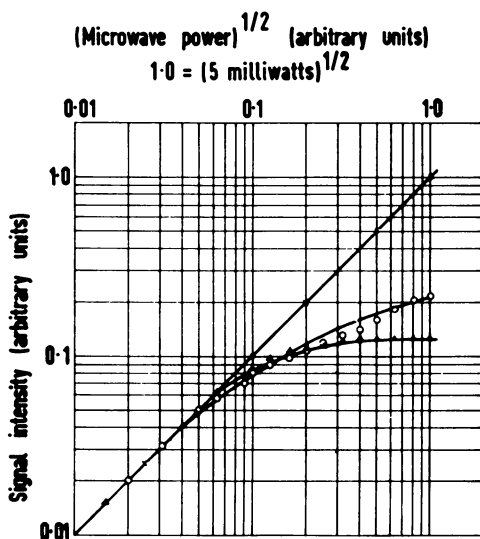


Figure 13. Microwave power saturation of O^- radical ion and trapped electron signals in γ -irradiated frozen aqueous alkali hydroxide solutions at 77°K. T^- in 3M NaOH/ H_2O (Δ); 3M NaOH/ D_2O (\circ); O^- (\times).

All the lines under consideration solely are caused by the presence of the alkali hydroxides as solutes and not by the presence of carbonate as an impurity. This was established by the results of experiments with Na_2CO_3 itself as the solute: the resulting spectrum (Figure 3f) is quite different from those obtained in the case of alkali hydroxides as solutes

(Figure 12a); also the Na_2CO_3 specimens are not blue after irradiation. Further, carbonate free NaOH prepared from distilled sodium metal gave the same results as AnalaR NaOH which contains about 2.5% NaCO_3 as an impurity. Finally, the new resonance signals found in the alkali hydroxide systems are not caused by a direct effect of radiation on the solute, since solid NaOH itself on γ -irradiation at 77°K . neither turns blue, nor shows the characteristic ESR spectra discussed above (16, 45).

From the experimental results discussed in the previous paragraph it follows that with alkali hydroxide as solute in ice there are two new paramagnetic species formed on γ -irradiation at 77°K . in addition to the OH radicals and a small yield of H atoms. It may be inferred that the two new paramagnetic species are caused by the reaction of the radiation-produced electrons and holes with the solute. In order to distinguish between these two species, their g -factors can be taken as guides. Thus in the case of NaOH in H_2O line A corresponds to a g -factor of 2.0006 while the spectrum of the other species comprising lines B and B' has $g = 2.073$ and $g = 2.0015$ (on the basis of Kneubühl's analysis (35)), so that $g_{av} = 2.049$ for this species. The center of line B corresponds to $g = 2.0597$. Similar results were obtained in the case of the other alkali metal hydroxides both in H_2O and D_2O (Table VIII). It thus follows that the former line with a negative g -shift, compared to the free electron value, must be assigned to the reaction product of the electrons while the other which exhibits a positive g -shift is caused by the reaction of the holes. Further confirmation of these conclusions is provided by the results on the effect of different electron scavengers on the intensities of these two signals. The results presented in Table IX clearly show that it is line A which is caused by a species formed by reaction of the electrons—a conclusion in agreement with the one arrived at before on the basis of g -factors alone. It is also seen that the blue color is "bleached" in the presence of the electron scavengers and therefore must be caused by the same species which gives rise to the line A.

Table IX. Effect of Different Electron Scavengers on the Yields of Trapped Electrons and O^- Radical Ions^a in γ -Irradiated 2.5M NaOH at 77°K .

Acceptor (0.1 moles/liter)	Color after irradiation	G_{O^-}	G_{T^-}
Nil	Deep blue	0.53	0.47
CrO_4^{2-}	Yellow (as before irradiation)	0.59	0
MnO_4^-	Purple (as before irradiation)	0.74	0
$\text{Fe}(\text{CN})_6^{3-}$	Yellow (as before irradiation)	0.42	0
$\text{ClCH}_2\text{CO}_2\text{H}^b$	Almost colorless	0.58	obscured
NO_2^-	Colorless	0.62	0
NO_3^-	Colorless	obscured	obscured
N_2O saturated at room temperature	No noticeable difference as compared to 2.5M NaOH	0.74	0.34

^a See footnote (a) to Table VIII.

^b Solutions mixed at $\sim 0^\circ \text{C}$. to minimize hydrolysis of $\text{ClCH}_2\text{CO}_2\text{H}$.

The Electron Deficient Center. It has been suggested by several authors (11, 16, 64) that the line at 3208 Gauss is to be attributed to a hydrated O^- radical ion; the large spin-orbit coupling as reflected by the

large positive g -shift and the large anisotropy in the g -tensor of this resonance line have been explained by these authors on the basis of the above assignment. This large spin-orbit coupling is also responsible for the rather short spin-lattice relaxation time for this species as a result of which it does not exhibit microwave power saturation. Reactions of the radiation produced holes with the hydroxyl ions according to:



followed by a proton transfer from a neighboring hydroxyl ion:



can, in fact, lead to the formation of the O^- ions. This reaction scheme also accounts for the observed increase in the yield of these species with increasing alkali hydroxide concentration (47) since with increasing OH^- Reaction 31 can compete to an increasing extent with the recombination reaction of the electrons and holes. The occurrence of Reaction 32 is also indicated by the observed increase in the intensity of line B on annealing the crystalline specimens at $\sim 110^\circ \text{K}$. when the OH radicals disappear. If the O^- ions are formed solely as a result of Reaction 32 as suggested by Schulte-Frohlinde and Eiben (57, 58) and Ershov *et al.*, (16), then with increasing alkali hydroxide concentration $G(\text{OH})$ should decrease. On the contrary it is found that $G(\text{OH})$ is constant in the region of $\text{NaOH} = 0-5M$, although the yield of O^- ions increases with solute concentration in this region (Figure 14). This indicates, that the O^- radical ions are also formed by another process, viz., Reaction 31 followed by Reaction 32. The model dealt with in greater detail below adequately accounts for the variation of the different radical yields with the alkali hydroxide concentration.

The Electron Excess Center. In their earlier paper Schulte-Frohlinde and Eiben (57) had assigned the line A to the O^- ion and the other line to the "stabilized electron"; subsequently they have reversed this assignment, and are therefore in agreement with other authors. However, the line with $g = 2.0006$ has been interpreted in different ways, although all interpretations relate it to the radiation-produced electron. Thus Schulte-Frohlinde and Eiben (57, 58) consider the species responsible for this line to be a "stabilized free electron," while Ershov *et al.* (16) and Henriksen (23) identify it with a "solvated electron" or a "polaron" in the same sense as these two terms are used in the radiation chemistry of water and aqueous solutions. According to the above authors, this species is not found in pure ice because of Reaction 30, whereas in alkaline systems such a reaction should not occur. (Henriksen does not offer any explanation about the specific role of alkali hydroxide in stabilizing the "solvated electron.") Both of these hypotheses can be shown to be incorrect. Thus, if Reaction 30 occurred to any extent in pure ice, one should be able to detect H atoms in neutral ice with a yield of at least as high as the maximum yield of the "solvated electrons," viz.,

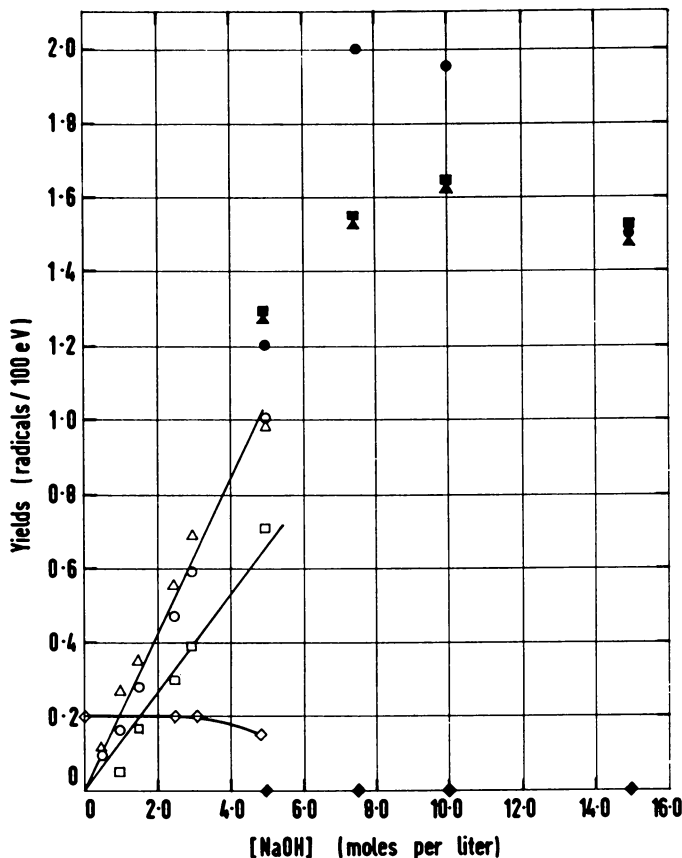


Figure 14. Variation of radical yields with solute concentration in γ -irradiated frozen aqueous NaOH solutions at 77°K. (○) $G(T^-)$ in polycrystalline phase; (●) $G(T^-)$ in glassy phase; (□) $G(O^-)$ in polycrystalline phase at 77°K.; (■) $G(O^-)$ in glassy phase at 77°K.; (△) $G(O^-)$ in polycrystalline phase after annealing at 110°K.; (▲) $G(O^-)$ in glassy phase after annealing at 110°K.; (◇) $G(OH)$ in polycrystalline phase; (◆) $G(OH)$ in glassy phase.

$G \approx 2$ (Figure 14) as found in irradiated alkaline ice. However, even at 4°K. the H atom yield in pure ice is only ~ 0.4 , while at 77°K., no H atoms are found. If, on the other hand, all the H atoms produced by Reaction 3 should combine to form H_2 gas, the yield of the latter should be of the order of $G(H_2) = 1$, whereas the observed yield of molecular hydrogen is only $G = 0.1$ (18). Further, a mere increase in the pH of the system to inhibit Reaction 30 does not result in the "stabilization" of the solvated electrons for it has been found (45) that aqueous Na_2CO_3 or NH_4OH solutions (which have $pH > 7$) on γ -irradiation at 77°K. do not

show the signals attributed to these species and the O^- ions as in the case of the alkali hydroxide solutions. It may be argued that in alkaline ice the occurrence of Reactions 31 and 32 protects a proportionate number of electrons that would otherwise have been consumed by a recombination reaction with the holes. Although as will be considered later, this is partly the reason for the stabilization of electrons in alkali hydroxide solutions, it does not prove to be the complete answer. It is seen from Figure 14 that over the range of concentrations up to $\sim 5M$ NaOH, there are also OH radicals present in addition to the O^- radical ions and the electrons. Also, at all concentrations of NaOH there is a measurable yield of H atoms (23). In view of the high reactivity of the radiation-produced electrons with both H atoms and OH radicals ($k \sim 5 \times 10^{10} M^{-1} \text{ sec.}^{-1}$) it is difficult to see how they can be present in these systems and yet not react with the H and OH radicals. Hence, as will be discussed below, one has to ascribe a more specific role to the alkali hydroxides in stabilizing the radiation-produced electrons.

Having thus concluded that the signal in the free spin field position is not caused simply by the solvated electron (polaron), we are left with the possibilities that it may be either caused by a reaction product of the electron, or by electrons bound in some trap and thereby rendered immobile. As the species from the reaction of the electrons in the alkali hydroxide solutions gives a single resonance line and not the H atom doublet, reaction of electrons with OH^- giving H-atoms can be ruled out. (H-atoms formed in low yields in the alkali hydroxide systems do not originate from the reaction of the electrons since their yields are found to be unaffected by the presence of electron scavengers.) Reaction with the alkali metal cations can also be considered unlikely for, if it were to occur in the case of the alkali hydroxides, it should also occur in the case of the sulfates and the halides. In fact, the ESR line at $g = 2.0006$ and the $585 m\mu$ absorption band are not observed in the case of these solutes. Also, the possibility that these species are colloidal alkali metal atoms formed according to:



can be ruled out since the ESR line and the blue color can be bleached by visible light.

Model for Electron Trapping in the Frozen Alkali Hydroxide Solutions. Since the line A and the associated $585 m\mu$ absorption band in γ -irradiated alkaline ice are not caused by either solvated electrons as such, or their reaction products, we are necessarily led to believe that they are to be attributed to trapped electrons. Any electropositive center can, in principle, be considered capable of functioning as an electron trap. (In this discussion any electron deficient center is considered electropositive.)

One of the first suggestions in this connection was made by Jortner and Sharf (28) according to whom the electron is trapped in an expanded orbital of the alkali metal cation. This view is, however, shown to be unsatisfactory by the experimental finding that electrons are not trapped

in the case of alkali metal sulfates, although here, as with the hydroxides, the holes can react with the SO_4^{-2} ions, thus making a proportionate number of electrons available for trapping on the expanded orbitals of the cations, if such is the case.

Obvious sites for trapping electrons would be electron vacancies. Blandamer, Shields, and Symons (10) suggested that in alkali hydroxide glasses such vacancies can be created by the radiation itself. The only radiation-produced electron deficient centers present in the frozen alkali hydroxide solutions are the OH radicals and the O^- ions. Of these, the former can be ruled out since the trapped electrons persist even on annealing the crystalline specimens at $\sim 110^\circ \text{K}$. when the OH radicals decay; whereas in the glassy specimens there are no OH radicals, yet the trapped electrons do exist. Moorthy and Weiss (47) therefore suggested that the O^- ions, formed according to Reactions 31 and 32 act as the traps for the electrons in the alkali hydroxide systems. More or less direct confirmation of the suggestion made by Moorthy and Weiss (47) was obtained from the results of experiments on the effect of KI as an acceptor solute in the alkali hydroxide systems. It was found that in presence of 1M KI, the O^- line is not present indicating that the I^- ions can compete with OH^- ions for the radiation-produced holes, thus inhibiting Reactions 31 and 32. At the same time the trapped electron signal at $g = 2.0006$ and the blue color are markedly reduced in intensity thus suggesting that the O^- ion is a specific trap for the electron. Contrary to what Blandamer *et al.* (11) conclude, it appears more likely that the residual broad signal near $g = 2.0006$ in presence of a large I^- concentration is an electron trapped at an I atom (formed by reaction of the radiation produced hole with I^-) rather than the original trapped electron center next to an interacting I^- ion. The ESR signal expected of the I atom is, however, not detected, which may be caused by unfavorable relaxation mechanisms. An indication of such a situation has also been obtained in the studies on irradiated frozen HCl, HBr, and HI. In all cases the irradiated specimens take on a green color, but an ESR signal, possibly owing to $(\text{Hal})_2^-$ could be observed only in the case of HCl but not in the case of HBr and HI. Experiments in presence of KI as a hole acceptor also revealed that line B' left behind on eliminating the trapped electron by photobleaching or by electron acceptors is a part of the O^- radical ion spectrum. Thus in presence of KI both lines B and B' were found to disappear, indicating that they both belong to the same species, viz., the O^- radical ion.

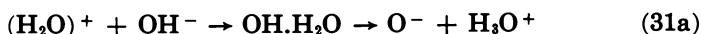
From the preceding discussion it may be concluded that the main resonance line at $g = 2.0006$ in irradiated frozen alkali hydroxide solutions is attributable to the radiation-produced electron trapped around a hydrated O^- radical ion. Insofar as the latter is an electron vacancy created by the reaction of the radiation produced holes with the OH^- ions, the trapped electron may be considered to be analogous to an F center formed in alkali halide crystals, where, however, the electron vacancies exist even prior to irradiation. The term trapped electron (symbolized T^-) has been used throughout the present paper. This model will be

discussed later in the light of the physical characteristics of the resonances, such as the g -factors, line widths, and microwave power saturation. It is also evident that the alkali hydroxide plays a dual role in "stabilizing" the radiation produced electrons in ice: first, as a result of the reaction of the holes with the OH^- ions, an equal number of electrons escape recombination with the holes; second, the hydrated O^- ions function as traps for the electrons. At first sight, it may seem surprising that O^- should act here as a trap. It should be borne in mind, however, that O^- is an electron deficient center and therefore can act as a hole around which the electron is trapped.

On the basis of the above model Moorthy and Weiss (47) have explained the dependence of the yields of the different paramagnetic species, viz., OH , O^- , and T^- on the alkali hydroxide concentration. Their treatment leads to the result:

$$G(\text{T}^-) = G(\text{O}^-) \propto [\text{OH}^-]$$

and $G(\text{OH}) = G(\text{OH})_0$, where the latter is the OH radical yield in pure ice. The experimental results in the crystalline specimens (Figure 14) were in agreement with the above equations, within the limits of uncertainties associated with the evaluation of absolute yields from ESR measurements. The surprising result, which is also borne out experimentally in the crystalline phase (Figure 14) is the constancy of the OH radical yield, having the same value as in pure ice. In view of this, it is suggested that the reaction of the radiation-produced holes with the OH^- ions to form O^- ions proceeds as represented by:

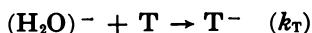


and that Reaction 32 does not occur in the crystalline phase at 77°K . As assumed previously (47), in the glassy specimens O^- ions are formed by conversion of all the OH radicals through Reaction 32, in addition to those formed according to 31a. In this reaction scheme the equations expressing the stationary state criteria for the radiation produced electrons and holes are:

$$\frac{d[(\text{H}_2\text{O})^-]}{dt} = EI - k_r[(\text{H}_2\text{O})^-] - k_T[\text{T}][(\text{H}_2\text{O})^-] = 0 \quad (34)$$

$$\frac{d[(\text{H}_2\text{O})^+]}{dt} = EI - k_r[(\text{H}_2\text{O})^+] - k_{31a}[\text{OH}^-][(\text{H}_2\text{O})^+] = 0 \quad (35)$$

where E is the efficiency of formation of electrons and holes, and the k 's the rate constants for the appropriate reactions. The electron-trapping process is represented by



where T , the electron trap, is the O^- ion formed in Reaction 31a. As will be considered in the next section the "recombination" of the elec-

trons and holes is a pairwise process so that $[(\text{H}_2\text{O})^-] \simeq [(\text{H}_2\text{O})^+]$. From Equations 34 and 35 it follows that $k_T[\text{T}][(\text{H}_2\text{O})^-] = k_{31a}[\text{OH}^-][(\text{H}_2\text{O})^+]$ i.e. $G(\text{T}^-) = G(\text{O}^-)$. Further, from Equation 31a it follows that:

$$G(\text{O}^-) = \frac{k_{31a}[(\text{H}_2\text{O})^+][\text{OH}^-]}{I} = \frac{E k_{31a}[\text{OH}^-]}{k_r + k_{31a}[\text{OH}^-]} \quad (36)$$

At low hydroxide concentrations such that $k_r \gg k_{31a}[\text{OH}^-]$, the observed linear variation of $G(\text{O}^-)$ and hence also of $G(\text{T}^-)$, is apparent from Equation 36. From the assumption already made regarding the glassy phase the yield equations become:

$$G(\text{OH}) = 0$$

$$G(\text{T}^-) \simeq E k_{31a}[\text{OH}^-], \text{ for low } [\text{OH}^-]$$

and

$$G(\text{O}^-) \simeq E k_{31a}[\text{OH}^-] + G(\text{OH})_0$$

As predicted by these equations, the O^- and T^- yields increase with the alkali hydroxide concentration. Although according to Equation 36 the yields should attain a limiting value at high alkali hydroxide concentration such that $k_r \ll k_{31a}[\text{OH}^-]$, above $\sim 10M$ there is actually a slow decrease which evidently must be owing to the fact that the energy absorbed by the water fraction gradually decreases in this region, while energy absorption in the solute does not lead to the formation of the same radicals. From the maximum in the yield *vs.* concentration plot, a lower limit for E can be given as ~ 2.0 electrons and holes each per 100 e.v. absorbed, a value close to the one arrived at from the maximum in the plots of H atom yield *vs.* acid concentration.

Useful insight into the interactions of the trapped electrons with their environment can be obtained by studying the physical characteristics of the ESR signals, such as g -factors, linewidths, and microwave power saturation.

Microwave Power Saturation and Line Widths. The plots of signal intensity of the trapped electron in both the alkaline H_2O and D_2O matrices *vs.* the square root of microwave power (Figure 13) have the shape predicted by Portis (54) for the case of inhomogeneous broadening. Moreover, inhomogeneously broadened lines are Gaussian and do not change either the shape or the width on saturation. This was found to be the case for the signal of the trapped electron in alkaline ice at 77°K . irrespective of the cation both in H_2O and D_2O . In the absence of inhomogeneities in the external magnetic field the causes of inhomogeneous broadening are: anisotropic interaction of the unpaired electron with the applied magnetic field, dipolar interaction between unpaired electrons with different Larmor precession frequencies (—i.e., free radicals with different g -factors), and unresolved hyperfine interaction. Anisotropic interaction with the external magnetic field, if present, should have in a polycrystalline or glassy matrix, given rise to an unsymmetrical resonance with clearly recognizable “kinks” corresponding to the different principal components of the anisotropic g -tensor. On the other hand, the trapped

electron signal is a symmetric single line, and therefore g -factor anisotropy can be ruled out as a cause of inhomogeneous broadening.

From the model already proposed for the trapping of the electron in the alkali hydroxide systems, it is apparent that the trapped electron experiences two types of local magnetic interactions: dipolar interaction with the unpaired electron on the O^- radical ion and nuclear hyperfine interaction with the protons (or deuterons) on the water molecules oriented around the O^- ion (i.e. the water molecules originally oriented around the OH^- ion from which the O^- ion is formed). The observed large decrease in the breadth of the trapped electron signal on going from H_2O to D_2O suggests the latter interaction to be the predominant one. From the results given in Table VIII, and the spins and magnetic moments of the alkali metal nuclei (e.g., (55)) it is also evident that electron spin-alkali metal nuclear spin interaction is much less important as compared with electron spin-proton (or deuteron) spin interactions in causing line broadening, and this also suggests that the model proposed by Jortner and Sharf (28) according to whom the electron is trapped on an expanded orbital of the alkali metal cations, does not hold. On the basis of the model proposed in this section (Figure 15) the absence of appreciable interaction with the alkali metal nuclei is obvious since the nearest neighbors of the O^- ion are the protons. Nevertheless, as shown in Figure 15, there is a small interaction with the alkali metal cations which is reflected by a small, but definite dependence of the line width on the nature of cation and also by the g -shifts (Table VIII).

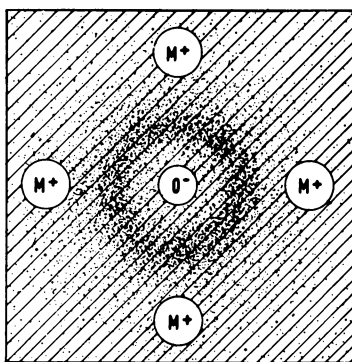


Figure 15. Schematic (two dimensional) representation of the F-center formed in γ -irradiated alkali hydroxide ice at $77^\circ K$. (the striations represent the ice matrix).

Assuming four water molecules to be coordinated to the O^- ions, eight protons can interact with the unpaired electron of T^- . Nuclear hyperfine interaction with eight equivalent protons should result in nine hyperfine components with an intensity distribution of 1:8:28:56:70:-

56:28:8:1. The separation between the individual components is proportional to the unpaired electron density on the interacting protons. An approximate value for this can be obtained by the procedure outlined by Kip *et al.* (34) for the F-centers in alkali halide crystals. According to their treatment the hyperfine separation is given by $(1/n)\zeta A$ where A is the hyperfine coupling constant for the free atom (H atoms in the present case), n , the number of nuclei (protons) interacting with the unpaired electron (eight for the trapped electron) and ζ is the fractional effective s character of the unpaired electron wave function on any of the interacting nuclei. In an earlier treatment (47) this was evaluated as follows. In a free hydrogen atom ζ is unity and the hyperfine coupling constant is 1420 Mc/s; while in the OH radical where the proton is chemically bound, this is 115 Mc/s which corresponds to $\zeta = 0.08$. As in the present case the protons interacting with the unpaired electron are chemically bound as in the OH radical, the value of ζ for the former can be considered to be approximately the same as that for the OH radical. The separation between the individual hyperfine lines in the trapped electron ESR spectrum will then be $1/8 \times 0.08 \times 1420$ Mc/s ≈ 5 Gauss. However, this procedure is not entirely correct, although it gives the correct magnitude for the separation between the individual hyperfine components. The refinement proposed here is as follows. The hydrogenic atomic orbitals making up the trapped electron M.O. are the 2s-orbitals so that the value of A to be taken is $|\Psi_{2s|r=0}|^2/|\Psi_{1s|r=0}|^2$ times the free atom value, i.e. $A = 0.125 \times 1420$ Mc/s. For ζ the value of 0.6 arrived at by Kip *et al.* (34) in the case of the F-center in alkali halide crystals can be taken. The separation between the hyperfine components then becomes $1/8 \times 0.6 \times 0.125 \times 1420$ Mc/s ≈ 5 Gauss, as before. When the ratio of the hyperfine component separation to component width is less than ~ 0.7 , the hyperfine structure will be completely obscured (5), and the observed spectrum will be the envelope of the individual lines. For nine lines with the intensity distribution of 1:2:28:56:70:56:28:8:1, and ~ 5 Gauss apart the envelope turns out to be very nearly Gaussian with a full width at half-maximum equal to ~ 17.5 Gauss. A similar treatment for D₂O leads to 4.4 Gauss for the width. These values are in satisfactory agreement with the experimentally observed values of 16.1 Gauss and 5.7 Gauss, respectively for the ESR spectrum of the trapped electron in the H₂O and D₂O matrices (Table VIII). This therefore, supports the suggestion that the width of the trapped electron is largely caused by unresolved hyperfine interaction, with the neighboring protons (or deuterons). A direct confirmation could only be obtained by the technique of electron nuclear double resonance (ENDOR, (26)). The above treatment can also be extended to include the contribution to the line width from hyperfine interaction with the more distant alkali metal nuclei. In view of the rather small dependence on these nuclei, however, this has not been included.

***g*-Shifts.** The closeness of the *g*-factors of the trapped electron to the free electron value in the different systems (Table VIII) suggests that

the unpaired electron of this center resides in an *s*-orbital, or if it is in a *p*-orbital the crystalline field quenches almost completely the orbital moment. The lowest empty orbital on the O⁻ radical ion in which the electron can be trapped is the 3*s*, and therefore it is reasonable to assume that the electron in the trapped electron center resides on this orbital. From the results given in Table VIII it is also seen that this center exhibits a negative *g*-shift of 10⁻³ units as compared with the free spin value. This can be explained by assuming a small admixture of the next higher 3*p*-state with the ground state 3*s* orbital. It is also found that $|\Delta g|$ increases from Li to K which can be explained by assuming admixture of *p*-states of the neighboring alkali metal cations as in the case of the F-center in alkali halide crystals (29). On the basis of the proposed treatment $|\Delta g|$ is proportional to $\lambda/\Delta E$, the ratio of the spin orbit coupling parameter to the *s-p* separation. The $\lambda/\Delta E$ values computed from spectroscopic data (38) show that the observed *g*-shifts follow the same trend as the former, although on this basis alone a larger variation in *g*-shifts might be expected. For the same cation the *g*-shifts are also found to be different for H₂O and D₂O as the matrices. As the variation of the *g*-shifts with the alkali metal nucleus and the hydrogen isotopes is small compared to the absolute magnitude of the *g*-shift, it is to be concluded that the major contribution to this quantity comes from the spin-orbit interaction resulting from the admixture of the 3*p* oxygen orbital with the 3*s* orbital on which the electron is trapped.

The O⁻ radical ion resonance has certain characteristic features different from those of the trapped electron. The observed large positive *g*-shift (Table VIII) indicates the presence of the odd electron with appreciable spin orbit coupling in a shell which is more than half-filled. As pointed out by Blandamer *et al.* (11) the form of the *g*-tensor suggests that the crystalline electric field acting on this species has axial symmetry. The decrease in the line width on substituting H₂O by D₂O is much less than in the case of the trapped electron, suggesting that unresolved hyperfine interaction with the proton (or deuteron) is not solely responsible for the large width of the O⁻ resonance. It may partly be owing to *g*-value anisotropy, and partly to a short relaxation time, which is evident from the fact that the O⁻ signal does not exhibit microwave power saturation, as in the case of the trapped electron, however, a small dependence of the widths and the *g*-shifts on the alkali metal nuclei is also apparent, thus suggesting that the odd electron in this radical ion interacts to some extent with the neighboring cations.

Nature of the Electrons and Holes in Irradiated Ice

From a detailed consideration of the kinetics of reactions of electrons and holes in γ -irradiated frozen aqueous solutions (45), it is inferred that any model proposed to describe the nature of these species and their interactions has to meet the following requirements in order to be able satisfactorily to explain the different experimental results: the electrons and holes normally undergo a primary recombination process and experi-

mental evidence suggests that this process is kinetically of the first order. An appreciable chemical reaction owing to these species is observed only when there are solutes present capable of reacting with both of these species in competition with the recombination process. Thus, for instance, in the case of the sulfates of the group II(b) metals, the holes react with SO_4^{-2} to form the SO_4^- radical ion, but this reaction does not occur in the case of the alkali metal sulfates, the difference being that only the above divalent metal ions can react with the electrons. Similarly, the reaction of the electrons with chromate does not take place to any extent unless an acceptor for the positive holes such as OH^- , H_2PO_4^- , HSO_4^- , HClO_4 is also present. These observations imply that even if a reaction were to occur with either the electron or the hole the other species will be close enough to react with the product of this reaction thus reforming the original solute, as shown by the following scheme (X and Y are electron and hole acceptors, respectively).

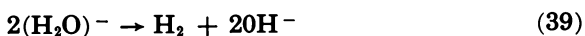


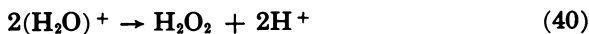
or



Such a process can be considered to be a catalyzed recombination of the electrons and holes via a suitable solute. On the other hand when there are two solutes (X and Y) capable of reacting with the electrons as well as with the holes, Reactions 38a and 37a can effectively compete with the back Reactions 37b and 38b. From these considerations it may be inferred that in irradiated ice and frozen aqueous solutions the electron is closely coupled to the hole and may be considered to be a polaron bound to a hole polaron (36). This would also account for the first-order nature of the recombination process.

Model for the Radiolysis Water and Aqueous Solutions. In the light of the currently accepted theories of the initial physical and chemical processes accompanying the passage of ionizing radiations through matter, in water or ice one would expect the initial formation of excited water molecules, and positive holes and electrons. Weiss (70) had suggested that both the parent positive hole $(\text{H}_2\text{O})^+$ and the electron polarize the medium and are stabilized by "self-trapping" in a manner analogous to the polarons in ionic crystals. It is further postulated that in the polarons the charges are delocalized over a relatively large number of water molecules, which is conveyed symbolically as $(\text{H}_2\text{O})_n^-$ and $(\text{H}_2\text{O})_n^+$ or more simply $(\text{H}_2\text{O})^-$ and $(\text{H}_2\text{O})^+$. In this model the predominant reactions of the polarons in the absence of suitable scavengers are:





Recent pulse radiolysis experiments (20, 30) have fully established the presence of the negative polarons (hydrated electrons) in irradiated water, and also have demonstrated the occurrence of Reaction 39 (15).

Dielectric Properties of Ice. Although the polaron model proposed by Weiss (70) for water is adequate to elucidate the role of the charged intermediates in irradiated ice and frozen aqueous solutions, consideration of the dielectric properties of ice as compared to water however indicate the necessity for certain modifications which seem to be justified by the present findings. The static dielectric constant of ice at -65°C . is ~ 95 (7), while for liquid water at 25°C . it is ~ 84 . The significant difference between the two phases is with respect to the relaxation time for orientation of the water dipoles. The value for water at 25°C . is 10^{-10} sec. and would clearly be very large for ice at -196°C . (7). This would mean that whereas in water the orientation of dipoles can follow the fields even up to very high frequencies this would not be the case in ice at 77°K . Consequently, the Coulombic attraction in ice is not governed by the static dielectric constant but by the high frequency limit $\epsilon_\infty = n^2 = 1.7$. This is to some extent offset by the fact that in ice at these temperatures the electron on thermalization (~ 0.006 e.v.) would be somewhat further away from the parent ion than in water (thermal energy ~ 0.025 e.v.). Another consequence of the long relaxation time for ice is the fact that neither the hole nor the electron can polarize the surrounding medium by re-orientation of the water dipoles which are so to speak "frozen in." Because of the greater electrostatic attraction between the electron and the hole polarons in ice, these two can be bound together in a manner somewhat analogous to the binding in an exciton (36). The possible existence of excitons in irradiated ice has been previously also suggested by Weiss (70).

At this stage, it would in fact, be pertinent to visualize the radiolysis of ice in terms of solid state concepts. According to these the ionization process is equivalent to the excitation of an electron into the conduction band continuum leaving behind a positive hole in the valence band. In the band picture neither the electron nor the hole is localized on any specific molecule; further, they can bring about electronic polarization of the surrounding medium and can exist in polaron states. The attractive potential between such electron (or negative) and hole polarons determines a series of stable bound states in the energy gap between the valence and conduction bands. It is postulated here that the polaron states have appreciable lifetimes during which reactions of the electrons and holes with suitable solutes can be observed. In the absence of such reactive solutes, the electrons subsequently drop into one of the stable exciton states and this process, rather than the annihilation of electrons and holes, is considered to be the first-order recombination process discussed above.

Luminescence Studies. The present model, apart from satisfactorily explaining the different experimental observations also adequately accounts for the observations on the fluorescence and thermoluminescence of γ -irradiated pure ice (17, 60). Non-Cerenkov fluorescence emission has been observed during γ -irradiation of ice at temperatures above 87° K., and the shape of the curve of fluorescence intensity versus temperature of irradiation definitely suggests that there should be fluorescence emission also at 77° K. On warming ice initially irradiated at 77° K., thermoluminescence was also observed between 103° and 263° K. On the basis of the model proposed here these observations can be interpreted as follows. The electrons are distributed among a number of exciton levels covering a wide energy range. The electrons bound in levels which are separated from the conduction band by energies less than the thermal energy can be thermally excited into the conduction band; following such an excitation the electrons and holes can undergo radiative recombination. From the point of view of the recombination process postulated above, this can now be considered to involve both a radiative annihilation of some of the electrons and holes and the transformation of others from the reactive polaron states to the bound exciton states.

Summary

Some general conclusions regarding the radiolysis of ice and frozen aqueous solutions at low temperatures (4°–77° K.) have been arrived at from the work reported here. The hydrogen atoms and hydroxyl radicals formed in irradiated pure ice at 4° K. as well as the OH radicals formed at 77° K., do not originate from the electrons and holes resulting from the action of radiation on ice. These radicals are probably formed by dissociation of excited water molecules in the tracks of the fast charged particles passing through the medium. In pure ice at 77° K., only OH radicals are found because of the occurrence of reactions: $\text{H}, \text{OH} \rightarrow \text{H}_2\text{O}$ and $\text{H} + \text{H} \rightarrow \text{H}_2$, whereas the $\text{OH} + \text{OH}$ reaction occurs only above $\sim 110^\circ \text{K}$. However, in the case of solutes with polynegative oxyanions such as SO_4^{-2} , HPO_4^{-2} , PO_4^{-3} , CO_3^{-2} etc., H atoms formed by the dissociation of water molecules in the hydration shell of these oxyanions are stable even at 77° K., as in this case the H atoms are presumably protected from recombination with the OH radicals which can react with the anions. There is another more important mechanism for the formation of H atoms in frozen aqueous solutions at 77° K., namely the reaction of the electrons (negative polarons) with acidic salts such as bisulfate, dihydrogen phosphate, or bicarbonate, or the corresponding acids as the solutes. These H atoms are also stable at 77° K. because they are not attacked by the holes (positive polarons) which under these conditions react with the anions. It was found that the divalent cations such as Mg^{+2} , Zn^{+2} , Cd^{+2} , and Hg^{+2} can react with the electrons to form the corresponding monovalent cations, identifiable by their characteristic ESR spectra. Similarly, reaction with chromate (or dichromate) gives a

pentavalent chromium species. In the alkali hydroxide systems the holes react with the OH^- ions to form O^- radical ions and the electrons are trapped in the form of F-centers, in an expanded orbital of the O^- radical ions. In all cases, however, an observable net reaction of the electrons or holes occurs only when there are solutes present capable of reacting with both of these species. With solutes which react with only one of these species no net reaction is observed since the reaction product in general is attacked by the second species in its proximity. In pure ice these charged species are mutually trapped in the form of bound electron-hole pairs of exciton-like character. Such a model is also kinetically compatible with the experimental results on radical yields and the effect of acceptor solutes on these yields.

Acknowledgment

One of us (PNM) thanks the Atomic Energy Establishment Trombay, Bombay, India, for the award of a Colombo Plan Fellowship during the tenure of which the present work has been performed.

Literature Cited

- (1) Adams, G. E., Baxendale, J. H., Boag, J. W., *Proc. Chem. Soc.* **241** (1963).
- (2) Adams, G. E., Boag, J. W., Michael, B. D., *Proc. Chem. Soc.* **411** (1964).
- (3) Allan, J. T., Scholes, G., *Nature* (London) **187**, 218 (1960).
- (4) Allen, A. O., Schwarz, H. A., *Proc. Second Intern. Conf. Peaceful Uses Atomic Energy*, United Nations, Geneva, **29**, 30 (1958).
- (5) Anderson, R. S., in "Methods of Exptl. Physics," Marton, L., ed., p. 441-500, Academic Press, New York, 1962.
- (6) Appleby, A., Scholes, G., Simic, M., *J. Am. Chem. Soc.* **85**, 3891 (1963).
- (7) Auty, R. P., Cole, R. H., *J. Chem. Phys.* **20**, 1309 (1952).
- (8) Avery, E. C., Grossweiner, L. I., *J. Chem. Phys.* **21**, 372 (1953).
- (9) Baxendale, J. H., *et al.*, *Nature* **201**, 468 (1964).
- (10) Blandamer, M. J., Shields, L., Symons, M. C. R., *Nature* (London) **199**, 902 (1963).
- (11) Blandamer, M. J., Shields, L., Symons, M. C. R., *J. Chem. Soc.* **1964**, 4352.
- (12) Blandamer, M. J., Catterall, R., Shields, L., Symons, M. C. R., *J. Chem. Soc.* **1964**, 4357.
- (13) Breit, G., Rabi, I. I., *Phys. Rev.* **38**, 2082 (1931).
- (14) Cotton, F. A., Wilkinson, G., in "Advanced Inorganic Chemistry," Interscience Publishers, New York, 1962.
- (15) Dorfman, L. M., Taub, I. A., *J. Am. Chem. Soc.* **85**, 2370 (1963).
- (16) Ershov, B. G., Pykaev, A. K., Glazunov, P. I., Spysin, Y., *Doklady Akad. Nauk S.S.S.R.* **149**, 363 (1963).
- (17) Ghormley, J. A., *J. Chem. Phys.* **24**, 1111 (1956).
- (18) Ghormley, J. A., Stewart, A. C., *J. Am. Chem. Soc.* **78**, 2934 (1956).
- (19) Gray, L. H., *J. Chim. Phys.* **48**, 172 (1951).
- (20) Hart, E. J., Boag, J. W., *J. Am. Chem. Soc.* **84**, 4090, 1962.
- (21) Hart, E. J., Gordon, S., Thomas, J. K., *J. Phys. Chem.* **68**, 1271 (1964).
- (22) Hart, E. J., Thomas, J. K., Gordon, S., *Rad. Res. Suppl.* **4**, 74 (1964).
- (23) Henriksen, T., *Rad. Res.* **23**, 63 (1964).
- (24) Hochanadel, C. J., *Rad. Res. Suppl.* **4**, 150 (1964).
- (25) Hughes, W. E., Moulton, W. G., *J. Chem. Phys.* **39**, 1359 (1963).
- (26) Ingram, D. J. E., in "Free Radicals as Studied by Electron Spin Resonance," Butterworths, London, 1958.
- (27) Jortner, J., Ottolenghi, M., Rabani, M., Stein, G., *J. Chem. Phys.* **37**, 2488 (1962).
- (28) Jortner, J., Sharf, B., *J. Chem. Phys.* **37**, 2506 (1962).
- (29) Kahn, A. H., Kittel, C., *Phys. Rev.* **89**, 315 (1953).
- (30) Keene, J. P., *Nature* (London), **197**, 47 (1962).

- (31) Kevan, L., in "Progress in Solid State Chemistry," ed. H. Reiss, Pergamon Press, London, 1964.
- (32) Kevan, L., Moorthy, P. N., Weiss, J. J., *Nature* (London), **199**, 689 (1963).
- (33) Kevan, L., Moorthy, P. N., Weiss, J. J., *J. Am. Chem. Soc.* **86**, 771 (1964).
- (34) Kip, A. F., Kittel, C., Levy, R. A., Portis, A. M., *Phys. Rev.* **91**, 1066 (1953).
- (35) Kneubühl, F. K., *J. Chem. Phys.* **33**, 1074 (1960).
- (36) Knox, R. S., in "Theory of Excitons," Solid State Physics Suppl. **5**, Academic Press Inc., New York, 1963.
- (37) Kon, H., *J. Inorg. and Nucl. Chem.* **25**, 933 (1963).
- (38) Landolt-Bornstein, Zahlenwerte und Funktionen, I., pp. 52 and 61, Springer, Berlin, 1950.
- (39) Lea, D. E., in "Actions of Radiations on Living Cells," Cambridge University Press, Cambridge, 1946.
- (40) Livingston, R., Zeldes, H., Taylor, E. H., *Phys. Rev.* **94**, 725 (1954).
- (41) Livingston, R., Zeldes, H., Taylor, E. H., *Disc. Far. Soc.* **19**, 166 (1955).
- (42) Livingston, R., Weinberger, A. J., *J. Chem. Phys.* **33**, 499 (1960).
- (43) Matheson, M. S., *Ann. Rev. Phys. Chem.* **13**, 77 (1962).
- (44) McMillan, J. A., Matheson, M. S., Smaller, B., *J. Chem. Phys.* **33**, 609 (1960).
- (45) Moorthy, P. N., Ph.D. Thesis, University of Durham (England), 1965.
- (46) Moorthy, P. N., Weiss, J. J., *Nature* (London) **201**, 1317 (1964).
- (47) Moorthy, P. N., Weiss, J. J., *Phil. Mag.* **10**, 659 (1964).
- (48) Moorthy, P. N., Weiss, J. J., *Nature* (London) **204**, 776 (1964).
- (49) Moorthy, P. N., Weiss, J. J., *J. Chem. Phys.* **42**, 3121 (1965).
- (50) Moorthy, P. N., Weiss, J. J., *J. Chem. Phys.* **42**, 3127 (1965).
- (51) Nafe, J. E., Nelson, E. B., *Phys. Rev.* **73**, 718 (1948).
- (52) Piette, L. H., Rempel, R. C., Weaver, H. E., Flournoy, J. M., *J. Chem. Phys.* **30**, 1623.
- (53) Platzman, R. L., in "Basic Mechanisms in Radiobiology," N.R.C., Publ. No. **305**, Washington, D.C., 1953.
- (54) Portis, A. M., *Phys. Rev.* **91**, 1071 (1953).
- (55) Ramsey, N. F., in "Experimental Nuclear Physics," Vol. I, E. Segre, ed., p. 434, John Wiley and Sons, New York, 1953.
- (56) Scholes, G., Simic, M., Weiss, J. J., *Disc. Far. Soc.* **36**, 214 (1963).
- (57) Schulte-Frohlinde, D., Eiben, K., *Z. Naturf.* **17 A**, 445 (1962).
- (58) Schulte-Frohlinde, D., Eiben, K., *Sixth Intern. Symp. Free Radicals*, Cambridge (England), Preprint AE., 1962.
- (59) Schulte-Frohlinde, D., Eiben, K., private discussion.
- (60) Sitharama Rao, D. N., Duncan, J. F., *J. Phys. Chem.* **67**, 2126 (1963).
- (61) Siegel, S., Baum, L. H., Skolnik, S., Flournoy, J. M., *J. Chem. Phys.* **32**, 1249 (1960).
- (62) Siegel, S., Flournoy, J. M., Baum, L. H., *J. Chem. Phys.* **34**, 1782 (1961).
- (63) Sharpay, V. A., in "Proceedings of the Tihany Symposium on Radiation Chemistry," pp. 463-476, Budapest, 1962.
- (64) Sharpay, V. A., Molin, Yu. N., *Russ. J. Phys. Chem.* **35**, 1465 (1961).
- (65) Smaller, B., Matheson, M. S., Yasaitis, E. L., *Phys. Rev.*, **94**, 202 (1954).
- (66) Sweet, J. P., Thomas, J. K., *J. Phys. Chem.* **68**, 1363 (1964).
- (67) Thomas, J. K., *J. Phys. Chem.* **67**, 2593 (1963).
- (68) Thomas, J. K., Gordon, S., Hart, E. J., *J. Phys. Chem.* **68**, 1524 (1964).
- (69) Weiss, J. J., Porret, D., *Nature* (London) **139**, 1019 (1937).
- (70) Weiss, J. J., *Nature* (London) **186**, 751 (1960).
- (71) Weiss, J. J., *Nature* (London) **199**, 589 (1963).
- (72) Weiss, J. J., *Rad. Res. Suppl.* **4**, 141 (1964).

RECEIVED May 14, 1965.

16

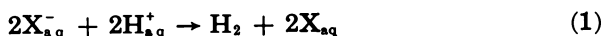
Solvated Electron Formation and Hydrogen Evolution in the Photochemistry of Aqueous Solutions

GABRIEL STEIN

Department of Physical Chemistry, Hebrew University, Jerusalem, Israel.

The nature of the first spectroscopic excited state of negative ions in aqueous solution is described and the evidence in favor of the theory considering the excited electron to be bound in the electronic polarization field of the organized medium is discussed. The experimental evidence concerning the dissociation of this excited, charge transfer to the solvent, state to yield a solvated electron is given, as well as the evidence that shows the thermal ionization of internal excited states of, for example, phenolate and β -naphtholate, to yield solvated electrons in competition with fluorescence. Recent experiments on aqueous solutions of ferrocyanide are used to discuss the nature of the photochemical scavenging processes and the reaction between the solvated electron and its parent ion. Experiments on β -naphthol are described to illustrate competition between fluorescence and solvated electron formation. The mechanisms producing molecular hydrogen from solvated electrons are described.

When deaerated aqueous solutions are illuminated, evolution of molecular hydrogen, originating from the water, may be observed. This photochemically induced water splitting produces hydrogen gas and thus corresponds to a two-electron equivalent change, schematically:



where X^- before the loss of one electron, may be neutral or bear a charge. What is the detailed mechanism of this relatively simple, basic process?

Obviously the absorption of a quantum affects one unit of X_{aq}^- only, leading to a spectroscopically recognizable state. What is the

nature of the first stage, how does it lead to a chemical one-equivalent reaction, how does this result in the final two equivalent product—these are the questions that a full answer must solve. For some years now we attempted step-by-step to elucidate the single reaction stages. In the present paper the evidence obtained in favor of the view that solvated electrons, formed in two distinct consecutive stages are in many cases essential intermediates in the process, is presented. This is followed by describing some reactions leading to the conversion of solvated electrons into hydrogen atoms. These, then acting as oxidizing agents, complete the process. Finally, some recent results are described which shed further light on the detailed kinetics of such photochemical systems involving inhomogeneous, diffusion-controlled kinetics in aqueous solutions containing solvated electrons.

*The Nature of the Primary Excited State.
Solvated Electrons of the First Kind*

The primary photochemical step, resulting from the absorption of the photon, must produce transition to a spectroscopically recognizable upper state—excitation or ionization, in which the Franck-Condon principle is observed. Which of these is involved in the process of hydrogen evolution could be clearly ascertained for one of the simple systems in which Reaction 1 occurs: O_2 -free aqueous solutions of iodide ions. The absorption spectrum of such solutions is well known, showing two bands with maxima at ~ 226 and ~ 194 $m\mu$. Photolytic light at 254 $m\mu$ is absorbed near the onset of the 226 $m\mu$ max. band.

Franck and Scheibe (8) were the first to interpret the absorption spectra of halide ions in solution as due to a charge transfer to the solvent (CTTS). The solvation configuration around the ion cannot change during the transition. Therefore the energy required for the transition at the band maximum:

$$h\nu_{\max} = E_X + H^- - H + \chi - B \quad (2)$$

where E_X is the electron affinity of the halogen atom, H^- and H heats of solvation of X^- and X . The Franck-Condon orientation strain, χ , is the energy required to create around the atom the same configuration of water dipoles as that around the ion and, B is the energy of binding of the electron in the excited state resulting after photon absorption. Franck and Scheibe considered the ion to be directly photoionized in the primary step and the electron removed into the water to a distance from the parent atom where only the electronic polarization of the otherwise undisturbed water molecules would bind it (9). The resultant value of B could not be calculated. This was done through the novel approach of Franck and Platzman (12), after many inconclusive attempts in the intervening years. They assumed the formation of a spherically symmetrical excited state centered on the parent atom. In this the excited electron is bound by $B = E_e + S_e$. E_e is the binding in a hydrogen like excited state owing to the atomic and orientation polarizations only of the oriented water molecules around X^- . These create a coulomb field with, according to Landau (26), an effective charge $Z_{\text{eff}} = 1/D_{\text{op}} - 1/D_e$. D_{op} and D_e

are the optical and static dielectric constants of water. S_e is caused by the electronic polarization of the medium by the excited electron in the expanded orbital. $B \cong 1 + 0.5 \cong 1.5$ e.v. In this theory the mean radius of such an electron = $5.8A.$, thus extending over the first hydration layer of the original Γ_q ion. The values of $h\nu_{\max}$ found and calculated now agreed well.

However Smith and Symons (43, 44, 45) found that the theory of Franck and Platzman did not account for environmental (temperature, solvents, added salts) effects on the spectrum. They proposed instead a theory based on an electron in a box of radius r . Absorption of $h\nu$ causes the resulting atom to contract, the electron preserving its radius as in the ground state. Environmental effects change this radius.

The radius thus calculated from the theory of Smith and Symons does not correspond to any known property of halide ions. However, when the acceptable physical model of Franck and Platzman is combined with the concept of a variable radius, as proposed by Smith and Symons, both absolute value and environmental effects can be accounted for. This was done in the theory of Stein and Treinin (18, 19, 47), using an improved energetic cycle to obtain absolute values of r , the spectroscopically effective radius of the cavity containing the X^- ion. These values were then found to correspond to the known partial ionic radii in solution, as did values of dr/dT to values obtained from other experiments. The specific effects of temperature, solvents, and added salts could be used to differentiate between internal and such CTTTS transitions where the electron interacts in the excited state strongly with the medium. These spectroscopic aspects of the theory were examined later in detail and compared with experiment by Treinin and his co-workers (3, 4, 32, 33, 42, 48).

The evidence is thus consistent with the primary formation of a first kind of solvated electron, still symmetrically centered on its parent atom, and expanded over an orbital involving the first hydration layer. Its radius is probably (47) less than the value proposed by Franck and Platzman.

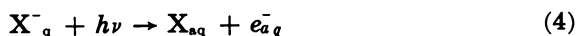
It will be shown that this first state, (in which the electron is solvated with an energy lower than in its final state), is short lived, and goes over in the next step of the reaction sequence into a second kind of solvated electron.

Thermal Dissociation of the Excited State. Formation of the Solvated Electron - Parent Atom Pair

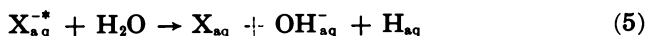
The spectroscopic evidence thus favors the formation of a bound excited state of the electron around the parent atom.



Does the kinetic evidence from studying the reaction mechanism support this, or favor instead a direct photoionization?



Alternatively, if it supports the spectroscopic evidence, does the first excited state interact directly with the formation of H atoms, for example with water

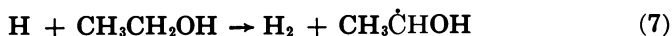


or with H_{aq}^+ :

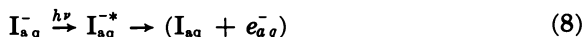


The answer was established in a series of investigations (20, 21, 22, 23) for I^- in water (20, 21) and other solvents (22), and for halide ions and OH^- in water (23).

H atom scavengers—i.e., alcohols, were added. However at neutral pH, hydrogen evolution according to



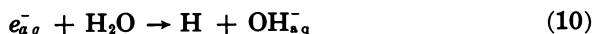
was not observed, thus excluding formation of H atoms according to Reaction 5. Electron scavengers, H_{aq}^+ , N_2O , acetone, and a series of Brönsted acids (24) particularly phosphate ion (21, 24), were now added in the presence or absence of added ethanol. The quantitative investigation of the effect of the various scavenger concentrations on the quantum yield of the products indicated (20) that the electrons are formed close to the parent atom. Thus direct ionization according to Reaction 4 with removal of the electron to a distance is not likely. This supports the spectroscopic evidence. The results also showed that Reaction 6, direct interaction between the scavengers and the spectroscopic state can be excluded, even at high concentrations of H_{aq}^+ . The results could be explained however in terms of a dissociation of the excited ion into a halogen atom, X, and a solvated electron, e_{aq}^- , formed in close proximity



Noyes (36) developed the quantitative treatment of the kinetics of reactions in which a pair of reactive intermediates is formed in close proximity in thermal or photochemical reactions. Geminate recombinations may now occur in competition with the diffusion of the gemini away from each other. Those escaping geminate recombination in the initially inhomogeneous distribution may eventually reach a homogeneous distribution in the bulk of the solution and lead to hydrogen evolution through recombination:



or through:



Hydrogen is evolved in the bulk forming a residual yield obtained even in the absence of scavengers. With scavengers present, these will compete with geminate recombination in the inhomogeneous distribution discussed above. The distinctive feature of this situation is that since

scavengers do not interact directly with the first excited state, the limiting quantum yield Φ does not approach 1 with increasing scavenger concentration $[S]$. It approaches a limiting value determined by the yield of Reaction 8, the dissociation of the excited state into X and e_{aq}^- . Noyes' treatment leads to a linear dependence of the quantum yield φ on $[S]^{1/2}$ over a range of $[S]$. Noyes' original theoretical treatment was extended (21) to make it applicable to a wider range of scavenger concentrations, and gave the dependence of φ the quantum yield of H_2 , on scavenger concentration, as follows:

$$\ln\left(1 - \frac{\varphi}{\Phi}\right) = \ln\beta' - \frac{2a}{\beta'}(\pi k_{8+} e_{aq}^- [S])^{1/2} \quad (11)$$

where a and β' are specific parameters in Noyes' treatment characterizing the chances that the initial pair will not recombine, but escape from each other. Using scavengers which convert e_{aq}^- into H atoms, such as the acids (24), H_{aq}^+ or $H_2PO_4^-$ (20, 24), Reaction 7 may now follow and H_2 evolution is observed, quantitatively obeying Equation 11. Rate constants $k_{8+} e_{aq}^-$ calculated from Reaction 11 were in good agreement (20, 24) with results obtained in radiolysis experiments.

The detailed kinetic evidence thus obtained led to the conclusion that a second form of solvated electron, e_{aq}^- is formed from the first state, in a distinct thermal step, Reaction 8. The apparent activation energy, resulting from competition between Reaction 8 and primary decay to the ground state:



was determined (23); it is of the order of 4 kcal./mole. For example, for I_{aq}^- with $\lambda = 2537\text{\AA}$, $\Phi_{25^\circ\text{C.}} = 0.29$ but only 0.19 at 5°C . For Cl^- at 1849\AA , $\Phi_{25^\circ\text{C.}} \rightarrow 1$. The existence of such an activation energy determining the value of Φ is also consistent with two distinct stages leading to the formation of e_{aq}^- . Another experimental fact (20) which strongly supports the proposed mechanism is that the quantum yield is independent of light intensity as required by Noyes' theory.

The solvated electron thus formed is no longer centered on the parent atom. To form two distinct entities an asymmetrization occurred either by movement of the I atom from the center or of the electron from the spherical symmetry. The electron e_{aq}^- is now the center of solvation, at first near to, but distinct in its diffusive properties from its parent atom. It is bound by oriented water molecules. This process must have occurred in less than the lifetime of the spectroscopic excited state; less than 10^{-10} sec. Fluorescence is not observed in solutions of I_{aq}^- , showing the short lifetime of the primary excited state.

Subsequently e_{aq}^- was observed by spectroscopic measurements in the flash photolysis of such systems by Matheson, Mulac, and Rabani (31). Flash photolysis provides no evidence as to the mechanism of e_{aq}^- formation.

The energy of solvation of e_{aq}^- was calculated by Baxendale (1) from a thermodynamic cycle and compared with its spectrum. The

energy of solvation is 1.75 e.v. The absorption peak is at $h\nu = 1.72$ e.v. The energy of solvation is thus somewhat higher than the 1.5 e.v. obtained in the first state. (The agreement between $h\nu$ at the absorption peak, and the energy of solvation as well as the wide extension of the band to higher energies would possibly indicate that light absorption results in a direct photoionization in this case.) In order to account for the possibility of a transition from the first state into the second in 10^{-10} sec., it appears necessary to assume that in the case of solvated ions showing CTTS transition sites pre-exist in water able to bind the electron with energies equal to or exceeding that available in the CTTS state. This may be the original site, from which the parent atom moved out. It will be similar to an anion vacancy.

It is interesting to note that in the photochemical evolution of hydrogen from aqueous solutions of Fe^{+2} ions (17) H atoms appear as intermediate, but preceding formation of e_{aq}^- could not be proved.

Recently Lehman and Weiss (27, 28) re-investigated the mechanism here proposed for the photochemical formation of e_{aq}^- from I_{aq}^- and confirmed it.

The mechanism by which H atoms formed in these systems lead finally to H_2 evolution were investigated separately (5, 6, 35, 46). It was shown that in the case of I_{aq}^- , H atoms react with H_{aq}^+ to yield H_{2aq}^+ . This oxidizes I_{aq}^- and gives H_2 , thus completing the process started with the formation of the first excited state by absorption of a quantum.

Formation of e_{aq}^- from Excited States Corresponding to Internal Molecular Transition. Competition with Fluorescence

In charge transfer to solvent transition the bound electron in the spectroscopically observed first excited state interacts strongly with the solvent oriented in the field of the ion. Will the formation of e_{aq}^- occur also when excitation results in an internal molecular transition? For instance, on illumination will aqueous solutions of aromatic molecules evolve H_2 through preceding e_{aq}^- formation?

Following the classical observation of Lewis and his school (29, 30, 34) of the photoionization of aromatic molecules in rigid solvents, Land, Porter and Strachan (25) proved such processes in the flash photolysis of aqueous solutions of phenols. It was suggested (7, 15, 25, 38) that the primary photochemical act involves electron ejection.

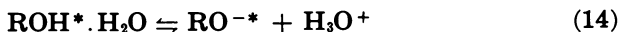
These systems were now re-investigated to elucidate the detailed mechanism. Phenol itself (16), at neutral and acid pH, gave a very low quantum yield of H_2 , so that quantitative investigations of the mechanism could not be carried out. At alkaline pH however, where the phenolate ion is present, the limiting quantum yield Φ rose to 0.23 with light of 2537Å and 0.30 with 2288Å., at 28°C. The investigation of the absorption spectrum of the phenolate ion above 210 $m\mu$ showed (16) that only internal molecular transitions are involved. Both photolytic wavelengths are absorbed in a $\pi \rightarrow \pi^*$ transition. Applying the criteria established (3, 4, 46) to distinguish between such transitions, and CTTS

bands (which show marked blue shifts on adding, for example, KF or sucrose) did not show that CTTS transitions are involved in the case of the phenolate ion, and no evidence was found even for a weak CTTS band hidden under the known transitions. The detailed kinetics showed that in the mechanism leading to H_2 evolution from phenolate solutions, direct interaction between electron scavengers and the primary excited state may be excluded here too; excellent agreement was found with the assumption that once again a two-step mechanism is involved, solvated electron formation preceding hydrogen evolution:



The added scavengers compete with the secondary recombination between C_6H_5O and e_{aq}^- according to the square root of concentration law.

What mechanism brings about the thermal detachment of the electron when strong interaction with the solvent in the excited state is not observed? Why is the yield for the anion larger than for the neutral molecule if the nature of the spectroscopic transition is similar? It occurred to us that a parallel investigation of fluorescence and solvated electron formation may give clues to the answer since fluorescence correlates with the lifetime of the emitting state. If the emitting state is related to the one yielding the solvated electron, further information would become available. Phenol and phenolate fluoresce very weakly, but β -naphthol and β -naphtholate fluoresce adequately. The correlation between fluorescence and pH has been investigated previously by Foerster (10, 11) and by Weller (51). The correlation between fluorescence and solvated electron formation as a function of pH was accordingly investigated for β -naphthol and β -naphtholate by Ottolenghi (37). He found a close parallel between the dependence of fluorescence efficiency and quantum yield of solvated electron formation over the pH range 0.4-14. The pK of β -naphthol is 9.23 at room temperature. In the excited state, as discussed by Foerster and by Weller (10, 11, 49, 50, 51) $pK^* = 2.8$, so that the system in the excited state tends towards the corresponding new equilibrium



Weller (49, 50, 51) established the relative fluorescence intensities of ROH^* and RO^{-*} as a function of pH. Ottolenghi (37) succeeded in showing that the quantum yield of direct H atom formation (from ROH^*) and solvated electron formation (from RO^{-*}) follow the identical relative pH dependence. Excitation was into the second singlet $\pi-\pi^*$ transition. Emission is known to occur from the first singlet. It was concluded (37) that both fluorescence of RO^{-*} and solvated electron formation originate from this state, in competition with each other.

To gain further detailed information on the mechanism of this competition, work is in progress, together with Mr. Z. Ludmer, on the effect of temperature changes on the aqueous β -naphthol system. Examination of temperature effect (16° to 69° C.) on the spectrum showed at $pH \geq 12$ that between 220 and 380 $m\mu$ there is no indication of a CTTS band in the

spectrum of the naphtholate ion. Fluorescence yields and solvated electron formation (using N_2O as the scavenger and measuring φ_{N_2}) were examined at different temperatures in the above range at pH 4.8 and 12. Varying p_{N_2O} it was shown that at no temperature or pressure did N_2O interact at either pH with the excited state, and did not affect directly the fluorescence yield. At pH 4.8 increasing the temperature from 16° to 69° C. increases by more than 50% both fluorescence and solvated electron formation. At this pH below the pK, this can be correlated with an increase in RO^{-*}/ROH^* mainly through a temperature shift in pK (10). This large effect obscured any specific differences that may exist between the two processes.

At pH = 12 however RO^{-*} is formed exclusively. Indeed, adding OH^- does not noticeably change, between pH 12 and 14, the spectrum, the fluorescence, or solvated electron yield at constant temperature. Significantly however, at this pH it was found that increasing temperature in the above range decreased the fluorescence by some 20% and caused a corresponding increase in solvated electron formation. These results therefore strengthen the view (37) that a common stage is involved in both processes. For fluorescence the lowest singlet excited state is ascertained to be the emitting one. Is it also the one for solvated electron formation? The general question of decrease of fluorescence with temperature was discussed by Bowen and Seaman (2), who represent it by an empirical equation, involving an apparent activation energy. They do not propose an exact theory to account for it; they do consider the possibility that increasing temperature facilitates transition from the lowest excited singlet to the lower triplet state, with loss of fluorescence. The question arises, therefore, whether increase with temperature of the solvated electron yield is caused by a direct transition from the lowest excited singlet, or through transition first to the relatively long lived triplet, which then yields the solvated electron. A survey of the existing evidence is consistent with this latter possibility. Experiments are now in progress to examine the direct formation of the triplet and possible formation of solvated electrons from it.

The results for phenolate and naphtholate show that internal transition may lead to solvated electron formation from aromatic anions. The fact that the products are the negatively charged solvated electron and a radical which is neutral (and not a positively charged one) may be partly responsible for the increased efficiency of anions over the undissociated molecules. Primary recombination may decrease in the absence of coulombic attraction. Moreover the ionization potential of the anion is lower.

CTTS transitions, in which the oriented solvent participates are absent in the spectrum of the aromatic solutes but the lifetime of the excited state, as shown by the existence of fluorescence is longer, probably 10^{-9} sec. During this extended lifetime, sufficient reorganization of the solvent may occur to enable the excited electron to be trapped, and to allow for the first relative diffusive displacement of the gemini, which is necessary for the observed kinetics to develop. The temperature ef-

fects, together with the quantitative dependence of quantum yield on scavenger concentration once again show that two distinct stages are involved in the formation of the solvated electron. The first stage, an excited electron in a molecular orbital, is clearly identified by spectroscopy.

For β -naphtholate at 25°C. the quantum yield of fluorescence is about 0.2; of solvated electron formation about 0.1. This solvated electron formation is a major factor competing with fluorescence for that part of the original quantum energy reaching the lowest singlet state. As previously stated (37), it may be a major factor leading to fluorescence quenching in polar solvents, and particularly in aqueous solutions.

The Mechanism of Solvated Electron Formation in Aqueous Solutions of Ferrocyanide

From the preceding it is apparent that the nature of the first excited state has been clarified for CTTS transitions of simple anions, and that both for these and for intramolecular processes following on primary excitation the events are known with some certainty up to the stage of asymmetrization. Also, after the pair of solvated electron and parent species have been established by at least one diffusive translation (so that at least one solvent molecule separates them) all steps following have been elucidated. There remains the question of the detailed nature of the processes in the time interval between 10^{-14} and 10^{-11} to 10^{-9} sec. after primary absorption.

To assist with this, we have for some years now investigated in detail the spectroscopy and photochemistry of the ferrocyanide in aqueous solution. This work was carried out together with Mrs. M. Shirom (40).

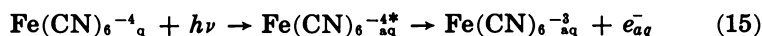
The ferrocyanide ion, stable at neutral pH, shows well understood optical transitions in the visible and near u.v. It carries four negative charges, which should facilitate solvated electron formation. A survey of its known photochemistry indicated that at neutral pH we may hope that solvated electron formation will be the only photochemical primary process. Indeed, after we commenced the work, Matheson, Mulac, and Rabani (31) found on flash photolysis the absorption spectrum of e_a^- in aqueous solutions of ferrocyanide.

To elucidate the details of the mechanism, we first studied the absorption spectrum. Using at neutral pH the method of environmental effects (3, 46), it was found that, in addition to the well known (13, 41) ligand field and so called charge or electron transfer transitions (which for such complexes denotes transition of an electron from the central metal ion to the ligands) a CTTS band was also observed—i.e., a transition which is strongly affected by changes owing to the solvent medium. This band, with λ_{\max} at about 255 m μ , is overlaid by two strong molecular transitions and becomes apparent only when changing temperature, solvent composition, and added KF or sucrose reveal opposite shifts in the different bands. Applying the theory as ex-

tended by Treinin for polyvalent anions (48), the effective charge of ferrocyanide has the apparent value of -2 .

Parallel with our investigations, Burak and Trenin (3, 4) also found a similar hitherto unknown CTTS band in the spectrum of the azide ion, situated between two molecular transitions and discussed it in detail. They also elucidated (not yet published) the details of the photochemistry of N_3^- , which involves the formation of a number of intermediate radicals.

In the case of $Fe(CN)_6^{4-}$, the investigation of the photochemistry showed that in neutral solution the only observable products were the ferricyanide ion, $Fe(CN)_6^{3-}$, and e_{aq}^- , thus simplifying the situation. Monochromatic light was used to investigate the quantum yield in various transitions, at room temperature with N_2O as electron scavenger. Starting with $\lambda = 365 \text{ m}\mu$, the absorption is mainly due to the $422 \text{ m}\mu$ max. d-d transition, $1_{A_{1g}} \rightarrow 3_{T_{1g}}$, with a small part ($\sim 3\%$) contributed by the $322 \text{ m}\mu$ d-d transition, $1_{A_{1g}} \rightarrow 1_{T_{1g}}$. The limiting quantum yield for e_{aq}^- formation $\Phi = 0.006$. At $313 \text{ m}\mu$ the absorption is mainly in the $322 \text{ m}\mu$ max. band, and Φ rises to 0.26. At $265 \text{ m}\mu$ absorption is partly by the $270 \text{ m}\mu$ max. d-d ligand field transition $1_{A_{1g}} \rightarrow 1_{T_{2g}}$, and partly in the CTTS band. Φ rises to 0.51. At $254 \text{ m}\mu$ absorption is to a large extent in the CTTS band; $\Phi = 1.0$. At $229 \text{ m}\mu$ and at $214 \text{ m}\mu$ absorption is in the metal to ligand transition, $1_{A_{1g}} \rightarrow 1_{T_{1u}}$, with λ_{max} at $218 \text{ m}\mu$. Φ for both these wavelengths decreases to 0.88–0.89. These measurements, in which special attention was paid to accurate actinometry, show that the limiting yield Φ of solvated electron formation—i.e., the percentage of primary excited states that according to:



form the separate solvated ferricyanide ion and solvated electron, rises to a maximum in the CTTS band. In the internal transition, even at higher quantum energies, Φ decreases. Thus in this system, where fluorescence is not observed, so that the lifetime of the primary excited state is short, the best chances for resultant electron solvation is in the transition which was characterized by an involvement of the solvent molecules.

According to Equation 11 we may now determine the Noyes parameters α and β' , using $H_2PO_4^-$ as the e_{aq}^- scavenger. As discussed previously (40), phosphate ions in this system mediate the conversion of e_{aq}^- into H atoms (21, 24) thus converting the reducing e_{aq}^- into the oxidizing H, leading to H_2 evolution in the presence of alcohols:

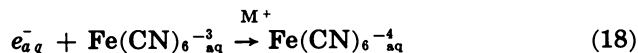


Plotting ϕH_2 according to Equation 11 vs. $[H_2PO_4^-]^{1/2}$, straight lines were obtained. From the slopes, $(2\alpha/\beta')(k_{H_2PO_4^-} + k_m)^{1/2}$ was obtained for the different wavelengths, giving the values of 0.51, 0.40, 0.47, 0.62, and 0.82 respectively for $\lambda = 313, 265, 254, 229,$ and $214 \text{ m}\mu$. The higher the value the greater the chance that the pair, once formed at an

initial separation r_0 , will escape, rather than recombine. Within the same electronic transition, the chances are indeed greater for this at the higher quantum energy of 214 than at 229 $m\mu$. However, the chance appears to reach a minimum around the CTTS band. The chances there are maximum for primary separation but also for secondary recombination. This indicates the influence of the type of electronic transition on the parameters of the photochemical mechanism, for which no explicit form is given in Noyes' treatment.

It is important to note that the constants $+k_{s+e_{aq}^-}$ derived from the ferrocyanide system, from these heterogeneous kinetics, agree very well indeed with the known constants obtained from the homogeneous kinetics in radiolysis experiments. Thus the scavenged species, e_{aq}^- , appears to have the same characteristics.

The residual yield φ_r , obtained by extrapolation from Equation 11 is zero in experiments using phosphate ion as the scavenger, but has a small positive value using N_2O , or acetone. We attribute this to a salt effect promoting recombination:



The results in the ferrocyanide system thus furnish information towards an answer to some of the remaining questions; they correlate electronic transitions with the specific parameters of the entities formed after 10^{-10} sec., and furnish conclusive evidence in favor of the mechanism delineated previously. They leave unproved the detailed nature of the process in which e_{aq}^- and the parent species separate in the first instance.

Literature Cited

- (1) Baxendale, *Rad. Res. Supplement* 4, 139 (1964).
- (2) Bowen, E. J., Seaman, D., in "Luminescence of Organic and Inorganic Materials," G. Porter, ed., p. 135, Wiley, New York, 1962.
- (3) Burak, I., Treinin, A., *Trans. Faraday Soc.* 59, 1490 (1963).
- (4) Burak, I., Treinin, A., *J. Chem. Phys.* 39, 189 (1963).
- (5) Czapski, G., Stein, G., *Nature* 182, 598 (1958).
- (6) Czapski, G., Stein, G., *J. Phys. Chem.* 63, 850 (1959); 64, 219 (1960).
- (7) Dobson, G., Grossweiner, L. I., *Trans. Faraday Soc.* 61, 708 (1965).
- (8) Franck, J., Scheibe, G., *Z. Physik. Chem. A.* 139, 22 (1928).
- (9) Farkas, A., Farkas, L., *Trans. Faraday Soc.* 34, 1120 (1938).
- (10) Foerster, Th., *Naturwiss.* 36, 186 (1949).
- (11) Foerster, Th., *Z. Elektrochem.* 54, 531 (1950).
- (12) Franck, J., Platzman, R. L., Farkas Memorial Volume, Jerusalem, 1952, p. 21; *Z. Physik*, 138, 411 (1954).
- (13) Gray, H. B., Beach, N. A., *J. Am. Chem. Soc.* 85, 2922 (1963).
- (14) Grossweiner, L., Swenson, G. W., Zwicker, E. F., *Science* 141, 805, 1042, 1180 (1963).
- (15) Grossweiner, L. I., Zwicker, E. F., *J. Chem. Phys.* 32, 305 (1960).
- (16) Jortner, J., Ottolenghi, M., Stein, G., *J. Am. Chem. Soc.* 85, 2712 (1963).
- (17) Jortner, J., Stein, G., *J. Phys. Chem.* 66, 1258, 1264 (1962).
- (18) Jortner, J., Raz, B., Stein, G., *Trans. Faraday Soc.* 56, 1273 (1960).
- (19) Jortner, J., Raz, B., Stein, G., *J. Chem. Phys.* 34, 1455 (1961).
- (20) Jortner, J., Ottolenghi, M., Levine, R., Stein, G., *J. Phys. Chem.* 65, 1232 (1961).
- (21) Jortner, J., Ottolenghi, M., Stein, G., *J. Phys. Chem.* 66, 2029, 2037, 2042 (1962).

- (22) Jortner, J., Ottolenghi, M., Stein, G., *J. Phys. Chem.* **67**, 1271 (1963).
- (23) Jortner, J., Ottolenghi, M., Stein, G., *J. Phys. Chem.* **68**, 247 (1964).
- (24) Jortner, J., Ottolenghi, M., Ranbani, J., Stein, G., *J. Chem. Phys.* **37**, 2488 (1962).
- (25) Land, E. J., Porter, G., Strachan, E., *Trans. Faraday Soc.* **57**, 1855 (1961).
- (26) Landau, L. D., *Phys. Z. Sowjetunion* **3**, 664 (1933); **9**, 158 (1936).
- (27) Lehman, H. P., Ph.D. Thesis, Newcastle, 1964.
- (28) Lehman, H. P., Weiss, J. J., to be published.
- (29) Lewis, G. N., Lipkin, D., *J. Am. Chem. Soc.* **64**, 2801 (1942).
- (30) Linschitz, H., Berry, M. G., Schweitzer, D., *J. Am. Chem. Soc.* **76**, 5833 (1954).
- (31) Matheson, M. S., Mulac, W. A., Rabani, J., *J. Phys. Chem.* **67**, 2613 (1963).
- (32) Meyerstein, D., Treinin, A., *Trans. Faraday Soc.* **57**, 2104 (1961).
- (33) Meyerstein, D., Treinin, A., *J. Phys. Chem.* **66**, 446 (1962).
- (34) Michaelis, L., Schubert, M. P., Granick, S., *J. Am. Chem. Soc.* **61**, 1981 (1939).
- (35) Navon, G., Stein, G., to be published.
- (36) Noyes, R. M., *J. Am. Chem. Soc.* **77**, 2042 (1955); **78**, 5486 (1956).
- (37) Ottolenghi, M., *J. Am. Chem. Soc.* **85**, 3557 (1963).
- (38) Porter, G., Strachan, *Trans. Faraday Soc.* **34**, 1595 (1958).
- (39) Roy, J. C., Williams, R. R., Hamill, W. H., *J. Am. Chem. Soc.* **76**, 3274 (1954).
- (40) Shirom, M., Stein, G., *Nature* **204**, 778 (1964).
- (41) Shulman, R. G., Sugano, S., *J. Chem. Phys.* **42**, 39 (1965).
- (42) Sperling, R., Treinin, A., *J. Phys. Chem.* **68**, 897 (1964).
- (43) Smith, M., Symons, M. C. R., *Discuss. Faraday Soc.*, **24**, 206 (1957).
- (44) Smith, M., Symons, M. C. R., *Trans. Faraday Soc.* **54**, 338, 346 (1958).
- (45) Smith, M., Symons, M. C. R., *J. Chem. Phys.* **25**, 1074 (1956).
- (46) Stein, G., *Discuss. Faraday Soc.* **29**, 235 (1960).
- (47) Stein, G., Treinin, A., *Trans. Faraday Soc.* **55**, 1087, 1091 (1959); **56**, 1393, (1960).
- (48) Treinin, A., *J. Phys. Chem.* **68**, 893 (1964).
- (49) Weller, A., *Z. Elektrochem.* **56**, 662 (1952).
- (50) Weller, A., *Z. Physik. Chem.* **15**, 438 (1958).
- (51) Weller, A., *Progress in Reaction Kinetics* **1**, 189 (1961).

RECEIVED May 26, 1965.

The Interconvertibility of e_{aq}^- and H

JOSEPH RABANI*

Argonne National Laboratory, Argonne, Ill.

The conversion of e_{aq}^- into H atoms and the reaction of H atoms with OH^- are reviewed. e_{aq}^- reacts with acids to form H atoms. The reactivity is correlated with the dissociation constants of the acids. The relation is in accordance with a general acid catalysis for the conversion of e_{aq}^- into H atoms. Only one base, OH^- , has been found as yet to be effective in converting H atoms into e_{aq}^- . The rate constant of $2.2 \times 10^7 M^{-1} sec^{-1}$ can be calculated from different results. From k_{H+OH^-} and k_{e+H_2O} , $pK = 9.6$ is calculated for the dissociation constant of the hydrogen atom.

Ionizing radiation provides the most convenient method of obtaining e_{aq}^- and H atoms in water. It is believed that homogeneously distributed e_{aq}^- , H, OH, H_3O^+ , OH^- , H_2O_2 , and H_2 are formed within 10^{-8} sec. as a result of the absorption of the ionizing radiation. Of these so-called "primary products," the last four are stable species and their properties are well known. Until 1960, the reactions of e_{aq}^- , H, and OH had been studied only indirectly. By adding various radical scavengers, rates of disappearance of these scavenger solutes could be studied, or the nature and rates of formation of stable products. In many cases, the immediate products of the scavenging reactions are also radicals. The mechanism may be very complicated and the final products only of little value understanding in the mechanism.

With the development of very high intensity radiation sources, the reactions of the primary species can now be followed directly (16). Both optical spectra and electrical conductivity have been used to follow chemical reactions induced by pulse radiolysis. e_{aq}^- and OH radicals have optical absorptions that can be easily followed. H atoms cannot be

* Permanent Address: Department of Physical Chemistry, The Hebrew University, Jerusalem, Israel.

observed directly, but very often the product of their reaction with a scavenger can be followed spectroscopically.

Among other methods of forming e_{aq}^- or H atoms in aqueous solutions, the more important are: (a) generation of H atoms by a discharge in H_2 gas. The partially dissociated gas is then bubbled through water. This method has been developed by Czapski and Stein (13) and has the advantage of forming initially only one type of reactive species—i.e., H atoms. The greatest disadvantage of this method is the inhomogeneous radical distribution in the water. There are higher concentrations near the surface of a bubble; (b) e_{aq}^- can easily be obtained photochemically. Jortner, Ottolenghi and Stein (32) have shown that e_{aq}^- is obtained in the photochemistry of halide and OH^- ions. Matheson, Mulac, and Rabani (38), and Grossweiner, Swenson, and Zwicker (22) confirmed this observation using a flash photolysis apparatus. CNS^- and $Fe(CN)_6^{4-}$ also formed e_{aq}^- upon absorption of light.

The Radiolytic Production of the Reducing Radicals

In the 1940's and early 1950's, H atoms were believed to be the only reducing radicals produced by irradiation (47, 54).

The possibility that e_{aq}^- may take part in a chemical reaction was also considered (19, 51, 55), but no experimental evidence was used to support this view until 1958.

Baxendale and Hughes (7) observed in aqueous methanol solutions a decrease in G_H going from 0.1N H_2SO_4 to neutral solutions. They concluded that at the higher pH a reducing species which is unable to dehydrogenate is produced, and suggested an equilibrium between e_{aq}^- and H, shifted towards H in the acid.

Hayon and Weiss (29) used chloroacetic acid as a scavenger for the reducing radicals in irradiated water. They found that dehydrogenation of chloroacetic acid was the major reaction in the very acid region, while in less acid solutions dechlorination took place at the expense of the dehydrogenation. The sum of dehydrogenation and dechlorination was constant throughout the region. This indicated two interconvertible species wherein one could be converted to the other by H_3O^+ .

Barr and Allen (6) measured the effect of O_2 on the chain reaction induced by ionizing radiation to combine H_2 and H_2O_2 to water. H_2O_2 can be reduced by both H and e_{aq}^- to OH.



OH radicals are converted to H atoms by their reaction with H_2 .



In this system, Reaction 3 supplies the reducing radicals which carry on the chain. Barr and Allen found that O_2 was very efficient, compared to H_2O_2 , in scavenging the reducing radicals formed by 3. This was in

contradiction with a ratio of 1.85 (3) between the scavenging efficiency of O_2 and H_2O_2 towards the reducing radicals produced directly by the radiation in neutral solutions. The result forced Barr and Allen (6) to conclude that the reducing species formed by Reaction 3 were different than the primary species formed by the radiation in neutral pH.

Allan and Scholes (2) obtained quantitative evidence that one form of the reducing radicals (they assumed it was e_{aq}^-) was converted to the other by reaction with H_3O^+ . Their competition experiments showed that acetone could be reduced by e_{aq}^- in competition with Reaction 4.



Many others confirmed later the existence of two different species, stoichiometrically equivalent to H atoms, but different in reactivity. An unequivocal proof, however, that the neutral form is e_{aq}^- , has been obtained by Czapski and Schwarz (12). They showed that the ionic strength effect on reactions of e_{aq}^- was indeed as expected with unit negatively charged species. This result was verified by other workers (11).

Finally, the development of pulse radiolysis enabled a direct observation of e_{aq}^- , and a direct distinction between e_{aq}^- and H could easily be made. Matheson (37) (with spectroscopic data obtained by Keene) suggested that e_{aq}^- has optical absorption in the visible. Hart and Boag (26) used spectrographic plates and studied this absorption. The effect of solutes, which were known as electron scavengers led to the conclusion that the absorption was due to e_{aq}^- . It was confirmed later, that the absorption belonged to unit negatively charged species by means of a salt effect (20), as well as by conductivity measurements (49). Many more papers on the absorption spectrum and rate constants of the hydrated electron have since appeared (16).

Evidence for an Independent Yield of H Atoms

Allan and Scholes (2) suggested an independent yield of H atoms in neutral solutions. As will be discussed later, e_{aq}^- can be converted to H atoms by reaction with H_3O^+ and other scavengers.

In the acid pH region, hydrogen atoms will dehydrogenate an appropriate organic solute, RH_2 , according to Reaction 5.



The experimental yield of H_2 is then, $G(H_2)$ equal to the sum of the radical yield of e_{aq}^- , G_e , of H, G_H and of the molecular yield of H_2 , G_{H_2} . Allan and Scholes (2) investigated 2-propanol solutions and have shown that an electron scavenger, acetone, could compete with H^+ for e_{aq}^- . A decrease of $G(H_2)$ was observed at lower $[H^+]/[\text{acetone}]$ ratios. However, under conditions that all e_{aq}^- were supposed to react with acetone without the formation of H or H_2 , $G(H_2) = 1.05$ was obtained. Allan and Scholes concluded $G_H = G(H_2) - G_{H_2} = 1.05 - 0.45 = 0.6$ molecules/(100 e.v.).

Rabani and Stein (43, 46) measured the relative rate constants of H atoms in neutral solutions with various scavengers and compared them to acid solutions. The relative reactivity of H atoms towards ferricyanide, 2-propanol, glucose, glycerol, formate, and methanol was the same in neutral and acid pH. (Formate results have been corrected for the dissociation of the acid.) Scholes and Simic (48) confirmed these observations and extended them to additional scavengers. There is now little doubt that G_{H} (the neutral yield of H atoms) $\simeq 0.5$, but there is no agreement about the precursor of these H atoms (4, 28, 35).

Conversion of e_{aq}^- to H

It has been mentioned that e_{aq}^- can be converted to H atoms by Reaction 4. Lifshitz (36) has found that dihydrogen phosphate ions increased $G(\text{H}_2)$ in neutral formate solutions and suggested Reaction 6 followed by 5. Her results were



confirmed by others (31), who used both ionizing radiation and ultraviolet light to produce e_{aq}^- . Other acids, were also reported to convert e_{aq}^- to H atoms. In Table I we present rate constants for the reaction of e_{aq}^- with an acid, as measured by different techniques.

We used for Table I the rate constants (16), $k_{e^+ \text{NO}_2^-} = 3.9 \times 10^9$, $k_{e^+ \text{NO}_3^-} = 9.0 \times 10^9$, $k_{e^+ \text{H}_3\text{O}^+} = 2.0 \times 10^{10}$ and $k_{e^+ \text{acetone}} = 5.2 \times 10^9 \text{ M}^{-1}\text{sec}^{-1}$ (slightly corrected [e.g. see (45)] for other parallel reactions, when such corrections had been neglected (17, 20, 27, 52)). The values (16), of $k_{e^+ \text{ferricyanide}}$ needed no correction of that type. These rate constants have been used in combination with competition work to calculate the rate constants in both columns 4 and 5. In column 5, the results have been calculated for zero ionic strength using the expression: $\log(k_{\mu}/k_0) = -Z \frac{\mu^{1/2}}{1 + \mu^{1/2}}$ where k_{μ} is the rate constant for e_{aq}^- with an ion of a charge Z , at the ionic strength μ . Although at high ionic strengths, the correction to $\mu = 0$ is less certain, the corrected results should be preferred to the uncorrected values.

The results based on ferricyanide were calculated with $k_{e^+ \text{ferricyanide}} = 1.1 \times 10^{10} \text{ M}^{-1}\text{sec}^{-1}$ (16), which can be obtained by an extrapolation from $\mu = 0.20$ to $\mu = 0.25$.

The photochemical results differ somewhat from the radiation chemical, probably because of the approximations in the photochemical model.

The phosphate results based on (31) were obtained at pH = 6.25 (HPO_4^{2-} present does not react with e_{aq}^-). If KH_2PO_4 alone was present, the H^+ in equilibrium with it is supposed to scavenge e_{aq}^- . The high result (52) for $k_{e^+ \text{H}_2\text{PO}_4^-} = 1.5 \times 10^9 \text{ M}^{-1}\text{sec}^{-1}$, obtained in $10^{-3} \text{MKH}_2\text{PO}_4$ alone (53) is surprising. We were unable to advance a logical explanation for the discrepancy, which would be in agreement with all the experimental data. Further investigation of e_{aq}^- decay in H_2PO_4^- is desired. Recent pulse radiolysis experiments in which the decay of e_{aq}^- was fol-

Table I. Rate Constants for Conversion of e_{aq}^- to H Atoms by Different Acids

Acid (HA)	Ionic Strength	pH	" $k_{e+HA \rightarrow H}$ " $M^{-1}sec.^{-1}$	$k_{e+HA \rightarrow H}$ at $\mu = 0$ / $M^{-1}sec.^{-1}$	Method and Reference
H ₂ O ⁺	~0	4.0-4.6	2.0×10^{10}	2.0×10^{10}	pulse radiolysis (20)
H ₂ O ⁺	~0	4.1-4.7	1.9×10^{10}	1.9×10^{10}	pulse radiolysis (17)
H ₂ O ⁺	<0.024	2.1-4.3	...	2.05×10^{10}	pulse radiolysis (34)
H ₂ PO ₄ ⁻	~0.25	6.25	4.9×10^6	4.9×10^6	radiation based on nitrite (31)
H ₂ PO ₄ ⁻	~0.25	6.25	2.5×10^6	4.7×10^6	radiation based on ferricyanide (31)
H ₂ PO ₄ ⁻	~0.25	6.25	9.0×10^6	4.3×10^6	radiation based on acetone (31)
H ₂ PO ₄ ⁻	~0.25	6.25	6.9×10^6	6.9×10^6	radiation based on nitrate (31)
H ₂ PO ₄ ⁻	0.15-0.35	6.25	4.9×10^7	1.2×10^7	photochemistry based on H ₂ O ⁺ (31)
H ₂ PO ₄ ⁻	0.3	not reported	1.7×10^7	1.7×10^7	radiation based on nitrate (5)
H ₂ PO ₄ ⁻	~0	not reported	1.5×10^8	...	pulse radiolysis (52)
HF and HF ₂ ⁻	0.46	5.03	1.1×10^8	4.3×10^7	radiation based on acetone (31)
HF and HF ₂ ⁻	0.6	5.03	8.0×10^7	1.8×10^7	photochemistry based on H ₂ O ⁺ (31)
NH ₄ ⁺	0.3	7.9	0.9×10^6	1.8×10^6	radiation based on acetone (31)
NH ₄ ⁺	0.09	8.3	6.4×10^6	1.1×10^6	radiation based on acetone (31)
NH ₄ ⁺	1.0	7.6	4.1×10^6	1.3×10^6	radiation based on acetone (31)
NH ₄ ⁺	up to 4	7.8	8.5×10^6	1.1×10^6	photochemistry based on H ₂ O ⁺ (31)
HCO ₂ H	...	5.0	1.2×10^8	1.2×10^8	pulse radiolysis (20)
CH ₃ CO ₂ H	...	5.4	1.5×10^8	1.5×10^8	pulse radiolysis (20)
H ₂ O	...	8.4	1.6×10^1	1.6×10^1	pulse radiolysis (25)
H ₂ O	2.5×10^1	Cs in ethylene diamine (15)

lowed in a solution containing both KH₂PO₄ and K₂HPO₄, gave $k_{e+H_2PO_4^-} = (5.5 \pm 0.9) \times 10^6 M^{-1} sec.^{-1}$ at $\mu = 0$. The presence of K₂HPO₄, which was inert to e_{aq}^- , is essential for buffering the solution. This value is in excellent agreement with the previous steady radiolytic work (31).

The results obtained with formic and acetic acids have been corrected as described before. There is evidence that in these two reactions, reduction takes place besides H atom formation. In formic acid (50), a limiting $G(H_2) = 2.2$ is obtained at concentrations of 5M and up.

This may indicate that only $\sim 30\%$ of e_{aq}^- are converted to H atoms by reaction with HCO_2H . In acetic acid (30), $G(\text{H}_2) = 2.1$ is obtained as a limiting value at $\text{pH} = 4.5$. This indicates again $\sim 30\%$ conversion of e_{aq}^- to H.

The results of Table I show a general decrease in efficiency of converting e_{aq}^- to H atoms with the decrease of the equilibrium constant of the acids.

In Figure 1 we present the data plotted according to Brönsted's equation (9). The slope of -0.51 in this plot is in agreement with the theory for general acid catalysis.

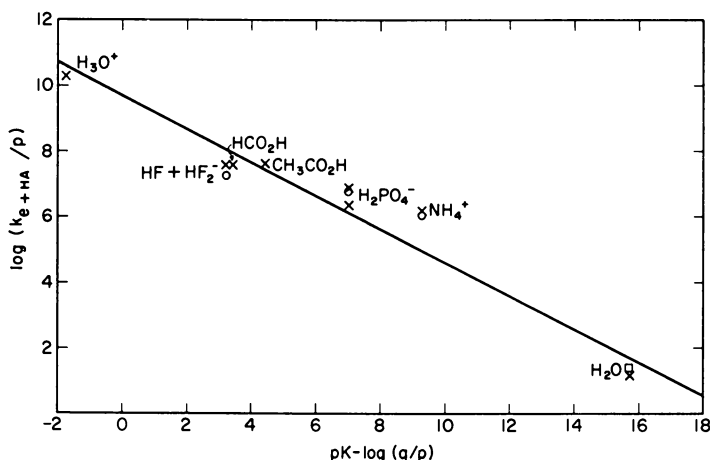


Figure 1. The Brönsted Law for acid catalysis in the conversion of e_{aq}^- to H.

X—radiation chemical data; O—photochemical data; □— H_2O in ethylene diamine.

Conversion of H Atoms to e_{aq}^-

Baxendale and Hughes (7) and Friedman and Zeltmann (18) suggested



in connection with the pH effects on hydrogen abstraction from different compounds. Jortner and Rabani (33) demonstrated Reaction 7 by using gas phase generated H atoms (13) in an aqueous solution of chloroacetate ions. As discussed before (29), H atoms react with chloroacetic acid to produce H_2 and Cl^- (most of the H atoms form H_2). But e_{aq}^- forms Cl^- exclusively. Only 10% of the H atoms reacted with chloroacetate ions to form Cl^- in neutral solutions (33).

However, in alkaline solutions, practically every H atom introduced led to Cl^- formation. This was interpreted as owing to Reaction 7. The effects of $\text{ClCH}_2\text{CO}_2^-$ concentration, pH and other conditions left no room

American Chemical Society
Library

1155 16th St., N.W.
Washington, D.C. 20036

for any alternative interpretation which would account for all the observations.

This was confirmed in another system (41) (same technique, but using nitrate) which showed an enhanced reduction rate in alkaline solutions as compared with the neutral pH.

Much work has been done using the neutral residual H atoms ($G \sim 0.5$). Allan, Robinson, and Scholes (1) measured $G(\text{H}_2)$ in alkaline solutions of 2-propanol, ethanol, or methanol, in the presence of $10^{-4} M$ acetone. In such a system, $G(\text{H}_2)$ can be used to determine the relative rate constants $k_{\text{H}+\text{RH}_2}/k_{\text{H}+\text{OH}^-}$, where RH_2 is the organic compound which forms H_2 by reaction with H atoms. Nehari and Rabani (42) used a similar technique with different organic solutes.

Table II presents relative rate constants for various organic compounds. The second column includes data obtained by direct competition with Reaction 7. HCO_2^- , acetone, and acetate were taken from (42), the others calculated from (1).

Table II. Reactivity of H Atoms ($G \sim 0.5$) with OH^-

RH_2	$k_{\text{H}+\text{RH}_2}/k_{\text{H}+\text{OH}^-}$	$k_{\text{H}^{\text{a}}+\text{RH}_2}$	$k_{\text{H}^{\text{b}}+\text{RH}_2}$	$k_{\text{H}^{\text{c}}+\text{RH}_2}$	$k_{\text{H}^{\text{d}}+\text{RH}_2}$
HCO_2^-	11	15	16	13.5 ^f	14
2-propanol	6.5	5.1	7.8; 4.0	...	4.4
ethanol	1.5	1.5	...	1.5	1.5
methanol	0.2	0.17	0.20	0.16	...
acetone	0.083 ^e	0.069 ^e	0.088 ^g
acetate	0.027	0.030

^a From (48) competition with DCO_2^- in neutral pH.

^b From (43) and (46), competition with ferricyanide in neutral pH.

^c From (8), competition with CuSO_4 in 0.1 N H_2SO_4 .

^d From (44) competition with ferricyanide in acid pH.

^e Rate constant for hydrogen abstraction.

^f $[\text{HCO}_2^-]$ concentration calculated from pK of the acid with a correction for an ionic strength effect on pK.

^g Calculated from (8) and (44).

The results in the last four columns have been normalized to $k_{\text{H}+\text{ethanol}} = 1.5$ or to $k_{\text{H}+\text{CH}_3\text{OH}} = 0.20$.

For the calculations in the fourth and sixth columns of Table II we used $k_{\text{H}+\text{ferricyanide}}/k_{\text{H}+\text{HCO}_2^-} = 20$. This was obtained from the previous results (44) in 0.047 M formic acid (no H_2SO_4) after $[\text{HCO}_2^-]$, calculated from the pK of formic acid, has been corrected for the effect of the ionic strength. In the more acid region, this correction is larger and less certain, but also would give $\frac{k_{\text{H}+\text{ferricyanide}}}{k_{\text{H}+\text{HCO}_2^-}}$ about 20. The ratio of 20 agrees well with the neutral results of 18 (43) and 27 (48). The results in Table II show good agreement for the relative rate constants.

To calculate an absolute rate constant for Reaction 7, we can use $\frac{k_{\text{H}+\text{ethanol}}}{k_{\text{H}+\text{OH}^-}} = 1.5$ which is supported by the other ratios. Combining this with $k_{\text{H}+\text{O}_2}/k_{\text{H}+\text{ethanol}} = 520 \pm 80$ (measured by direct competition between O_2 and ethanol in 0.1 M HClO_4) (23) one gets $k_{\text{H}+\text{O}_2}/k_{\text{H}+\text{OH}^-} = 780$. Using (21) $k_{\text{H}+\text{O}_2} = 2 \times 10^{10} M^{-1}\text{sec}^{-1}$, $k_{\text{H}+\text{OH}^-} = 2.6 \times 10^7 M^{-1}\text{sec}^{-1}$ results. It is possible also to use $k_{\text{H}+\text{O}_2}/k_{\text{H}+\text{HCO}_2^-}$ as calculated (44) from Hart's direct competition (24). This calculation gives the values

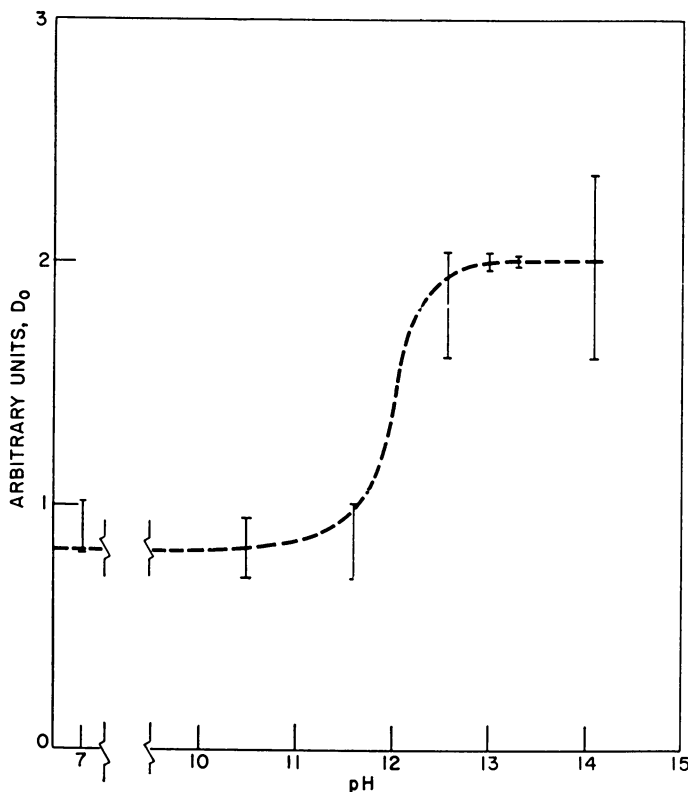


Figure 2. Effect of pH on initial optical density at 5780 Å. (39).

$k_{\text{H}+\text{OH}^-} = 1.7 \times 10^7$ and $2.4 \times 10^7 \text{ M}^{-1}\text{sec.}^{-1}$ based on ethanol (taking $\frac{k_{\text{H}+\text{HCO}_2^-}}{k_{\text{H}+\text{ethanol}}} = 10$) and formate respectively. In the light of the difficulties with the pH sensitive formic acid $-\text{O}_2$ system, the value of $k_{\text{H}+\text{OH}^-} = 2.6 \times 10^7 \text{ M}^{-1}\text{sec.}^{-1}$ seems to be better established.

The conversion of H atoms into electrons was directly demonstrated by Matheson and Rabani (39). They pulse irradiated solutions of $\sim 0.1 \text{ M H}_2$, which converts all the OH radicals into H atoms. At pH = 11.6, the optical density (due to e_{aq}^- absorption) showed an initial increase with time, before it decayed to zero. This was explained as being caused by Reaction 7, which under the appropriate conditions produces more electrons than the amount initially decaying. From (39) Figure 5, $k_{\text{H}+\text{OH}^-} = 1.8 \times 10^7 \text{ M}^{-1} \text{ sec.}^{-1}$ has been calculated. Fielden and Hart find recently $k_{\text{H}+\text{OH}^-} = 2.3 \times 10^7 \text{ M}^{-1} \text{ sec.}^{-1}$ by direct observation of the formation of e_{aq}^- in alkaline H_2 solutions. Since the decay of e_{aq}^- , under the conditions of the experiments, was mainly by second order reactions with other species produced by the radiation, the initial increase in optical absorption showed dependency on both the pH and

the pulse intensity. In less basic solutions—e. g., pH \sim 10, a decay was observed immediately after the pulse because Reaction 7 was not important. At pH 13.3 a similar result was obtained because Reaction 7 was too fast, and most of the H atoms were converted to e_{aq}^- during the pulse. At intermediate pH values such as 11.6, Reaction 7 could be followed directly when the pulse intensity was small, and the second-order reactions by which e_{aq}^- decayed were slowed down. With higher intensities at the same pH, only a decay was observed. Another demonstration of Reaction 7 has been done by the measurements of the initial optical density vs. pH. When Reaction 7 becomes fast so that H atoms are converted to e_{aq}^- during the pulse, the initial optical density increases. At pH 13–14, the initial optical density was over twice as high as compared with that of pH 7–11. This is shown in Figure 2. The amount of increase in D_0 is in accordance with Reaction 7 and with the expected ratio of $\frac{G_H + G_{OH}}{G_e}$.

Recently, a similar technique has been used (40) to demonstrate the conversion of the neutral H atoms ($G \sim 0.5$) to e_{aq}^- . Figure 3 shows an oscilloscope trace obtained with $2.4 \times 10^{-2} M OH^-$ at 5780 Å., optical path = 80 cm. (no H_2). (See (45) for details about the technique.) The initial small increase in optical density is caused by the Reaction 7. This increase is very small, because $G_H \approx 0.2 G_e$. The results agree with those obtained with $\sim 0.1 M H_2$, but we did not make any quantitative analysis.

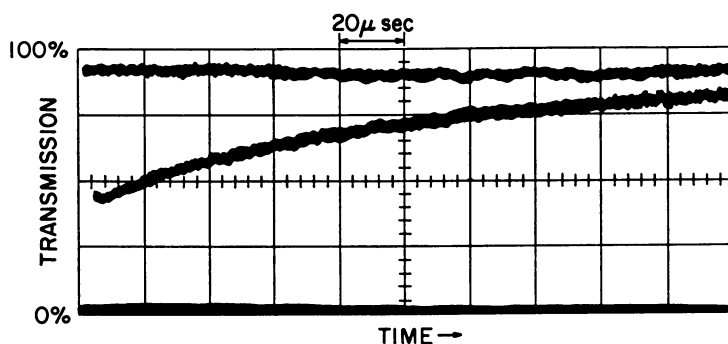


Figure 3. An oscilloscope trace showing e_{aq}^- absorption at 5780 Å. in $2.4 \times 10^{-2} M OH^-$.

(5 mole % $Ba(OH)_2$ in $NaOH$). Optical path—80 cm.

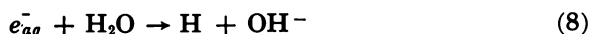
The conversion of H into e_{aq}^- agrees with other observations. Thus, Cheek and Swinnerton (10) find a radiation induced chain reaction between H_2 and N_2O . $G(N_2)$ is much greater in alkaline solutions than in neutral. The chain propagation is by the reaction of e_{aq}^- or H atoms with N_2O , to form OH (in alkaline solutions $-O^-$), and OH^- reacts with H atoms to form e_{aq}^- . In alkaline solutions the reaction is enhanced, owing

to Reaction 7, since e_{aq}^- is very reactive towards N_2O , in contrast to H atoms.

Dainton and Peterson (14) find an increase in $G(N_2)$ in alkaline solutions containing N_2O . This again agrees with the conversion of H ($G_H \approx 0.5$) to e_{aq}^- as demonstrated in Figure 3.

The pK of H

We can now obtain the dissociation constant of H atoms as a ratio of k_7 and k_8



The best value (25) for k_8 has been measured with pulse radiolysis in pre-irradiated (to reduce reactive impurities) aqueous H_2 solutions. This value, $16 \pm 1 M^{-1}sec.^{-1}$, combined with $k_{H+OH^-} = 2.2 \times 10^7 M^{-1}sec.^{-1}$ (average of 1.8 and 2.6×10^7) gives $pK = 9.6$.

Acknowledgment

The author wishes to thank Dr. M. S. Matheson for many helpful discussions, and W. A. Mulac and J. L. Weeks for invaluable aid in the preparation of the paper.

Literature Cited

- (1) Allan, J. T., Robinson, M. G., Scholes, G., *Proc. Chem. Soc.* **1962**, 381.
- (2) Allan, J. T., Scholes, G., *Nature* **187**, 218 (1960).
- (3) Allen, A. O., Schwarz, H. A., *2nd Internat. Conf.*, Geneva **29**, 30 (1958).
- (4) Anbar, M., Meyerstein, D., *J. Phys. Chem.* **68**, 1713 (1964).
- (5) Appleby, A., Scholes, G., Simic, M., *J. Am. Chem. Soc.* **85**, 3891 (1963).
- (6) Barr, N. F., Allen, A. O., *J. Phys. Chem.* **63**, 928 (1959).
- (7) Baxendale, J. H., Hughes, G., *Z. Physik. Chem. N. F.*, **14**, 306, 323 (1958).
- (8) Baxendale, J. H., Smithies, D. H., *Z. Physik. Chem. N. F.*, **7**, 242 (1956).
- (9) Bell, R. P., "The Proton in Chemistry," Cornell University Press, Ithaca, 1959.
- (10) Cheek, C. H., Swinnerton, J. W., *J. Phys. Chem.* **68**, 1429 (1964).
- (11) Collinson, E., Dainton, F. S., Smith, D. R., Tazuke, S., *Proc. Chem. Soc.* **1962**, 40.
- (12) Czapski, G., Schwarz, H. A., *J. Phys. Chem.* **66**, 471 (1962).
- (13) Czapski, G., Stein, G., *J. Phys. Chem.*, **63**, 850 (1959).
- (14) Dainton, F. S., Peterson, D. B., *Proc. Roy. Soc.* **267A**, 443 (1962).
- (15) Dewald, R. R., Dye, J. L., Eigen, M., DeMaeyer, L., *J. Chem. Phys.* **39**, 2388 (1963).
- (16) Dorfman, L. M., Matheson, M. S., Chapter on "Pulse Radiolysis" in Vol. 3 of *Progress in Reaction Kinetics*, ed., G. Porter, 1965.
- (17) Dorfman, L. M., Taub, I. A., *J. Am. Chem. Soc.* **85**, 2370 (1963).
- (18) Friedman, H. L., Zeltmann, A. H., *J. Chem. Phys.* **28**, 878 (1958).
- (19) Frohlich, H., Platzman, R. L., *Phys. Rev.* **92**, 1152 (1953).
- (20) Gordon, S., Hart, E. J., Matheson, M. S., Rabani, J., Thomas, J. K., *J. Am. Chem. Soc.* **85**, 1375 (1963).
- (21) Gordon, S., Hart, E. J., Thomas, J. K., *J. Phys. Chem.* **68**, 1262 (1964).
- (22) Grossweiner, L. I., Swenson, G. W., Zwicker, E. F., *Science* **141**, 805 (1963).
- (23) Halpern, J., Rabani, J., unpublished results.
- (24) Hart, E. J., *J. Am. Chem. Soc.* **76**, 4312 (1954).
- (25) Hart, E. J., private communication.
- (26) Hart, E. J., Boag, J. W., *J. Am. Chem. Soc.* **84**, 4090 (1962).
- (27) Hart, E. J., Gordon, S., Thomas, J. K., *J. Phys. Chem.* **68**, 1271 (1964).

- (28) Hayon, E., *Trans. Faraday Soc.* **60**, 1059 (1964).
- (29) Hayon, E., Weiss, J., *Sec. Int. Conf.*, Geneva, **29**, 80 (1958).
- (30) Hayon, E., Weiss, J., *J. Chem. Soc.* **1960**, 5091.
- (31) Jortner, J., Ottolenghi, M., Rabani, J., Stein, G., *J. Chem. Phys.* **37**, 2488 (1962).
- (32) Jortner, J., Ottolenghi, M., Stein, G., *J. Phys. Chem.* **68**, 247 (1964).
- (33) Jortner, J., Rabani, J., *J. Phys. Chem.* **66**, 2081 (1962).
- (34) Keene, J. P., *Rad. Res.* **22**, 1 (1964).
- (35) Lifshitz, C., *Can. J. Chem.* **40**, 1903 (1962).
- (36) Lifshitz, C., Ph.D. Thesis, The Hebrew Univ., Jerusalem, Israel (1961).
- (37) Matheson, M. S., *Ann. Rev. Phys. Chem.* **13**, 77 (1962).
- (38) Matheson, M. S., Mulac, W. A., Rabani, J., *J. Phys. Chem.* **67**, 2613 (1963).
- (39) Matheson, M. S., Rabani, J., *J. Phys. Chem.* **69**, 1324 (1965).
- (40) Matheson, M. S., Rabani, J., unpublished data.
- (41) Navon, G., Stein, G., *J. Phys. Chem.* **69**, 1384 (1965).
- (42) Nehari, S., Rabani, J., *J. Phys. Chem.* **67**, 1609 (1963).
- (43) Rabani, J., *J. Am. Chem. Soc.* **84**, 868 (1962).
- (44) Rabani, J., *J. Phys. Chem.* **66**, 361 (1962).
- (45) Rabani, J., Mulac, W. A., Matheson, M. S., *J. Phys. Chem.* **69**, 53 (1965).
- (46) Rabani, J., Stein, G., *J. Chem. Phys.* **37**, 1865 (1962).
- (47) Samuel, H. A., Magee, J. L., *J. Chem. Phys.* **21**, 1080 (1953).
- (48) Scholes, G., Simic, M., *J. Phys. Chem.* **68**, 1738 (1964).
- (49) Schmidt, K., private communication.
- (50) Smithies D., Hart, E. J., *J. Am. Chem. Soc.* **82**, 4775 (1960).
- (51) Stein, G., *Discussions Faraday Soc.* **12**, 227, 289 (1952).
- (52) Thomas, J. K., Gordon, S., Hart, E. J., *J. Phys. Chem.* **68**, 1524 (1964).
- (53) Thomas, J. K., private communication.
- (54) Weiss, J., *Nature* **153**, 748 (1944).
- (55) Weiss, J., *Nature* **174**, 78 (1954).

RECEIVED May 10, 1965. Based on work performed under the auspices of the U.S. Atomic Energy Commission.

Submicromolar Analysis of Hydrated Electron Scavengers

EDWIN J. HART and E. M. FIELDEN

Department of Chemistry, Argonne National Laboratory, Argonne, Ill.

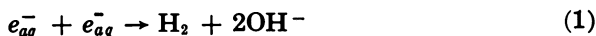
The analysis of typical e_{aq}^- scavengers such as oxygen, hydrogen peroxide, nitrous oxide, acetone, and thymine in the concentration range from 10^{-8} to 10^{-6} M is reported. These compounds react with e_{aq}^- with rate constants that vary from $4 \times 10^9 M^{-1} \text{sec.}^{-1}$ for thymine to $1.9 \times 10^{10} M^{-1} \text{sec.}^{-1}$ for oxygen. Hydrated electrons are introduced into an aqueous, hydrogen-saturated matrix at pH 11 by 2 rad x-ray pulses of 0.4 to 2 μ sec. duration. From the half-life of e_{aq}^- obtained by absorption spectrophotometry, the concentration of the dissolved species may be estimated. Some results are reported on the effectiveness of standard evacuation and irradiation techniques for the removal of oxygen from aqueous solutions. The mechanisms of the e_{aq}^- initiated $\text{H}_2\text{O}_2 + \text{H}_2$ and $\text{N}_2\text{O} + \text{H}_2$ chain reactions are briefly discussed.

During the course of recent work (8), it became evident that the hydrated electron, (e_{aq}^-), possesses many of the characteristics of an ideal analytical reagent. It is readily generated, highly reactive, deeply colored, and capable of rapid and precise determination. By utilizing these properties, it is possible to analyze a wide variety of inorganic and organic compounds at submicromolar concentrations with 5 to 10×10^{-9} $M e_{aq}^-$ formed by pulsed x-rays. This paper describes the techniques used to analyze oxygen, hydrogen peroxide, nitrous oxide, acetone, and thymine in an aqueous matrix at pH 11.

Basis of Method

Hydrated electrons, generated by short pulses of x-rays or electrons absorbed in water, react with many molecules and ions with high rate

constants (3, 6, 9, 10). Consequently, in the presence of such e_{aq}^- scavengers, decay of e_{aq}^- is rapid. On the other hand, especially in hydrogen-saturated alkaline solutions where H^+ is neutralized and OH is rapidly converted to H and then to e_{aq}^- (see Reactions 4 and 5 below), the decay of e_{aq}^- is comparatively slow at concentrations $< 10^{-8} M$. The decay reaction is



whereas in the presence of an excess of an electron scavenger—i.e., O_2 , the decay is predominantly



At an $[e_{aq}^-]$ of $10^{-8} M$, the theoretical $\tau_{1/2}$ owing to Reaction 1 alone is 10 msec. compared to 0.35 msec. in the presence of $10^{-7} M O_2$. Since absorption spectrophotometry by photoelectric recording techniques (4, 6, 11) will readily follow half-lives of the order of 10^{-6} sec., measurements under these conditions are routine.

Experimental

Preparation of Matrix. Our standard matrix consists of an H_2 saturated 0.001*N* NaOH solution rendered free of O_2 and e_{aq}^- scavengers by degassing and irradiation techniques (8, 14). About 700 ml. of triply distilled water is given a preliminary degassing in a one liter evacuation chamber in order to remove most of the O_2 and CO_2 . Then 1.0*N* NaOH is added to make the solution 0.001*N*. The solution need not be carbonate free, but it is advisable to minimize this ion because it forms an absorbing transient ion by reacting with the OH radical (1). Next, the solution is saturated with H_2 , degassed (cycle repeated twice), and finally saturated with H_2 . This solution is then forced into H_2 purged 100 (or 50) ml. syringes. The residual O_2 and e_{aq}^- scavengers are removed by 15 min. Co^{60} γ -ray irradiation to a total dose of $\sim 100 \mu M e_{aq}^-$ (8).

Preparation of Solutions. Standard solutions of O_2 , H_2O_2 , N_2O , thymine, and acetone are prepared either in the pre-irradiated matrix or pre-irradiated H_2 saturated water at concentrations ~ 10 to $50 \mu M$. Aliquots of these solutions are then micropipetted into the irradiation cell containing the matrix (Figure 1). The microsyringe is filled from a larger syringe by forcing the solution to be analyzed into the needle, up through the microsyringe barrel, and out of the top. After flowing freely for some seconds, the plunger is reinserted. This technique thoroughly eliminates air from the syringe, a serious contaminant because of its oxygen.

Irradiation Cell Assembly. Our 13.2 ml. irradiation cell (2.2 cm. diameter, 4 cm. length), provided with a glass encased magnet, is shown in Figure 1. This cell is mounted in a multiple reflection assembly (13). In normal practice this cell is used with 16 light passes giving an optical path length of 64 cm. The matrix, stored in a 100 ml. syringe, is introduced into the He-purged cell through stopcock A. After two complete replacements, 5/20 cone B on the He line is replaced by microsyringe C containing the sample. Because traces of oxygen and other impurities may have been introduced with the solution, it is pulse irradiated until a

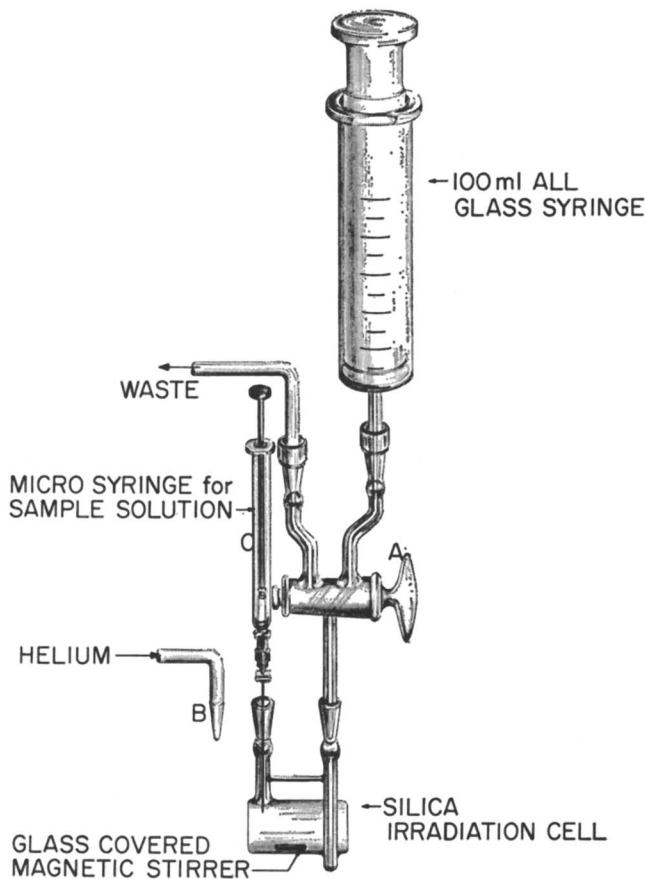


Figure 1. Irradiation cell assembly for e_{aq}^- spectrophotometry.

See reference (7) for optical arrangement and reference (13) for multiple reflection cell details.

constant decay of e_{aq}^- results ($\tau_{1/2} \sim 8-10$ msec.). This treatment usually requires about twenty $7 \text{ nM} \cdot e_{aq}^-$ pulses. (nM signifies nanomolar (10^{-9} M)). After this final irradiation, the sample is injected and the solution mixed by agitating the stirrer several times with a magnet. The solution is now homogeneous and ready for the x-ray or electron-analyzing pulse. Figure 2 shows the decay of a typical solution before and after injecting 13 nM O_2 .

Because low concentrations of oxygen ($\sim 100 \text{ nM}$) are analyzed many samples may be run without changing the matrix. Irradiation with 100–500 pulses usually restores the solution to its original $\tau_{1/2}$ because the final reduction product is water. Other scavengers, too, can often be removed by repeated pulsing so that the matrix may be reused.

Recording of e_{aq}^- Decay. The intensity of the light passing through the reaction cell is monitored by a conventional, monochromator/photo-

multiplier/oscilloscope combination. The photomultiplier was an RCA-7102 with associated pre-amplifier. The rise time of the pre-amplifier could be controlled by switching in various integrating capacitors. This has the effect of removing the high frequency components of the random noise fluctuations present in the signal. Care was always taken to ensure that the band width of the electronic circuitry was adequate to display the transient absorption being recorded. In practice the rise time of the recording system was never greater than 5% of the half-life of the transient signal. For example in the oscilloscope traces of Figure 2 the rise time (sometimes called response time or integrating time) of the complete recording system was 100 $\mu\text{sec.}$ and the half-lives of the two decays are 8000 and 2000 $\mu\text{sec.}$ Reducing the rise time to 10 $\mu\text{sec.}$ did not affect the experimental half-lives showing that negligible distortion had been produced by the 100 $\mu\text{sec.}$ rise time.

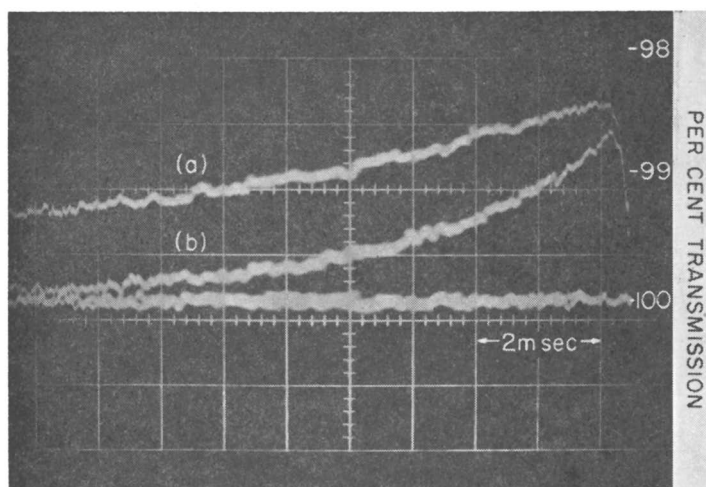


Figure 2. Decay of e_{aq}^- absorption band at 6900 Å. in a hydrogen-saturated solution at pH 11 (a) O_2 -free (b) $1.3 \times 10^{-8} M O_2$.

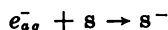
Decay is from right to left. The lower horizontal trace was recorded 30 msec. before the x-ray pulse and represents 100% transmission.

The standard procedure for taking a picture like Figure 2 is to adjust the photomultiplier pre-amplifier output to be 2 volts—i.e., the difference between 100% and zero light is represented by this voltage. The signal is then amplified by a known factor (50 in the case of Figure 2), and the radiation pulse is triggered. The upper line in Figure 2 represents the 100% light-level and is recorded 30 msec. before the radiation pulse occurs. The two lower traces are superposed examples of transient absorptions produced by the pulse.

Irradiation Source. One to two rad electron or x-ray pulses are required to produce 6 to 12 nM e_{aq}^- . We use 1 $\mu\text{sec.}$ pulses of 16 m.e.v. tungsten x-rays generated with an ARCO electron accelerator. The pulse must, however, be introduced in a time short compared to the measured half-lives. Any similarly pulsed x-ray beam of 150 to 200 k.e.v. would serve equally well since there is no rigid requirement of uniform irradiation.

tion. With x-ray pulses of lower energy, more pulses may be required in order to clean out the scavenger between runs. Alternatively, a steady x-ray or γ -ray source may be substituted for the pulsed x-rays for this purpose.

Calculation of Results. By considering the loss of e_{aq}^- as two psuedo-first-order reactions, namely, a decay by the matrix, m , and decay by the scavenger, s



we have

$$-\frac{d(e_{aq}^-)}{dt} = k_m(e_{aq}^-)(m) + k_s(e_{aq}^-)(s)$$

where k_m and k_s are rate constants for matrix and solute, respectively.

$$\ln(e_{aq}^-) = [k_m(m) + k_s(s)]t$$

for $(e_{aq}^-) = 1/2 (e_{aq}^-)_0$ and since $k_m(m) = 0.693/\tau_{1/2}$

$$s = \frac{.693}{k_s} \left(\frac{1}{t_{1/2}} - \frac{1}{\tau_{1/2}} \right)$$

k_s is the rate constant for the scavenger, s , $t_{1/2}$ is the half-life of the solute reaction, and $\tau_{1/2}$ is the half-life of the matrix. The matrix reaction only approximates first-order since Reaction 1 in an absolutely pure matrix is second-order. In general, trace impurities improve the first-order approximation. Since the matrix reaction only accounts for a small fraction of the decay in the presence of scavengers, the errors involved in this approximation are negligible compared to other experimental errors.

Results

Analysis of e_{aq}^- scavengers at concentrations in the range from 10^{-8} to $10^{-6} M$ has been demonstrated for oxygen, hydrogen peroxide, nitrous oxide, acetone, and thymine at pH 11. In principle, any inorganic or organic compound reacting with e_{aq}^- with rate constants $> 10^9 M^{-1} \text{sec}^{-1}$ may be analyzed with similar results. For compounds with lower rate constants the sensitivity of the method diminishes by a factor of 10 for each order of magnitude decrease in rate constant.

Oxygen. The results of several runs carried out at O_2 concentrations from 18-190 nM are shown in Figure 3. While there is some scatter in the points, considering the extremely low concentrations dealt with and the difficulties in handling gas solutions, this calibration curve provides a satisfactory demonstration of the feasibility of e_{aq}^- analyses. The ordinate in Figure 3 represents the calculated oxygen concentrations in the irradiation cell based on the experimental e_{aq}^- decay half-life and the value for $k_{e_{aq}^-} + O_2$ of $1.9 \times 10^{10} M^{-1} \text{sec}^{-1}$ (7). The points should lie on the indicated line if the above rate constant is correct under these conditions.

To illustrate a practical use of our method, we have measured the "O₂-equivalent concentrations" of some matrix solutions after different

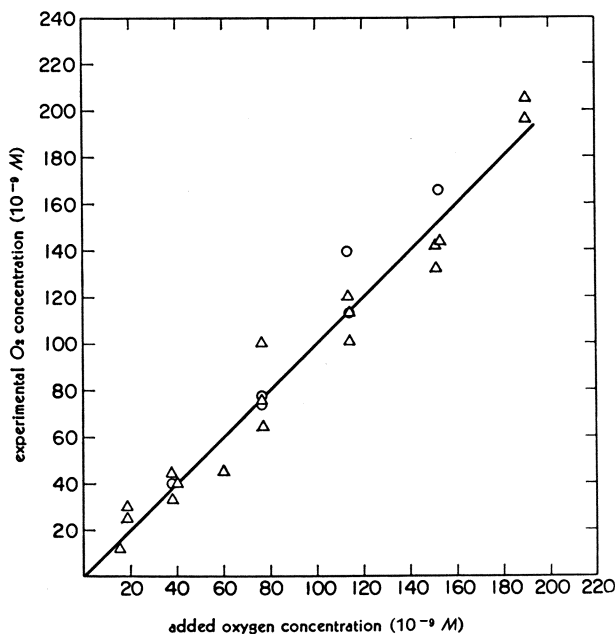


Figure 3. Determination of oxygen from e_{aq}^- half-life measurements.

Δ pH 11, H_2 -saturated matrix
 ○ pH 11, 0.001 M CH_3OH matrix.

treatments. For example, how effective are our evacuation and irradiation techniques for removing O_2 ? How much O_2 is introduced into the irradiation cell by a typical transfer of matrix from a 100 ml. syringe into a He-purged cell? For the first time, we can place an upper limit on the oxygen content of aqueous solutions treated in these ways.

The effect of a number of evacuations on oxygen removal is shown in experiments 1-3 of Table I. Calculation of the oxygen concentration is based on the assumption that O_2 is the only e_{aq}^- scavenger present. The results show that little is to be gained by more than one evacuation and subsequent hydrogen saturation.

γ -ray irradiation is an extremely effective method of removing O_2 in our H_2 -saturated matrix. See Experiments 4 and 5 of Table I. Irradiation with about $25 \mu M e_{aq}^-$ reduces the O_2 concentration to $< 0.03 \mu M O_2$. Further irradiation does not lower the O_2 level. This result indicates that some air or impurities leak into the syringe.

Pulse irradiation is the most effective way of removing the final traces of oxygen from the reaction cell. Experiments 6a-6g display the progress of $8 nM e_{aq}^-$ x-ray pulses in removing oxygen from sample 6 that had previously been Co^{60} irradiated with $75 \mu M e_{aq}^-$. Experiments 7-7d show the disappearance of oxygen after $69 nM$ had been injected into matrix

Table I. Oxygen Measurements in pH 11 Matrix

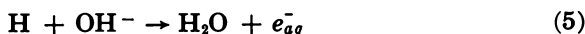
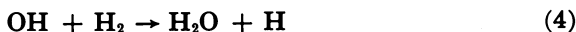
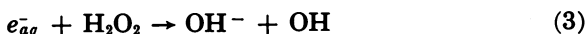
Exp. No.	(O_2) nM	$\Delta(O_2)^a$ nM	$(e_{aq}^-)^b$ nM	$(e_{aq}^-)/$ $\Delta(O_2)$	Pretreatment		
					No. of Evacua- tions	No. of H_2 equilibra- tions	$\mu M(e_{aq}^-)$ ($Co^{60}\gamma$ - rays)
1	2500	..	0	...	1	1	..
2	2500	..	0	...	2	2	..
3	1200	..	0	...	3	3	..
4	30	..	0	...	3	3	25
5	41	..	0	...	3	3	50
6	69	..	0	...	3	3	75
6a	69	..	16	...			
6b	48	20	80	4.0			
6c	28	40	160	4.0			
6d	11	58	240	4.1			
6e	6	63	320	5.1			
6f	2	66	400	6.1			
6g	0	69	800	11.6			
7	69	0	8	...			
7a	60	9	40	4.5			
7b	46	23	80	3.5			
7c	26	43	200	4.7			
7d	4	65	600	9.2			

^a Decrease in O_2 concentration during pulse irradiation in Experiments 6 and 7.

^b Accumulated dose of (e_{aq}^-) introduced by x-ray pulses.

6g. Note in column 5 that each of these groups of experiments requires 4 e_{aq}^- /molecule O_2 in the initial stages of O_2 removal. This is the theoretical number of e_{aq}^- needed to convert O_2 into $2O^{-2}$.

Other e_{aq}^- Scavengers. Calibration curves in Figure 4 for hydrogen peroxide, nitrous oxide, acetone, and thymine illustrate the precision and versatility of the method. As with O_2 , H_2O_2 may be satisfactorily analyzed at concentrations below 100 nM. Acetone, nitrous oxide, and thymine with somewhat lower e_{aq}^- rate constants are less sensitive, but 5–10% precision is possible for solutions of 500 nM concentrations. The ordinate in Figure 4 is the experimental quantity $(1/t_{1/2} - 1/\tau_{1/2})$, and the slopes of the calibration curves are a measure of the rate constants of the e_{aq}^- scavenger reactions. Table II lists rate constants obtained from the data in Figures 3 and 4 compared to previous literature values. Estimation of nitrous oxide and hydrogen peroxide presents a special problem in that a product of their reactions with hydrated electrons is an OH radical. One of the features of the hydrogen-saturated pH 11 matrix is the conversion of OH radicals into e_{aq}^- , so that with these solutes decomposition will occur by a chain reaction—i.e., for H_2O_2 :



and for nitrous oxide:



followed by (4) and (5).

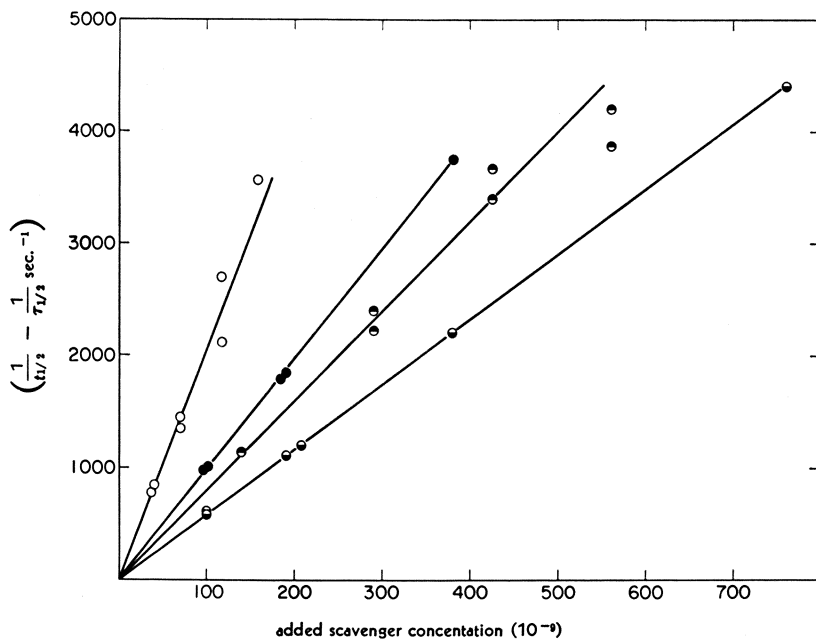


Figure 4. Calibration curves for some e_{aq}^- scavengers at pH 11.

$t_{1/2}$ = half-life with scavenger; $\tau_{1/2}$ = half-life of matrix.

○ H_2O_2 in 0.001 M CH_3OH ; solid line, $k_{eaq}^- + H_2O_2 = 1.3 \times 10^{10} M^{-1} sec^{-1}$

● Acetone in sat. H_2 ; solid line, $k_{eaq}^- + acetone = 6.9 \times 10^9 M^{-1} sec^{-1}$

● N_2O in 0.001 M CH_3OH ; solid line, $k_{eaq}^- + N_2O = 5.6 \times 10^9 M^{-1} sec^{-1}$

● Thymine in sat. H_2 ; solid line, $k_{eaq}^- + thymine = 4.0 \times 10^9 M^{-1} sec^{-1}$

Chain decomposition in these solutions has been observed by other workers (5). This disadvantage has been overcome by adding methanol to the matrix in sufficient concentration to scavenge the OH radicals to the exclusion of Reaction 4, thus preventing further steps in the reaction chain. Hydrogen peroxide and nitrous oxide were generally determined in the presence of 0.001M methanol in the matrix. The effect of methanol on the matrix was to speed up the decay of e_{aq}^- roughly by a factor of two, and this factor was taken into account in estimating the amount of e_{aq}^- scavenger present from its half-life.

Experiments on these scavengers in the absence of methanol were not very reproducible, and the average chain length was surprisingly short, indicating the presence of at least one unaccounted for non-chain reaction, possibly involving an intermediate such as N_2O^- or $H_2O_2^-$. The irreproducibility precluded using a calibration curve to study these scavengers in the absence of methanol where the chain reaction was allowed to occur. Any other OH scavenger with a low reactivity towards e_{aq}^- could be used instead of methanol.

Table II. Comparison of Present and Published e_{aq}^- Rate Constants

Reaction	Rate Constant (pH 11)		Published Rate Constants	
	$M^{-1} \text{ sec.}^{-1}$	pH	$M^{-1} \text{ sec.}^{-1}$	
$e_{aq}^- + O_2$	1.9×10^{10}	7	1.88×10^{10} (7);	2.16×10^{10} (12)
$e_{aq}^- + H_2O_2$	1.3×10^{10}	7	1.23×10^{10} (7);	1.36×10^{10} (12)
$e_{aq}^- + N_2O$	5.6×10^9	7	8.7×10^9 (7);	5.6×10^9 (12)
$e_{aq}^- + \text{Acetone}$	6.9×10^9	11	5.8×10^9 (2)	
$e_{aq}^- + \text{Thymine}$	4.05×10^9	6	1.7×10^{10} (9)	
$e_{aq}^- + \text{Thymine}$...	12	2.7×10^9	

Complex molecules such as acetone and especially thymine require much larger doses of radiation to render them inactive. In some cases it is preferable to start with a fresh sample of matrix for each estimation.

Limitations. At the present stage of development, analyses are confined to solutions containing but a single e_{aq}^- scavenger of known composition. Furthermore, since oxygen in the sample needs to be lowered to negligible concentrations, anaerobic conditions must prevail at all stages of the analysis. And since use is made of the favorable conditions existing in H_2 saturated solutions buffered at pH 11, the sample must be stable at this pH.

Potential in Analytical Chemistry. The method has already found applications in radiation chemistry. In addition to the oxygen analyses herein reported, hydrogen peroxide generated by intense 15 m.e.v. electron pulses has been measured from the decay of e_{aq}^- by subsequent low intensity x-ray pulses.

By the very nature of the method, the analysis of unknown samples is not feasible. Fortunately, in many cases one knows the qualitative composition of the sample and if the sample can be purified or treated so that a single e_{aq}^- scavenger is present, the method applies. If one component is a gas such as O_2 or N_2O , it may be removed by purging with N_2 or by degassing. In other cases a chemical treatment such as precipitation, complexing, or a change in pH may be effective.

The hydrated electron may well find use in analytical chemistry laboratories. Not only have we shown that e_{aq}^- is a valuable species for measuring submicromolar concentrations of its scavengers, but we have also demonstrated that satisfactory results may be obtained by very feeble x-ray pulses. While we irradiated our samples with 16 m.e.v. electrons or x-rays from a linear accelerator, an inexpensive pulsed x-ray unit of 150–200 k.e.v., capable of delivering 1 to 2 r/pulse, should serve equally well. Furthermore only minimal shielding is required under these conditions, thereby greatly facilitating manipulations needed for carrying out routine analyses.

Acknowledgment

We wish to thank Messers B. E. Clift and E. R. Backstrom for their skillful operation of the Linac for these studies.

Literature Cited

- (1) Adams, G. E., Boag, J. W., *Proc. Chem. Soc.* **1964**, 112.
- (2) Anbar, M., Hart, E. J., *J. Phys. Chem.* **69**, 973 (1965).
- (3) Baxendale, J. H., *et al.*, *Nature* **201**, 468 (1964).
- (4) Boag, J. W. In "Actions Chimiques et Biologiques des Radiations," Series VI Chap. I, 4-70, Haissinsky, M., ed., Masson et Cie, Paris, 1963.
- (5) Cheek, C. H., Swinnerton, J. W., *J. Phys. Chem.* **68**, 1429 (1964).
- (6) Dorfman, L. M., Matheson, M. S., "Pulse Radiolysis," in *Progress in Reaction Kinetics*, G. Porter, ed., Pergamon, London, 1965.
- (7) Gordon, S., *et al.*, *Discuss. Faraday Soc.* No. **36**, 193 (1963).
- (8) Hart, E. J., Gordon, S., Fielden, E. M., *J. Phys. Chem.*, submitted.
- (9) Hart, E. J., *Science* **146**, 19 (1964).
- (10) Hart, E. J., *Ann. Rev. Nuc. Sci.*, in press.
- (11) Keene, J. P., *J. Sci. Instr.* **41**, 493 (1964).
- (12) Keene, J. P., *Radiation Research* **22**, 1 (1964).
- (13) Rabani, J., Mulac, W. A., Matheson, M. S., *J. Phys. Chem.* **69**, 53 (1965).
- (14) Senvar, C. B. Hart, E. J., *Proc. 2nd Intern. Conf. Peaceful Uses At. Energy, Geneva* **29**, 19 (1958).

RECEIVED April 30, 1965. Based on work performed under the auspices of the U. S. Atomic Energy Commission.

Kinetic Evidence that "Excited Water" is Precursor of Intraspur H_2 in the Radiolysis of Water

THOMAS J. SWORSKI

Chemistry Division, Oak Ridge National Laboratory, Oak Ridge, Tenn. 37831

Homogeneous kinetics is used instead of diffusion kinetics to express the dependence of intraspur G_{H_2} on solute concentration. The rate-determining step for H_2 formation is not the combination of reducing species, but first-order disappearance of "excited water." Two physical models of "excited water" are considered. In one model, the $H_2O + OH$ radical pair is assumed to undergo geminate recombination in a first-order process with H_2O combination to form H_2 as a concomitant process. In this model, solute decreases G_{H_2} by reaction with H_2O . In the other model, "excited water" yields freely diffusing $H_2O + OH$ radicals in a first-order process and solute decreases G_{H_2} by reaction with "excited water." The dependence of intraspur G_{H_2} on solute concentration indicates $\tau_{H_2O^*} = 10^{-9} - 10^{-10}$ sec.

It was believed that G_{H_2} and $G_{H_2O_2}$ were independent of solute concentration until it was demonstrated (40, 41) experimentally for Co^{60} γ -radiation that $G_{H_2O_2}$ was markedly decreased by Br^- and Cl^- . Furthermore, $G_{H_2O_2}$ was shown (40, 41) to decrease linearly with the cube root of $[Br^-]$ and $[Cl^-]$ within experimental error in the concentration range from 10^{-5} to 10^{-1} M. This empirical relationship stimulated theoretical effort to explain quantitatively the dependence of G_{H_2} and $G_{H_2O_2}$ on solute concentration by diffusion kinetics using the Samuel-Magee (34) model.

The numerical and approximate analytical treatments using the Samuel-Magee model and an intercomparison of the results have been presented in an excellent review of diffusion kinetics by Kuppermann (19). He has pointed out that there is a quantitative inconsistency between the model and experiment: although the agreement can be

made reasonable, the curvature of the experimental and theoretical curves for the dependence of yields on solute concentration is different and invariant with respect to most of the pertinent parameters. It was suggested (42) in a preliminary communication that this quantitative inconsistency could be attributed to two factors: (a) H_2 in water irradiated with Co^{60} γ -radiation is formed by two processes—intraspur and interspur—in contrast with only intraspur processes in the isolated spur of the Samuel-Magee model, and (b) the precursor of H_2 disappears by a pseudo-unimolecular process. The objective of this paper is to present the results of a detailed analysis of the pertinent literature which supports this suggestion.

Results

Effect of NO_3^- on $G(Ce^{+3})$. There is a striking effect (43) of NO_3^- on Ce^{+4} reduction in sulfuric acid solutions. Tl^+ increases (44) $G(Ce^{+3})$ from $2G_{H_2O_2} + G_H - G_{OH}$ to $2G_{H_2O_2} + G_H + G_{OH}$. NO_3^- at concentrations greater than $0.01M$ markedly enhances $G(Ce^{+3})$ both in the presence and absence of Tl^+ , the effect being approximately equal in both cases. Mahlman (24) confirmed this effect and extended the study from $0.5M$ to $5.0M$. The enhancement, $\Delta G(Ce^{+3})$, for NO_3^- concentrations from $0.1M$ to $5.0M$ is quantitatively expressed by Equation 1 as shown in Figure 1.

$$1/\Delta G(Ce^{+3}) = 0.185 + 0.0804/[NO_3^-] \quad (1)$$

Equation 1, with constants obtained by the method of least squares as for all subsequent equations, is based on the data of Mahlman (24) for Ce^{+4}

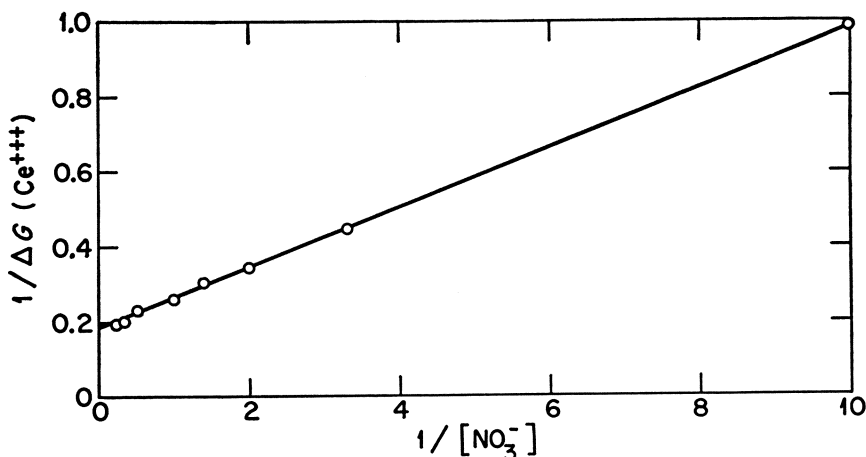


Figure 1. Dependence of $1/\Delta G(Ce^{+3})$ on $1/[NO_3^-]$ for Co^{60} γ -Radiation.

solutions containing Tl^+ and on the value of 7.92 (44) for $G(Ce^{+3})$ in the absence of NO_3^- .

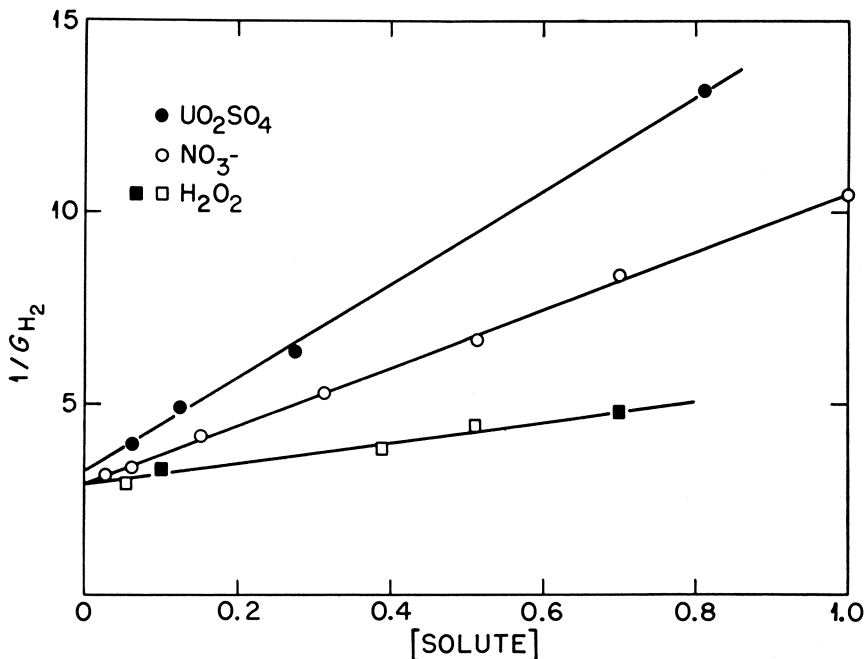


Figure 2. Dependence of $1/G_{H_2}$ on [Solute] for Co^{60} γ -Radiation: \blacksquare H_2O_2 (Ghormley and Hochanadel); \square H_2O_2 (Anderson and Hart).

This effect of NO_3^- ion is quantitatively consistent with a reaction mechanism (43) in which NO_3^- interacts with an electronically excited water molecule before it undergoes collisional deactivation by a pseudo-unimolecular process (the NO_3^- effect is temperature independent (45) and not proportional to T/η (37)). Equation 1, according to this mechanism, yields a lifetime for H_2O^* of 4×10^{-10} sec., based on a diffusion-controlled rate constant of 6×10^9 for reaction with NO_3^- .

Dependence of G_{H_2} on Solute Concentration. Another effect of NO_3^- in aqueous solutions is a decrease in G_{H_2} with increase in NO_3^- concentration (5, 25, 26, 38, 39). This decrease in G_{H_2} is generally believed to result from reaction of NO_3^- with reducing species before they combine to form H_2 . These effects of NO_3^- on $G(Ce^{+3})$ and G_{H_2} raise the question as to whether or not they are both caused by reaction of NO_3^- with the same intermediate.

γ -Radiation. The decrease in G_{H_2} for NO_3^- concentrations from 0.01M to 1.0M is quantitatively expressed for Co^{60} γ -radiation by Equation 2 as shown in Figure 2.

$$1/G_{H_2} = 2.93 + 7.53[NO_3^-] \quad (2)$$

Equation 2 is based on the data of Boyle and Mahlman (25, 26). These results agree with the *ad hoc* mechanism considered above for the effect of NO_3^- on $G(Ce^{+3})$, with the added assumption that H_2 results from the

first-order disappearance of H_2O^* . Equation 2 also yields a lifetime for H_2O^* of 4×10^{-10} sec. in excellent agreement with Equation 1. Therefore, the NO_3^- effect on $G(\text{Ce}^{+3})$ is caused by reaction of NO_3^- with the precursor of H_2 .

The decrease in G_{H_2} for H_2O_2 and UO_2SO_4 concentrations from 0.01M to 1.0M is quantitatively expressed for Co^{60} γ -radiation by Equations 3 and 4 as also shown by Figure 2.

$$1/G_{\text{H}_2} = 2.90 + 2.72[\text{H}_2\text{O}_2] \quad (3)$$

$$1/G_{\text{H}_2} = 3.24 + 12.2[\text{UO}_2\text{SO}_4] \quad (4)$$

Equation 3 is based on the data of Ghormley and Hochanadel (12) and Anderson and Hart (3). Equation 4 is based on the data of Boyle, Kieffer, Hochanadel, Sworski, and Ghormley (6). Similarly, though not shown in Figure 2, the decrease in G_{H_2} for NO_2^- and Cu^{+2} concentrations from 0.01M to 1.0M is quantitatively expressed for Co^{60} γ -radiation by Equations 5 and 6.

$$1/G_{\text{H}_2} = 2.83 + 4.19[\text{NO}_2^-] \quad (5)$$

$$1/G_{\text{H}_2} = 3.08 + 25.8[\text{Cu}^{+2}] \quad (6)$$

Equations 5 and 6 are based on the data of Schwarz (36) with only G_{H_2} at 0.394M KNO_3 showing significant deviation.

It is currently believed (1) that $G_{\text{H}_2} = 0.45$ in neutral and acid solutions. The intercept values of Equations 2-6 are significantly higher and correspond to about $G_{\text{H}_2} = 0.33 \pm 0.2$. The remainder of the "molecular" H_2 yield is more easily scavenged and suggests two processes for H_2 formation. A similar viewpoint has been presented by Mahlman (26) and supported by Hayon (14) and is based on the departure from linearity of G_{H_2} on $[\text{NO}_3^-]^{1/3}$ at concentrations greater than 1.0M (38).

Fission-Recoils. G_{H_2} for UO_2SO_4 , UO_2F_2 , and $\text{U}(\text{SO}_4)_2$ solutions is quantitatively expressed for fission-recoil radiation by Equations 7-9 as shown by Figure 3.

$$1/G_{\text{H}_2} = 0.571 + 0.645[\text{UO}_2\text{SO}_4] \quad (7)$$

$$1/G_{\text{H}_2} = 0.600 + 0.338[\text{UO}_2\text{F}_2] \quad (8)$$

$$1/G_{\text{H}_2} = 0.605 + 0.891[\text{U}(\text{SO}_4)_2] \quad (9)$$

Equations 7-9 are based on the data of Boyle, Kieffer, Hochanadel, Sworski, and Ghormley (6). In sharp contrast with the dependence of G_{H_2} on solute concentration for Co^{60} γ -radiation, G_{H_2} is quantitatively expressed by Equations 7-9 over the entire concentration range investigated. For UO_2SO_4 solutions, this corresponded to concentrations ranging from 1.1×10^{-3} to 2.2M. Thus we have the surprising result that H_2 formation appears to occur by two processes for Co^{60} γ -radiation, but by only one process for fission-recoil radiation. Limiting values for G_{H_2} indicated by intercept values of Equations 7, 8, and 9 are 1.75, 1.67, and 1.65.

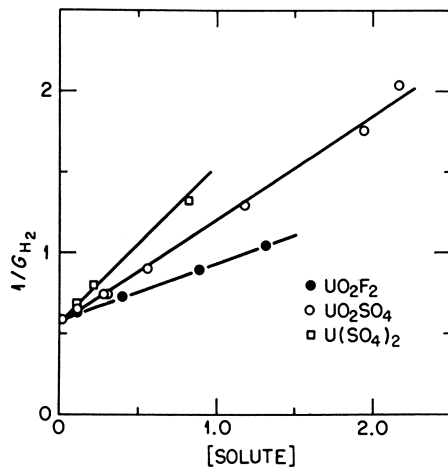


Figure 3. Dependence of $1/G_{H_2}$ on [Solute] for Fission Recoils.

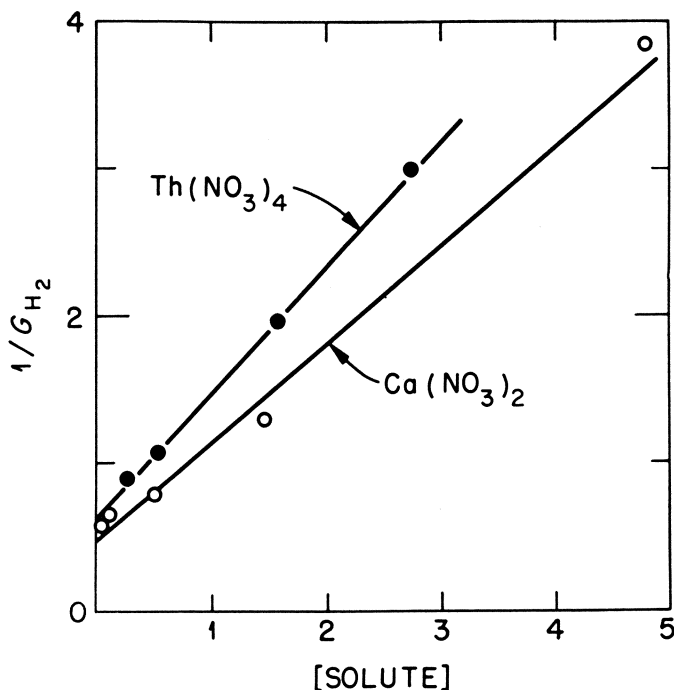


Figure 4. Dependence of $1/G_{H_2}$ on [Solute] for Fission Recoils.

G_{H_2} for $Th(NO_3)_4$ and $Ca(NO_3)_2$ solutions is quantitatively expressed for fission-recoil radiation by Equations 10 and 11 as shown in Figure 4.

$$1/G_{H_2} = 0.634 + 0.864[\text{Th}(\text{NO}_3)_4] \quad (10)$$

$$1/G_{H_2} = 0.493 + 0.343[\text{NO}_3^-] \quad (11)$$

Equation 10 is based on the data of Boyle and Mahlman (5). Equation 11 is based on the data of Sowden (39). Although excellent agreement between the results from $\text{Th}(\text{NO}_3)_4$ and $\text{Ca}(\text{NO}_3)_2$ solutions is indicated (39) in a plot of G_{H_2} against $[\text{NO}_3^-]^{1/3}$ assuming total dissociation of both solutes, Equations 10 and 11 markedly disagree in the limiting value of G_{H_2} for infinitely dilute solutions: Equation 10 indicates $G_{H_2} = 1.58$, and Equation 11 indicates $G_{H_2} = 2.03$.

Reactor Radiation. G_{H_2} for $\text{Ca}(\text{NO}_3)_2$ solutions from 0.01M to 1.0M is quantitatively expressed for reactor radiation by Equation 12.

$$1/G_{H_2} = 1.49 + 3.51[\text{NO}_3^-] \quad (12)$$

Equation 12 is based on the data of Sowden (38) for the Harwell experimental reactor BEPO. Equation 12 indicates two processes for H_2 formation similar to the results from γ -radiation: Equation 12 indicates $G_{H_2} = 0.67$ for infinitely dilute solutions while the measured value is 0.82.

18.9 m.e.v. D^+ . G_{H_2} for H_2O_2 solutions from 0.01M to 1.0M is quantitatively expressed for 18.9 m.e.v. D^+ radiation by Equation 13.

$$1/G_{H_2} = 2.10 + 2.05[\text{H}_2\text{O}_2] \quad (13)$$

Equation 13 is based on the data of Anderson and Hart (3). Again, two processes are indicated for H_2 formation: Equation 13 indicates $G_{H_2} = 0.476$ for infinitely dilute solutions, while the measured value at $3 \times 10^{-5} \text{M}$ H_2O_2 is 0.675.

Dependence of $G(\text{H}_2 + \text{Cl}^-)$ on CH_2ClCOOH Concentration. The sum of $G(\text{H}_2)$ and $G(\text{Cl}^-)$ at moderately low concentrations of chlorinated compounds indicates (17) that all reducing species react to yield either H_2 or Cl^- . The enhancement, $\Delta G(\text{H}_2 + \text{Cl}^-)$, at concentrations of CH_2ClCOOH from 0.1M to 2.5M is quantitatively expressed for Co^{60} γ -radiation by Equation 14 as shown in Figure 5.

$$1/\Delta G(\text{H}_2 + \text{Cl}^-) = 0.545 + 0.280/[\text{CH}_2\text{ClCOOH}] \quad (14)$$

Equation 14 is based on the data of Hayon and Allen (17) at pH 1.0. $\Delta G(\text{H}_2 + \text{Cl}^-)$ was taken as the increase over $G(\text{H}_2 + \text{Cl}^-)$ of 3.65 for 0.001M CH_2ClCOOH .

Discussion

Hart and Boag's discovery (13) of the broad optical absorption band of the e_{aq}^- in irradiated water confirmed the conclusion (7, 8) that the e_{aq}^- , instead of the H atom, is the principal reducing intermediate in the bulk of the solution. Understandably, the Lea-Platzman (31) viewpoint of the primary physical processes of energy absorption gained currency over the Samuel-Magee (34) viewpoint. Their disagreement concerned the fate of the electron from primary ionization of water: Platzman (31)

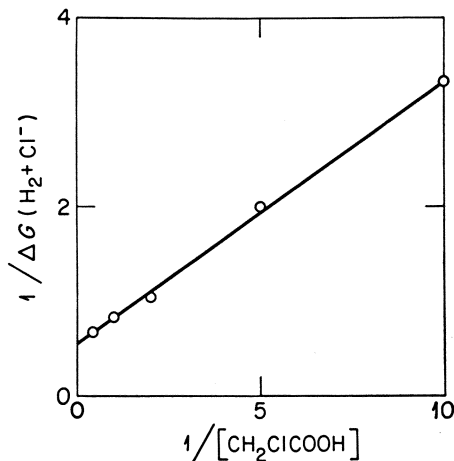
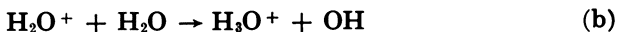
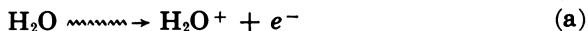


Figure 5. Dependence of $1/\Delta G(H_2 + Cl^-)$ on $1/[CH_2ClCOOH]$ for Co^{60} γ -radiation.

has accepted Lea's viewpoint (20) that the electron escapes from the parent positive ion, while Samuel and Magee (34) have deduced that the electron does not escape.

Plausible arguments have been presented (14, 29, 35) for the e_{aq}^- , not the H atom, as the main precursor of H_2 . Assume that it is the reaction of NO_3^- with the e_{aq}^- which causes both enhancement of $G(Ce^{+3})$ and decrease in G_{H_2} . Then, Equations 1 and 2 would yield a lifetime for e_{aq}^- of 5×10^{-10} sec., based on a rate constant (4) for reaction of NO_3^- with e_{aq}^- of $8.15 \times 10^9 M^{-1} \text{ sec.}^{-1}$. This is much longer than the lifetime of 8×10^{-11} sec. to be expected for the e_{aq}^- in 0.8N sulfuric acid ($[H^+_{aq}] \sim 0.6M$ (46)) owing to reaction with H^+_{aq} alone. This, together with the absence of any marked influence of pH on the effect of NO_3^- on either $G(Ce^{+3})$ [0.08N to 0.8N H_2SO_4 (45)] or G_{H_2} (27) forces the conclusion that the NO_3^- effects are not attributable to reaction of NO_3^- with e_{aq}^- . Therefore, the precursor of H_2 cannot be the e_{aq}^- . This agrees with conclusions (2, 21) based on the absence of any effect of H^+_{aq} on isotopic enrichment of hydrogen with light hydrogen from H_2O - D_2O mixtures.

Magee (22) proposed that three consecutive elementary processes, occurring in about 10^{-13} sec., yield OH and H_3O as the primary chemical intermediates in the radiolysis of water



and that H_3O is the precursor of e_{aq}^- .



The results summarized by Equations 1-14 are interpreted in this paper by reaction mechanisms which include reaction of solute with H_3O .

There is sufficient recent theoretical and experimental evidence to justify serious consideration of H_3O as an intermediate in the radiolysis of water. Bernstein (15) has presented thermochemical evidence for the stability of H atom adducts such as H_3O and NH_4 and estimated (16) the stability of H_3O with respect to $H_2O + H$ in the gas phase as about 5 kcal./mole. C. E. Melton and P. S. Rudolph of this Laboratory have demonstrated to H. A. Mahlman and the author, by mass spectrometric techniques, the existence of H_3O , D_3O , and D_2HO in the gas phase. These species were presumably desorbed from the instrument walls. The ratio $[H_3O]/[H_2O]$ was 1/200 at a background pressure of 10^{-8} torr in an ion source designed to eliminate ion-molecule reactions.

Effect of LET. It is commonly assumed in comparative studies using radiations which lose energy at different rates, e.v./A. denoted as linear energy transfer or LET, that the chemical effects differ only as a result of spatial distribution of the primary chemical intermediates. In the Samuel-Magee model, these intermediates are assumed to be in isolated spheres for Co^{60} γ -radiation and in a cylinder—the length of the track—for particles of higher LET for which higher G_{H_2} values are observed. The variations in G_{H_2} with variations in LET are correlated in the Samuel-Magee model with variations in the initial density of intermediates in the cylinder.

A different model to explain the variations in G_{H_2} with LET is induced here. The failure of Equations 2-6 for Co^{60} γ -radiation, Equation 12 for reactor radiation, and Equation 13 for 18.9 m.e.v. D^+ to represent quantitatively the dependence of G_{H_2} on solute concentrations less than 0.01M is interpreted as evidence that H_2 formation for these radiations results from two reactions: intraspur and interspur reactions. In interspur reactions, intermediates from one spur react with intermediates from an adjacent spur before they escape into the bulk of the solution.

If we denote the G -value for H_2 formed in intraspur reactions by $G_{H_2}^0$, then the G -value for H_2 formed in interspur reactions is equal to $G_{H_2} - G_{H_2}^0$. The variations in G_{H_2} , $G_{H_2}^0$ and $G_{H_2} - G_{H_2}^0$ with increase in LET, shown in Table I, result from a concomitant decrease in average distance between spurs in a particle track. $G_{H_2} - G_{H_2}^0$ increases from

Table I. Dependence of G_{H_2} , $G_{H_2}^0$, and $G_{H_2} - G_{H_2}^0$ on LET

Radiation	G_{H_2}	$G_{H_2}^0$	$G_{H_2} - G_{H_2}^0$
Fission Recoil	1.67	1.67 ^a	0
Harwell Reactor	0.84	0.67	0.17
18.9 m.e.v. D^+	0.675	0.476	0.199
Co^{60} γ 's	0.45	0.33	0.12
"Isolated Spur"	≤ 0.33	≤ 0.33	0

^a Intercept values for Equations 7-9 and 11 indicate $G_{H_2}^0$ for fission recoils is about 1.67 ± 0.09 .

zero for an "isolated spur" to a maximum value for some intermediate value of LET and then decreases to zero for fission recoils since essentially all spurs initially overlap adjacent spurs. $G_{H_2}^0$ increases continuously

with increase in LET since the probability for adjacent spurs to overlap each other initially, increases.

Pucheault and Ferradini (33) have also presented arguments for spurs in an α -particle track which do not overlap adjacent spurs initially. They quantitatively interpreted a wide variety of experimental results assuming that H_2 and H_2O_2 are formed in intraspur reactions and destroyed in interspur reactions.

Applicability of Homogeneous Kinetics. The applicability of homogeneous kinetics to the reaction of solute with H_2O in the spur raises the question as to whether Equations 1-14 are only an approximation of the dependence on solute concentration which would result from treatment of intraspur reactions by diffusion kinetics. An answer is provided by Figure 6. The slope and intercept values in Equation 15

$$1/G_{H_2}^0 = 1 + 4.42[X] \quad (15)$$

were selected to yield the same value for $G(R_2)/G(R_2)_0$ of 0.43 at $[X] = 0.3$ as shown in Figure 1 of Schwarz's (36) paper. There is a large disagreement in the curvature of the dependence of $G(R_2)$ on solute concentration between the results from Schwarz's treatment and Equation 17.

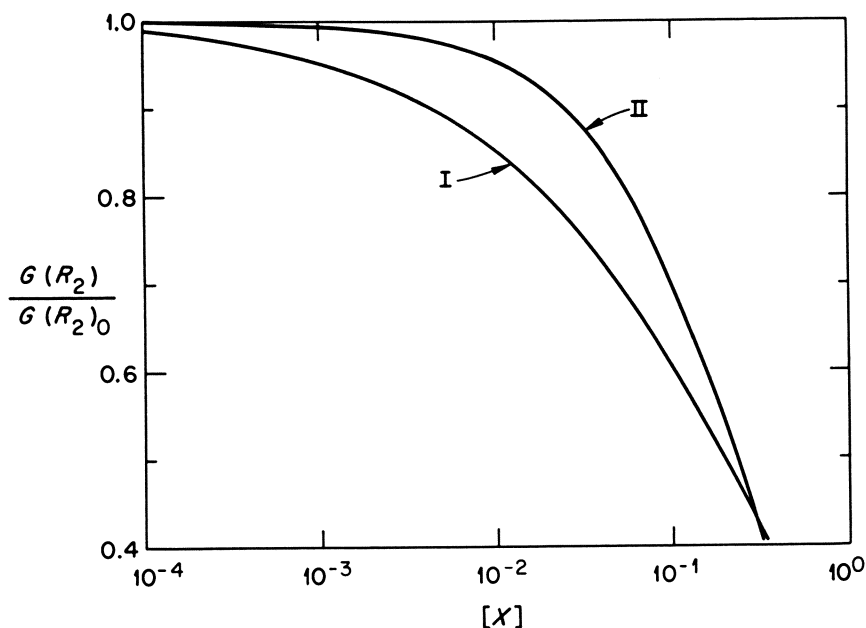


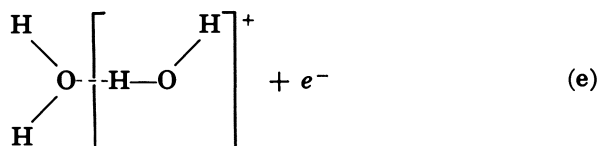
Figure 6. Dependence of $G(R_2)/G(R_2)_0$ on $[X]$: I. Schwarz's treatment; II. Equation 15.

Since the shape of the curves in diffusion kinetics is invariant with respect to most of the pertinent parameters (19), the conclusion is reached that diffusion kinetics can not quantitatively express the dependence of $G_{H_2}^0$ on solute concentration. Therefore, the question arises as to whether a

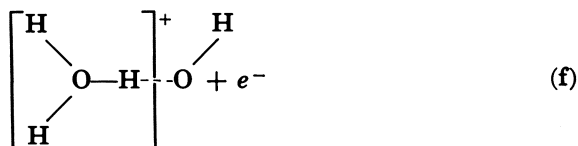
fundamental and simple reason exists for the applicability of homogeneous kinetics.

Equations 1-14 demonstrate that some effects of solute which are commonly attributed to reaction with e_{aq}^- can be quantitatively expressed by a reaction mechanism in which bimolecular reaction of the precursor with solute is in competition with precursor disappearance by a first-order process. The first observation that such a reaction mechanism may be applicable in water was made by Dainton and Peterson (9) who proposed H_2O^* and its reaction with H^{+}_{aq} to explain the increase in radical pair yield for Co^{60} γ -radiation with increase in sulfuric acid concentration. Dainton and Watt (10) proposed the alternative hypothesis that H^{+}_{aq} makes available to solutes isolated radical pairs $[H + OH]$ which would otherwise revert to water. Hayon (18), however, has normalized the increase in radical pair yield by a wide variety of solutes with reference to H^{+}_{aq} on the basis of their reactivity towards e_{aq}^- and concluded that the increase in radical pair yield is caused by reduction of the back reaction to form water in the spur.

A strong correlation exists in the Magee proposal (22, 23). Consider primary ionization to occur in one of two molecules of water with a hydrogen bond:



Proton transfer occurs which is effectively an ion-molecule reaction:



Charge neutralization yields H_3O and OH with a hydrogen bond:



Reactions e, f, and g more clearly present the Magee proposal represented above by Reactions a, b, and c.

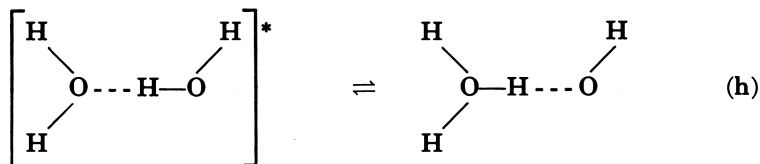
The applicability of homogeneous kinetics is attributed to first-order disappearance of H_2O^* , "excited water," as the rate-determining step for H_2 formation, instead of the combination of reducing species as commonly assumed when using the Samuel-Magee model. Two alternative physical models of H_2O^* are proposed. In one, H_2O^* is the $H_3O + OH$ radical pair which is assumed to undergo geminate recombination with

H_2O combination to form H_2 as a concomitant process. In this model, solute decreases $G_{\text{H}_2^0}$ by reaction with H_3O . In the other model, H_2O^* yields freely diffusing $\text{H}_3\text{O} + \text{OH}$ radicals in a first-order process, and solute decreases $G_{\text{H}_2^0}$ by reaction with H_2O^* .

Geminate Recombination of $\text{H}_3\text{O} + \text{OH}$. Noyes (30) has discussed the kinetics of competitive processes when reactive fragments are produced in pairs. Geminate recombination [original partners such as $\text{H}_3\text{O} + \text{OH}$] occurs within about 10^{-9} sec., and significant competition with this combination is not expected unless solute concentration is 0.01M or greater, even for diffusion-controlled reactions. Therefore, the kinetic dependence expressed by Equations 1-14 occurs at concentrations when competition with geminate recombination becomes possible. If such competition does occur, Noyes (30) has pointed out that the amount of additional reaction varies approximately as the square root of the concentration of scavenger. This is just the concentration dependence originally reported (6) for G_{H_2} in the decomposition of water by fission recoils. Since $G_{\text{H}_2} = G_{\text{H}_2^0}$ for fission recoils, the conclusion is drawn that solutes decrease $G_{\text{H}_2^0}$ by reaction with H_3O in competition with H_3O disappearance by geminate recombination.

Let geminate recombination volume denote that volume within which the $\text{H}_3\text{O} + \text{OH}$ radical pair can diffuse before geminate recombination occurs. The spur is then a number of $\text{H}_3\text{O} + \text{OH}$ radical pairs whose geminate recombination volumes initially overlap each other. Intraspur formation of H_2 results from combination of H_3O radicals from pairs whose geminate recombination volumes overlap each other. We assume, just as Dainton and Watt (10) have assumed, that an isolated radical pair disappears approximately by a first-order process to reform water. Then for first-order kinetics to be approximately valid for geminate recombination in the spur, the concentration of foreign radicals in each geminate recombination volume must vary only slowly with time during the lifetime, $\tau_{\text{H}_3\text{O}^*}$, of the $\text{H}_3\text{O} + \text{OH}$ radical pair.

The Role of Excitation. It would be surprising if excitation played no role in the radiolysis of water. This is implied, however, by attributing all the effects of radiation either to charge separation which yields OH and e_{aq} , or to charge neutralization which yields $\text{H}_3\text{O} + \text{OH}$. Therefore, the suggestion is made here that excitation may also result in forming the $\text{H}_3\text{O} + \text{OH}$ radical pair.



Superexcited states of water (32) would certainly provide as much energy for Reaction h as charge neutralization. Superexcited states are not required, however, for Reaction h to proceed, since charge neutralization undoubtedly produces H_3O^* . Assume Reaction h to be reversible.

Then ionization which yields $\text{H}_2\text{O} + \text{OH}$ by the sequence of Reactions e, f, and g would result in formation of "excited water" by the reverse of Reaction h. Thus, the effect of both ionization and excitation would be formation of H_2O^* .

Assume that the lifetime of H_2O^* is longer than the lifetime of the radicals which disappear in intraspur reactions. Then the rate-determining step for inhibition of intraspur H_2O formation would be reaction of solute with H_2O^* . Let us assume that the rate constant $k_{\text{R,R}}$ for intraspur combination of freely diffusing radicals is about $10^{10} \text{ sec.}^{-1}$, and that the lifetime of H_2O^* is about $4 \times 10^{-10} \text{ sec.}$ Then the concentration of radicals during intraspur formation of H_2 must be greater than $0.25M$ which is not unreasonable.

Lifetime for "Excited Water." $\tau_{\text{H}_2\text{O}^*} k_{\text{S,H}_2\text{O}^*}$, where $k_{\text{S,H}_2\text{O}^*}$ is the rate constant reaction of solute with "excited water" (reaction of solute with H_2O in one model and with H_2O^* in the other model), is a constant which can be derived from results summarized by Equations 1-14 as discussed below and which is independent of any constant errors in absolute dosimetry. Let $G_{\text{H}_2\text{O}^*}$ denote the yield of H_2O^* which disappears intraspur by a first-order process with resultant H_2 , H_2O_2 , and H_2O formation. Let a denote the number of H_2 molecules formed for each H_2O^* which disappears intraspur.

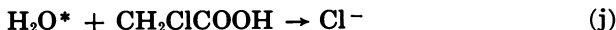


A reaction mechanism in which Reaction i competes with reaction of solute with H_2O^* , $k_{\text{S,H}_2\text{O}^*} [\text{H}_2\text{O}^*][\text{S}]$, yields the following kinetic relationship:

$$1/G_{\text{H}_2}^0 = 1/aG_{\text{H}_2\text{O}^*} + k_{\text{S,H}_2\text{O}^*}[\text{S}]/k_i a G_{\text{H}_2\text{O}^*} \quad (16)$$

The ratio of slope to intercept from a plot of $1/G_{\text{H}_2}^0$ against $[\text{S}]$ yields $\tau_{\text{H}_2\text{O}^*} k_{\text{S,H}_2\text{O}^*}$, where $\tau_{\text{H}_2\text{O}^*}$ is $1/k_i$. Equations 2-13 are of the form of Equation 16, and the values of $\tau_{\text{H}_2\text{O}^*} k_{\text{S,H}_2\text{O}^*}$ obtained from them are listed in Table II.

Equations 1 and 14 are of a different form than Equations 2-13. Let $G^0(\text{Cl}^-)$ denote the yield of Cl^- formed by intraspur reaction of H_2O^* with CH_2ClCOOH .



We assume that $G^0(\text{Cl}^-) = b\Delta G(\text{H}_2 + \text{Cl}^-)$ for the experimental data expressed by Equation 14 where b is a proportionality constant. A reaction mechanism in which Reaction i competes with Reaction j yields the following kinetic relationship:

$$1/\Delta G(\text{H}_2 + \text{Cl}^-) = b/G_{\text{H}_2\text{O}^*} + bk_i/G_{\text{H}_2\text{O}^*} k_j [\text{CH}_2\text{ClCOOH}] \quad (17)$$

Equations 1 and 14 are of this form, and the ratio of intercept to slope yields the values for $\tau_{\text{H}_2\text{O}^*} k_{\text{S,H}_2\text{O}^*}$ listed in Table II.

There is excellent agreement between the three values for $\tau_{\text{H}_2\text{O}^*} k_{\text{S,H}_2\text{O}^*}$ obtained for NO_3^- with Co^{60} γ -radiation and reactor radiation,

Table II. Constants Derived From Equations 1-14

Radiation	Solute	$\tau_{\text{H}_2\text{O}^*} k_{\text{S},\text{H}_2\text{O}^*}$
Co ⁶⁰ γ	NO ₃ ⁻ (1) ^a	2.30
	NO ₃ ⁻ (2) ^a	2.57
	H ₂ O ₂	0.938
	UO ₂ SO ₄	3.77
	NO ₂ ⁻	1.48
	Cu ⁺²	8.38
Fission-Recoils	CH ₂ ClCOOH	1.95
	UO ₂ SO ₄	1.13
	UO ₂ F ₂	0.563
	U(SO ₄) ₂	1.47
	Th(NO ₃) ₄	1.36
Reactor 18.9 m.e.v. D ⁺	NO ₃ ⁻ (11) ^a	0.70
	NO ₃ ⁻ (12) ^a	2.36
	H ₂ O ₂	0.976

^a Parenthetical notation indicates which Equation in the text was used.

and between the two values obtained for H₂O₂ with Co⁶⁰ γ -radiation and 18.9 m.e.v. D⁺. The corresponding values obtained for fission recoils are significantly lower. $\tau_{\text{H}_2\text{O}^*} k_{\text{S},\text{H}_2\text{O}^*}$ obtained for NO₃⁻ and UO₂SO₄ with Co⁶⁰ γ -radiation, reactor radiation, and 18.9 m.e.v. D⁺ is about 3.4 times as large as for fission recoils. This is attributed either to a marked increase in the degree of overlapping of geminate recombination volumes in one model or to reaction of H₂O* with primary intermediates in the other model.

The values of $\tau_{\text{H}_2\text{O}^*} k_{\text{S},\text{H}_2\text{O}^*}$ in Table II indicate a value for $\tau_{\text{H}_2\text{O}^*}$ ranging from 10⁻⁹ to 10⁻¹⁰ sec., based on a value for $k_{\text{S},\text{H}_2\text{O}^*}$ of 6 × 10⁹ M⁻¹ sec.⁻¹ from Debye's equation (11). The constants in Table II are also a measure of the relative reactivity of solute with H₂O* for any particular form of radiation for which $\tau_{\text{H}_2\text{O}^*}$ can be considered a constant. The relative reactivities of solute with H₂O* and e_{aq}^- for Co⁶⁰ γ -radiation differ slightly but significantly as shown in Table III. Relative reactivities with e_{aq}^- are based on measurements of absolute rate constants by pulsed-radiolysis techniques (4).

Table III. Relative Reactivities of H₂O* and e_{aq}^- for Co⁶⁰ γ -Radiation

Solute	$k_{\text{S},\text{H}_2\text{O}^*}/k_{\text{H}_2\text{O}_2,\text{H}_2\text{O}^*}$	$k_{\text{S},e_{aq}^-}/k_{\text{H}_2\text{O}_2,e_{aq}^-}$
H ₂ O ₂	1	1
NO ₂ ⁻	1.6	0.3
NO ₃ ⁻	2.6	0.6
UO ₂ ⁺²	4.0	5.4
Cu ⁺²	8.9	2.1
CH ₂ ClCOOH	2.1	

Some of the data used to obtain Equations 1-14 is shown in Figure 7. κ is a normalized factor for solute concentration and is equal to a ratio of constants obtained from Table II. The correlation for fission recoils and γ -radiation is very good over the entire concentration range. The curves in Figure 7 are theoretical and represent Equation 8 for fission recoils, Equation 12 for reactor radiation, Equation 13 for 18.9 m.e.v. D⁺, and Equation 3 for γ -radiation. Figure 7 emphasizes that the

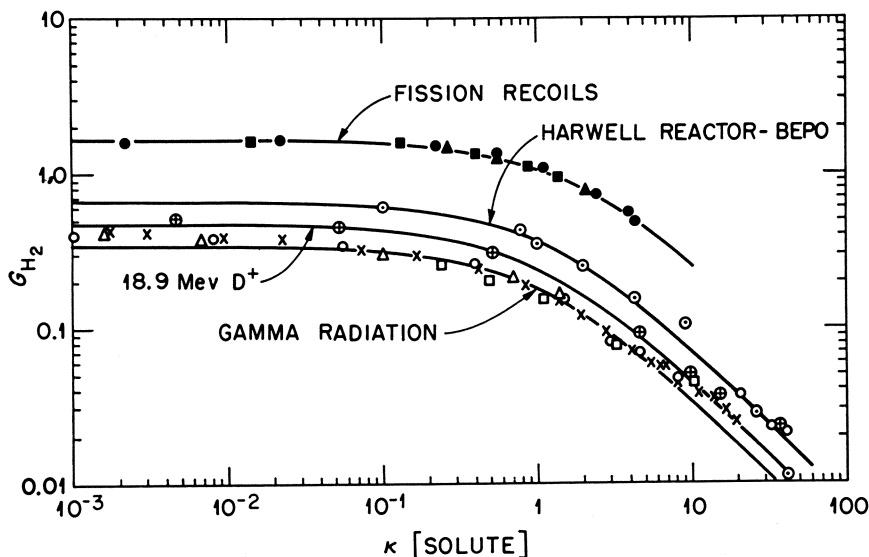


Figure 7. Dependence of G_{H_2} on [Solute]. Fission Recoils: \blacksquare UO_2F_2 , $\kappa = 1.0$; \bullet UO_2SO_4 , $\kappa = 2$; \blacktriangle $U(SO_4)_2$, $\kappa = 2.6$. Harwell Reactor-BEPO: \circ NO_3^- , $\kappa = 2.7$. 18.9 m.e.v. D^+ : \oplus H_2O_2 , $\kappa = 1.0$. Gamma Radiation: \triangle H_2O_2 , $\kappa = 1.0$ (Ghormley and Hohanadel); \circ H_2O_2 , $\kappa = 1.0$ [Anderson and Hart]; \times NO_3^- , $\kappa = 2.7$; \square UO_2SO_4 , $\kappa = 4.0$.

dependence of $G_{H_2}^0$ on solute concentration is similar for all forms of radiation for solute concentrations from 0.01M to 1.0M. Deviation from the theoretical line for solute concentrations greater than 1.0M (up to 7.0M for NO_3^- and 41M for H_2O_2) is evident in Figure 7 for Co^{60} γ -radiation.

Intraspur Yields for Co^{60} γ -Radiation. $G_{H_2O^*}$ can be estimated from Equation 14. The limiting value for $\Delta G(H_2 + Cl^-)$, from the intercept value in Figure 5 and Equation 14, of 1.83 together with $G_{H_2}^0 = 0.33$ yields a limiting value for $G_{Cl^-}^0$ and $G_{H_2O^*}$ of 2.16. Since $G_{H_2}^0 = 0.33$, the yield for reforming water by intraspur reactions must be $G_{H_2O^*}^0 = 1.50$. This estimate for $G_{H_2O^*}$ and $G_{H_2O^0}$ is probably low since Cl^- can react (41) with OH radical in the spur at pH = 1.0. This minimal value for $G_{H_2O^0}$ is very large when compared with $G_{H_2}^0 = 0.33$ and indicates a strong correlation between H_2O and OH radicals in the spur initially. Such a correlation exists in forming H_3O and OH by Reactions a-c, but cannot be reasonably understood with the Lea-Platzman (31) model.

It was tacitly assumed in the preliminary communication (42) that values for $G_{H_2O^*}$ of 3.04 and for $G_{H_2O^0}$ of 2.38 could be estimated from the limiting value for $\Delta G(Ce^{+3})$ from Equation 1. This assumption was implied (42) by attributing the NO_3^- effect to a decrease in G_{H_2} and concomitant increase in $G_{H_2O_2}$ with implied formation of NO_2^- by intraspur reaction of NO_2 radicals. This estimate would be too high if there were NO_2^- formation without NO_2 precursors, either by reaction (43) with H_2O^* or by direct action (28).

Interspur Yields for Co⁶⁰ γ -Radiation. H₂ formed by interspur combination of H₃O radicals with a *G*-value of 0.12 is much more easily inhibited by solute than H₂ formed by intraspur combination of H₃O radicals. The data of Boyle and Mahlman (5) on the dependence of *G*_{H₂} on NO₃⁻ concentrations up to 0.01*M* yields an interspur lifetime for H₃O of 150/*k*_{NO₃⁻,H₃O} based on values of *G*_{H₂} = 0.45 and *G*_{H₃} = 0.33. This is only a rough approximation since a value of 300/*k*_{NO₃⁻,H₃O} was reported in the preliminary communication (42) based on *G*_{H₃}⁰ = 0.34.

Since some H₃O radicals combine to form H₂ by an interspur reaction, it is reasonable to conclude that some H₃O radicals may also disappear by an interspur reaction with OH radicals to reform water. Furthermore, reformation of water may also occur by reaction of OH radical with e_{aq}⁻, produced by Reaction d, in an interspur reaction. Hayon (18) attributed the increase in radical yield with increase in sulfuric acid concentration to reaction of H⁺_{aq} with e_{aq}⁻



in the spur to inhibit reformation of water. The data of Dainton and Peterson (9) yields a lifetime for these e_{aq}⁻'s of 125/*k*₁₉. This is in excellent agreement with the interspur lifetime for H₃O of 150/*k*_{NO₃⁻,H₃O} and indicates that Reaction k is an interspur reaction and not an intraspur reaction. The increase in radical yield with decrease in pH must be caused by Reaction k since an important argument against the e_{aq}⁻ as precursor of H₂ is the conclusion that H₃O does not react with H⁺_{aq}. The *G*-value for reforming water by reaction of OH with e_{aq}⁻ is 0.75 according to Dainton and Peterson (9). No estimate is available for the yield of H₃O radicals which combine with OH radical in an interspur reaction.

Acknowledgment

The author thanks A. O. Allen, J. W. Boyle, H. A. Mahlman, and R. G. Sowden for providing numerical values from published Figures and expresses his appreciation to C. J. Hochanadel and H. A. Mahlman for many stimulating discussions.

Literature Cited

- (1) Allen, A. O., "The Radiation Chemistry of Water and Aqueous Solutions," Van Nostrand, Princeton, 1961.
- (2) Anbar, M., Meyerstein, D., *J. Phys. Chem.* **69**, 698 (1965).
- (3) Anderson, A. R., Hart, E. J., *J. Phys. Chem.* **65**, 804 (1961).
- (4) Baxendale, J. H., Fielden, E. M., Capellos, C., Francis, J. M., Davies, J. V., Ebert, M., Gilbert, C. W., Keene, J. P., Land, E. J., Swallow, A. J., Nosworthy, J. M., *Nature* **201**, 468 (1964).
- (5) Boyle, J. W., Mahlman, H. A., *Nucl. Sci. Eng.* **2**, 492 (1957).
- (6) Boyle, J. W., Kieffer, W. F., Hochanadel, C. J., Sworski, T. J., Ghormley, J. A., *Proc. Intern. Conf. Peaceful Uses Atomic Energy* **7**, 576 (1956).
- (7) Collinson, E., Dainton, F. S., Smith, D. R., Tazuke, S., *Proc. Chem. Soc.* **1962**, 140.
- (8) Czapski, G., Schwarz, H. A., *J. Phys. Chem.* **66**, 471 (1962).

- (9) Dainton, F. S., Peterson, D. B., *Proc. Roy. Soc. (London)* **A267**, 443 (1962).
- (10) Dainton, F. S., Watt, W. S., *Proc. Roy. Soc. (London)* **A275**, 447 (1963).
- (11) Debye, P., *Trans. Electrochem. Soc.* **82**, 265 (1942).
- (12) Ghormley, J. A., Hochanadel, C. J., *Radiation Research* **2**, 227 (1955).
- (13) Hart, E. J., Boag, J. W., *J. Am. Chem. Soc.* **84**, 4000 (1962).
- (14) Hayon, E., *Nature* **194**, 737 (1962).
- (15) Bernstein, H. J., *J. Am. Chem. Soc.* **85**, 484 (1963).
- (16) Bernstein, H. J., private communication.
- (17) Hayon, E., Allen, A. O., *J. Phys. Chem.* **65**, 2181 (1961).
- (18) Hayon, E., *J. Phys. Chem.* **68**, 1242 (1964).
- (19) Kuppermann, A., in "The Chemical and Biological Action of Radiations," M. Haissinsky, ed., Vol. 5, Academic Press, New York, 1961.
- (20) Lea, D. E., "Actions of Radiations on Living Cells," Cambridge University Press, Cambridge, 1946.
- (21) Lifschitz, C., *Canadian J. Chem.* **41**, 2175 (1963).
- (22) Magee, J. L., *Radiation Res. Suppl.* **4**, 20 (1964).
- (23) Magee, J. L., "Summary of Proceedings of Informal Conferences on the Radiation Chemistry of Water," Radiation Laboratory, University of Notre Dame, Notre Dame, Ind., 1959 and 1961.
- (24) Mahlman, H. A., *J. Phys. Chem.* **64**, 1598 (1960).
- (25) Mahlman, H. A., Boyle, J. W., *J. Chem. Phys.* **27**, 1434 (1957).
- (26) Mahlman, H. A., *J. Chem. Phys.* **32**, 601 (1960).
- (27) Mahlman, H. A., Chemistry Division Annual Progress Report, Oak Ridge National Laboratory, Oak Ridge, Tenn., ORNL-3488, 1963.
- (28) Mahlman, H. A., *J. Phys. Chem.* **67**, 1466 (1963).
- (29) Nehari, S., Rabani, J., *J. Phys. Chem.* **67**, 1609 (1963).
- (30) Noyes, R. M., *J. Am. Chem. Soc.* **77**, 2042 (1955).
- (31) Platzman, R. L., in "Radiation Biology and Medicine," W. D. Claus, ed., Addison-Wesley, New York, 1958.
- (32) Platzman, R. L., *Radiation Research* **17**, 419 (1962).
- (33) Pucheault, J., Ferradini, C., *Proc. Intern. Conf. Peaceful Uses Atomic Energy* **29**, 24 (1958).
- (34) Samuel, A., Magee, J. L., *J. Chem. Phys.* **21**, 1080 (1953).
- (35) Schwarz, H. A., *Radiation Res. Suppl.* **4**, 89 (1964).
- (36) Schwarz, H. A., *J. Am. Chem. Soc.* **77**, 4960 (1955).
- (37) Smoluchowski, M. V., *Z. Physik. Chem. (Leipzig)* **92**, 129 (1918).
- (38) Sowden, R. G., *J. Am. Chem. Soc.* **79**, 1263 (1957).
- (39) Sowden, R. G., *Trans. Faraday Soc.* **55**, 2084 (1959).
- (40) Sworski, T. J., *J. Am. Chem. Soc.* **76**, 4687 (1954).
- (41) Sworski, T. J., *Radiation Research* **2**, 227 (1955).
- (42) Sworski, T. J., *J. Am. Chem. Soc.* **86**, 5034 (1964).
- (43) Sworski, T. J., *J. Am. Chem. Soc.* **77**, 4689 (1955).
- (44) Sworski, T. J., *Radiation Research* **4**, 483 (1956).
- (45) Sworski, T. J., unpublished results.
- (46) Young, T. F., Maranville, L. F., Smith, H. M., in "The Structure of Electrolytic Solutions," W. J. Hamer, ed., Wiley and Sons, New York, 1959.

RECEIVED April 26, 1965. Research sponsored by the U. S. Atomic Energy Commission under contract with the Union Carbide Corporation.

Optical Generation of Hydrated Electrons from Aromatic Compounds

LEONARD I. GROSSWEINER and HANS-INGO JOSCHEK

Department of Physics, Illinois Institute of Technology, Chicago, Ill. 60616

A flash photolysis investigation of aromatic compounds has shown that photoionization in aqueous solution occurs for a number of benzene derivatives with electron-donating substituents, aryl carboxylic acids, and heterocyclics with five-member rings. Thermodynamic estimates for several benzene derivatives indicate that electron ejection is feasible and is competitive with bond rupture. It is suggested that the lowest π - π^* state of the ring system populates a charge transfer intermediate which can release an electron to the solvent. Comparing the hydrated electron yields with scavenging rate constants show that the molecules which are not readily photoionized in solution tend to react most rapidly with hydrated electrons.

Photoionization in condensed systems has been considered for many years in connection with the absorption spectra of halide ions in solution and the photolysis of aromatic compounds in rigid glasses. Recently, Jortner *et al.* (15) proposed that hydrated electrons are an initial product of the ultraviolet-light photolysis of aqueous phenolate ion, based on the effects of scavengers on the quantum yield. This explanation was confirmed by the work of Grossweiner and co-workers (10, 29) who reported a direct observation of the hydrated electron absorption band by flash photolysis of phenol derivatives and aromatic amino acids. A more detailed investigation of aqueous phenol and the cresols by Dobson and Grossweiner (6) showed that hydrated electrons are an initial photochemical product of both the neutral molecules and the anions, although the initial yields from the former were lower by an order of magnitude. The purpose of this investigation was to survey representative aromatic compounds for optical generation of the hydrated electron, in order to clarify the relationship between molecular structure and photoionization

in solution. Radical spectra are reported only for the compounds noted in the text. A more complete discussion of the radicals will be given elsewhere.

Experimental Data

The experimental arrangement and our procedures for flash photolysis have been described previously (5, 6). The hydrated electron was identified by its strong absorption from 600 to 900 m μ , where the longer-lived radicals are often transparent, and the scavenging by dissolved oxygen and hydrogen ions. Subsidiary runs with organic solvents aided in separating the hydrated electron absorption from other transients. Table I summarizes the results for the occurrence of the hydrated electron band in spectra taken at 5 μ sec. peak-to-peak delay. The observed initial yield of hydrated electrons is designated as follows: (++) prominent band-photographic density difference > 1; (+) less intense but clearly visible band-photographic density difference from 0.2 to 1; (f) faint but detectable band-photographic density difference from 0.05 to 0.2; (-) hydrated electron band not detected; (Δ) indeterminate case because of an overlapping radical absorption. The minimum detectivity was $\approx 0.1 \mu\text{Me}_{\text{aq}}^-$. All data refer to irradiation in Vycor cells with unfiltered light from fused-silica flash lamps. Radical spectra measured in selected cases are summarized in Table II. A determination of the wavelength effect for several benzene derivatives showed that optical excitation in the secondary band (1L_b) is responsible for electron generation; this data will be reported in detail with the other radical spectra.

Table I. Optical Production of Hydrated Electron from Aromatic Compounds in Aqueous Solution

(A) Oxygen compounds ^{a, b}	<i>m</i> -methoxyphenol; H ₂ O (+)
phenol; H ₂ O (+); pH 11.7 (+)	<i>p</i> -methoxyphenol; H ₂ O (+)
benzyl alcohol; H ₂ O (-)	<i>o</i> -phenoxyphenol; H ₂ O (-)
β -phenylethyl alcohol; H ₂ O (-)	<i>m</i> -phenoxyphenol; H ₂ O (-)
<i>o</i> -cresol; H ₂ O(+); pH 11.7 (++)	<i>p</i> -phenoxyphenol; H ₂ O (-)
<i>m</i> -cresol; H ₂ O (+); pH 11.7 (++)	diphenylether; H ₂ O-EtOH (1:1) (-)
<i>p</i> -cresol; H ₂ O (+); pH 11.7 (++)	benzoic acid; pH 9.2 (+)
catechol; H ₂ O (+)	phenylacetic acid; pH 8.4 (+)
resorcinol; H ₂ O (+)	β -phenylpropionic acid; pH 8.4 (+)
hydroquinone; H ₂ O (+)	γ -phenylbutyric acid; pH 8.6 (+)
2,2'-dihydroxybiphenyl; H ₂ O (Δ)	δ -phenylvaleric acid; pH 8.7 (+)
2,4'-dihydroxybiphenyl; H ₂ O (+)	phenoxyacetic acid; pH 9.0 (f)
4,4'-dihydroxybiphenyl; H ₂ O (Δ)	<i>p</i> -methoxy-phenoxyacetic acid; pH 8.9 (+)
3,3'-dihydroxybiphenyl; H ₂ O (+)	<i>o</i> -hydroxy-phenylacetic acid; pH 8.6 (++)
anisole; H ₂ O (++) ; pH 9.2 (++)	β -(<i>p</i> -hydroxy)phenyl propionic acid; pH 11.7 (+)
ethoxybenzene; H ₂ O (+)	α -naphthol; pH 8.9 ^c
benzylmethyl ether; H ₂ O (f)	benzoquinone; H ₂ O (-)
β -phenylethyl-methyl ether; H ₂ O (f)	diphenoquinone; H ₂ O; (Δ)
styrene oxide; H ₂ O (-)	benzaldehyde; H ₂ O-EtOH (8:2) (-)
<i>o</i> -dimethoxybenzene; H ₂ O (++)	acetophenone; H ₂ O (-)
<i>m</i> -dimethoxybenzene; H ₂ O (++)	methyl benzoate; H ₂ O (-)
<i>p</i> -dimethoxybenzene; H ₂ O (+); pH 9.2 (+)	<i>t</i> -butyl peroxybenzoate; H ₂ O (-)
<i>o</i> -methoxyphenol; H ₂ O (+)	

(B) Sulfur Compounds

thiophenol; H₂O (+ +)
 benzyl mercaptan; H₂O—EtOH (1:1)
 (—)
 α -phenyl-ethyl mercaptan; H₂O—
 EtOH (1:1) (—)
 thioanisole; H₂O (f); pH 8.9 (+)
 diphenylsulfide; H₂O—EtOH (8:2)
 (—)

(C) Nitrogen Compounds

aniline; H₂O (+ +)
 benzylamine; H₂O (—)
 β -phenylethylamine; H₂O (f)
 γ -phenylpropylamine; H₂O (—)
 diphenylamine; H₂O (Δ)
 triphenylamine; H₂O (Δ)
 dimethylaniline; H₂O (+)
 trimethylphenylammonium chloride;
 (H₂O) (—)
 p -phenylenediamine; H₂O (+)
 azobenzene; H₂O—EtOH (9:1) (—)
 nitrobenzene; H₂O—EtOH (99.5:0.5)
 (—)
 benzonitrile; H₂O (—)
 benzyl nitrile; H₂O (—)

(D) Phosphorus Compounds

phenylphosphine; H₂O (—)
 triphenylphosphine; H₂O—EtOH
 (1:1) (—)
 triphenylphosphine oxide; H₂O—EtOH
 (9:1) (—)

(E) Halogen Compounds

fluorobenzene; H₂O—EtOH (1:1) (—)
 chlorobenzene; H₂O—EtOH (1:1) (—)

bromobenzene; H₂O—EtOH (7:3) (—)
 $\alpha\alpha\alpha$ -trifluorotoluene; H₂O (—)

(F) Hydrocarbons

benzene; H₂O—EtOH (8:2) (f)
 toluene; H₂O—EtOH (7:3) (f)
 i -propylbenzene; H₂O—EtOH (6:4) (f)
 t -butylbenzene; H₂O—EtOH (6:4) (f)
 p -xylene; H₂O—EtOH (7:3) (+ +)
 styrene; H₂O—EtOH (1:1) (—)
 naphthalene; H₂O—EtOH (9:1)^c

(G) Other Benzene Derivatives

o -bromophenol; H₂O (—)
 p -bromophenol; H₂O (—)
 p -bromoanisole; H₂O (—)
 p -nitrophenol; H₂O (—)
 p -nitroanisole; H₂O (—)
 benzamide; H₂O (—)
 benzaldoxime; pH 8.8 (—)
 phenylalanine; H₂O (f), pH 11.7 (+)
 tyrosine; H₂O (+); pH 11.7 (+)

(H) Heterocyclic Compounds

benzofuran; pH 8.2 (+)
 thiophene; H₂O—EtOH (99.5:0.5) (f)
 benzothiophene; H₂O (+)
 pyridine; H₂O—EtOH (99.5:0.5) (—)
 quinoline; H₂O (—); pH 8.7 (—)
 acridine; pH 8.9 (+)
 pyrrole; H₂O (+)
 indole; pH 8.6 (+ +)
 2-methyl indole; H₂O (+)
 3-methyl indole; H₂O (+)
 3-indole carboxylic acid; pH 9.0 (+)
 3-indole acetic acid; pH 8.6 (+ +)
 3-indole propionic acid; pH 9.0 (+ +)
 tryptophan; H₂O (f); pH 11.7 (+)
 benzimidazole; H₂O (—)

^a All solutions were evacuated to 5×10^{-6} mm. Hg. The runs indicated as H₂O were made with triply distilled water, those indicated as pH 8.4 to pH 9.2 were made with Na₂B₄O₇ buffer solution, and those indicated as pH 11.7 were made with 0.04M Na₂PO₄ in which case the incident light was filtered with concentrated buffer solution to suppress photolysis of the solvent. The compounds used were the best available commercial grades and were purified by crystallization or distillation when deemed necessary. Solutions subject to oxidation by the atmosphere were handled under nitrogen prior to evacuation. The solute concentrations were selected to give absorbance (1 cm.) ≈ 1 at the maxima of the longest wavelength absorption bands.

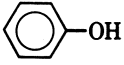
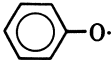
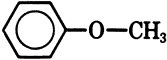
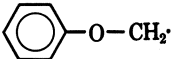
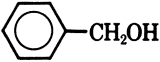
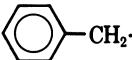

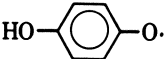
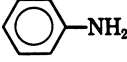
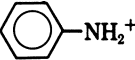
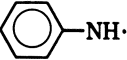

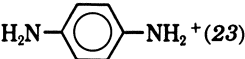
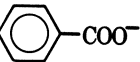

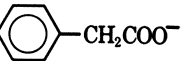
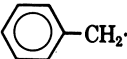
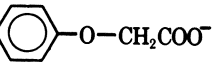
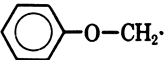
^b In some runs water-ethanol mixtures were used to obtain adequate solubility. Work in this laboratory by K. Youtsey has shown that the solvated electron is produced by flash photolysis of p -cresol in water-ethanol solutions with a decreasing yield as the water fraction decreases. The initial electron-to-radiation ratio in dry ethanol is two-tenths of that in water.

^c See footnote-a of Table V.

Discussion

Our observation of the hydrated electron band at a 5 μ sec. delay cannot be attributed to the thermal reaction: $H + OH^- \rightarrow e_{aq}^- + H_2O$, because the rate constant of $1.8 \times 10^7 M^{-1} \text{sec.}^{-1}$ (21) permits only a negligible conversion of H atoms below pH 10. Therefore, the cases indicated as (+) and (+ +) are taken as definite proof of photoionization. The cases indicated as (f) are less certain, although a photographic density difference of proper lifetime was measured densitometrically because the weak absorptions made the delineation from other transients, such as short-lived triplets, less certain. The absence of the hydrated electron

Table II. Radical Spectra from Flash Photolysis of Aromatic Compounds in Evacuated, Aqueous Solution

Parent Molecule ^a	Transient Absorption Maxima ^b	Radical Assignment and Reference
 (1.0)	398(n), 383(n), 362(n)	 (9,17)
 (0.6)	400(n), 380(n), ≈330(b)	 <i>this work</i>
 (9)	316(n)	 (24)
 (0.06)	429(n), 408(n), 401(n), <400(vb)	 (c)
 (1)	425(n) 402(n)	 (18) 
 (0.2)	475(b)	 (23)
 (0.1)	440(b), <340(vb)	 (d)
 (10)	316(n)	 (24)
 (0.7)	400(n), 382(n), ≈330(b)	 <i>this work</i>

^a The number below each formula is the solute concentration in millimolar.

^b Wavelength maxima are in m μ . The approximate half-band width is given as: n-narrow (<10 m μ); b-broad (10 to 50 m μ); vb-very broad (>50 m μ).

^c Benzoquinone and hydroquinone give the same radical spectra in ethanol (9), EPA glass (17), and water (*this work*).

^d The phenyl radical in the gas phase consists of a system of double-headed bands in the region 430–530 m μ (25). The assignment of the spectrum reported here is tentative pending further work.

band may indicate either an alternative photochemical process or the rapid scavenging of hydrated electrons by the parent molecules. A back reaction of hydrated electrons with the primary radicals would not suppress the hydrated electron band at 5 μ sec. delay, but a local recapture by the parent radical-ion could not be distinguished from negative production.

It is not feasible to categorize the molecules that give optical production of hydrated electrons by an unambiguous set of characteristics. With some exceptions they fall into the following classes: (a) benzene derivatives with electron-donating substituents; (b) aryl carboxylic acids; (c) certain heterocyclics with five-member rings. As shown in Table III, the observed yield was largest for molecules of low gas-phase photoionization potential. The relatively good correspondence indicates that the ease of electron ejection is a significant factor in solution. Comparing the hydrated electron yields from monosubstituted benzene derivatives with the Hammett substituent constants (σ_p) in Table IV indicates, for this group of compounds, that substituents of high electron

Table III. Correlation of Optical Hydrated Electron Production with Gas-Phase Photoionization Potentials

compound	PIP (e.v.)	e_{ea}^- yield
<i>N,N</i> -dimethylaniline	7.14 ^{b,c}	+
<i>p</i> -phenylenediamine	7.15 ^d	+
triphenylphosphine	7.36 ^b	—
aniline	7.70 ^a , 8.69 ^b	+ +
acridine	7.78 ^b	+
α -naphthol	$\approx 7.8^e$	^o
naphthalene	8.12 ^a , 8.14 ^b	^o
ethoxybenzene	8.13 ^f	+
anisole	8.22 ^a	+ +
quinoline	8.30 ^b	—
thiophenol	8.33 ^a	+ +
<i>p</i> -xylene	8.44 ^{a,b}	+ +
styrene	8.47 ^a	—
phenol	8.50 ^a , 8.52 ^b	+
benzylamine	8.64 ^b	—
<i>t</i> -butylbenzene	8.68 ^a	f
<i>i</i> -propylbenzene	8.69 ^a	f
toluene	8.83 ^a , 8.81 ^b	f
thiophene	8.86 ^a	f
pyrrole	8.90 ^a	+
bromobenzene	8.98 ^a	—
chlorobenzene	9.07 ^a	—
fluorobenzene	9.19 ^a	—
pyridine	9.23 ^a , 9.40 ^b	—
benzene	9.24 ^{a,b}	f
acetophenone	9.27 ^a , 9.65 ^b	—
benzaldehyde	9.53 ^a , 9.60 ^b	—
$\alpha\alpha\alpha$ -trifluorotoluene	9.68 ^a	—
<i>p</i> -benzoquinone	9.68 ^b	—
benzonitrile	9.71 ^a	—
nitrobenzene	9.92 ^a	—

^a Taken from the values selected by Streitwieser (28).

^b Taken from Terenin and Vilesov (32).

^c Taken from Vilesov (34).

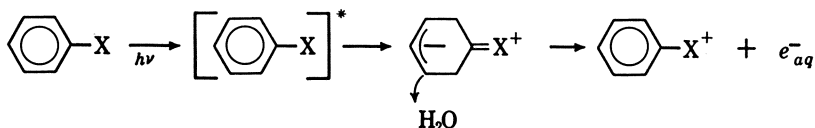
^d Taken from Briegleb and Czekalla (3).

^e Taken from Forster and Nishimoto (8).

^f Taken from Watanabe *et al.* (35).

^o See footnote a of Table V.

donating power in the ground state favor photoionization in solution; while those of high electron-withdrawing power suppress it. (The σ^+ values are probably more suitable for this comparison, but the distinction is not significant for qualitative purposes.) These correlations suggest that the site of electron release is the aromatic part of the molecule. A possible explanation is the production of a charge transfer intermediate via the lowest $\pi-\pi^*$ excited singlet state, which can then release an electron to the solvent:



The essential step is believed to be the escape of the electron from the coulomb-valence force potential well. A subsequent proton transfer from the radical cation to the solvent should depend on its acidity. For example, the transient spectra in Table II show that proton transfer takes place for phenol and anisole, in which cases the radicals were identified as neutral phenoxyl and phenoxymethyl, respectively. On the other hand, irradiating aniline gave both the neutral and protonated

Table IV. Correlation of Optical Hydrated Electron Production from Monosubstituted Benzene Derivatives with Hammett Substituent Constants

substituent	σ_p^a	e_{aq}^- yield
—N(CH ₃) ₂	—0.83	+
—NH ₂	—0.66	++
—O [—]	—0.519 ^b	++
—OH	—0.37	+
—OCH ₃	—0.268	++
—OC ₂ H ₅	—0.24	+
—C(CH ₃) ₃	—0.197	f
—CH ₃	—0.170	f
—CH(CH ₃) ₂	—0.151	f
—OC ₆ H ₅	—0.028 ^b , —0.320 ^a	—
—SCH ₃	0.00	+
—COO [—]	0.00	+
—H	0	f
—CH ₂ OH	0.00 ^c	—
—CH ₂ CN	+0.077 ^b	—
—F	+0.062	—
—SH	+0.15	++
—CHO	+0.216 ^b	—
—Cl	+0.227	—
—Br	+0.232	—
—COOCH ₃	+0.385 ^d	—
—COCH ₃	+0.502	—
—CF ₃	+0.54	—
—N=NC ₆ H ₅	+0.640 ^b	—
—CN	+0.660	—
—NO ₂	+0.778	—
—N(CH ₃) ₃ ⁺	+0.82	—

^a Taken from McDaniel and Brown (22) unless noted otherwise.

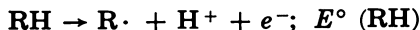
^b Taken from Jaffé (13).

^c Taken from Kwok *et al.* (16).

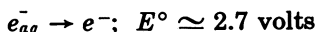
^d Taken from van Bekkum *et al.* (33).

anilino radicals, while *p*-phenylenediamine gave the protonated Wurster's salt. Of course, for phenolate ion only the electron transfer is necessary to give phenoxy radical.

The energy requirements of the overall process can be estimated by combining the oxidation potential of the substrate:



with the redox potential of the hydrated electron as calculated by Baxendale (2):



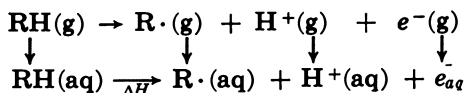
to give:

$$\Delta F \text{ (e.v.)} = -F[E^\circ (\text{RH}) - 2.7] - 0.41$$

where *F* is the faraday and the last term corrects the result to pH 7. The values given below, based on Fieser's estimates of the oxidation potentials (7), show that the energy associated with the longest wavelength π - π^* absorption (last column) exceeds the free energy requirements for typical substituted benzenes.

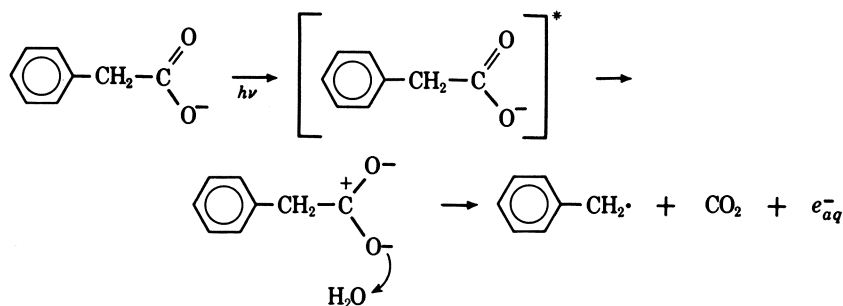
	$-E^\circ$ (volts)	$\Delta F(\text{pH } 7)$ (e.v.)	$h\nu$ (e.v.)
phenol	1.225	3.5	4.6
<i>p</i> -cresol	1.175	3.4	4.5
resorcinol	1.179	3.4	4.5
<i>p</i> -methoxyphenol	0.984	3.2	4.3
aniline	1.271	3.5	4.4

An alternative approach based on the cycle:



gives: $\Delta H \simeq D(\text{R}-\text{H}) + I(\text{H}) + S(\text{RH}) - S(\text{R}\cdot) - S(\text{H}^+) - S(e_{aq}^-)$, where *D* is the gas-phase bond-dissociation energy, *I*(H) is the hydrogen atom ionization potential (13.5 e.v.), and *S* is the hydration energy. Taking $S(\text{H}^+) \simeq 11.7$ e.v. (based on Randles' (26) value for the free energy), $S(e_{aq}^-) \simeq 1.7$ e.v. (2), and $S(\text{RH}) \approx S(\text{R}\cdot)$ gives: $\Delta H \simeq D(\text{R}-\text{H}) + 0.1$ e.v. Therefore, within the limits of this calculation, photoionization in aqueous solution is competitive with bond rupture.

The surprising occurrence of photoionization in aryl carboxylic acids may be explained by the transfer of excitation energy from the ring system to the carboxyl group to give an intermediate with charge separation at the side-chain terminus—e.g.,



Some support for this mechanism derives from our observation of benzyl radical from phenylacetic acid, phenoxyethyl radical from phenoxyacetic acid, and possibly the phenyl radical from benzoic acid. Radical spectra were not found for several aryl acids with longer side chains; but this is not inconsistent because the β -phenylethyl and higher radicals are not expected to absorb strongly above 300 $m\mu$. The case of the heterocyclics is complicated by the possibility of excitation either via the π -system or a lone pair electron on the heteroatom, and discussion of this group will be deferred until additional experimental data are obtained.

Any realistic mechanism must explain why optical electron production from aromatic molecules in organic solvents occurs with much lower yields than in water. We found that the radicals obtained from anisole, thioanisole, and *p*-cresol in ethanol, methanol, and cyclohexane were comparable in type and yield with the results in aqueous solution, while the solvated electron band was either faint or absent in each case. However, the pulse radiolysis work of Dorfman and associates (31, 27) has shown that solvated electrons are stabilized in aliphatic alcohols and furthermore, Grossweiner and co-workers (11, 5) have observed that optical solvated electron production takes place readily from halide ions in ethanol. (An experiment in which iodide ion was photolyzed to give solvated electrons in ethanol containing *p*-cresol established that the solvated electrons are not scavenged rapidly by *p*-cresol.) It can be concluded that the electron transfer act is less likely for aromatics in organic solvents. It is probable that the lower solvation energies of the radical ion and the electron in fluid organic solvents favor bond rupture over photoionization. Furthermore, electron release will be suppressed by the deeper coulombic well in low dielectric constant solvents. Since the radical yields were not appreciably different in organic and aqueous solvents, it does not appear that deactivation of the excited state is strongly solvent dependent. It has been established that electron ejection from aromatic compounds does take place in rigid hydrocarbon (19) and polar (20) organic glasses and in frozen aqueous solutions (4, 14); hence, this aspect of the process remains obscure.

The essential question concerning the compounds that did not give detectable hydrated electron spectra is whether photoionization was absent in those cases or whether the electron was released and scavenged

by the parent molecule in a fast reaction. Table V compares the maximum hydrated electron lifetimes, as calculated from the actual solute concentrations and the scavenging rate constants, with the results in Table I. With the exception of naphthalene and α -naphthoate, all positive cases for which the comparison can be made are within the resolving time of the apparatus (see footnote *a*). Although the molecules which did not give the hydrated electron band are most reactive, it cannot be concluded that all cases of negative electron production were caused to scavenging. For example, the transient spectra show that benzyl alcohol gives benzyl radical and that *p*-benzoquinone gives the *p*-hydroxyphenoxy radical. The first almost certainly occurs by bond rupture and the second via hydrogen abstraction in the excited state. Furthermore, the flash irradiation of bromobenzene and chlorobenzene caused a pH decrease owing to splitting-off of halogen atoms. As Table V shows, benzoic acid anion with an actual lifetime $< 3 \mu\text{sec.}$ gave a prominent hydrated electron band, which indicates that the electron would have been detected with less effective scavengers had it been produced. For these reasons we believe that, in general, the compounds which do not photoionize in solution tend to react most rapidly with hydrated electrons.

Table V. Comparison of Optical Hydrated Electron Production with Reactivity toward Hydrated Electrons

<i>compound</i>	<i>scavenging rate constant</i> $M^{-1}\text{sec.}^{-1}$	<i>maximum</i> e_{aq}^- <i>lifetime</i> $\mu\text{sec.}$	e_{aq}^- <i>yield</i>
phenol	4.0×10^8 (30)	250	+
thiophenol	4.7×10^7 (1)	215	++
aniline	$<2 \times 10^7$ (12)	>50	++
hydroquinone	$<10^7$ (12)	>50	+
thiophene	6.5×10^7 (30)	48	f
phenylalanine	$<10^7$ (12)	>33	+
benzene	1.4×10^7 (1)	32	f
toluene	1.2×10^7 (1)	24	f
benzoquinone	1.25×10^9 (12)	14	-
β -phenylpropionic acid anion	1.1×10^7 (30)	9	+
phenylacetic acid anion	1.4×10^7 (30)	7	+
fluorobenzene	6.0×10^7 (1)	6	-
styrene	1.3×10^{10} (30)	5	-
benzoic acid anion	3.1×10^9 (30)	2.4	+
pyridine	1.0×10^9 (12)	1.3	-
α -naphthoate	6.1×10^9 (1)	1.3	^a
benzyl alcohol	1.3×10^8 (1)	0.9	-
naphthalene	5.4×10^9 (1)	0.7	^a
nitrobenzene	3.0×10^{10} (12)	0.2	-
chlorobenzene	5.0×10^8 (1)	0.2	-
$\alpha\alpha\alpha$ -trifluorotoluene	1.8×10^9 (1)	0.1	-
benzotrile	1.6×10^{10} (1)	0.05	-
bromobenzene	4.3×10^9 (1)	0.03	-
benzamide	1.7×10^{10} (1)	0.03	-

Transients absorbing in the red region of lifetime $< 50 \mu\text{sec.}$ and quenched by oxygen were observed which are believed to be due to triplet states.

Acknowledgment

The authors wish to acknowledge helpful discussions concerning this work with Prof. S. I. Miller of the IIT Department of Chemistry.

Literature Cited

- (1) Anbar, M., Hart, E. J., *J. Am. Chem. Soc.* **86**, 5633 (1964).
- (2) Baxendale, J. H., *Radiation Research Supplement* **4**, 139 (1964).
- (3) Briegleb, G., Czekalla, J., *Z. Elektrochem.* **63**, 6 (1959).
- (4) Debye, P., Edwards, J. O., *Science* **116**, 143 (1952); *J. Phys. Chem.* **20**, 236 (1952).
- (5) Dobson, G., Grossweiner, L. I., *Radiation Research* **23**, 290 (1964).
- (6) Dobson, G., Grossweiner, L. I., *Trans. Faraday Soc.* **61**, 708 (1965).
- (7) Fieser, L. F., *J. Am. Chem. Soc.* **52**, 5204 (1930).
- (8) Forster, L. S., Nishimoto, K., *J. Am. Chem. Soc.* **87**, 1459 (1965).
- (9) Grossweiner, L. I., Mulac, W. A., *Radiation Research* **10**, 515 (1959).
- (10) Grossweiner, L. I., Swenson, G. W., Zwicker, E. F., *Science* **141**, 805 (1963).
- (11) Grossweiner, L. I., Zwicker, E. F., Swenson, G. W., *Science* **141**, 1180 (1963).
- (12) Hart, E. J., Gordon, S., Thomas, J. K., *J. Phys. Chem.* **68**, 1271 (1964).
- (13) Jaffé, H. H., *Chem. Rev.* **53**, 191 (1953).
- (14) Jortner, J., Sharf, B., *J. Chem. Phys.* **37**, 2506 (1962).
- (15) Jortner, J., Ottolenghi, M., Stein, G., *J. Am. Chem. Soc.* **85**, 2712 (1963).
- (16) Kwok, W. K., More O'Ferrall, R. A., Miller, S. I., *Tetrahedron* **20**, 1913 (1964).
- (17) Land, E. J., Porter, G., Strachan, E., *Trans. Faraday Soc.* **57**, 1885 (1961).
- (18) Land, E. J., Porter, G., *Trans. Faraday Soc.* **59**, 2027 (1963).
- (19) Lewis, G. N., Lipkin, D., *J. Am. Chem. Soc.* **64**, 2801 (1942).
- (20) Linschitz, H., Berry, M. G., Schweitzer, D., *J. Am. Chem. Soc.* **76**, 5833 (1954).
- (21) Matheson, M. S., Rabani, J., *J. Phys. Chem.* **69**, 1324 (1965).
- (22) McDaniel, D. H., Brown, H. C., *J. Org. Chem.* **23**, 420 (1958).
- (23) Michaelis, L., Schubert, M. P., Granick, S., *J. Am. Chem. Soc.* **61**, 1981 (1939).
- (24) Porter, G., Wright, F. J., *Trans. Faraday Soc.* **51**, 1469 (1955).
- (25) Porter, G., Ward, B., *Proc. Chem. Soc.* **1964**, 288.
- (26) Randles, J. E. B., *Trans. Faraday Soc.* **52**, 1573 (1956).
- (27) Sauer, M. C., Arai, S., Dorfman, L. M., *J. Chem. Phys.* **42**, 708 (1965).
- (28) Streitwieser, Jr., A., "Progress in Physical Organic Chemistry," ed. S. G. Cohen, A. Streitwieser, Jr., R. W. Taft, pp. 1-30, Interscience, New York, 1963.
- (29) Swenson, G. W., Zwicker, E. F., Grossweiner, L. I., *Science* **141**, 1042 (1963).
- (30) Szutka, A., Thomas, J. K., Gordon, S., Hart, E. J., *J. Phys. Chem.* **69**, 289 (1965).
- (31) Taub, I. A., Sauer, Jr., M. C., Dorfman, L. M., *Disc. Faraday Soc.* No. **36**, 206 (1963).
- (32) Terenin, A., Vilesov, F., "Advances in Photochemistry," Vol. 2, pp. 385-421, ed. W. A. Noyes, Jr., G. S. Hammond, and J. N. Pitts, Jr., Interscience, New York.
- (33) van Bekkum, H., Verkade, P. E., Wepster, B. M., *Rec. trav. Chim.* **78**, 815 (1959).
- (34) Vilesov, F. I., *Zhur. Fiz. Khim.* **35**, 2010 (1961).
- (35) Watanabe, K., Nakayama, T., Mottl, J., "Final Report on Ionization Potentials of Molecules by a Photoionization Method," December, 1959, Dept. Army No. 5B-99-01-004, ORD TB2-0001-OOR-1624.

RECEIVED April 28, 1965. Supported by Public Health Service Research Grant GM-10038 from the National Institutes of Health.

Reactions of the Hydrated Electron with Substances of Biological Importance

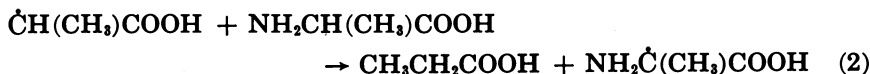
M. EBERT and A. J. SWALLOW

Paterson Laboratories, Christie Hospital and Holt Radium Institute, Manchester 20, England

Re-examination of the radiolysis of aqueous solutions of alanine (absence of oxygen) shows that electrons react rapidly with the cationic form, less rapidly with the zwitterion, and much less rapidly with the anionic form. These conclusions have been confirmed by pulse radiolysis. Rate constants for amino acids, peptides, proteins, and numerous other substances have been obtained. Critical evaluation of these and correlation with molecular properties is now well under way. In living systems the reactions of the hydrated electron vary with the part of the cell concerned, with the developmental stage of the cell, and possibly with the nature of any experimentally added substances.

Aqueous solutions of substances which are biologically important have been irradiated with high energy radiations since the beginning of the century. By 1958–1962 the nature of the overall changes occurring had been elucidated in many cases (1, 23), and substantial progress had been made in working out the reaction mechanism on a basis of the primary decomposition of water into H atoms, OH radicals, and other products. In the last few years it has become clear that hydrated electrons are primary radiolysis products from water, and that in the case of many reactions previously attributed to H atoms, we are in fact dealing with the reactions of hydrated electrons. Classical radiation chemistry, when suitably reinterpreted, can now provide much information about the reactions of hydrated electrons, especially about the nature of the products formed and about the role played in the overall mechanism.

An important instance of this development is the case of amino acids. For alanine, it had previously been supposed (26) that propionic acid was formed by the reactions:

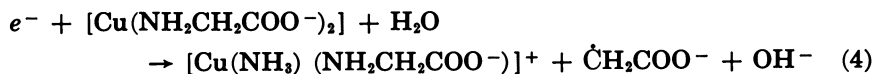


If electrons rather than hydrogen atoms are the principal reducing species in irradiated water, then one might suppose either that electrons are converted into hydrogen atoms which then react as previously supposed, or that electrons react directly giving the same products as had been attributed to H atom reactions (24). Weeks, Cole, and Garrison added formate, which reacts with H atoms but not with electrons, to a neutral solution of alanine and found that the propionic acid yield remained unaffected at $G \sim 1.0$. Hence, the electrons must be reacting directly with alanine (12, 25). By adding chloracetate, a known electron scavenger, to the alanine-formate system, Garrison and colleagues were able to estimate that the rate constant for the reaction of the hydrated electron with the zwitterion form of alanine, now written:



was about $1/100$ of the reaction rate with chloracetate—i.e., $k \sim 10^8 M^{-1} \text{ sec.}^{-1}$. By studying the effect of pH on the propionic acid yield they found that the rate constant for the reaction with the cationic form was about $1/3$ the rate constant for reaction with H^+ —i.e., was in the region of $10^{10} M^{-1} \text{ sec.}^{-1}$ (25). The original pH obtained for glycine by Stein and Weiss in 1949 (21), and confirmed for alanine by Maxwell, can be explained if the electron is relatively unreactive with the anionic form of the amino acids (13).

More recently Willix, Weeks, and Garrison have shown that β -amino acids are relatively unreactive towards electrons regardless of the ionic form (28). Willix and Garrison have also shown that electrons react with the bis-glycinato-Cu(II) chelate leading to chemical change in the ligand (27)



Although it is necessary to re-examine all mechanisms based on H atoms, many will be found to be still correct because hydrated electrons are readily converted into hydrogen atoms by hydrogen ions ($k = 2 \times 10^{10}$) and by other reagents acting as Brönsted acids. In particular Jortner, Ottolenghi, Rabani, and Stein have shown that at neutral pH, the ion H_2PO_4^- can convert electrons into hydrogen atoms (18). Substances of biological importance in neutral solutions are thus not necessarily being exposed to the action of hydrated electrons on irradiation. It is known that solutions containing nicotinamide adenine dinucleotide

(NAD) and an excess of pyrophosphate buffer (pH 7.8) and ethanol give hydrogen with $G = 3.2$ on irradiation (22). If the electrons had reacted with the NAD the yield of hydrogen would have been expected to be only the molecular yield $G \sim 0.5$ plus a small contribution owing to H atom reactions. Presumably the pyrophosphate ions converted the electrons into hydrogen atoms which were then able to dehydrogenate ethanol as proposed in the original mechanism:



Evidence from Pulse Radiolysis

In the last two or three years the application of the pulse radiolysis technique has provided a wealth of information about rate constants which without pulse radiolysis could have been obtained only with very great difficulty. Lists of rate constants obtained by pulse radiolysis have been given elsewhere (3, 10). The published values for alanine and glycine, including the most recent data, are given in Table I.

Table I. Rate Constants for Reaction with the Hydrated Electron (room temperature)

Substance	pH	Rate Constant	Reference
Alanine	Neutral or alkaline	$8 \times 10^7 M^{-1} \text{ sec.}^{-1}$	(16)
	Neutral or alkaline	$<10^7$	(15)
	6.8	5×10^6	(7)
	6.4	5.9×10^6	(9)
Glycine	Neutral or alkaline	1.2×10^8	(16)
	Neutral or alkaline	$<10^7$	(15)
	neutral	$<10^7$	(5)
	6.4	8×10^6	(7)
	6.3	8.5×10^6	(9)
		(mean value)	
	8.5	5.5×10^6	(9)
9.5	4.1×10^6	(9)	
11.0	1.8×10^6	(9)	

Rate constants for reactions of the hydrated electron are usually obtained by measuring the rate of disappearance of the absorption 5000 – 7000 Å., the exact wavelength chosen depending on the characteristics of the analyzing light. Two assumptions are made: (1) the absorption is in fact caused by the hydrated electron, and (2) the electron is disappearing by reaction with the solute of interest, in this case, alanine or glycine. In the work by Davies, Ebert, and Swallow (9) the first assumption was checked by noting that the position and height of the absorption peak agreed with that of the hydrated electron, and that air, N_2O , or hydrogen ions caused the absorption to disappear, commensurate with the known rate constants. Hence, the possibility could be excluded that the absorption was caused by some other species, formed, for example, by attack of OH radicals or the hydrated electrons themselves on glycine. The second assumption, particularly delicate in view of the low apparent reactivity of the materials, was justified by careful deaeration, by exhaustive purification of the amino acids, and by the use of sufficiently low doses and high solute concentrations to eliminate reaction

of electrons with other electrons or radicals. Accordingly, and in view of the agreement with the other most recent value obtained independently by Braams (7), we can conclude that in neutral solution, the rate constant for reaction with alanine is $6 \pm 1 \times 10^6 M^{-1} \text{ sec.}^{-1}$ and with glycine $8.5 \pm 0.5 \times 10^6 M^{-1} \text{ sec.}^{-1}$. The value for alanine is about 20 times less than that concluded by Garrison and colleagues; but in view of the direct nature of the measurement, the lower value seems preferable, especially since reactive impurities can increase the apparent value of a rate constant obtained by pulse radiolysis but can never decrease it.

The effect of ionic form on the reaction of the hydrated electron with amino acids has been examined. The cationic form could not be examined since appreciable amounts of H^+ would have to be present, and with currently available techniques the electron would disappear too rapidly. But by making the solutions alkaline it has been possible to study the anionic form. For glycine (Table I), and several other amino acids and peptides (7), it has been shown that the amino acids are less reactive in the anionic form, agreeing with the conclusion drawn by Garrison. The results for glycine however cannot be interpreted on the basis of the known pK together with assumed rate constants for zwitterion and anion. Other factors are evidently present, and further work is required.

The most recent values for reactions of the hydrated electron with amino acids and peptides are now in fairly good agreement (7, 9), and attempts are being made to relate the values to other properties of the compounds. It is noted that peptides are more reactive than amino acids. This might be taken to indicate that the electron is reacting with the peptide group itself; but Braams has shown that acetyl alanine and acetyl glycine are relatively unreactive (7). Braams suggests that reactivity can be correlated with the pK of the amino group. Substances with a low pK react more rapidly, possibly because the proton is relatively weakly bound. Hence the protonated amino groups are the reaction sites. We can extend this idea to explain why the cationic form of alanine is more reactive than the zwitterion if we say that reaction with the proton on the carboxyl group is fast. Aromatic amino acids such as tryptophan, phenylalanine, or tyrosine are very reactive, and here the electron appears to be reacting with the side group (6, 9).

Other correlations of reactivity are being made, not only for substances of biological importance, but also for all other substances. Particularly important in this connection is the large reactivity of neutral $-SH$ and $-SS-$ groups (7). Also, thiourea reacts rapidly with electrons, with $k = 3 \times 10^9 M^{-1} \text{ sec.}^{-1}$ (8, 15). The high reactivity of thiourea has been related to the protection it affords polymers in aqueous solutions (8). In the absence of polymer, thiourea accepts both electrons and OH radicals, and the reduced and oxidized free radicals so produced then react with each other to regenerate the original material. When polymer is present, the OH radicals can attack the polymer, and

the electrons can attack the thiourea. Reaction between the two types of radical so produced then appears to lead to a degree of protection.

The rate constant for reaction of the electron with biological polymers such as nucleic acids (11) and proteins (7) have been examined. When calculated on a per mole basis the rate constants can be quite high—e.g., ribonuclease (pH 6.8) $k = 1.3 \times 10^{10} M^{-1} \text{ sec.}^{-1}$, lysozyme (pH 6.2) $k = 7.5 \times 10^{10} M^{-1} \text{ sec.}^{-1}$), but they are much less than if the constituent units were in free solution. For ribonuclease an attempt has been made to estimate the rate constant from the rate constants for the constituent units (6). Allowance was made for the decrease in collision radius in going from the constituent units to the protein, and for the number of positive charges on the protein molecule. The estimated value agreed with the measured value to within a factor of two or three. If this approach is accepted, one can conclude that the strongest contribution to the reactivity arises from —SS groups, and this conclusion is in line with other evidence from radiation chemistry.

Among other reactions of the hydrated electron may be mentioned the reaction with methylene blue. Methylene blue may be regarded as the prototype of easily reducible biological substances such as NAD, cytochrome-c, etc. The preliminary value for the rate constant for reaction with the hydrated electron (5) has now been shown to be too high, and the more reasonable value of $2.5 \times 10^{10} M^{-1} \text{ sec.}^{-1}$ has been obtained (19). It is thus no longer necessary to attribute special properties to methylene blue.

As well as for substances of exclusively biological importance, it is necessary, for a full understanding, to know the reactivity of hydrated electrons with substances such as H^+ , O_2 , CO_2 , water, etc. which are equally present in biological systems. Many of these rate constants are known, but unfortunately the rate constant for reaction with water itself is still not entirely certain, although it has been investigated recently by two independent groups (4, 14).

To summarize, there is still a need for carefully determining more rate constants for various substances of biological interest in their various charged forms. This phase of the subject will be complete when critically chosen values have passed into the Tables and when theoretical correlations have been sufficiently developed to enable rate constants for unexamined substances to be reliably predicted. There is also still a need to correlate the reactivity of the hydrated electron with the reactivity of free radicals such as H, OH, organic radicals, peroxy radicals, etc., so as to be able to predict the reactivity of unexamined free radicals. Another need is to establish the influence of conditions on the rate constants. The influence of ionic strength is now well known, but other factors, such as the dielectric properties of the medium, have been shown to have an effect in some cases (2, 20). Also, the effect of temperature has been investigated in only a few cases (9).

Reactions of the Hydrated Electron in Vivo.

In order to apply the chemical results to radiation biology, we must consider the structure of the living cell at various stages of the mitotic

cycle as revealed by electron micrographs. A maze of cytoplasmic membranes is present, presumably consisting of lipid molecules with the hydrophilic groups pointing into the aqueous area. This area contains a great many water-soluble proteins, metabolites, and katabolites of both low and high molecular weight. The concentration cannot be homogeneous and must be extremely inhomogeneous at the sites of organized enzymatic activity. Some of the enzymes are locked up in the nonaqueous volumes of cellular organelles, such as mitochondria and ribosomes and other submicroscopic particles of the cell. One consequence of the structured nature of the cell may be that much of the water is bound up; hence, the nature and reactivity of hydrated electrons may be quantitatively somewhat different from in dilute solutions, in the same way that hydrated electrons in strong salt solutions are different (2, 20).

Reactions of the hydrated electron can be important for radiation biology only if the molecules attacked play a vital role in the life of the cell—e.g., if they are unique or in very low numbers, or have a template function in the duplicating mechanism. This draws attention to compounds such as DNA, RNA, messenger RNA, or enzymes. Further, enzyme systems can be blocked by some antimetabolites, and this may be one way in which a chemically changed small molecule in the aqueous part of the cell may have disastrous effects. Unfortunately, although many workers have looked at this question, there is still no clear evidence on which are the important chemical changes as far as radiation biology is concerned. Nevertheless, whatever the biologically important molecules, the hydrated electrons, like any other reactive entity from the water, must be produced within about 30 Å. if they are to produce an effect (17). If a macromolecule changes its shape from linear to spherical, or from coiled to uncoiled during the life cycle of the cell, then the attack by hydrated electrons will alter, partly because of the varying volume of water involved, and partly because different chemical groups may be exposed to the electrons. It is in fact observed that the radiation sensitivity of synchronous cell cultures depends on the developmental stage of the cell. This does not prove that hydrated electrons are causing cell damage, but it shows that the possibility can still be considered.

Reactions of the hydrated electron possibly may be somewhat relevant to the action of dose-modifying agents such as O₂, NO, CO₂, and sulfhydryl compounds. It can safely be assumed that these exert their influence at the radiation-chemical level, and it is notable that many of them react rapidly with hydrated electrons. Table II, taken from a paper by Braams (6), compares the rate constant for reaction with the hydrated electron with the concentration at which certain compounds have been used as protective agents. It can be seen that, at the concentrations used in biological systems, those substances which are effective as protectors can compete favorably with oxygen for hydrated electrons. Penicillamine was not a good protector at the concentration used and did not compete as favorably as the other substances for hydrated electrons. Higher concentrations of penicillamine could not be

given to the animal with safety. It does not, of course, necessarily follow that it is reaction of the electron with oxygen which gives rise to the biological damage. Substances which react readily with the hydrated electron may well react readily with other free radicals. Among the possibilities is that macromolecular free radicals, formed for example, by direct ionization or by OH attack, may give rise to biological damage if they react with oxygen, but may be repaired in the absence of oxygen or by reaction with the protective compounds.

Table II. Correlation between Reactivity with Hydrated Electrons and in Vivo Protective Power

Substance, <i>S</i>	$k_e^- + S$ ($M^{-1} \text{ sec.}^{-1}$)	Concentration, <i>C</i> , When Used as Protective Agent (<i>mM</i>)	Protection	<i>kC</i>
Cysteine	8.7×10^9	1	+2	9×10^6
Cysteamine	2×10^{10}	2	+2	40×10^6
Cystamine	4×10^{10}	1	+2	40×10^6
MEG	2×10^{10}	0.7	+2	14×10^6
Penicillamine	5.1×10^9	1	0	5×10^6
Oxygen	2×10^{10}	0.25	—	5×10^6

Conclusion

The discovery of the hydrated electron in irradiated aqueous solutions has made it necessary to re-examine the mechanisms proposed for the irradiation of aqueous solutions of substances which are biologically important. The new technique of pulse radiolysis has provided a breakthrough in many ways, particularly in determining absolute rate constants. These advances have made it possible to begin working out the reactivity of solvated electrons in vivo, although it is not yet possible to specify the precise role of the reactions in radiation biology.

Acknowledgment

The authors are grateful to Drs. R. Braams and W. M. Garrison for sending them manuscripts in advance of publication.

Literature Cited

- (1) Allen, A. O., "The Radiation Chemistry of Water and Aqueous Solutions," Van Nostrand, Princeton, 1961.
- (2) Anbar, M., Hart, E. J., private communication.
- (3) Anbar, M., Neta, P., *Int. J. Appl. Rad. Isotopes* **16**, 227 (1965).
- (4) Baxendale, J. H., Ebert, M., Keene, J. P., Swallow, A. J., *Proc. Symp. Pulse Radiolysis*, Manchester, England, (in press).
- (5) Baxendale, J. H., Fielden, E. M., Capellos, C., Francis, J. M., Davies, J. V., Ebert, M., Gilbert, C. W., Keene, J. P., Land, E. J., Swallow, A. J., Nosworthy, J. M., *Nature* **201**, 468 (1964).
- (6) Braams, R., *Proc. Symp. Pulse Radiolysis*, Manchester, England, (in press).
- (7) Braams, R., to be published.
- (8) Charlesby, A., Fydeler, P. J., Kopp, P. M., Keene, J. P., Swallow, A. J., *Proc. Symp. Pulse Radiolysis*, Manchester, England, (in press).

- (9) Davies, J. V., Ebert, M., Swallow, A. J., *Proc. Symp. Pulse Radiolysis*, Manchester, England, (in press).
- (10) Dorfman, L. M., Matheson, M. S., *Progr. Reaction Kinetics* **3**, (in press).
- (11) Ebert, M., Scholes, G., Shaw, P., Willson, R. L., *Proc. Symp. Pulse Radiolysis*, Manchester, England, (in press).
- (12) Garrison, W. M., *Rad. Res. Suppl.* **4**, 158 (1964).
- (13) Garrison, W. M., *Rad. Res. Suppl.* **4**, 170 (1964).
- (14) Gordon, S., Hart, E. J., *Proc. Symp. Pulse Radiolysis*, Manchester, England, (in press).
- (15) Hart, E. J., Gordon, S., Thomas, J. K., *J. Phys. Chem.* **68**, 1271 (1964).
- (16) Hart, E. J., Thomas, J. K., Gordon, S., *Rad. Res. Suppl.* **4**, 75 (1964).
- (17) Hutchinson, F., *Rad. Res.* **7**, 473 (1957).
- (18) Jortner, J., Ottolenghi, M., Rabani, J., Stein, G., *J. Chem. Phys.* **37**, 2488 (1962).
- (19) Keene, J. P., Land, E. J., Swallow, A. J., *Proc. Symp. Pulse Radiolysis*, Manchester, England, (in press).
- (20) Revetti, L. M., Swallow, A. J., unpublished work.
- (21) Stein, G., Weiss, J., *J. Chem. Soc.* **1949**, 3256.
- (22) Swallow, A. J., *Biochem. J.* **61**, 197 (1955).
- (23) Swallow, A. J., "Radiation Chemistry of Organic Compounds," Pergamon Press, Oxford, 1960.
- (24) Swallow, A. J., *Proc. Int. Conf. Rad. Res.*, p. 49, Natick, Mass., 1963.
- (25) Weeks, B. M., Cole, S. A., Garrison, W. M., UCRL 11213, (1964).
- (26) Weeks, B. M., Garrison, W. M., *Rad. Res.* **9**, 291 (1958).
- (27) Willix, R. L. S., Garrison, W. M., *J. Phys. Chem.*, (in press).
- (28) Willix, R. L. S., Weeks, B. M., Garrison, W. M., *Rad. Res.*, (in press).

RECEIVED May 7, 1965.

INDEX

- A**
- Absorption spectra 202
 in the alcohols 37
 in ethylamine, potassium, and
 rubidium 151
 of metal-amines 164
 of sodium-ammonia solutions 29
 Absorption spectrum of e_{aq}^- 46
 identification 46
 Acetic acid 66, 73
 Acetone 74
 analysis 259
 Activated complex 140, 147
 Active metals 163
 Activity coefficient in metal am-
 monia solutions 90
 Acyl amides 73
 Affinity, electron 146
 Alanine, reactions of hydrated
 electron with 290
 Alcohols 73
 absorption coefficients in 38
 absorption spectra in 37
 rate constants in 41
 reaction rates of e_{aq}^- in 58
 yields in 39
 Aldehydes and ketones 73
 Alkali hydroxides, reactions of
 electrons and holes in frozen
 aqueous solutions of 210
 Alkali metals
 deuteroammonia solutions of 125
 in liquid ammonia 1
 electrical conductivity of 97
 the volume expansion of 111
 nature of electronide and spinide
 solutions of 1
 with water, reactions of 167
 Alkaline earth metal, deuteroam-
 monia solutions 126
 Alkoxides 34
 Amines 73
 absorption spectra of metal- 164
 Amino acids, reactions of hydrated
 electron with 289
 Ammonia
 deutero- *See* Deuteroammonia
 dielectric constant of liquid 131
 electrolytes in 82
 solutions, flash photolysis of 150
 spectrum of liquid 126
 Ammoniated electron 28
 with NH_4^+ , reaction of 33
 Ammoniated metal anion 29
 Ammonium ions 66
 Analysis by hydrated electrons
 of acetone 259
 of hydrogen peroxide 259
 of oxygen 257
 of thymine 259
 Analysis of hydrated electron
 scavengers, submicromolar 253
 Apparent molar volume of all
 alkali metals in ammonia 117
 Aqueous solutions of Fe^{+2} ions 235
 Arnold and Patterson model 121
 Aromatic anions, solvated electron
 formation from 237
 Aromatic carboxylic acids 75
 Aromatic compounds 75
 in aqueous solution, photoioni-
 zation of 297
 reduction of 33
 Aromatic free radicals, spectra of 282
 Aromatic molecules in rigid sol-
 vents, photoionization of 235
 Asymmetrization 234, 238
 Atom transfer reaction 145
 Atomic conductance of sodium in
 $NH_3(l)$ 2, 3
- B**
- Becker, Lindquist, and Alder
 model 4, 120, 122
 Benzene, reduction of 33
 Biological substances, reactions of
 hydrated electron with 289
 BLA model 4, 120, 122
 Blue shifts 236
 Bound state of excess electrons in
 liquids 7
 Br_2^- 62
 BrO_3^- 69
 BrO_3^{+2} 70
 Brönsted acids 65, 233
 Bubble model for a localized elec-
 tron 16
 Butadiene 76
- C**
- Carbonic acid 66
 Carboxylate ions 74
 Cation-centered monomer in am-
 monia 161

Cavity formation	9
models	16
CCl_4	59
Cd^{+1} radical ions	206
Cd^{+2}	60, 71
Cd^{+2} on the H atom yield, effect of	206
Ceric perchlorate	204
Cesium	
with ammonium, bromide, reaction of	167, 169
with ethanol, reaction of	167, 169
with HCl, reaction of	167, 169
with methanol, reaction of	167
with water, reaction of	167
rate constants	168
CF_3Cl	74
Charge of e_{aq}^-	47
Charge transfer reactions in frozen aqueous solutions, photochemical	195
Charge transfer to the solvent (CTTS)	231
CHCl_3	59
$(\text{CH}_3)_2\text{COH}$	63
Chemiluminescence	144, 147
CH_2OH	63
Chromate on the yields, effect of	210
Citric acid	66, 74
Cl_2^-	62
Cleaning procedure for glassware	165
ClO_3^-	69
ClO_3^{2-}	70
$\text{C}(\text{NO}_2)_3^-$	60
CO	67
CO^-	67
CO_2	68
CO_2^-	68
Comparison of k with e_{aq}^-	41
Competition kinetics in e_{aq}^- reactions	57
Competition with fluorescence	235
Conductance of sodium in $\text{NH}_3(\text{l})$	3
Conductance and structure	1
Conduction processes in concentrated metal-ammonia solutions	96
$\text{Co}(\text{NH}_3)_6^{+3}$	60
Continuum model	20
Continuum theory	142
COOH	68
Coulombic compounds	1, 2
force	5
interactions	4
in solutions	2
Cr^{+2}	71
$\text{Cr}(\text{CN})_6^{-3}$	60
$\text{Cr}(\text{C}_2\text{O}_4)_3^{-3}$	60
$\text{Cr}_2\text{O}_7^{-2}$	60
CS_2	59, 68
CS_2^-	68
CTTS	231
bands	235
transitions	232
Cu^{+2}	71

D

Debye-Hückel theory	97
Degassing, efficiency of	258
Density dependence of well depth	19
Deuteroammonia	
dielectric constant of liquid	131
preparation of	127
spectroscopy of metal solutions	125
spectrum of liquid	126
Diffusion	233
coefficient in metal ammonia solutions	92
constant of e_{aq}^-	50
control	140
controlled encounter rates of e_{aq}^-	51
controlled rate constants of e_{aq}^-	52
controlled reactions of e_{aq}^-	59
Dimer model for solvated electrons, solvent	173
Dimer species, M_2	29
Disodium spinide	5
Dissociation of the excited ion	233
Dissociation of the spinide	5
Distribution, initially inhomogeneous	233
Disulfide, reactions of hydrated electron with	292
Dose-modifying agents	294

E

e_{aq}^-	
in concentrated electrolyte solutions	58
equilibrium with H atoms in water	48
rate constants with acids	246
reaction, effect of ionic strength on the rate of	47
reaction with	
e_{aq}^-	59, 63
H	63
H^+	60
H_2O	64
H_2O_2	59
H_3O^+	65
I_2	59, 62, 69
MnO_4^-	60
NO_3^-	69
O_2	59
OH	63
tetranitromethane	47, 59
reactions, competition kinetics	57
e_{solv}^- in alcohols, reaction rates of	58
Effect of	
Cd^{+2} on the H atom yield	206
chromate on the yields	210
different electron scavengers on H atom yields	187
ionic strength on rate of e_{aq}^- reaction	58
temperature changes	236
Effective charge	239

- Effective (*continued*)
 electron mass 100
 mass for translation of the sol-
 vated electron 143
 mass of electron 10
- Electrical conductance 87, 89
 of electrolyte solutions 83
 of metals in amines 83, 87
 of metals in ammonia 83
 of sodium in ammonia 86
 temperature effect 88
- Electrical conductivities
 of alkali metals in ammonia 97
 of metals in ammonia 102
- Electrons 1, 3
- Electrochemical electron transfer
 reactions 146
- Electrolyte solutions 85
 e_{aq}^- in concentrated 58
 in ammonia 82
 in water 82
- Electron
 affinity 146
 attachment reactions, kinetics of . 163
 binding in polar solvents 22
 bubble model for a localized 16
 conductance 87
 entropy in ammonia 94
 polarization 141
 scavengers 186, 215, 233
 solvent interactions in liquid
 rare gases 9
 transfer
 from metal amide to metal ion . 160
 reactions 138, 143
 theory 138
- Electron trapping 218
- Electronic energies for localized
 state 18
- Electronic wave function of a sol-
 vated electron 140
- Electronide solutions of alkali
 metals in $NH_3(l)$ 1
- Electronides 1, 4
- Electrons
 formation and reactions of 180
 heat of transport 93
 and holes in irradiated ice 224
- EMF of metal ammonia solutions . . 90
- Energies for localized state, elec-
 tronic 18
- Energy levels of hydrated electron . . 23
- Energy of solvation of e_{aq}^- 234
- Energy surface, potential 139
- Environment, equilibrium of e_{aq}^-
 with its ionic 58
- Environmental effects 238
 on the spectrum 232
- Enzymes, reactions of hydrated
 electron with 294
- Equilibrium of e_{aq}^- with its ionic
 environment 58
- Equilibrium with metal ions, sol-
 vated electrons in 57
- Equivalent ionic conductance of
 e_{aq}^- 50
- ESR spectra 182
- ESR spectrum, potassium in
 ethylamine 152
- Ethylamine, absorption spectra in . . 151
- Ethylenediamine, reactions in 164
- Exchange energy 71
- Exchange reaction, $NH_3 + NH_4^+$. . 33
- Exchange reactions, homogeneous
 electron 145
- Excited ion, dissociation of the 233
- Excited state
 lifetime of the 237
 spectroscopic 234
 lowest singlet 237
 thermal dissociation of the 232
- Excited water 263, 272
- Expanded metal
 dimer model 29
 model 29
- Extinction coefficients
 of amide and metal solutions . . . 153
 of solvated electrons 135
 in the alcohols 38, 39

F

- Fast reactions of solvated electrons . 163
- Fe^{+2} 195
- Fe^{+2} ions, aqueous solutions of 235
- Ferrocyanide 71, 238
 flash photolysis of 238
 photochemistry of 238
 solvated electron formation in . . . 238
 spectroscopy of 238
- F, F^1 , and F_2 centers 89
- Flash photolysis 234
 of aqueous solutions of phenols . . 235
 of ferrocyanide 238
 hydrated electron generation 297
 of metal-amine or ammonia solu-
 tions 150
 of potassium amide 156
- Fluorescence 234
 competition with 235
 and solvated electron forma-
 tion 236, 237
 and thermoluminescence 227
- Formaldehyde 74
- Formation of
 ClO_2 radical 201
 e_{aq}^- 235
 electrons and holes 180
 HPO_4^- radical ion 200
 SO_4^- radical ion 198
 solvated electron 56
 Formic acid 66
- Franck-Condon principle 231
- Free electron model 13
- Free energy 142
 in metal ammonia solutions 91
- Freeze-purification 165
- Frozen aqueous solutions, reduc-
 tion of metal ions in 205
- Furan 76

G	
G_{H_2}	265
<i>g</i> -Factors, line widths and	213
<i>g</i> -Shifts.....	223
Gamma-irradiated frozen aqueous solutions.....	180
Gamma-irradiated ice.....	180
Gas-phase PIP, correlation with optical hydrated electron production.....	283
Geminate recombination.....	233
of $\text{H}_2\text{O} + \text{OH}^-$	273
Glassware, cleaning procedure for.....	165
Glycine, reactions of hydrated electron with.....	291
H	
H atom.....	63
<i>See also</i> Hydrogen scavengers.....	233
yields.....	183, 186
effect of Cd^{+2} on the.....	206
effect of different electron scavengers on.....	187
H atoms.....	59
conversion to e_{aq}^-	242, 247
dissociation constant in water.....	251
evidence for formation by radiation.....	244
independent yield of.....	244
rate constants of.....	248
reaction with OH^-	247
H^+_{aq}	235
Halide ions.....	233
Hall effect.....	97, 102
Haloaliphatic compounds.....	74
Hammitt substituent constant, correlation with optical hydrated electron production.....	284
H/D isotope effect.....	65, 66
Heterocyclic compounds.....	76
Hg^{+1} radical ion.....	208
HO_2	63
$\text{H}_2\text{O}_{\text{aq}}$	65
H_2O formation.....	269, 272
Holes.....	
formation and reactions of.....	180
reaction of the positive.....	196
Homogeneous electron exchange reactions.....	145
H_2PO_4^-	66
HSO_4^-	66
Hydrated electron.....	
comparison of scavenging with optical production.....	287
conversion to H.....	242, 245
production of.....	256
reactions of.....	55, 289
in radiation chemistry.....	45
scavengers, submicromolar analysis of.....	253
<i>in vivo</i> , reactions of.....	293
Hydrated electrons.....	
analysis by.....	253
Hydrated electrons (continued)	
from aromatic compounds, optical generation of.....	297
in chain reactions.....	259
as product of interaction of hydroxide ions with hydrogen atoms.....	57
in water, decay of.....	254
Hydration energy of electron.....	49
Hydration shell, reaction in the.....	187
Hydrocarbons.....	73
Hydrogen.....	67
abstraction by amine radicals.....	160
atom formation.....	182
atom yields.....	184
evolution in photochemistry of aqueous solutions.....	230
peroxide analysis.....	259
peroxide, chain decomposition.....	260
photochemical evolution of.....	235
Hydroxy complexes.....	72
Hydroxyl ammonium ions.....	66
I	
I^-	195, 233
I_2^-	69
Imidazole.....	76
Indole.....	76
Inhomogeneous, diffusion-controlled kinetics.....	231
Initially inhomogeneous distribution.....	233
Interconvertibility of e_{aq}^- and H.....	242
Interspur yields.....	277
Intraspur H_2 in radiolysis of water.....	263
Intraspur yields.....	276
Intrinsic reorganization factor.....	142
IO_3^-	69
Ion pair of sodium ion and electron.....	4
Ion pairs.....	85
Ion triplets.....	89
Ionic aggregates in ammonia.....	29
Ionic strength.....	
on rate constant of $e_{\text{aq}}^- + \text{ferrocyanide}$, effect of.....	48
on the rate of the e_{aq}^- reaction, effect of.....	58
on reaction rates of e_{aq}^- , effect of.....	47
Isopropyl alcohol.....	74
K	
Ketones, aldehydes and.....	73
Kinetic motion.....	52
Kinetics.....	
of ammonium-electron reaction.....	31
of electron-attachment reactions.....	163
inhomogeneous, diffusion-controlled.....	231
L	
Lactic acid.....	66, 74
LCAO-MO scheme for solvent dimer model.....	176

- LET effects 270
 Lifetime of the excited state 237
 Lifetime of the spectroscopic excited state 234
 Ligand field 71
 Light intensity vs. quantum yield 234
 Limiting conductance of sodium in $\text{NH}_3(\text{l})$ 3
 Line widths and g -factors 213
 Liquid ammonia, sodium in 3
 Liquid ammonia, volume expansion of alkali metals in 111
 Liquids at equilibrium, structure of 8
 Lithium in $\text{NH}_3(\text{l})$ 112
 Localized excess electron 9
 states in polar solvents 20
 Lowest singlet excited state 237
- M**
- Magnetic susceptibility 106
 Magneto-resistance 105
 Mass action constants 86
 of metals in amines 84
 Mechanisms of H atom formation and stabilization 186, 191
 Metal amide, extinction coefficients 153
 Metal-amine
 flash-photolysis of 150
 solutions, electrical transport properties of metal-ammonia and 82
 Metal-ammonia
 and metal-amine solutions, electrical transport properties of 82
 solutions
 conduction processes in concentrated 96
 stability of 131
 structure and kinetics 27
 Metal-deuteroammonia solution, spectroscopy of dilute 125
 Metal dimer
 in ethylamine 152
 model, expanded 29
 Metal-ethylenediamine systems 170
 Metal ions
 in frozen aqueous solutions, reduction of 206
 solvated electrons in equilibrium with 57
 Metal model, expanded 29
 Metal monomer in ethylamine 152
 Metal solutions
 formation of 149
 photochemistry of 149
 Methylene blue, reactions of hydrated electron with 293
 Mg^{+1} and Zn^{+1} radical ions 208
 Mg^{+2} 70
 Micro Wien effect 5, 85, 89
 Mn^{+2} 71
 Mobile species, nature of the 191
 Mobility of e_{aq}^- 50
- Mobility of electron 9, 10, 11
 Molar extinction coefficient of e_{aq}^- 47
 Molecular geometry of liquids 8
 Monomer 164
 species, M 29
 Multiple scattering effects 14
- N**
- β -Naphthol 236
 Nature of the mobile species 191
 NH_4^+ 66
 NH_4OH 66
 Nicotinamide adenine dinucleotide, reactions of hydrated electron with 290
 Nitrogen 67
 Nitrous oxide, chain decomposition 260
 NO 59, 63
 NO_2 63, 69
 NO_2^- 69
 NO_3 60
 N_2O 67
 N_2O^- 67
 Nucleic acids, reactions of hydrated electron with 293
- O**
- O^- radical ion 215
 O^- radical ions, yields of trapped electrons and 215
 O_2^- 64
 OH 59, 63
 OH^- 182, 233
 Olefins 73
 Optical generation of hydrated electrons from aromatic compounds 297
 Organic liquids, solvated electron in 36
 Oscillator strength of e_{aq}^- 47
 Oxalic acid 66, 74
 Oxygen
 analysis 257
 removal by pre-irradiation 258
- P**
- Pair correlation function 8
 Penicillamine, reaction with hydrated electron 294
 Pentavalent chromium 209
 Peptides, reactions of hydrated electron with 292
 Persulfonate ions 70
 Phase effects 194
 Phenolate ion 235
 Phenols, flash-photolysis of aqueous solutions of 235
 Photochemical
 bleaching in acid glasses 203
 charge transfer reactions in frozen aqueous solutions 195

Photochemical (<i>continued</i>)	
evolution of hydrogen	235
formation of e_{aq}^- from I_{aq}^-	235
reaction	204
Photochemistry of	
aqueous solutions	230
ferrocyanide	238
metal solutions	149
Photoionization	
of aromatic molecules in rigid solvents	235
in solution, energetics of	285
Photolytically generated solvated electron	56
Photoregeneration	151
pK of e_{aq}^-	48
Plane wave electrons in He, energy of	15
Plumbate (II)	72
Polarization	
electron	20
energy	94
solvent	141
Polaron	22, 29, 143
theory	146
Positive holes in ice	197
Potassium	
absorption spectra in	151
dimer in ethylamine	155
in ethylamine, ESR spectrum	152
in liquid ammonia	113, 114
volume minimum for	118
monomer in ethylamine	155
Potential barrier of He to electrons	9
Potential energy surface	139
Properties of hydrated electron	47
Proteins, reactions of hydrated electron with	293
Proton conductance	87
Proton transfer	171
Pseudopotential	11
Purines	76
Pyridine	76
Pyrimidines	76
Pyrrole	76
Q	
Quantized vortex rings	10
Quantum mechanics	142
Quantum yield <i>vs.</i> light intensity	234
Quasi-free state of excess electrons in liquids	7
R	
R-band excitation	152
Radial distribution function	8
Radiation chemistry, hydrated electron in	45
Radiation protection <i>vs.</i> reactivity with hydrated electrons	295
Radiolysis of ice and frozen aqueous solutions	180
Radiolysis of water	263
Radiolytically generated solvated electron	56

Radius of charge distribution of e_{aq}^-	48
Rare earth	70
Rate constants	140, 141, 147, 192
in the alcohols	41
of hydrated electron	50
significance in diffusion theory of water radiolysis	52
of transients in water radiolysis	51
Reaction	
of cesium	
and ammonium bromide	169
and ethanol	167, 169
and HCl	167, 169
and NH_4Br	167
and rubidium with methanol	167
coordinate	140
of e_{aq}^-	
and ferricyanide	48
and H^+	60
and hydrogen ion, activation energy	52
and hydrogen ion, redox potential of	48
and H_2O_2	59
and MnO_4^-	60
and O_2	59
and tetranitromethane	47, 59
in the hydration shell	187
of the positive holes	196
rates of e_{aq}^- in alcohols	58
of rubidium and methanol	169
Reactions of	
alkali metals with water	167
e_{aq}^- , diffusion controlled	59
the electron, relative rates of	193
electrons and holes	180, 182, 210
the hydrated electron	55
solvated electrons, fast	163
Reducing radicals, radiolytic production of	243
Reduction	
by alcohols and alkali metals in $NH_3(l)$	33
of aromatic compounds	33
of benzene	33
of metal ions in frozen aqueous solutions	205
Re-irradiation or removal of oxygen	258
Relative rates of reactions of the electron	193
Reorganization factor, intrinsic	142
Rotons, interaction between electrons and	9
Rubidium	
in ethylamine solutions, absorption spectrum of	151
with methanol, reaction of	167, 169
S	
Scattering lengths of electrons	13
Scavengers	193
submicromolar analysis of hydrated electron	253

- Scavengers (*continued*)
- which convert e_{aq}^- 234
 - Screening 24
 - Shedlovsky conductance function 88
 - Singlet and triplet states of the electron pair 30
 - $S_2O_8^{2-}$ 60
 - Sodium
 - ammonia solutions, absorption spectra of 29
 - with ethanol in $NH_3(l)$, reaction of 31
 - in $NH_3(l)$ 2, 3
 - volume minimum for 118
 - salt effect on spectrum in liquid ND_3 134
 - spectrum in $ND_3(l)$ 132
 - and water rate constants 168
 - Solvated electron 87, 111
 - binding energies of 177
 - comparison of cavity, cation trap, and solvent dimer models 173
 - dimension of dimer skeleton 177
 - dissociation of metals into ions and 117
 - effective mass for translation of 143
 - electronic wave function of 140
 - in equilibrium with metal ions 57
 - of the first kind 231
 - formation of 56
 - from aromatic anions 237
 - in ferrocyanide 238
 - in photochemistry of aqueous solutions 230
 - kinetics of formation 174
 - minimized 96
 - model for 173, 174
 - in ND_3 , extinction coefficient of 135
 - in NH_3 , extinction coefficient of 56
 - photolytically generated 56
 - radiolytically generated 56
 - reaction rates 171
 - the solvent dimer model 173
 - solvent dipoles and 176
 - species: HX , H_2Y , H_3Z , H_4W 176
 - spectral transitions of 177
 - standard oxidation potential 145
 - standard potential for 145
 - various species of 175
 - Solvent polarization 141
 - Spectra 212
 - in amines and ethers 43
 - Spectrophotometry, low temperature dewar 127
 - Spectroscopic excited state, lifetime of the 234
 - Spectroscopically effective radius of ion 232
 - Spectroscopy of
 - ferrocyanide 238
 - metal-deuteroammonia solutions 125
 - Spectrum, environmental effects on the 232
 - Spin coupling in the ionic clusters 30
 - Spin-paired species 111
 - Spinide 1, 4, 5
 - dissociation 4
 - solutions of alkali metals in $NH_3(l)$ 1
 - Spinions 1, 5
 - Stages in formation of solvated electron, two 238
 - Standard oxidation potential of the solvated electron 145
 - Standard potential for the solvated electron 145
 - Statistical mechanics 142
 - Stopped-flow technique 164
 - Structure of liquids at equilibrium 8
 - Styrene 76
 - Sulfhydryl, reactions of hydrated electron with 292, 294
 - Symons' confined model 122
- T**
- $T_{H_2O}^{*}$ 275
 - Tellurite ions 70
 - Temperature changes, effect of 236
 - Temperature coefficient of resistance 89
 - Theoretical studies 7
 - Thermal conductivity of metals in ammonia 108
 - Thermal dissociation of the excited state 232
 - Thermalized nonsolvated electrons 58
 - Thermodynamic and mechanistic studies of reactions 30
 - Thermodynamic functions for species in $NH_3(l)$ 30
 - Thermoelectric
 - effect in metal ammonia solutions 93
 - effect in mixed salt-metal-ammonia solutions 93
 - power 105
 - Thiophene 76
 - Thiourea, reactions of hydrated electron with 292
 - Thomas-Fermi model 97
 - Thymine analysis 259
 - Transfer reaction
 - atom 145
 - electrochemical 146
 - electron 138, 143
 - Transfer theory, electron 138
 - Transference numbers
 - of electrons 90
 - of metal ammonia solutions 90
 - Transient absorption, recording of 255
 - Transition
 - metal ions 71
 - to metallic state 23
 - $\pi \rightarrow \pi^*$ 235
 - Translation of the solvated electron, effective mass for 143
 - Transport properties of metal-ammonia and metal-amine solutions, electrical 82
 - Trapped electrons 218
 - and O^- radical ions, yields of 215

Trapped hole.....	203
yield of.....	204
Triplet state.....	237
Tunnelling mechanism.....	93
Two stages in formation of e_{sol}^-	238
Two-step mechanism.....	236

V

V-band excitation.....	152
Valence electron wave function.....	11
Volume change	
of cesium in ammonia.....	116
of potassium in ammonia.....	115
Volume expansion	
of alkali metals in liquid ammonia.....	111, 112
of metal solutions.....	117
minimum.....	118
for solutions of sodium in ammonia.....	112

W

Walden product.....	83, 87
Water-soluble polyesters.....	93
Wave function of a solvated electron, electronic.....	140
Wien effect.....	5, 86
in metal ammonia solutions.....	89

Y

Yield of trapped holes.....	204
Yields in the alcohols.....	39
Yields of trapped electrons and O^- radical ions.....	215

X

Zn^{+1} radical ions, Mg^{+1} and.....	208
Zn^{+2}	71